



**MONASH** University

# **The Development of New Treatments for Multi-Drug Resistant Tuberculosis**

Lisa Barbaro

*B. Pharm. Sci. (Hons)*

A thesis submitted for the degree of Doctor of Philosophy at

Monash University in 2019

Monash Institute of Pharmaceutical Sciences

## Copyright notice

© Lisa Barbaro (2019).

## **Dedication**

This thesis is dedicated to my parents.

To my mother, Giulia

who was a constant pillar of support through this journey.

To the memory of my late father, Carmine

who did not get the chance to see me realise this dream.

## Abstract

Tuberculosis (TB) is an ancient disease resulting from infection with *Mycobacterium tuberculosis* (*M.tb*). Largely fuelled by the recent rise in multi-drug resistant (MDR) infections, TB has re-emerged as a major global health concern and is currently responsible for more deaths annually than any other infectious disease. In response to the urgent need for new therapies to combat drug resistance, bedaquiline (BDQ, developed by Janssen) received accelerated approval from the United States Food and Drug Administration (FDA) in 2012. Despite being highly efficacious against MDR-TB as a result of a novel mode of action, BDQ has been associated with significant toxicities and liabilities which have limited its widespread clinical use. Of most concern is cardiotoxicity resulting from the inhibition of the human ether-a-go-go-related gene (hERG)-encoded channel, however other adverse effects include including phospholipidosis, hepatotoxicity and drug-drug interactions. Additionally, BDQ possesses an extremely long terminal elimination half-life (5.5 months after dosing), which can prolong adverse effects, thus contributing to toxicity.

Bedaquiline's various liabilities can be attributed to specific structural and physicochemical features. In particular, BDQ is highly lipophilic (cLogP 7.25), a property which is well-documented to significantly contribute to drug toxicity and pharmacokinetic (PK) issues. As such, the primary objective of this project was to investigate whether modifying BDQ's structure to reduce lipophilicity could result in equipotent derivatives with improved safety and PK profiles.

Our initial strategy to lower lipophilicity was to replace BDQ's quinoline ring (region A) with the less lipophilic pyridine heterocycle. Given that Janssen's SAR was invariably dependant the quinoline throughout their development of BDQ, this also allowed us to enter into novel IP space. To access these novel derivatives, new synthetic methods were developed to facilitate the incorporation of alternate heterocycles in this region, resulting in the synthesis of a library of substituted pyridyl derivatives. This study confirmed that potent *in vitro* activity could be achieved despite replacement of the quinoline ring in this region. Although attempts were made to lower lipophilicity by introducing polar substituents to the ring, only pyridine derivatives substituted with an additional phenyl moiety in the C5 position were found to return potent activity comparable to BDQ. As such, only minor reductions in lipophilicity were achieved using this strategy.

With novel IP in hand, the second phase of this project aimed to explore additional lipophilicity lowering modifications to the diaryl region of BDQ (regions B and C). Somewhat fortuitously, an optimised second-generation BDQ analogue (TBAJ-587) was disclosed by a competing research group which provided more polar moieties in these B and C regions for us to trial. As such, the second phase of this project was focused on incorporating these polar B and C regions of TBAJ-587 with our novel



pyridine A region. A considerable effort went into devising a synthetic pathway that would enable these additional modifications, resulting in a series of highly potent hybrid structures with significantly reduced lipophilicities. Two hybrid derivatives were further assessed for their hERG channel inhibition, which identified one compound with a significantly reduced risk of cardiotoxicity in comparison to BDQ and TBAJ-587. Interestingly, the least lipophilic analogue of the pair exhibited very potent hERG inhibition, thus highlighting that lipophilicity is not the sole property responsible for a compound's interaction with the channel.

In the last study of this thesis, we aimed to extend the SAR of our hybrid series to incorporate more polar diazine rings (pyrazine and pyridazine) in place of the A region pyridine. Although not completed within the time-frame of this project, substantial progress was made towards establishing new pathways which will allow for future investigation into the effects of these novel modifications.

## **Declaration**

This thesis is an original work of my research and contains no material which has been accepted for the award of any other degree or diploma at any university or equivalent institution and that, to the best of my knowledge and belief, this thesis contains no material previously published or written by another person, except where due reference is made in the text of the thesis.

Signature: Lisa Barbaro

Date: July 23<sup>rd</sup>, 2019

## Achievements during enrolment

### Publications:

**Barbaro, L.**; Priebbenow, D. L.; Che, D.; Baell, J. B. *Antibacterial Compounds and Methods of Use*, Australian Provisional Patent Application 2018903291, filed Sep 4th **2018** by Monash University.

Priebbenow, D. L.; **Barbaro, L.**; Baell, J. B. *New Synthetic Approaches towards Analogues of Bedaquiline*. *Org. Biomol. Chem.* **2016**, 14 (40), 9622–9628.

### Conference presentations:

Royal Australian Chemical Institute Medicinal Chemistry and Chemical Biology Conference, Brisbane, Australia, **2018** (Poster Presentation)

European Federation for Medicinal Chemistry 5th Young Medicinal Chemist Symposium, Ljubljana, Slovenia, **2018** (Flash Presentation)

XXV European Federation for Medicinal Chemistry International Symposium on Medicinal Chemistry, Ljubljana, Slovenia, **2018**, (Poster Presentation)

Royal Australian Chemical Institute 42nd Annual Synthesis Symposium, Melbourne, Australia, **2017**, (Oral Presentation)

Tuberculosis Centre of Research Excellence Conference, Sydney, Australia, **2017**, (Oral Presentation)

Royal Australian Chemical Institute National Centenary Congress, Melbourne, Australia, **2017**, (Oral Presentation)

### Awards:

Best Poster Prize, XXV European Federation for Medicinal Chemistry International Symposium on Medicinal Chemistry, Ljubljana, Slovenia, **2018**

Second Place Oral Presentation, Monash Postgraduate Symposium, **2017**

## Acknowledgements

Completing this PhD over the past four years has been nothing short of a marathon - a true product of persistence, determination and resilience. Integral to me realising this goal is the endless support that I have been so fortunate to have received throughout this experience. I would like to take this opportunity to thank all the people who have made this incredible journey possible.

Firstly, I would like to express my sincere gratitude to my supervisors Prof. Jonathan Baell and Dr. Daniel Priebbenow for their unlimited support, guidance, and inspiration. Jonathan, thank you for allowing me to undertake a PhD within your group. It has been a great privilege filled with many valuable experiences and opportunities. Your constant enthusiasm, positive outlook and unique sense of humour are all qualities I've appreciated along the way, especially when things didn't always go as planned. Thank you for believing in me. Dan, thank you for inspiring me to strive for nothing less than perfect and for pushing me to make the most of this PhD. I can't thank you enough for being so generous with your time to provide endless feedback, coaching, advice and general chemistry wisdom. You have played such an integral part in what I have achieved and learned throughout this PhD - you are truly a super star.

I would also like to acknowledge and thank all the collaborators who have contributed to this project. Thanks to Prof. Jamie Triccas and Dr. Gayathri Nagalingam (Centenary Institute, Sydney) for performing the majority of our REMA assays, and for dealing with an overwhelmingly large number of test compounds. Many thanks to Assoc. Prof. Nick West and Dr. Lendl Tan (University of Queensland) for taking over recent responsibility of the REMA assay and for ensuring this was completed in time for inclusion within this thesis. Thanks to Dr. Daqing Che and his team at HangZhou (China) for performing all our diastereomeric separations. Many thanks to Dr. Mrinal Kundu and his team at TCG Lifesciences (India) for performing all chiral separations, and for bending over backwards to ensure that our samples were returned in time to include within this thesis. Thanks to Dr. Robert Gable at the University of Melbourne who undertook the crystallography study presented in this thesis.

I would also like to extend my gratitude to Dr. Jason Dang for providing me with the opportunity to develop in-depth NMR, LC and Mass Spec knowledge as a member of his team. Thank you for all your generous support, it truly means a lot.

A big thank you to all the members of the Baell group, both past present, for making these four years an enjoyable and sometimes crazy experience. There are far too many of you to name individually, but each and every one of you have had a very unique impact on my time in his group, for which I appreciate and cherish.

To all the fellow students I have shared this PhD experience with. Thank you for being such great company and for all the special memories. We all share a special bond stemming from this collective journey that I hope will never be lost.

Thank you to all my friends for your love, support and patience. I am truly blessed to have such a beautiful network of people in my life. Thank you for always bringing me back to centre and make me smile, especially when I needed it the most.

To my family, for your unconditional love and encouragement. Thank you for continuously showing an interest in what I've been up to in my PhD, even if it didn't really make much sense. I love you all so very much.

## Abbreviations

|                                 |   |
|---------------------------------|---|
| °C                              | Degrees centigrade                              |
| 2D                              | 2-Dimensional                                   |
| Å                               | Angstrom  |
| Ac                              | Acetyl  |
| ADME                            | Absorption, distribution, metabolism, excretion |
| Ar                              | Aryl  |
| ATP                             | Adenosine triphosphate                          |
| B <sub>2</sub> pin <sub>2</sub> | Bis(pinacolato)diboron                          |
| BDQ                             | Bedaquiline                                     |
| CDCl <sub>3</sub>               | Deuterated chloroform                           |
| CDI                             | 1,1'-Carbonyldiimidazole                        |
| Cryo-EM                         | Cryogenic electron microscopy                   |
| CYP                             | Cytochrome P450                                 |
| CYP3A4                          | Cytochrome P450 isoenzyme 3A4                   |
| Da                              | Dalton  |
| DARQ                            | Diarylquinoline                                 |
| DMA                             | <i>N,N</i> -Dimethylacetamide                   |
| DMAP                            | 4-Dimethylaminopyridine                         |
| DME                             | 1,2-Dimethoxyethane                             |
| DMF                             | Dimethylformamide                               |
| DMSO                            | Dimethylsulfoxide                               |
| DMSO- <i>d</i> <sub>6</sub>     | Deuterated dimethyl sulfoxide                   |
| DoM                             | Directed <i>ortho</i> -metalation               |
| dr                              | Diastereomeric ratio                            |
| ECG                             | Electrocardiogram                               |
| ESI                             | Electrospray ionisation                         |

|                  |   |
|------------------|---|
| EtOAc            | Ethyl acetate   |
| FDA              | Food and Drug Administration                                    |
| Glu              | Glutamate   |
| h                | Hours   |
| H37Rv            | Virulent laboratory strain of <i>Mycobacterium tuberculosis</i> |
| HC               | Heterocycle   |
| hERG             | Human <i>ether-a-go-go</i> -related gene                        |
| HIV              | Human immunodeficiency virus                                    |
| HPLC             | High-performance liquid chromatography                          |
| HR-MS            | High resolution mass spectrometry                               |
| IC <sub>50</sub> | The concentration of a drug that gives a half-maximal response  |
| IP               | Intellectual property   |
| IPA              | Isopropyl alcohol   |
| L                | Litres  |
| LAH              | Lithium aluminium hydride                                       |
| LCMS             | Liquid chromatography mass spectrometry                         |
| LDA              | Lithium diisopropylamide  |
| LiHMDS           | Lithium bis(trimethylsilyl)amide                                |
| LogD             | Octanol-water distribution coefficient                          |
| LogP             | Octanol-water partition coefficient                             |
| LR-MS            | Low resolution mass spectrometry                                |
| LTMP             | Lithium tetramethylpiperidide                                   |
| <i>M.tb</i>      | <i>Mycobacterium tuberculosis</i>                               |
| M2               | <i>N</i> -monodesmethyl metabolite of bedaquiline               |
| MDR              | Multi-drug resistant  |
| MeCN             | Acetonitrile  |
| MeOD             | Deuterated methanol   |

|                                    |  |
|------------------------------------|--|
| mg                                 | Milligram  |
| MIC <sub>90</sub>                  | Concentration of drug which inhibits 90% of bacterial growth |
| min                                | Minutes  |
| mL                                 | Millilitres  |
| MP                                 | Melting point  |
| MW                                 | Molecular weight   |
| <i>MW</i>                          | Microwave  |
| Naph                               | Naphthyl   |
| NBS                                | <i>N</i> -bromosuccinimide                                   |
| NIS                                | <i>N</i> -iodosuccinimide                                    |
| NMR                                | Nuclear magnetic resonance                                   |
| Pd(dppf)Cl <sub>2</sub>            | [1,1'-Bis(diphenylphosphino)ferrocene]dichloropalladium(II)  |
| Pd <sub>2</sub> (dba) <sub>3</sub> | Tris(dibenzylideneacetone)dipalladium(0)                     |
| Pet. Sp.                           | Petroleum spirits  |
| Ph                                 | Phenyl   |
| PhMe                               | Toluene  |
| Pin                                | Pinacol  |
| PK                                 | Pharmacokinetic  |
| Pydz                               | Pyridazine   |
| Pyr                                | Pyridine   |
| Pyz                                | Pyrazine   |
| REMA                               | Resazurin microtiter assay                                   |
| rt                                 | Room temperature   |
| SAR                                | Structure-activity relationship                              |
| TB                                 | Tuberculosis   |
| TFA                                | Trifluoroacetic acid   |
| THF                                | Tetrahydrofuran  |



|      |                                    |
|------|------------------------------------|
| TLC  | Thin layer chromatography          |
| TMDS | Tetramethyldisiloxane              |
| TPSA | Topological polar surface area     |
| Ts   | Toluenesulfonyl                    |
| TsCl | <i>p</i> -Toluenesulfonyl chloride |
| WHO  | World Health Organisation          |
| XDR  | Extensively-drug resistant         |

## Table of Contents

|   |           |
|---|-----------|
| Abstract .....  | iii       |
| Declaration .....                                       | v         |
| Achievements during enrolment .....                     | vi        |
| Acknowledgements .....                                  | vii       |
| Abbreviations .....                                     | ix        |
| Table of Contents .....                                 | xiii      |
| <b>Chapter 1: Project Introduction .....</b>            | <b>1</b>  |
| 1.1 Introduction .....                                  | 1         |
| 1.2 Tuberculosis .....                                  | 1         |
| 1.2.1 Epidemiology.....                                 | 1         |
| 1.2.2 Aetiology .....                                   | 2         |
| 1.2.3 Clinical presentation .....                       | 3         |
| 1.2.4 Pathogenesis and progression .....                | 3         |
| 1.2.5 Diagnosis and detection.....                      | 4         |
| 1.2.6 Treatment .....                                   | 5         |
| 1.3 Bedaquiline .....                                   | 6         |
| 1.3.1 Discovery and development .....                   | 7         |
| 1.3.2 Synthesis of BDQ.....                             | 9         |
| 1.3.3 Target and mechanism of action .....              | 11        |
| 1.3.4 Clinical efficacy.....                            | 14        |
| 1.3.5 Safety of bedaquiline .....                       | 15        |
| 1.3.5.1. Cardiotoxicity .....                           | 15        |
| 1.3.5.2. Drug-drug interactions.....                    | 17        |
| 1.3.5.3. Hepatotoxicity.....                            | 17        |
| 1.3.5.4. Long half-life .....                           | 17        |
| 1.4 Drug-like properties .....                          | 18        |
| 1.4.1 Lipophilicity related toxicity .....              | 18        |
| 1.4.1.1. hERG inhibition .....                          | 19        |
| 1.4.1.2. Phospholipidosis .....                         | 20        |
| 1.4.1.3. CYP inhibition .....                           | 21        |
| 1.4.1.4. Hepatotoxicity.....                            | 21        |
| 1.5 Project objectives.....                             | 21        |
| 1.6 References .....                                    | 25        |
| <b>Chapter 2: Pyridine Analgues of Bedaquiline.....</b> | <b>30</b> |

|  |           |
|--|-----------|
| 2.1 Introduction .....   | 30        |
| 2.2 Pyridine analogues of BDQ bearing a phenyl ring at unit C .....              | 37        |
| 2.2.1 Synthesis .....  | 37        |
| 2.2.2 Validation of the 2,6-dimethoxypyridine core as a bioactive template ..... | 43        |
| 2.2.3 Extended SAR of the pyridine core .....                                    | 44        |
| 2.3 Pyridine analogues of BDQ bearing a naphthyl ring at unit C.....             | 50        |
| 2.3.1 Alpha arylation strategy with bromopyridine.....                           | 51        |
| 2.3.2 Suzuki–Miyaura strategy with pyridyl boronic acid .....                    | 54        |
| 2.3.3 SAR of the pyridine core at the C5 position .....                          | 58        |
| 2.4 Conclusion .....   | 63        |
| 2.5 References .....   | 65        |
| <b>Chapter 3: Pyridine Hybrids of TBAJ-587 .....</b>                             | <b>67</b> |
| 3.1 Introduction .....   | 67        |
| 3.2 Synthesis of a model pyridine-TBAJ-587 hybrid .....                          | 69        |
| 3.2.1 Synthesis of the southern subunit of the model analogue.....               | 71        |
| 3.2.2 Synthesis of northern subunit of model analogue .....                      | 73        |
| 3.2.2.1. Pathway A .....   | 73        |
| 3.2.2.2. Pathway B .....   | 75        |
| 3.2.2.3. Pathway C .....   | 76        |
| 3.2.2.4. Pathway D .....   | 78        |
| 3.2.3 Addition between southern and northern subunits.....                       | 80        |
| 3.3 Synthesis of expanded series TBAJ-587 pyridine analogues.....                | 82        |
| 3.3.1 Optimised route to southern subunit.....                                   | 82        |
| 3.3.1.1. Directed <i>ortho</i> -lithiation .....                                 | 83        |
| 3.3.1.2. Halogen-metal exchange .....  | 85        |
| 3.3.2 Optimised route to northern subunit .....                                  | 88        |
| 3.3.3 Addition and synthesis of a library of hybrid analogues.....               | 89        |
| 3.4 <i>In vitro</i> testing .....  | 94        |
| 3.4.1 Testing protocol overview .....  | 94        |
| 3.4.2 Stage one .....  | 94        |
| 3.4.3 Stage two .....  | 97        |
| 3.4.4 Stage three <i>in vitro</i> evaluation.....                                | 98        |
| 3.4.4.1. Inhibitory activity against <i>M.tb</i> .....                           | 98        |
| 3.4.4.2. Inhibitory activity at hERG .....                                       | 99        |
| 3.5 Conclusion.....  | 101       |
| 3.6 References .....   | 103       |

|   |            |
|---|------------|
| <b>Chapter 4: Diazine Hybrids of TBAJ-587 .....</b>                   | <b>105</b> |
| 4.1 Introduction .....  | 105        |
| 4.2 Synthesis of pyrazine analogues .....                             | 106        |
| 4.2.1 Directed <i>ortho</i> -metalation .....                         | 107        |
| 4.2.1.1. Directed <i>ortho</i> -lithiation .....                      | 107        |
| 4.2.1.2. Directed <i>ortho</i> -magnesiatio.....                      | 111        |
| 4.2.2 Halogen-metal exchange .....                                    | 112        |
| 4.2.3 Completion of the southern subunit .....                        | 114        |
| 4.2.4 Addition of the northern and southern subunits.....             | 114        |
| 4.3 Synthesis of pyridazine analogues .....                           | 116        |
| 4.4 Conclusion.....   | 119        |
| 4.5 References .....  | 120        |
| <b>Chapter 5: Conclusions and Future Directions .....</b>             | <b>122</b> |
| 5.1 Project summary.....  | 122        |
| 5.2 Future directions.....  | 124        |
| <b>Chapter 6: Experimental Methods .....</b>                          | <b>125</b> |
| 6.1 Chemistry .....   | 125        |
| 6.1.1 General experimental methods .....                              | 125        |
| 6.1.2 General methods .....   | 127        |
| 6.1.2.1. Method A .....   | 127        |
| 6.1.2.2. Method B .....   | 128        |
| 6.1.2.3. Method C .....   | 128        |
| 6.1.2.4. Method D .....   | 129        |
| 6.1.2.5. Method E.....  | 129        |
| 6.1.3 Chapter 2 compounds.....  | 130        |
| 6.1.4 Chapter 3 compounds.....  | 182        |
| 6.1.5 Chapter 4 compounds.....  | 221        |
| 6.2 Biological assays.....  | 230        |
| 6.2.1 Resazurin microtitre assay .....                                | 230        |
| 6.2.2 <i>In vitro</i> hERG inhibition assay .....                     | 231        |
| 6.3 References .....  | 233        |
| <b>Appendices.....</b>  | <b>235</b> |
| Appendix 1: Characterisation for representative final compounds ..... | 235        |
| A1.1 Compound 2.045-B .....   | 235        |
| A1.2 Compound 2.106-B.....  | 237        |
| A1.3 Compound 3.02-B .....  | 239        |

|   |     |
|---|-----|
| Appendix 2: NMR assignments for selected compounds .....        | 241 |
| A2.1 Compounds 3.44 and 3.47 .....                              | 241 |
| A2.2 Compound 3.50 .....  | 247 |
| Appendix 3: Report of crystal structure for compound 4.04 ..... | 250 |

## Chapter 1: Project Introduction

### 1.1 Introduction

Tuberculosis (TB) is one of the most ancient and deadliest diseases known to mankind.<sup>[1]</sup> Despite being a curable disease, it still kills more people worldwide than any other single infectious agent.<sup>[2]</sup> Effective eradication of TB is complicated by its ability to remain in persistent lesions, requiring extended regimens of multiple drugs. Furthermore, the emergence of multi- and extensively-drug resistant strains (MDR- and XDR-TB) has added to the global control burden.<sup>[2]</sup> Cases of resistance are increasingly difficult to manage with the dwindling pool of poor-quality treatments reserved for these instances, and as such, drug-resistant strains are associated with increased morbidity and mortality.<sup>[2]</sup> Given the shortcomings of the currently available therapies, there exists an urgent need for new TB drugs that can simplify treatment.

The development of bedaquiline (BDQ, trade-name Sirturo, **Figure 1.1**), the first new anti-TB drug commercialised in over 40 years, promised to revolutionise the treatment of MDR-TB due to its novel mode of action against mycobacterial adenosine triphosphate (ATP) synthase.<sup>[3]</sup> Despite this promise, serious adverse effects including cardiotoxicity have limited its use to that of a last resort treatment.<sup>[4]</sup> The observed toxicities seen with the administration of BDQ are linked to certain structural and physicochemical features of the drug, including its lipophilicity, basicity and molecular weight.<sup>[5]</sup>

This project is focused on optimising the structure of BDQ to improve its safety profile, with the overall aim of developing a new-generation of candidates for the treatment of MDR-TB.

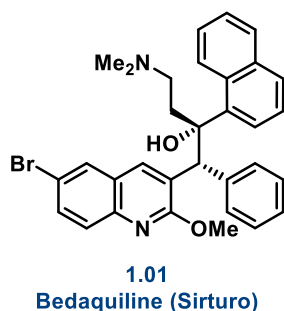


**Figure 1.1.** The molecular structure of BDQ.

### 1.2 Tuberculosis

#### 1.2.1 Epidemiology

Tuberculosis currently represents one of the most significant public health threats to the global population. The most recent report from the World Health Organisation (WHO) estimated that 10 million new cases of active infection occurred in 2017.<sup>[2]</sup> Even more concerning was that 1.7 billion

people (approximately one-quarter of the world's population) were estimated to be infected subclinically, presenting a large reservoir of potential infection.<sup>[6]</sup>

Despite the emergence of anti-TB drugs more than half a century ago, TB remains the biggest infectious killer in the world with an estimated 1.6 million TB-related deaths occurring in 2017.<sup>[2]</sup> Furthermore, it is the leading cause of death in persons co-infected with the human immunodeficiency virus (HIV), accounting for approximately 40% of fatalities in this population.<sup>[7]</sup> Given that TB is a curable disease, the number of associated deaths is unacceptably high.

Tuberculosis is a disease fuelled by poverty, predominantly affecting the most vulnerable populations in the poorest countries. The regions of South-East Asia and Africa currently account for close to 70% of overall TB cases seen globally.<sup>[2]</sup> In Australia, the situation is significantly less problematic, having maintained one of the lowest rates of TB in the world for the last three decades (5 to 6 cases per 100 000 population).<sup>[8]</sup> Despite this, Australia's proximity to many high-incidence countries and its ever increasing migrant intake from these regions means that continued vigilance is required.

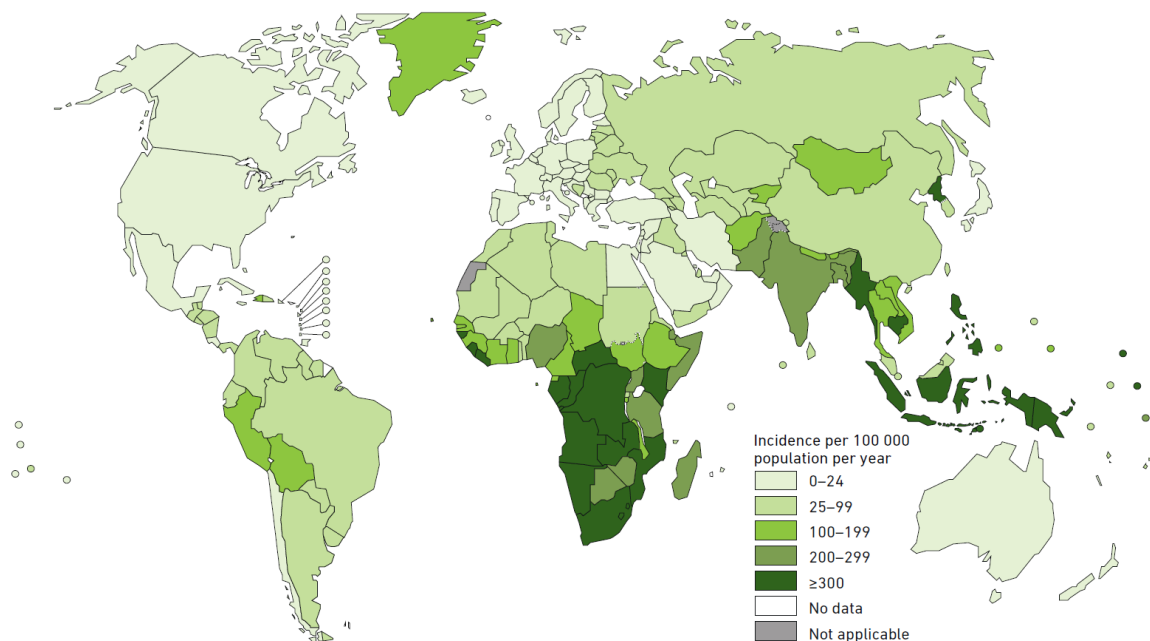


**Figure 1.2.** Estimated global TB incidence rates in 2017, image courtesy of the WHO (from ref 2).

### 1.2.2 Aetiology

The causative agents of human and mammalian TB are all closely related species within the *Mycobacteria* genera grouped into what is termed the *Mycobacterium tuberculosis* (*M.tb*) complex which includes *M.tb*, *Mycobacterium africanum*, *Mycobacterium bovis*, *Mycobacterium microti*, and *Mycobacterium canetti*.<sup>[9]</sup> Of these species, *M.tb* is the principal pathogen leading to TB in humans. First discovered by Robert Koch in 1882<sup>[1]</sup>, these rod-shaped bacteria are characterised by a complex

and highly impermeable lipid-rich cell wall<sup>[10]</sup>, and a considerably slow growth-rate. In comparison with *Escherichia coli*, which divides every 20 min, *M.tb* has a doubling time of approximately 12 to 24 h and colonies are not visible on plates for 4 to 6 weeks.<sup>[11]</sup>

### 1.2.3 Clinical presentation

Infection with *M.tb* primarily occurs within the lung (pulmonary TB), however extrapulmonary TB also exists and represents up to a third of all cases.<sup>[12]</sup> Symptoms relating to pulmonary TB include chronic cough, persistent fatigue, low-grade fever, loss of appetite, and muscle and tissue wasting. If an active infection is left untreated, uncontrolled *M.tb* growth results in extensive lung damage that ultimately leads to death.<sup>[13]</sup>

### 1.2.4 Pathogenesis and progression

The development of TB is characterised by multiple stages, as illustrated in **Figure 1.3**. The factors that regulate the progression and outcome of infection are multifaceted, and involve a complex interplay between the host immune response and survival strategies employed by the bacilli.<sup>[14]</sup>

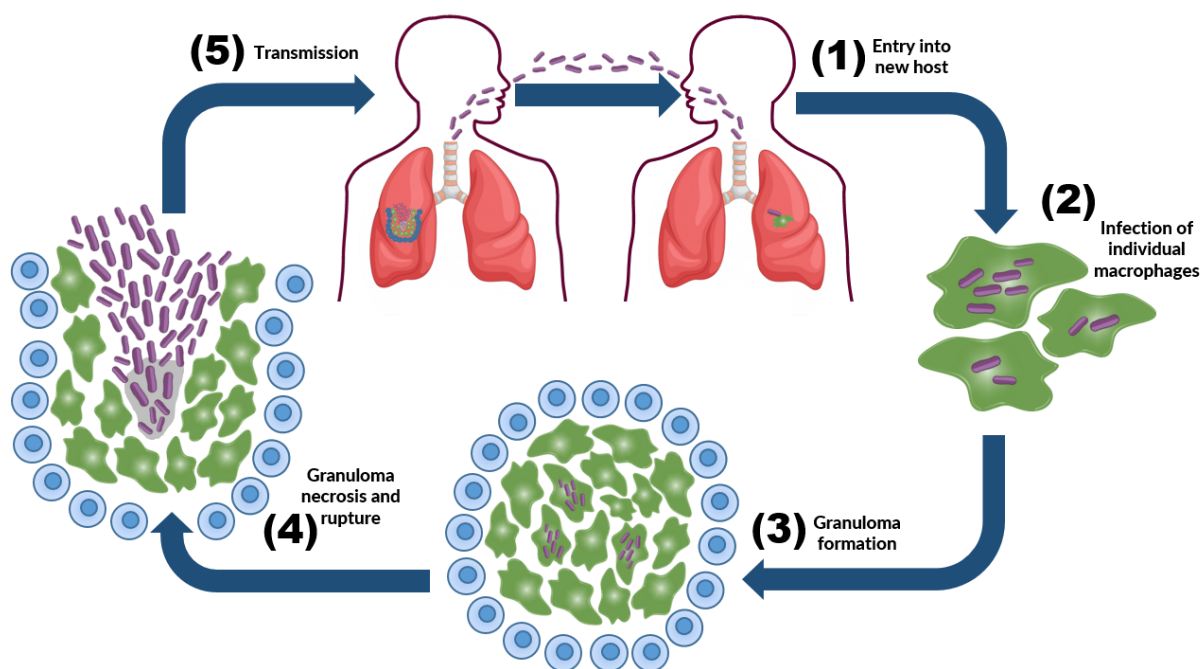


**Figure 1.3.** Pathogenic life-cycle of *M.tb*. 1) Initial infection arises from inhalation of viable bacteria. 2) *M.tb* is engulfed alveolar macrophages. 3) Infected macrophages recruit other immune cells help attack the infection, resulting in the formation of a granuloma. 4) If the infection overcomes the immune system, the granuloma breaks down, releasing *M.tb* into the lung. 5) Fine aerosol particles containing the bacteria are coughed up by an individual with active infection, resulting in disease transmission (adapted from ref 15).

Infection is initiated by inhalation of droplet particles containing viable *M.tb*, expectorated from an individual presenting with active pulmonary TB. Given that particles can remain airborne for several hours and that as little as 1–10 bacilli are needed to initiate infection, TB is relatively contagious.<sup>[16]</sup>



Once in the lungs, *M.tb* is primarily engulfed by resident alveolar macrophages as part of the host's innate immune response. Although macrophages are usually successful in providing an initial defence against infection, *M.tb* has evolved numerous strategies that allow it to evade destruction and survive within these cells.<sup>[14]</sup>

In an attempt to further control the infection, an adaptive immune response is developed by the host, resulting in the formation of an enclosed and organised cluster of inflammatory cells known as a granuloma. This structure serves to contain the spread of *M.tb* and is the hallmark pathological feature of the disease.<sup>[14]</sup> At this stage, the fate of the infection is determined by the strength of the host immune response.

In immunocompetent individuals, immediate progression to active primary disease is rare, and containment of infection occurs in over 90% of people.<sup>[17]</sup> This containment phase, defined as latent TB, is characterised by a state of dormancy within the granuloma, where bacilli persist but do not proliferate. Although these individuals remain infected with *M.tb*, they are clinically asymptomatic and not infectious.<sup>[17]</sup> Latent carriers retain an estimated 10% lifetime risk of disease, with the highest risk within the first few years post-infection.<sup>[18,19]</sup> The precise mechanisms responsible for the transition to a resumed secondary infection is presently unclear, however the risk of reactivation is substantially higher in individuals with disturbed immune function, such as those co-infected with the human immunodeficiency virus (HIV).<sup>[14]</sup>

During active infection, the enclosed nature of the granuloma leads to accumulation of necrotic debris within the central region.<sup>[20]</sup> As the disease progresses, the granuloma becomes increasingly necrotic until it weakens to the extent of rupture, releasing *M.tb* into the lung airways and leading to the formation of secondary granulomas.<sup>[21]</sup> In terms of transmission, this results in a productive cough which facilitates a new cycle of infection.

### **1.2.5 Diagnosis and detection**

Rapid and accurate detection of active infection is critical in the control of TB. The diagnosis of TB is definitively established by isolation of *M.tb* from a bodily secretion or tissue biopsy.<sup>[22]</sup> The gold standard in TB diagnosis is the culture assay, which involves the growing of colonies from a collected clinical sample, most often sputum (coughed up phlegm).<sup>[23]</sup> In addition to initial diagnosis, culture assays are also used to monitor the response to treatment. Culture conversion from positive to negative signals treatment success, with cure usually defined as sustained culture conversion for >12 months.<sup>[24]</sup>

### 1.2.6 Treatment

The persistent nature of *M.tb* gives rise to the need for long and complicated treatment regimens with a cocktail of drugs. The drugs used for the treatment of TB are grouped by the World Health Organisation (WHO) according to their effectiveness, experience of use, safety and drug class (**Table 1.1**).<sup>[4]</sup> Of all the classes, Group 1 first-line oral agents are the most potent and safest, thus forming the core of any drug treatment program so long as they remain effective. All other classes (Groups 2–5) are reserved for drug-resistant cases and are in general less effective and more toxic.

**Table 1.1.** Current drugs recommended for the treatment of tuberculosis (adapted from ref 4).

| GROUP NAME  | ANTI-TB AGENT   |
|---|---|
| <b>Group 1.</b> First-line oral agents  | Isoniazid<br>Rifampicin<br>Ethambutol<br>Pyrazinamide   |
| <b>Group 2.</b> Injectable anti-TB drugs  | Kanamycin<br>Amikacin<br>Capreomycin  |
| <b>Group 3.</b> Fluoroquinolones  | Levofloxacin<br>Moxifloxacin<br>Gatifloxacin  |
| <b>Group 4.</b> Oral bacteriostatic second-line drugs   | Ethionamide<br>Prothionamide<br>Cycloserine<br>Terizidone<br>Para-aminosalicylic acid<br>Para-aminosalicylate sodium  |
| <b>Group 5.</b> Anti-TB drugs with limited data of efficacy and/or long term safety in the treatment of drug resistant TB | Bedaquiline<br>Delamanid<br>Linezolid<br>Clofazimine<br>Amoxicillin/clavulanate<br>Imipenem/cilastatin<br>Meropenem<br>High-dose isoniazid<br>Thioacetazone<br>Clarithromycin |

A fundamental problem in the treatment of TB is the long duration of therapy required for complete eradication. The current recommended treatment regimen for drug-susceptible TB is of at least 6 months in duration using a combination all four first-line oral agents.<sup>[4]</sup> The need for such prolonged therapy is thought to result from altered mycobacterial metabolism in response to local environment pressures. A theory initially proposed by Mitchison<sup>[25]</sup> suggests that mycobacteria exist within a spectrum of metabolic states during active infection ranging anywhere from actively replicating to quiescent. This variation complicates therapeutic intervention as drugs that can target each of these

states effectively are required. Furthermore, targeting dormant populations efficiently remains a difficult hurdle to overcome as many anti-TB drugs depend on bacterial replication for their mode of action.<sup>[26]</sup>

Although progress has been achieved in reducing the global incidence of TB, the emergence of MDR-TB and XDR-TB strains over the past decade has fuelled new concern regarding the global control of TB. The current definition of MDR-TB is the resistance of a patient to the two most potent first-line drugs isoniazid and rifampicin.<sup>[27]</sup> Additional resistance to any fluoroquinolone (**Table 1.1**, Group 3) and at least one injectable agent (**Table 1.1**, Group 2) is classed separately as XDR-TB and is exceedingly difficult to cure. The rise in drug-resistance is primarily regarded as a man-made incidence resulting from poor treatment management of initial drug-susceptible infections. When incomplete sterilisation of all bacterial populations occurs, selection pressure can favour the proliferation of drug-resistant subpopulations that arise from normal low-frequency spontaneous mutations.<sup>[28]</sup> The spread of MDR-TB from person to person occurs just as readily as drug-susceptible TB, and as such, the majority of new MDR cases now occur as the result of this primary transmission.<sup>[29]</sup>

Treatment of MDR-TB is associated with much poorer outcomes than observed for cases of drug-susceptible TB. The most recent data from the WHO reported that only 54% of all new MDR-TB and 30% of XDR-TB patients were successfully treated in 2017<sup>[2]</sup>, statistics that clearly highlight the lack of quality treatment options remaining once the most potent first-line regimens have been exhausted. The majority of these drugs (**Table 1.1**, Groups 2–5) are much less effective, especially at targeting persisting dormant populations. As a result, treatment of MDR-TB is much more intensive and involves daily dosing of multiple drugs for up to 24 months, presenting a significant burden to those affected.<sup>[27]</sup> These drugs are also linked with severe toxicities and drug-drug interactions, further restricting treatment options. Without effective drugs, resistant strains could become the dominant form of TB disease in the near future. Given the current scenario, there is an urgent need for new anti-*M.tb* agents, particularly those that operate *via* novel modes of action as to treat the growing drug-resistance epidemic.

### 1.3 Bedaquiline

In recognition of the dire need for new treatment options for MDR-TB, the Federal Food and Drug Administration (FDA) granted accelerated conditional approval for BDQ (**Figure 1.1**, *vide supra*) in December 2012 as a new drug for the treatment of MDR-TB.<sup>[30]</sup> Bedaquiline is a first-in-class diarylquinoline (DARQ) that acts to selectively inhibit mycobacterial ATP synthase, thus eliminating infection by depleting *M.tb* energy stores.<sup>[31]</sup> A direct result of this unique mode of action is equipotent *in vitro* activity against all mycobacterial subpopulations, a characteristic that is not met to the same

extent by any other available anti-*M.tb* drug.<sup>[32]</sup> Although BDQ promised to potentially shorten and simplify treatment regimens for MDR-TB, its use is currently limited to a last resort option due safety concerns revealed during Phase II clinical trials.<sup>[4]</sup>

### 1.3.1 Discovery and development

Bedaquiline was discovered in 1996 at Janssen Pharmaceutica (Johnson & Johnson), by a team led by Koen Andries.<sup>[3]</sup> Their research program towards the discovery of BDQ was initiated through a whole-cell phenotypic screen of more than 70,000 compounds from the Janssen medicinal chemistry library, which were tested for antimycobacterial activity against the *M.tb* surrogate *Mycobacterium smegmatis*.<sup>[33]</sup> From this campaign, hit compounds from 23 clusters were evaluated for their drug-like properties including antimycobacterial activity, an absence of cytotoxicity, and favourable ADME (Absorption Distribution Metabolism Excretion) and pharmacokinetic (PK) profiles. This evaluation resulted in the selection of the DARQ singleton **1.02 (Figure 1.4)** as a promising structure warranting further optimisation.

Janssen's lead optimisation effort produced a series of over 200 DARQ derivatives with *in vitro* whole-cell activity against both *M. smegmatis* and *M.tb*.<sup>[33,34]</sup> As summarised in **Figure 1.4**, their effort mainly focused on modifications to regions B, C and D including substitutions to the aromatic rings (B and C) or their replacement with other functionalised groups, and the modulation of the chain length and basicity in region D. Interestingly, the quinoline core (region A) was maintained throughout their entire series, which was only explored through varying substituents on the quinoline ring. Additionally, given the presence of two stereogenic centres (classified as *R* or *S* using the Cahn–Ingold–Prelog priority system), synthesis of these derivatives led to a mixture of four stereoisomers distributed as racemic mixtures of two diastereomers (*RR*, *SS* and *SR*, *RS*). To facilitate a clear understanding of the structure-activity relationship (SAR), the two diastereomers were separated using silica-gel flash chromatography, and the individual enantiomers of the diastereomer of interest were further separated by chiral chromatography.<sup>[33]</sup>

Overall, the features deemed to be particularly important for activity included:

- the correct relative and absolute configuration at both stereocentres (*RS* for BDQ),
- a basic tertiary amine at the end of the region D chain, requiring a pKa >8 and a 2-carbon chain length,
- the presence of two adjacent lipophilic groups, ring C preferring electron-deficient aromatics, and
- substitution of the quinoline at C6 and C2, preferably by bromo and methoxy substituents respectively.

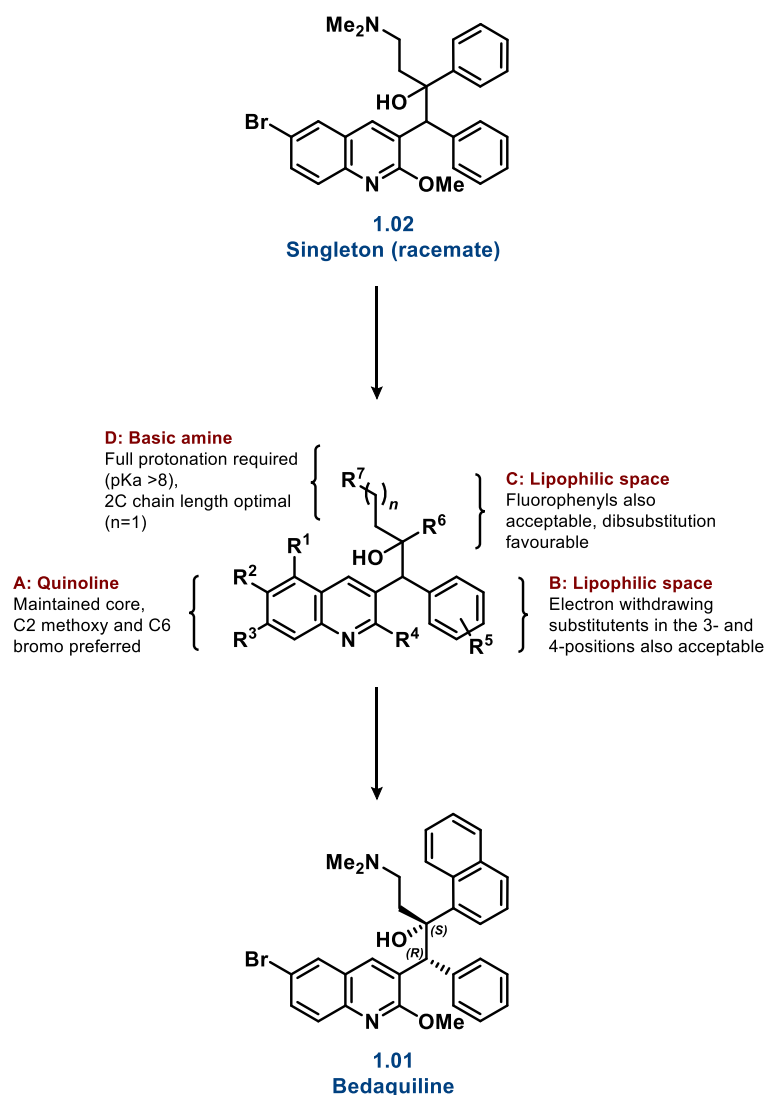


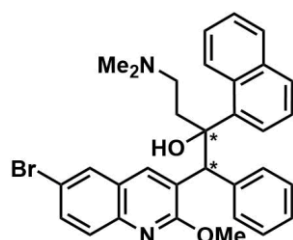
**Figure 1.4.** Summary of Janssen's hit-to-lead campaign from singleton **1.02** to BDQ.

Compounds were assessed *in vitro* for their ability to inhibit 90% of bacterial growth (minimum inhibitory concentration = MIC<sub>90</sub>). Following assessment, 20 derivatives of the DARQ series were found to possess an MIC<sub>90</sub> below 0.5 µg/mL (against *M.tb* strain H37rv). Further investigation of three shortlisted structures in an *in vivo* mouse infection model identified BDQ to be the most promising candidate of the DARQ class.<sup>[3]</sup>

During lead optimisation, it was discovered that activity within the DARQ class varied between diastereomers, and also enantiomers. Specifically, the *RS*, *SR* diastereomer was observed to be 10- to 100-fold more active than the *RR*, *SS* diastereomer. For the BDQ scaffold, the *RS*, *SR* diastereomer was 25-fold more active than the *RR*, *SS* form (**Table 1.2**, entries 1 and 4).<sup>[33]</sup> Separation of the enantiomers *RS* from *SR* revealed that the eutomer was in fact the enantiomer with the *RS* absolute configuration returning an MIC<sub>90</sub> of 0.03 µg/mL (0.05 µM, entry 2) which was *ca.* 300-fold more potent than the *SR*

enantiomer (i.e. the distomer). These differences in activity were subsequently explained by conformational and modelling studies (discussed in **Section 1.3.3**, *vide infra*).

**Table 1.2.** Antimycobacterial activity of the various isomers of BDQ.



| Entry | Configuration | <i>M.tb</i> (H37rv)<br>MIC <sub>90</sub> (μg/mL) |
|-------|---------------|--|
| 1     | <i>RS, SR</i> | 1.8  |
| 2     | <i>RS</i>     | 0.03   |
| 3     | <i>SR</i>     | 8.8  |
| 4     | <i>RR, SS</i> | 44.1   |
| 5     | <i>RR</i>     | 4.4  |
| 6     | <i>SS</i>     | 8.8  |

### 1.3.2 Synthesis of BDQ

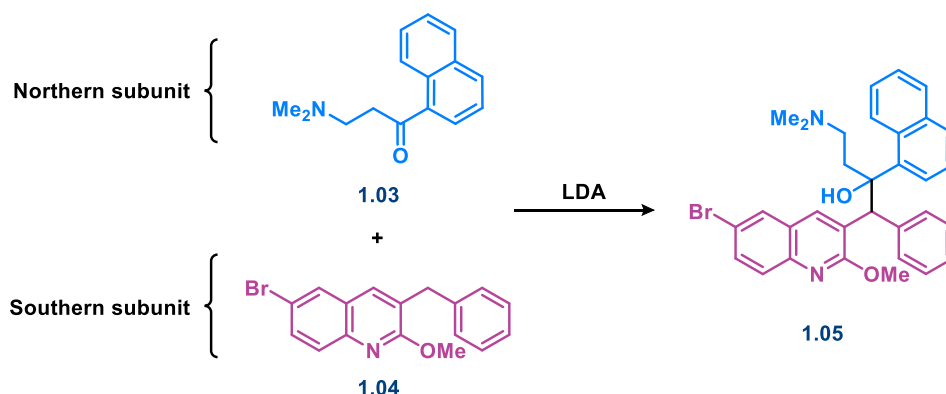
Janssen employed a relatively convergent synthesis towards BDQ and related analogues in their original discovery route, of which the final step required the LDA-mediated addition of the southern benzylquinoline fragment **1.04** to the northern naphthyl β-ketoamine fragment **1.03** (**Scheme 1.1** and **1.2**).<sup>[33,35]</sup>

Synthesis of the hydrochloride salt of fragment **1.03** was straight-forward and involved a Mannich reaction of 1-acetonaphthone **1.06** with the iminium ion generated *in situ* from condensation of formaldehyde and dimethylamine hydrochloride. Neutralisation of **1.07** using sodium hydroxide converted this to the northern subunit **1.03**.

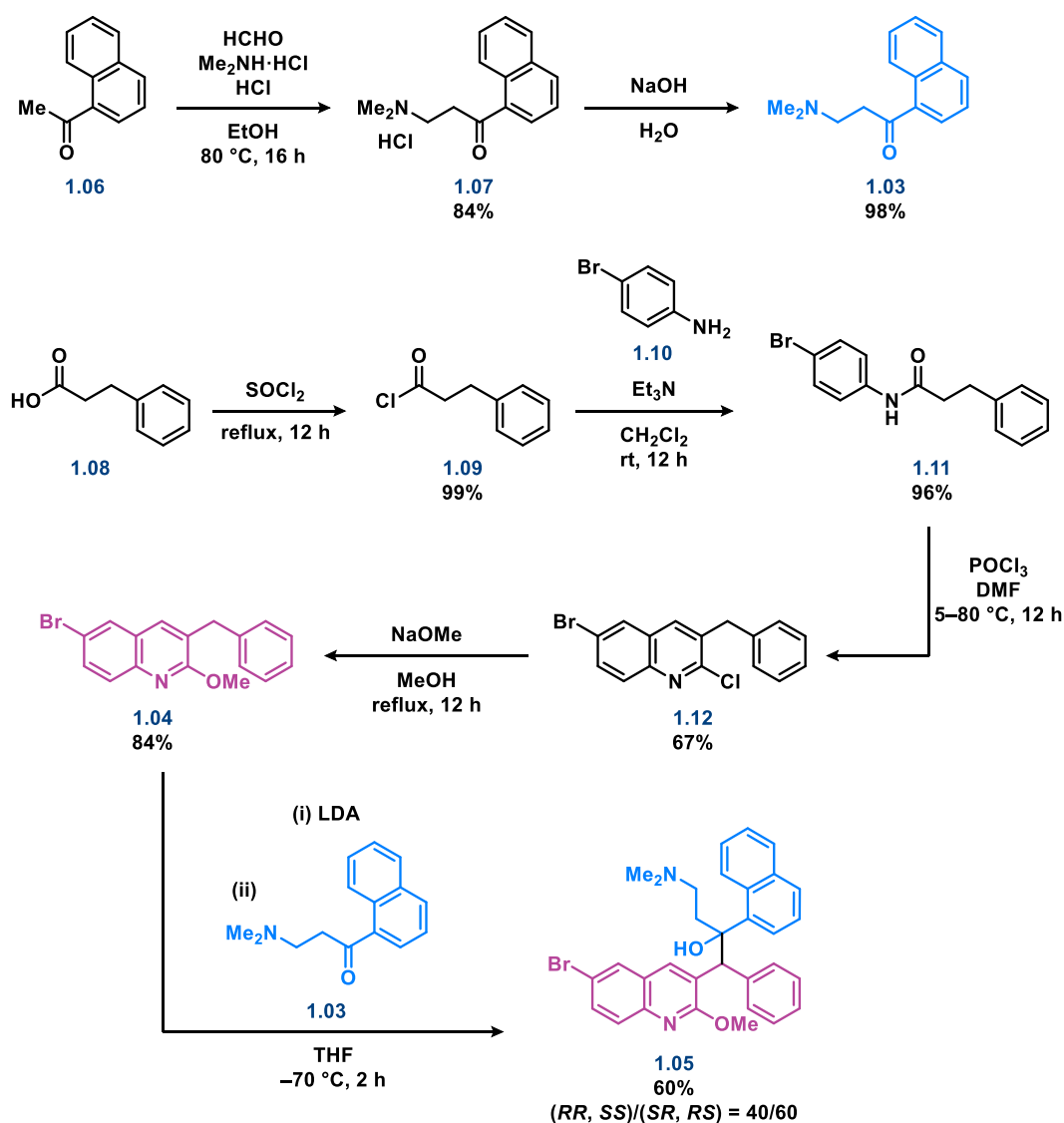
For the southern fragment **1.04**, the requisite diphenylpropionamide **1.11** was prepared in two steps from commercially available 3-phenylpropionic acid (**1.08**) and 4-bromoaniline (**1.10**). Vilsmeier–Haak formylation then followed to produce the 2-chloroquinoline intermediate **1.12** through cyclisation and chlorination. The synthesis of this fragment was then completed with S<sub>N</sub>Ar conversion of the quinoline C2 chloride of **1.12** to a methoxy substituent.

The combination of the northern and southern fragments was accomplished with initial lithium diisopropylamide (LDA) deprotonation of fragment **1.04**, followed by 1,2-carbonyl addition to fragment **1.03**. This resulted in **1.05** as a mixture of four isomers, distributed as a 40:60 mixture of two racemic diastereomers (*RR, SS*):(*RS, SR*). The pairs of diastereomers were separable over silica gel by virtue of their differing physicochemical properties and the pure enantiomers (*RS, SR, RR, SS*) were further isolated using chiral high-performance liquid chromatography (HPLC) using an amylose *tris*(3,5-dimethylphenylcarbamate) stationary phase (Chiralpak AD, **Scheme 1.3**). Without the ability

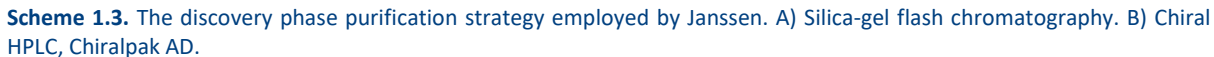
to select for the desired stereochemistry during synthesis, this route remains highly inefficient as 75% of the final product is lost as undesired stereoisomers.



**Scheme 1.1.** Overall synthetic strategy employed by Janssen towards BDQ.



**Scheme 1.2.** The detailed synthetic pathway employed by Janssen towards the initial synthesis of BDQ.



Bedaquiline is a first-in-class inhibitor of mycobacterial ATP synthase, a transmembrane enzyme responsible for the production of intracellular energy (ATP) through the flux of protons across an electrochemical gradient.<sup>[36]</sup> Despite ATP synthase being a ubiquitous enzyme found in all cells, BDQ is 20000-fold more selective for the mycobacterial enzyme ( $IC_{50} = 0.01 \mu M$ ) over the human homologue ( $IC_{50} = >200 \mu M$ ).<sup>[37]</sup>

The diagram illustrates the structure and function of the F<sub>1</sub>F<sub>0</sub> ATP synthase complex in a Mycobacterium cell wall. On the left, a whole Mycobacterium cell is shown with its characteristic thick, multi-layered cell wall. A callout provides a detailed view of the F<sub>1</sub>F<sub>0</sub> complex embedded in the inner membrane.

The complex is divided into two main parts: the F<sub>1</sub> portion in the cytoplasm and the F<sub>0</sub> portion embedded in the inner membrane. The F<sub>1</sub> part consists of several subunits labeled  $\alpha$ ,  $\beta$ ,  $\gamma$ ,  $\delta$ , and  $\epsilon$ . The F<sub>0</sub> part is embedded in the inner membrane and includes subunits  $a$ ,  $b$ ,  $c$ , and  $\epsilon$ . A red arrow indicates the rotation of the transmembrane disk and central stalk, which is driven by the flow of protons ( $H^+$ ) from the periplasmic space through the  $c$  subunits. This rotation is coupled to the synthesis of ATP from ADP in the cytoplasm.

The cell wall structure is also shown, with the outer membrane (mycolic acids) and the periplasmic space (containing protons) clearly delineated. The inner membrane is the site where the F<sub>0</sub> complex is embedded.

Bacterial ATP synthase is composed of two major structural domains, a catalytic domain ( $F_1$ ) and a proton-translocating domain ( $F_0$ ) which together act as a biological rotary motor (**Figure 1.5**). These domains are further comprised of multiple subunits –  $F_1$  is composed of subunits  $\alpha\beta\gamma\delta\epsilon$ , and is



located in the cytoplasm where it generates ATP, and  $F_0$  spans the membrane and contains subunits  $a$ ,  $b_2$ ,  $c_{9-12}$  arranged in a symmetrical disk.<sup>[40]</sup> During normal functioning, protons enter the enzyme through subunit- $a$  and are translocated to a  $c$ -subunit glutamate residue in the ion-binding site (Glu-61 in *M.tb*).<sup>[39,41]</sup> This proton translocation causes rotation of the  $c$ -ring, and the transfer of this rotational energy to the catalytic domain induces a series of conformational changes which are ultimately responsible for ATP synthesis.<sup>[41]</sup>

Bedaquiline's target was first proposed by Andries *et al.* through whole-genome sequencing of BDQ resistant mutant strains of both *M.tb* and *M. smegmatis*.<sup>[3]</sup> Through comparative analysis of the genome sequences of susceptible and resistant strains, they were able to identify two different point mutations in the *atpE* gene, which encodes the  $c$ -subunit of ATP synthase.

Without a crystal structure of the  $F_0$  binding domain initially available, genetic, biochemical and docking studies were performed which all provided further evidence of subunit- $c$  as the BDQ binding site, pointing to the essential acidic residue Glu-61 as the specific binding region.<sup>[31,39,42–44]</sup> In 2015, Preiss *et al.*<sup>[45]</sup> published the first X-ray co-crystal structure (1.7 Å) of the highly conserved mycobacterial ATP synthase  $c$ -ring in the related species *Mycobacterium phlei* (83.7% homology) together with BDQ (**Figure 1.6**). In agreement with previous studies, the BDQ molecule was observed to specifically bind to the  $c$ -ring's ion-binding site *via* numerous interactions. The most important of these interactions was considered to be the charge assisted H-bond from the protonated dimethylamino group to the Glu-65 (Glu-61 in *M.tb*) carboxyl sidechain within the  $c$ -ring ion-binding site (2.5 Å). Additionally, a water bridged H-bond from the tertiary alcohol to Glu-65 was observed as well as an extensive number of van der Waals interactions within a stretch of nine residues provided by two adjacent  $c$ -units. In particular, the quinoline and naphthalene units appeared to play a role in correctly positioning the dimethylamino side chain into ion-binding site.

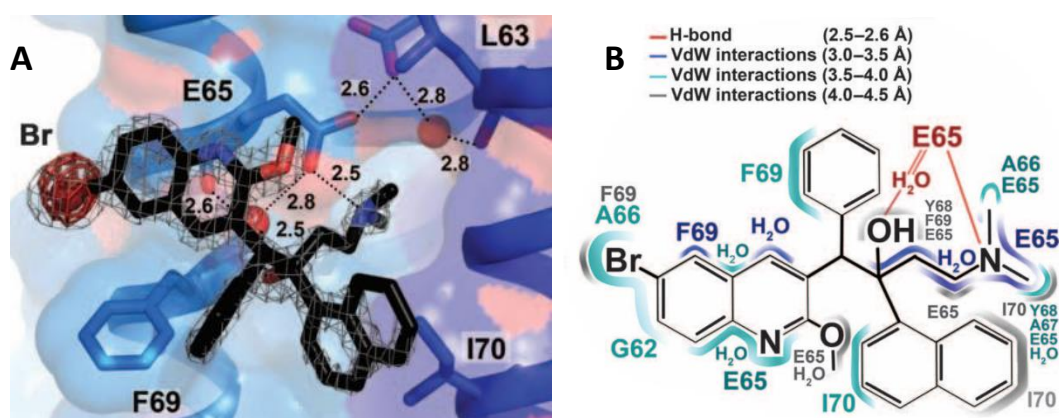


**Figure 1.6.** Crystal structure of the *M. phlei*  $c$ -ring in complex with BDQ. A) Slanted view of the mycobacterial ion-binding site showing the interaction of BDQ with the  $c$ -ring. B) Two-dimensional plot indicating the interactions between BDQ and the  $c$ -ring. Adapted from ref 45.

To explain the stereospecificity of the binding site, Andries and his team evaluated the binding modes of all four enantiomers of BDQ through docking into the modelled binding site, with the best docking orientations shown in **Figure 1.7**.<sup>[43]</sup> In agreement with the observed experimental results (**Table 1.2**, *vide supra*), calculation of the interaction energies found the *RS* stereoisomer to be the most strongly bound configuration as a result of this being able to form an additional H-bond between the hydroxyl moiety and Glu-61 of the c-subunit.

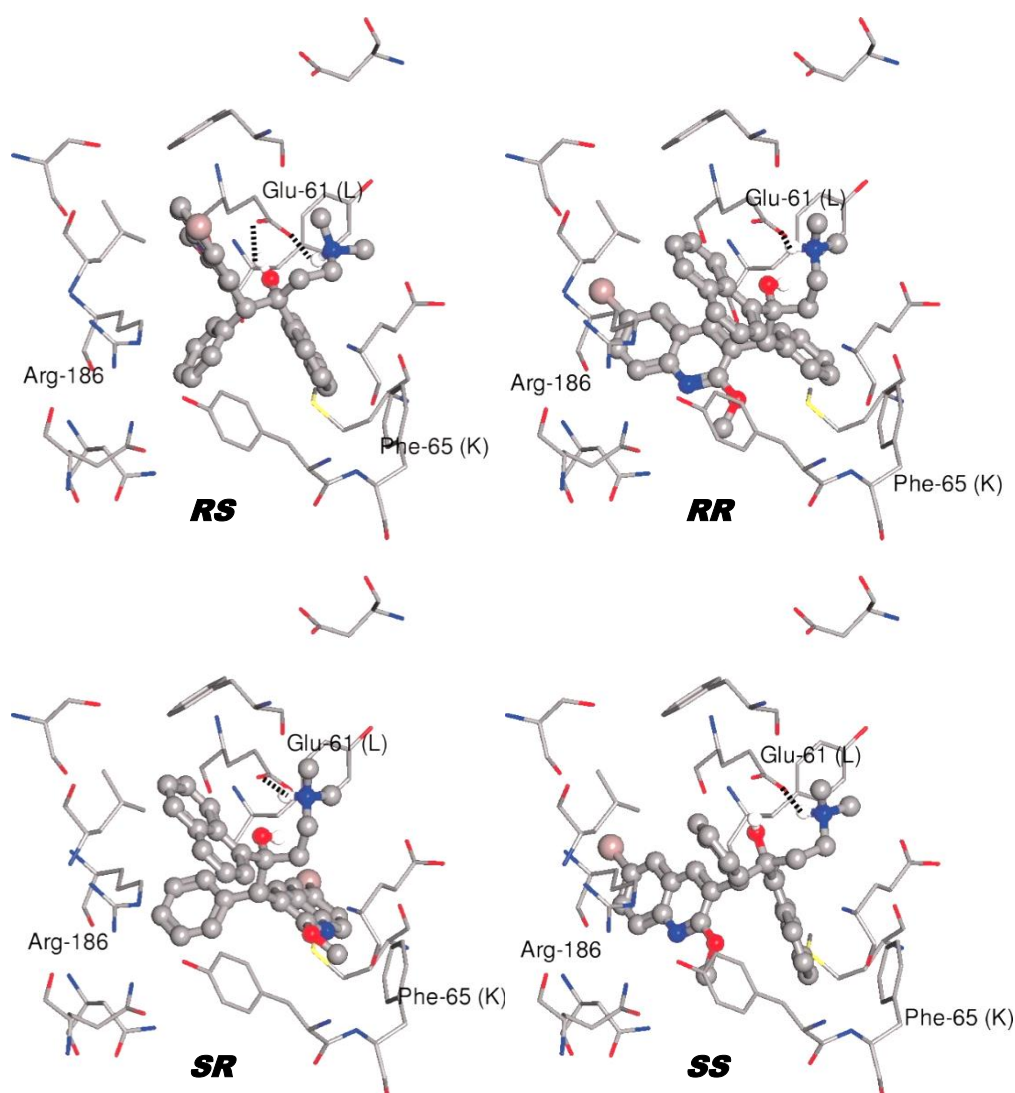


**Figure 1.7.** Proposed binding mode of all enantiomers of BDQ in a constructed homology model of *M.tb* ATP synthase. The *RS* stereoisomer is the only configuration able to form the additional H-bond between the hydroxyl moiety and Glu-61. Adapted from ref 43.

Bedaquiline's potent inhibition of ATP synthase is proposed to arise as a result of its ability to hinder rotation of the c-ring.<sup>[45]</sup> As illustrated in **Figure 1.8**, upon binding of a single molecule of BDQ between the cleft of two adjacent c-ring subunits, the bulky molecule is sterically and energetically disfavoured from passing the a-c subunit interface, effectively acting as a wedge to stall further rotation. Without

rotation, ion-exchange and ultimately ATP synthesis is halted, resulting in pronounced bacterial killing through depletion of *M.tb* energy stores.

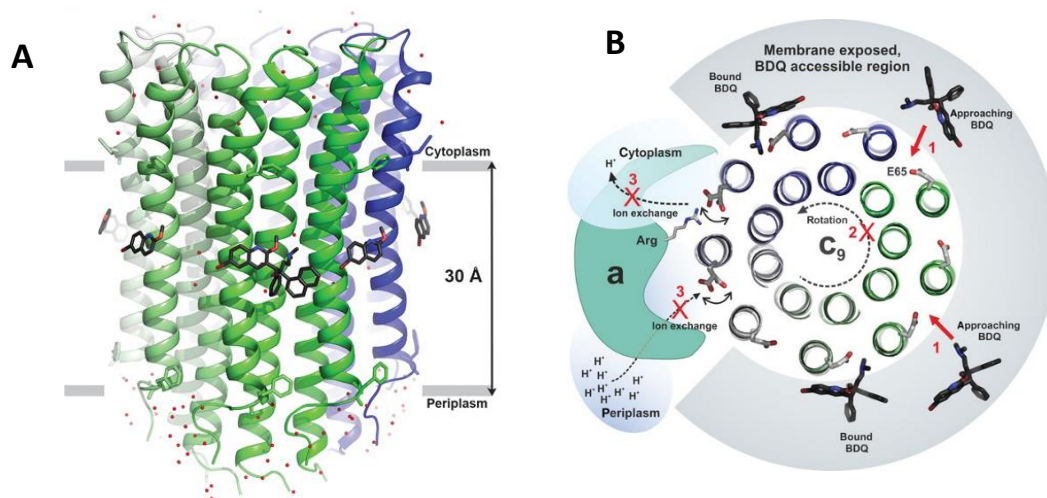


**Figure 1.8.** Structure of the *M. phlei* c-ring in complex with BDQ. A) Side view of the c-ring with BDQ bound. B) Top view of the c-ring (cartoon representation) with bound BDQ molecules. BDQ is proposed to act as a wedge once it approaches the a-c subunit interface. Adapted from ref 45.

### 1.3.4 Clinical efficacy

Evidence for the efficacy of BDQ in the treatment of MDR-TB was first derived from Phase IIb trial C208 which ultimately led to its accelerated approval by the FDA in 2012.<sup>[46]</sup> As illustrated in the Kaplan–Meier plot (**Figure 1.9**), BDQ added to a standard second-line background regimen for 24 weeks resulted in a substantially improved rate to culture conversion, with a higher proportion of subjects achieving culture conversion in comparison with the placebo arm (background regimen alone).

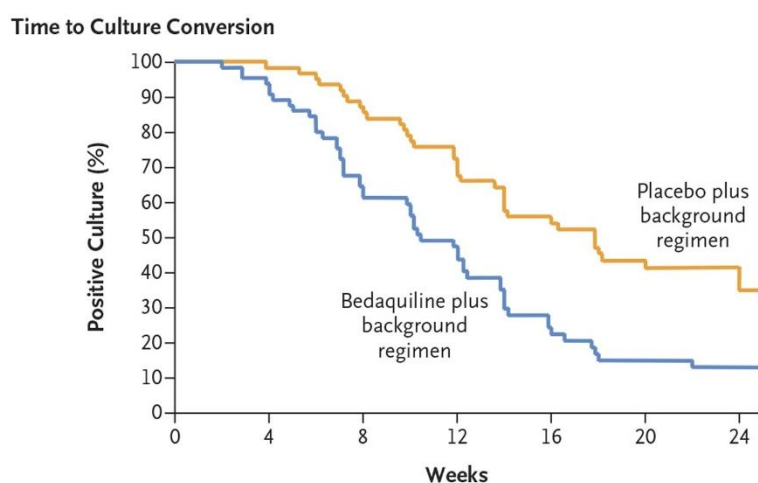


**Figure 1.9.** Time to sputum-culture conversion in Phase IIb trial C208 stage 2 (adapted from ref 46).

To measure the long-term significance of this result, after the 24 week investigational period with BDQ, the study subjects continued the background regimen for an additional 96 week follow-up period. At the end of the study (120 weeks), almost twice as many patients in the BDQ group were cured in comparison with the control group with placebo (**Table 1.3**), demonstrating the BDQ's effect was durable and long ranging. Additionally, it was noted that inclusion of BDQ in the treatment regimen also markedly decreased the risk of acquiring resistance to other background drugs. Bedaquiline's promising efficacy has also been mirrored in multiple post-marketing studies<sup>[47–54]</sup>, and is currently being further evaluated in multiple Phase III clinical trials.<sup>[55]</sup> Overall these studies demonstrate that the inclusion of BDQ in the treatment of MDR-TB leads to improvements in treatment outcomes, with the potential to reduce treatment duration and relapse rates.

**Table 1.3.** Summary of evidence for the efficacy of bedaquiline in the treatment of MDR-TB (adapted from ref 56).

| Parameters                                     | Bedaquiline | Placebo  |
|--|-------------|----------|
| Median time to sputum culture conversion       | 83 days     | 125 days |
| Proportion of patients with culture conversion |             |          |
| Week 24  | 78.8%       | 57.6%    |
| Week 72  | 71.2%       | 56.1%    |
| Week 120                                       | 62.1%       | 43.9%    |
| Proportion cured                               | 57.6%       | 31.8%    |

### 1.3.5 Safety of bedaquiline

Despite promising to shorten and simplify treatment regimens, due to safety concerns raised during clinical evaluation, BDQ's widespread use for MDR-TB is currently limited to 24 weeks in cases where all other therapies have previously failed.<sup>[46]</sup> Of particular concern was a significantly higher rate of mortality observed during one Phase II trial, with death occurring in 11.4% (9/79) of patients receiving BDQ in comparison to 2.5% (2/81) of those receiving placebo.<sup>[57]</sup> Although the specific cause of these additional deaths remains unclear, great caution is warranted with the use of BDQ and therefore it is currently prescribed with an FDA "black box" warning highlighting an increased risk of mortality.<sup>[57]</sup> Additional observed adverse effects included cardiotoxicity, drug-drug interactions and hepatotoxicity, which may be exacerbated by its long terminal elimination half-life.

#### 1.3.5.1. Cardiotoxicity

The most serious safety concern noted during clinical trials was cardiotoxicity arising from BDQ's interference with the heart's electrical activity. This is measured as QT prolongation on the electrocardiogram (ECG) which predisposes individuals to potentially fatal arrhythmia (known as torsades de pointes).<sup>[58]</sup> During a healthy heartbeat, the heart displays an ordered spread of depolarisation which gives rise to the characteristic ECG trace (**Figure 1.10**, A). The QT interval is

defined as the time between the beginning of the Q wave and the end of the T wave which estimates the duration of the ventricular action potential. As such, lengthening of this interval reflects a delay in cardiac repolarisation that increases the risk of rapid irregular heartbeats (torsades de pointes) that can lead to fainting and sudden death (**Figure 1.10, B**).

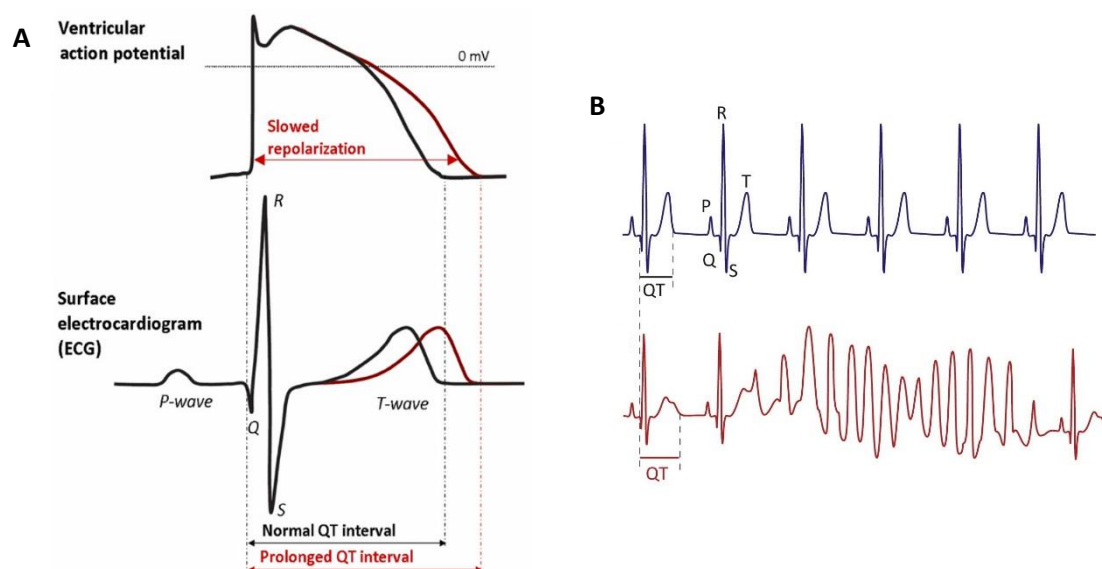


**Figure 1.10.** Ventricular action potential and the related ECG signal. A) Normal and prolonged ventricular action potential are reflected on the ECG recording, with lengthening of the QT interval B) Schematised ECG recording presenting the onset of torsades de pointes in a patient with long QT syndrome (red line). Adapted from refs 59 and 60.

Almost all cases of drug-induced QT prolongation can be attributed to blockade of the cardiac Kv11.1  $K^+$  ion channel encoded by the human ether-a-go-go related gene (hERG).<sup>[61]</sup> This channel is critical for the repolarisation of the cell membrane during a ventricular action potential with the release of  $K^+$  ions out of the cell. Inhibition of the hERG channel therefore delays repolarisation of the membrane giving rise to an increased QT interval. In recent years, a number of marketed drugs have been withdrawn or restricted due to safety issues relating to QT prolongation, and as such it is of great concern to the pharmaceutical industry and regulatory agencies.<sup>[62]</sup>

For an individual patient, a QTc (QT corrected for heart rate) interval of >500 ms or an increase in the QTc of >60 ms from reference is generally considered to confer a high risk of ventricular arrhythmia.<sup>[63]</sup> Additionally, in the setting of a clinical trial, a mean increase in QTc of 5 ms compared with placebo is considered of concern to regulators.<sup>[63]</sup> The use of BDQ during Phase IIb trial C208 was associated with moderate QT prolongation, with a mean increase of 15.4 ms at week 24 compared to an increase of 3.3 ms in the placebo group.<sup>[46]</sup> Additionally, more patients experienced QTc increases >60 ms from reference values as compared with the placebo group (9.1% vs. 2.5%), however only a single patient in the BDQ group was observed to develop a QTc interval of 500 ms.

### **1.3.5.2. Drug-drug interactions**

Considering BDQ is always dosed in combination with multiple drugs as part of complex regimens, the potential for drug-drug interactions is of particular concern. In relation to cardiotoxicity, combination with other drugs which also demonstrate QT prolongation presents a particular risk of cardiotoxicity due to the additive or synergistic effects that may result. In Phase II study C209, mean increases in QTc were more pronounced in the subject group who were receiving BDQ in combination with the second-line anti-TB drug clofazimine, with a mean change of 31.9 ms at week 24 in comparison to 12.3 ms for those who were taking BDQ without clofazimine.<sup>[50]</sup>

In addition to drug-drug interactions related to cardiotoxicity, metabolism related interactions are also of concern. Bedaquiline is primarily hepatically metabolized by cytochrome P450 isoenzyme 3A4 (CYP3A4) into the less active yet more toxic *N*-monodesmethyl metabolite (M2).<sup>[57,64]</sup> As a consequence, co-administration of BDQ with drugs that either induce or inhibit this enzyme results in altered drug bioavailability and must be avoided as to not interfere with its therapeutic effect or lead to increased toxicity. Given that many antiretroviral drugs such as lopinavir and ritonavir are potent CYP3A4 inhibitors, and that co-infection of TB and HIV is pronounced, the use of BDQ is highly limited in these settings due to the potential for increased toxicity.<sup>[65]</sup> Additionally, BDQ is not recommended for concomitant use with other rifamycin antimycobacterial drugs (E.g. rifampicin) as a result of their CYP3A4 inducing activity which has been demonstrated to result in sub-therapeutic concentrations of BDQ.<sup>[65]</sup>

### **1.3.5.3. Hepatotoxicity**

Pooled safety data from Phase IIb trial C208 (stages 1 and 2) revealed a higher incidence of hepatic related toxicity in the BDQ group (8.8%) as compared to the placebo group (1.9%), with elevated serum transaminases discovered in the majority of these cases.<sup>[56]</sup> Two patients taking BDQ in the pooled Phase II studies had grade 3 or 4 liver function test abnormalities close to the time of death, however it is unclear whether these fatalities were BDQ-related.<sup>[57]</sup> Furthermore, in a detailed analysis over 120 weeks in the single-arm Phase II trial C209, 1.7% of patients were identified to have hepatic events related to BDQ.<sup>[50]</sup> As such, BDQ is recommended to be used with caution in patients with severe hepatic impairment, and it is advised that a combination of BDQ together with alcohol or other hepatotoxic drugs should be avoided.<sup>[57]</sup>

### **1.3.5.4. Long half-life**

Bedaquiline possess an extremely long terminal elimination half-life of 5.5 months mainly due to its propensity to distribute extensively into tissues.<sup>[66]</sup> As a result, BDQ is dosed initially at 400 mg once daily for the first 14 days of treatment, followed by 200 mg three days a week.<sup>[57]</sup> Although less



frequent dosing is advantageous, adverse events may also be prolonged after drug cessation, therefore contributing to toxicity. Given the potential for over-proportional accumulation within tissue, the full exploration of BDQ's potential dose range has not been explored.<sup>[57]</sup>

Bedaquiline's extensive tissue distribution is thought to arise from its tendency to specifically accumulate and remain trapped within the lysosomes of cells.<sup>[66]</sup> Once inside the lysosome, the drug can form indigestible drug-phospholipid aggregates giving rise to what is identified as phospholipidosis.<sup>[67]</sup> It is hypothesised that as a result of this phenomenon, BDQ accumulates and is slowly released from peripheral tissue compartments giving rise to the observed extended terminal elimination half-life. Indeed, BDQ and its active metabolite M2 were both found to be inducers of phospholipidosis during preclinical studies.<sup>[68]</sup>

## **1.4 Drug-like properties**

In order for a drug to have a high chance of success in making it into the clinic, it must simultaneously satisfy a number of criteria relating to potency, PK and safety. Some of the compound properties which have been used by medicinal chemists to define the properties which constitute 'drug-like' compounds include molecular weight (MW), lipophilicity, topological polar surface area (TPSA), number of hydrogen bond donors and acceptors, number of rotatable bonds, fraction of sp<sup>3</sup> carbons and the number of aromatic rings.<sup>[69]</sup> Of all these properties, control of lipophilicity is recognised as one of the most important to consider in maintaining a compound within desired ADME and toxicological parameters.<sup>[70]</sup>

### **1.4.1 Lipophilicity related toxicity**

Lipophilicity is defined as the affinity of a drug for a lipid environment. It may be determined experimentally as the octanol-water partition coefficient (LogP) or the distribution coefficient (LogD). Whereas LogP describes the partition of an unionised solute between a water and octanol phase, the LogD takes ionisation into consideration and therefore describes partition at a specific pH (usually physiological pH, 7.4). Larger LogP or LogD values correspond to greater lipophilicity. In practice, a calculated value of LogP (cLogP) is most often used as a quick estimation of lipophilicity, instead of measuring LogP experimentally.<sup>[70]</sup>

There is increasing evidence to suggest that control of lipophilicity within a defined optimal range can improve compound quality and the likelihood of success. According to 'Lipinski's Rule of 5' the desirable LogP of a compound intended for oral administration should be <5 for optimal pharmacokinetics, in addition to a molecular weight <500 Da, hydrogen bond donors <5, or hydrogen bond acceptors <10.<sup>[71]</sup> More recently, Gleeson has revised some of these parameters, suggesting that

compounds with a LogP <4 and a molecular weight <400 stand an even greater chance of success.<sup>[72]</sup> In general, high lipophilicity frequently leads to compounds with poor solubility and therefore poor absorption, and an increased likelihood of receptor promiscuity, toxicity and rapid clearance.<sup>[70]</sup>

The specific effect of lipophilicity on drug toxicity has been well documented in a range of studies analysing pharma datasets.<sup>[73–75]</sup> Perhaps the most significant study is what led to the 3/75 rule, derived from the investigation of 245 Pfizer preclinical candidates for *in vivo* tolerability in rats and dogs. In this study it was demonstrated that compounds with both high lipophilicity (cLogP >3) and low polarity (TPSA <75 Å<sup>2</sup>) were 6 times more likely to be associated with adverse events in comparison to compounds that exhibited both low lipophilicity (cLogP <3) and high polarity (TPSA >75 Å<sup>2</sup>).<sup>[73]</sup>

Three specific examples of drug-induced toxicity that correlate to lipophilicity include inactivation of the hERG cardiac potassium channel, drug-induced cellular phospholipidosis, cytochrome P450 (CYP) superfamily inhibition and hepatotoxicity.

#### 1.4.1.1. hERG inhibition

The hERG cardiac potassium channel is known to potently bind and be inactivated by a wide variety of chemotypes with high promiscuity. As mentioned previously, this can lead to cardiotoxicity as a result of QT prolongation. Inhibition of hERG has been shown to be related to compound lipophilicity and is exacerbated with compounds containing a basic amine element.

In a study by Waring *et al.*<sup>[76]</sup>, an analysis of 7685 AstraZeneca compounds associated with hERG inhibition data was performed. The data were analysed and presented as the probability of achieving a compound with a hERG IC<sub>50</sub> of >10 µM as a function of lipophilicity for different ionisation classes, with lipophilic bases demonstrating the lowest probability to achieve a hERG IC<sub>50</sub> of >10 µM. Their findings suggested that a cLogP of <2 was required to have a >70% chance of avoiding potent hERG inhibition. Similar findings have also been reported across a range of other dataset studies.<sup>[72,77]</sup>

A number of studies have been undertaken to explore the SAR of hERG based on pharmacophores and molecular descriptors (extensively reviewed by Jing *et al.*<sup>[78]</sup>). Although the large structural diversity of hERG inhibitors preclude the use of one specific pharmacophore model to predict hERG inhibition, many strongly correlate drug lipophilicity with hERG binding, with at least once hydrophobic or aromatic ring feature in addition to a cationic group. Despite this, some drugs that do not conform to these features also inhibit the channel at therapeutically relevant concentrations.<sup>[79]</sup>

Since the crystal structure of the hERG channel is yet to be solved, a number of mutagenesis studies and homology models have been used to distinguish key residues that may interact directly with hERG-blocking drugs.<sup>[78,80]</sup> Many of these studies have highlighted Tyr-652 and Phe-656 lining the pore of



the channel to be of particular importance, which were originally suggested to interact with drugs through cation- $\pi$  interactions to the protonated amine or  $\pi$ -stacking interactions to the hydrophobic regions. Many other additional residues have been implicated, including Thr-623 and Ser-624.<sup>[80]</sup> Very recently, the high resolution cryogenic electron microscopy (cryo-EM) structure of the open state structure of the hERG channel revealed the unexpected presence of four unique hydrophobic pockets in the central cavity which include these key residues.<sup>[81]</sup> Given this new insight, it has been suggested that drugs may bind within these pockets through hydrophobic interactions rather than interactions specific to the aromatic nature of these residues. Although the cryo-EM structure represents a major breakthrough in the quest to understand the molecular basis of hERG inhibition, drug bound structures are yet to be solved. As such the precise mechanisms underlying the binding of such a wide variety of drugs to hERG are complex and remain to be fully understood, and therefore precise predictive tools are not yet available.

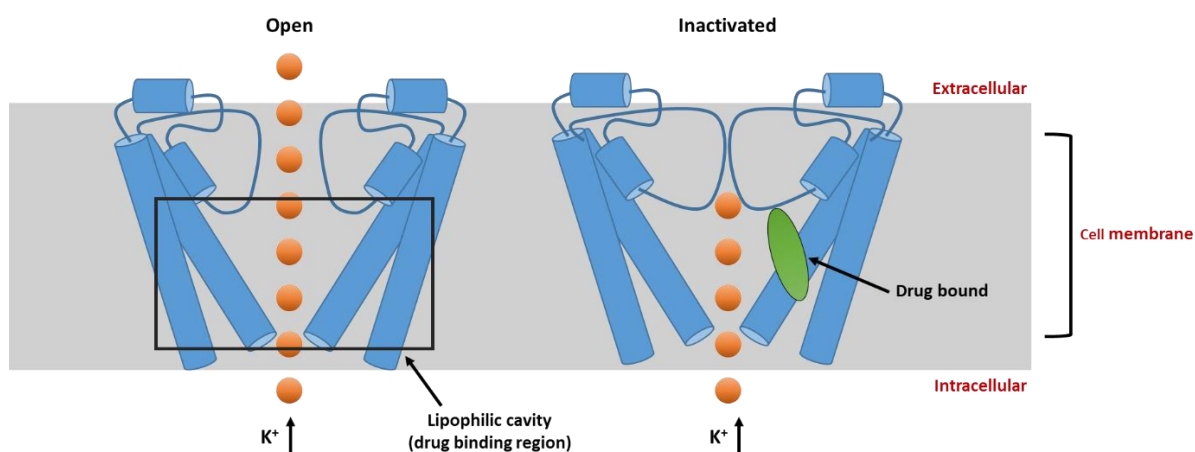


**Figure 1.11.** Schematic depiction of the hERG channel key structural elements. Most drugs that inhibit hERG are believed to bind to residues lining the large lipophilic central cavity of the channel, stabilising the inactive state (adapted from ref 82).

#### 1.4.1.2. Phospholipidosis

Similar to drugs which inhibit hERG, drug-induced phospholipidosis also appears to be strongly correlated with lipophilic basic amines.<sup>[83]</sup> As mentioned previously, drug-induced phospholipidosis is believed to result from lysosomal trapping, which is proposed to occur as a result of drug entry and protonation within the acidic environment of the lysosome, which restricts reverse diffusion of the cationic drug back across the lysosomal membrane.<sup>[84]</sup> Therefore, in order to induce phospholipidosis, a drug must have a degree of lipophilicity to passively diffuse across the membrane, whilst also possessing a basic moiety that is able to be protonated at pH 4–5. Although the direct relationship between phospholipidosis and drug toxicity remains poorly understood, it remains a concern to regulatory agencies.<sup>[85]</sup>

In a study by Ploemen *et al.*, it was demonstrated that the risk of phospholipidosis induced by a drug increases if the sum of  $\text{LogP}^2$  and  $\text{pKa}^2$  is  $>90$ .<sup>[86]</sup> Furthermore, Tomizawa *et al.* have suggested that a high risk of drug-induced phospholipidosis exists for compounds with a net charge of 1 and a  $\text{LogP} > 2.75$ .<sup>[87]</sup> Following from these studies, multiple computational methods to predict the likelihood of phospholipidosis have been developed using additional molecular properties, however lipophilicity and basicity remain as important correlating factors throughout.<sup>[88]</sup>

#### 1.4.1.3. CYP inhibition

The CYP superfamily of enzymes is a very large and diverse group of enzymes which play important and dominant role in the metabolism of drugs. Of all the isoforms, CYP3A4 is responsible for ~30% of drug metabolism.<sup>[89]</sup> It therefore follows that inhibition of this enzyme results in drug-drug interactions due to restricted metabolism of other CYP3A4 substrates.

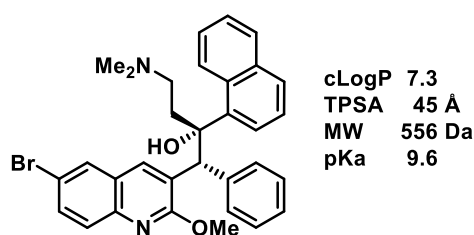
Compound lipophilicity has been shown to be fundamentally important to CYP substrate selectivity, affinity and inhibition.<sup>[90–93]</sup> In a 2008 study by Gleeson analysing the effect that close to 50000 GlaxoSmithKline compounds had on CYP inhibition, a strong correlation was found to exist with  $\text{cLogP}$  across all the isoforms investigated, with an increase in  $\text{cLogP}$  associated with an increase in the mean  $\text{pIC}_{50}$  values.<sup>[72]</sup> For CYP3A4, large neutral drugs were found to be more potent inhibitors.

#### 1.4.1.4. Hepatotoxicity

The precise mechanism of BDQ-related hepatotoxicity remains to be determined, however it has been suggested that large doses of highly lipophilic drugs (which require greater hepatic metabolism) are associated with an increased propensity for liver toxicity through the saturation of clearance processes or the build-up of reactive metabolites. On analysis of 154 drugs in the LTKB benchmark dataset, Chen *et al.* reported a significantly higher incidence of drug-induced hepatotoxicity with drugs that were dosed daily at  $\geq 100$  mg, in combination with a  $\text{LogP} \geq 3$ .<sup>[94]</sup>

### 1.5 Project objectives

When assessing BDQ's physicochemical profile, it is quite clear that it possesses some key properties which give rise to its adverse toxicological and pharmacokinetic profiles. As shown in **Figure 1.12**, it has a very high MW for a drug (556 Da), it is a highly lipophilic basic amine ( $\text{cLogP}$  7.3,  $\text{pKa}$  9.6) and has very low TPSA (45 Å). In particular, its extreme lipophilicity combined with its basicity is thought to be a major contributing factor regarding hERG-mediated cardiotoxicity, as well as the induction of phospholipidosis (which likely contributes to BDQ's long terminal half-life). Additionally, BDQ's metabolism by CYP3A4, and hepatotoxicity are also thought to be driven by its lipophilicity.



| Adverse effects and risks                | Implicated properties |
|--|-----------------------|
| hERG mediated cardiotoxicity             | cLogP, pKa            |
| Phospholipidosis/long terminal half-life | cLogP, pKa            |
| CYP3A4 mediated drug-drug interactions   | cLogP, MW             |
| Hepatotoxicity                           | cLogP                 |

**Figure 1.12.** The relationship between BDQ's physicochemical profile and its observed adverse effects.

In light of these shortcomings, it is clear that there exists an exciting opportunity to discover novel and improved drugs inspired by BDQ, yet without its associated liabilities. More specifically, given that many of these toxicities are likely related to BDQ's lipophilicity coupled with basicity, it is hypothesised that modifying the structure to reduce these influences could significantly improve BDQ's side-effect and PK profiles. Additionally, it is also expected that these properties can be altered whilst retaining or even increasing BDQ's potent inhibitory activity.

Interestingly, since BDQ's structure was revealed in 2005, very few examples of modified analogues have been published in the literature. The lack of effort in this space is most likely due to the stereostructural complexity of BDQ resulting from its two contiguous stereogenic centres, making the synthesis of analogues very challenging and time-consuming. In response to its complexity, the few studies that have arisen have focused on simplifying the chemical structure to make the synthesis more tractable.<sup>[95–98]</sup> One such study by Jain *et al.*<sup>[96]</sup> reported novel achiral arylquinoline derivatives which were designed using the essential pharmacophoric features of BDQ in combination with computer modelling to best match BDQ's lowest energy conformations (**Figure 1.13**). Despite being quite imaginative work resulting in simplified structures with a significant lowering of lipophilicity (cLogP 5.4), releasing the rigid conformation of BDQ was shown to be detrimental to activity (2.28 vs. 0.03 µg/mL).

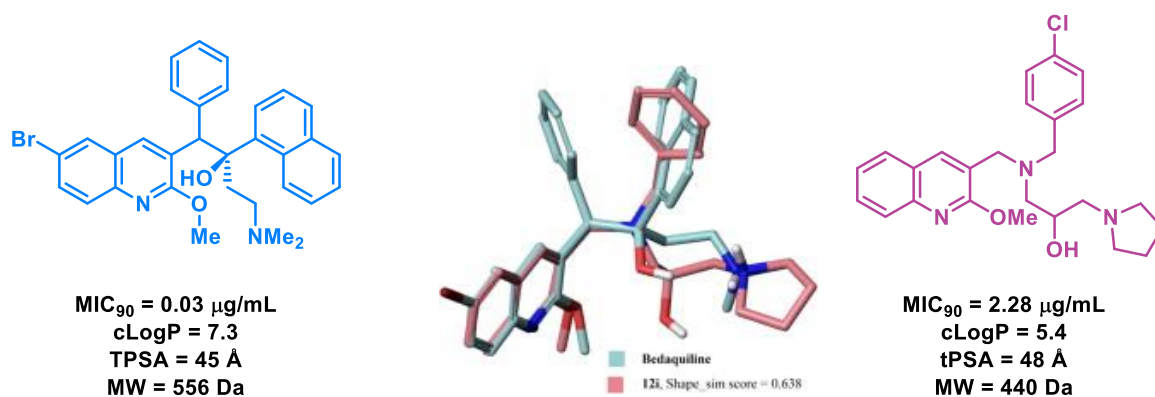


**Figure 1.13.** A series of arylquinoline derivatives were designed by Jain *et al.*<sup>[96]</sup> to retain the significant pharmacophoric features and three dimensional geometry of BDQ.

Since BDQ's rigid conformation appears to be significantly correlated with its potency, the focus of this project is to retain BDQ's core configuration, while improving drug-like properties by optimising the main structural regions A, B, C and D (**Figure 1.14**). Specifically, this could be achieved by (i) reducing lipophilicity through further modifications to regions A, B and C, and/or (ii) attenuating basicity through modifications to the amino group in region D.

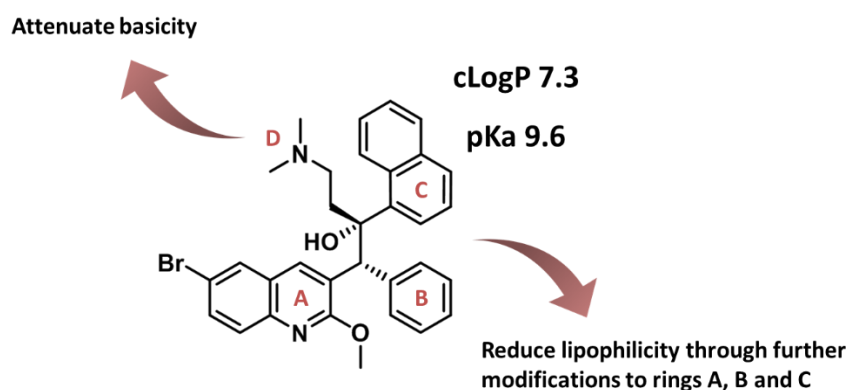


**Figure 1.14.** Strategies identifies to improve upon BDQ's toxicological profile.

To reduce lipophilicity, ring A was selected as the most the most attractive region to begin optimising as Janssen's interrogation of this region was relatively limited. As mentioned previously, their SAR was invariably dependent on the quinoline in this region throughout their entire series. Given that there was no evidence to suggest that the quinoline was specifically required for activity, it is envisaged that it could be replaced with a variety of less lipophilic *N*-heterocycles (E.g. pyridine, pyrazine or pyridazine), therefore allowing us to reduce lipophilicity whilst also providing an opportunity to access novel intellectual property (IP) space.

In addition to exploring region A, a secondary strategy to improve BDQ's side-effect profile would be to investigate lowering the basicity of the region D amino functionality. Considering that Janssen's

interrogation of this region concluded that activity significantly decreased with a  $pK_a < 8$ , this strategy is only planned if significant improvements in activity in comparison with BDQ can be achieved through modifications to the A-ring to compensate.

Throughout this project, all synthesised target compounds will be evaluated for inhibitory activity *in vitro* against *M.tb* in order to determine whether potency can be maintained despite the incorporated structural modifications. The results provided by these preliminary assays will help guide the synthesis of future analogues.

Shortlisted compounds which demonstrate activity close to that of BDQ's will also be profiled for compound safety, the most important assay being the measurement of hERG inhibition. Additional assays aimed at assessing metabolic stability and phospholipidosis will also be of value.

The specific objectives of this PhD project are therefore to:

- synthesise potent, novel analogues of BDQ with improved properties by reducing lipophilicity, and potentially basicity,
- profile synthesised analogues for *in vitro* inhibition of *M.tb* in comparison to BDQ, and
- evaluate the most potent analogues for safety in comparison to BDQ (E.g. hERG inhibition).

## 1.6 References

- [1] T. M. Daniel, *Respir. Med.* **2006**, *100*, 1862–70.
- [2] World Health Organization, *Global Tuberculosis Report*, **2018**.  
[https://www.who.int/tb/publications/global\\_report/en/](https://www.who.int/tb/publications/global_report/en/) (retrieved 14 April 2019).
- [3] K. Andries, P. Verhasselt, J. Guillemont, H. W. H. Göhlmann, J.-M. Neefs, H. Winkler, J. Van Gestel, P. Timmerman, M. Zhu, E. Lee, et al., *Science* **2005**, *307*, 223–7.
- [4] World Health Organisation, *Companion Handbook to the WHO Guidelines for the Programmatic Management of Drug-Resistant Tuberculosis*, **2014**.  
[https://www.who.int/tb/publications/pmdt\\_companionhandbook/en/](https://www.who.int/tb/publications/pmdt_companionhandbook/en/) (retrieved 12 December 2015).
- [5] H. Patel, R. Pawara, K. Pawara, F. Ahmed, A. Shirkhedkar, S. Surana, *Tuberculosis* **2019**, *117*, 79–84.
- [6] R. M. G. J. Houben, P. J. Dodd, *PLOS Med.* **2016**, *13*, e1002152.
- [7] R. K. Gupta, S. B. Lucas, K. L. Fielding, S. D. Lawn, *AIDS* **2015**, *29*, 1987–2002.
- [8] C. Toms, R. Stapledon, C. Coulter, P. Douglas, *Commun. Dis. Intell. Q. Rep.* **2017**, *41*, E247–E263.
- [9] S. D. Lawn, A. I. Zumla, *Lancet* **2011**, *378*, 57–72.
- [10] V. Jarlier, H. Nikaido, *FEMS Microbiol. Lett.* **1994**, *123*, 11–18.
- [11] M. I. Voskuil, I. L. Bartek, K. Visconti, G. K. Schoolnik, *Front. Microbiol.* **2011**, *2*, 105.
- [12] M. K. Ozvaran, R. Baran, M. Tor, I. Dilek, D. Demiryontar, S. Arinç, N. Toker, E. U. Chousein, O. Soğukpınar, *Ann. Thorac. Med.* **2007**, *2*, 118–21.
- [13] I. Smith, *Clin. Microbiol. Rev.* **2003**, *16*, 463–96.
- [14] T. C. Zahrt, *Microbes Infect.* **2003**, *5*, 159–167.
- [15] C. J. Cambier, S. Falkow, L. Ramakrishnan, *Cell* **2014**, *159*, 1497–1509.
- [16] D. G. Russell, P.-J. Cardona, M.-J. Kim, S. Allain, F. Altare, *Nat. Immunol.* **2009**, *10*, 943–948.
- [17] C. Nunes-Alves, M. G. Booty, S. M. Carpenter, P. Jayaraman, A. C. Rothchild, S. M. Behar, *Nat. Rev. Microbiol.* **2014**, *12*, 289–99.
- [18] E. Vynnycky, *Am. J. Epidemiol.* **2000**, *152*, 247–263.
- [19] J. R. Andrews, F. Noubary, R. P. Walensky, R. Cerda, E. Losina, C. R. Horsburgh, *Clin. Infect. Dis.* **2012**, *54*, 784–91.
- [20] D. G. Russell, *Immunol. Rev.* **2011**, *240*, 252–68.
- [21] M.-J. Kim, H. C. Wainwright, M. Locketz, L.-G. Bekker, G. B. Walther, C. Dittrich, A. Visser, W. Wang, F.-F. Hsu, U. Wiehart, et al., *EMBO Mol. Med.* **2010**, *2*, 258–74.
- [22] M. Pai, M. P. Nicol, C. C. Boehme, in *Tuberc. Tuber. Bacillus, Second Ed.*, American Society Of Microbiology, **2016**, pp. 363–378.

- [23] Y. J. Ryu, *Tuberc. Respir. Dis.* **2015**, 78, 64–71.
- [24] K. F. Laserson, L. E. Thorpe, V. Leimane, K. Weyer, C. D. Mitnick, V. Riekstina, E. Zarovska, M. L. Rich, H. S. F. Fraser, E. Alarcón, et al., *Int. J. Tuberc. Lung Dis.* **2005**, 9, 640–5.
- [25] D. A. Mitchison, *Chest* **1979**, 76, 771–81.
- [26] P. Brennan, D. Young, B. Robertson, *Tuberculosis* **2008**, 88, 85–6.
- [27] World Health Organisation, *Guidelines for the Programmatic Management of Drug-Resistant Tuberculosis*, **2011**. <https://www.who.int/tb/publications/tb-drugresistant-guidelines/en/> (retrieved 12 December 2015).
- [28] D. A. Mitchison, *Int. J. Tuberc. Lung Dis.* **1998**, 2, 10–5.
- [29] N. R. Gandhi, P. Nunn, K. Dheda, H. S. Schaaf, M. Zignol, D. van Soolingen, P. Jensen, J. Bayona, *Lancet* **2010**, 375, 1830–43.
- [30] J. Cohen, *Science* **2013**, 339, 130.
- [31] A. Koul, N. Dendouga, K. Vergauwen, B. Molenberghs, L. Vranckx, R. Willebrords, Z. Ristic, H. Lill, I. Dorange, J. Guillemont, et al., *Nat. Chem. Biol.* **2007**, 3, 323–4.
- [32] A. Koul, L. Vranckx, N. Dendouga, W. Balemans, I. Van den Wyngaert, K. Vergauwen, H. W. H. Göhlmann, R. Willebrords, A. Poncelet, J. Guillemont, et al., *J. Biol. Chem.* **2008**, 283, 25273–25280.
- [33] J. Guillemont, C. Meyer, A. Poncelet, X. Bourdrez, K. Andries, *Future Med. Chem.* **2011**, 3, 1345–1360.
- [34] J. E. G. Guillemont, J. F. E. Van Gestel, M. G. Venet, L. F. B. Decrane, D. F. J. Vernier, F. C. Odds, I. C. F. Csoka, K. J. L. M. Andries, *Quinoline Derivatives and Their Use as Mycobacterial Inhibitors*, **2004**, WO011436.
- [35] J. Guillemont, C. Meyer, A. Koul, K. Andries, in *Compr. Chirality* (Eds.: E. M. Carreira, H. Yamamoto), Elsevier, Amsterdam, **2012**, pp. 54–69.
- [36] J. P. Abrahams, A. G. W. Leslie, R. Lutter, J. E. Walker, *Nature* **1994**, 370, 621–628.
- [37] A. C. Haagsma, R. Abdillahi-Ibrahim, M. J. Wagner, K. Krab, K. Vergauwen, J. Guillemont, K. Andries, H. Lill, A. Koul, D. Bald, *Antimicrob. Agents Chemother.* **2009**, 53, 1290–2.
- [38] S. C. Goolooze, A. F. Cohen, R. Rissmann, *Br. J. Clin. Pharmacol.* **2015**, 80, 182–184.
- [39] A. C. Haagsma, I. Podasca, A. Koul, K. Andries, J. Guillemont, H. Lill, D. Bald, *PLoS One* **2011**, 6, e23575.
- [40] D. Stock, A. G. W. Leslie, J. E. Walker, *Science* **1999**, 286, 1700–1705.
- [41] J. E. Walker, D. Keilin, A. P. Halestrap, P. Mitchell, P. Mitchell, S. Iwata, C. Ostermeier, B. Ludwig, H. Michel, T. Tsukihara, et al., *Biochem. Soc. Trans.* **2013**, 41, 1–16.
- [42] S. Petrella, E. Cambau, A. Chauffour, K. Andries, V. Jarlier, W. Sougakoff, *Antimicrob. Agents Chemother.* **2006**, 50, 2853–6.
- [43] M. R. de Jonge, L. H. M. Koymans, J. E. G. Guillemont, A. Koul, K. Andries, *Proteins Struct. Funct. Bioinforma.* **2007**, 67, 971–980.

- [44] E. Segala, W. Sougakoff, A. Nevejans-Chauffour, V. Jarlier, S. Petrella, *Antimicrob. Agents Chemother.* **2012**, *56*, 2326–34.
- [45] L. Preiss, J. D. Langer, O. Yildiz, L. Eckhardt-Strelau, J. E. G. Guillemont, A. Koul, T. Meier, *Sci. Adv.* **2015**, *1*, e1500106–e1500106.
- [46] A. H. Diacon, A. Pym, M. P. Grobusch, J. M. de Los Rios, E. Gotuzzo, I. Vasilyeva, V. Leimane, K. Andries, N. Bakare, T. De Marez, et al., *N. Engl. J. Med.* **2014**, *371*, 723–732.
- [47] N. Ndjeka, F. Conradie, K. Schnippel, J. Hughes, N. Bantubani, H. Ferreira, G. Maartens, D. Mametja, G. Meintjes, X. Padanilam, et al., *Int. J. Tuberc. Lung Dis.* **2015**, *19*, 979–985.
- [48] L. Guglielmetti, D. Le Du, M. Jachym, B. Henry, D. Martin, E. Caumes, N. Veziris, N. Metivier, J. Robert, C. Andrejak, et al., *Clin. Infect. Dis.* **2015**, *60*, 188–194.
- [49] L. Guglielmetti, D. Le Dû, N. Veziris, E. Caumes, D. Marigot-Outtandy, Y. Yazdanpanah, J. Robert, M. Fréchet-Jachym, *Eur. Respir. J.* **2016**, *48*, 582–5.
- [50] A. S. Pym, A. H. Diacon, S.-J. Tang, F. Conradie, M. Danilovits, C. Chuchottaworn, I. Vasilyeva, K. Andries, N. Bakare, T. De Marez, et al., *Eur. Respir. J.* **2016**, *47*, 564–574.
- [51] E. Pontali, G. Sotgiu, L. D’Ambrosio, R. Centis, G. B. Migliori, *Eur. Respir. J.* **2016**, *47*, 394–402.
- [52] S. E. Borisov, K. Dheda, M. Enwerem, R. Romero Leyet, L. D’Ambrosio, R. Centis, G. Sotgiu, S. Tiberi, J.-W. Alffenaar, A. Maryandyshev, et al., *Eur. Respir. J.* **2017**, *49*, 1700387.
- [53] O. Olayanju, J. Limberis, A. Esmail, S. Oelofse, P. Gina, E. Pietersen, M. Fadul, R. Warren, K. Dheda, *Eur. Respir. J.* **2018**, *51*, 1800544.
- [54] C. Hewison, M. Bastard, N. Khachatryan, T. Kotrikadze, A. Hayrapetyan, Z. Avaliani, N. Kiria, L. Yegiazaryan, N. Chumburidze, O. Kirakosyan, et al., *Int. J. Tuberc. Lung Dis.* **2018**, *22*, 766–772.
- [55] D. R. Silva, M. Dalcolmo, S. Tiberi, M. A. Arbex, M. Munoz-Torrico, R. Duarte, L. D’Ambrosio, D. Visca, A. Rendon, M. Gaga, et al., *J. Bras. Pneumol.* **2018**, *44*, 153–160.
- [56] The World Health Organisation, *The Use of Bedaquiline in the Treatment of Multidrug-Resistant Tuberculosis: Interim Policy Guidance*, **2003**.
- [57] Prescribing Information for Sirturo (bedaquiline) (PDF).  
[http://www.accessdata.fda.gov/drugsatfda\\_docs/label/2012/204384s000lbl.pdf](http://www.accessdata.fda.gov/drugsatfda_docs/label/2012/204384s000lbl.pdf) (retrieved 20 January 2015).
- [58] M. C. Sanguinetti, M. Tristani-Firouzi, *Nature* **2006**, *440*, 463–469.
- [59] L. S. Grilo, P.-A. Carrupt, H. Abriel, *Front. Pharmacol.* **2010**, *1*, 137.
- [60] J. I. Vandenberg, E. Perozo, T. W. Allen, *Trends Pharmacol. Sci.* **2017**, *38*, 899–907.
- [61] R. Pearlstein, R. Vaz, D. Rampe, *J. Med. Chem.* **2003**, *46*, 2017–2022.
- [62] M. J. Waring, J. Arrowsmith, A. R. Leach, P. D. Leeson, S. Mandrell, R. M. Owen, G. Pairaudeau, W. D. Pennie, S. D. Pickett, J. Wang, et al., *Nat. Rev. Drug Discov.* **2015**, *14*, 475–486.



- [63] E14 Clinical Evaluation of QT/QTc Interval Prolongation and Proarrhythmic Potential for Non-Antiarrhythmic Drugs <https://www.fda.gov/media/71372/download> (retrieved 20 April 2019).
- [64] M. C. Rouan, N. Lounis, T. Gevers, L. Dillen, R. Gilissen, A. Raoof, K. Andries, *Antimicrob. Agents Chemother.* **2011**, *56*, 1444–1451.
- [65] E. M. Svensson, K. E. Dooley, M. O. Karlsson, *Antimicrob. Agents Chemother.* **2014**, *58*, 6406–6412.
- [66] A. H. Diacon, P. R. Donald, A. Pym, M. Grobusch, R. F. Patientia, R. Mahanyele, N. Bantubani, R. Narasimooloo, T. De Marez, R. van Heeswijk, et al., *Antimicrob. Agents Chemother.* **2012**, *56*, 3271–6.
- [67] N. Anderson, J. Borlak, *FEBS Lett.* **2006**, *580*, 5533–5540.
- [68] N. Mesens, M. Steemans, E. Hansen, G. R. Verheyen, F. Van Goethem, J. Van Gompel, *Toxicol. Vitro.* **2010**, *24*, 1417–1425.
- [69] M. Segall, *Expert Opin. Drug Discov.* **2014**, *9*, 803–817.
- [70] J. A. Arnott, S. L. Planey, *Expert Opin. Drug Discov.* **2012**, *7*, 863–875.
- [71] C. A. Lipinski, F. Lombardo, B. W. Dominy, P. J. Feeney, *Adv. Drug Deliv. Rev.* **2001**, *46*, 3–26.
- [72] M. P. Gleeson, *J. Med. Chem.* **2008**, *51*, 817–834.
- [73] J. D. Hughes, J. Blagg, D. A. Price, S. Bailey, G. A. DeCrescenzo, R. V. Devraj, E. Ellsworth, Y. M. Fobian, M. E. Gibbs, R. W. Gilles, et al., *Bioorg. Med. Chem. Lett.* **2008**, *18*, 4872–4875.
- [74] P. D. Leeson, B. Springthorpe, *Nat. Rev. Drug Discov.* **2007**, *6*, 881–890.
- [75] J. J. Sutherland, J. W. Raymond, J. L. Stevens, T. K. Baker, D. E. Watson, *J. Med. Chem.* **2012**, *55*, 6455–6466.
- [76] M. J. Waring, C. Johnstone, *Bioorg. Med. Chem. Lett.* **2007**, *17*, 1759–1764.
- [77] U. Zachariae, F. Giordanetto, A. G. Leach, *J. Med. Chem.* **2009**, *52*, 4266–4276.
- [78] Y. Jing, A. Easter, D. Peters, N. Kim, I. J. Enyedy, *Future Med. Chem.* **2015**, *7*, 571–586.
- [79] L. C. Macdonald, R. Y. Kim, H. T. Kurata, D. Fedida, *Sci. Rep.* **2018**, *8*, 289.
- [80] M. V Helliwell, Y. Zhang, A. El Harchi, C. Du, J. C. Hancox, C. E. Dempsey, *J. Biol. Chem.* **2018**, *293*, 7040–7057.
- [81] W. Wang, R. MacKinnon, *Cell* **2017**, *169*, 422–430.e10.
- [82] J. I. Vandenberg, M. D. Perry, M. J. Perrin, S. A. Mann, Y. Ke, A. P. Hill, *Physiol. Rev.* **2012**, *92*, 1393–1478.
- [83] H. Sun, M. Xia, S. A. Shahane, A. Jadhav, C. P. Austin, R. Huang, *Bioorg. Med. Chem. Lett.* **2013**, *23*, 4587–90.
- [84] F. Kazmi, T. Hensley, C. Pope, R. S. Funk, G. J. Loewen, D. B. Buckley, A. Parkinson, *Drug Metab. Dispos.* **2013**, *41*, 897–905.
- [85] M. J. Reasor, K. L. Hastings, R. G. Ulrich, *Expert Opin. Drug Saf.* **2006**, *5*, 567–583.

- [86] J.-P. H. T. M. Ploemen, J. Kelder, T. Hafmans, H. van de Sandt, J. A. van Burgsteden, P. J. M. Salemink, E. van Esch, *Exp. Toxicol. Pathol.* **2004**, *55*, 347–55.
- [87] K. Tomizawa, K. Sugano, H. Yamada, I. Horii, *J. Toxicol. Sci.* **2006**, *31*, 315–24.
- [88] S. S. Choi, J. S. Kim, L. G. Valerio, N. Sadrieh, *Toxicol. Appl. Pharmacol.* **2013**, *269*, 195–204.
- [89] U. M. Zanger, M. Schwab, *Pharmacol. Ther.* **2013**, *138*, 103–141.
- [90] D. A. Smith, *Eur. J. Pharm. Sci.* **1994**, *2*, 69–71.
- [91] D. A. Smith, H. van de Waterbeemd, *Curr. Opin. Chem. Biol.* **1999**, *3*, 373–8.
- [92] D. A. Smith, M. J. Ackland, B. C. Jones, *Drug Discov. Today* **1997**, *2*, 406–414.
- [93] D. A. Smith, M. J. Ackland, B. C. Jones, *Drug Discov. Today* **1997**, *2*, 479–486.
- [94] M. Chen, J. Borlak, W. Tong, *Hepatology* **2013**, *58*, 388–396.
- [95] R. S. Upadhyaya, J. K. Vandavasi, N. R. Vasireddy, V. Sharma, S. S. Dixit, J. Chattopadhyaya, *Bioorg. Med. Chem.* **2009**, *17*, 2830–2841.
- [96] P. P. Jain, M. S. Degani, A. Raju, M. Ray, M. G. R. Rajan, *Bioorg. Med. Chem. Lett.* **2013**, *23*, 6097–6105.
- [97] S. Singh, K. K. Roy, S. R. Khan, V. K. Kashyap, A. Sharma, S. Jaiswal, S. K. Sharma, M. Y. Krishnan, V. Chaturvedi, J. Lal, et al., *Bioorg. Med. Chem.* **2015**, *23*, 742–752.
- [98] C. He, L. Preiss, B. Wang, L. Fu, H. Wen, X. Zhang, H. Cui, T. Meier, D. Yin, *ChemMedChem* **2017**, *12*, 106–119.

## Chapter 2: Pyridine Analgues of Bedaquiline

### 2.1 Introduction

In order to address the safety concerns associated with BDQ, and in particular hERG channel inhibition, the key focus of this project was to reduce lipophilicity whilst retaining potent anti-*M.tb* activity. Given that very limited SAR existed around the unit A quinoline heterocycle, we initially aimed to explore structural modification in this region in an effort to target lipophilicity whilst also accessing novel IP space. Specifically, at the commencement of this project there was no evidence to indicate whether the quinoline ring was essential for activity as other heterocyclic or carbocyclic variants had not been reported. Given this, the first aim of this project was to substitute the quinoline heterocycle with other appropriate nitrogen-containing heterocycles as a means to explore this region.

The first heterocyclic motif chosen to explore the effect of quinoline substitution was the closely related pyridyl ring. The pyridine moiety is a commonly employed heterocyclic scaffold featured in over 100 marketed pharmaceuticals including the blockbuster drugs esomeprazole (Nexium) and loratadine (Claritin) (**Figure 2.1**).<sup>[1]</sup> It was initially anticipated that the reduction in lipophilicity provided by employing a pyridine ring in place of a quinoline could reduce drug toxicity and improve overall properties, however it was unknown what effect this would have on the activity against *M.tb*.

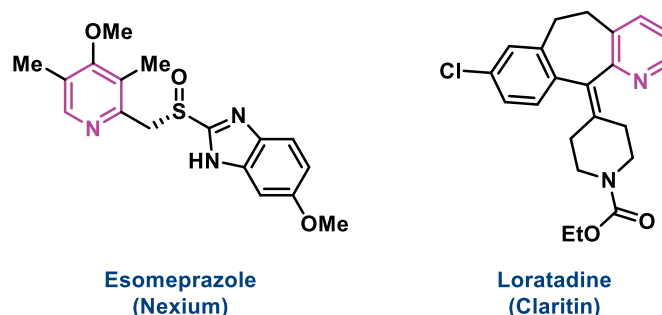


**Figure 2.1.** Examples of pharmaceutical drugs that contain the pyridine scaffold.

Initial work within the group had focused on the use of 2-methoxypyridine as a quinoline replacement, with further diversification explored at the pyridyl C5 position (**Figure 2.2**).

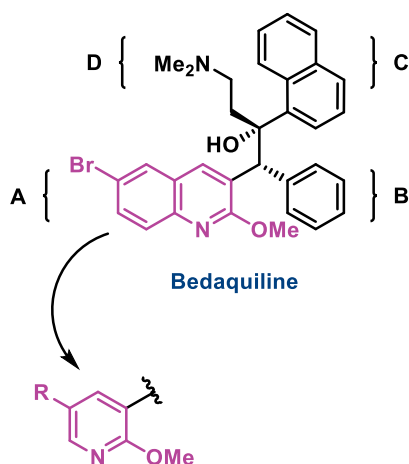
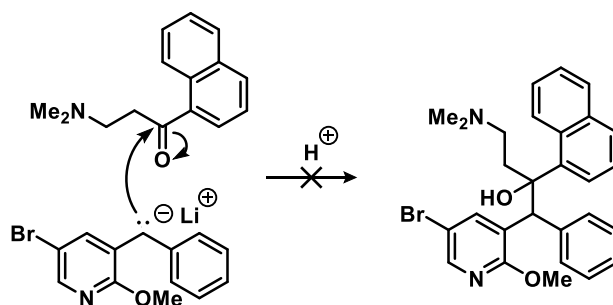


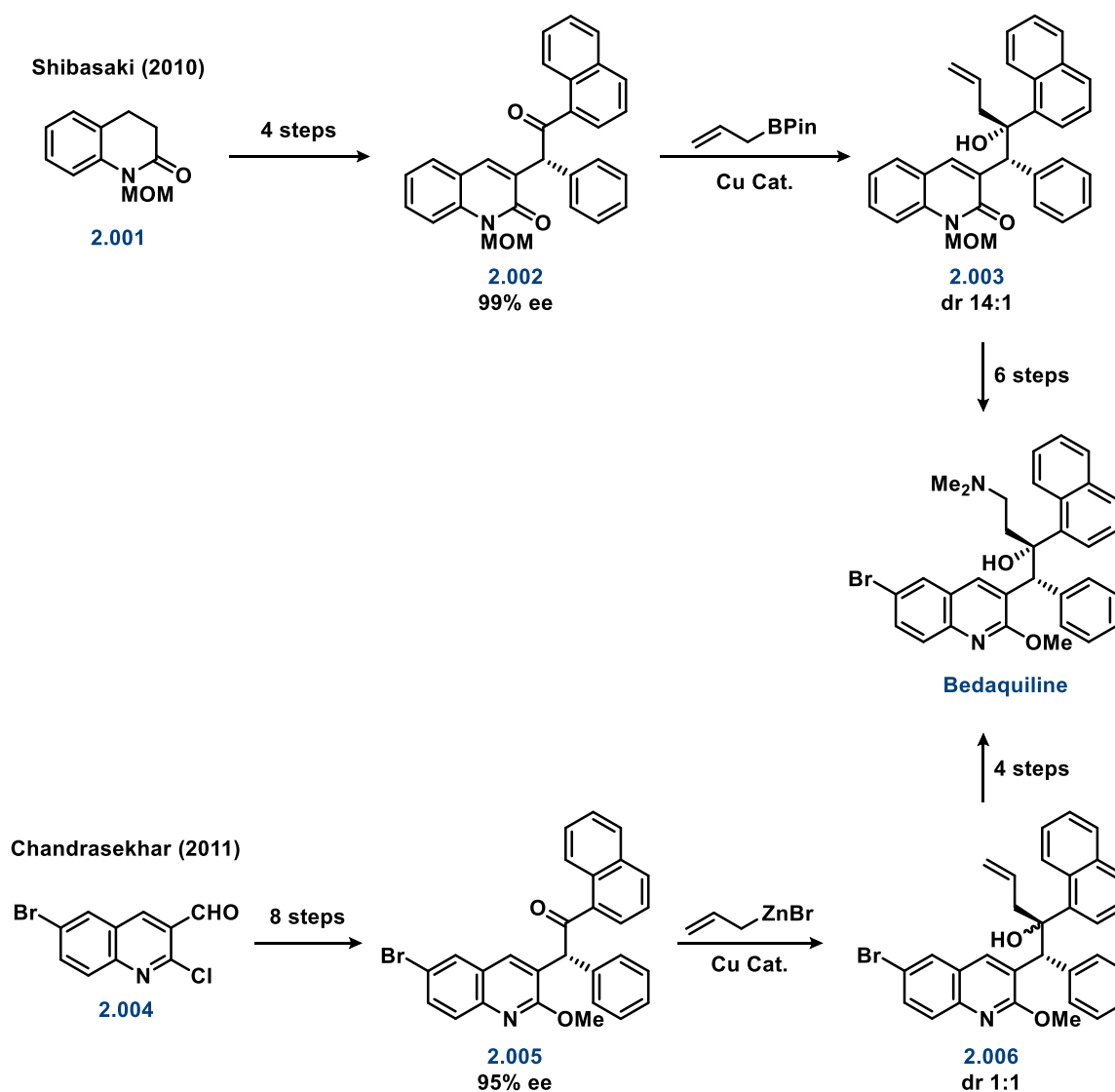
**Figure 2.2.** Previous work within the group had investigated the use of 2-methoxypyridine as a quinoline replacement in region A of BDQ.

To access pyridyl analogues of BDQ in an efficient manner, appropriate synthetic strategies were required. Early work in our group focused on accessing pyridyl analogues of BDQ using the original Janssen discovery route.<sup>[2]</sup> As described in Chapter 1 (**Scheme 1.2**), this synthetic route involved a late stage LDA-mediated 1,2-carbonyl addition reaction of a carbanion generated from the southern “AB” benzylquinoline subunit to the carbonyl group of the northern “CD” naphthyl  $\beta$ -amino ketone subunit. Although this reaction was successfully employed to synthesise BDQ, initial attempts in our group to access pyridinyl analogues of BDQ using this approach proved ineffective, specifically during the coupling of the northern and southern fragments (**Scheme 2.1**).



**Scheme 2.1.** The attempted LDA-mediated addition reaction previously trialed in the group towards ring A pyridine analogues of BDQ.

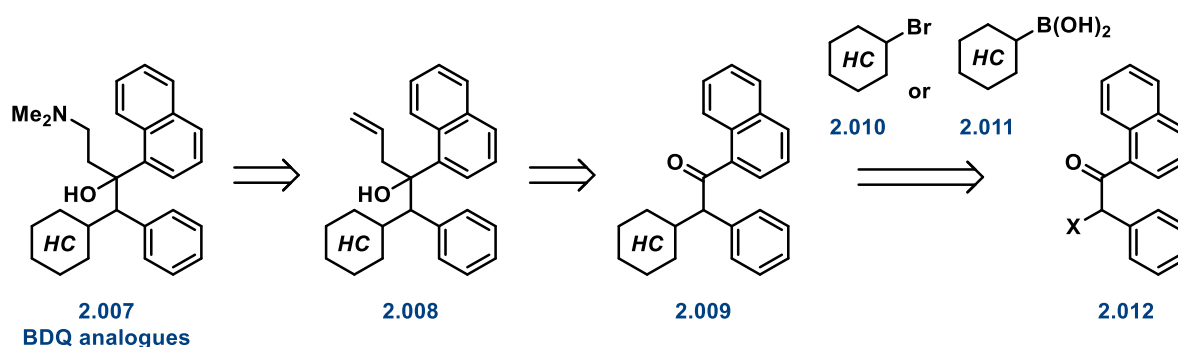
A review of the literature to identify alternate synthetic routes revealed that in addition to Janssen’s procedure, two asymmetric syntheses of BDQ had been published, first by the group of Shibasaki in 2010<sup>[3]</sup>, followed by Chandrasekhar and colleagues in 2011<sup>[4]</sup> (**Scheme 2.2**). Both synthetic routes shared a common strategy in that they relied on the synthesis of a key triarylketone intermediate (**2.002** and **2.005**), followed by allylation to install a terminal alkene (**2.003** and **2.006**) from which the dimethylamino chain could then be incorporated.



**Scheme 2.2.** The two reported asymmetric syntheses towards BDQ.

The key steps in the Shibasaki synthesis to install chirality were a catalytic enantioselective proton migration followed by a diastereoselective allylation, whereas Chandrasekhar employed a Sharpless asymmetric epoxidation followed by copper-mediated ring-opening of the epoxide with an aryl Grignard. Although both reports demonstrated elegant strategies to access enantiomerically pure BDQ, their applicability to this project was limited as they were very lengthy (>12 steps) and linear. Additionally, the quinoline motif was installed at an early stage which did not facilitate the practical substitution of the quinoline ring with alternate heterocycles (the aim of this study). Considering these limitations, prior work in our group had focused on the discovery of new synthetic pathways inspired by this general strategy that could readily facilitate the inclusion of alternative heterocycles in the ring A position at a later stage.<sup>[5]</sup>

During this early study, retrosynthetic analysis of BDQ analogues identified a novel synthetic strategy allowing for efficient quinoline substitution in a modular fashion (**Scheme 2.3**). This strategy progresses through the formation of a key triarylketone intermediate **2.009** which can accommodate the inclusion of the requisite heterocycle to  $\alpha$ -bromoketone **2.012** from the corresponding heteroaryl halide **2.010** or boronic acid **2.011** coupling partners. In a similar fashion to Chandrasekhar's asymmetric synthesis of BDQ<sup>[4]</sup>, it was envisaged that the dimethylamino tether could be installed *via* allylation to afford the secondary key intermediate **2.008**, with the final analogues **2.007** accessed through the subsequent conversion of the terminal alkene to the requisite amine.



**Scheme 2.3.** Retrosynthetic analysis towards the synthesis of ring A analogues of BDQ. HC = heterocycle.

This strategy was first validated in the group through the incorporation of 2-methoxypyridine at heterocyclic unit A from the corresponding pyridyl boronic acid (**Figure 2.3**). As Janssen had reported that a phenyl in place of the naphthyl ring at unit C was also tolerated (*M.tb* H37rv MIC<sub>90</sub> = 0.16  $\mu$ g/mL compared with 0.07  $\mu$ g/mL for *RS*, *SR* racemates, respectively)<sup>[6]</sup>, this additional substitution was deemed acceptable for early investigation of SAR in the unit A region as having two identical ring in the B and C regions simplified the synthetic strategy.

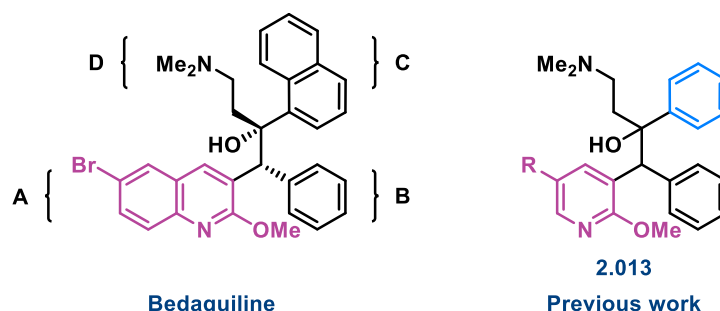
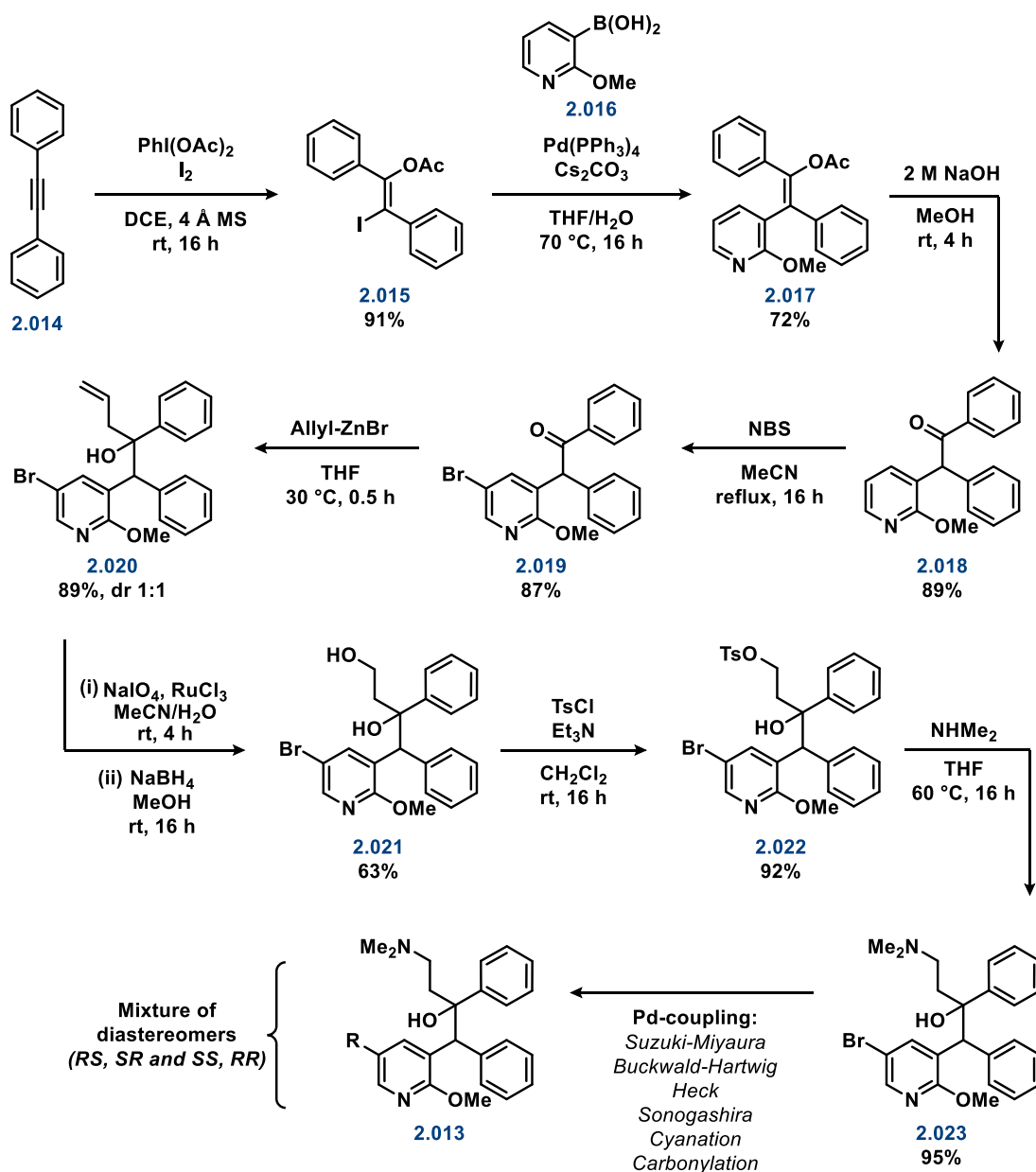


**Figure 2.3.** Previous work in the group synthesised 2-methoxypyridine analogues of BDQ bearing a phenyl ring in region C (series **2.013**).

To summarise this synthetic pathway (**Scheme 2.4**), the requisite iodoalkene **2.015** was prepared from diphenylacetylene (**2.014**) utilising a novel iodoacyloxylation protocol with iodobenzene diacetate and

iodine.<sup>[7]</sup> This method facilitated the introduction of both a halide and acetoxy group to afford **2.015** which readily underwent Suzuki–Miyaura cross-coupling with pyridyl boronic acid **2.016**. Hydrolysis of the resulting substituted enol-acetate **2.017** afforded the key triarylketone **2.018** in 89% yield. From here, the C5 bromine was selectively installed to serve as handle for later diversification (**2.019**), and addition of allyl-ZnBr across the ketone resulted in the allylated product **2.020** as a 1:1 mixture of diastereomers. In the next step, oxidative cleavage of the terminal alkene afforded an aldehyde intermediate which was subsequently reduced to the primary alcohol using sodium borohydride (**2.021**). To complete this pathway, the alcohol was activated, followed by installation of the dimethylamino group *via* nucleophilic substitution to give key intermediate **2.023**.



**Scheme 2.4.** The first pathway developed in the group towards the synthesis of 2-methoxypyridine analogues of BDQ bearing a phenyl ring in region C.

As the early stage of this project was focused on exploring the SAR of the ring A region, and more specifically exploring whether the quinoline could be substituted with a retention of activity, analogues were synthesised in the group from intermediate **2.023** through a variety of Pd-catalysed cross-coupling reactions including Suzuki–Miyaura, Buchwald–Hartwig, Heck, and Sonogashira cross-coupling reactions as well as cyanation and carbonylation procedures. It should be noted that the presence of two stereocentres meant that these analogues were isolated as a mixture of four stereoisomers (*RR*, *SS*, *SR*, *RS*). At this early stage, chiral purity was not deemed necessary as the primary aim was to identify whether quinoline substitution was tolerated in terms of anti-tubercular activity, and therefore all analogues were isolated and tested as mixtures of all four stereoisomers.

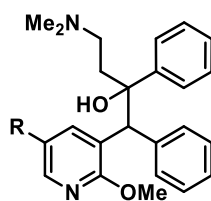
The preliminary *in vitro* activity data for these analogues against replicating *M.tb* (H37rv strain) using the resazurin microtiter assay (REMA) is summarised in **Table 2.1**. In this assay, *M.tb* (H37Rv strain) was incubated in the presence of sample (100–0.2  $\mu$ M, serially diluted in a 96-well plate format) for 7 days at 37 °C and under aerobic conditions. After this time, resazurin (a redox indicator dye) was added to each sample well. When viable cells come into contact with resazurin, the dye is reduced, which gives rise to a change in fluorescence. Therefore this assay measures fluorescence to detect cellular metabolic activity (viability). Changes in fluorescence relative to positive control wells (*M.tb* with no inhibitor) minus negative control wells (no *M.tb*) were used to determine the percentage inhibition at the various sample concentrations. The MIC<sub>90</sub> was determined using non-linear regression to produce a line of best fit, with the MIC<sub>90</sub> defined as the sample concentration which resulted in a 90% inhibition of bacterial growth.

It is important to highlight that although the MIC<sub>90</sub> (*M.tb* strain H37Rv) of BDQ was reported by Janssen as 0.05  $\mu$ M (0.03  $\mu$ g/mL)<sup>[6]</sup>, in our collaborator's hands this assay consistently reported BDQ's MIC<sub>90</sub> 10-fold higher (0.5  $\mu$ M). It was observed from this series that the presence of polar groups in the C5 position of the pyridine resulted in a complete loss in activity (**Table 2.1**, entries 2–6). In contrast, aromatic groups in this region were found to possess more favourable activity (**Table 2.1**, entries 8–9), suggesting this region prefers larger lipophilic functional groups. Given that activity was demonstrated for the aromatic analogues, these early results validated the strategy to explore this region given that the quinoline could be substituted. In particular, **2.029** represented an attractive template for further modification. It might be pointed out that BDQ is 40-fold more potent than **2.029**, however it should be borne in mind that BDQ is enantiomerically pure (*RS*) and that the eutomer of **2.029** would be expected to be close to four times as potent as the parent racemic mixture. Compound **2.029** also represents a template which is approximately 30-fold less lipophilic than BDQ (cLogP 5.70 vs 7.25, respectively). Moreover, the naphthyl ring in the unit C region is known to contribute to its potency, while **2.029** bears a phenyl group in this region. Finally, varying the nature of the substituents



on the quinoline ring is known to significantly modulate the bioactivity of BDQ. At this stage, it was thought that it was highly unlikely that this biaryl moiety in the region A of **2.029** was coincidentally optimised. Rather we saw **2.029** as a template upon which we could obtain useful assay readouts through modifications to either to the C5 phenyl ring or the core pyridyl ring.

**Table 2.1.** Preliminary *in vitro* activity of 2-methoxypyridine analogues (series **2.013**) of BDQ tested as racemic mixtures of all 4 stereoisomers.



**2.013**  
Racemate (*RR*, *SS*, *SR*, *RS*)

| Entry | Compound     | R | <i>M.tb</i> H37Rv<br>MIC <sub>90</sub> (μM) | cLogP |
|-------|--------------|---|---|-------|
| 1     | BDQ          |   | 0.54 ± 0.05 <sup>a</sup>                    | 7.25  |
| 2     | <b>2.023</b> |   | >100  | 4.71  |
| 3     | <b>2.024</b> |   | >100  | 3.38  |
| 4     | <b>2.025</b> |   | >100  | 3.50  |
| 5     | <b>2.026</b> |   | >100  | 4.91  |
| 6     | <b>2.027</b> |   | >100  | 3.96  |
| 7     | <b>2.028</b> |   | 57.5  | 5.02  |
| 8     | <b>2.029</b> |   | 20.0  | 5.70  |
| 9     | <b>2.030</b> |   | 23.5  | 6.45  |

<sup>a</sup>Value expressed as mean ± standard error of the mean (*n* = 7).

Guided by the promising preliminary results achieved for the 2-methoxypyridine analogues (**2.013**), the focus of this candidate's project was to further expand upon the SAR in of the ring A region of BDQ. While SAR for the 2-methoxypyridine analogues continued to be investigated within the group, this candidate's contribution to this study was to design and synthesise analogues bearing a unique 2,6-dimethoxypyridine core to explore whether substitution at the C6 position of the pyridine ring was

also tolerated. It was anticipated that if these analogues were active, then this would provide a useful synthetic handle that could open up access to a distinct new series of analogues whereby variations of the C6 ether, or substitution of the C6 ether for other functional groups including aryl, alkyl, or amino tethers could be explored. Furthermore, the introduction of polar groups at this position (in this case a methoxy group) also provides an increase in polar surface area which has been previously correlated with reduced drug toxicity.<sup>[8]</sup>

To explore the effect of an additional methoxy group at the C6 position of the pyridine ring, the first half of this chapter (**Section 2.2**) details the synthesis and preliminary *in vitro* inhibitory activity of 2,6-dimethoxypyridine analogues of BDQ bearing a phenyl ring at unit C (**2.031**, **Figure 2.4**). In the second half of this chapter (**Section 2.3**), the development of an alternative synthetic pathway which can accommodate two different groups in regions B and C is also detailed which was used to synthesise analogues bearing a naphthyl ring in region C as a direct comparison to BDQ (**2.032**, **Figure 2.4**).

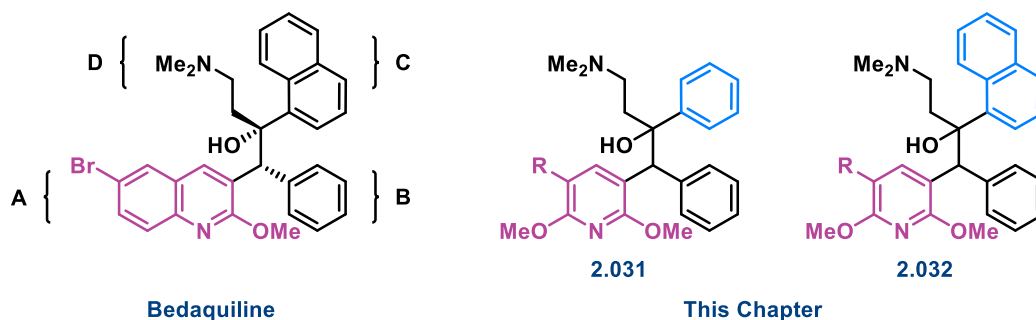
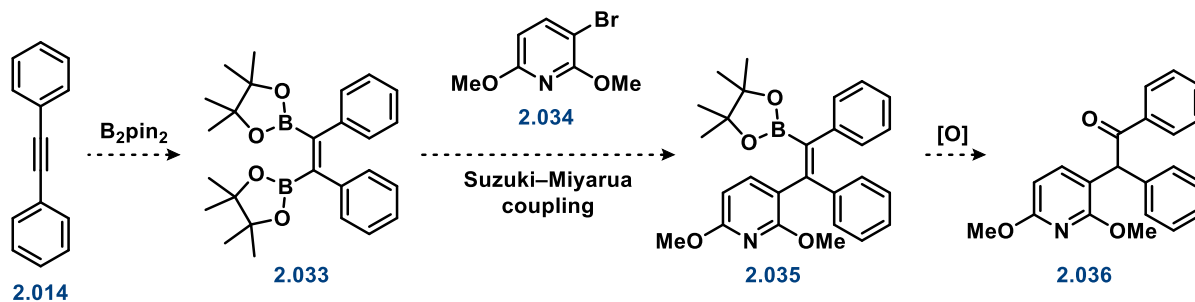


**Figure 2.4.** The general structure of the 2,6-dimethoxypyridine analogues of BDQ synthesised in this chapter.

## 2.2 Pyridine analogues of BDQ bearing a phenyl ring at unit C

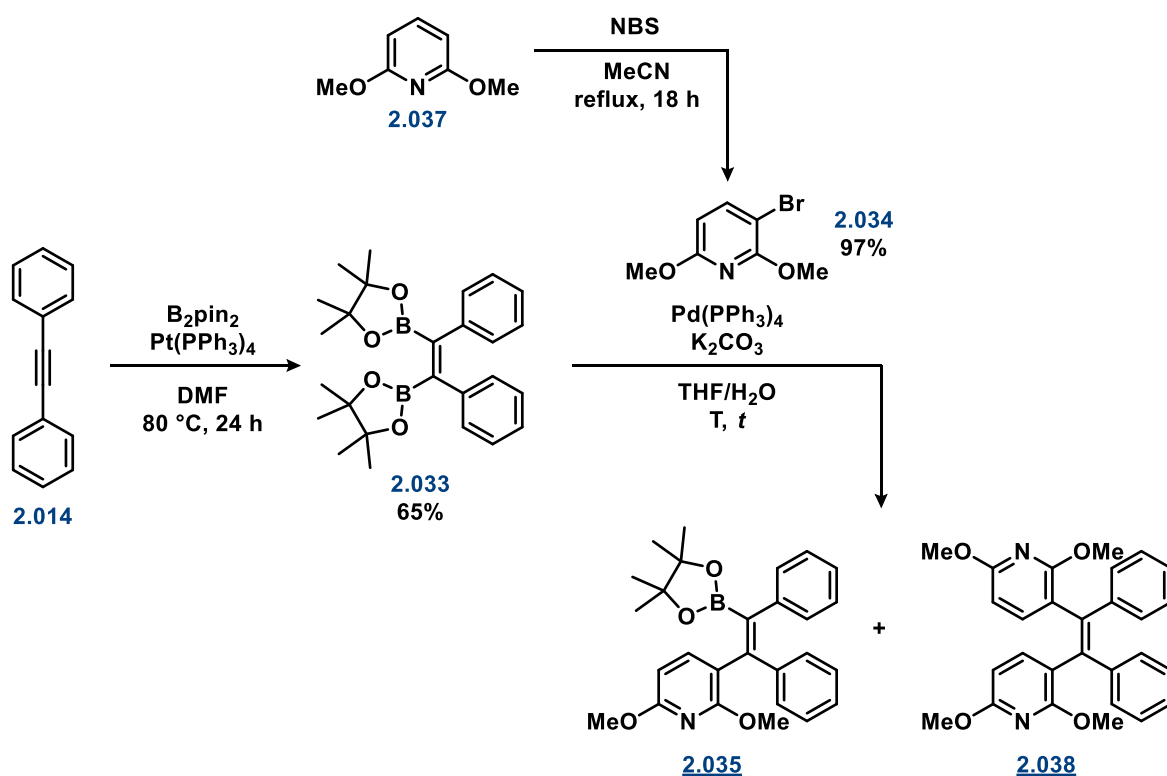
### 2.2.1 Synthesis

As was identified during retrosynthetic analysis (**Scheme 2.3**, *vide supra*), the pyridine heterocycle could be incorporated as either the pyridyl boronic acid or the bromopyridine. Although the synthetic strategy chosen for the 2-methoxypyridine analogues had employed the pyridyl boronic acid substrate in the cross-coupling process (**Scheme 2.4**, *vide supra*), an alternative strategy was explored to incorporate the heterocycle as the heteroaryl halide (specifically 3-bromo-2,6-dimethoxypyridine) as this was more readily accessible than the corresponding pyridyl boronic acid. As shown in **Scheme 2.5**, this newly proposed strategy proceeds *via* Suzuki–Miyaura cross-coupling of bromopyridine **2.034** with a diboronate alkene **2.033** derived from diphenylacetylene (**Scheme 2.5**). It was proposed that oxidation of the boronate group (a masked enol) would then provide key intermediate **2.036**.



**Scheme 2.5.** Novel strategy towards key triarylketone intermediate **2.036** in incorporating 2,6-dimethoxypyridine as the heteroaryl halide.

To conduct this synthesis, diphenylacetylene **2.014** was reacted with bis(pinacolato)diboron ( $B_2pin_2$ ) using the procedure first performed in the group of Suzuki<sup>[9]</sup> to afford the *vic*-diborylalkene **2.033** in 65% yield (**Scheme 2.6**). The boronate **2.033** was then subjected to palladium-catalysed Suzuki–Miyaura cross-coupling to bromopyridine **2.034** using conditions adapted from a procedure developed by Shimizu *et al.*<sup>[10]</sup> In their study, the reaction of 2 equivalents of *o*-bromotoluene to 1 equivalent of **2.033** was reported to achieve the homocoupled product with 100% selectivity, suggesting that coupling of a second equivalent of aryl halide was unfavourable. In our hands, although this reaction was relatively selective for **2.035** on a 1 mmol scale (**Table 2.2**, entry 1), when the reaction scale was increased to 4 mmol the formation of di-coupled product **2.038** was observed as the major product (**Table 2.2**, entry 2) as exemplified in the  $^1H$  NMR spectrum of the crude reaction mixture (**Figure 2.5**). In an attempt to optimise this reaction, a lower loading of **2.034** (1.25 equivalents) was trialed, and the reaction was performed in a microwave (*MW*) reactor at 100 °C for 2 h (**Table 2.2**, entry 3). Although a small quantity of the di-coupled product was observed by  $^1H$  NMR, the reaction predominantly afforded mono-coupled alkene in a much shorter reaction time.



**Scheme 2.6.** Synthetic scheme for the synthesis of intermediate **2.035**.

**Table 2.2.** Conditions used to optimise the Suzuki–Miyaura cross-coupling reaction between **2.033** and **2.034** to give intermediate **2.035**.

| Entry | Scale (mmol) | Equivalents of <b>2.034</b> | Conditions (T, t) | Ratio of <b>2.035</b> : <b>2.038</b> <sup>a</sup> | Yield of <b>2.035</b> (%) |
|-------|--------------|-----------------------------|-------------------|---|---------------------------|
| 1     | 1            | 2                           | 60 °C, 39 h       | 96:4  | 88                        |
| 2     | 4            | 2                           | 60 °C, 24 h       | 30:70   | 31                        |
| 3     | 4            | 1.25                        | 100 °C, 2 h (MW)  | 92:8  | 71                        |

<sup>a</sup>Determined using the  $^1\text{H}$  NMR spectrum of the crude reaction mixture.

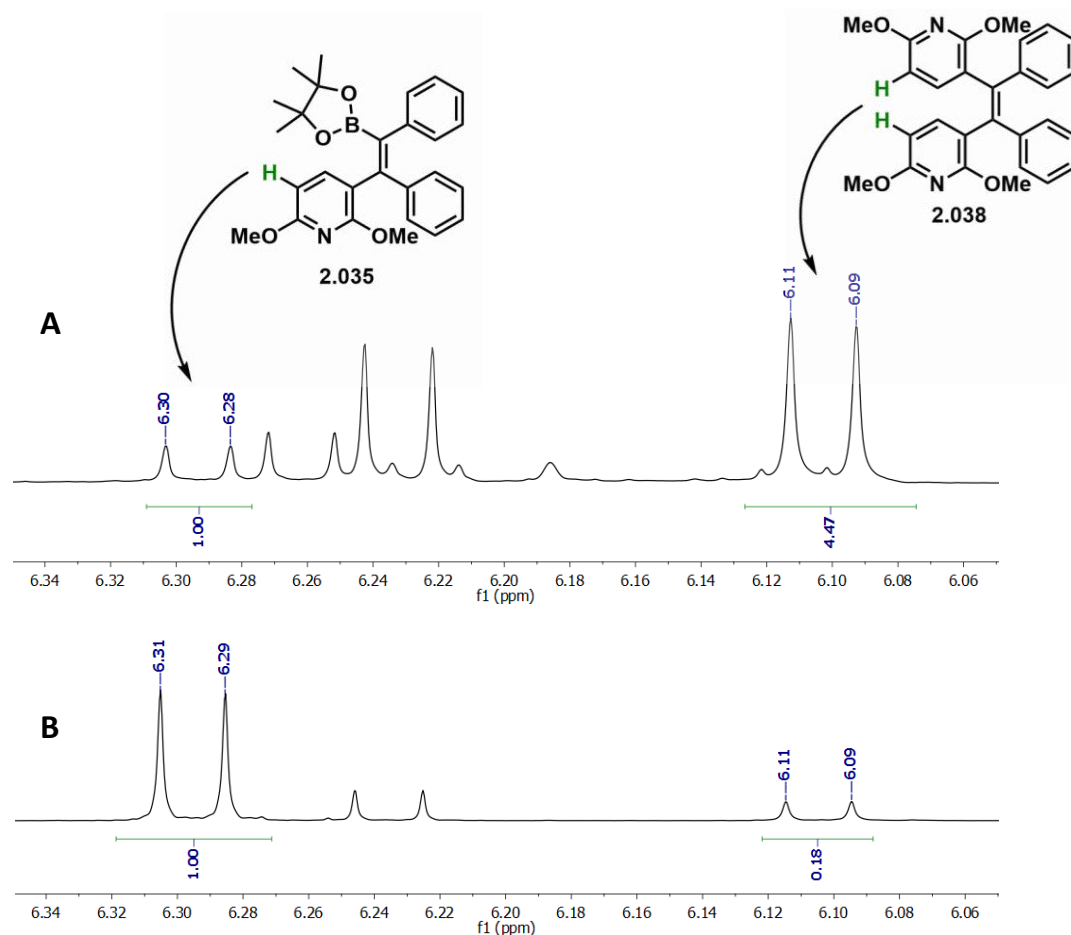
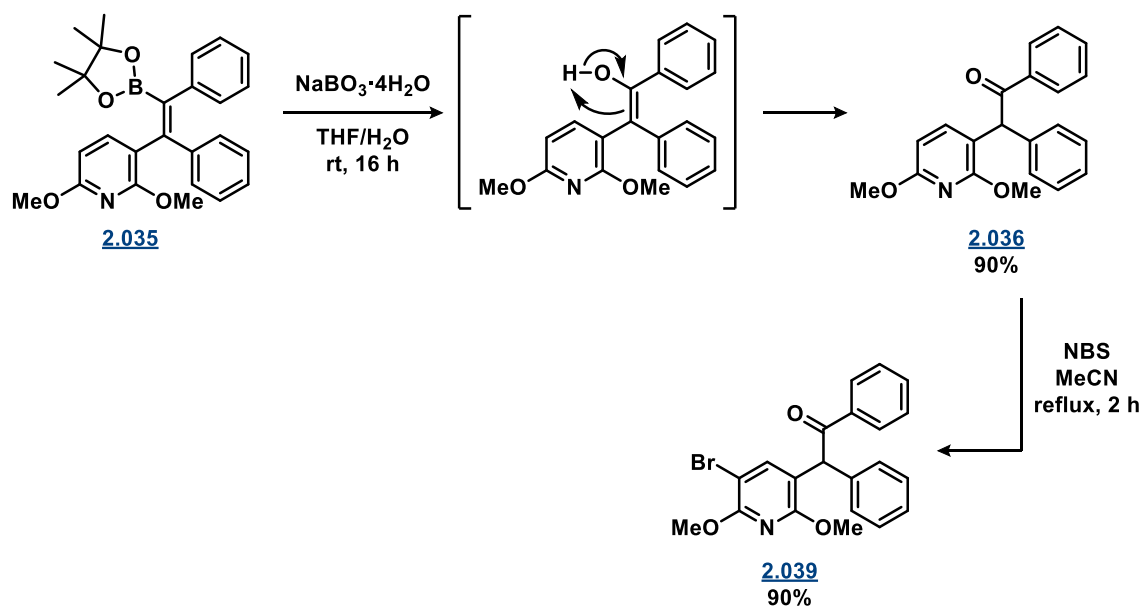


**Figure 2.5.** The  $^1\text{H}$  NMR spectra of the crude reaction mixtures obtained from the Suzuki–Miyaura cross-coupling reaction between **2.033** and **2.034**, indicating the ratio between desired product **2.035** and di-coupled by-product **2.038**. A) 4 mmol scale, 2 equivalents of **2.034**, 60 °C, 24 h (entry 2, Table 2.2). B) 4 mmol scale, 1.25 equivalents of **2.034**, 100 °C, 2 h (MW).

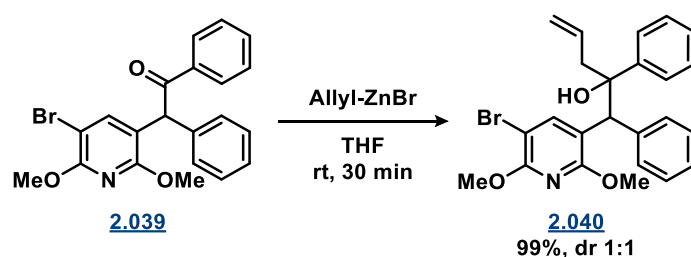
The vinyl boronic ester **2.035** can be considered a masked enolate, and therefore it readily tautomerised to the triarylketone following oxidation of the boronate group using sodium perborate (Scheme 2.7).<sup>[11]</sup> From here, reaction of **2.28** with *N*-bromosuccinimide (NBS) regioselectively installed a bromine atom at the pyridine C5 position to serve as a handle for subsequent elaboration. Selectivity occurred at the C5 position due to activation at the *ortho/para* positions relative to the electron donating methoxy substituents.<sup>[12]</sup>



**Scheme 2.7.** Synthetic scheme for the synthesis of intermediate **2.039**.

With synthetic methods in hand to prepare trisubstituted ketone **2.039** containing the requisite pyridine heterocycle, attention turned to installing the dimethylamino tether. Although this pathway was previously optimised within the group for the 2-methoxypyridine scaffold (**Scheme 2.4**, *vide supra*), it was unknown if a similar strategy would be applicable when moving to the more electron rich 2,6-dimethoxypyridine heterocyclic core.

To explore the allyl addition to this new substrate, allyl-ZnBr was prepared and reacted with ketone intermediate **2.039** resulting in allylated tertiary alcohol **2.040** in a 1:1 diastereomeric ratio (dr, **Scheme 2.8**).<sup>[13]</sup> During repeated attempts of this reaction it was found that quantitative yields could be obtained with careful addition of the allyl bromide to the activated zinc solution to ensure that the internal temperature of the mixture remained close to ambient temperature.



**Scheme 2.8.** Allylation of triarylketone intermediate **2.039** to **2.040**.

It can be seen from the  $^1\text{H}$  NMR spectrum in **Figure 2.6** that all the peaks are in duplicate and are clearly in a 1:1 ratio. To assist with understanding the  $^1\text{H}$  NMR spectrum, the signals corresponding to

each diastereomer are highlighted, with diastereomer A in yellow, diastereomer B in blue, and regions of signal overlap highlighted in green.

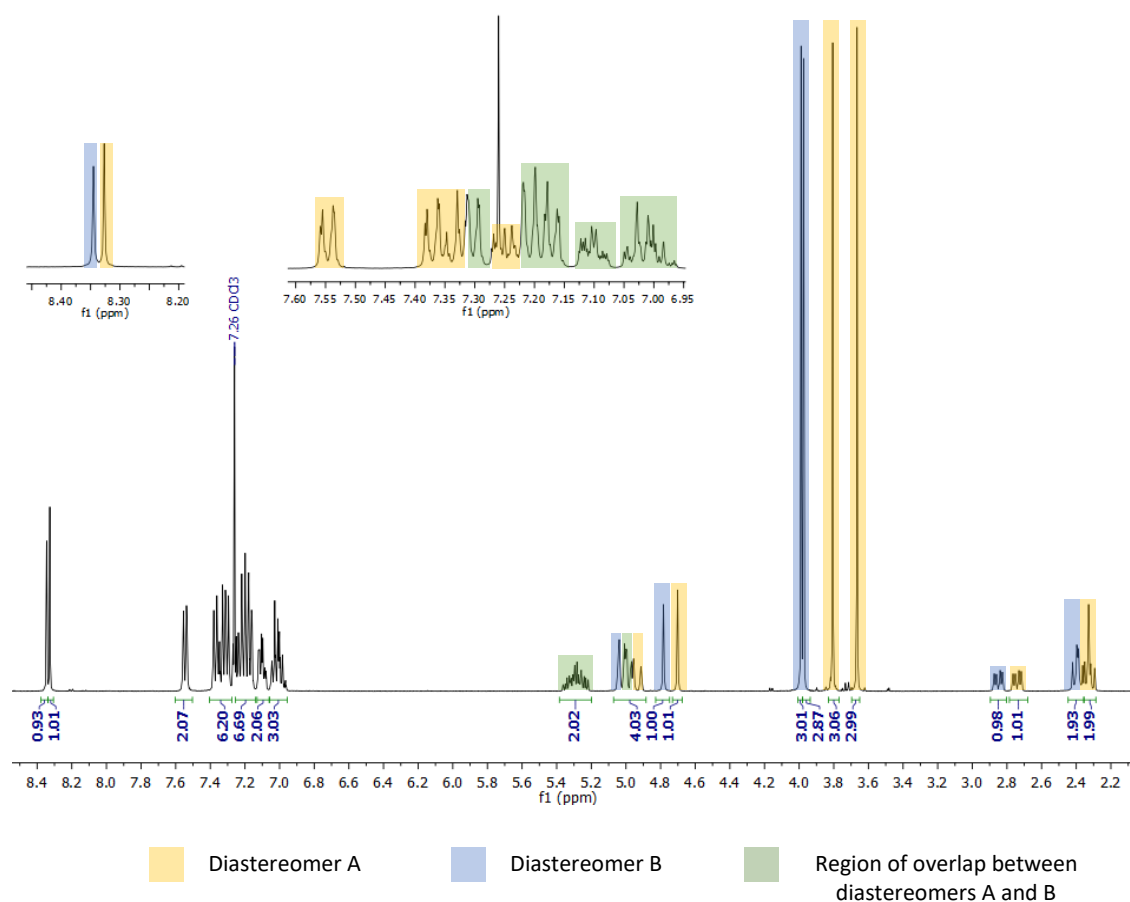
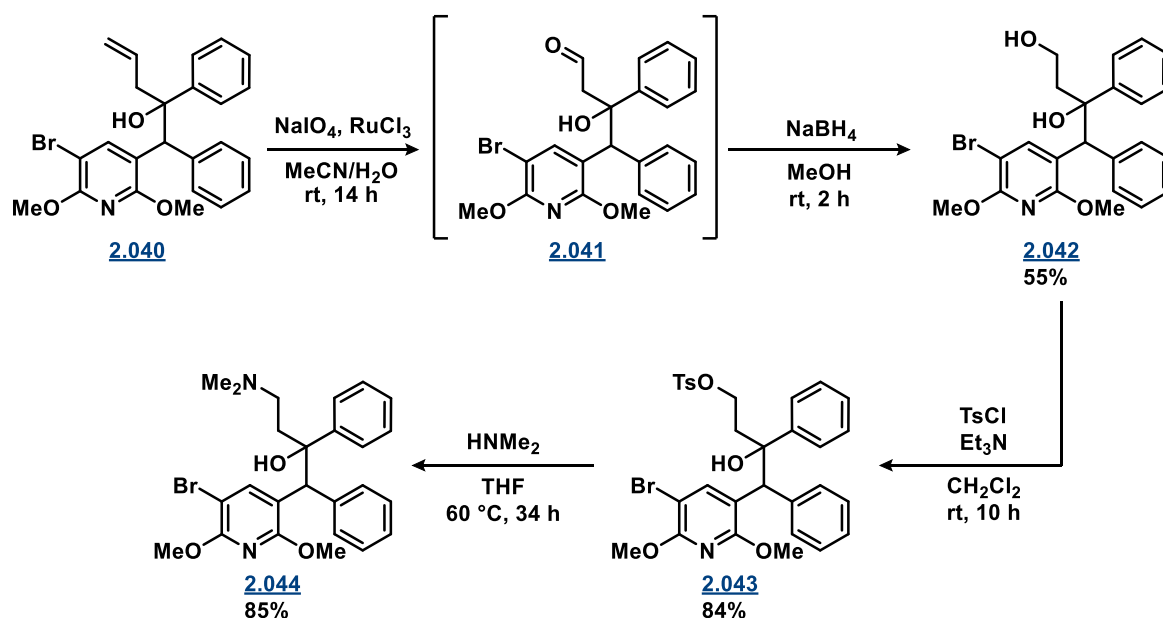


**Figure 2.6.**  $^1\text{H}$  NMR spectrum of intermediate **2.040** showing a mixture of diastereomers A and B in a 1:1 ratio.

With the allyl motif installed, the next step was oxidative cleavage of the terminal alkene in **2.040** to access an aldehyde intermediate **2.041** (Scheme 2.9). This was performed using a mild procedure which employed ruthenium trichloride ( $\text{RuCl}_3$ ) and sodium periodate ( $\text{NaIO}_4$ ) in an acetonitrile/water solvent system.<sup>[14]</sup> From the aldehyde, the amine could be installed either *via* reductive amination, or through a 3-step process involving reduction of the aldehyde to the alcohol, activation (i.e. tosylation to generate a better leaving group) and displacement of the leaving group with nucleophilic amine. Previous work conducted in the group using the 2-methoxypyridine substrate had investigated reductive amination as a means of installing the dimethylamine from the aldehyde, however this was observed to regenerate the triarylketone **2.039** by means of a retro-aldol process. Given this prior outcome, the alternate strategy was utilised, and therefore subsequent reduction of **2.041** with sodium borohydride ( $\text{NaBH}_4$ ) then afforded diol **2.042** in 55% yield over 2-steps.

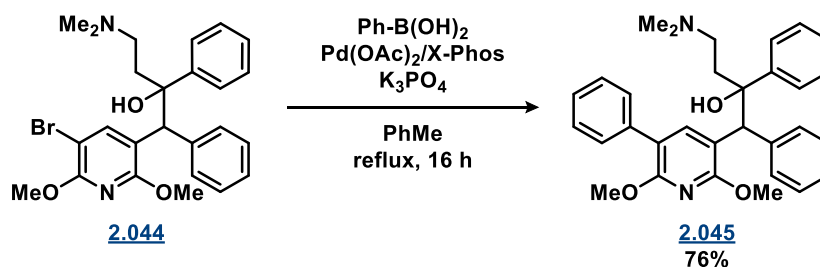
The final stages of this pathway involved tosylation of the primary alcohol to generate a leaving group that was subsequently displaced by dimethylamine to afford key intermediate **2.044**. Although these steps resulted in moderate to good yields, complete conversion to the product was not always achieved, however in each case unreacted starting material could be recovered during purification.



**Scheme 2.9.** Synthetic scheme towards key intermediate **2.044**.

### 2.2.2 Validation of the 2,6-dimethoxypyridine core as a bioactive template

Similarly to the 2-methoxypyridine series, multiple structures could be accessed through Pd-catalysed coupling reactions to the C5 bromine of intermediate **2.044**. Considering it was unknown what effect the additional methoxy group at the C6 position would have on activity against *M.tb*, intermediate **2.044** and the phenyl substituted analogue **2.045** were initially planned to be assessed for *in vitro* activity.



**Scheme 2.10.** Suzuki–Miyaura cross-coupling between **2.044** and phenylboronic acid to give analogue **2.045**.

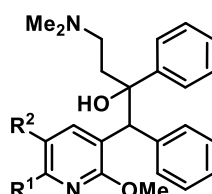
The Suzuki–Miyaura cross-coupling reaction towards phenyl-coupled product **2.045** progressed smoothly in 76% yield. As was the case for intermediates **2.040–2.043**, during the purification of this analogue it was found that the two diastereomers (*RR*, *SS* and *SR*, *RS*) could not be separated using



conventional silica-gel flash chromatography despite trialling a range of eluent conditions as well as the use of a finer particle grade silica (15–40µm, 60Å). Although the  $^1\text{H}$  NMR of the crude reaction mixture indicated product was formed in a 1:1 diastereomeric ratio, due to the difficulties encountered during purification the diastereomeric ratio within the final isolated sample became unequal (2:3).

As shown in **Table 2.3**, the 2,6-dimethoxypyridine derivatives **2.044** and **2.045** were both observed to possess relatively potent activity, thus indicating that the pyridine ring with an additional methoxy extension at the C6 ( $\text{R}^1$ ) position was a valid template for further elaboration. Specifically, when comparing the bromo derivatives, the C6 ( $\text{R}^1$ ) methoxy derivative was found to be significantly more active than its des-methoxy counterpart (entries 1 and 3). It should be noted that as the diastereomeric ratio for **2.045** (entry 4) was slightly skewed in favour of one of the diastereomers (the identity of which was unknown), it was not completely accurate to directly compare its  $\text{MIC}_{90}$  value (12.5 µM) with the other measured values which were all in an equal ratio (entries 1–3). For this reason, it was realised that if we were to continue to test samples that mixtures of all 4 isomers in the future, then it would be of particular importance to maintain a relatively equal diastereomeric ratio for all samples to facilitate accurate comparison.

**Table 2.3.** Preliminary *in vitro* activity of the 2,6-dimethoxypyridine derivatives **2.044** and **2.045**.



| Entry | Compound     | $\text{R}^1$ | $\text{R}^2$ | <i>M.tb</i> H37Rv<br>$\text{MIC}_{90}$ (µM) | Diastereomeric<br>ratio |
|-------|--------------|--------------|--------------|---|-------------------------|
| 1     | <b>2.023</b> | H            |              | >100  | 1:1                     |
| 2     | <b>2.029</b> | H            |              | 20  | 1:1                     |
| 3     | <b>2.044</b> | OMe          |              | 26.4  | 1:1                     |
| 4     | <b>2.045</b> | OMe          |              | 12.5  | 2:3                     |

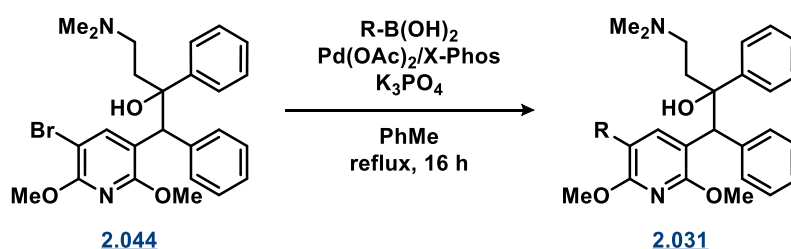
### 2.2.3 Extended SAR of the pyridine core

In response to the promising preliminary results summarised in **Table 2.3**, a more in-depth analysis of the SAR in the C5 region of the pyridine ring was planned. As we had previously experienced long turn-

around times to obtain assay results, it was decided that it would be more efficient to synthesise a larger selection of analogues to gain insight on the SAR in this region.

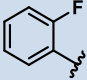
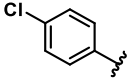
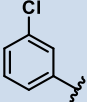
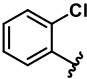
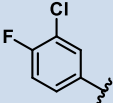
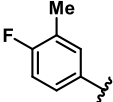
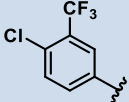
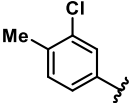
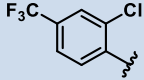
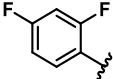
Considering early results for the 2-methoxypyridine series (**2.013**) suggested that compounds containing phenyl rings in this region exhibited enhanced potency (**Table 2.1, *vide supra***), the majority of analogues were synthesised *via* Suzuki–Miyaura cross-coupling employing a variety of commercially available aryl boronic acids (**Table 2.4**). While the overall aim of this project was to develop novel BDQ analogues with reduced lipophilicity, potent activity against *M.tb* could not be compromised. As such, a variety of boronic acid coupling partners with various hydrophobicities were selected to allow us to explore the effects of incorporating these groups on activity.

**Table 2.4.** Synthesis of C5 substituted pyridine analogues of BDQ (series **2.031**) using Suzuki–Miyaura cross-coupling.

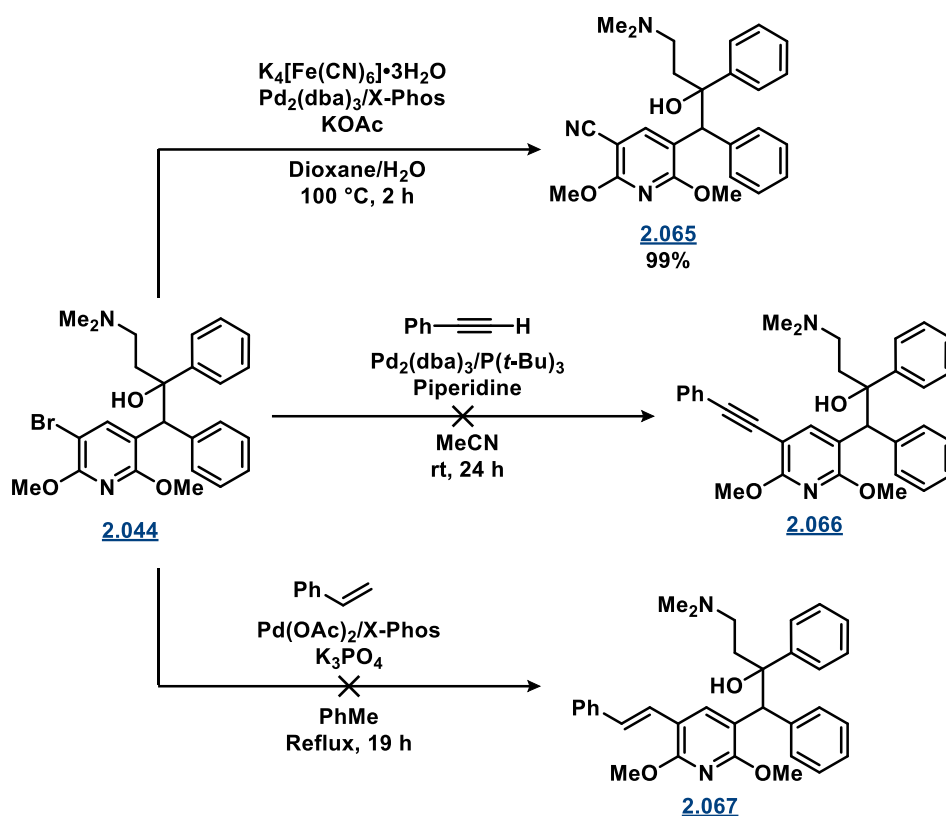


| Entry | Compound     | R | Yield (%) |
|-------|--------------|---|-----------|
| 1     | <b>2.046</b> |   | 96        |
| 2     | <b>2.047</b> |   | 91        |
| 3     | <b>2.048</b> |   | 98        |
| 4     | <b>2.049</b> |   | 94        |
| 5     | <b>2.050</b> |   | 69        |
| 6     | <b>2.051</b> |   | 94        |
| 7     | <b>2.052</b> |   | 48        |
| 8     | <b>2.053</b> |   | 52        |
| 9     | <b>2.054</b> |   | 83        |

Table 2.4. (continued)

| Entry | Compound     | R   | Yield (%) |
|-------|--------------|---|-----------|
| 10    | <u>2.055</u> |    | 92        |
| 11    | <u>2.056</u> |    | 96        |
| 12    | <u>2.057</u> |    | 70        |
| 13    | <u>2.058</u> |    | 66        |
| 14    | <u>2.059</u> |    | 66        |
| 15    | <u>2.060</u> |    | 91        |
| 16    | <u>2.061</u> |   | 49        |
| 17    | <u>2.062</u> |  | 51        |
| 18    | <u>2.063</u> |  | 63        |
| 19    | <u>2.064</u> |  | 55        |

In addition to the Suzuki–Miyaura cross-coupling reaction, Pd-catalysed cyanation, Sonogashira and Heck reactions were also performed from intermediate **2.044** using identical procedures to those trialled previously for the 2-methoxypyridine scaffold (**Scheme 2.11**). Although the cyanation reaction provided analogue **2.065** in quantitative yield, the Sonogashira and Heck protocols failed to afford any of the desired products and at this stage were not further pursued.



**Scheme 2.11.** Additional Pd-catalysed reactions trialled from intermediate **2.044**.

In many cases it was observed that the Suzuki–Miyaura cross-coupling reactions did not progress to completion despite increasing the loading of boronic acid and reaction times. In these instances, remaining starting material and product were present as an inseparable mixture which were unable to be purified by column chromatography despite clear separation on TLC. Due to the difficulty encountered in the purification of desired product from unreacted starting material, whilst also maintaining an equal diastereomeric ratio, it was decided that the diastereomers would be separated using preparative high performance liquid chromatography (HPLC) prior to evaluation against *M.tb*. This ensured complete purity, as well as providing a closer estimate of the true MIC<sub>90</sub> of the most active stereoisomer.

The resulting separated diastereomers were denoted as either A or B following HPLC purification, where A was the first to elute from the column, and B was the second to elute. Interestingly, when comparing the <sup>1</sup>H NMR spectra of the separated diastereomers A and B, the relative chemical shifts were consistent for all analogues synthesised, which is exemplified for analogues **2.065** and **2.057** in **Figure 2.7**. Most notably, for diastereomer B (second to elute from the HPLC column), the pyridine proton ( $\text{H}_{1\text{B}}$ ) was consistently shifted upfield relative to the pyridine proton in diastereomer A ( $\text{H}_{1\text{A}}$ ). Additionally, both the methoxy protons ( $\text{H}_{3\text{B}}/\text{H}_{4\text{B}}$ ) and the bridged proton ( $\text{H}_{2\text{B}}$ ) were consistently shifted downfield in all <sup>1</sup>H NMR spectra for diastereomer B relative to diastereomer A. By comparison

to the relative  $^1\text{H}$  NMR chemical shifts that were reported by Chandrasekhar for both diastereomers of BDQ<sup>[4]</sup>, this would render diastereomer A the *RR*, *SS* pair, and diastereomer B the *RS*, *SR* pair. Although attempts were made to obtain a crystal structure of a representative analogue to be certain of the relative stereochemistry, crystals were not able to be grown.

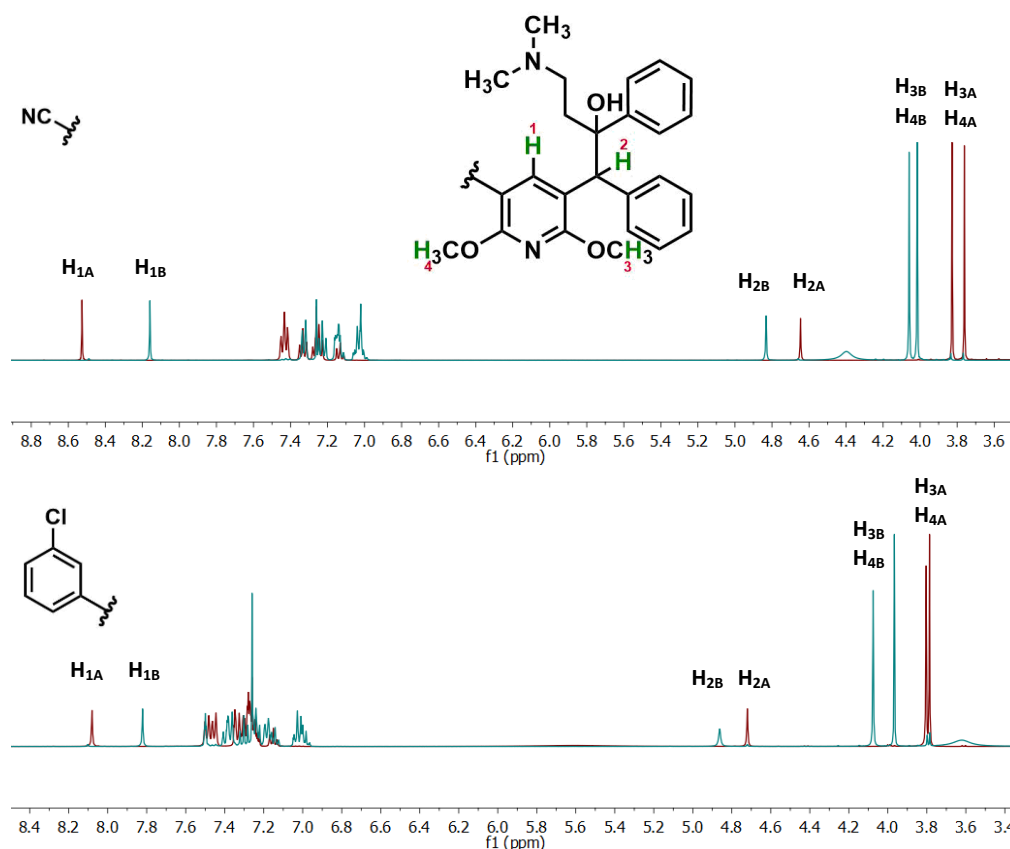


**Figure 2.7.** Representative overlaid  $^1\text{H}$  NMR spectra of diastereomer A (red) and diastereomer B (teal) for cyano derivative **2.065** and meta-chloro derivative **2.057** demonstrating the relative peak shifts for key protons  $\text{H}_1\text{--H}_4$ .

Prior to determining the  $\text{MIC}_{90}$ , a preliminary drug inhibition screen was performed by our collaborators at the Centenary Institute (University of Sydney) on all separated pyridine diastereomers. In this preliminary screen, *M.tb* (H37Rv strain) was incubated in the presence of the test sample in three concentrations (1, 10 and 100  $\mu\text{M}$ ) for 7 days at 37  $^\circ\text{C}$  and under aerobic conditions. After this time, cell viability was measured using a fluorescence-based assay that detected cellular metabolic activity (REMA assay). Changes in fluorescence relative to positive control wells (*M.tb* with no inhibitor) minus negative control wells (no *M.tb*) were used to determine the percentage inhibition at the three test sample concentrations. As is shown in **Figure 2.8**, the results from this screen allowed us to compare diastereomers A to B to help select the active diastereomer to progress for further determination of the  $\text{MIC}_{90}$ . Considering the *RS* configuration of BDQ was found to be significantly more active in all other isomers (*SR*, *RR*, *SS*), it was assumed that the most active diastereomer was the *RS*, *SR* pair by analogy to BDQ. In all cases except for BDQ, both diastereomers

were inactive at 1  $\mu\text{M}$  (100% survival at this concentration), and therefore to simplify interpretation this concentration is not included in the graph. As can be seen from the graphed results, diastereomer B was generally more active in comparison to diastereomer A except for **2.044**, **2.051** and **2.055**. For analogues **2.065**, **2.057**, **2.058**, **2.062**, **2.063** and **2.064**, a distinction in the activity between the two diastereomers was not possible at the concentrations tested (100% inhibition at 100  $\mu\text{M}$  and 100% survival at 10  $\mu\text{M}$ ), and therefore  $\text{MIC}_{90}$  would need to be measured for both diastereomers to establish the active pair.

In addition to assisting with shortlisting the active diastereomers, this activity screen also offered a coarse assessment of SAR. Although it is not a substitute for  $\text{MIC}_{90}$ , it allowed us to see some general trends between all the analogues tested. Firstly, in comparison to the bromo and cyano substituted pyridine rings (**2.044** and **2.065** respectively), the phenyl substituted derivatives were in general more active thus supporting the preference of a phenyl ring in this region as was observed previously for the 2-methoxypyridine series. Additionally, in comparison to the unsubstituted phenyl ring **2.045** which is estimated to have an  $\text{MIC}_{90}$  of *ca.* 10  $\mu\text{M}$  as highlighted by the dotted line (which represents 90% inhibition), rings substituted with electron withdrawing groups such as halogens and cyano appeared to be slightly more favourable, with a fluorine atom in the *meta*-position generating the most potent compound from this preliminary inhibitory screen (100% inhibition at 10  $\mu\text{M}$ ). In contrast, although electron donating groups (e.g. methoxy) were tolerated, a loss in potency was typically observed when compared with **2.045**. Disubstitutions to the pyridyl C5 phenyl ring were also investigated however in general these did not offer any improvements over the mono-substituted derivatives, and in some cases were highly deleterious to activity.

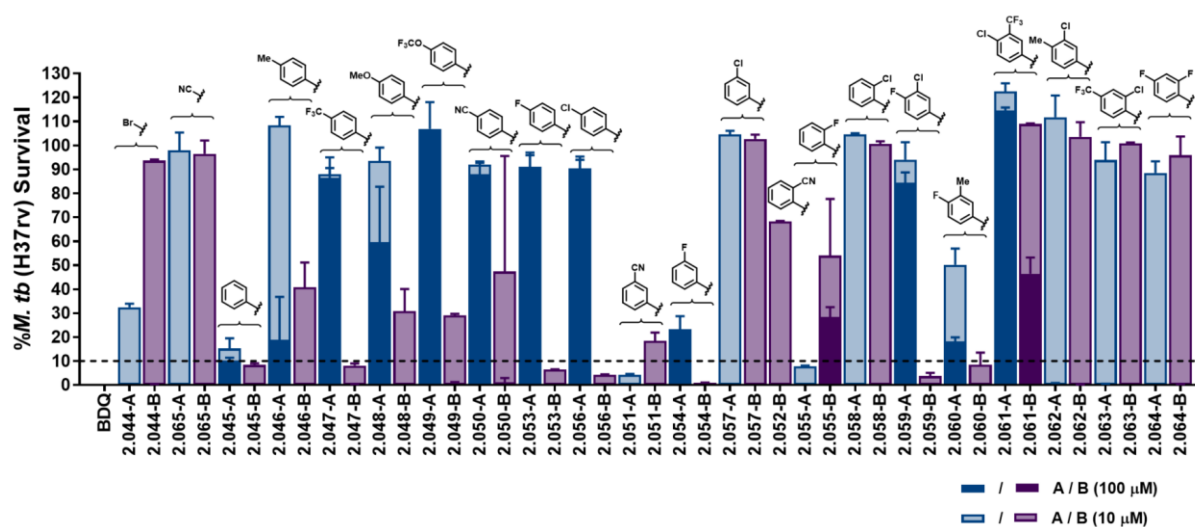


**Figure 2.8.** Preliminary activity screen of the synthesised 2,6-dimethoxypyridine derivatives (series **2.031**), indicating percentage survival of *M.tb* at 10  $\mu\text{M}$  (translucent) and 100  $\mu\text{M}$  (solid) for diastereomers A (blue) and B (purple).

As mentioned previously, in conjunction with this candidate's study into the 2,6-dimethoxypyridine scaffold (**2.031**), additional work in the group was focused on further expanding on the SAR in the C5 position of 2-methoxypyridine scaffold (**2.013**). In combining all the preliminary screening data for the two scaffolds (**Figure 2.9**), we were also able to make a rough analysis on the relative activity between the two series. Similarly to the data shown in **Figure 2.8**, all derivatives were inactive at 1  $\mu\text{M}$  and so for ease of interpretation this concentration was omitted. As shown in the chart, in most cases the 2-methoxypyridine derivatives (red) appeared to be more active than their 2,6-dimethoxypyridine counterparts (blue), however it was difficult to discern the general trend in activity within the 2-methoxypyridine series as the majority of analogues demonstrated close to 100% inhibition at 10  $\mu\text{M}$ , yet 100% survival at 1  $\mu\text{M}$ .

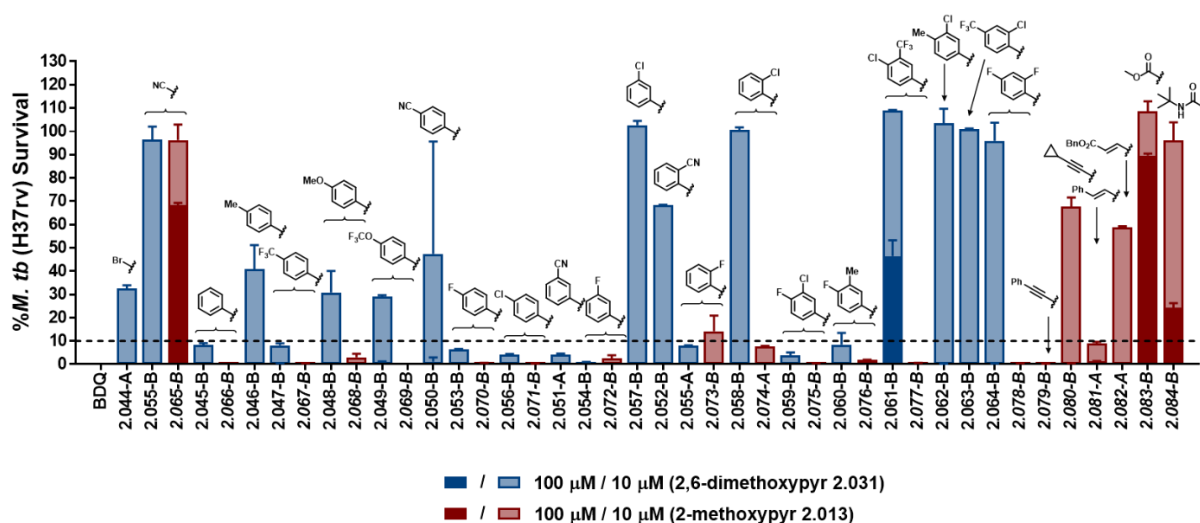


**Figure 2.9.** Preliminary activity screen of the synthesised 2,6-dimethoxypyridine series **2.031** (blue) in comparison with the 2-methoxypyridine series **2.013** (red) indicating percentage survival of *M.tb* at 10  $\mu\text{M}$  (translucent) and 100  $\mu\text{M}$  (solid).

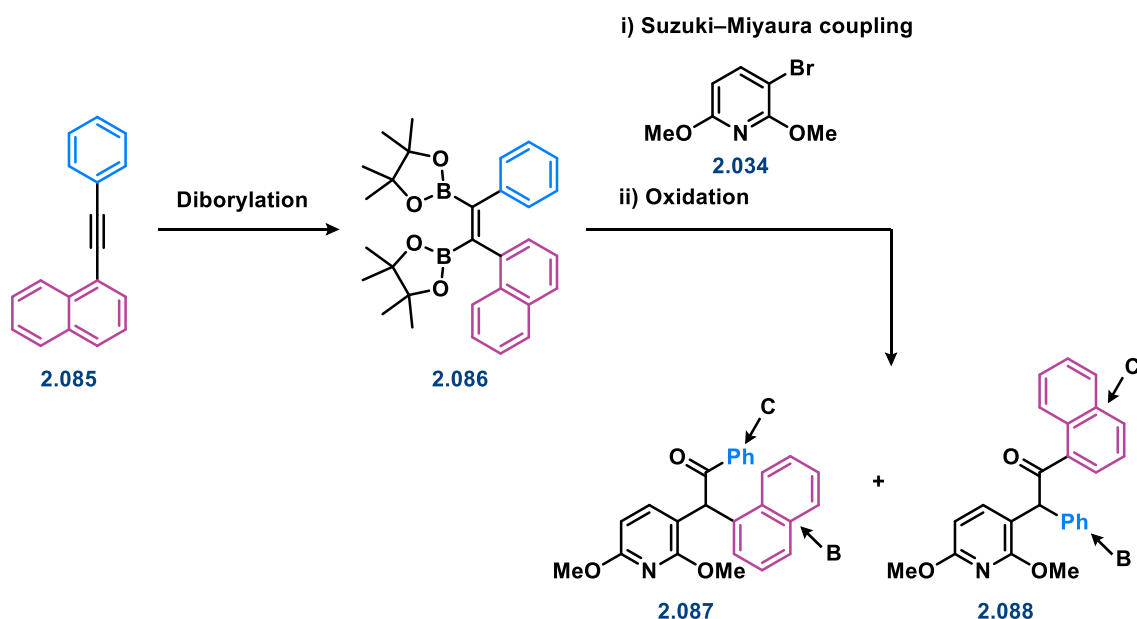
Due to shifting project priorities (see Chapter 3) in addition to our collaborators having a limited capacity to test all our samples,  $\text{MIC}_{90}$  values were not measured for these analogues, however given that the most active derivatives (<10% survival as indicated by the dotted line) were 100% inactive at 1  $\mu\text{M}$ , it was estimated that the majority of these analogues (as racemates) possessed activity closer to 10  $\mu\text{M}$  than to 1  $\mu\text{M}$ .

### 2.3 Pyridine analogues of BDQ bearing a naphthyl ring at unit C

Simultaneous to developing the synthesis detailed in **Section 2.2.1** to access BDQ analogues of type **2.031** bearing identical phenyl rings in regions B and C, an alternative strategy was sought which would enable installation and variation of alternative groups in these two positions. Specifically, a pathway that would allow for the synthesis of analogues bearing a naphthyl ring in region C would allow us to directly compare the SAR of the ring A region relative to BDQ. Additionally, such a synthesis would

also enable future exploration of the B and C regions to further improve upon BDQ's physicochemical profile in conjunction to variations in the A region.

As shown in **Scheme 2.12**, the strategy developed in **Section 2.2.1** towards key triarylketone intermediate **2.088** was not optimised for different groups present in the B and C regions. Specifically, regioselectivity would be difficult to control during the Suzuki–Miyaura cross-coupling reaction between bromopyridine **2.034** and diborylalkene **2.086**. As such, this section details an alternative synthetic strategy that more easily accommodates variations in these two regions to specifically synthesise pyridine analogues bearing a naphthyl ring at unit C.

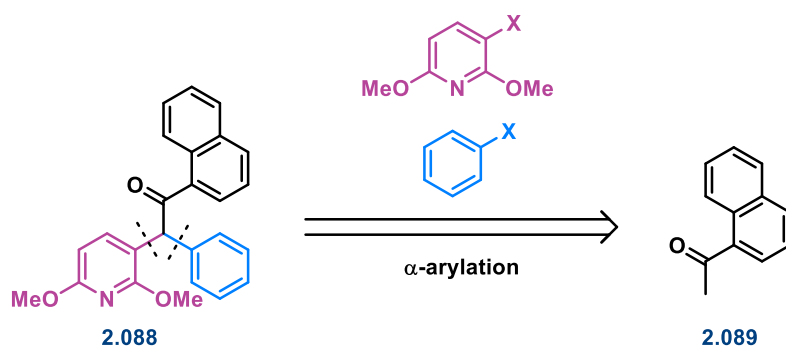


**Scheme 2.12.** It was anticipated that regioselectivity would be difficult to control using the synthetic scheme developed in section 2.2.1 when different groups were present in regions B and C.

### 2.3.1 Alpha arylation strategy with bromopyridine

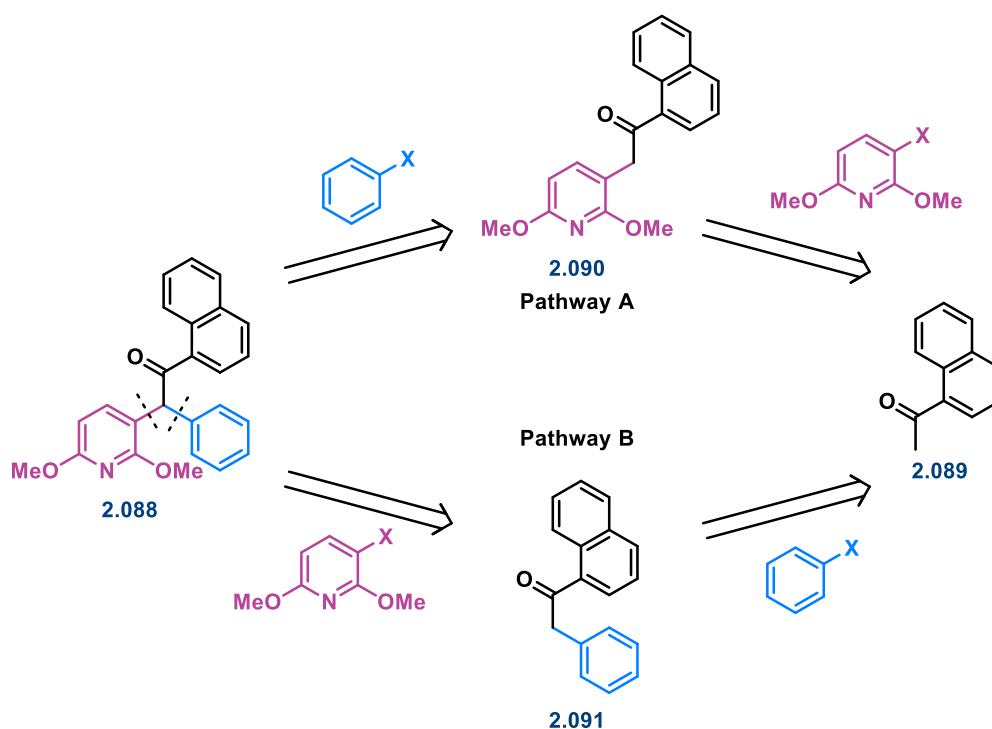
An alternative strategy to facilitate access to the key triarylketone intermediate **2.088** was proposed through the use of two successive  $\alpha$ -arylation cross-coupling reactions to the relevant methyl aryl ketone (**Scheme 2.13**). Reported independently in 1997 by the groups of Buchwald<sup>[15]</sup>, Hartwig<sup>[16]</sup> and Miura<sup>[17]</sup>, the Pd-catalysed  $\alpha$ -arylation of ketones is a very versatile reaction which allows for direct cross-coupling of aryl and heteroaryl halides with an alkene component in the form of an enolate generated *in situ*.<sup>[18]</sup>





**Scheme 2.13.** Retrosynthesis identified  $\alpha$ -arylation from methyl aryl ketone **2.089** as an alternative strategy towards triarylketone **2.088**.

As shown in the more detailed retrosynthetic analysis **Scheme 2.14**, either aryl halide could be initially reacted with acetonaphthone to give a diarylketone intermediate (either **2.090** or **2.091**), which could then be further reacted with the second aryl halide to give key triarylketone intermediate **2.088**. Although previous work in the group had successfully utilised both pathways with 3-bromo-2-methoxyquinoline<sup>[5]</sup>, application of this strategy to the 2,6-dimethoxypyridine scaffold had not been validated.

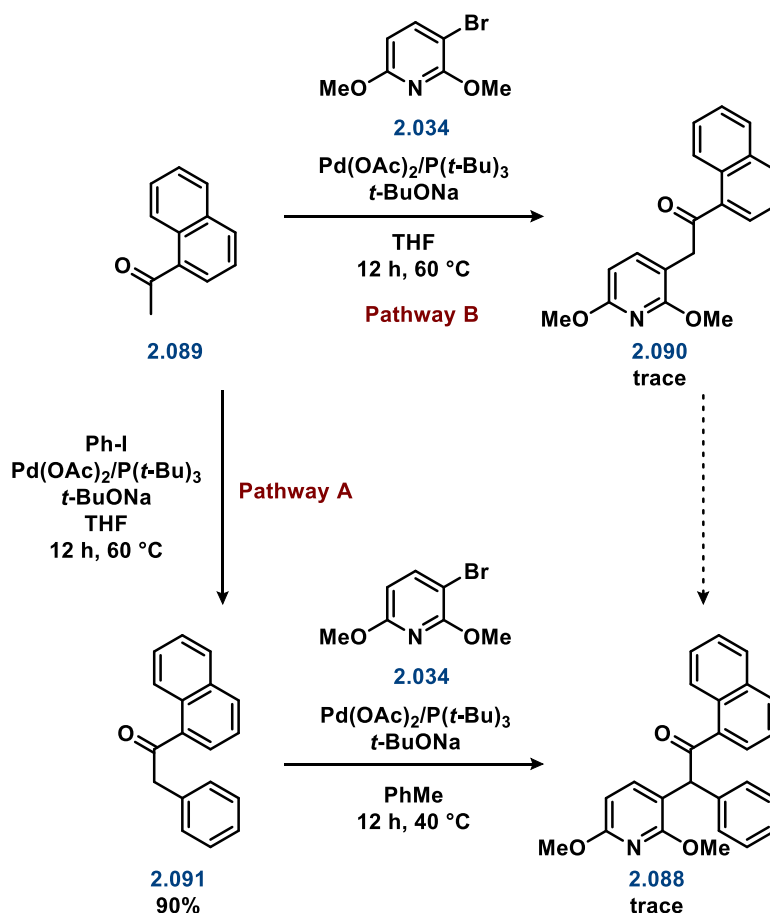


**Scheme 2.14.** A more in-depth retrosynthetic analysis identified two alternative pathways towards triarylketone **2.088** using an  $\alpha$ -arylation strategy from methyl aryl ketone **2.089**.

To explore this strategy, initial efforts focused on the Pd-catalysed  $\alpha$ -arylation between the enolate of acetonaphthone (**2.089**) and iodobenzene to afford the requisite  $\alpha$ -substituted ketone **2.091** in 90%

yield (**Scheme 2.15, Pathway A**). From this substituted ketone (**2.091**), the second cross-coupling reaction in pathway A was attempted with bromopyridine **2.034** using reaction conditions that had previously been optimised for the quinoline scaffold.<sup>[5]</sup> Although a trace amount of the desired product **2.088** was identified by LCMS, the <sup>1</sup>H NMR spectrum of the crude reaction mixture indicated the majority of the starting materials remained unreacted. Furthermore, following subsequent reaction attempts, no desired product was able to be isolated.

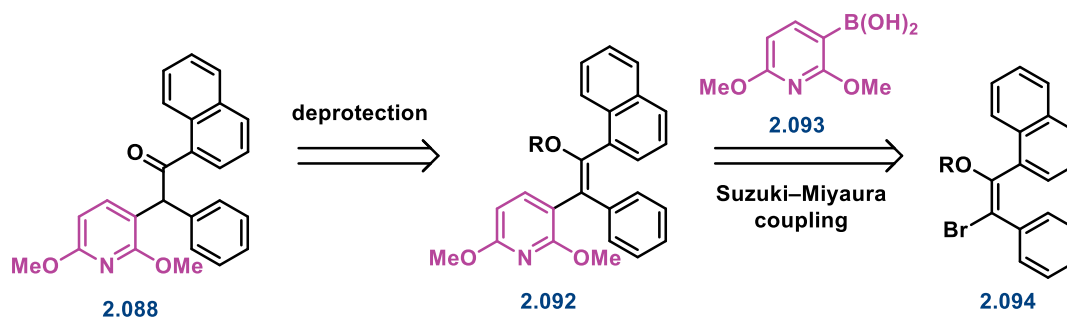
As an alternate strategy, the reverse sequence towards **2.088** was also trialled (**Scheme 2.15, Pathway B**). Using the identical reaction conditions to those employed for the synthesis of intermediate **2.087**,  $\alpha$ -arylation between acetophenone **2.089** and bromopyridine **2.034** was attempted however this repeatably produced only trace amounts of intermediate **2.090**, meaning the desired triarylketone was not accessible using this pathway. Given that the coupling with bromopyridine **2.034** performed poorly in both pathways, these results suggested that the chosen catalytic system was potentially not well suited to this specific pyridine coupling partner. Indeed, it has been well documented that cross-coupling reactions with heterocyclic substrates can be problematic as the heteroatoms can coordinate to the metal centre, therefore deactivating the catalyst.<sup>[19,20]</sup> Although P(*t*-Bu)<sub>3</sub> has been described as a versatile ligand for electron rich, electron neutral, electron poor, sterically hindered, or sterically unhindered arylhalides<sup>[21]</sup>, a report by Itoh and Mase<sup>[22]</sup> indicated that bulky monodentate ligands such as P(*t*-Bu)<sub>3</sub> are more susceptible to deactivation by heterocyclic substrates. As such, further exploration of the literature identified a variety of different ligands which were successfully employed in the coupling of methyl aryl ketones to halopyridine substrates and therefore revealing a range of complexes that were less susceptible to heteroatom deactivation.<sup>[23–27]</sup> Although a ligand screen may have assisted to optimise the coupling reactions with bromopyridine **2.034**, at this stage of the project an alternative strategy (detailed in **Section 2.3.2**) was discovered which successfully produced key intermediate **2.088**, and therefore no further optimisation of this pathway was explored.



**Scheme 2.15.** The attempted synthesis of triarylketone **2.088** using two  $\alpha$ -arylation strategies from acetophenone **2.089**.

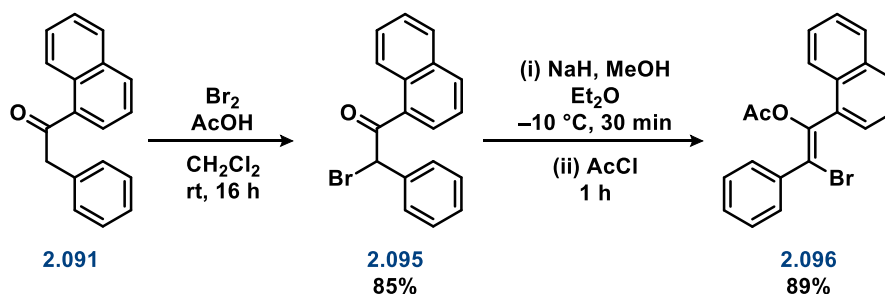
### 2.3.2 Suzuki–Miyaura strategy with pyridyl boronic acid

An alternative strategy identified to access pyridine analogues bearing two different groups in the B and C regions is outlined in **Scheme 2.16**. In contrast to the pathway described in **Section 2.3.1**, which incorporated the heterocycle as the heteroaryl halide, this pathway was designed to introduce the pyridine from the respective pyridyl boronic acid **2.093** using Suzuki–Miyaura cross-coupling with a vinylic halide (**2.094**).

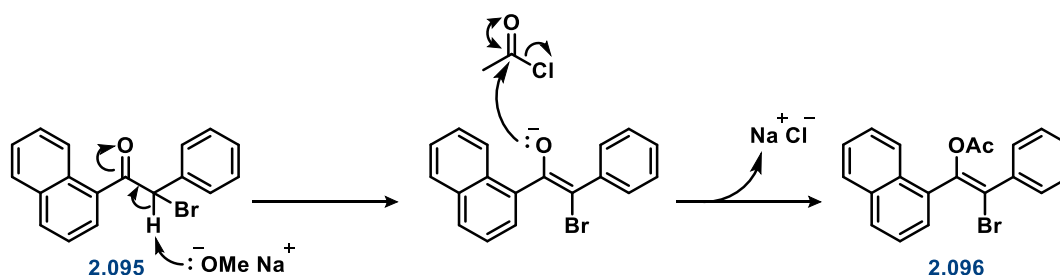


**Scheme 2.16.** Alternative strategy identified to access key intermediate **2.085** which incorporates the requisite pyridine moiety *via* Suzuki–Miyaura cross-coupling with a vinyl halide intermediate.

To enable introduction of the pyridine *via* Suzuki–Miyaura cross-coupling, the vinyl halide could be incorporated as the bromo-enol acetate **2.096** using a modified procedure first reported by Cooper *et al.*<sup>[28]</sup> (**Scheme 2.17**). In this procedure, intermediate **2.095** resulting from the bromination of **2.091** (previously prepared in **Scheme 2.15**) is reacted with *in situ* generated sodium methoxide (NaH with MeOH), followed by trapping of the enol with acetyl chloride to give **2.096** (**Scheme 2.18**).

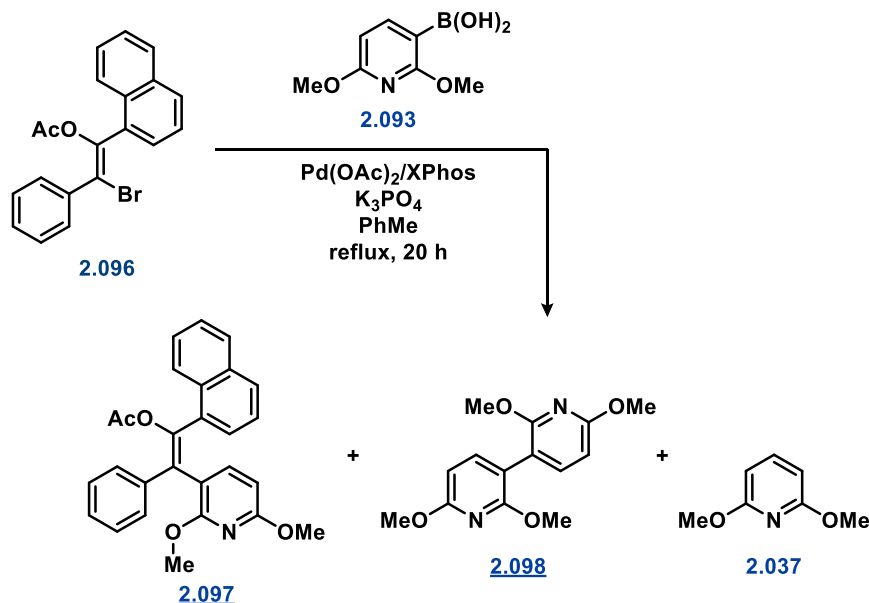


**Scheme 2.17.** Synthetic pathway towards bromo-enol acetate intermediate **2.096**.



**Scheme 2.18.** The mechanism towards bromo-enol acetate intermediate **2.096**.

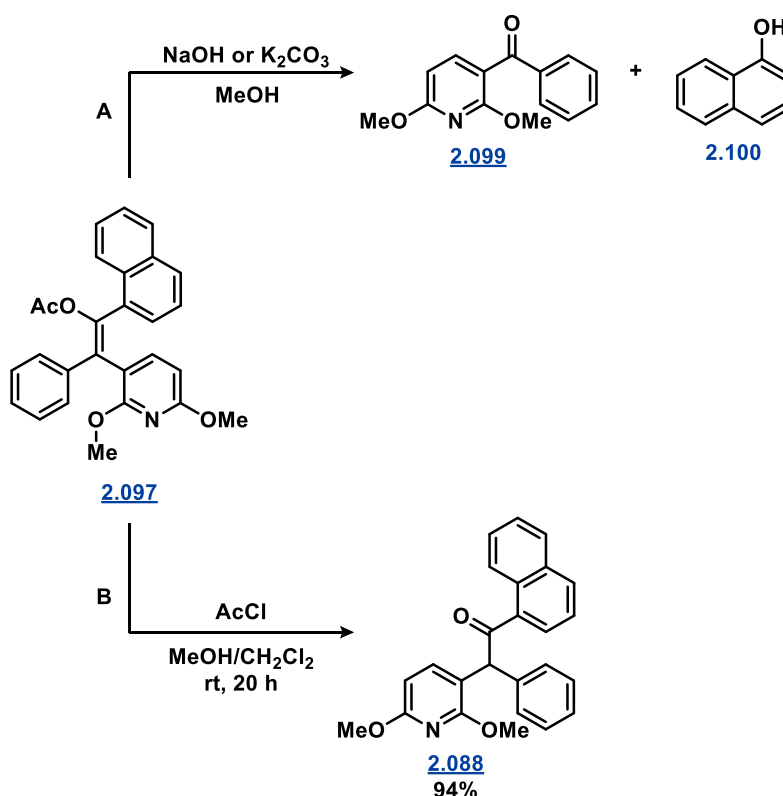
Suzuki–Miyaura cross-coupling of pyridine boronic acid **2.093** and intermediate **2.096** was performed using a catalytic system of palladium acetate and X-Phos in the presence of potassium phosphate and toluene under reflux for 20 h (**Scheme 2.19**). In the first attempt of this reaction, 2 equivalents of boronic acid **2.093** was used to produce intermediate **2.097** in 40% yield. In addition to the desired product, homocoupled boronic acid **2.098** (14%), and dimethoxypyridine **2.037** (14%, as a result of protodeboronation of **2.093**) were also isolated. In a repeated attempt of this reaction, increasing the amount of boronic acid to 3 equivalents slightly improved the yield of **2.097** to 50%, however no unreacted starting material **2.096** was observed, suggesting degradation of **2.096** had occurred. Although this reaction was not repeated, it is possible that a reduction in reaction temperature could at least partially improve yield by limiting potential thermal degradation of the starting materials.



**Scheme 2.19.** Suzuki–Miyaura cross-coupling between bromo-enol acetate **2.096** and pyridyl boronic acid **2.093**.

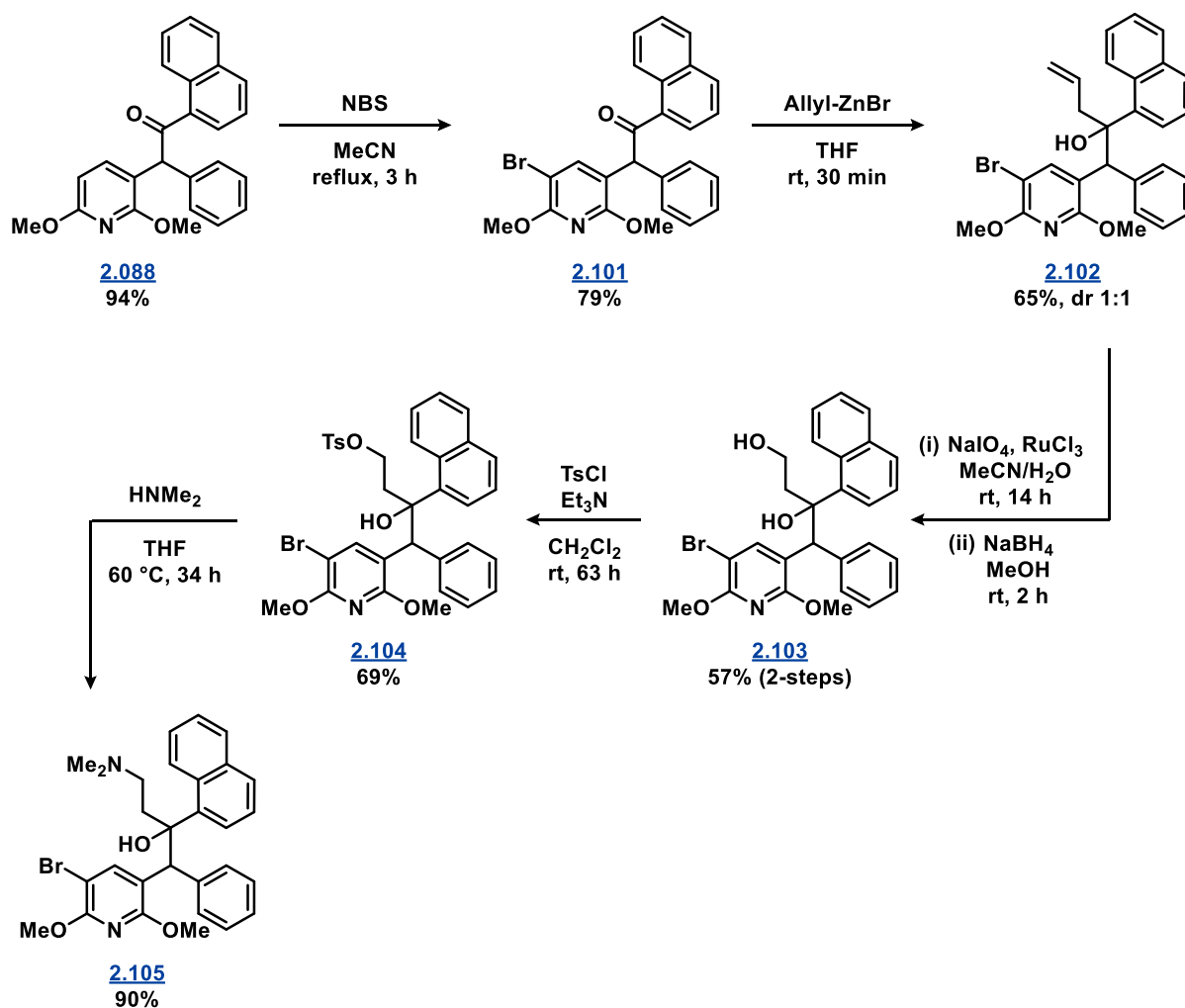
Interestingly, when the analogous Suzuki–Miyaura cross-coupling reaction had been performed within our research group using quinolyl boronic acid, *in situ* hydrolysis of the enol acetate occurred to directly afford the free ketone<sup>[5]</sup>, however this was not observed with intermediate **2.097**. Attempts to deacetylate intermediate **2.097** under basic conditions (aqueous solutions of NaOH or  $\text{K}_2\text{CO}_3$ ) proved unsuccessful, and instead led to the formation of diarylketone **2.099** (Scheme 2.20, A). The mechanism leading to the formation of this product remains unknown, however naphthol (**2.100**) was also isolated from the aqueous phase during workup accounting for the naphthyl portion of the molecule that was cleaved during this process.

Given that base-mediated hydrolysis led to substrate decomposition, attention turned to exploring deacetylation using non-basic conditions. A thorough search of the literature revealed a mild acid mediated deacetylation protocol using HCl generated *in situ* by addition of acetyl chloride to MeOH.<sup>[29]</sup> Although the literature report outlining this approach detailed that a catalytic amount of acetyl chloride (15 mol%) was sufficient for a range of substrates, in our hands a total of 2 equivalents was required for full conversion to cleanly provide deacetylated triarylketone **2.088** in excellent yield (94%, Scheme 2.20, B).



**Scheme 2.20.** Deacetylation of intermediate **2.097** was attempted using both A) basic conditions, or B) acidic conditions.

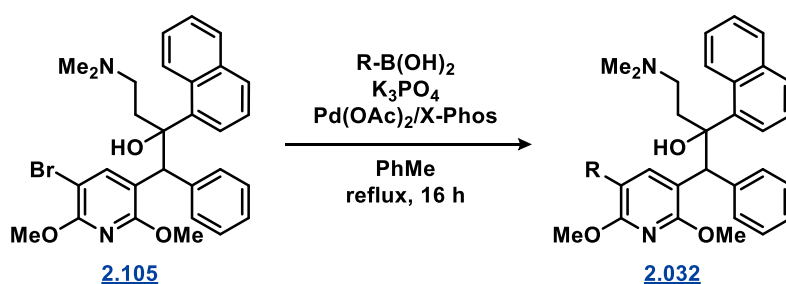
With synthetic methods now in hand to prepare triarylketone **2.088** containing the requisite pyridine heterocycle, the remaining steps in the synthesis towards the key intermediate **2.105** (**Scheme 2.21**) were analogous to those previously optimised for the synthesis of intermediate **2.044** (**Section 2.2.1**). In general, these reactions progressed similarly when applied to this scaffold, however some minor differences were noted possibly as a result of the additional steric bulk imparted by the naphthyl ring in region C. Firstly, in contrast to the allylation in **Scheme 2.8** (**Section 2.2.1**) where product was obtained quantitatively, yields greater than 65% were not achieved for the allylation of intermediate **2.101** to **2.102**. Despite this, unreacted starting material was readily recovered. Additionally, the rate of tosylation of intermediate **2.103** to **2.104** was found to be significantly slower and did not proceed to completion despite a considerable excess of tosyl chloride (10 equivalents) over a period of 63 h. In a repeated attempt of this reaction, catalytic DMAP (10 mol%) was included to assist with activation, however no improvement in conversion rate or yield was observed, although some unreacted starting material was able to be recovered.



**Scheme 2.21.** Synthetic scheme from intermediate triarylketone **2.088** to key intermediate **2.105**.

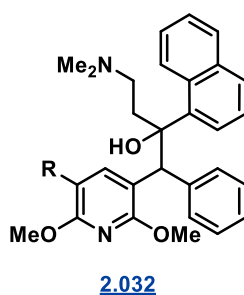
### 2.3.3 SAR of the pyridine core at the C5 position

Similarly to intermediate **2.044** (Scheme 2.10, Section 2.2.1), a variety of structures could be accessed through transition metal-catalysed coupling reactions (E.g. Suzuki–Miyaura cross-coupling) to the C5 bromine on the 2,6-dimethoxypyridyl ring. At this stage of the project we had not received bioactivity data for the parallel C5 substituted pyridine series bearing a phenyl ring at unit C (class **2.031**), as discussed earlier in Section 2.2.3. Therefore, it was planned to incorporate a small selection of *para*-substituted phenyl rings to allow for comparison between these two series once all preliminary *in vitro* testing had been completed. Suzuki–Miyaura cross-coupling (Scheme 2.22) provided analogues in Table 2.5 as a 1:1 mixture of diastereomers which were separated by preparative HPLC into diastereomer A (first to elute) and diastereomer B (second to elute).



**Scheme 2.22.** Diversification of intermediate **2.105** using Suzuki–Miyaura cross-coupling towards 2,6-dimethoxypyridine analogues of class **2.032**.

**Table 2.5.** Product yields of all analogues of type **2.032** synthesised *via* Suzuki–Miyaura cross-coupling.



| Entry | Compound     | R | Yield |
|-------|--------------|---|-------|
| 1     | <b>2.106</b> |   | 71%   |
| 2     | <b>2.107</b> |   | 96%   |
| 3     | <b>2.108</b> |   | 94%   |
| 4     | <b>2.109</b> |   | 93%   |
| 5     | <b>2.110</b> |   | 77%   |
| 6     | <b>2.111</b> |   | 61%   |

In a similar fashion to the phenyl series **2.031** described in **Section 2.2.3**, these analogues were first assessed in a preliminary inhibition screen at three drug concentrations (1, 10 and 100  $\mu M$ ) to determine the active diastereomer prior to being analysed to determine the  $MIC_{90}$ . Shown in **Figure 2.10** is the most active diastereomer of each naphthyl-bearing analogue synthesised in this series (**2.032**, green) compared with the previous series (**2.031**, blue) at both 10 and 1  $\mu M$  (all analogues demonstrated 100% inhibition at 100  $\mu M$ ).



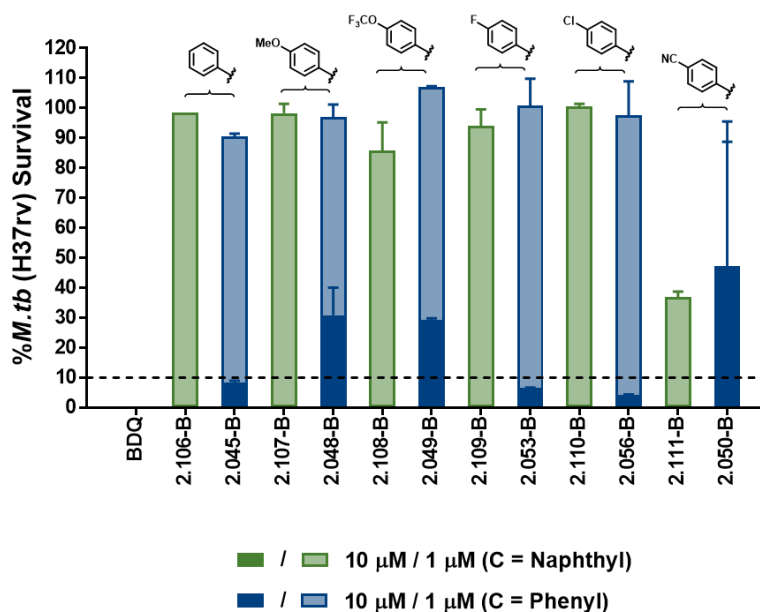


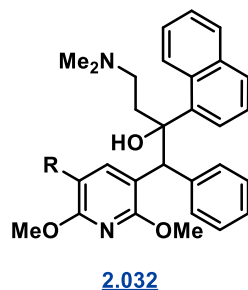
**Figure 2.10.** Preliminary activity screen of the synthesised 2,6-dimethoxypyridine analogues bearing a naphthyl ring in region C (series **2.032**, green) in comparison to the 2,6-dimethoxypyridine analogues of BDQ bearing a phenyl ring in region C (series **2.031**, blue) indicating percentage survival of *M.tb* at 10 µM (solid) and 1 µM (translucent). Only the most active diastereomer is shown.

In comparison to the previous series **2.031** which contained a phenyl ring region C (blue), the naphthyl bearing analogues **2.032** (green) were all more potent as demonstrated by a 100% inhibition of *M.tb* at 10 µM. These preliminary results indicated that the additional extension in bulk in both regions A and C was not detrimental to activity. Interestingly, the cyano analogue **2.111-B** demonstrated *ca.* 60% inhibition at 1 µM (40% survival) making it the most potent of all the 2,6-dimethoxypyridine analogues that had been screened to this point.

From here, further analysis to determine the MIC<sub>90</sub> of these analogues was performed using the REMA assay (described in **Section 2.1**), with the results summarised in **Table 2.6**. General observations from this series indicated that a slight improvement in activity (2- to 3-fold) could be achieved with the inclusion of *para*-substituents to the ring (entries 4, 5 and 7) in comparison the unsubstituted phenyl ring (entry 2). Additionally, when relating activity to cLogP it can be seen that activity did not necessarily correlate with lipophilicity, with the *para*-cyano derivative being the most potent of this series (entry 7, 1.24 µM) despite possessing the lowest cLogP value of 6.15. Considering that cyano derivative **2.111-B** (entry 7) was tested as a racemic mixture of two enantiomers (presumably *RS*, *SR* by analogy to BDQ), it is anticipated that the activity of the eutomer (presumably *RS*) could be close to half this value (*ca.* 0.6 µM), and therefore potentially matching BDQ's potency in this assay. At this stage, this result was very promising as it provided evidence that we could obtain potent anti-*M.tb* activity comparable to BDQ by using new heterocyclic cores in the ring A region. Furthermore, derivative **2.111-B** provides a relatively substantial reduction in cLogP (>10-fold) and a marked

increase in TPSA in comparison to BDQ (78 vs. 45, respectively) as a result of the polar cyano substituent on the phenyl ring, as well and the methoxy substituent at the C6 pyridyl position .

**Table 2.6.** Preliminary *in vitro* activity of 2,6-dimethoxypyridine series **2.032** bearing a naphthyl ring in region C.



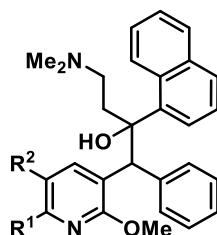
| Entry | Compound     | R | <i>M.tb</i> H37Rv MIC <sub>90</sub> (μM) <sup>a</sup> |                   | cLogP |
|-------|--------------|---|---|-------------------|-------|
| 1     | BDQ          |   | 0.54 ± 0.05 <sup>b</sup>                              |                   | 7.25  |
|       |              |   | A   | B                 |       |
| 2     | <b>2.106</b> |   | 5.31  | 3.88 <sup>c</sup> | 6.71  |
| 3     | <b>2.107</b> |   | N.D.  | 4.35 ± 0.61       | 6.72  |
| 4     | <b>2.108</b> |   | N.D.  | 2.34 ± 0.07       | 7.83  |
| 5     | <b>2.109</b> |   | 4.99  | 2.41 <sup>c</sup> | 6.85  |
| 6     | <b>2.110</b> |   | N.D.  | 3.44 ± 0.55       | 7.42  |
| 7     | <b>2.111</b> |   | 24.88   | 1.24 <sup>c</sup> | 6.15  |

<sup>a</sup>Values are expressed as mean ± standard error of the mean (n = 3), <sup>b</sup>n = 7, <sup>c</sup>n = 1

Simultaneous work conducted in the group which was focused on the synthesis of the related 2-methoxypyridine analogues is included in **Table 2.7** for comparison (R<sup>1</sup> = H). Although this presents a relative small data set, in directly comparing both classes where R<sup>2</sup> is maintained, the additional methoxy group at R<sup>1</sup> appears to generally confer an improvement in activity (2 to 3-fold) despite a *ca.* 2-fold reduction in cLogP (entries 2, 3, 5 and 6). The only exception to this trend is the *para*-fluoro analogue of the 2-methoxypyridine class (entry 9) which was found to be the most potent derivative of this entire study with an MIC<sub>90</sub> of 0.80 μM. This analogue was 3-fold more potent than its C6 (R<sup>1</sup>) methoxy counterpart (entry 8) and 7-fold more potent than its related unsubstituted phenyl ring (entry 3). Given that this compound was evaluated as a racemic mixture of two enantiomers, it is expected that the activity of the eutomer could be equivalent to that of BDQ (0.54 μM) once purified.

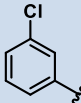
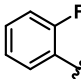
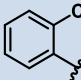
Another observation that can be made from the 2-methoxypyridine class is the comparative effect of *ortho*, *meta* and *para* halogen substitution to the phenyl ring. Whereas the *para*-fluoro position (entry 9) was the most favoured in comparison to the *ortho* and *meta* positions (entries 12 and 14), for the chloro derivatives, the *ortho*-substituted ring was most potent (entry 15).

**Table 2.7.** Combined preliminary *in vitro* activity of all tested pyridine analogues of BDQ bearing a naphthyl ring in region C. Only compounds where R<sup>1</sup> = OMe were synthesised by this candidate, whereas compounds with R<sup>2</sup> = H were synthesised by Dr. Daniel Priebbenow.



| Entry | Compound       | R <sup>1</sup> | R <sup>2</sup> | <i>M.tb</i> H37Rv<br>MIC <sub>90</sub> (μM) <sup>a</sup> | cLogP |
|-------|----------------|----------------|----------------|--|-------|
| 1     | BDQ            |                |                | 0.54 ± 0.05  | 7.25  |
| 2     | <b>2.106-B</b> | OMe            |                | 3.88 <sup>c</sup>  | 6.71  |
| 3     | <b>2.112-B</b> | H              |                | 5.51 ± 0.08 <sup>b</sup>                                 | 6.87  |
| 4     | <b>2.107-B</b> | OMe            |                | 4.35 ± 0.61  | 6.72  |
| 5     | <b>2.108-B</b> | OMe            |                | 2.34 ± 0.07  | 7.83  |
| 6     | <b>2.113-B</b> | H              |                | 6.77 ± 0.78  | 8.00  |
| 7     | <b>2.111-B</b> | OMe            |                | 1.24 <sup>c</sup>  | 6.15  |
| 8     | <b>2.109-B</b> | OMe            |                | 2.41 <sup>c</sup>  | 6.85  |
| 9     | <b>2.114-B</b> | H              |                | 0.80 ± 0.12 <sup>b</sup>                                 | 7.02  |
| 10    | <b>2.110-B</b> | OMe            |                | 3.44 ± 0.55  | 7.42  |
| 11    | <b>2.115-B</b> | H              |                | 6.94 ± 2.42 <sup>b</sup>                                 | 7.59  |
| 12    | <b>2.116-B</b> | H              |                | 2.41 <sup>c</sup>  | 7.02  |

Table 2.7. (continued)

| Entry | Compound | R <sup>1</sup> | R <sup>2</sup>  | <i>M.tb</i> H37Rv<br>MIC <sub>90</sub> (μM) <sup>a</sup> | cLogP |
|-------|----------|----------------|---|--|-------|
| 3     | 2.117-B  | H              |  | 7.90 <sup>c</sup>  | 7.59  |
| 14    | 2.118-B  | H              |  | 2.51 <sup>c</sup>  | 7.02  |
| 15    | 2.119-B  | H              |  | 4.52 <sup>c</sup>  | 7.34  |

<sup>a</sup>Values are expressed as mean  $\pm$  standard error of the mean ( $n = 3$ ), <sup>b</sup> $n = 2$ , <sup>c</sup> $n = 1$

## 2.4 Conclusion

This section of the project was focused on exploring synthetic strategies to further expand the SAR in ring A region of BDQ to determine if potency could be retained following quinoline substitution. Two synthetic pathways were successfully identified and optimised to enable successful incorporation of a pyridine in the ring A region from either the pyridine boronic acid or halopyridine. Due to their modular nature, it can be envisaged that these synthetic pathways could be further extended to incorporate a variety of heteroaryl halides or boronic acids.

In terms of the SAR studies in the ring A region, this candidate's contribution was to synthesise analogues incorporating a 2,6-dimethoxypyridine core to investigate whether additional substitution and/or extension in the C6 (R<sup>1</sup>) position of the pyridine ring could be tolerated. Additionally, SAR in the C5 (R<sup>2</sup>) region was also simultaneously expanded. Through the synthesis of these analogues it was established that a methoxy group in the C6 (R<sup>1</sup>) position of the ring was tolerated, with potent analogues achieved with the inclusion of this substituent. Furthermore, in exploring the C5 region (R<sup>2</sup>), it was found that substitutions to the incorporated phenyl ring could in some cases lead up to a 3- to 7-fold increase in potency compared with the unsubstituted ring. The most potent analogues of this study (**2.111-B** and **2.114-B**) are anticipated to possess close to equipotent activity to BDQ as the eutomer. Furthermore, the potency observed for derivative **2.111-B** was particularly promising as this compound was less lipophilic and more polar than BDQ, thus providing a potentially safer derivative in comparison.

Overall, it was demonstrated that novel and potent compounds could be furnished following replacement of the quinoline ring in region A with a substituted phenyl-pyridine moiety. Despite achieving a single analogue with that was highly potency and less lipophilic, due to the additional requirement of the phenyl ring at the C5 (R<sup>2</sup>) position, we were not able to achieve large reductions in cLogP, which remained relatively high for the majority of derivatives tested. However, with

relatively active analogues in hand (and in new IP space) we were now well placed to focus our attention towards targeting lipophilicity. At this stage it was proposed that this could be achieved by:

- (i) further exploring the pyridine C5 ( $R^2$ ) region with heterocyclic moieties in place of the phenyl rings described herein,
- (ii) exploring the SAR at the pyridine C6 ( $R^1$ ) position to introduce more polar groups,
- (iii) investigating more polar heterocyclic moieties in the ring A region for example pyrazine and pyridazine (see Chapter 4), or
- (iv) exploring substitution of the B and C rings to incorporate more polar moieties for example heterocycles and polar substituents (see Chapters 3 and 4).

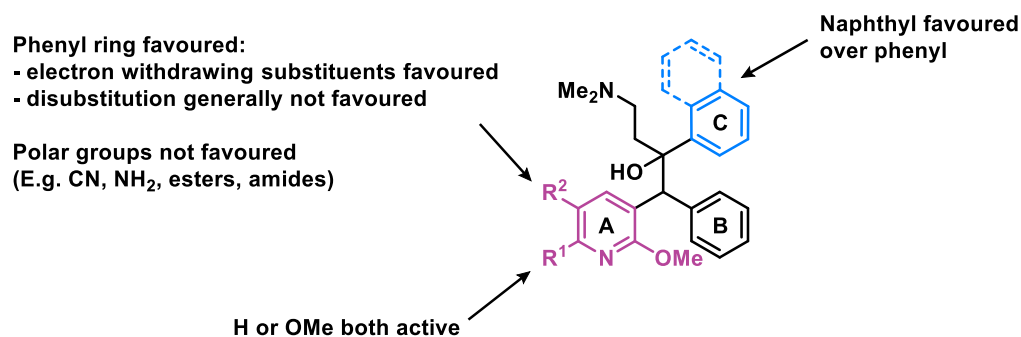


**Figure 2.11.** Generalised summary of the SAR obtained in this chapter.

## 2.5 References

- [1] A. E. Goetz, N. K. Garg, *Nat. Chem.* **2013**, *5*, 54–60.
- [2] J. E. G. Guillemont, J. F. E. Van Gestel, M. G. Venet, L. F. B. Decrane, D. F. J. Vernier, F. C. Odds, I. C. F. Csoka, K. J. L. M. Andries, *Quinoline Derivatives and Their Use as Mycobacterial Inhibitors*, **2004**, WO011436.
- [3] Y. Saga, R. Motoki, S. Makino, Y. Shimizu, M. Kanai, M. Shibasaki, *J. Am. Chem. Soc.* **2010**, *132*, 7905–7907.
- [4] S. Chandrasekhar, G. S. K. Babu, D. K. Mohapatra, *European J. Org. Chem.* **2011**, *2011*, 2057–2061.
- [5] D. L. Priebbenow, L. Barbaro, J. B. Baell, *Org. Biomol. Chem.* **2016**, *14*, 9622–9628.
- [6] J. Guillemont, C. Meyer, A. Poncelet, X. Bourdrez, K. Andries, *Future Med. Chem.* **2011**, *3*, 1345–1360.
- [7] D. L. Priebbenow, R. W. Gable, J. Baell, *J. Org. Chem.* **2015**, *80*, 4412–8.
- [8] J. D. Hughes, J. Blagg, D. A. Price, S. Bailey, G. A. DeCrescenzo, R. V. Devraj, E. Ellsworth, Y. M. Fobian, M. E. Gibbs, R. W. Gilles, et al., *Bioorg. Med. Chem. Lett.* **2008**, *18*, 4872–4875.
- [9] T. Ishiyama, N. Matsuda, N. Miyaura, A. Suzuki, *J. Am. Chem. Soc.* **1993**, *115*, 11018–11019.
- [10] M. Shimizu, I. Nagao, Y. Tomioka, T. Hiyama, *Angew. Chem. Int. Ed. Engl.* **2008**, *47*, 8096–9.
- [11] H. R. Kim, J. Yun, *Chem. Commun.* **2011**, *47*, 2943–2945.
- [12] V. Cañibano, J. F. Rodríguez, M. Santos, M. A. Sanz-Tejedor, M. C. Carreño, G. González, J. L. García-Ruano, *Synthesis* **2001**, *2001*, 2175–2179.
- [13] Y. Zhang, X. Jia, J.-X. Wang, *European J. Org. Chem.* **2009**, *2009*, 2983–2986.
- [14] D. Yang, C. Zhang, *J. Org. Chem.* **2001**, *66*, 4814–4818.
- [15] M. Palucki, S. L. Buchwald, *J. Am. Chem. Soc.* **1997**, *119*, 11108–11109.
- [16] B. C. Hamann, J. F. Hartwig, *J. Am. Chem. Soc.* **1997**, *119*, 12382–12383.
- [17] T. Satoh, Y. Kawamura, M. Miura, M. Nomura, *Angew. Chemie Int. Ed. English* **1997**, *36*, 1740–1742.
- [18] D. A. Culkin, J. F. Hartwig, *Acc. Chem. Res.* **2003**, *36*, 234–245.
- [19] R. H. Crabtree, *Chem. Rev.* **2015**, *115*, 127–150.
- [20] A. S. Guram, X. Wang, E. E. Bunel, M. M. Faul, R. D. Larsen, M. J. Martinelli, *J. Org. Chem.* **2007**, *72*, 5104–5112.
- [21] M. Kawatsura, J. F. Hartwig, *J. Am. Chem. Soc.* **1999**, *121*, 1473–1478.
- [22] T. Itoh, T. Mase, *Tetrahedron Lett.* **2005**, *46*, 3573–3577.
- [23] D. Wang, J. Hu, J. Zhao, M. Shen, Y. Wang, P. Yu, *Tetrahedron* **2018**, *74*, 4100–4110.
- [24] M. R. Biscoe, S. L. Buchwald, *Org. Lett.* **2009**, *11*, 1773–1775.

- [25] A. J. DeAngelis, P. G. Gildner, R. Chow, T. J. Colacot, *J. Org. Chem.* **2015**, *80*, 6794–6813.
- [26] C. Cao, L. Wang, Z. Cai, L. Zhang, J. Guo, G. Pang, Y. Shi, *European J. Org. Chem.* **2011**, *2011*, 1570–1574.
- [27] P. R. Melvin, A. Nova, D. Balcells, W. Dai, N. Hazari, D. P. Hruszkewycz, H. P. Shah, M. T. Tudge, *ACS Catal.* **2015**, *5*, 3680–3688.
- [28] D. J. Cooper, L. N. Owen, *J. Chem. Soc. C* **1966**, *0*, 533–540.
- [29] C.-E. Yeom, S. Lee, Y. Kim, B. Kim, *Synlett* **2005**, *2005*, 1527–1530.

## Chapter 3: Pyridine Hybrids of TBAJ-587

### 3.1 Introduction

As demonstrated in Chapter 2, substitution of the ring A quinoline revealed that this moiety was not critical for potent anti-*M.tb* activity. As deviation from the quinoline ring had not been previously explored, this discovery enabled us to enter into novel IP space through the incorporation of alternate heterocyclic moieties in this region.

Given that the key focus of this project was to synthesise novel analogues of BDQ which were less lipophilic yet potent against *M.tb*, our initial strategy to reduce BDQ's lipophilicity involved replacement of the quinoline with the smaller pyridyl heterocycle. Despite our best efforts, our SAR study determined that an additional phenyl ring in the C5 ( $R^2$ ) position of the ring was required to maintain potent anti-*M.tb* activity within this series, and therefore at this stage of the project our most potent analogues remained quite lipophilic (cLogP >6). Despite this observation, we were well placed to continue to explore additional strategies to delineate lipophilicity from activity to improve upon the safety profile of BDQ analogues. As summarised in **Figure 3.1**, the strategies that were proposed to achieve this included further derivatisation of the ring A pyridine including heterocyclic variants at the C5 ( $R^2$ ) position and more polar functionalities in the C6 ( $R^1$ ) position. Additionally, we were also interested in modulating the polarity in the B and C regions of the structure.

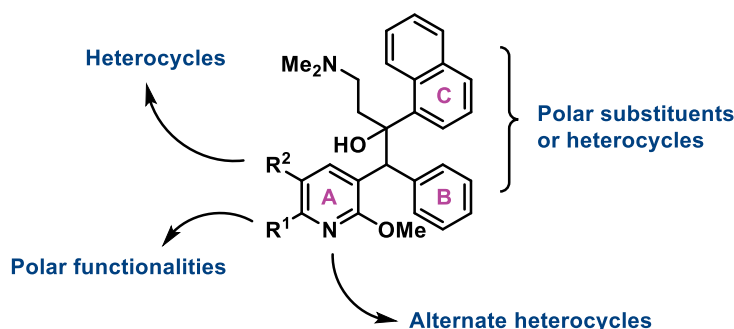


**Figure 3.1.** Proposed strategies towards further reducing the lipophilicity of our ring A pyridine analogues of BDQ.

Rather unexpectedly, at this stage of the project we were made aware of a complementary research program led by Prof. William Denny at the University of Auckland. In analogy to our efforts, their project also predominantly focused on reducing the lipophilicity of BDQ as a means to improve BDQ's safety and PK profiles.<sup>[1–6]</sup> Denny first disclosed the structure of their efforts towards their preclinical candidate TBAJ-587 (**Figure 3.2**) at the 2017 Gordon Research Conference on Tuberculosis Drug Discovery and Development<sup>[7]</sup>, which was recently published.<sup>[5]</sup> Somewhat fortuitously and in contrast to our program, the Denny group predominantly focused on further exploring the SAR of the diaryl



component of BDQ (rings B and C). To the best of our knowledge, they did not explore the more synthetically challenging concept of substituting the A ring as we have demonstrated in Chapter 2. It is important to note that although the absolute configuration of TBAJ-587 was identical to that of BDQ, the change in the stereoassignment (*SS* as opposed to *RS*) is due to the inclusion of the *ortho*-fluoro substituent on ring B in accordance with the Cahn–Ingold–Prelog priority rules.

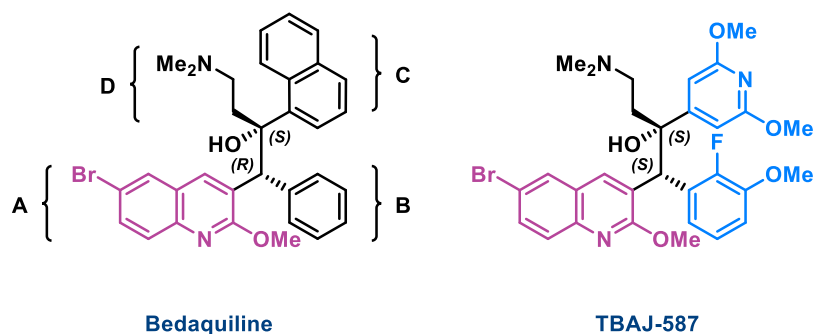


**Figure 3.2.** The comparative structures of BDQ and TBAJ-587.

As shown in **Table 3.1**, TBAJ-587 possesses superior *in vitro* and *in vivo* activity, pharmacokinetic properties and safety profiles in comparison to BDQ. Of particular significance, TBAJ-587 has reduced potency at hERG and a lower predicted efficacious exposure, providing a lower risk of QTc prolongation. Interestingly, Denny discovered that a reduction in lipophilicity was not sufficient on its own to significantly reduce hERG inhibition. Instead, they discovered that the inclusion of a pyridyl ring at region C was a major factor in achieving the desired reduction in hERG inhibition within their series. As a result of their extensive medicinal chemistry effort which cumulated in the synthesis of over 1000 analogues, TBAJ-587 is expected to enter phase 1 clinical trials in 2020.

**Table 3.1.** The predictive safety and efficacy comparison between BDQ and TBAJ-587.

| Compound Data  | BDQ  | TBAJ-587 |
|--|------|----------|
| cLogP  | 7.3  | 5.8      |
| MIC <sub>90</sub> (μg/mL) <sup>a[5]</sup>              |      |          |
| MABA   | 0.04 | 0.006    |
| LORA   | 0.08 | <0.02    |
| hERG IC <sub>50</sub> (μM) <sup>[5]</sup>              | 1.6  | 13       |
| Phospholipidosis AC <sub>50</sub> (μM) <sup>b[7]</sup> | 5    | 4        |
| CYP3A4 IC <sub>50</sub> (μM) <sup>[7]</sup>            | >10  | 24       |
| Mouse PO t <sub>1/2</sub> (h) <sup>c[7]</sup>          | 44   | 16       |
| Δlog <sub>10</sub> CFU <sup>d[5]</sup>                 | 6.1  | 5.2      |

<sup>a</sup>*M.tb* strain H37Rv, determined under replicating; (MABA) or non-replicating (LORA) conditions; <sup>b</sup>Concentration at which an assay is at 50% of that for a control compound; <sup>c</sup>Half-life in mice; <sup>d</sup>Log reduction in lung colony forming units (CFU) compared to vehicle at 20 mg/kg daily in mice for 12 days, beginning 10 days after *M.tb* inoculation via the aerosol route.

Inspired by the Denny group's efforts to improve BDQ's properties, we saw this as the perfect opportunity to begin development on a novel class of analogues through the combination of our unique pyridine A region with Denny's optimised B and C regions. In particular, this provided us with a great opportunity to further lower lipophilicity of our BDQ-like analogues by virtue of the increased polarity that these novel B and C rings would provide.

In a similar fashion to our previous series (described in Chapter 2), our initial aim was to investigate various substituents at the C5 position of the ring A pyridine to see if a similar trend in the SAR of this region could be achieved for this novel series. As such, this chapter details the synthesis and preliminary SAR of pyridine ring A hybrids of TBAJ-587 to access new therapeutic candidates that exhibit potency against *M.tb* with the aim to improve upon the safety profile and overall properties of BDQ-type compounds (**Figure 3.3**).

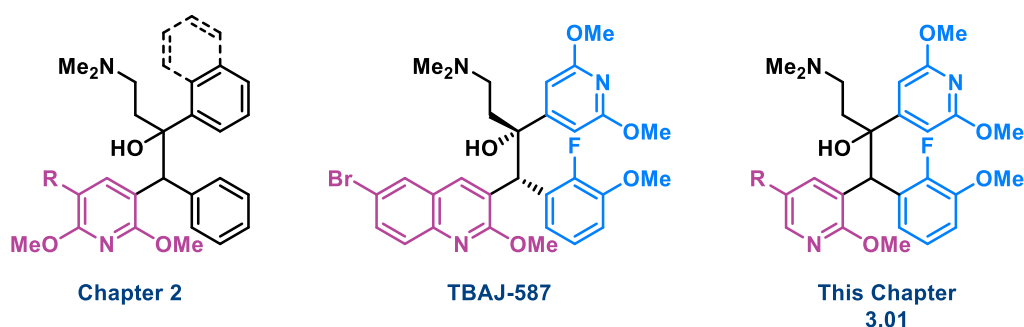


**Figure 3.3.** This chapter is focused on the synthesis of a novel class of BDQ analogues (**3.01**) as a result of combining our prior work described in Chapter 2 with the Denny candidate TBAJ-587.

### 3.2 Synthesis of a model pyridine-TBAJ-587 hybrid

Prior to synthesising a library of pyridine-TBAJ-587 hybrids, we first set out to design and optimise a new synthetic pathway that would enable the synthesis of a single representative compound to confirm if potency could be achieved with this novel class of compounds. As shown in **Figure 3.4**, the first analogue that we designed was the 2-methoxypyridine derivative **3.02** containing a *para*-trifluoromethoxyphenyl group at the C5 position of the ring A pyridine. This derivative was specifically chosen as at this stage of the project the limited results that we had obtained from our collaborators had suggested this was a potent combination to include in the A region.

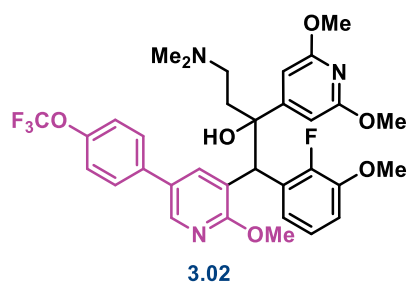
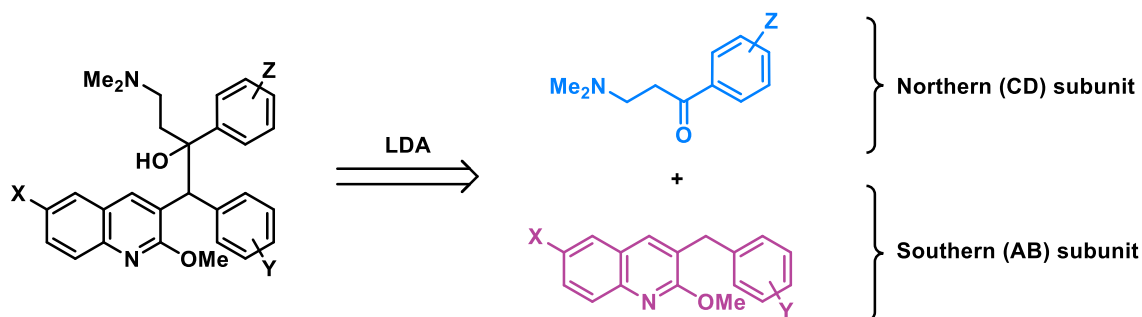


**Figure 3.4.** The structure of the first model derivative that was synthesised as part of this novel analogue class (**3.01**).

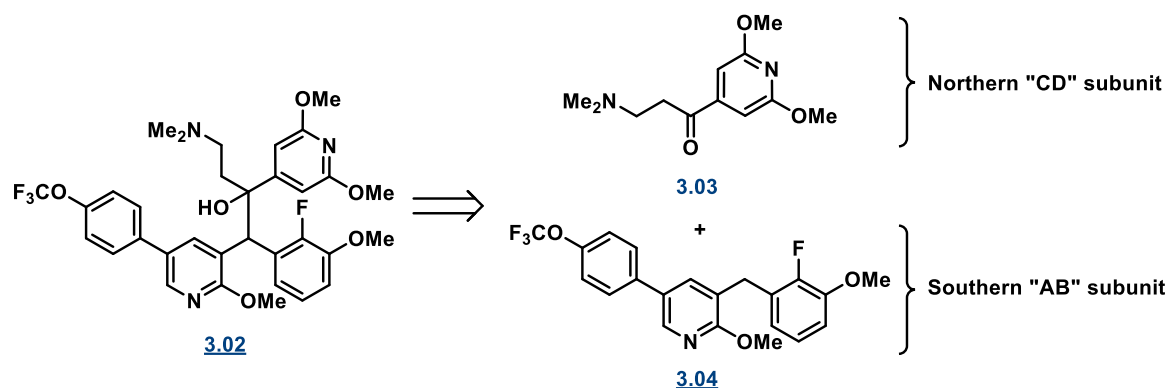
Although the specific synthetic pathway used to access TBAJ-587 wasn't fully disclosed during the Denny group presentation, they did provide a generalised scheme which indicated that their strategy was a convergent route very similar to that utilised by the Janssen in the synthesis of BDQ. As shown in **Scheme 3.1**, this strategy required the synthesis of both a northern (CD) subunit and a southern (AB) subunit, which were coupled together at the final stage by employing an LDA-mediated 1,2-carbonyl addition reaction.



**Scheme 3.1.** The general synthetic strategy utilised by the Denny group towards TBAJ-587 and related compounds.

As mentioned in Chapter 2, previous work in our group had determined this route to be inefficient for preparing a library of BDQ analogues where the quinoline ring was substituted with a pyridine at ring A due to issues encountered during the final LDA-mediated addition. While investigating alternative pathways to access to analogues of TBAJ-587, we discovered a patent recently filed by Cisen Pharmaceuticals in China.<sup>[8]</sup> Much to our surprise, this patent disclosed a range of pyridine ring A analogues of BDQ which were almost identical to our first series. Interestingly, one of the synthetic pathways detailed in this patent also progressed *via* a final LDA-mediated addition between northern and southern subunits.

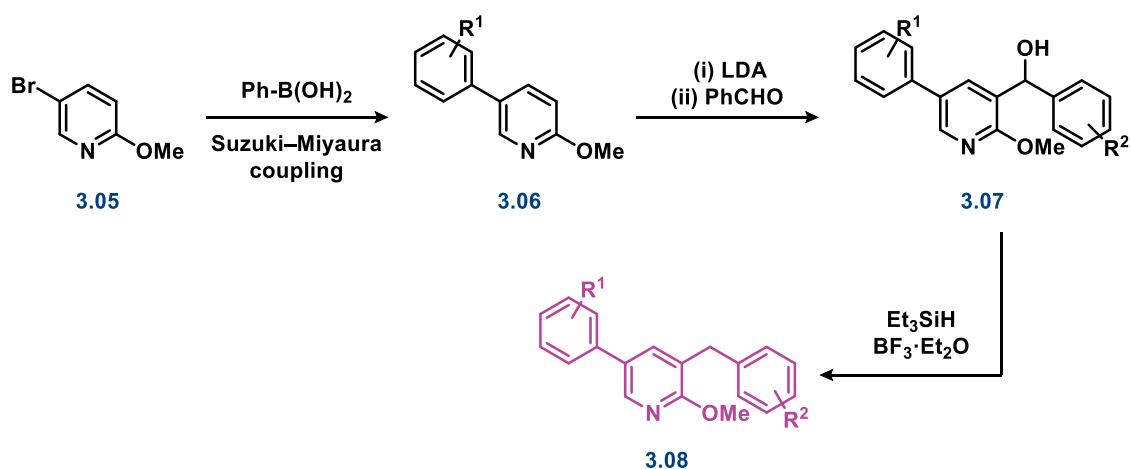
Given that both Cisen Pharmaceuticals and the Denny group had both employed this convergent strategy, we decided that an attempt at synthesising derivative **3.02** using a combination of these two strategies was worthy of trialling before investigating other strategies (**Scheme 3.2**).



**Scheme 3.2.** Proposed convergent strategy towards model compound **3.02**.

### 3.2.1 Synthesis of the southern subunit of the model analogue

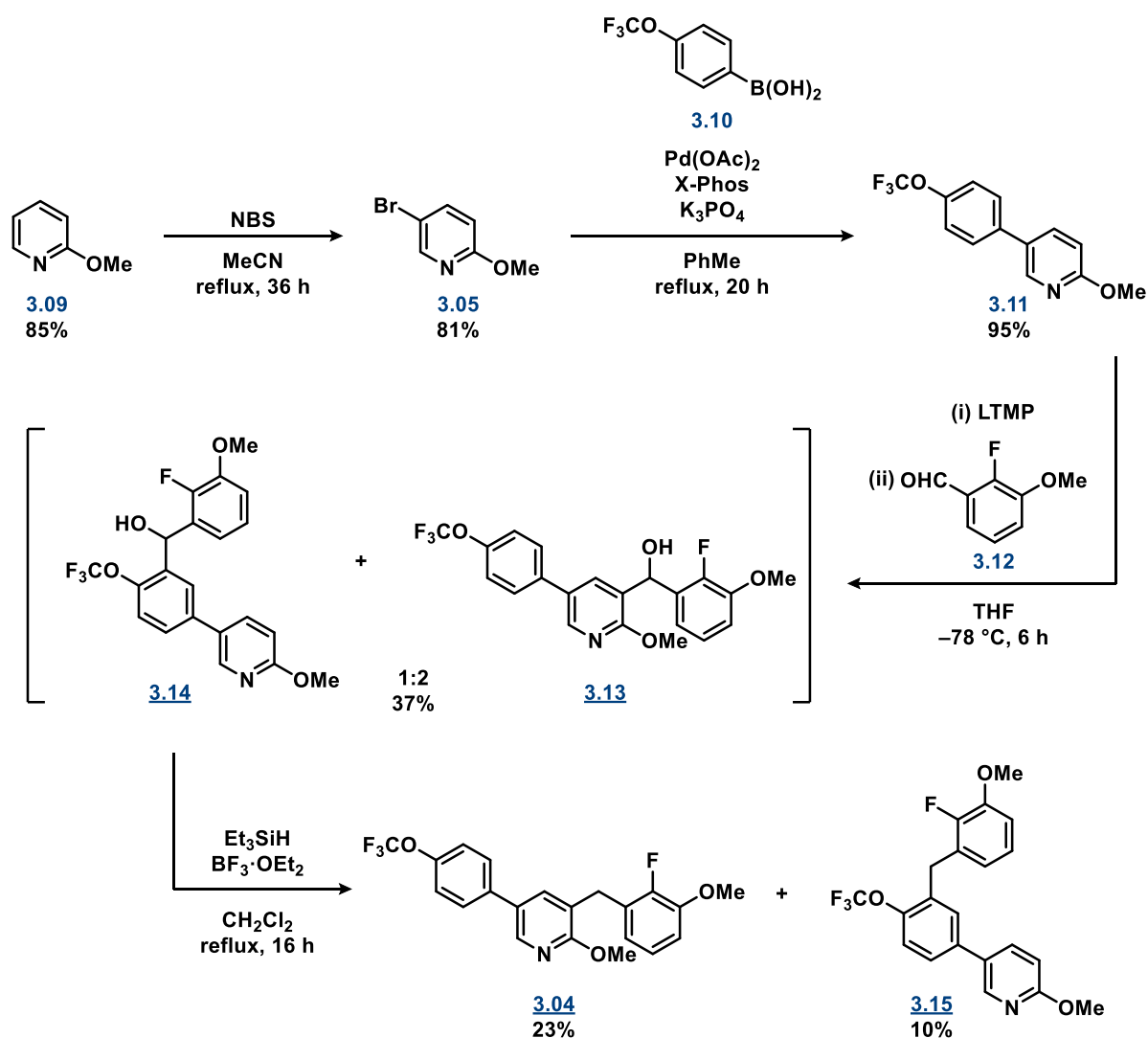
The synthetic strategy that was designed to access the southern portion of compound **3.02** was modelled on the pathway described in the Cisen Pharmaceuticals patent.<sup>[8]</sup> As summarised in **Scheme 3.3**, Cisen first incorporated the C5 phenyl ring to the pyridine core *via* Suzuki–Miyaura cross-coupling to give **3.06**, followed by selective LDA-mediated addition of the B ring moiety to C3 of the pyridine ring (**3.07**). Reduction of the benzylic alcohol afforded the completed southern subunit **3.08**.



**Scheme 3.3.** The procedure published by Cisen Pharmaceuticals towards their pyridine southern subunit.

To begin our analogous synthesis as summarised in **Scheme 3.4**, we employed selective bromination at the C5 position of methoxypyridine using NBS gave **3.05** in 81% yield. This was followed by Suzuki–Miyaura cross-coupling with boronic acid **3.10** which afforded intermediate **3.11** in excellent yield. Introduction of the second aromatic ring was then trialled using benzaldehyde derivative **3.12** as the electrophile. Employing a directed *ortho*-metalation (DoM) strategy, LDA was used to deprotonate the C3-position of the pyridyl ring to generate a nucleophile that could react with the aldehyde, however only a trace amount of the desired product was observed from this reaction by LCMS. When

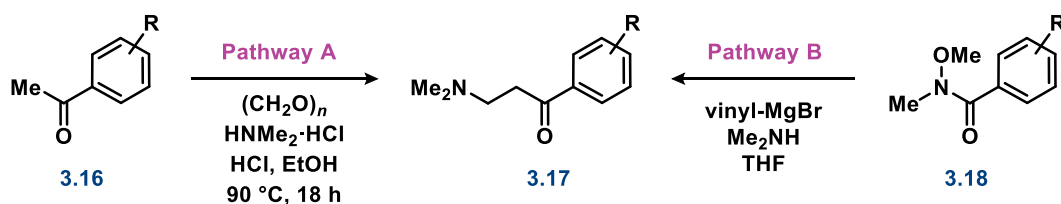
investigating the literature regarding the lithiation of methoxypyridines, it was discovered that an unfavourable equilibrium results when LDA is employed as the base with these substrates.<sup>[9]</sup> In an attempt to improve the efficiency of the lithiation step, the stronger lithium base LTMP (lithium tetramethylpiperidide) was utilised, which led to 37% conversion of the starting material to addition product. Upon analysis of this reaction, a 2:1 mixture of addition regioisomers **3.13** and **3.14** was observed, with the minor product generated as a result of competing addition *ortho* to the aryl trifluoromethoxy group. As these regioisomers were inseparable using silica-gel chromatography, the mixture of **3.13** and **3.14** was carried forward to the next step. Following silyl-mediated reduction of the hydroxy group, separation of the regioisomers was achievable resulting in isolation of the completed southern subunit **3.04** in 23% yield over two-steps. Although this pathway was clearly suboptimal at this early stage of the study, this provided a sufficient amount of the southern subunit towards the production of the model compound for preliminary testing purposes.



**Scheme 3.4.** Pathway used towards the synthesis of the southern subunit **3.04** of model analogue **3.02**.

### 3.2.2 Synthesis of northern subunit of model analogue

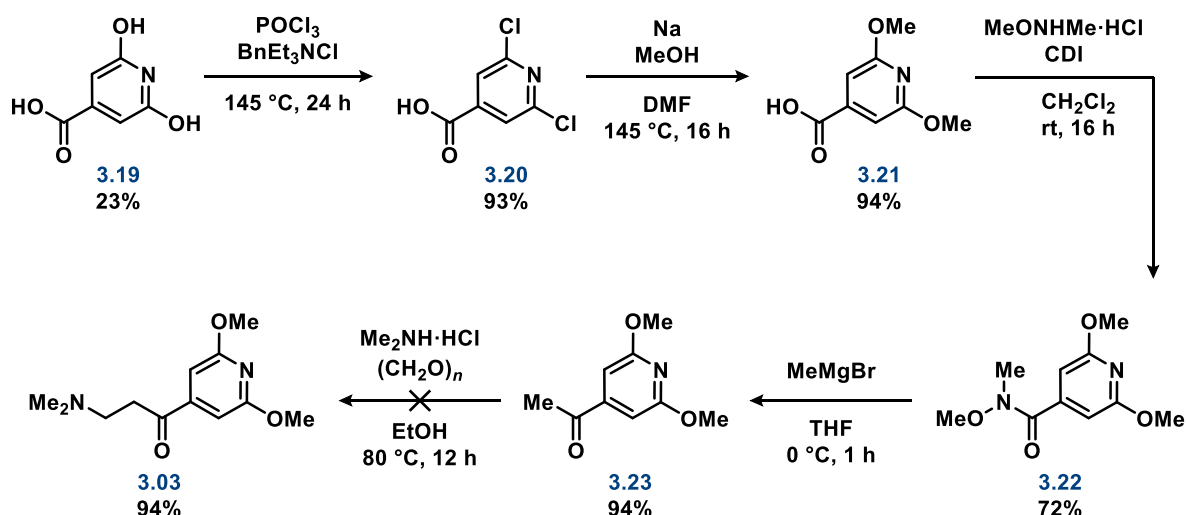
As shown in **Scheme 3.5**, the Denny group had described two alternate generalised routes which they used towards the synthesis of their northern subunits **3.17**.<sup>[7]</sup> Whereas the key transformation in Pathway A was a Mannich addition analogous to the strategy employed by Janssen in the synthesis of BDQ,<sup>[10]</sup> Pathway B installed a reactive vinyl group from Weinreb amide **3.18**, followed by Michael addition of dimethylamine to the resulting vinyl ketone. As it wasn't clear which pathway was used to synthesise the northern subunit of TBAJ-587, both pathways were investigated along with two additional pathways C and D.



**Scheme 3.5.** The two general strategies that the Denny group used towards the synthesis of their BDQ analogues. Pathway A = Mannich addition, Pathway B = Grignard and Michael addition.

#### 3.2.2.1. Pathway A

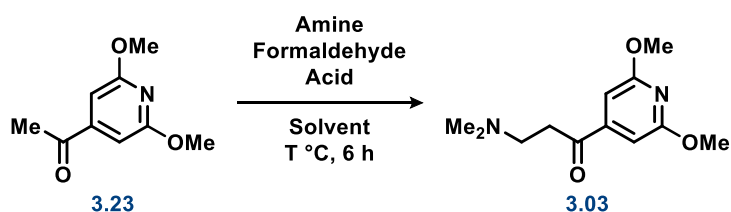
The initial route trialled towards the synthesis of the northern subunit **3.03** is illustrated **Scheme 3.6**. In this pathway, the key acetylpyridine intermediate **3.23** was prepared to allow for Mannich addition. Starting from **3.19**, literature reported procedures were used to provide **3.20** and **3.21** in excellent yields (93 and 94%, respectively).<sup>[11,12]</sup> To access the requisite acetylpyridine **3.23**, intermediate **3.21** was then converted to the corresponding Weinreb amide **3.22**, followed by nucleophilic addition of methylmagnesium bromide ( $\text{MeMgBr}$ ). From the resulting intermediate **3.23**, conventional Mannich conditions were trialled (with formation of the iminium ion *in situ*)<sup>[13,14]</sup>, however no reaction was observed and only starting material was recovered.



**Scheme 3.6.** Pathway A trialled towards the northern subunit **3.03**.

In light of this unsuccessful reaction attempt, a variety of Mannich conditions described in the literature using pyridyl ketones were trialled (**Table 3.2**).<sup>[15,16]</sup> Although a trace amount of product could be achieved when 1,4-dioxane was used as the solvent (entries 2 and 4), improvement in product yield could not be achieved by varying the reagents and conditions in accordance with the literature reports.

**Table 3.2.** Attempted reagents and conditions for the optimisation of the Mannich reaction.



| Entry | Aldehyde                         | Amine                       | Acid | Solvent        | Temp (°C)           | Outcome         |
|-------|----------------------------------|-----------------------------|------|----------------|---------------------|-----------------|
| 1     | (CH <sub>2</sub> O) <sub>n</sub> | Me <sub>2</sub> NH·HCl      | HCl  | <i>i</i> -PrOH | 90 °C               | No reaction     |
| 2     | (CH <sub>2</sub> O) <sub>n</sub> | Me <sub>2</sub> NH·HCl      | HCl  | Dioxane        | 110 °C              | Trace product   |
| 3     | (CH <sub>2</sub> O) <sub>n</sub> | Me <sub>2</sub> NH·HCl      | HCl  | Dioxane        | 130 °C <sup>a</sup> | 13% <b>3.25</b> |
| 4     | CH <sub>2</sub> O                | Me <sub>2</sub> NH (40% aq) | AcOH | Dioxane        | 110 °C              | Trace product   |

<sup>a</sup>Reacted for 2 h in a microwave reactor

Additionally, if the reaction temperature was increased to 130 °C as was reported by Ozaki et al.<sup>[16]</sup> (entry 3), propanone Mannich base **3.25** was produced in 13% yield, as confirmed by LCMS and <sup>1</sup>H

NMR (**Figure 3.5**). This by-product is thought to have formed *via* a bis-Mannich reaction to generate intermediate **3.24** followed by subsequent elimination to afford **3.25** (**Scheme 3.7**).<sup>[17,18]</sup>

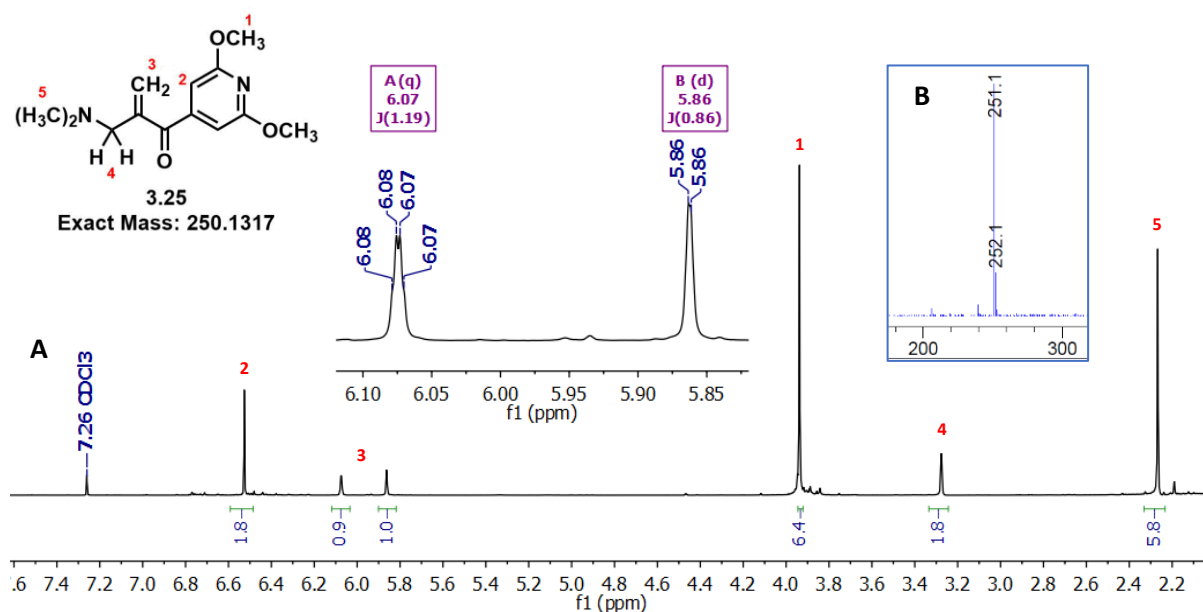
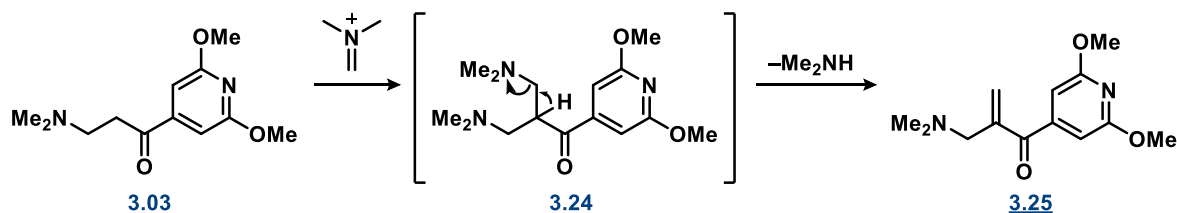


**Figure 3.5.** The A) <sup>1</sup>H NMR spectrum and B) LR-MS confirming propanone Mannich base by-product **3.25**.



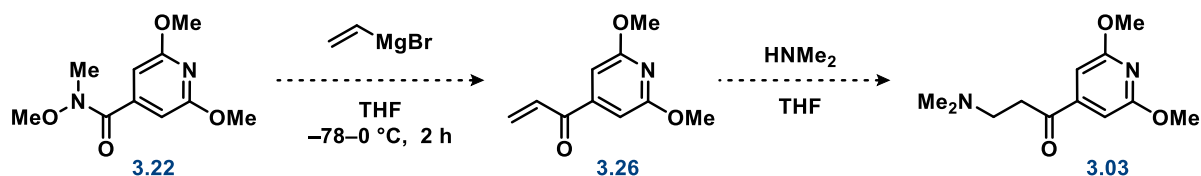
**Scheme 3.7.** Proposed mechanism towards propanone Mannich base by-product **3.25**.

Despite some literature precedence for the use of the Mannich reaction to generate pyridyl  $\beta$ -aminoketones from acetylpyridine substrates, this reaction appeared to be unsuitable for our specific system and therefore this route was not pursued any further.

### 3.2.2.2. Pathway B

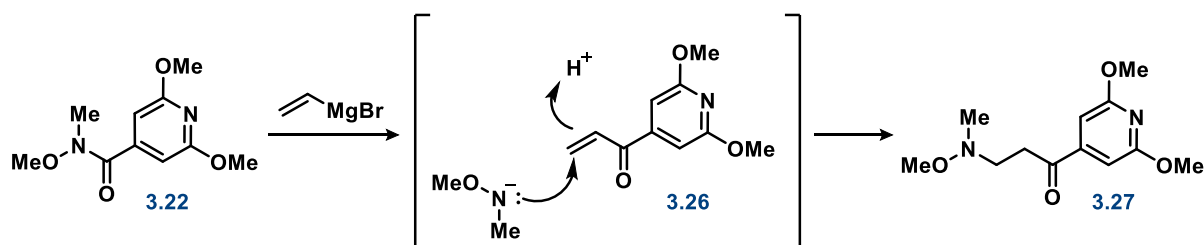
The alternative route identified to access the northern subunit was through use of a Michael addition between dimethylamine to a reactive vinyl-pyridylketone intermediate **3.26** (**Scheme 3.8**). Similar to Pathway A, this intermediate could also be accessed *via* Grignard addition to the key Weinreb amide **3.22**.





**Scheme 3.8.** The proposed towards northern subunit **3.03** utilising Pathway B.

Initial attempts at isolating vinylketone intermediate **3.26** proved to be difficult. Although **3.26** appeared to be formed when monitoring the reaction between **3.22** and vinyl magnesiumbromide by LCMS, it degraded following aqueous workup and was unable to be isolated. On further inspection of the literature, it was revealed that a common by-product resulting from this method was  $\beta$ -aminoketone **3.27** (Scheme 3.9) formed as a result of conjugation of the liberated *N,O*-dimethylhydroxylamine to the highly reactive pyridyl-vinylketone.<sup>[19,20]</sup> With this in mind as a possible reason for the loss of **3.26**, additional trials of this reaction were quenched at  $0$  °C with 2 M HCl to circumvent the formation of this by-product, however the desired pyridyl-vinylketone remained unable to be isolated. Given the difficulty in isolating vinylketone **3.26**, it was hypothesised that this system was too unstable and therefore in a final attempt at this pathway, an excess of dimethylamine was reacted with vinylketone *in situ* in a similar fashion to the work described by Gomtsyan and co-workers.<sup>[21]</sup> Unfortunately, this reaction attempt led to a complex mixture of products and the desired pyridyl  $\beta$ -aminoketone **3.03** was not isolated following chromatography.



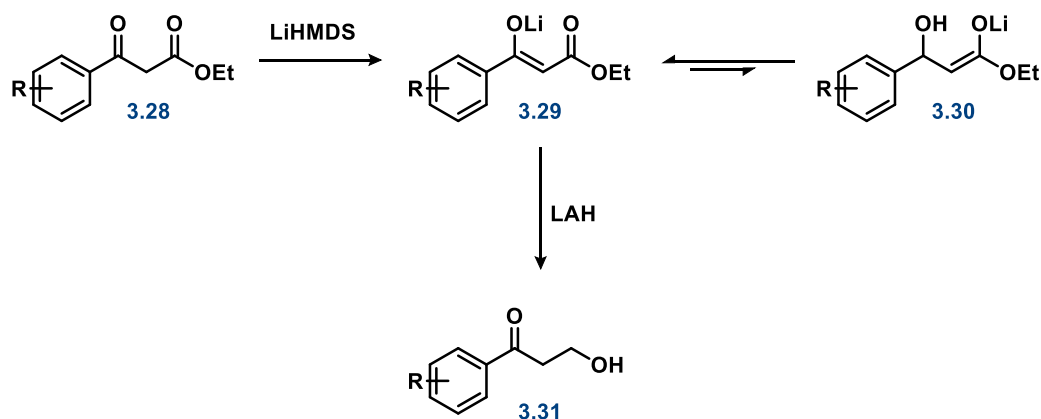
**Scheme 3.9.** Mechanism towards the formation of possible by-product **3.27** during vinyl-Grignard addition to Weinreb amide **3.22**.

Given the difficulties that were encountered in exploring this pathway, other synthetic strategies were prioritised, however a recent publication from the Denny group has in fact confirmed that Pathway B was the route that they used to access the northern subunit of TBAJ-587, which in their hands afforded **3.03** from **3.22** in 57% yield.<sup>[5]</sup>

### 3.2.2.3. Pathway C

Pathway C was inspired by a publication authored by Sivagurunathan *et al.*,<sup>[22]</sup> who described a one-pot process for the chemoselective reduction of esters in aryl  $\beta$ -keto esters. In this article, the authors

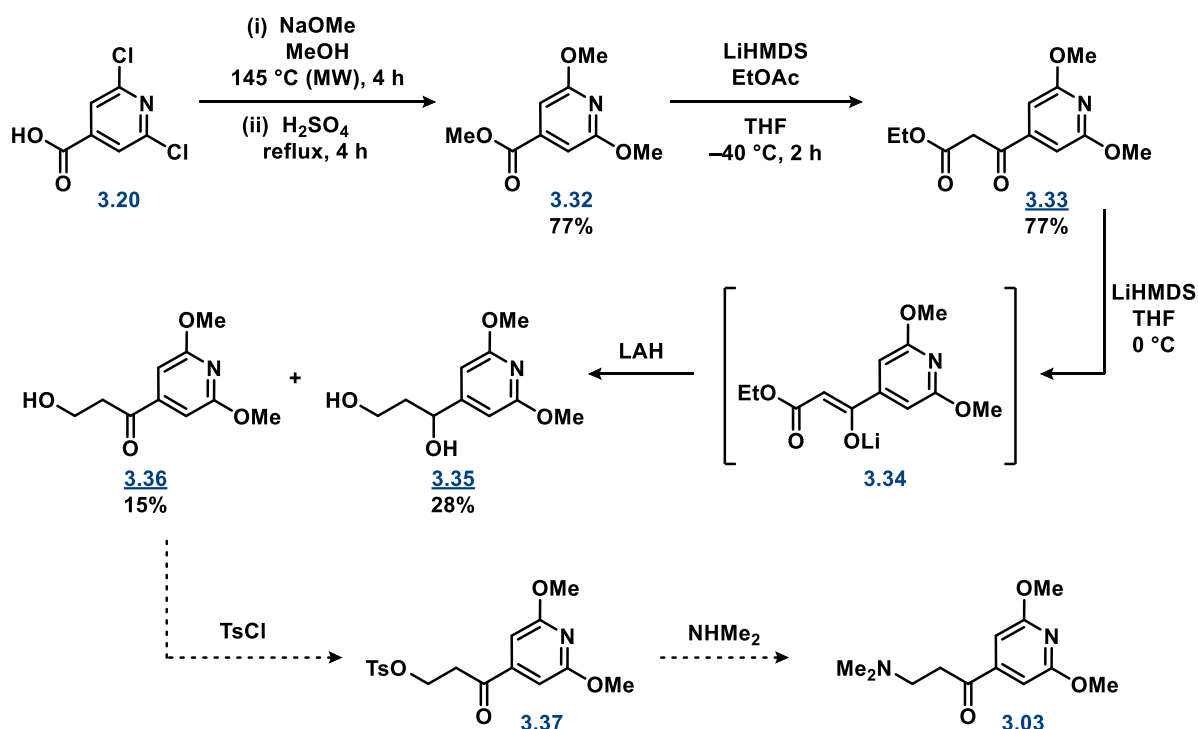
demonstrated that the reactivity of the ketone functionality could be greatly reduced by forming the aryl stabilised ketone enolate **3.29** prior to reduction (**Scheme 3.10**).



**Scheme 3.10.** The chemoselective one-pot reduction procedure of esters in aryl  $\beta$ -keto esters as reported by Sivagurunathan *et al.*<sup>[22]</sup>

To explore the suitability of this protocol for our system, the requisite pyridyl  $\beta$ -keto ester intermediate **3.33** was synthesised in three steps (**Scheme 3.11**). Starting from intermediate **3.20**, an  $S_NAr$  reaction under microwave irradiation followed by esterification afforded methoxylated intermediate **3.32** in good yield. A subsequent Li-mediated Claisen condensation between EtOAc and **3.32** furnished the requisite  $\beta$ -keto ester **3.33** in 77% yield.

Although the scope reported by Sivagurunathan *et al.* included a variety of substituted phenyl and pyridyl  $\beta$ -keto esters, in our hands this procedure suffered from poor yield and poor selectivity (2:1 ratio of **3.35** to **3.36**). Considering the suboptimal yield of intermediate **3.36** and the increased length of this overall reaction sequence, this strategy was deprioritised to give way to Pathway D.



**Scheme 3.11.** Pathway C trialled towards the northern subunit **3.03**.

#### 3.2.2.4. Pathway D

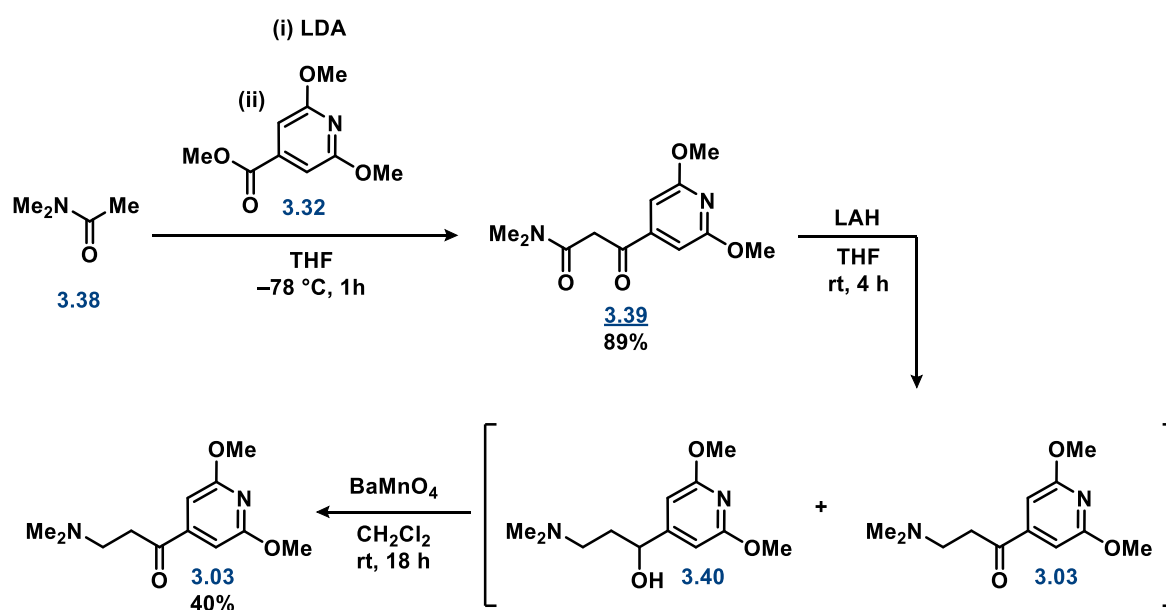
The final strategy identified towards northern subunit **3.03** is illustrated in **Scheme 3.12**. This pathway was in part inspired by Pathway C, however instead of installing the dimethylamine functionality at the final stage, this strategy could directly afford the tethered dimethylamine group *via* reduction of a  $\beta$ -ketoamide intermediate (**3.39**). The key  $\beta$ -ketoamide intermediate **3.39** could be accessed in very good yield from the condensation reaction between dimethylacetamide **3.38** and methoxylated intermediate **3.32** (previously synthesised in Pathway C).

Further analysis of **3.39** by <sup>1</sup>H NMR (CDCl<sub>3</sub>) found that this intermediate predominantly existed in its enol form **3.41** (*ca.* 1:4 ratio of keto to enol, **Figure 3.6**) which is due to stabilisation of the enol by the extended conjugated  $\pi$ -system and the intramolecular hydrogen-bond.<sup>[23]</sup> It is well established that interconversion between keto-enol tautomers of  $\beta$ -dicarbonyls is slow on the <sup>1</sup>H NMR time-scale<sup>[24]</sup>, hence why separate resonances are observed for each tautomer. On the other hand, proton exchange between the different enol forms (**3.41a** and **3.41b**) is too fast to be distinguishable on the <sup>1</sup>H NMR time-scale and therefore an average of these peaks is observed.

Considering there was little precedent for chemoselective amide reduction in the presence of ketones reported in the literature, it was decided to reduce **3.39** without prioritising selectivity as it was anticipated that the resulting amino alcohol **3.40** could be easily re-oxidised to the ketone under mild conditions. Interestingly, when analysing the crude reaction mixture after reduction with lithium

aluminium hydride (LAH), a 1:2 ratio of amino alcohol **3.40** to amino ketone **3.03** was observed. This observation suggests that some protection of the  $\beta$ -keto group may have been afforded as a result of this intermediate predominantly existing as the enol tautomer **3.41a**. Indeed selectivity in this manner has been previously demonstrated for  $\beta$ -dicarbonyl compounds, with electron withdrawing groups being shown to stabilise the adjacent enol form and thus offering protection.<sup>[25]</sup>

Subsequent oxidation of the amino alcohol intermediate **3.40** in the crude reaction mixture was performed using barium manganate ( $\text{BaMnO}_4$ ), which successfully afforded the requisite pyridyl  $\beta$ -aminoketone **3.03** in 40% yield over two steps. On further analysis of this key intermediate, it was observed that it was prone to degradation, presumably as a result of deamination ( $\beta$ -elimination), which is known to occur with  $\beta$ -aminoketones.<sup>[26]</sup> To limit degradation, intermediate **3.03** was freshly prepared prior to the final coupling reaction between the northern and southern subunits, however it could be envisaged that formation of the hydrochloride salt may potentially enhance the stability and shelf-life of this intermediate, although this was not attempted.



**Scheme 3.12.** Pathway D towards the northern subunit **3.03**.

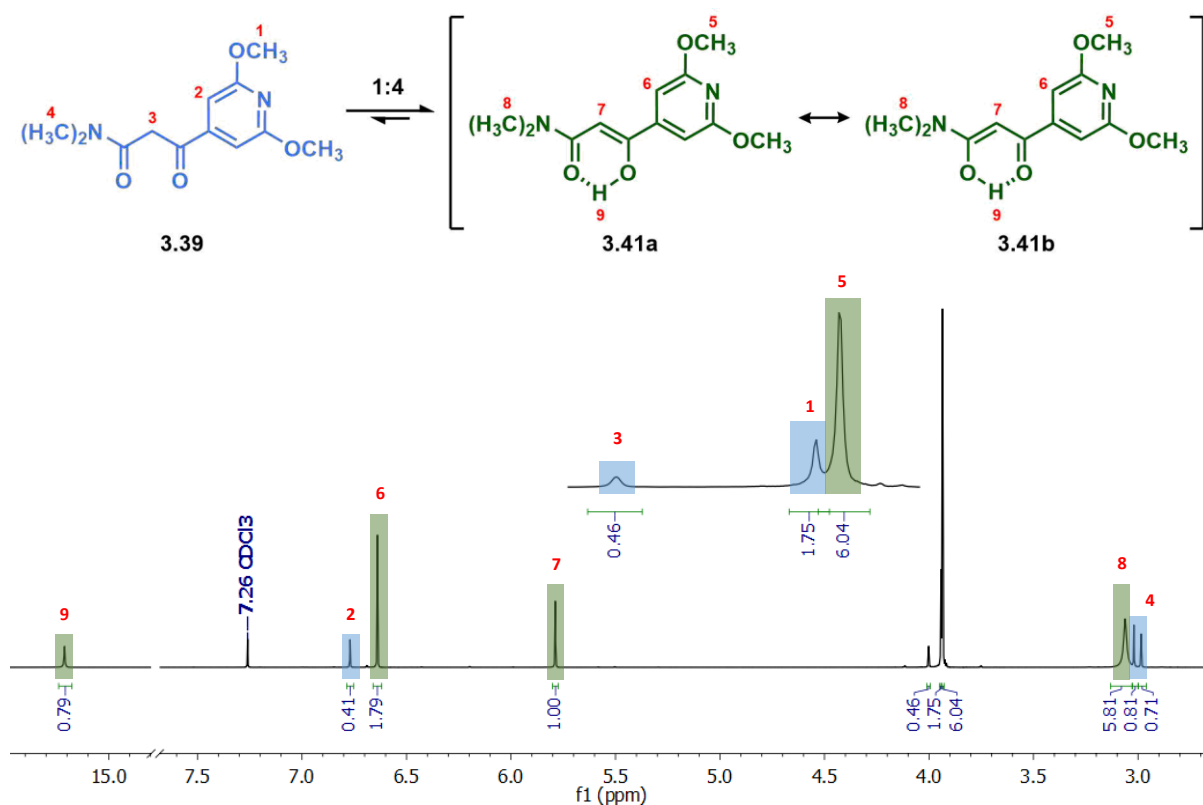
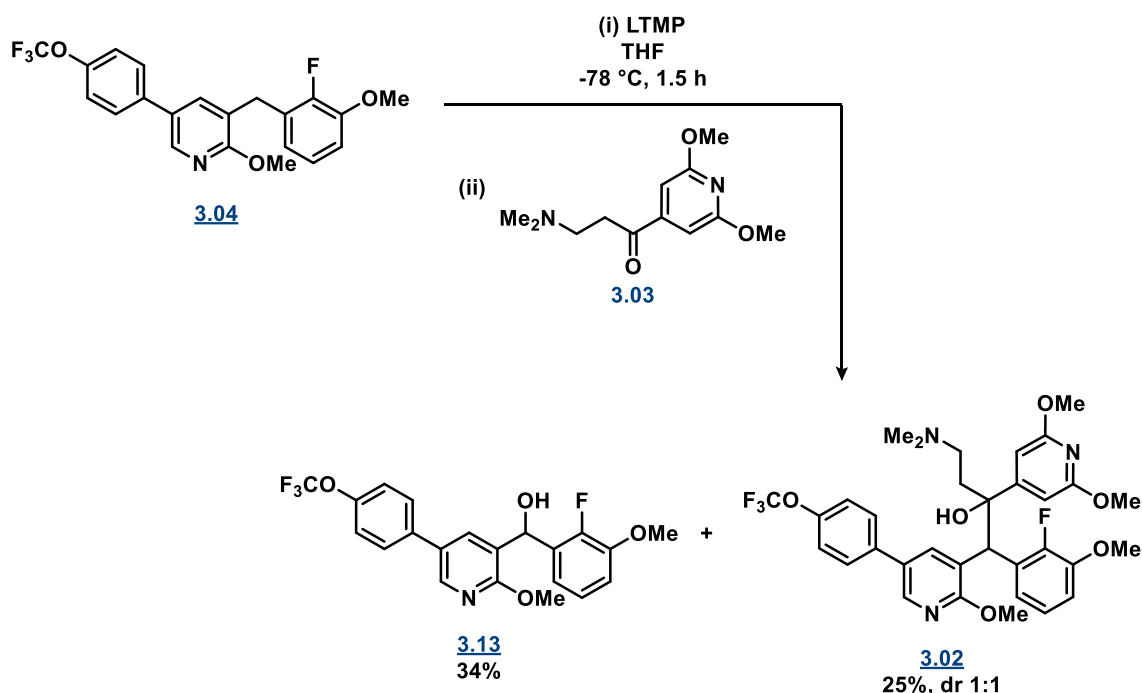


**Figure 3.6.** Intermediate **3.39** predominantly exists in its enol form (**3.41**) in CDCl<sub>3</sub> as confirmed by <sup>1</sup>H NMR.

### 3.2.3 Addition between southern and northern subunits

With both components now synthesised, model analogue **3.02** was prepared through LTMP-mediated addition of the southern subunit **3.04** to the northern subunit **3.03** which afforded the requisite analogue **3.02** in 25% yield. Although low yielding, unreacted starting material was also recovered. Interestingly, diaryl alcohol intermediate **3.13** was also regenerated as a by-product (34% yield), which contributed to the low yield of desired product **3.02**. As for the previous analogues described in Chapter 2, model derivative **3.02** was formed as a racemic mixture of four stereoisomers which were subsequently separated into two diastereomer pairs using preparative HPLC, denoted as A (first to elute) and B (second to elute).



**Scheme 3.13.** Addition reaction of southern subunit **3.04** to northern subunit **3.03** to give the model analogue **3.02**.

Prior to determining the MIC<sub>90</sub>, a preliminary drug inhibition screen was performed by our collaborators at the Centenary Institute (Sydney) for both diastereomers. As described previously in Chapter 2, *M.tb* (H37Rv strain) was incubated in the presence of the test sample at 1, 10 and 100 µM, followed by using the REMA assay to determine the percentage survival of the bacteria<sup>[27]</sup>. As shown in **Figure 3.7**, the results from this screen revealed that diastereomer B was the most active diastereomer (100% inhibition of *M.tb* at 1 µM) and therefore this diastereomer was selected for further *in vitro* assessment. Subsequent measurement of the MIC<sub>90</sub> for this analogue demonstrated very potent activity of 1.09 µM. Considering **3.02** was tested as a racemic mixture of two stereoisomers (presumably *RR* and *SS*), it was anticipated that the pure eutomer (*SS*, identical absolute configuration to BDQ and TBAJ-587) of this analogue would have activity close to that of BDQ (MIC<sub>90</sub> = 0.54 µM). Given that potent activity was confirmed for this representative derivative, a larger series of pyridine-TBAJ-587 hybrids were planned to further explore the SAR of this novel compound class.

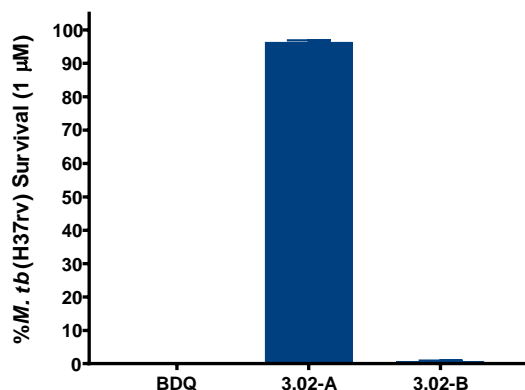


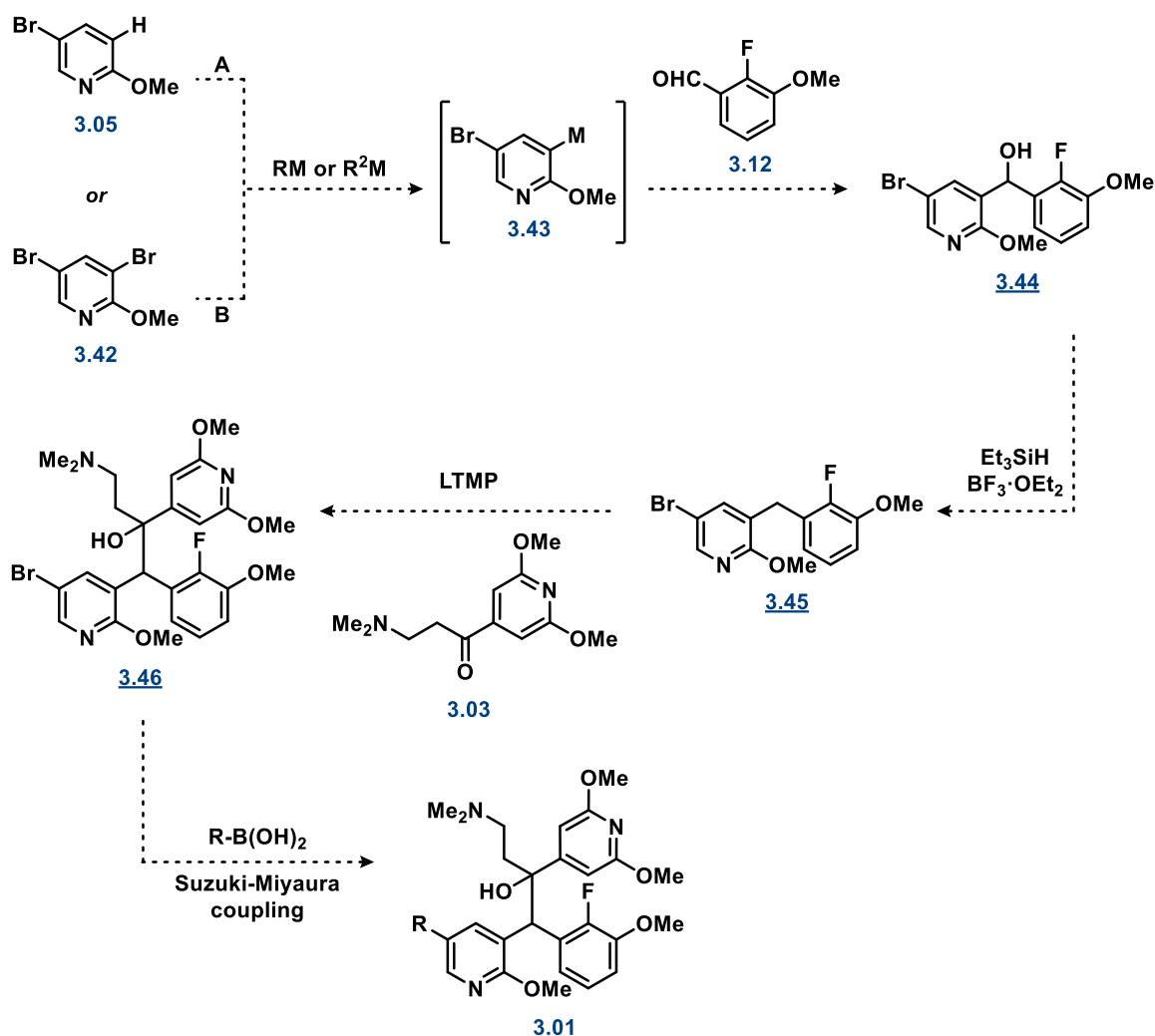
**Figure 3.7.** Preliminary drug inhibition screen of the A and B diastereomers of model compound **3.02**, indicating percentage survival of *M.tb* at 1  $\mu$ M.

### 3.3 Synthesis of expanded series TBAJ-587 pyridine analogues

Considering the pathway developed to synthesise model analogue **3.02** was not optimised, time was invested into improving the synthetic route prior to scaling up to synthesise the entire series.

#### 3.3.1 Optimised route to southern subunit

To circumvent the issues observed during the synthesis of this subunit in **Section 3.2.1**, an optimised pathway was proposed. As shown in **Scheme 3.14**, this synthetic pathway would introduce the aryl ring at the C5-position of the pyridine core after addition of the benzaldehyde at the C3-position, preventing the regioselectivity issues experienced previously during the Li-mediated addition of the B ring. Additionally, this route would also facilitate the late stage derivatisation of the pyridine core from intermediate **3.46**, therefore providing a more efficient means to prepare a small library of analogues.

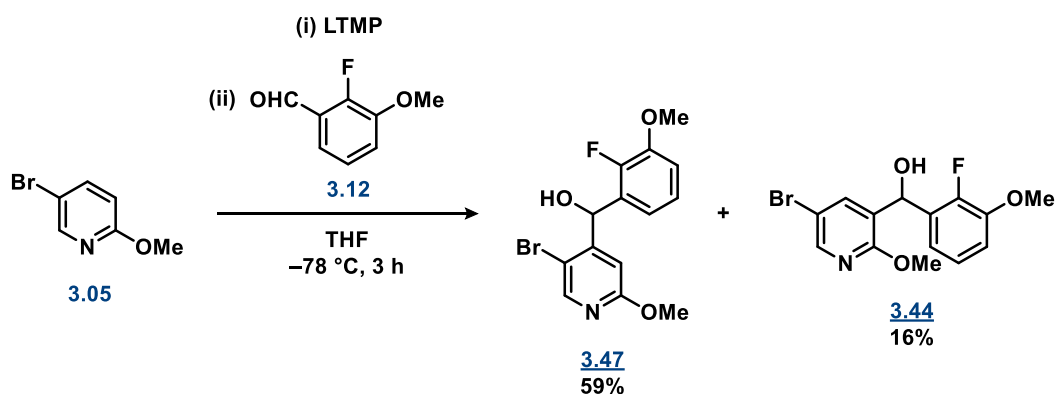


**Scheme 3.14.** Proposed route optimisation towards the southern subunit **3.45** to be used for the efficient synthesis of a library of analogues of type **3.01**.

### 3.3.1.1. Directed *ortho*-lithiation

Given that a small quantity of 5-bromo-2-methoxypyridine (**3.05**) still remained from the synthesis described in **Scheme 3.4** (**Section 3.2.1**), the first reaction trialled towards intermediate **3.45** was an LTMP-mediated DoM strategy (**Scheme 3.15**). Despite the methoxy group generally being regarded as a better directing group than the bromo group<sup>[28,29]</sup>, in the case of **3.05** the increased acidity of the pyridine at the C4-position<sup>[30,31]</sup> combined with the inductive electron withdrawing effect of the adjacent bromo group meant that a mixture of regioisomers were produced, with the major product resulting from C4 addition to **3.05** (59% of **3.47** versus 16% of **3.44**).





**Scheme 3.15.** Directed *ortho*-metalation pathway trialled from 5-bromo-2-methoxypyridine (**3.05**) towards **3.44**.

The identity of each product from this reaction was confirmed using a combination of the  $^1\text{H}$  NMR and 2D NMR (HMBC). As shown in the  $^1\text{H}$  NMR spectra of both isomers in  $\text{CDCl}_3$  (**Figure 3.8**), the pyridine protons on C6 and C4 in regioisomer **3.44** display  $J_{\text{meta}}$  coupling with each other as expected ( $J = 2.5$  Hz), whereas regioisomer **3.47** has an absence of splitting between the pyridine protons. Furthermore, the C3 proton of regioisomer **3.47** is significantly shifted upfield in relative to the C3 proton of regioisomer **3.44** due to the adjacent electron donating methoxy group. Additional HMBC experiments also supported these assignments, with **3.44** displaying a unique  $^3J$  C-H cross-peak between H7 and C2, and **3.47** displaying a unique  $^3J$  C-H cross-peak between H7 and C5 (refer to **Appendix A2.1**).

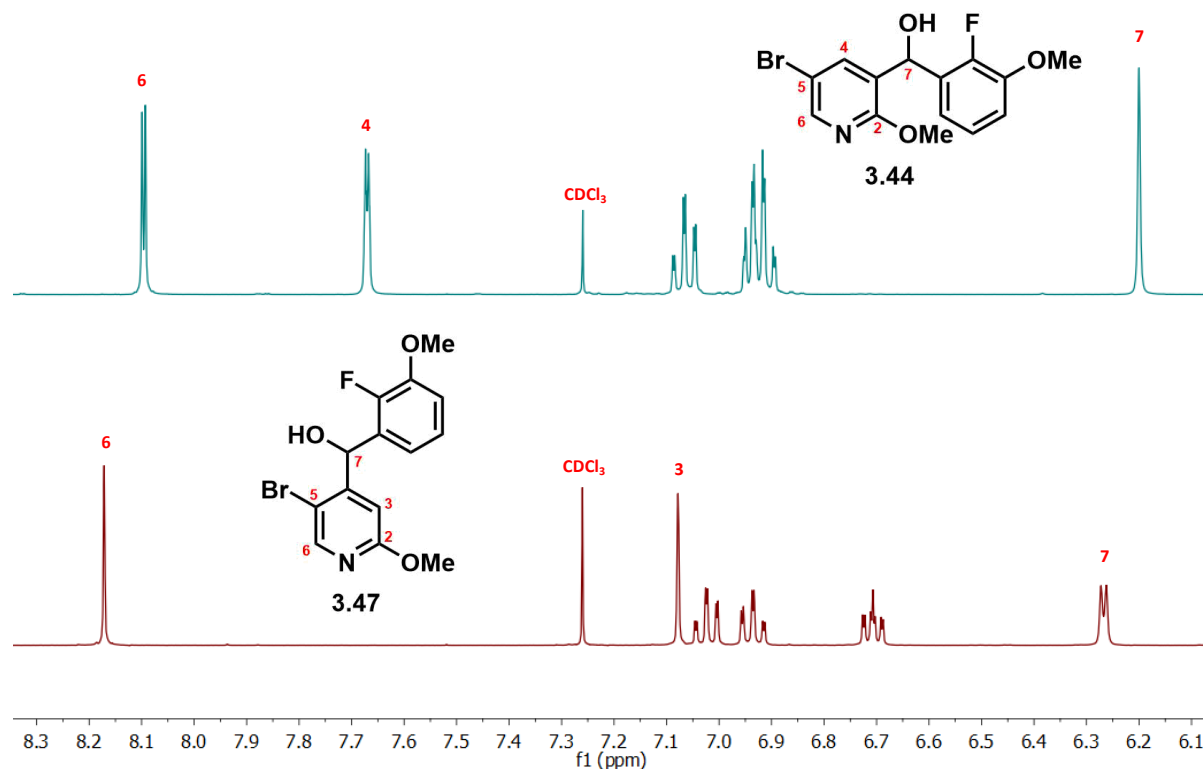
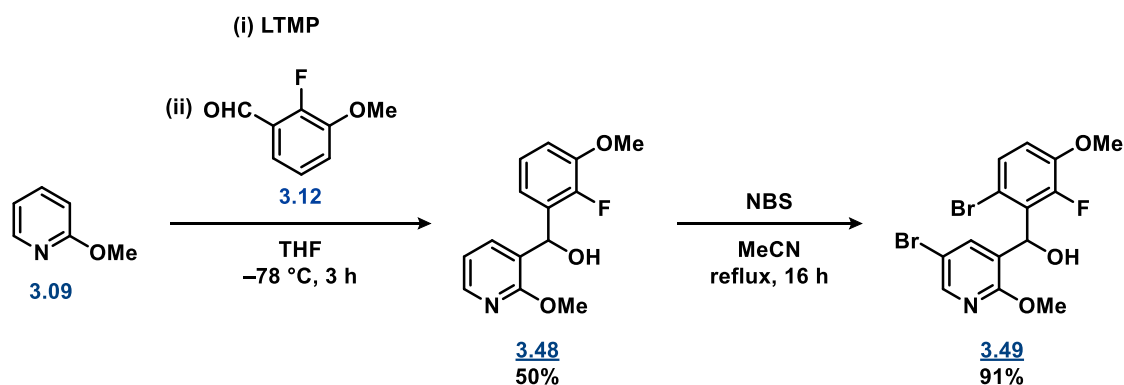


**Figure 3.8.** Structural identification of regioisomers **3.44** and **3.46** using  $^1\text{H}$  NMR.

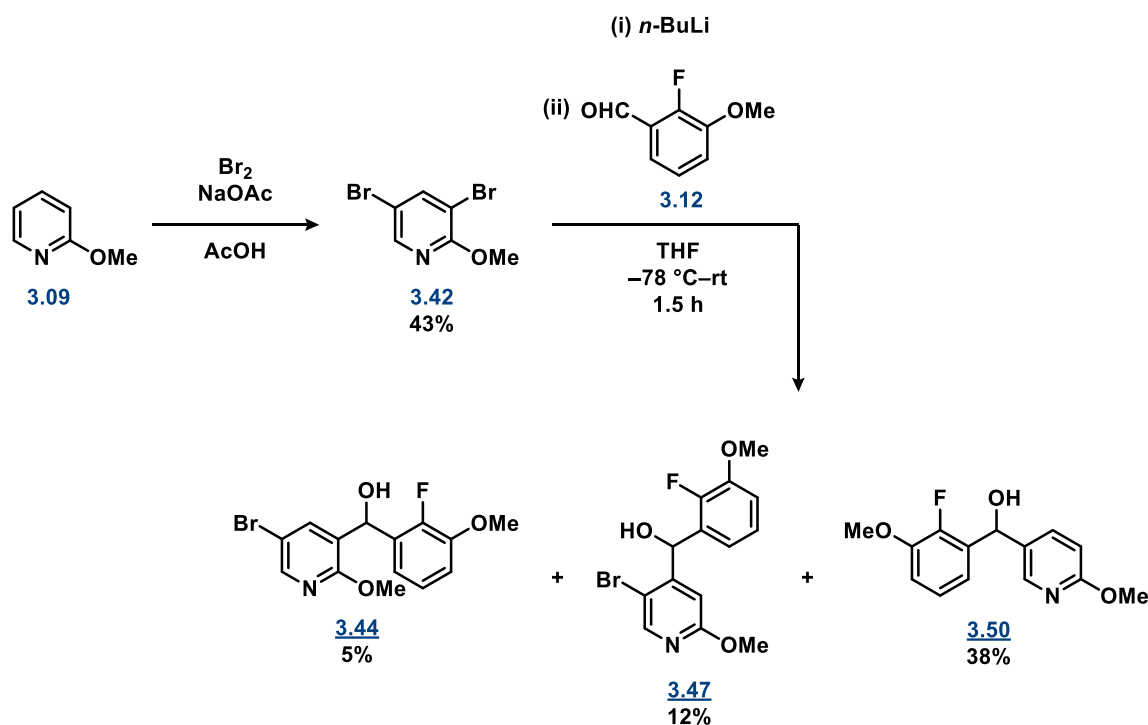
Due to the regioselectivity issues encountered when starting from **3.05**, the alternative sequence starting from 2-methoxypyridine (**3.09**) detailed in **Scheme 3.16** was explored. In this pathway, the pyridine was successfully functionalised with the benzaldehyde at the C3 position to give intermediate **3.48** in 50% yield, however perhaps not surprisingly bromination in the subsequent step was not selective for the pyridine ring, with a bromo group also installed *para* to the phenyl methoxy group to give di-bromo product **3.49**.



**Scheme 3.16.** Attempted synthesis of **3.44** using a directed *ortho*-metalation pathway starting from 2-methoxypyridine (**3.09**).

### 3.3.1.2. Halogen-metal exchange

An alternative method explored to access intermediate **3.44** was *via* halogen-metal exchange from dibromopyridine **3.42**. Despite there being literature precedence for lithiation at the C3 position with the use of *n*-BuLi<sup>[32,33]</sup>, in our hands this reaction repeatably provided only trace amounts of desired product **3.44** as observed by  $^1\text{H}$  NMR (**Scheme 3.17**). Instead, this reaction was found to be selective for exchange at the C5 position, with further *in situ* lithiation at C3 resulting in the isolation of des-bromo intermediate **3.50** as the major product following aqueous workup (refer to **Appendix A2.2**). Interestingly, 12% of intermediate **3.47** was also isolated (confirmed by comparison to the previously solved  $^1\text{H}$  NMR, **Figure 3.8**) as a result of DoM at the pyridine C4 position followed by Li/Br exchange and protonation at the C3 position.

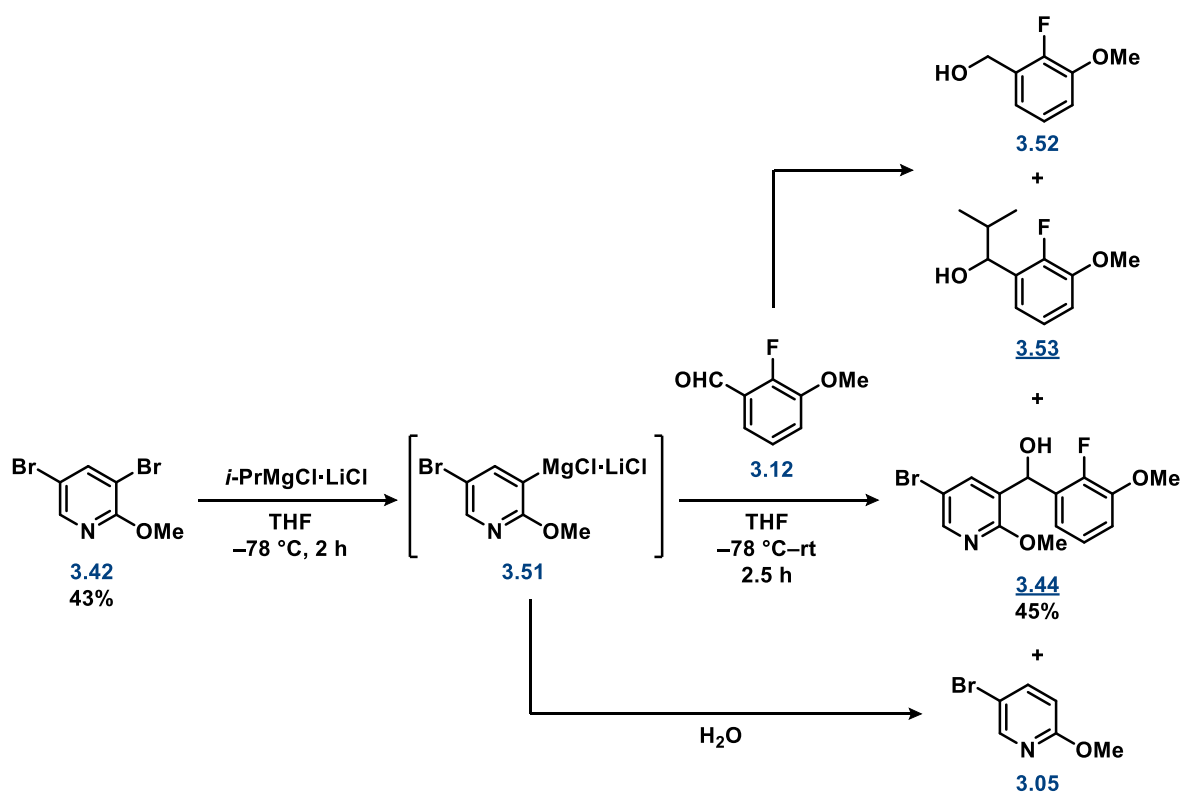


**Scheme 3.17.** Attempted synthesis of **3.44** from 3,5-dibromomethoxypyridine (**3.42**) using halogen-metal exchange with *n*-BuLi.

Curious to investigate whether regioselectivity for the C3 position was possible from **3.42**, an alternative approach utilising the Grignard reagent *i*-PrMgCl·LiCl (Turbo-Grignard) was explored (**Scheme 3.18**). The use of this reagent was first introduced by the group of Knochel<sup>[34]</sup> as a very efficient reagent for halogen-Mg exchange, which was also demonstrated to be particularly suitable for electron poor *N*-heterocyclic compounds such as pyridines. Following a literature reported procedure<sup>[35]</sup>, Turbo-Grignard was added to **3.42** at  $-78\text{ }^\circ\text{C}$  and reacted for 2 h. Following this initial metalation time, benzaldehyde **3.12** was added dropwise to the reaction mixture, which was then allowed to warm to room temperature after 30 min and reacted for a total time of 12 h. On analysis of the crude reaction mixture by  $^1\text{H}$  NMR, complete regioselectivity for the desired product **3.44** was observed (confirmed by comparison to previously solved  $^1\text{H}$  NMR, **Figure 3.8**), indicating that the methoxy group was able to direct exchange though complexation with the Grignard reagent.<sup>[36]</sup> In addition to product, unreacted starting material **3.42** was also isolated.

In a repeated attempt of this reaction, to aid the initial metalation process the reaction was allowed to warm from  $-78$  to  $0\text{ }^\circ\text{C}$  after addition of the Grignard, followed by cooling again to  $-78\text{ }^\circ\text{C}$  prior to the addition of the benzaldehyde. Interestingly, despite the starting material being completely consumed using these modified reaction conditions, the overall isolated yield of desired product **3.44** was not increased. On further analysis of the crude reaction mixture by  $^1\text{H}$  NMR, it was found that although unreacted starting material no longer remained, an increase in des-brominated starting

material **3.05** was discovered. Additionally, by-products **3.52** and **3.53** were also discovered as a result of reduction/ $\beta$ -hydride transfer (**3.52**) and competitive addition of the Grignard isopropyl group (**3.53**) to the benzaldehyde. These reaction products suggested that although all starting material was reacting with the Grignard in the first step to sufficiently form metalated intermediate **3.51**, complete reaction with the benzaldehyde was not occurring either due to insufficient benzaldehyde remaining to react as a result of by-product formation, or insufficient reactivity of the Grignard towards the benzaldehyde. In a subsequent attempt of this reaction, increasing the amount of benzaldehyde **3.12** from 1.1 to 1.5 equivalents had no effect on the yield, therefore suggesting that insufficient reactivity of **3.51** towards the benzaldehyde was the most likely cause.



**Scheme 3.18.** Synthesis of **3.44** from 3,5-dibromomethoxypyridine (**3.42**) using halogen-metal exchange with *i*-PrMgCl·LiCl.

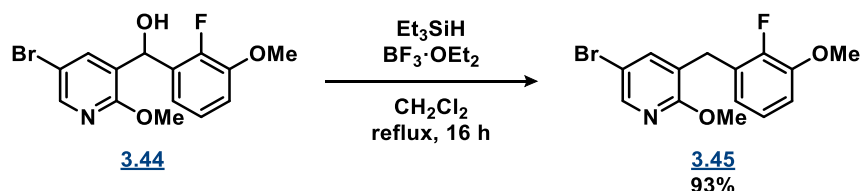
**Table 3.3.** Conditions trialled during the metalation of 3,5-dibromopyridine (**3.42**) using halogen-metal exchange with *i*-PrMgCl·LiCl.

| Entry | Metalation conditions | Ratio of <b>3.44</b> : <b>3.42</b> : <b>3.05</b> | Yield of <b>3.44</b> |
|-------|-----------------------|--|----------------------|
| 1     | -78 °C, 2 h           | 53:42:5  | 43%                  |
| 2     | -78 °C → 0 °C, 2 h    | 70:3:30  | 45%                  |

Considering that the original metalation conditions (entry 1) allowed recovery of unreacted starting material **3.42** with no significant change to the yield of desired product **3.44**, all remaining attempts

of this reaction were carried out with these original conditions and no further efforts at optimising this reaction was trialled.

With intermediate **3.44** now in hand, silane reduction progressed smoothly to give optimised southern subunit **3.45** in excellent yield.

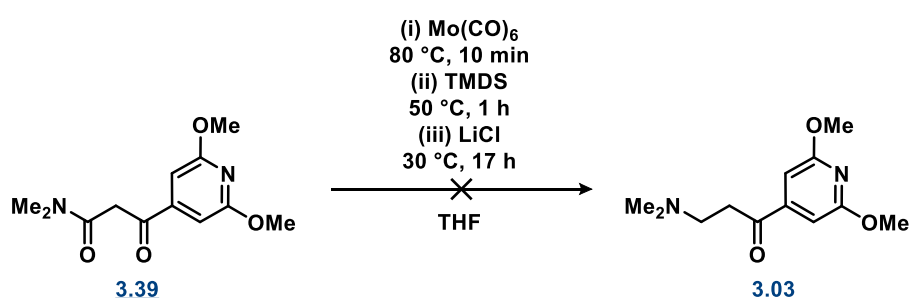


**Scheme 3.19.** Silane-mediated reductive deoxygenation of intermediate **3.44** to complete the optimised southern subunit **3.45**.

### 3.3.2 Optimised route to northern subunit

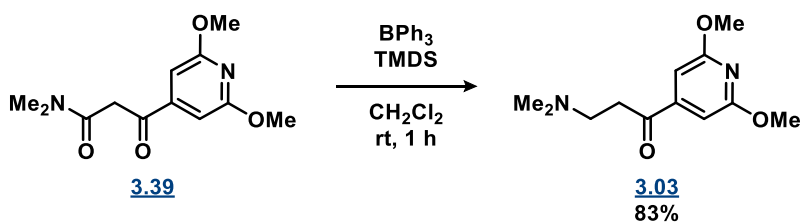
To improve the efficiency of the pathway towards the northern subunit, we decided to further investigate the limited number of literature protocols that described the chemoselective reduction of amides in the presence of a ketone.

In our initial attempt we followed a protocol by Tinnis and co-workers<sup>[37]</sup> which described the use of tetramethyldisiloxane (TMDS) in combination with catalytic  $\text{Mo}(\text{CO})_6$  to selectively reduce tertiary amides in the presence of ketones and aldehydes. Despite reporting two examples where selective amide reduction was achieved in molecules which also possessed a ketone functionality (73 and 82% yield), in our hands starting material remained unreacted with no evidence of conversion to the desired product (**Scheme 3.20**).



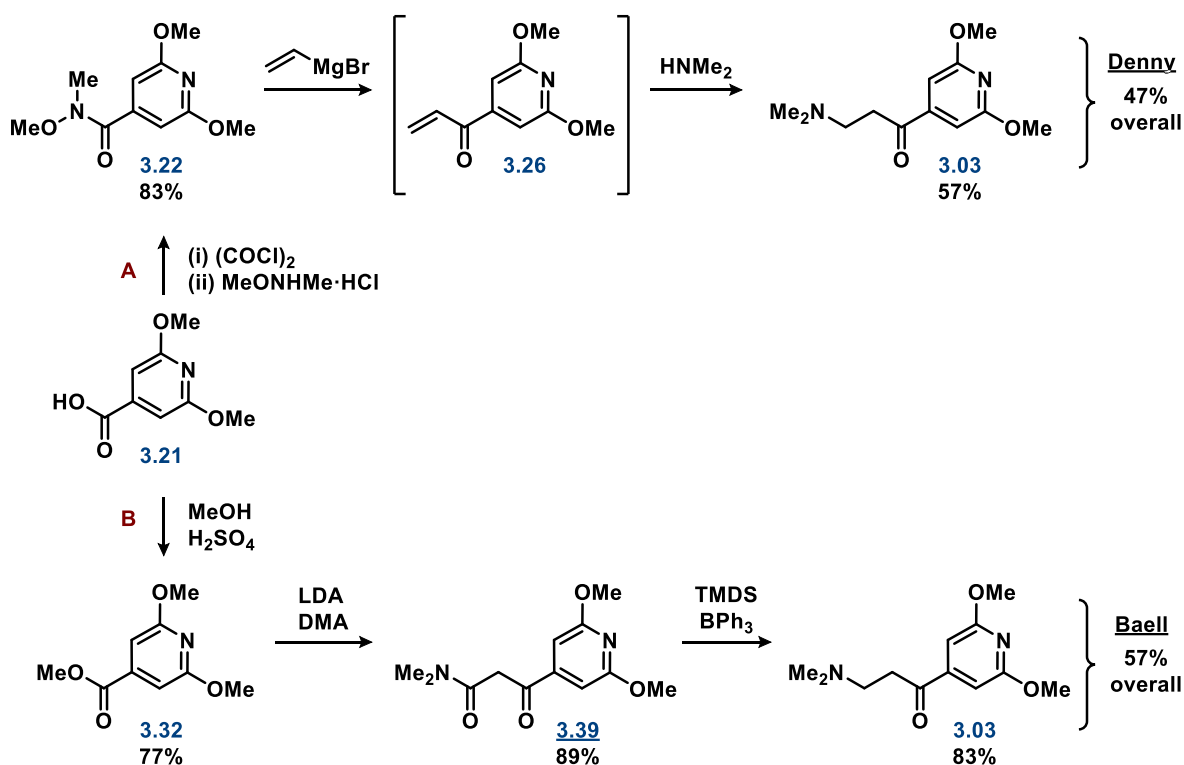
**Scheme 3.20.** Attempted chemoselective reduction of **3.39** using the protocol as reported by Tinnis *et al.*<sup>[37]</sup>

In a separate procedure reported by the group of Okuda<sup>[38]</sup>, 10 mol% of triphenylborane ( $\text{BPh}_3$ ) was used to catalyse the reduction of tertiary amides with hydrosilanes to provide the respective amines with high chemoselectivity in the presence of ketones. Much to our delight, using this protocol with TMDS as the hydride source selectively converted **3.39** to **3.03** in very good yield (83%) within 1 h (**Scheme 3.21**).



**Scheme 3.21.** The chemoselective reduction of **3.39** to **3.03** using TMDS and catalytic BPh<sub>3</sub>.

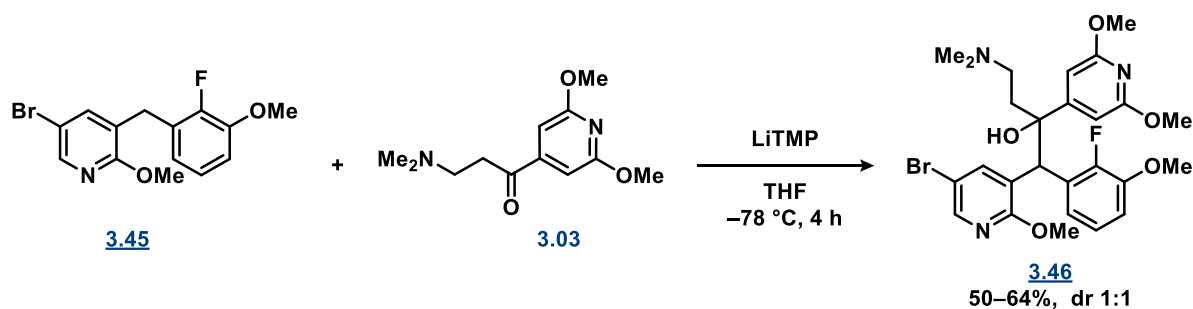
In comparison to the recently published Denny group procedure that reported the synthesis of **3.03** in an overall yield of 47%<sup>[5]</sup>, our optimised sequence produced **3.03** in a greater yield of 57% over 3-steps (**Scheme 3.22**). Additionally, this pathway is much more robust as it avoids progressing through the highly reactive vinylketone intermediate.



**Scheme 3.22.** The comparison between A) The Denny reported pathway towards **3.03** (47% overall yield), and B) our optimised pathway towards **3.03** (57% overall yield).

### 3.3.3 Addition and synthesis of a library of hybrid analogues

With the synthesis of the two requisite subunits **3.03** and **3.45** now optimised, LTMP mediated addition was then employed to access intermediate **3.46** in preparation for derivatisation. Using similar reaction conditions to those previously utilised to synthesise the model compound **3.02**, intermediate **3.46** was prepared in moderate yield (50–64%) as a 1:1 mixture of diastereomers (**Scheme 3.23**). Interestingly, in contrast to **Scheme 3.13** (*vide supra*) towards model compound **3.02**, no diarylalcohol **3.44** (analogous to **3.13**) was observed as a by-product during this reaction.

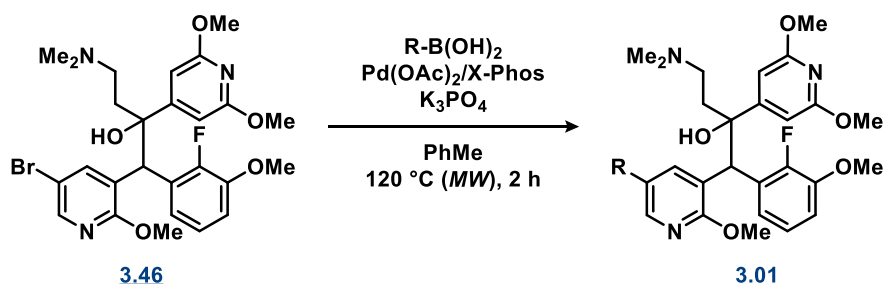


**Scheme 3.23.** Addition reaction of southern subunit **3.45** to northern subunit **3.03** to give key intermediate **3.46**.

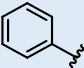
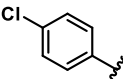
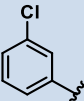
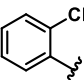
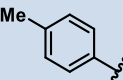
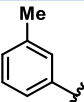
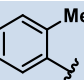
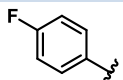
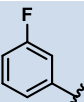
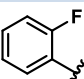
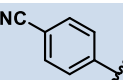
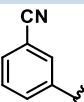
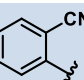
In a similar fashion to that previously described in Chapter 2, a small library of analogues were prepared from intermediate **3.46** using Suzuki–Miyaura cross-coupling with a variety of substituted phenyl boronic acids (**Table 3.4**). Judicious choice of coupling partners enabled us to explore the effects of electron withdrawing and electron donating substituents with various hydrophobicities at the *ortho*, *meta* and *para* positions on the ring. Although the SAR of C5 position on the pyridine ring had been explored in Chapter 2 for the pyridine ring A analogues of BDQ, at this stage it was unknown if a similar trend in SAR would be obtained for this series considering the change in both rings B and C.

In contrast to the Suzuki–Miyaura cross-coupling conditions established to access the previous series described in Chapter 2 (reflux, 16 h), it was discovered that reaction time could be greatly reduced for the analogues detailed in **Table 3.4** using microwave irradiation at 120 °C for 2 h (**Scheme 3.24**). Interestingly, when these conditions were used in conjunction with *para*-chlorophenylboronic acid, di-coupled product **3.67** was also observed by LCMS as a result of *in situ* Suzuki–Miyaura cross-coupling occurring between the product **3.55** and remaining boronic acid (**Scheme 3.9**). As this by-product was very difficult to separate from the desired product **3.55**, the reaction conditions were slightly modified for the chlorophenyl boronic acids, with a reduction in the amount of boronic acid used from 2 to 1.2 equivalents, and a reduction in reaction time from 2 h to 10 min, found to be optimal in limiting the amount of di-coupled by-product formed.

**Scheme 3.24.** The optimised Suzuki–Miyaura cross-coupling conditions used to synthesise hybrid analogues of type **3.01**.



**Table 3.4.** Product yields and diastereomeric ratios of all analogues of type **3.01** synthesised by Suzuki–Miyaura cross-coupling in **Scheme 3.24**.

| Entry | Compound                | R   | Yield (%) | Diastereomers A:B |
|-------|-------------------------|---|-----------|-------------------|
| 1     | <b>3.54</b>             |    | 75        | 55:45             |
| 2     | <b>3.55<sup>a</sup></b> |    | 66        | 52:48             |
| 3     | <b>3.56<sup>a</sup></b> |    | 77        | 52:48             |
| 4     | <b>3.57<sup>a</sup></b> |    | 88        | 50:50             |
| 5     | <b>3.58</b>             |    | 91        | 50:50             |
| 6     | <b>3.59</b>             |    | 91        | 50:50             |
| 7     | <b>3.60</b>             |   | 87        | 50:50             |
| 8     | <b>3.61</b>             |  | 86        | 50:50             |
| 9     | <b>3.62</b>             |  | 79        | 50:50             |
| 10    | <b>3.63</b>             |  | 85        | 50:50             |
| 11    | <b>3.64</b>             |  | 55        | 57:43             |
| 12    | <b>3.65</b>             |  | 42        | 67:33             |
| 13    | <b>3.66</b>             |  | 45        | 50:50             |

<sup>a</sup>The reaction time for these analogues was reduced to 10 min.



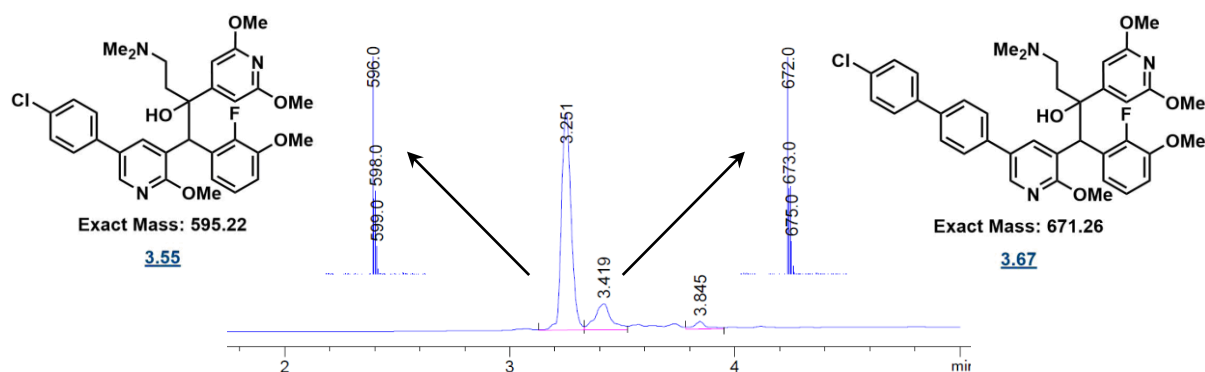
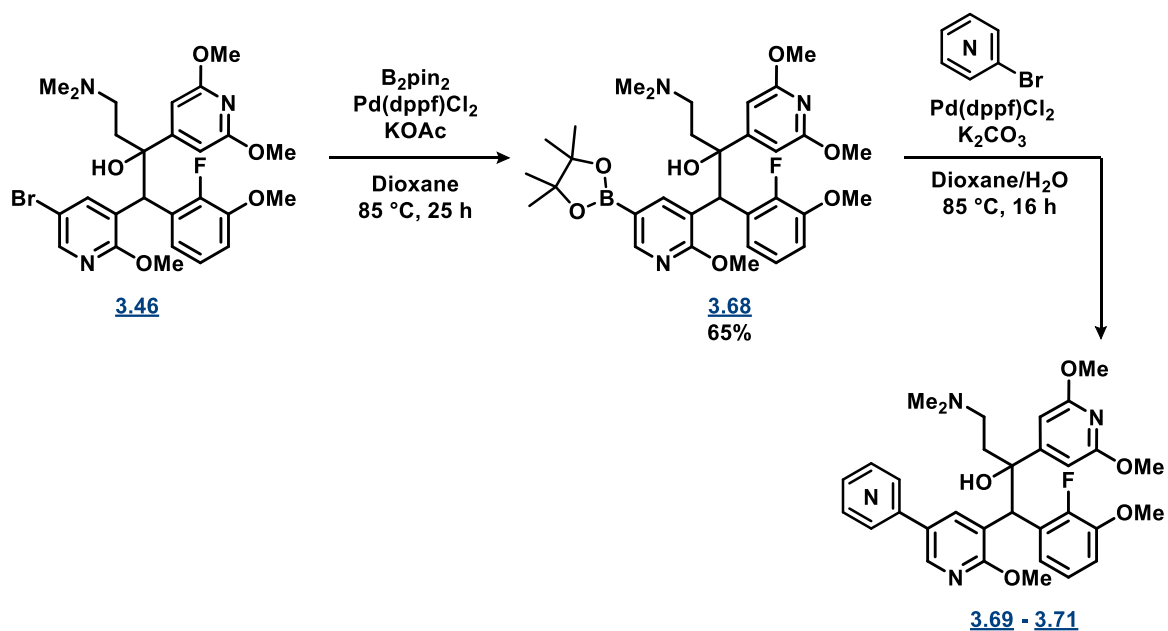


**Figure 3.9.** Di-coupled by-product **3.67** was observed by LCMS during the synthesis of **3.55** via Suzuki–Miyaura cross-coupling between **3.46** and *para*-chlorophenylboronic acid.

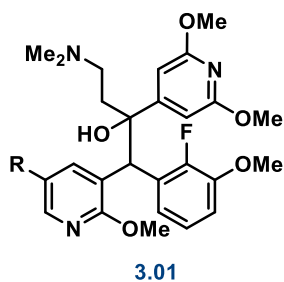
In addition to the phenyl analogues shown above, analogues containing 2-, 3- and 4-pyridinyl groups at the C5 position (**Table 3.5**) were also targeted to investigate whether heteroaromatic motifs might be tolerated in this region considering they would aid with increasing polarity and reducing lipophilicity. Initially, attempts to synthesise the 3- and 4-pyridinyl variants using the optimised Suzuki–Miyaura cross-coupling conditions in **Scheme 3.24** proved to be unsuccessful. Given the lack of reactivity, a repeated attempt at a lower temperature (80 °C) was trialed as it was hypothesised that these pyridyl boronic acids may be more prone to temperature related degradation, however this also failed to yield the desired product. As it is well documented that 2-pyridyl boronic acids are inherently unstable and cannot be employed in Suzuki–Miyaura cross-coupling reactions<sup>[39,40]</sup>, the Suzuki–Miyaura cross-coupling reaction with this boronic acid was not attempted.

Given the difficulty in accessing these pyridyl analogues from intermediate **3.46**, an alternative strategy was devised which involved formation of the boronate ester at the C5-position of the 2-methoxypyridine core. This would subsequently enable the 2-, 3- and 4-pyridinyl groups to be introduced using the respective pyridyl bromides. To this end, key intermediate **3.46** was readily converted to aryl boronate **3.68** in 65% yield, and subsequently reacted with 2-, 3- and 4-bromopyridine to afford the requisite bipyridine analogues **3.69** to **3.71** (**Table 3.5**).



**Scheme 3.25.** The synthetic pathway utilised to synthesise bipyridine analogues **3.69** to **3.71**.

**Table 3.5.** Product yields of all analogues of type **3.01** synthesised by Suzuki–Miyaura cross-coupling from boronate ester **3.68**.



| Entry | Compound    | R | Yield (%) |
|-------|-------------|---|-----------|
| 1     | <b>3.69</b> |   | 92        |
| 2     | <b>3.70</b> |   | 57        |
| 3     | <b>3.71</b> |   | 92        |

### 3.4 *In vitro* testing

#### 3.4.1 Testing protocol overview

Given the long turn-around times that were experienced during *in vitro* assessment of our previous analogue series (Chapter 2), we designed a more time-efficient testing protocol for this series of hybrid derivatives which was organised into three stages (**Figure 3.10**). In the first stage, all analogues were tested as a mixture of all four stereoisomers to generate a rank order based on potency. The only exception to this were the pyridine analogues (**3.69** to **3.71**) which were not synthesised in time for this initial phase of testing. In the second stage, all shortlisted analogues were separated into their two diastereomers (A and B) *via* preparative HPLC (performed by HangZhou, China). The potency for all separated diastereomers was then determined to allow us to select the most active diastereomer for each derivative (either A or B), as well as assisting us to select our top three analogues. In the final stage of this protocol, our top three derivatives were subjected to enantiomeric purification (performed by TCG Lifesciences, India), and each purified stereoisomer was evaluated for potency against *M. tb* to identify the eutomer.

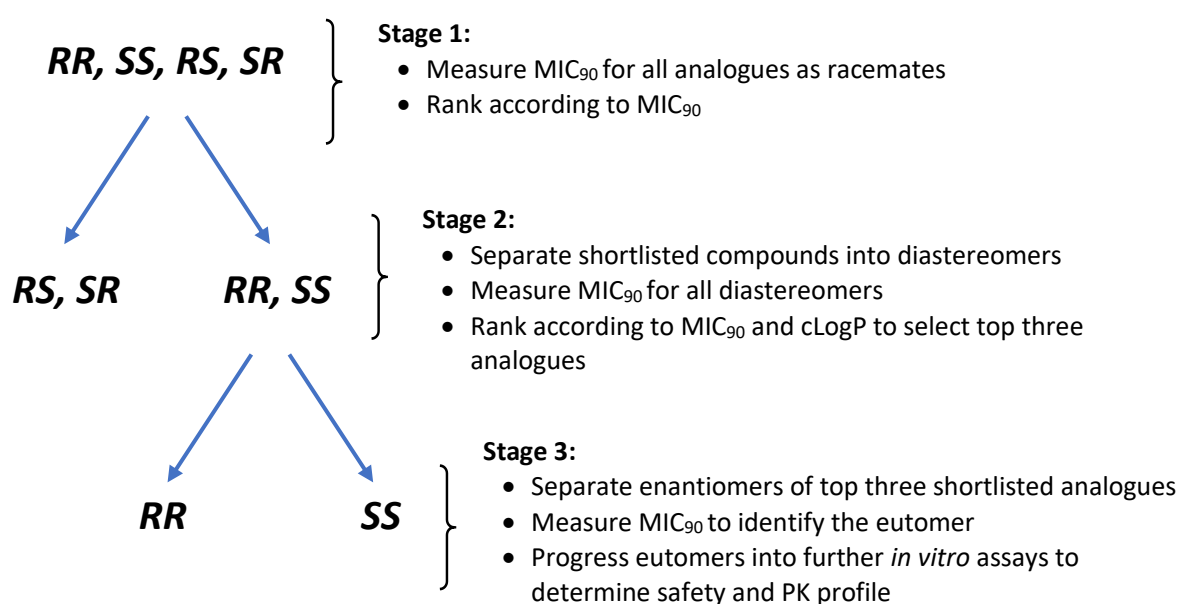


**Figure 3.10.** The three-tier testing protocol which we designed to efficiently evaluate all analogues of this series.

#### 3.4.2 Stage one

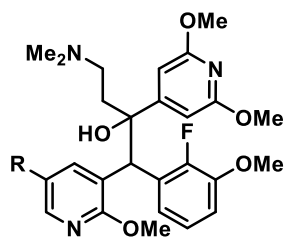
The first stage of our evaluation protocol involved determining the MIC<sub>90</sub> for the racemic mixtures (*RR*, *SS*, *SR*, *RS*) of all our synthesised analogues. Considering that we were to rank these analogues against each other, extra care had been taken during purification to maintain a relatively equal distribution of the diastereomers (**Table 3.4**, *vide supra*).

The results that we obtained from this initial testing protocol are summarised in **Table 3.6**. Firstly, in comparison to the C5 bromo derivative **3.46** (entry 1), the addition of the unsubstituted phenyl ring led to an increase in potency (2-fold, entry 2). This result thus indicated that the incorporation of the aryl group within this novel series also formed favourable interactions to the binding site as was observed with our initial BDQ pyridine analogues described in Chapter 2.

When assessing the relative effect of the substituent position on the phenyl ring, a clear trend in potency was observed. For each substituent tested, the *para*-substituted derivatives were in general the most potent (entries 3 to 6) in comparison to their *ortho* and *meta* counterparts. The only exception to this is the *meta*-cyano derivative **3.65** (entry 10) which was observed to have comparable activity to the *para*-cyano derivative **3.64** (entry 6), however this can in part be attributed to its disproportionate diastereomeric ratio (A:B = 67:33) as a result of the difficulties encountered during purification. In contrast, all of the *ortho*-substituted derivatives were the least active (*ca.* 2- to 5-fold decrease in activity, entries 11 to 14), presumably due to a penalty resulting from the sterically induced distortion in planarity between the two rings.

Lastly, when comparing the various functional groups explored at the *para*-position of the phenyl ring (entries 3 to 6), it appeared that the more lipophilic substituents led to more potent analogues, with the chloro-derivative **3.55** (entry 3) demonstrating the greatest activity against *M.tb* with an MIC<sub>90</sub> of 1.9  $\mu$ M. Although this relationship between cLogP and potency was not as clear in our previous analogue series reported in Chapter 2, this correlation is very typical of mycobacterial inhibitors due to their enhanced ability to cross the distinctively lipophilic cell wall of this bacterial genus.<sup>[41,42]</sup>

As a result of the observed trends in potency, all *para*-substituted derivatives (entries 3 to 6) and the unsubstituted phenyl derivative **3.54** (entry 2) were all selected to progress into the second phase of our evaluation protocol.

**Table 3.6.** Inhibitory activity of all pyridine analogues of type **3.01** tested as a mixture of diastereomers in stage one of our testing protocol.**3.01**Racemate (*RR*, *SS*, *RS*, *SR*)

| Entry | Compound                    | R | <i>M.tb</i> MIC <sub>90</sub> (μM) <sup>a</sup> | cLogP |
|-------|-----------------------------|---|---|-------|
| 1     | <a href="#"><u>3.46</u></a> |   | 10.8 ± 1.8                                      | 4.43  |
| 2     | <a href="#"><u>3.54</u></a> |   | 5.7 ± 0.0                                       | 5.42  |
| 3     | <a href="#"><u>3.55</u></a> |   | 1.9 ± 0.1                                       | 6.14  |
| 4     | <a href="#"><u>3.58</u></a> |   | 3.7 ± 0.3                                       | 5.92  |
| 5     | <a href="#"><u>3.61</u></a> |   | 4.3 ± 0.3                                       | 5.57  |
| 6     | <a href="#"><u>3.64</u></a> |   | 6.0 ± 0.1                                       | 4.88  |
| 7     | <a href="#"><u>3.56</u></a> |   | 8.3 ± 1.4                                       | 6.14  |
| 8     | <a href="#"><u>3.59</u></a> |   | 7.9 ± 0.4                                       | 5.92  |
| 9     | <a href="#"><u>3.62</u></a> |   | 6.4 ± 0.4                                       | 5.57  |
| 10    | <a href="#"><u>3.65</u></a> |   | 6.2 ± 0.5                                       | 4.88  |
| 11    | <a href="#"><u>3.57</u></a> |   | 9.8 ± 2.2                                       | 5.89  |
| 12    | <a href="#"><u>3.60</u></a> |   | 10.0 ± 2.5                                      | 5.62  |
| 13    | <a href="#"><u>3.63</u></a> |   | 10.0 ± 2.7                                      | 5.57  |
| 14    | <a href="#"><u>3.66</u></a> |   | 16.8 ± 5.5                                      | 4.88  |

<sup>a</sup>Values expressed as mean ± standard error of the mean (*n* = 2).

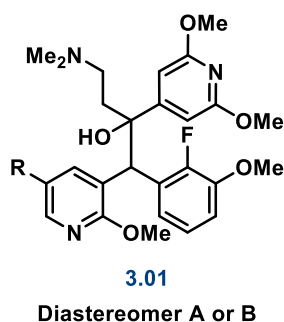
### 3.4.3 Stage two

The shortlisted analogues identified in stage one were then progressed to the next phase of analysis which involved evaluation of the separated diastereomers (A and B). All separated diastereomers were tested for inhibitory activity ( $MIC_{90}$ ) which allowed us to identify the active diastereomer of the pair, as well as allowing us to form a second shortlist of our top three analogues to submit for chiral separation in stage three. Additionally, the C5-pyridinyl analogues that were not included in stage one were also separated and included in this assay (entries 7 to 9).

As shown in **Table 3.7**, from these results we were able to determine that diastereomer B (second to elute from the HPLC column) was the most active diastereomer for every analogue tested (generally 3- to 7-fold more potent than A). By analogy to TBAJ-587, it is therefore expected that diastereomer B is a racemic mixture of the *RR* and *SS* stereoisomers.

Similarly to the trend in potency that was observed for the racemates tested in stage one of our testing protocol (**Figure 3.8**, *vide supra*), the inclusion of phenyl rings with more lipophilic substituents were in general more potent. For example, the *para*-trifluoromethoxyphenyl and *para*-chlorophenyl derivatives (entries 2 and 3) were the most potent in this testing phase ( $MIC_{90}$  = 1.09  $\mu$ M and 1.45  $\mu$ M), and also the most lipophilic with a cLogP of 6.54 and 6.14, respectively. Interestingly, the only exception to this trend was the *para*-cyanophenyl derivative **3.64** (entry 6) which displayed activity comparable to the phenyl and *para*-tolyl derivatives (entries 1 and 4) despite a significantly lower cLogP of 4.88. Analysis of the pyridyl analogues that were included in this assay (entries 7 to 9) indicated that the additional heterocyclic moiety in the C5 position of the core pyridine ring was detrimental to activity, with a 3- to 7-fold increase in the  $MIC_{90}$  value being observed when compared to the phenyl analogue **3.54** (entry 1). Given that the Denny group had reported a sharp decline in potency in their series when  $cLogP \leq 4$ <sup>[4]</sup>, it is unknown whether this reduction in potency is specifically due to this region not accommodating more polar heterocyclic rings, or if this is a result of the overall increase in polarity which could limit diffusion through the lipid-rich membrane which is required to access to the binding site.

Taking all these results into consideration, derivatives **3.02-B**, **3.55-B** and **3.64-B** were identified as the top three analogues to progress for further chiral separation and *in vitro* analysis. Specifically, **3.02-B** and **3.55-B** were chosen as they were most potent derivatives of this series, whereas **3.64-B** was selected for its balance between lipophilicity and potency.

**Table 3.7.** Inhibitory activity of all pyridine analogues of type **3.01** tested as either diastereomer A or B in stage two of our testing protocol.

| Entry | Compound    | R | <i>M.tb</i> H37Rv MIC <sub>90</sub> (μM) <sup>a</sup> |                          | cLogP |
|-------|-------------|---|---|--------------------------|-------|
|       |             |   | A   | B                        |       |
| 1     | <u>3.54</u> |   | 10.50   | 2.54 ± 0.86 <sup>a</sup> | 5.41  |
| 2     | <u>3.02</u> |   | ND  | 1.09 ± 0.30 <sup>a</sup> | 6.54  |
| 3     | <u>3.55</u> |   | 10.47   | 1.45 ± 0.51 <sup>a</sup> | 6.14  |
| 4     | <u>3.58</u> |   | 15.31   | 1.99 ± 0.73 <sup>a</sup> | 5.92  |
| 5     | <u>3.61</u> |   | 13.67   | 4.56 ± 1.29 <sup>a</sup> | 5.57  |
| 6     | <u>3.64</u> |   | 11.16   | 2.25 ± 0.90 <sup>a</sup> | 4.88  |
| 7     | <u>3.69</u> |   | 28.06   | 11.42                    | 4.03  |
| 8     | <u>3.70</u> |   | 19.16   | 17.11                    | 4.03  |
| 9     | <u>3.71</u> |   | 22.55   | 7.65                     | 4.24  |

<sup>a</sup>Values expressed as mean ± standard error of the mean (*n* = 2).

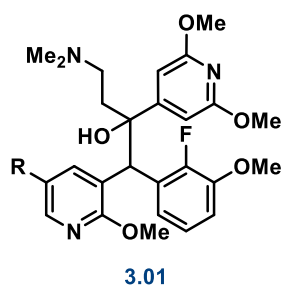
### 3.4.4 Stage three *in vitro* evaluation

#### 3.4.4.1. Inhibitory activity against *M.tb*

In stage three of our evaluation protocol, racemic diastereomer B derivatives **3.02-B**, **3.55-B** and **3.64-B** were separated into their respective enantiomers using chiral HPLC (performed by TCG Lifesciences, India). The separated enantiomers were denoted as B1 (first to elute from the column) and B2 (second to elute from the column).

Once resolved, the enantiomers were tested for inhibitory activity (REMA) against *M.tb* (H37rv) by our new collaborators at the University of Queensland (the group of Assoc. Prof Nick West), which allowed us to determine the eutomer and distomer for each derivative. As shown in **Table 3.8**, enantiomer B2 was found to possess the greatest activity (eutomer) for each analogue, which is expected to be the *SS* configuration by analogy to TBAJ-587. Much to our delight, derivatives **3.02** and **3.55** (entries 2 and 3, respectively) appear to possess comparable activity to that of BDQ despite substitution of the quinoline ring and a reduction in lipophilicity ( $MIC_{90} = 0.60 \mu M$  and  $0.76 \mu M$ , versus  $0.70 \mu M$  for BDQ). Of particular interest was the *para*-cyanophenyl derivative **3.64** (entry 4) which retained potent anti-*M.tb* activity ( $MIC_{90} = 0.98 \mu M$ ), despite being >200-fold less lipophilic than BDQ.

**Table 3.8.** Inhibitory activity of the enantiomers B1 and B2 of shortlisted pyridine analogues of type **3.01**.



| Entry | Compound    | R | <i>M.tb</i> H37Rv $MIC_{90}$ ( $\mu M$ ) |      | cLogP |
|-------|-------------|---|--|------|-------|
| 1     | BDQ         |   | 0.70 <sup>a</sup>                        |      | 7.25  |
|       |             |   | B1                                       | B2   |       |
| 2     | <b>3.02</b> |   | >10                                      | 0.60 | 6.54  |
| 3     | <b>3.55</b> |   | >10                                      | 0.76 | 6.14  |
| 4     | <b>3.64</b> |   | >10                                      | 0.98 | 4.88  |

<sup>a</sup>The  $MIC_{90}$  for BDQ was slightly higher in this assay performed by our new collaborators, however it is important to note that this was a single replicate ( $n=1$ ).

#### 3.4.4.2. Inhibitory activity at hERG

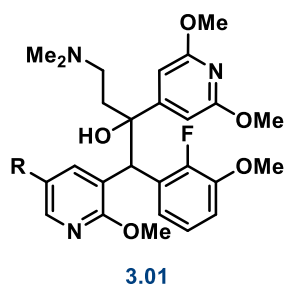
Chiral separation of derivatives **3.02-B**, **3.55-B** and **3.64-B** resulted in a much lower than expected recovery of separated enantiomers (*ca.* 5% mass recovery of B1 + B2). As such, an insufficient quantity of the chirally resolved samples remained to assess in additional assays to predict safety (such as the hERG inhibition assay), and therefore these assays were not completed for the eutomers within the timeframe of this project. Despite this, we were still in possession of a sufficient quantity of the



diastereomer B racemates **3.02-B** and **3.55-B**, and therefore these samples were used gain some insight into their hERG potency.

The *in vitro* effects of these samples on the hERG K<sup>+</sup> channel current (a surrogate for I<sub>Kr</sub>, the rapidly activating, delayed rectifier cardiac potassium current) expressed in mammalian cells were evaluated using the QPatch HT<sup>®</sup>, an automatic parallel patch clamp platform (Charles River Laboratories, US) The test articles were screened in at least 2 cells (n ≥ 2) in a dose-response fashion across seven concentrations, with exposure maintained for at least 5 minutes per concentration. Cisapride was used as a positive control to confirm the sensitivity of the test system to hERG inhibition. Further details regarding the assay protocol can be found in Chapter 5.

In **Table 3.9**, the hERG assay results are shown for the tested analogues in comparison to BDQ. Much to our delight, derivative **3.55-B** (entry 2) exhibited a marked reduction in hERG potency in comparison to BDQ (ca. 6-fold). Although we were also interested in benchmarking against TBAJ-587 in this assay, after much discussion with the TB Alliance (now in full possession of TBAJ-587), we were unable to obtain a sample for this assay due to legal complexities. Despite this, the reported literature hERG IC<sub>50</sub> value of TBAJ-587 is 13 μM<sup>[5]</sup> (as the *S,S* enantiomer), indicating that **3.55-B** may be superior in terms of predicted cardiac safety as a result in a change of topology in the A region. Interestingly, the *para*-cyanophenyl derivative **3.64-B** was found to be a very potent inhibitor of the hERG channel (IC<sub>50</sub> = 2.21 μM, entry 3) despite being significantly less lipophilic than BDQ and **3.55-B** (cLogP = 4.88). This result highlights that although a reduction in lipophilicity can aid in reducing the risk of hERG inhibition, it is not the sole property that drives a compound's interaction with the channel. Indeed, even subtle structural modifications have been demonstrated to considerably impact a compounds potential for hERG inhibition.<sup>[43]</sup> Following on from this, it is also important to note that stereochemistry can also have an impact of a compound's ability to inhibit hERG. We therefore cannot rule out the possibility that the distomer could potentially bind to the hERG channel selectively and result in a false-positive result for the **3.64** eutomer. As such, it still remains an important future goal to submit the purified eutomer of each derivative for hERG assessment.

**Table 3.9.** hERG channel inhibitory activity of racemic derivatives **3.55-B** and **3.65-B**.

| Entry | Compound      | R | hERG IC <sub>50</sub> (μM) | cLogP |
|-------|---------------|---|----------------------------|-------|
| 1     | BDQ           |   | 3.50                       | 7.25  |
| 2     | <b>3.55-B</b> |   | 22.23                      | 6.14  |
| 3     | <b>3.64-B</b> |   | 2.21                       | 4.88  |

### 3.5 Conclusion

This chapter was focused on the design and synthesis of a novel series of BDQ-like compounds in part inspired by the recently disclosed second-generation BDQ analogue TBAJ-587, developed within the Denny research group. Specifically, our derivatives were designed as a hybrid between our novel aryl-pyridine A region, with Denny's optimised B and C regions.

A number of new synthetic pathways were investigated and optimised during this study, resulting in the synthesis of 16 novel ring A derivatives which all possessed reduced lipophilicity in comparison with BDQ. These derivatives were subjected to an efficient testing protocol which allowed us to shortlist compounds based on their *in vitro* *Mt.b* inhibitory activity.

Multiple analogues were found to possess potent *anti-M.tb* activity despite substitution of the ring A quinoline with our novel aryl-pyridine moiety, as well as an overall lowering of lipophilicity. More specifically, *para*-substituted phenyl rings at the C5 position of the pyridine core were found to return the most potent analogues, with increased activity largely correlated with an increase in substituent lipophilicity (except for derivative **3.64**).

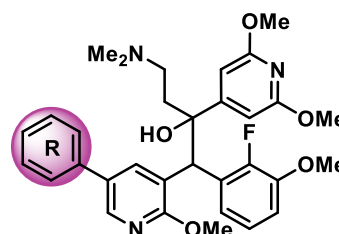
Three shortlisted analogues (**3.02**, **3.55** and **3.64**) were chirally purified allowing us to determine the potency of the eutomer, thus conclusively confirming that potent inhibitory activity similar to that of BDQ could be achieved despite quinoline ring A substitution. Furthermore, hERG assay results obtained for derivative **3.55-B** very promisingly revealed hERG channel inhibition that is >6-fold

weaker than that of BDQ ( $IC_{50} = 22.2 \mu M$  versus  $3.5 \mu M$ ) and *ca.* 2-fold weaker than the published value for TBAJ-587.

Overall this study has further demonstrated that structural modifications to the ring A region is a well-tolerated strategy leading to novel BDQ-like compounds with promising *in vitro* activity. Additionally, these modifications in combination with the Denny group's optimised B and C regions have allowed us to access a compound with significantly reduced hERG channel inhibition (derivative **3.55**). The future priority regarding this series will be to submit the chirally purified compounds for further assessment at hERG as well as a range of additional safety and PK assays to benchmark against BDQ and TBAJ-587.

Phenyl ring favoured:  
*p*-substitution with lipophilic groups preferred  
*p*-cyano tolerated

Pyridine heterocycle not favoured



| Compound | R | <i>M.tb</i> H37Rv<br>MIC <sub>90</sub> ( $\mu M$ )<br>(eutomer) | hERG IC <sub>50</sub> ( $\mu M$ )<br>(diastereomer B) | cLogP |
|----------|---|---|---|-------|
| 3.02     |   | 0.60  | N.D.  | 6.54  |
| 3.55     |   | 0.76  | 22.23   | 6.14  |
| 3.64     |   | 0.98  | 2.21  | 4.88  |

### 3.6 References

- [1] A. S. T. Tong, P. J. Choi, A. Blaser, H. S. Sutherland, S. K. Y. Tsang, J. Guillemont, M. Motte, C. B. Cooper, K. Andries, W. Van Den Broeck, et al., *ACS Med. Chem. Lett.* **2017**, *8*, 1019–1024.
- [2] P. J. Choi, H. S. Sutherland, A. S. T. Tong, A. Blaser, S. G. Franzblau, C. B. Cooper, M. U. Lotlikar, A. M. Upton, J. Guillemont, M. Motte, et al., *Bioorganic Med. Chem. Lett.* **2017**, *27*, 5190–5196.
- [3] H. S. Sutherland, A. S. T. Tong, P. J. Choi, D. Conole, A. Blaser, S. G. Franzblau, C. B. Cooper, A. M. Upton, M. U. Lotlikar, W. A. Denny, et al., *Bioorganic Med. Chem.* **2018**, *26*, 1797–1809.
- [4] A. Blaser, H. S. Sutherland, A. S. T. Tong, P. J. Choi, D. Conole, S. G. Franzblau, C. B. Cooper, A. M. Upton, M. Lotlikar, W. A. Denny, et al., *Bioorganic Med. Chem.* **2019**, *27*, 1283–1291.
- [5] H. S. Sutherland, A. S. T. Tong, P. J. Choi, A. Blaser, D. Conole, S. G. Franzblau, M. U. Lotlikar, C. B. Cooper, A. M. Upton, W. A. Denny, et al., *Bioorganic Med. Chem.* **2019**, *27*, 1292–1307.
- [6] A. M. Upton, C. B. Cooper, K. J. L. Marcel, J. E. G. Guillemont, W. M. M. Van Den Broeck, B. D. Palmer, Z. Ma, *Antibacterial Compounds and Uses Thereof*, **2017**, WO155909.
- [7] W. A. Denny, B. D. Palmer, A. Blaser, P. J. Choi, D. Conole, H. S. Sutherland, A. S. T. Tong, C. B. Cooper, M. U. Lotlikar, A. M. Upton, Presented at the Tuberculosis Drug Discovery and Development Conference, Gordon Research Conference, Lucca (Barga), Italy, June 25 – 30, **2017**.
- [8] Z. Dings, S. Chen, Z. Huang, W. Luo, Z. Cai, Y. Wang, D. Tang, *Pyridine Derivatives and Anti-Mycobacterial Use Thereof*, **2015**, WO 2016/008381 A1.
- [9] D. L. Comins, D. H. LaMunyon, *Tetrahedron Lett.* **1988**, *29*, 773–776.
- [10] J. E. G. Guillemont, J. F. E. Van Gestel, M. G. Venet, L. F. B. Decrane, D. F. J. Vernier, F. C. Odds, I. C. F. Csoka, K. J. L. M. Andries, *Quinoline Derivatives and Their Use as Mycobacterial Inhibitors*, **2004**, WO011436.
- [11] E. L. Stogryn, *J. Heterocycl. Chem.* **1974**, *11*, 251–253.
- [12] C. Klein, E. Baranoff, M. Grätzel, M. K. Nazeeruddin, *Tetrahedron Lett.* **2011**, *52*, 584–587.
- [13] J. M. Snell, S. M. McElvain, *J. Am. Chem. Soc.* **1934**, *56*, 1612–1614.
- [14] F. Chung, C. Tisné, T. Lecourt, B. Seijo, F. Dardel, L. Micouin, *Chem. - A Eur. J.* **2009**, *15*, 7109–7116.
- [15] T. Kolasa, M. A. Matulenko, A. A. Hakeem, M. V. Patel, K. Mortell, P. Bhatia, R. Henry, M. Nakane, G. C. Hsieh, M. A. Terranova, et al., *J. Med. Chem.* **2006**, *49*, 5093–5109.
- [16] S. Ozaki, E. Ebisui, K. Hamada, J.-I. Goto, A. Z. Suzuki, A. Terauchi, K. Mikoshiba, *Bioorg. Med. Chem. Lett.* **2010**, *20*, 1141–1144.
- [17] U. Girreser, D. Heber, M. Schütt, *Synthesis*. **1998**, *1998*, 715–717.
- [18] D. Zampieri, M. G. Mamolo, L. Vio, E. Banfi, G. Scialino, M. Fermeglia, M. Ferrone, S. Pricl, *Bioorg. Med. Chem.* **2007**, *15*, 7444–7458.
- [19] P. G. M. Wuts, S. R. Putt, A. R. Ritter, *J. Org. Chem.* **1988**, *53*, 4503–4508.

- [20] V. Stockmann, S. J. Kaspersen, A. Nicolaisen, A. Fiksdahl, *J. Heterocycl. Chem.* **2012**, *49*, 613–620.
- [21] A. Gomtsyan, R. J. Koenig, C.-H. Lee, *J. Org. Chem.* **2001**, *66*, 3613–3616.
- [22] K. Sivagurunathan, S. Raja Mohamed Kamil, S. Syed Shafi, F. Liakth Ali Khan, R. V. Ragavan, *Tetrahedron Lett.* **2011**, *52*, 1205–1207.
- [23] V. Bertolasi, V. Ferretti, P. Gilli, X. Yao, C.-J. Li, *New J. Chem.* **2008**, *32*, 694.
- [24] J. Emsley, in *Complex Chem.*, Springer Berlin Heidelberg, Berlin, Heidelberg, **1984**, pp. 147–191.
- [25] M. T. Barros, C. F. G. C. Geraldles, C. D. Maycock, M. I. Silva, *Tetrahedron* **1988**, *44*, 2283–2287.
- [26] M. Tramontini, L. Angiolini, *Tetrahedron* **1990**, *46*, 1791–1837.
- [27] L. Collins, S. G. Franzblau, *Antimicrob. Agents Chemother.* **1997**, *41*, 1004–9.
- [28] D. W. Slocum, C. A. Jennings, *J. Org. Chem.* **1976**, *41*, 3653–3664.
- [29] M. Schlosser, F. Mongin, *Tetrahedron Lett.* **1996**, *37*, 6551–6554.
- [30] J. A. Elvidge, J. R. Jones, C. O'Brien, E. A. Evans, H. C. Sheppard, *Adv. Heterocycl. Chem.* **1974**, *16*, 1–31.
- [31] B. S. Schafman, P. G. Wenthold, *J. Org. Chem.* **2007**, *72*, 1645–1651.
- [32] T. M. Bargar, J. K. Dulworth, M. T. Kenny, R. Massad, J. K. Daniel, T. Wilson, R. N. Sargent, *J. Med. Chem.* **1986**, *29*, 1590–1595.
- [33] J. M. Evans, G. Stemp, *Synth. Commun.* **1988**, *18*, 1111–1118.
- [34] A. Krasovskiy, P. Knochel, *Angew. Chemie Int. Ed.* **2004**, *43*, 3333–3336.
- [35] M. Peters, M. Trobe, R. Breinbauer, *Chem. - A Eur. J.* **2013**, *19*, 2450–2456.
- [36] D. S. Ziegler, B. Wei, P. Knochel, *Chem. - A Eur. J.* **2019**, *25*, 2695–2703.
- [37] F. Tinnis, A. Volkov, T. Slagbrand, H. Adolfsson, *Angew. Chemie Int. Ed.* **2016**, *55*, 4562–4566.
- [38] D. Mukherjee, S. Shirase, K. Mashima, J. Okuda, *Angew. Chemie Int. Ed.* **2016**, *55*, 13326–13329.
- [39] L.-C. Campeau, K. Fagnou, *Chem. Soc. Rev.* **2007**, *36*, 1058–1068.
- [40] M. Hapke, L. Brandt, A. Lützen, *Chem. Soc. Rev.* **2008**, *37*, 2782.
- [41] D. Machado, M. Girardini, M. Viveiros, M. Pieroni, *Front. Microbiol.* **2018**, *9*, 1367.
- [42] J. P. Sarathy, V. Dartois, E. J. D. Lee, *Pharmaceuticals* **2012**, *5*, 1210–35.

## Chapter 4: Diazine Hybrids of TBAJ-587

### 4.1 Introduction

The synthesis of ring A analogues of BDQ in chapter 2 (**Figure 4.1, A**) and TBAJ-587 in chapter 3 (**Figure 4.1, B**) successfully demonstrated that the quinoline moiety in this position could be replaced with various phenyl substituted pyridine rings to produce highly potent compounds. Additionally, *in vitro* hERG activity was found to be significantly reduced by moving to the TBAJ-587 scaffold. Building on this success, we were curious to further explore the ring A region with alternative *N*-heterocycles. Considering that the lipophilicity remained relatively high for our most potent inhibitors, our focus shifted to the design of analogues that incorporated the more polar heterocyclic rings pyrazine or pyridazine at ring A (**Figure 4.1, C**).

Diazines including pyrazine and pyridazine constitute an important scaffold previously incorporated in various pharmaceuticals which possess a broad range of biological activities including antimycobacterial (e.g. pyrazinamide<sup>[1]</sup>), antibacterial (e.g. sulfamethoxypyridazine<sup>[2]</sup>), antidiabetic (glipizide<sup>[3]</sup>), anticancer (bortezomib<sup>[4]</sup>), antihypertensive (e.g. hydralazine<sup>[5]</sup>) and hypnotic sedative (zopiclone<sup>[6]</sup>) agents. It was hypothesised that these rings would serve as a bioisosteric substitute of the pyridyl or quinolyl ring without loss of activity, with the additional nitrogen further reducing lipophilicity and improving overall properties.<sup>[7,8]</sup>

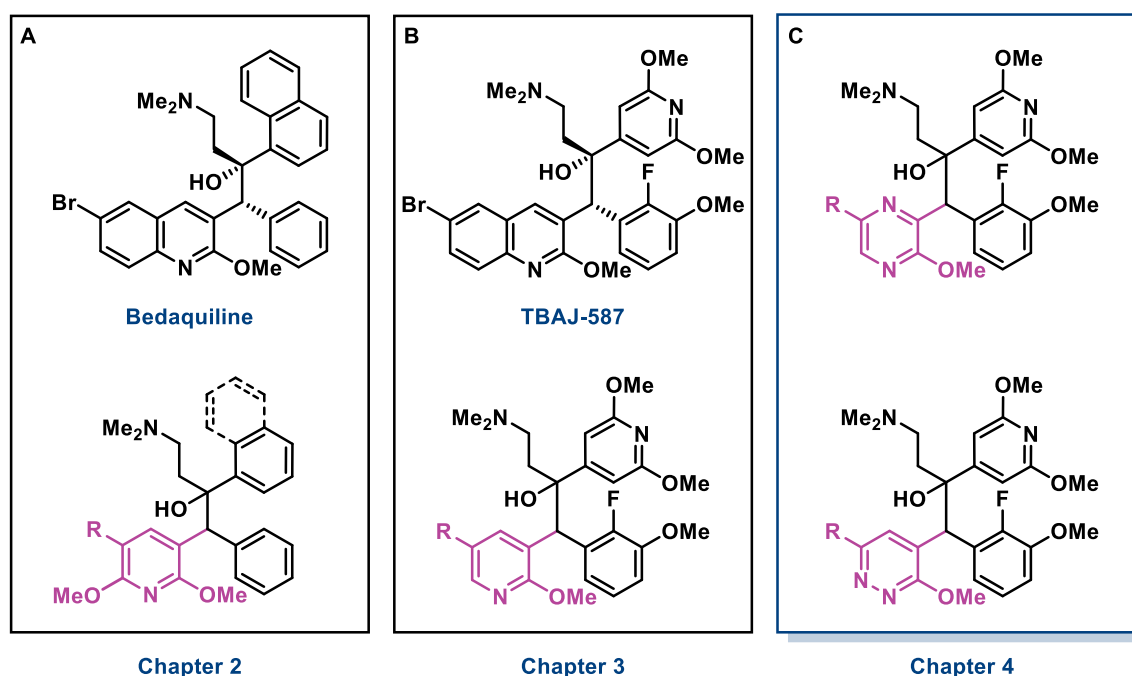
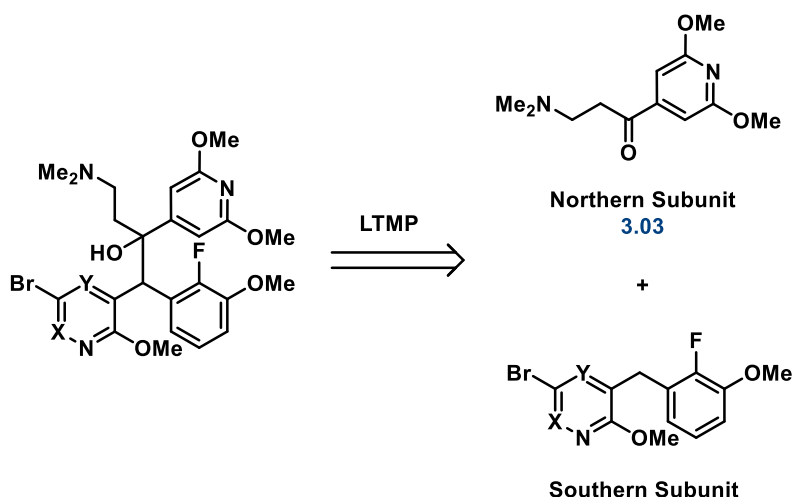


**Figure 4.1.** This chapter is focused towards the synthesis of diazine analogues of TBAJ-587 (Box C).

The synthetic strategy designed to access these diazine analogues was similar to that developed to access the pyridine hybrid analogues of TBAJ-587, previously described in Chapter 3 (**Scheme 4.1**). Given that the synthesis of the northern subunit **3.03** was already established, this chapter predominantly details efforts to synthesise the southern subunits containing the diazine cores. Of particular importance to both diazine analogues was the regioselective incorporation of the 2-fluoro-3-methoxybenzene ring, and hence a significant portion of this chapter is focused on exploring the various metalation reactions that provide regioselective control over this process.

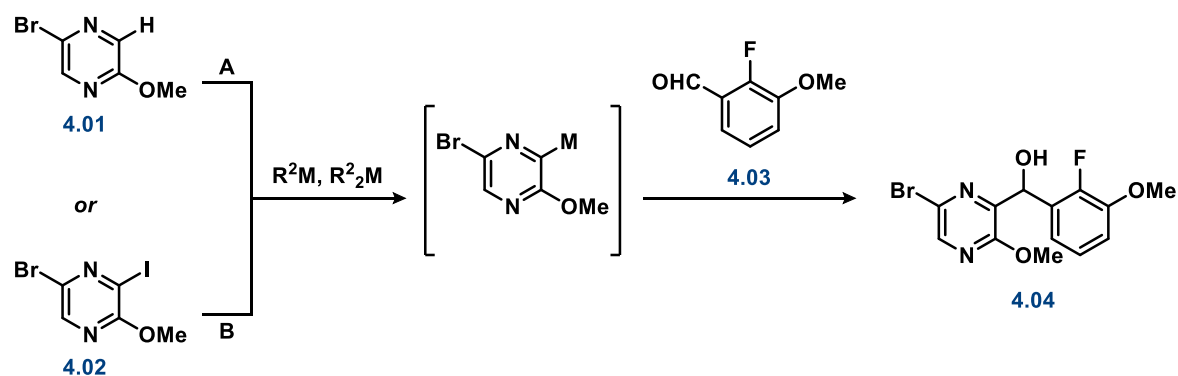
Due to time constraints, the synthetic pathways to access both diazine analogues were not completely optimised, however initial progress indicates that these pathways show promise, and future strategies to access these structures are proposed.



**Scheme 4.1.** Retrosynthetic strategy towards the synthesis of the diazine hybrids of TBAJ-587. Pyrazine analogues X = C, Y = N. Pyridazine analogues X = N, Y = C.

## 4.2 Synthesis of pyrazine analogues

In a similar fashion to that previously described for the pyridine analogues of TBAJ-587, both directed *ortho*-metalation (DoM) strategies from **4.01** (section 4.2.1) and halogen-metal exchange from **4.02** (section 4.2.2) were explored for the regioselective addition of benzaldehyde **4.03** to afford the  $\alpha$ -hydroxy intermediate **4.04** (**Scheme 4.2**).



**Scheme 4.2.** Metalation strategies explored towards the synthesis of the pyrazine southern subunit. A) Directed *ortho*-metalation, B) halogen-metal exchange. M = Li or Mg.

## 4.2.1 Directed *ortho*-metalation

### 4.2.1.1. Directed *ortho*-lithiation

The majority of the literature published regarding the metalation of pyrazines was established in the group of Quéguiner utilising conventional DoM with hindered lithium dialkylamide bases (e.g. LDA and LTMP).<sup>[9]</sup> Interestingly, despite their extensive investigation into the metalation of various substituted pyrazines including 2,6-disubstituted pyrazines, no examples exist for the metalation of 2,5-disubstituted pyrazines.

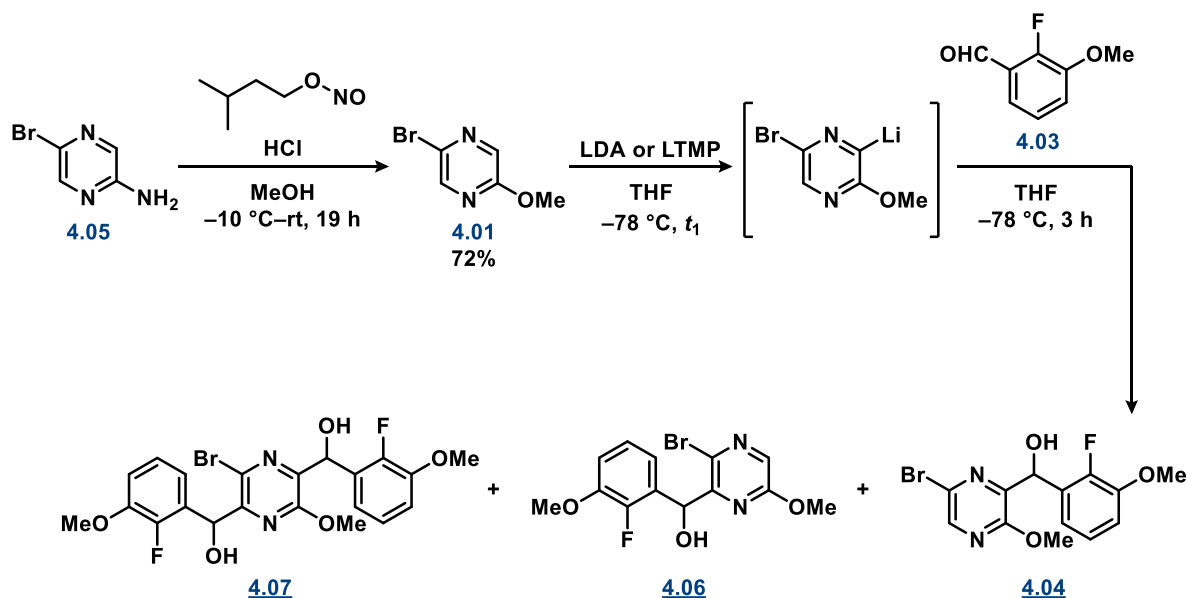
Beginning from 2-amino-5-bromopyrazine (**4.05**, **Scheme 4.3**), the amino group was converted to a methoxy group *via* Knoevenagel diazotization in acidic methanol.<sup>[10]</sup> From the resulting intermediate **4.01**, metalation with LDA and LTMP was compared using the conditions established by the group of Quéguiner as a guide.<sup>[11]</sup> Although their study determined that metalation of 2,5-disubstituted pyrazines with LDA provided greater yields in comparison to LTMP, in our case we did not observe any great differences in the yields between the two lithium bases (**Table 4.1**, entries 1–2).

Using <sup>1</sup>H NMR analysis of the crude reaction mixture, we were able to establish that the selectivity of desired regioisomer **4.04** over **4.06** remained the same for both bases (**Figure 4.2**). Interestingly in contrast to LDA, when LTMP was employed as the base an almost equivalent amount of the disubstituted product **4.07** was also formed (**Table 4.1**, entry 2). As the metalating base was used in excess, it was anticipated that by reducing the number of equivalents of LTMP, we could limit the additional metalation at C3 and therefore increase yield of the desired product. Interestingly, although the yield of **4.04** was improved when the amount of LTMP was reduced to 1.2 equivalents, the disubstituted product **4.07** was still formed (**Table 4.1**, entry 3). This result indicates that formation of **4.07** is not due to simultaneous dimetalation of **4.01**, and is instead a result of *in situ* lithiation of **4.04** by LTMP. Finally, reducing the metalation time (*t*<sub>1</sub>) to 5 min had little effect on the yield of **4.04** or the



amount of disubstituted product **4.07** formed, and this decrease in reaction time proved slightly detrimental to the regioselectivity of **4.04** over **4.06** (Table 4.1, entry 4).

At this point, additional optimisation of the LTMP-mediated addition was not conducted, however exploration of the optimal metalation and reaction times ( $t_1$  and  $t_2$ ) as well as reaction concentration and solvent type would be worth investigating in future work.



**Scheme 4.3.** Pyrazine functionalisation using the directed *ortho*-lithiation strategy with either LDA or LTMP.

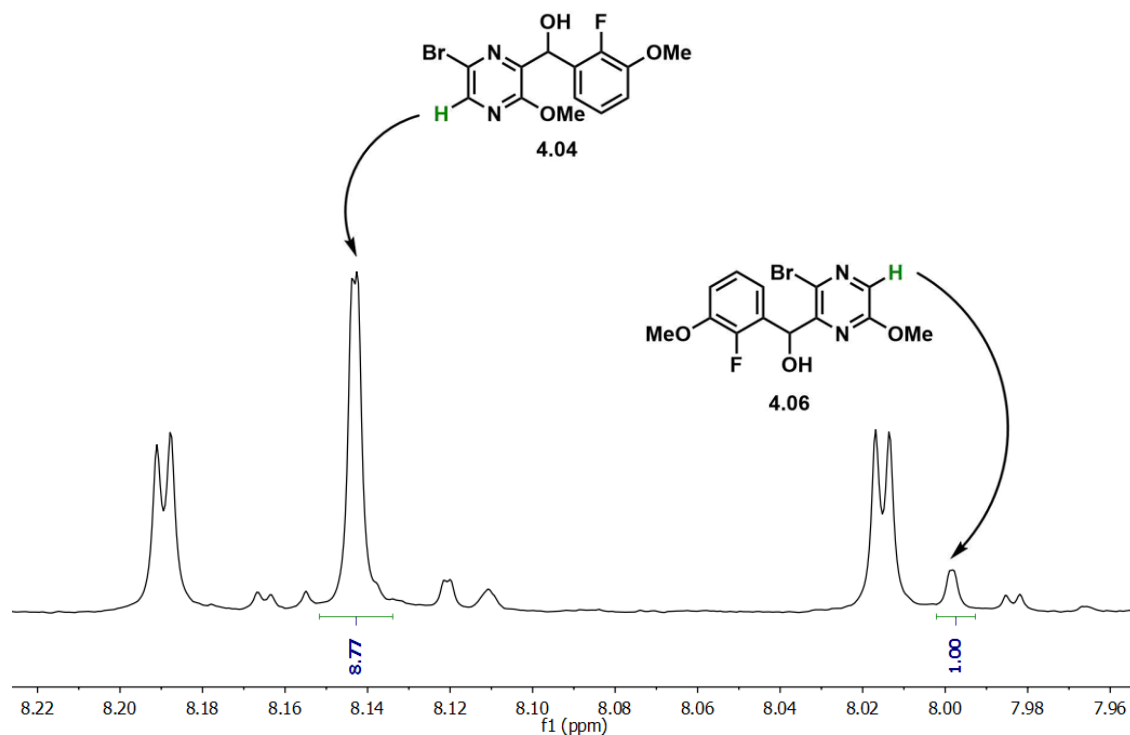


**Figure 4.2.**  $^1\text{H}$  NMR spectrum of crude reaction mixture demonstrating the ratio between **4.04** and **4.06**.

**Table 4.1.** Conditions trialed in the optimisation of the directed *ortho*-lithiation of pyrazine **4.01**.

| Entry | Base | Equivalents of base | $t_1$ | Yield of <b>4.04</b> (%) | Ratio of <b>4.04:4.06<sup>a</sup></b> | Ratio of ( <b>4.04+4.06</b> ): <b>4.07<sup>a</sup></b> |
|-------|------|---------------------|-------|--------------------------|---------------------------------------|--|
| 1     | LDA  | 2.2                 | 2 h   | 9                        | 91:9                                  | 100:0  |
| 2     | LTMP | 2.2                 | 2 h   | 13                       | 90:10                                 | 52:48  |
| 3     | LTMP | 1.2                 | 2 h   | 26                       | 90:10                                 | 61:39  |
| 4     | LTMP | 2.2                 | 5 min | 14                       | 84:16                                 | 54:46  |

<sup>a</sup>Determined using the <sup>1</sup>H NMR spectrum of the crude reaction mixture.

Quéguiner and co-workers have established the order of *ortho*-directing power in the diazine series to be F > OMe > Cl.<sup>[12]</sup> Given that the *ortho*-directing ability of the bromo group is considered relatively equivalent to that of the chloro group<sup>[13,14]</sup>, the major product of this reaction was expected to be the desired regioisomer **4.04** with addition at C6 (*ortho* to the methoxy group). To confirm this was the case, 2D NMR experiments (HMBC and NOESY) were conducted. As shown in **Figure 4.3 A**, the results from the HMBC experiment of **4.04** proved inconclusive as <sup>2</sup>J, <sup>3</sup>J and <sup>4</sup>J C–H couplings around the heterocyclic ring could be fit to either structure. Similarly, the NOESY spectrum of **4.04** (**Figure 4.3, B**) did not assist in identification due to the absence of a cross-peak between the pyrazine methoxy protons (H16) and either the α-proton (H18) or the pyrazine proton (H14).

Due to the inability of the 2D experiments to conclusively identify the major regioisomer formed during the metalation process, a crystal structure was obtained which unequivocally confirmed that **4.04** was indeed the major regioisomer with addition at C6 (**Figure 4.4**, see **Appendix A4 for full report**). A search through the crystal structure database<sup>[4]</sup> found only one similar compound, (4-bromophenyl)(pyridin-3-yl)methanol<sup>[5]</sup>.

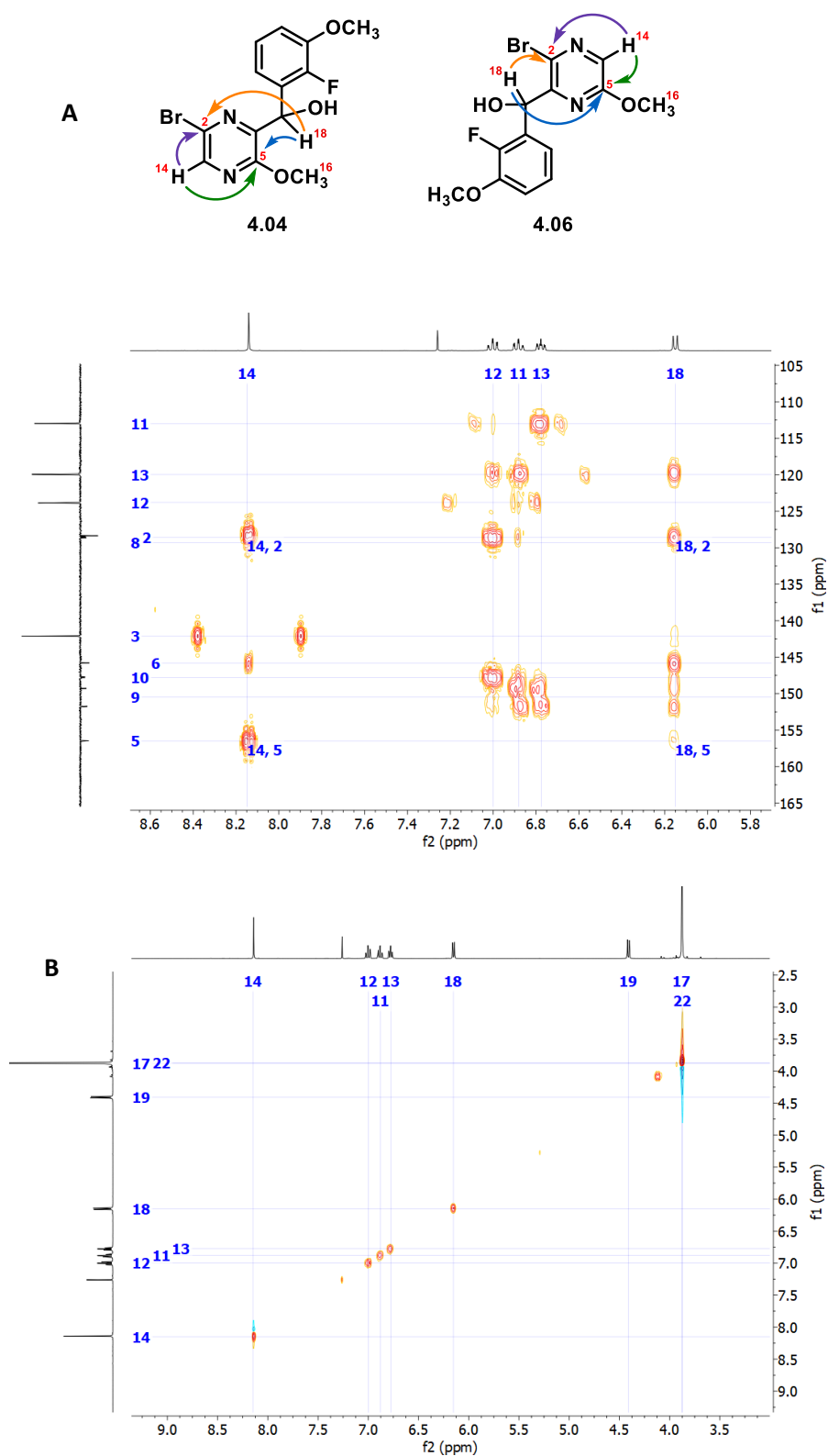


**Figure 4.3.** Structural investigation of **4.04** using 2D NMR. A) HMBC C–H cross-peaks can be fit to both structures. B) No cross-peaks were found between H16 and either H18 or H14 in the NOESY spectrum.

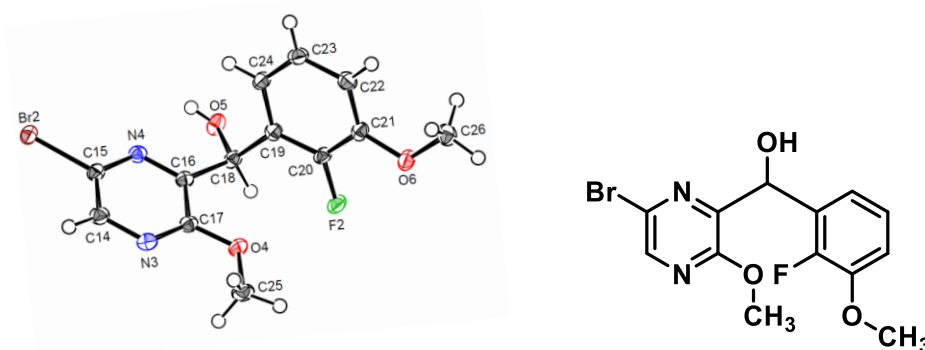
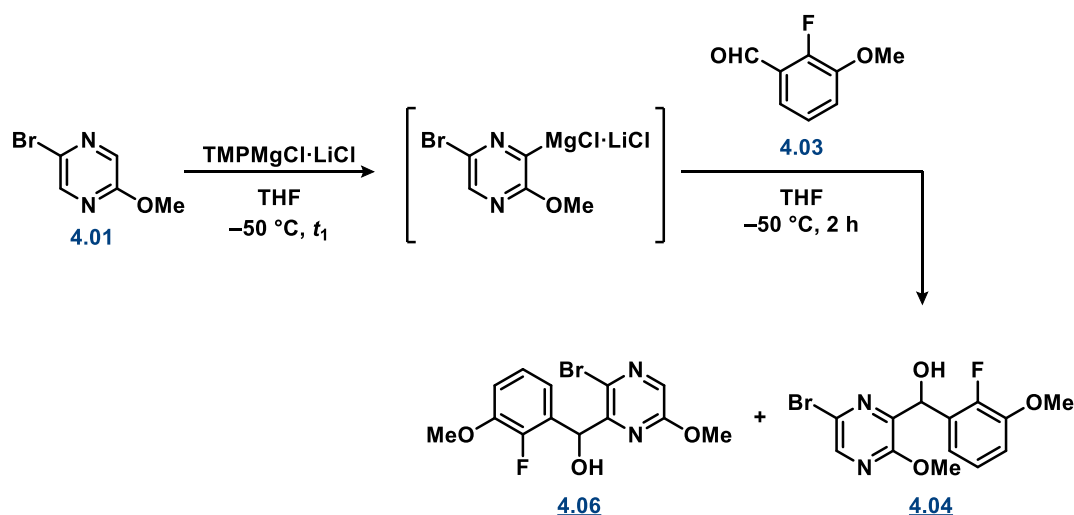


**Figure 4.4.** The crystal structure of **4.04** indicating that the regioisomer obtained is a result of addition at C6. The crystals of **4.04** were analysed by Dr. Robert Gable (University of Melbourne).

#### 4.2.1.2. Directed ortho-magnesiation

Metalation of diazines with lithium amides and their successive reactions with electrophiles are often associated with poor yields due to the instability of the lithiated heterocycles.<sup>[15,16]</sup> As an alternative, mixed lithium-magnesium bases such the turbo-Hauser base  $\text{TMPMgCl}\cdot\text{LiCl}$  and the more reactive  $\text{TMP}_2\text{MgCl}\cdot 2\text{LiCl}$  have proven especially effective as alternative metalating agents for the deprotonation of sensitive  $\pi$ -deficient heterocycles such as pyrazines.<sup>[17]</sup>

Using the method as first reported by Knochel<sup>[18]</sup>, the metalation of pyrazine intermediate **4.01** was carried out at  $-50\text{ }^\circ\text{C}$  for 2 h, followed by the addition of benzaldehyde **4.03** (Scheme 4.4). In comparison to directed lithiation using LTMP, the use of 1.2 equivalents of  $\text{TMPMgCl}\cdot\text{LiCl}$  resulted in a similar yield of the desired product **4.04** (20–22%), however the reaction was less regioselective towards **4.04** (Table 4.2, entry 1). Shortening the metalation time to 30 min reduced the yield and did not lead to enhanced regioselectivity (Table 4.2, entry 2). Interestingly, it was observed that an increase in the scale of the reaction was associated with slight improvement in the ratio of **4.04** to **4.06**, however this was not associated with an increase in the overall yield of **4.04** (Table 4.2, entries 3 and 4). At this point, no further optimisation of this reaction was attempted as **4.04** and **4.06** were separable using silica-gel chromatography, however increasing the addition reaction time ( $t_2$ ), equivalents of base and temperature would also be worth exploring. Additionally, the dimeric  $\text{TMP}_2\text{MgCl}\cdot 2\text{LiCl}$  is a more reactive mixed-metal base<sup>[17,19]</sup> and could be trialled as the metalating base in future attempts of the reaction.



**Scheme 4.4.** Pyrazine functionalisation using directed *ortho*-magnesiation with TMPMgCl·LiCl.

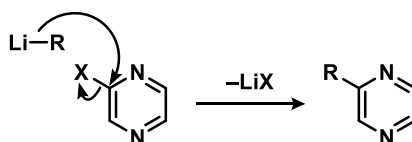
**Table 4.2.** Conditions trailed in the directed *ortho*-magnesiation of **4.01** using TMPMgCl·LiCl.

| Entry | Scale (mmol) | $t_1$ (h) | Yield of <b>4.04</b> (%) | Ratio <b>4.04</b> : <b>4.06</b> <sup>a</sup> |
|-------|--------------|-----------|--------------------------|--|
| 1     | 1            | 2         | 20%                      | 72:28  |
| 2     | 1            | 0.5       | 8%                       | 71:29  |
| 3     | 3            | 2         | 22%                      | 74:26  |
| 4     | 9.7          | 2         | 22%                      | 78:22  |
| 5     | 10           | 2         | 22%                      | 79:21  |

<sup>a</sup>Determined using the <sup>1</sup>H NMR spectrum of the crude reaction mixture.

### 4.2.2 Halogen-metal exchange

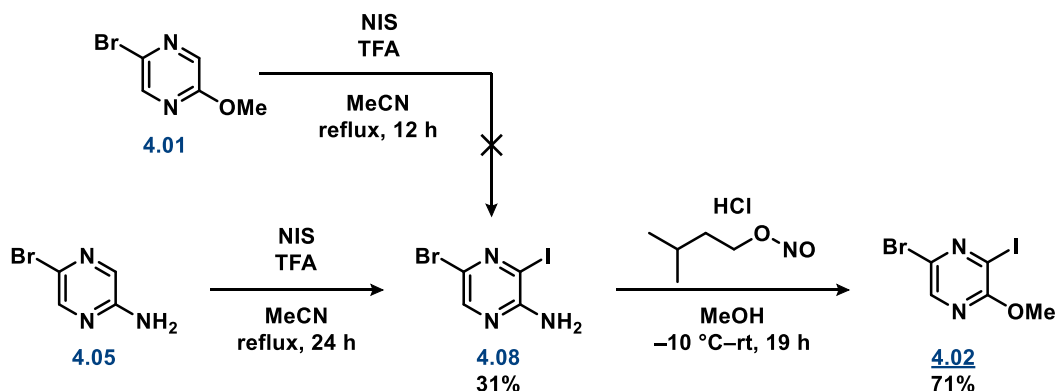
Although the DoM procedure was more straightforward, poor yields led us to explore halogen-metal exchange as an alternative strategy to access **4.04**. Due to the increased sensitivity of  $\pi$ -deficient rings such as pyrazines to competitive nucleophilic substitution as a result of their low LUMO energy, Grignard reagents are generally considered a better choice for the halogen-metal exchange as they are less nucleophilic than alkyllithium metalating agents such as *n*-BuLi (**Scheme 4.5**).<sup>[16,20]</sup>



**Scheme 4.5.** Competing nucleophilic substitution pathway commonly observed when alkyllithium metalating agents are used with  $\pi$ -deficient rings.

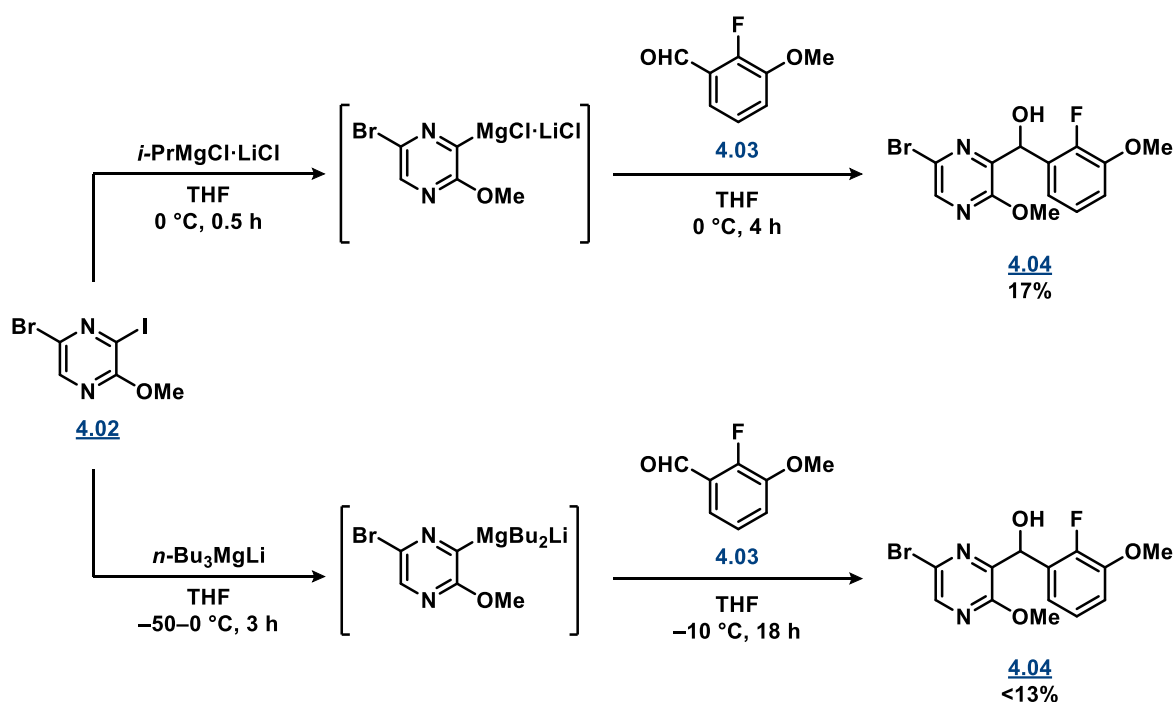
Interestingly, a search of the literature uncovered relatively few examples for the magnesiation of pyrazines *via* halogen exchange. Of the examples found, the vast majority of the reactions proceeded

via Mg/I exchange.<sup>[21–26]</sup> Given this, incorporation of an iodo group at C6 was planned as this would also provide greater selectivity over addition to the C2 bromo due to its greater rate of exchange.<sup>[27]</sup> Starting from **4.01**, iodination using *N*-iodosuccinimide (NIS) was attempted however no reaction was observed, and therefore the iodination of **4.05** was performed prior to methoxylation to afford **4.02** in 22% yield over 2 steps (**Scheme 4.6**).



**Scheme 4.6.** Pathway towards C6 iodination of pyrazine in preparation for iodine-magnesium exchange.

From iodinated intermediate **4.02** (**Scheme 4.7**), halogen-metal exchange using *i*-PrMgCl·LiCl was attempted using the conditions reported by Quéguiner and co-workers.<sup>[21]</sup> Although the reaction proceeded cleanly, only 17% of the product was formed with the majority of the starting material remaining unreacted. As an alternative to the classic Grignard reaction, a more recent strategy employed towards the halogen-metal exchange of pyrazine has been reported by the group of Turck.<sup>[22]</sup> In their report, halogen-metal exchange to a variety of diazines was performed using the magnesium “ate complex” *n*-Bu<sub>3</sub>MgLi. In this procedure, *n*-Bu<sub>3</sub>MgLi is prepared *in situ* by reacting *n*-BuMgCl with 2 equivalents of *n*-BuLi, followed by reaction with the electrophile. Despite good yields reported in their study using 2-iodopyrazine (70–86%), in our hands this reaction proved to be low yielding (<13%) when starting from compound **4.02**.

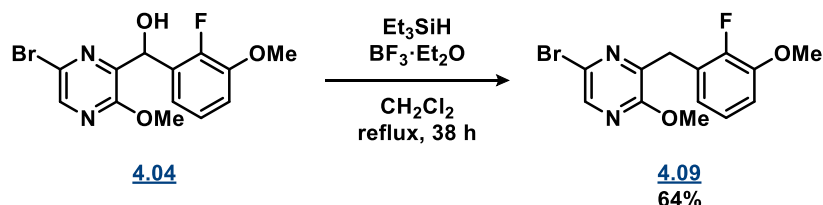


**Scheme 4.7.** Halogen-metal exchange reactions used to access compound **4.04**.

### 4.2.3 Completion of the southern subunit

At this point, the metalation with TMPMgCl·LiCl was selected as the best method to access intermediate **4.04** as it was the most time efficient reaction with a comparable yield to the optimised *ortho*-lithiation procedure.

Similarly to the pyridine series, the synthesis of the southern subunit was completed with the reductive deoxygenation of the benzylic hydroxyl group using an Et<sub>3</sub>SiH and BF<sub>3</sub>·Et<sub>2</sub>O system (**Scheme 4.8**). In comparison to the pyridine series, this reaction was very sluggish and required the addition of 12 equivalents of silane over the course of 38 h to enable complete consumption of starting material, as monitored by LCMS.



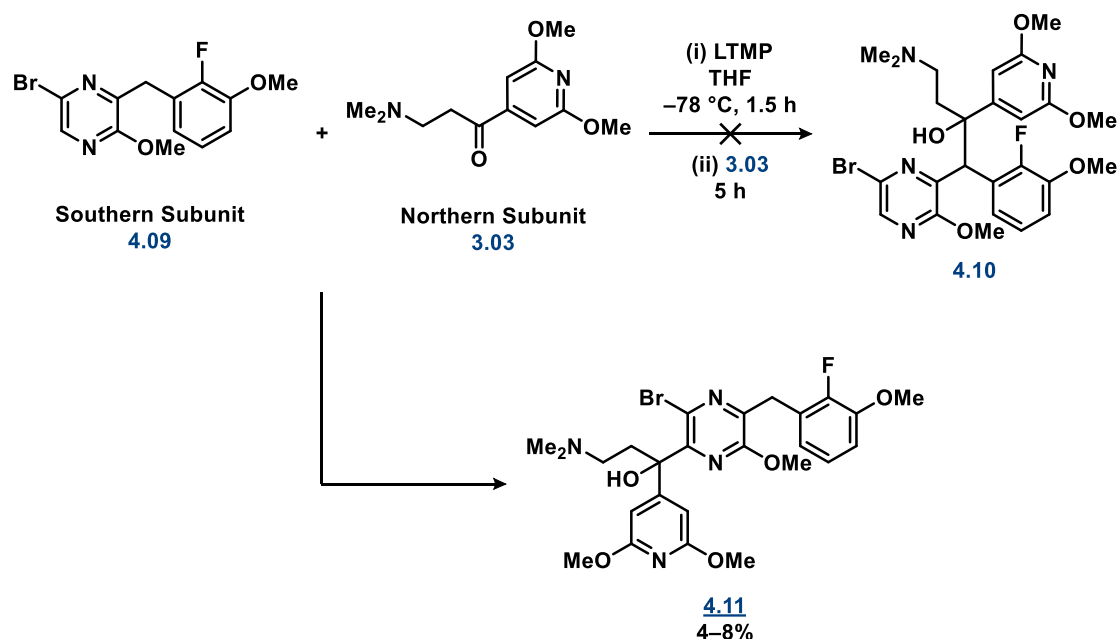
**Scheme 4.8.** Reductive deoxygenation of intermediate **4.04** to complete the southern subunit **4.09**.

### 4.2.4 Addition of the northern and southern subunits

The addition of the northern and southern subunits was attempted with identical conditions to that of the pyridine series in Chapter 3. Using 1.2 equivalents of LTMP, the benzylpyrazine (**4.09**, **Scheme**

**4.9**) was deprotonated at  $-78\text{ }^{\circ}\text{C}$  and stirred for 1.5 h, followed by addition to the pyridyl  $\beta$ -aminoketone **3.03** to react for a further 5 h. Although the majority of the starting materials remained unreacted, mass analysis using LCMS indicated a small amount of what was first thought to be desired product **4.10**. Interestingly, isolation and subsequent NMR analysis of this minor product (8% yield) identified this compound as isomer **4.11** (Scheme 4.9), resulting from addition of **3.02** to the pyrazine ring rather than at the benzylic proton. When this reaction was repeated a second time, only 4% of **4.11** was isolated with no evidence of **4.10** or bis-substituted product. Given this result, it is likely that the enhanced acidity of the pyrazine proton resulting from the additional nitrogen prevents this reaction from occurring selectively at the benzylic position as was achieved in the pyridine series (Chapter 3).

Although the synthesis of **4.10** was not able to be completed during the time-frame of this project, an alternative strategy worthy of exploring in the future to circumvent the issue of selectivity would be to block the C6 position on the pyrazine ring with another functional group so that deprotonation would only occur at the benzylic position. One such option would be to use a trimethylsilyl group, which could then be subsequently removed in the following step. Alternatively, if the group employed was an additional methoxy group, the resulting symmetry would impart the additional advantage of avoiding any regioselectivity issues in the earlier steps of the synthesis so long as the equivalents of the metalating agent were carefully controlled.



**Scheme 4.9.** Attempted addition of the northern and southern subunits towards pyrazine hybrids of TBAJ-587.



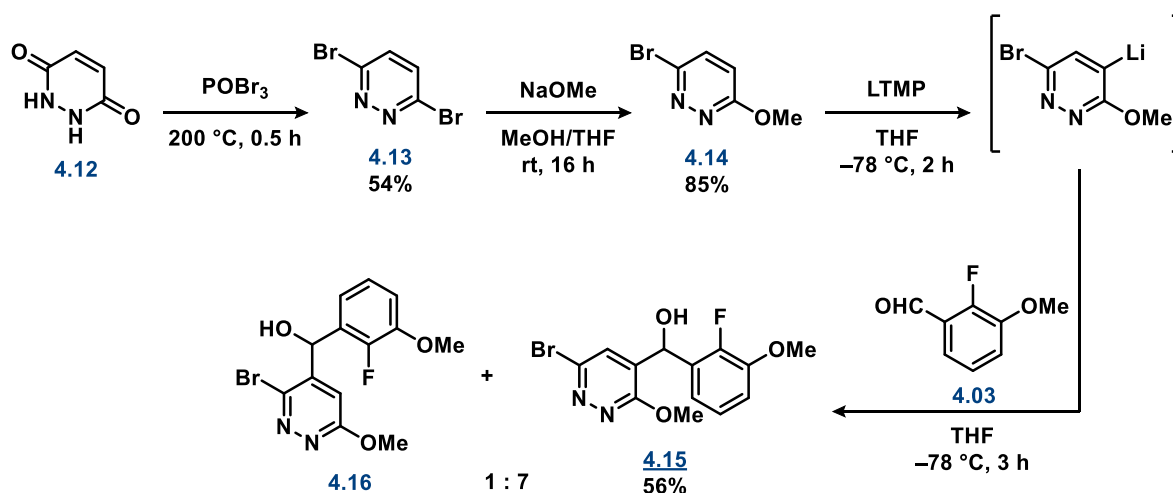
### 4.3 Synthesis of pyridazine analogues

As was the case for the pyrazine analogues (Section 4.2), the majority of the literature published regarding the metalation of pyridazine scaffolds has been established by the group of Quéguiner utilising DoM with hindered lithium dialkylamide bases.<sup>[9]</sup> Although no examples specifically utilising 3-bromo-6-methoxypyridazine **4.14** exist, a detailed study into the lithiation of 3-chloro-6-methoxypyridazine indicated that more hindered lithium bases led to better regioselectivity for the lithiation at C5 (*ortho* to the methoxy group).<sup>[11]</sup>

Starting from commercially available maleic hydrazide (**4.12**, Scheme 4.10), bromination followed by mono-methoxylation afforded key intermediate **4.14**.<sup>[28,29]</sup> Using the conditions as described by the group of Quéguiner<sup>[11]</sup>, lithiation of **4.14** with LTMP followed by trapping with **4.03** provided an 80:20 mixture of **4.15** and **4.16**, respectively. Although the two regioisomers were inseparable on column, recrystallisation from EtOH enabled **4.15** to be isolated in 56% yield. Quéguiner and co-workers reported that the regioselectivity for the C5 position of 3-chloro-6-methoxypyridazine (*ortho* to the methoxy group) could be further improved with the use of an even bulkier base<sup>[11]</sup>, however at this point no other bases were explored with **4.14** to further optimise selectivity for **4.15**.

When the scale of this reaction was increased from 1 to 5 mmol, the yield of **4.15** decreased to 21% and 24% (2 reaction attempts), however regioselectivity was not affected. Despite very careful control of reaction temperature, this reduction in yield could be due to temperature mediated degradation of the highly reactive lithiated pyridazine intermediate at this scale, and so in the future even lower metalation temperatures may be worth exploring if larger scale reactions are required. As an alternative, the use of TMPMgCl·LiCl could also be investigated as metalations with this base tend to be less sensitive to temperature.<sup>[17,18]</sup>

As was the case for the pyrazine series, the major product was expected to be the desired regioisomer **4.15** with addition at the carbon adjacent to the methoxy group due to the directing power of the methoxy group over the bromo.<sup>[12–14]</sup> Although no crystal structure was obtained, the <sup>1</sup>H NMR spectra of the two regioisomers (Figure 4.5) were similar to those published in the literature for the closely related 3-chloro-6-methoxypyridazine<sup>[11]</sup>, with the chemical shift of the pyrazine proton of **4.15** (7.90 ppm, CDCl<sub>3</sub>) shifted downfield in comparison to **4.16** (7.38 ppm, CDCl<sub>3</sub>) due to the electron-withdrawing inductive effect of the neighbouring C3 bromo substituent.



**Scheme 4.10.** Pyridazine functionalisation with **4.03** using directed *ortho*-lithiation.

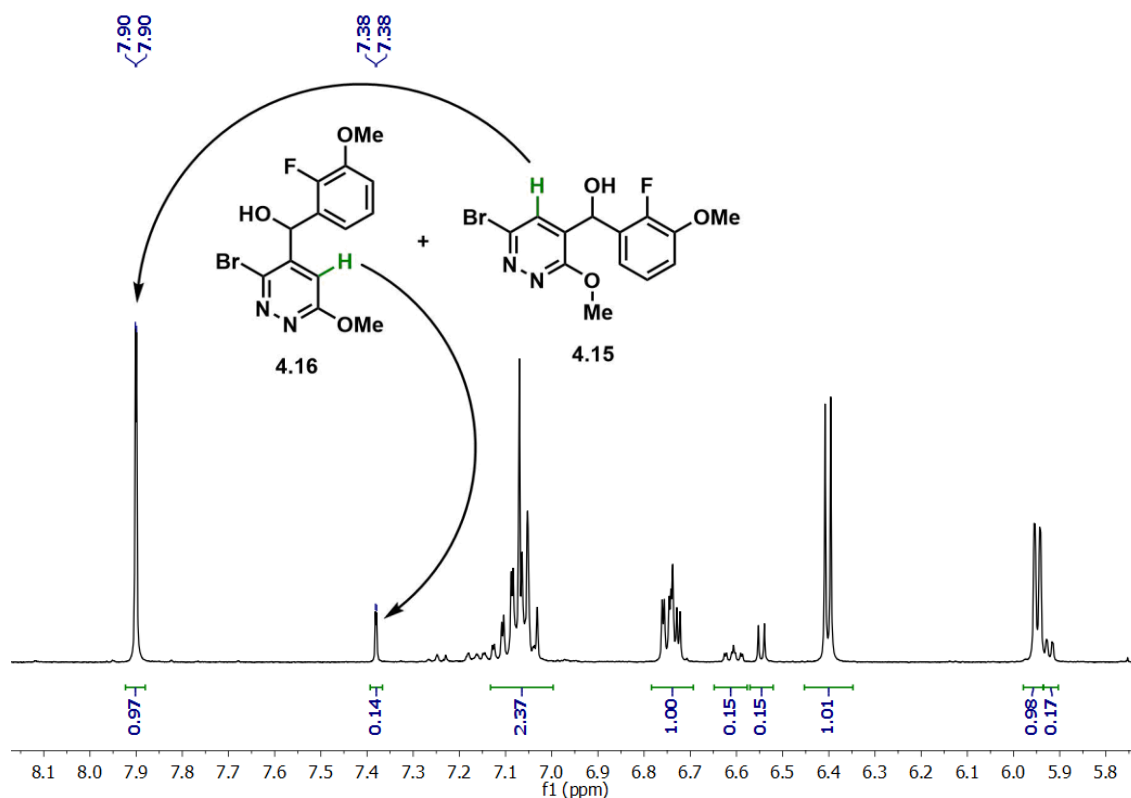
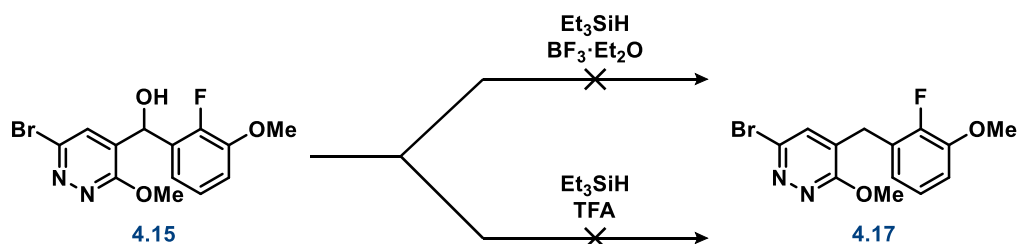


**Figure 4.5.**  $^1\text{H}$  NMR spectrum of the mixture of regioisomers **4.15** and **4.16** demonstrating that the large difference in the chemical shift of the pyridazine proton in each structure is able to be used for identification.

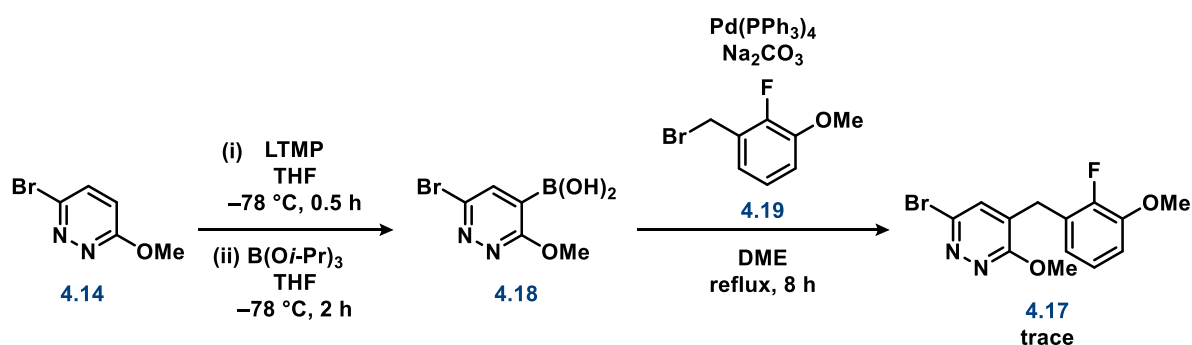
The final step towards the pyridazine southern subunit was the reductive deoxygenation of the diarylmethanol **4.15** (**Scheme 4.11**). Similarly to the pyridine and pyrazine syntheses, silane reduction using an  $\text{Et}_3\text{SiH}/\text{BF}_3\cdot\text{OEt}_2$  system in  $\text{CH}_2\text{Cl}_2$  at reflux was trialled however no reaction was observed. An alternative procedure was attempted using  $\text{Et}_3\text{SiH}$  and TFA, however once again the starting material

remained unreacted. At this point, other conditions to mediate this reduction were not explored however it would be worth investigating either TFA/NaBH<sub>4</sub><sup>[30]</sup>, ZnI<sub>2</sub>-NaBH<sub>3</sub>CN<sup>[31]</sup>, H<sub>3</sub>PO<sub>2</sub>/I<sub>2</sub><sup>[32]</sup>, PBr<sub>3</sub><sup>[33]</sup>, Mo(CO)<sub>6</sub>-Lawesson's reagent<sup>[34]</sup>, and Barton–McCombie deoxygenation<sup>[35]</sup> in the future.



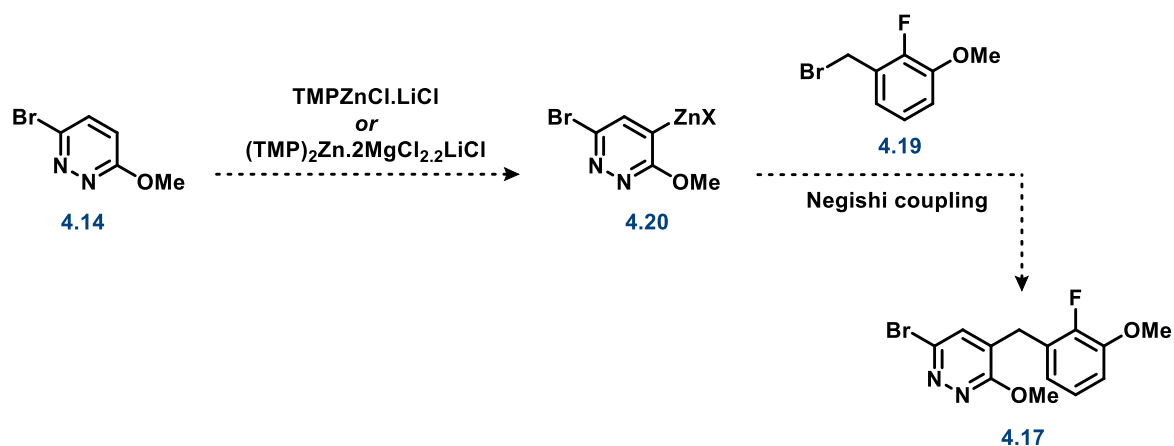
**Scheme 4.11.** Attempted reactions towards **4.17** using silane reduction.

As employed for the synthesis of TBAJ-587, an alternative strategy was investigated to access **4.17** which circumvented the need for reductive deoxygenation by using an Suzuki-Miyaura cross-coupling reaction between benzylbromide **4.19** and pyridazine boronic acid **4.18** (**Scheme 4.12**). Directed *ortho*-lithiation of **4.14** with LTMP followed by addition of triisopropylborate afforded the boronic acid derivative **4.18** following acidic workup, however the subsequent Suzuki-Miyaura cross-coupling produced a complex mixture with only trace amounts of the product **4.17** observed by LCMS.



**Scheme 4.12.** Attempted alternative strategy towards **4.17** using Suzuki-Miyaura cross-coupling.

An alternative procedure that would be worth exploring in the future is Negishi cross-coupling of **4.20** to the benzyl bromide, which has been previously explored by the group of Knochel with diazine substrates (**Scheme 4.13**).<sup>[15,36–38]</sup>



**Scheme 4.13.** Proposed alternative strategy towards **4.17** using Negishi coupling.

#### 4.4 Conclusion

The synthesis of the pyrazine and pyridazine ring A analogues of TBAJ-587 were explored in this chapter using procedures modelled on those described in Chapter 3 towards pyridine analogues. It is anticipated that with further optimisation, the progress achieved in this chapter will constitute to a great number of unique analogues of BDQ with improved physicochemical properties.

With regard to the pyrazine series, a significant effort into the regioselective metalation of the ring was conducted. A survey of various metalation strategies discovered that optimised conditions for DoM utilising either LTMP or  $\text{TMPMgCl} \cdot \text{LiCl}$  were superior to other methods trialled, however the yield for these processes remained low (22 and 26% respectively) and further optimisation is warranted. Furthermore, as the LTMP mediated addition of the two subunits failed to produce product **4.10**, this reaction also warrants further investigation. Since this is most likely a result of the increased acidity of the pyrazine ring proton, future work with this position blocked (e.g. a methoxy group) would be a strategy forward in completing this novel series.

Progress was also made towards the design and optimisation of a new synthetic pathway to access the novel pyridazine series, however this route was not completed in the time frame of this study due to difficulties encountered in the reductive deoxygenation of **4.15**. Future work towards the completion of the southern subunit **4.17** should focus on either (i) exploring alternative deoxygenation procedures; or (ii) a Pd-mediated cross-coupling approach using the benzylbromide **4.19**.

## 4.5 References

- [1] S. Kushner, H. Dalalian, J. L. Sanjurjo, F. L. Bach, S. R. Safir, V. K. Smith, J. H. Williams, *J. Am. Chem. Soc.* **1952**, *74*, 3617–3621.
- [2] *N. Engl. J. Med.* **1958**, *258*, 48–49.
- [3] V. Ambrogi, K. Bloch, S. Daturi, W. Logemann, M. A. Parenti, *J. Pharm. Sci.* **1972**, *61*, 1483–1486.
- [4] J. Adams, M. Kauffman, *Cancer Invest.* **2004**, *22*, 304–311.
- [5] M. R. Kandler, G. T. Mah, A. M. Tejani, S. N. Stabler, D. M. Salzwedel, *Cochrane Database Syst. Rev.* **2011**.
- [6] M. G. Terzano, M. Rossi, V. Palomba, A. Smerieri, L. Parrino, *Drug Saf.* **2003**, *26*, 261–282.
- [7] T. J. Ritchie, S. J. F. Macdonald, S. Peace, S. D. Pickett, C. N. Luscombe, *Medchemcomm* **2012**, *3*, 1062.
- [8] C. G. Wermuth, *Medchemcomm* **2011**, *2*, 935.
- [9] A. Turck, N. Plé, F. Mongin, G. Quéguiner, *Tetrahedron* **2001**, *57*, 4489–4505.
- [10] V. Lotti, G. A. Showell, *Substituted Pyrazines, Pyrimidines and Pyridazines for Use in the Treatment of Glaucoma*, **1991**, US5219849A.
- [11] L. Mojovic, A. Turck, N. Plé, M. Dorsy, B. Ndzi, G. Quéguiner, *Tetrahedron* **1996**, *52*, 10417–10426.
- [12] F. Toudic, A. Turck, N. Plé, G. Quéguiner, M. Darabantu, T. Lequeux, J. C. Pommelet, *J. Heterocycl. Chem.* **2003**, *40*, 855–860.
- [13] F. Mongin, M. Schlosser, *Tetrahedron Lett.* **1997**, *38*, 1559–1562.
- [14] S. Luliński, J. Serwatowski, *J. Org. Chem.* **2003**, *68*, 9384–9388.
- [15] S. Wunderlich, P. Knochel, *Chem. Commun.* **2008**, *0*, 6387.
- [16] F. Chevallier, F. Mongin, *Chem. Soc. Rev.* **2008**, *37*, 595–609.
- [17] B. Haag, M. Mosrin, H. Ila, V. Malakhov, P. Knochel, *Angew. Chemie Int. Ed.* **2011**, *50*, 9794–9824.
- [18] A. Krasovskiy, V. Krasovskaya, P. Knochel, *Angew. Chemie Int. Ed.* **2006**, *45*, 2958–2961.
- [19] G. C. Clososki, C. J. Rohbogner, P. Knochel, *Angew. Chemie Int. Ed.* **2007**, *46*, 7681–7684.
- [20] N. Plé, C. Fruit, Springer, Berlin, Heidelberg, **2012**, pp. 131–170.
- [21] A. Leprêtre, A. Turck, N. Plé, P. Knochel, G. Quéguiner, *Tetrahedron* **2000**, *56*, 265–273.
- [22] F. Buron, N. Plé, A. Turck, F. Marsais, *Synlett* **2006**, *2006*, 1586–1588.
- [23] N. A. Paras, J. Brown, Y. Cheng, S. Hitchcock, T. Judd, P. Lopez, A. E. Minatti, T. Nixey, T. Powers, C. M. Tegley, et al., *Amino Heteroaryl Compounds as Beta-Secretase Modulators and Methods of Use*, **2011**, WO2011090911A1.

- [24] J. A. Balog, A. Huang, U. Velaparthi, P. Liu, *Substituted Bicyclic Heteroaryl Compounds*, **2012**, WO2013049263A1.
- [25] O. Payen, F. Chevallier, F. Mongin, P. C. Gros, *Tetrahedron: Asymmetry* **2012**, 23, 1678–1682.
- [26] K. Babaoglu, G. Brizgys, J. Cha, X. Chen, H. Guo, R. L. Halcomb, X. Han, R. Huang, H. Liu, R. Mcfadden, et al., *Benzothiazol-6-Yl Acetic Acid Derivatives and Their Use for Treating an Hiv Infection*, **2013**, WO2013159064A1.
- [27] R. G. Jones, H. Gilman, in *Org. React.*, John Wiley & Sons, Inc., Hoboken, NJ, USA, **2011**, pp. 339–366.
- [28] N. J. Dewdney, Y. Lou, E. B. Sjogren, M. Soth, *Novel Phenyl-Imidazopyridines and Pyridazines*, **2009**, WO2010006947A1.
- [29] W. P. Dankulich, D. G. McGarry, C. Burns, T. F. Gallagher, F. A. Volz, *Substituted (Aminoiminomethyl or Aminomethyl) Benzoheteroaryl Compounds*, **1999**, WO2000039087A2.
- [30] G. W. Gribble, R. M. Leese, B. E. Evans, *Synthesis*. **1977**, 1977, 172–176.
- [31] C. K. Lau, C. Dufresne, P. C. Belanger, S. Pietre, J. Scheigetz, *J. Org. Chem.* **1986**, 51, 3038–3043.
- [32] P. E. Gordon, A. J. Fry, *Tetrahedron Lett.* **2001**, 42, 831–833.
- [33] Y. Nishigaya, K. Umei, D. Watanabe, Y. Kohno, S. Seto, *Tetrahedron* **2016**, 72, 1566–1572.
- [34] X. Wu, A. K. Mahalingam, M. Alterman, *Tetrahedron Lett.* **2005**, 46, 1501–1504.
- [35] D. H. R. Barton, S. W. McCombie, *J. Chem. Soc. Perkin Trans. 1* **1975**, 1574.
- [36] M. Mosrin, P. Knochel, *Org. Lett.* **2009**, 11, 1837–1840.
- [37] M. Mosrin, T. Bresser, P. Knochel, *Org. Lett.* **2009**, 11, 3406–3409.
- [38] A. Unsinn, M. J. Ford, P. Knochel, *Org. Lett.* **2013**, 15, 1128–1131.

## Chapter 5: Conclusions and Future Directions

### 5.1 Project summary

The overall aim of this project was to synthesise novel derivatives of BDQ to optimise its physicochemical, safety and PK profiles whilst retaining potent anti-*M.tb* activity. In particular, the parameter considered most important to address was BDQ's extreme lipophilicity, which is well-established to be associated with a range of adverse effects.

To achieve reductions in lipophilicity, our primary strategy was to interrogate the A ring of BDQ as modifications to this region (specifically replacement of the quinoline) simultaneously provided an excellent opportunity to access novel IP space. As it was unknown whether the inclusion of alternate heterocyclic moieties in this region would be tolerated in terms of potency against *M.tb*, we initially focused our attention on exploring the SAR in this region to establish if this was a viable strategy.

In Chapter 2, the first heterocycle explored as a quinoline replacement was the smaller pyridine ring. The majority of the SAR established for these pyridine analogues was through extension in the C5 position of the ring, however we also investigated the effect of introducing more polar groups to the pyridine through inclusion of a C6 methoxy group. It was established from this study that replacement of the quinoline in BDQ is tolerated, with substituted phenyl rings at the C5 position of the pyridine ring producing potent compounds. Furthermore, some of these novel derivatives exhibited a similar level of potency to BDQ. The inclusion of the C6 methoxy group was also found to be a well-tolerated strategy to further increase the polarity of the ring. Overall, one of the most potent analogues of this series (**2.111-B**, **Figure 5.1**) exhibited a 10-fold reduction in lipophilicity, which implied that potency was not necessarily correlated with BDQ's lipophilicity.

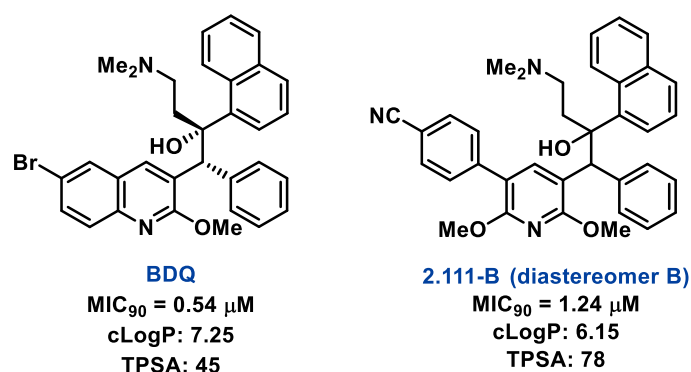


**Figure 5.1.** The most potent analogue synthesised by this candidate in Chapter 2 of this PhD thesis.

In the second stage of this project (Chapter 3), we shifted our attention to the recently disclosed BDQ analogue TBAJ-587, which provided more polar rings to incorporate in the B and C regions of our novel

ring A derivatives. A significant effort went into establishing efficient synthetic pathways to access these hybrid compounds, facilitating the synthesis of multiple, highly potent anti-*M.tb* compounds with improved physicochemical properties. Furthermore, promising preliminary results were obtained when investigating the potential to inhibit the hERG K<sup>+</sup> channel (implicated in BDQ's cardiotoxicity). Specifically, compound **3.55** (**Figure 5.2**) exhibited a >6-fold reduction in potency at hERG in comparison with BDQ, and a *ca.* 2-fold improvement in comparison with the reported value for TBAJ-587.

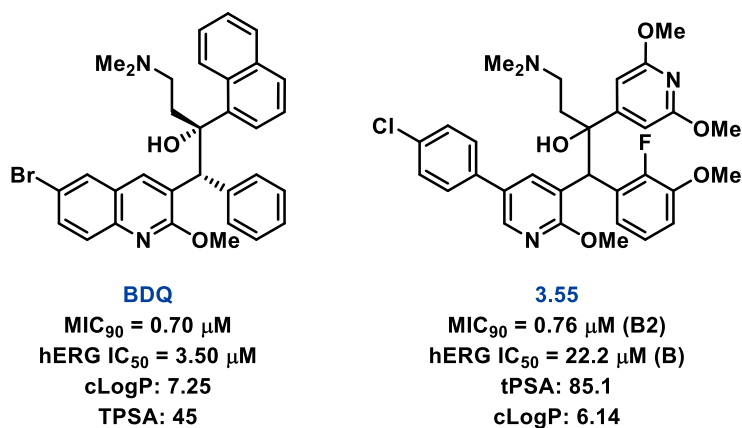


**Figure 5.2.** The most promising derivative synthesised in Chapter 3 of this PhD thesis. The  $\text{MIC}_{90}$  of BDQ was found to be relatively similar in this assay, which was performed by our new collaborators at the University of Queensland.

The final stage of this project aimed to build upon the SAR of the ring A region of the hybrid analogues by including the more polar heterocyclic moieties pyrazine and pyridazine. Although the synthesis of fully derivatised analogues was not completed, it is anticipated that with further optimisation, the significant progress achieved as a result of this study will constitute to a great number of novel derivatives with improved properties.



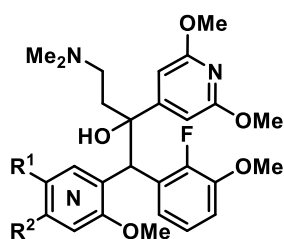
## 5.2 Future directions

In light of the very promising results obtained through this PhD project, it remains of great interest to scale up the eutomers of compounds **3.02**, **3.55** and **3.64** so that more extensive profiling and benchmarking studies may be performed.

These include in depth studies encompassing:

- stereochemical and physicochemical profiling, including absolute configuration, experimental cLogP and kinetic solubility,
- *in vitro* safety, including hERG inhibition, phospholipidosis and CYP3A4 inhibition,
- *in vitro* activity, including activity against slowly replicating *M.tb* populations (LORA assay) and ability to kill *M.tb* residing within macrophage cells (intracellular killing);
- DMPK (drug metabolism and pharmacokinetics), and
- *in vivo* activity and toxicity within a murine model of the disease.

Additionally, further expansion of the SAR of our hybrid derivatives remains of great interest to ensure that we have captured the best compounds to progress into further profiling studies. As mentioned, considerable progress has been made to facilitate the inclusion of diazine rings in place of the ring A pyridine. Additionally, it would also be of interest to further expand on the SAR in the C5 ( $R^1$ ) position of the heterocyclic ring (E.g. with a range of substituted heterocycles), and to explore extension at the C6 ( $R^2$ ) position with additional polar moieties.



$R^1$  = phenyl, heteroaryl (substituted)  
 $R^2$  = diverse polar substituents

**Figure 5.3.** Generalised targeted structural modifications for future studies.

## Chapter 6: Experimental Methods

### 6.1 Chemistry

#### 6.1.1 General experimental methods

All solvents used were of analytical grade: acetone, acetonitrile (MeCN), dichloromethane (CH<sub>2</sub>Cl<sub>2</sub>), dimethylformamide (DMF), dimethylsulfoxide (DMSO), ethanol (EtOH), ether (Et<sub>2</sub>O), ethyl acetate (EtOAc), isopropyl alcohol (IPA), methanol (MeOH), petroleum spirits (Pet. Sp.), tetrahydrofuran (THF), toluene (PhMe). Anhydrous solvents were either purchased in Sure/Seal bottles from Sigma-Aldrich, or alternatively were dried using activated molecular sieves (3 Å or 4 Å, Sigma-Aldrich). All commercially available chemicals were purchased from Advanced Molecular Technologies, AK Scientific, Alfa-Aesar, Ark Pharm, Boron Molecular, Chem-Impex, Combi-Blocks, Matrix Scientific, Merck, Precious Metals Online, Sigma-Aldrich, and stored appropriately and used as required. Analytical thin-layer chromatography (TLC) was performed on silica gel 60 F<sub>254</sub> pre-coated aluminium sheets (0.25 mm, Merck). TLC plates were visualised under UV illumination at 254 nm and 366 nm and with the aid of a potassium permanganate staining solution when appropriate. Flash column chromatography was carried out using Davisil silica gel LC60A (40–63 µm).

All described compounds were characterised at least by <sup>1</sup>H NMR. All novel compounds (distinguished by an underlined compound number) were fully characterised by <sup>1</sup>H and <sup>13</sup>C NMR, low resolution mass spectrometry (LR-MS), high resolution mass spectrometry (HR-MS) and melting point (MP) analysis (when recrystallised).

Small molecule <sup>1</sup>H and <sup>13</sup>C NMR spectra were acquired at 400.13 MHz and 100.62 MHz, respectively, on an Avance III Nanobay 400 MHz Bruker spectrometer at 298 K, coupled to the BACS 60 automatic sample changer and equipped with a 5 mm PABBO BB-1H/ D Z-GRD probe. Data acquisition and processing was managed using XWINNMR (Bruker) software package version 3.5 and plotting was managed using MestReNova version 11.0.4–18998. All NMR spectroscopy chemical shifts (δ) were measured in parts per million (ppm) referenced to an internal standard of residual proteo-solvent: CDCl<sub>3</sub> (7.26 ppm for <sup>1</sup>H and 77.16 ppm for <sup>13</sup>C), MeOD (3.31 ppm for <sup>1</sup>H and 49.0 ppm for <sup>13</sup>C), DMSO-*d*<sub>6</sub> (2.50 ppm for <sup>1</sup>H and 39.52 ppm for <sup>13</sup>C). Solvents used for NMR spectroscopy studies were purchased from Cambridge Isotope Laboratories. Each proton resonance was assigned according to the following convention: chemical shift (δ), multiplicity, coupling constant (*J* Hz) number of protons, assignment. Each carbon resonance was assigned according to the following convention: chemical shift (δ), multiplicity (where no multiplicity is assigned a singlet peak was observed) and coupling constants (*J* Hz) for carbon-fluorine coupling. Multiplicity is quoted as br (broad), s (singlet), d (doublet), t (triplet), q (quartet), p (pentet) and m (multiplet). Where possible, proton and carbon

peaks were assigned with the aid of HSQC and HMBC experiments using the following nomenclature: aromatic (Ar), phenyl (Ph), naphthyl (Naph), pyridine (Pyr), pyrazine (Pyz), pyridazine (Pydz), pinacol (Pin). Missing and/or overlapping  $^{13}\text{C}$  peaks were identified by HSQC and HMBC experiments and are indicated with a † symbol after the identified signal.

Analysis by LR-MS was performed on an Agilent 6120 Series Single Quadrupole LCMS coupled with an Agilent 1260 Infinity series ultra-HPLC, 1200 series G1312B quaternary pump, 1260 series G1367E HiP ALS autosampler and a 1290 series G4212A photodiode array detector. Acquisition and analysis were performed using the Chemstation software Rev.B.04.03 coupled with Masshunter Easy Access. The conditions for liquid chromatography were – column: Agilent Poroshell 120 EC-C18 2.7  $\mu\text{m}$  (3  $\times$  500 mm) 120 Å; column temperature: 35 °C; injection volume: 1  $\mu\text{L}$ ; solvent A: 0.1% formic acid in ultrapure  $\text{H}_2\text{O}$ ; solvent B: 0.1% formic acid in MeCN; flow rate: 0.5 mL/min; gradient: 5–100% of solvent B in solvent A over 2.5 min, then maintained for a further 3.8 min; detection: 254 nm and 214 nm. The conditions for mass spectrometry were – quadrupole ion source; ion mode: API-ES; drying gas temp: 350 °C; vaporiser temperature: 200 °C; capillary voltage: 3000 V (positive and negative); scan range: 100–1000 m/z; step size: 0.1 sec; acquisition time: 5 min.

All HR-MS analyses were acquired on an Agilent 6224 TOF LCMS Mass Spectrometer coupled to an Agilent 1290 Infinity series ultra-HPLC. All data were acquired and reference mass corrected *via* a dual-spray electrospray ionisation (ESI) source. Each scan or data point on the Total Ion Chromatogram (TIC) is an average of 13,700 transients, producing a spectrum every second. Mass spectra were created by averaging the scans across each peak and background subtracted against the first 10 seconds of the TIC. Acquisition was performed using the Agilent Mass Hunter Data Acquisition software version B.05.00 Build 5.0.5042.2 and analysis was performed using Mass Hunter Qualitative Analysis version B.05.00 Build 5.0.519.13. The conditions for mass spectrometry were: ion mode: ESI; drying gas flow: 11 L/min; nebuliser: 45 psi; drying gas temperature: 325 °C; capillary voltage: 4000 V; fragmentor (160 V), skimmer (65 V); octupole RFV (750 V), scan range: 100–1500 m/z; internal reference ions: positive ion mode = m/z = 121.050873 & 922.009798. The conditions for liquid chromatography were: reverse phase HPLC analysis fitted with an Agilent Zorbax SB-C18 Rapid Resolution HT 1.8  $\mu\text{m}$  (2.1  $\times$  50 mm) 80Å column; solvent A: 0.1% formic acid in ultrapure  $\text{H}_2\text{O}$ ; solvent B: 0.1% formic acid in MeCN; flow rate: 0.5 mL/min; gradient: 5–100% of solvent B in solvent A over 3.5 min.

Compound purity was determined using an Agilent 1260 Infinity Analytical HPLC (1260 Infinity G1322A Degasser, 1260 Infinity G1312B Binary pump, G1367E HiP ALS autosampler, 1260 Infinity G1316A Thermostatted Column Compartment, and 1260 Infinity G4212B DAD detector. The conditions for

liquid chromatography were – column: Agilent Zorbax Eclipse Plus C18 Rapid Resolution 3.5  $\mu\text{m}$  (4.6  $\times$  100 mm) 95  $\text{\AA}$ ; column temperature: 35  $^{\circ}\text{C}$ ; injection volume: 1  $\mu\text{L}$ ; solvent A: 0.1% trifluoroacetic acid (TFA) in ultrapure  $\text{H}_2\text{O}$ ; solvent B: 0.1% TFA in MeCN; flow rate: 1.0 mL/min; gradient: 5–100% of solvent B in solvent A over 9 min, then maintained for a further 1 min; detection: 254 nm and 214 nm.

Compound purity for derivatives separated by our collaborators at HangZhou (China) was determined using a Shimadzu LC-2010AHT system. The conditions for liquid chromatography were – column: Agilent Zorbax Eclipse XDB-C8 (2.7  $\mu\text{m}$ , 150 mm  $\times$  4.6 mm); column temperature: ambient; injection volume: 50  $\mu\text{L}$ ; solvent A: 0.05% TFA in ultrapure  $\text{H}_2\text{O}$ ; solvent B: 0.05% TFA in MeOH; isocratic ratio: variable; run time: variable; detection: 290 nm.

Preparative HPLC was performed using an Agilent 1260 Infinity Preparative HPLC system (G1361A DEAAF00598 and G1361A DEAAF00601 pumps, G2260A DEACR00301 ALS autosampler, G1315D DEAX03798 DAD detector, G1364B DEACS00435 fraction collector). Acquisition and analysis were performed using the Chemstation software Rev.B.03.02. The conditions for liquid chromatography were – column: Phenomenex Luna C8(2) (5  $\mu\text{m}$ , 250  $\times$  21.2 mm, 100  $\text{\AA}$ ); column temperature: ambient; solvent A: 0.1% TFA in ultrapure  $\text{H}_2\text{O}$ ; solvent B: 0.1% TFA in MeCN; flow rate: 20 mL/min; gradient: variable; run time: variable; detection: 254 nm.

Chiral HPLC (purity and separation) was performed by our collaborators at TCG Lifesciences (India) using an Agilent 1200 Infinity Analytical HPLC system (G1311A DE62960039 Quaternary Pump, G1367A DE11100750 WPALS autosampler, G1315B DE54627040 DAD detector). Acquisition and analysis were performed using the Chemstation software Rev.B.03.02. The conditions for liquid chromatography were – column: Chiralpak IG (5  $\mu\text{m}$ , 250  $\times$  4.6 mm); column temperature: ambient; mobile phase: variable; flow rate: 1 mL/min; program: isocratic; run time: variable; detection: variable.

Melting points were recorded using a Mettler Toledo MP50 melting point system with a heating rate of 2  $^{\circ}\text{C}/\text{min}$ .

Microwave reactions were conducted in a CEM Discover SP microwave reactor according to the manufacturer's instructions.

## 6.1.2 General methods

### 6.1.2.1. Method A

*General procedure to produce analogues of **2.044** using Suzuki–Miyaura cross-coupling*

To a reaction tube under an atmosphere of nitrogen were added  $\text{Pd}(\text{OAc})_2$  (2.31 mg, 5 mol%), X-Phos (9.82 mg, 10 mol%),  $\text{K}_3\text{PO}_4$  (131 mg, 0.618 mmol) and PhMe (4 mL). After stirring for 5 min, boronic acid (0.412 mmol) and **2.044** (100 mg, 0.206 mmol) were added, and the reaction mixture was stirred

at reflux for 16 h. After this time the reaction was cooled to room temperature, diluted with EtOAc and filtered through a pad of Celite with the aid of EtOAc. The filtrate was washed with a solution of  $\text{NH}_4\text{Cl}$  (saturated, aqueous), the layers separated and the aqueous layer extracted with EtOAc ( $\times 3$ ). The combined organic layers were washed with brine, dried over anhydrous  $\text{MgSO}_4$ , filtered, and concentrated under reduced pressure. Purification by silica gel flash chromatography (0–5%  $\text{MeOH}/0.1\% \text{NH}_3$  in  $\text{CH}_2\text{Cl}_2$ ) afforded the desired product as a mixture of diastereomers (A:B).

A portion of this product was further subjected to purification by preparative HPLC to isolate the individual diastereomers as the TFA salt. This was performed using a gradient of 30 to 100% solvent B in solvent A over 12 min.

#### 6.1.2.2. Method B

*General procedure to produce analogues of **2.105** using Suzuki–Miyaura cross-coupling*

To a reaction tube under an atmosphere of nitrogen were added  $\text{Pd}(\text{OAc})_2$  (2.80 mg, 5 mol%), X-Phos (11.9 mg, 10 mol%),  $\text{K}_3\text{PO}_4$  (159 mg, 0.750 mmol) and PhMe (1 mL). After stirring for 5 min, boronic acid (0.5 mmol) and **2.105** (134 mg, 0.250 mmol) were added, and the reaction mixture was stirred at reflux for 16 h. After this time the reaction was cooled to room temperature, diluted with EtOAc and filtered through a pad of Celite with the aid of EtOAc. The filtrate was washed with a solution of  $\text{NH}_4\text{Cl}$  (saturated, aqueous), the layers separated and the aqueous layer extracted with EtOAc ( $\times 3$ ). The combined organic layers were washed with brine, dried over anhydrous  $\text{MgSO}_4$ , filtered, and concentrated under reduced pressure. Purification by silica gel flash chromatography (0–5%  $\text{MeOH}$  in  $\text{CH}_2\text{Cl}_2$ ) afforded the desired product as a mixture of diastereomers (A:B).

A portion of this product was further subjected to purification by preparative HPLC to isolate the individual diastereomers as the TFA salt. This was performed using a gradient of 30 to 100% solvent B in solvent A over 12 min.

#### 6.1.2.3. Method C

*General procedure to produce analogues of **3.46** using Suzuki–Miyaura cross-coupling*

To a microwave tube was added **3.46** (282 mg, 0.500 mmol),  $\text{Pd}(\text{OAc})_2$  (5.61 mg, 5 mol%), X-Phos (23.8 mg, 10 mol%),  $\text{K}_3\text{PO}_4$  (318 mg, 1.50 mmol), the boronic acid (1.0 mmol) and toluene (2 mL, degassed). The reaction mixture was heated in a microwave reactor at 120 °C for 2 h. After this time the reaction mixture was filtered through a pad of Celite with the aid of EtOAc, and the filtrate washed with a solution of  $\text{NH}_4\text{Cl}$  (saturated, aqueous). The layers were separated, the aqueous layer extracted with EtOAc ( $\times 2$ ), and the combined organic layers were washed with brine, dried over anhydrous  $\text{MgSO}_4$ ,

filtered, and concentrated under reduced pressure. Purification by silica gel flash chromatography (0–5% MeOH in CH<sub>2</sub>Cl<sub>2</sub>) afforded the desired product as a mixture of diastereomers (A:B).

#### 6.1.2.4. Method D

*General procedure to produce chlorophenyl analogues of 3.46 using Suzuki–Miyaura cross-coupling*

To a microwave tube was added **3.46** (282 mg, 0.500 mmol), Pd(OAc)<sub>2</sub> (5.61 mg, 5 mol%), X-Phos (23.8 mg, 10 mol%), K<sub>3</sub>PO<sub>4</sub> (318 mg, 1.50 mmol), the boronic acid (0.600 mmol) and toluene (2 mL, degassed). The reaction mixture was heated in a microwave reactor at 120 °C for 10 min. After this time the reaction mixture was filtered through a pad of Celite with the aid of EtOAc, and the filtrate washed with a solution of NH<sub>4</sub>Cl (saturated, aqueous). The layers were separated, the aqueous layer extracted with EtOAc (×2), and the combined organic layers were washed with brine, dried over anhydrous MgSO<sub>4</sub>, filtered, and concentrated under reduced pressure. Purification by silica gel flash chromatography (0–5% MeOH in CH<sub>2</sub>Cl<sub>2</sub>) afforded the desired product as a mixture of diastereomers (A:B).

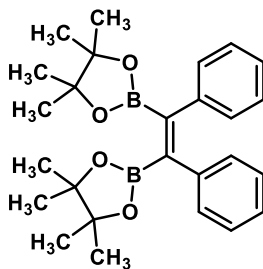
#### 6.1.2.5. Method E

*General procedure to produce analogues of 3.68 using Suzuki–Miyaura cross-coupling*

To a reaction tube was added **3.68** (122 mg, 0.200 mmol), Pd(dppf)Cl<sub>2</sub> (14.6 mg, 10 mol%), K<sub>2</sub>CO<sub>3</sub> (82.9 mg, 0.600 mmol), the pyridyl bromide (0.300 mmol) and 1,4-dioxane/water (4:1, 1 mL, degassed). The reaction mixture was heated at 80 °C for 16 h. After this time the reaction mixture was cooled to room temperature and filtered through a pad of Celite with the aid of EtOAc. The filtrate washed with a solution of NH<sub>4</sub>Cl (saturated, aqueous), the aqueous layer extracted with EtOAc (×2), and the combined organic layers were washed with brine, dried over anhydrous MgSO<sub>4</sub>, filtered, and concentrated under reduced pressure. Purification by silica gel flash chromatography (0–5% MeOH in CH<sub>2</sub>Cl<sub>2</sub>) afforded the desired product as a mixture of diastereomers (A:B).

A portion of this product was further subjected to purification by preparative HPLC to isolate the individual diastereomers as the TFA salt. This was performed using a gradient of 10 to 100% solvent B in solvent A over 12 min.

## 6.1.3 Chapter 2 compounds

**(Z)-1,2-diphenyl-1,2-bis(4,4,5,5-tetramethyl-1,3,2-dioxaborolan-2-yl)ethene**<sup>[1]</sup> (**2.033**)

To a degassed solution of DMF (80 mL) under nitrogen was added diphenylacetylene (9.80 g, 55.0 mmol), bis(pinacolato)diboron (12.7 g, 50.0 mmol) and  $\text{Pt}(\text{PPh}_3)_4$  (1.24 g, 1.00 mmol). After stirring at 80 °C for 24 h, the reaction mixture was cooled to room temperature, diluted with EtOAc and filtered through a pad of Celite with the aid of EtOAc. The reaction mixture was washed with cold saturated aqueous  $\text{NH}_4\text{Cl}$  (×5) to remove DMF, dried over anhydrous  $\text{MgSO}_4$ , filtered and concentrated under reduced pressure. Recrystallisation from EtOH afforded the title compound as a peach-white powder (14.01 g, 32.4 mmol, 65%). Spectroscopic data are in agreement with the literature reported values.<sup>[1]</sup>

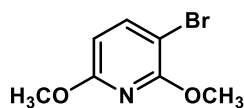
$^1\text{H}$  NMR (400 MHz,  $\text{CDCl}_3$ )  $\delta$  = 7.10 – 6.99 (m, 6H, Ph $\underline{\text{H}}$ ), 6.97 – 6.92 (m, 4H, Ph $\underline{\text{H}}$ ), 1.32 (s, 24H, Pin $\underline{\text{CH}}_3$ );

$^{13}\text{C}$  NMR (101 MHz,  $\text{CDCl}_3$ )  $\delta$  = 141.4 (Ph $\underline{\text{C}}$ ), 129.4 (Ph $\underline{\text{CH}}$ ), 127.6 (Ph $\underline{\text{CH}}$ ), 125.9 (Ph $\underline{\text{CH}}$ ), 84.2 (Pin $\underline{\text{C}}$ ), 25.0 (Pin $\underline{\text{CH}}_3$ ), missing boron bound quaternary carbons;

LR-MS (ESI+)  $m/z$ : mass not found;

HR-MS (ESI+)  $m/z$  [ $\text{M} = \text{C}_{26}\text{H}_{34}\text{B}_2\text{O}_4$ ]: [ $\text{M}+\text{H}$ ] $^+$  calc'd 455.2545, found 455.2556;

MP: 174.9 – 177.6 °C.

**3-bromo-2,6-dimethoxypyridine**<sup>[2]</sup> (**2.034**)

To a solution of 2,6-dimethoxypyridine (6.96 g, 50.0 mmol) in MeCN (200 mL) was added *N*-bromosuccinimide (8.90 g, 50.0 mmol), and the reaction stirred at 80 °C for 18 h. After this time, the solvent was evaporated under reduced pressure, and the residue purified by silica gel flash chromatography (0–6%  $\text{Et}_2\text{O}$  in Pet. Sp.) to afford the title compound as a clear-peach oil (10.6 g, 48.4 mmol, 97%). Spectroscopic data are in agreement with the literature reported values.<sup>[2]</sup>

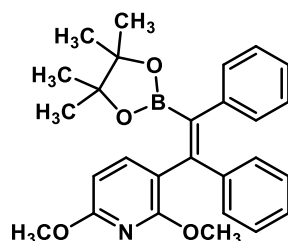
$^1\text{H}$  NMR (400 MHz,  $\text{CDCl}_3$ )  $\delta$  = 7.62 (d,  $J$  = 8.3 Hz, 1H, 4-Pyr $\underline{\text{H}}$ ), 6.22 (d,  $J$  = 8.3 Hz, 1H, 5-Pyr $\underline{\text{H}}$ ), 3.99 (s, 3H, 2-PyrO $\underline{\text{CH}}_3$ ), 3.89 (s, 3H, 6-PyrO $\underline{\text{CH}}_3$ );

$^{13}\text{C}$  NMR (101 MHz,  $\text{CDCl}_3$ )  $\delta$  = 162.2 (2-PyrC-OCH<sub>3</sub>), 158.6 (6-PyrC-OCH<sub>3</sub>), 143.8 (4-PyrC), 102.8 (5-PyrC), 95.5 (PyrC-Br), 54.4 (2-PyrOCH<sub>3</sub>), 53.9 (6-PyrOCH<sub>3</sub>);

LR-MS (ESI+)  $m/z$ : 218.9/220.9  $[\text{M}+\text{H}]^+$ ;

Analytical HPLC (254 nm):  $t_R$  = 7.4 min, 95%.

**(E)-3-(1,2-diphenyl-2-(4,4,5,5-tetramethyl-1,3,2-dioxaborolan-2-yl)vinyl)-2,6-dimethoxypyridine<sup>[3]</sup>**  
**(2.035)**



To a microwave tube under nitrogen were added **2.033** (1.98 g, 4.00 mmol), **2.034** (1.09 g, 5.00 mmol),  $\text{K}_2\text{CO}_3$  (3.32 g, 24.0 mmol),  $\text{Pd}(\text{PPh}_3)_4$  (0.231 g, 5 mol%) to a degassed solution of THF/water (10.5/3.5 mL). After stirring for 5 min at room temperature, the reaction mixture was heated at 100 °C for 2 h in a microwave reactor. After this time, the reaction mixture was cooled to room temperature, diluted with EtOAc, washed with  $\text{NH}_4\text{Cl}$  (saturated, aqueous) and the aqueous layer extracted with EtOAc ( $\times 3$ ). The combined organic layers were washed with brine, dried over anhydrous  $\text{MgSO}_4$ , filtered and concentrated under reduced pressure. Purification by silica gel flash chromatography (0–20% EtOAc in Pet. Sp.) afforded the title compound as a white solid (1.44 g, 3.24 mmol, 71%). A portion of this product was further recrystallised from EtOH to give a white powder for melting point analysis.

$^1\text{H}$  NMR (400 MHz,  $\text{CDCl}_3$ )  $\delta$  = 7.50 (d,  $J$  = 7.9 Hz, 1H, 4-PyrH), 7.18 – 6.92 (m, 10H, PhH), 6.30 (d,  $J$  = 7.9 Hz, 1H, 5-PyrH), 3.92 (s,  $J$  = 5.2 Hz, 3H, PyrOCH<sub>3</sub>), 3.79 (s, 2H, PyrOCH<sub>3</sub>), 1.07 (s,  $J$  = 10.8 Hz, 12H, PinCH<sub>3</sub>);

$^{13}\text{C}$  NMR (101 MHz,  $\text{CDCl}_3$ )  $\delta$  = 162.7 (PyrC-OCH<sub>3</sub>), 160.4 (PyrC-OCH<sub>3</sub>), 146.8 (Pyr-C=C), 142.9 (4-PyrCH), 141.6 (PhC), 141.2 (PhC), 130.1 (PhCH), 129.8 (PhCH), 128.0 (PhCH), 127.5 (PhCH), 126.6 (PhCH), 125.9 (PhCH), 119.1 (3-PyrC), 99.8 (5-PyrCH), 83.6 (PinC-CH<sub>3</sub>), 53.7 (PyrOCH<sub>3</sub>), 53.6 (PyrOCH<sub>3</sub>), 24.7 (PinCH<sub>3</sub>), boron bound quaternary carbon not seen;

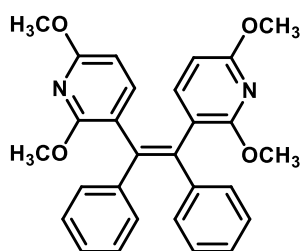
LR-MS (ESI+)  $m/z$ : 444.3  $[\text{M}+\text{H}]^+$ ;

HR-MS (ESI+)  $m/z$  [ $\text{M} = \text{C}_{27}\text{H}_{30}\text{BNO}_4$ ]:  $[\text{M}+\text{H}]^+$  calc'd 444.2345, found 444.2346;

Analytical HPLC (254 nm):  $t_R$  = 9.7 min, 91%;

MP: 114.9 – 116.9 °C.



**(Z)-1,2-bis(2,6-dimethoxypyridin-3-yl)-1,2-diphenylethene (2.038)**

This compound was isolated from the synthesis of **2.035** as an off-white solid which was further recrystallised from EtOH to give white crystals for melting point analysis.

$^1\text{H}$  NMR (400 MHz,  $\text{CDCl}_3$ )  $\delta$  = 7.21 (d,  $J$  = 8.0 Hz, 2H, PyrH), 7.11 – 6.98 (m, 10H, PhH), 6.11 (d,  $J$  = 8.0 Hz, 2H, PyrH), 3.84 (s, 6H, PyrOCH<sub>3</sub>), 3.66 (s, 6H, PyrOCH<sub>3</sub>);

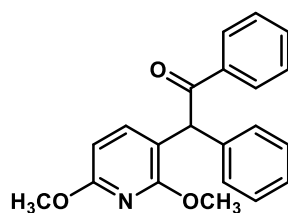
$^{13}\text{C}$  NMR (101 MHz,  $\text{CDCl}_3$ )  $\delta$  = 161.9 (PyrC–OCH<sub>3</sub>), 159.6 (PyrC–OCH<sub>3</sub>), 142.8 (4-PyrCH), 142.4 (C=), 136.8 (C), 130.7 (PhCH), 127.5 (PhCH), 126.3 (PhCH), 118.4 (3-PyrC), 100.0 (5-PyrCH), 53.6 (PyrOCH<sub>3</sub>), 53.2 (PyrOCH<sub>3</sub>);

LR-MS (ESI+)  $m/z$ : 455.2  $[\text{M}+\text{H}]^+$ ;

HR-MS (ESI+)  $m/z$  [ $\text{M} = \text{C}_{28}\text{H}_{26}\text{N}_2\text{O}_4$ ]:  $[\text{M}+\text{H}]^+$  calc'd 455.1965, found 455.1976;

Analytical HPLC (254 nm):  $t_R$  = 9.8 min, 94%;

MP: 157.8 – 160.5 °C.

**2-(2,6-dimethoxypyridin-3-yl)-1,2-diphenylethan-1-one<sup>[4]</sup> (2.036)**

To **2.035** (1.42 g, 3.24 mmol) in THF (25 mL) and water (25 mL) was added sodium perborate tetrahydrate (2.24 g, 14.6 mmol). The reaction mixture was stirred vigorously at room temperature for 16 h. After this time, the reaction was quenched with water and extracted with EtOAc (×3). The combined organic layers were washed with brine, dried over anhydrous  $\text{MgSO}_4$ , filtered and concentrated under reduced pressure. Purification by silica gel flash chromatography (5%  $\text{Et}_2\text{O}$  in Pet. Sp.) afforded the title compound as a white solid (0.973 g, 2.92 mmol, 90%). A portion of this product was further recrystallised from EtOH to give a white powder for melting point analysis.

$^1\text{H}$  NMR (400 MHz,  $\text{CDCl}_3$ )  $\delta$  = 8.04 – 7.95 (m, 2H, Ph $\underline{\text{H}}$ ), 7.53 – 7.48 (m, 1H, Ph $\underline{\text{H}}$ ), 7.44 – 7.37 (m, 2H, Ph $\underline{\text{H}}$ ), 7.37 – 7.23 (m, 5H, Ph $\underline{\text{H}}$ ), 7.18 (d,  $J$  = 8.1 Hz, 1H, 4-Pyr $\underline{\text{H}}$ ), 6.23 (d,  $J$  = 8.1 Hz, 1H, 5-Pyr $\underline{\text{H}}$ ), 6.19 (s, 1H, Pyr- $\underline{\text{CH}}$ -Ph), 3.91 (s, 3H, PyrO $\underline{\text{CH}}_3$ ), 3.89 (s, 3H, PyrO $\underline{\text{CH}}_3$ );

$^{13}\text{C}$  NMR (101 MHz,  $\text{CDCl}_3$ )  $\delta$  = 198.7 (C=O), 162.3 (Pyr $\underline{\text{C}}$ -OCH $_3$ ), 159.5 (Pyr $\underline{\text{C}}$ -OCH $_3$ ), 141.1 (4-Pyr $\underline{\text{CH}}$ ), 137.8 (Ph $\underline{\text{C}}$ ), 137.0 (Ph $\underline{\text{C}}$ ), 133.0 (Ph $\underline{\text{CH}}$ ), 129.5 (Ph $\underline{\text{CH}}$ ), 128.9 (Ph $\underline{\text{CH}}$ ), 129.0 (Ph $\underline{\text{CH}}$ ), 128.7 (Ph $\underline{\text{CH}}$ ), 127.4 (Ph $\underline{\text{CH}}$ ), 113.7 (3-Pyr $\underline{\text{C}}$ ), 100.6 (5-Pyr $\underline{\text{CH}}$ ), 53.7 (PyrO $\underline{\text{CH}}_3$ ), 53.7 (PyrO $\underline{\text{CH}}_3$ ), 52.0 (Pyr- $\underline{\text{CH}}$ -Ph);

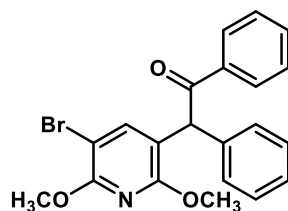
LR-MS (ESI+)  $m/z$ : 334.2  $[\text{M}+\text{H}]^+$ ;

HR-MS (ESI+)  $m/z$  [ $\text{M} = \text{C}_{21}\text{H}_{19}\text{NO}_3$ ]:  $[\text{M}+\text{H}]^+$  calc'd 334.1438, found 334.1440;

Analytical HPLC (254 nm):  $t_R$  = 8.7 min, 94%;

MP: 91.1 – 93.6 °C.

### 2-(5-bromo-2,6-dimethoxyphenyl)-1,2-diphenylethan-1-one<sup>[2]</sup> (**2.039**)



To a solution of **2.036** (1.32 g, 3.96 mmol) in MeCN (35 mL) was added *N*-bromosuccinimide (0.775 g, 4.36 mmol). The resulting mixture was stirred at reflux for 16 h. After this time, the solvent was evaporated under reduced pressure, and the residue purified by silica gel flash chromatography (5% EtOAc in Pet. Sp.) to afford the title compound as a white solid upon standing (1.53 g, 3.71 mmol, 94%). A portion of this product was further recrystallised from EtOH to give a light-yellow powder for melting point analysis.

$^1\text{H}$  NMR (400 MHz,  $\text{CDCl}_3$ )  $\delta$  = 8.02 – 7.97 (m, 2H, Ph $\underline{\text{H}}$ ), 7.54 – 7.49 (m, 1H, Ph $\underline{\text{H}}$ ), 7.44 – 7.27 (m, 8H, Ph $\underline{\text{H}}$ , 4-Pyr $\underline{\text{H}}$ ), 6.15 (s, 1H, Pyr- $\underline{\text{CH}}$ -Ph), 3.98 (s, 3H, PyrO $\underline{\text{CH}}_3$ ), 3.90 (s, 3H, PyrO $\underline{\text{CH}}_3$ );

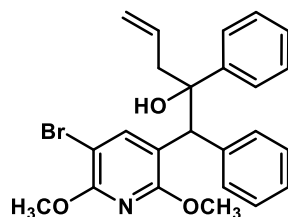
$^{13}\text{C}$  NMR (101 MHz,  $\text{CDCl}_3$ )  $\delta$  = 198.1 ( $\underline{\text{C}}=\text{O}$ ), 158.5 (Pyr $\underline{\text{C}}$ -OCH $_3$ ), 157.6 (Pyr $\underline{\text{C}}$ -OCH $_3$ ), 143.7 (Pyr $\underline{\text{CH}}$ ), 136.9 (Ph $\underline{\text{C}}$ ), 136.8 (Ph $\underline{\text{C}}$ ), 133.1 (Ph $\underline{\text{CH}}$ ), 129.4 (Ph $\underline{\text{CH}}$ ), 129.3 (Ph $\underline{\text{CH}}$ ), 128.9 (Ph $\underline{\text{CH}}$ ), 128.7 (Ph $\underline{\text{CH}}$ ), 127.7 (Ph $\underline{\text{CH}}$ ), 115.7 (3-Pyr $\underline{\text{C}}$ ), 95.5 (4-Pyr $\underline{\text{C}}$ ), 54.5 (PyrO $\underline{\text{CH}}_3$ ), 54.1 (PyrO $\underline{\text{CH}}_3$ ), 52.0 (Pyr- $\underline{\text{CH}}$ -Ph);

LR-MS (ESI+)  $m/z$ : 412.0/414.1  $[\text{M}+\text{H}]^+$ ;

HR-MS (ESI+)  $m/z$  [ $\text{M} = \text{C}_{21}\text{H}_{18}\text{BrNO}_3$ ]:  $[\text{M}+\text{H}]^+$  calc'd 412.0546, found 412.0549;

Analytical HPLC (254 nm):  $t_R$  = 9.3 min, 92%;

MP: 127.1 – 129.1 °C.

**1-(5-bromo-2,6-dimethoxypyridin-3-yl)-1,2-diphenylpent-4-en-2-ol<sup>[5]</sup> (2.040)****Step (i) – Preparation of allylzinc bromide:**

To an oven-dried reaction tube under nitrogen was added zinc powder (0.671 g, 10.3 mmol), which was then heated to 65 °C. After 2 min, 1,2-dibromoethane (88.4  $\mu$ L, 1.03 mmol) in THF (1.7 mL, anhydrous) was added, and the temperature was maintained for 10 min. The reaction mixture was then cooled to room temperature, followed by the addition of trimethylsilyl chloride (86.8  $\mu$ L, 0.684 mmol) in THF (0.855 mL, anhydrous). The mixture was stirred at room temperature for 15 min. After this time, allyl bromide (740  $\mu$ L, 8.55 mmol) in THF (4 mL, anhydrous) was added dropwise over 30 min.

**Step (ii) – Addition of allylzinc bromide:**

In an open atmosphere, **2.039** (2.82 g, 6.84 mmol) was added to the freshly prepared solution of allyl zinc bromide and stirred for 30 min at room temperature. After this time, the reaction was quenched by the addition of water (10 mL), diluted with EtOAc (15 mL), and the organic layer separated. The aqueous layer was extracted with EtOAc ( $\times 3$ ) and the combined organic layers were washed with brine, dried over anhydrous  $\text{MgSO}_4$ , filtered and concentrated under reduced pressure. Purification by silica gel flash chromatography (25–50% Pet. Sp. in PhMe) afforded the title compound as an off-white solid (3.06 g, 6.73 mmol, 98%, A:B = 48:52).

LR-MS (ESI+)  $m/z$ : 454.1/456.1  $[\text{M}+\text{H}]^+$ ;

HR-MS (ESI+)  $m/z$   $[\text{M} = \text{C}_{24}\text{H}_{24}\text{BrNO}_3]$ :  $[\text{M}+\text{H}]^+$  calc'd 454.1012, found 454.1016;

Analytical HPLC (254 nm):  $t_R$  = 9.5 min, 43% (A); 9.6 min, 52% (B);

**Diastereomer A:**

$^1\text{H}$  NMR (400 MHz,  $\text{CDCl}_3$ )  $\delta$  = 8.32 (s, 1H, 4-PyrH), 7.59 – 7.51 (m, 2H, PhH), 7.42 – 7.30 (m, 4H, PhH), 7.28 – 7.18 (m, 3H, PhH), 7.10 (t,  $J$  = 7.3 Hz, 1H, PhH), 5.40 – 5.11 (m, 1H, CH=CH<sub>2</sub>), 5.07 – 4.85 (m, 2H, CH=CH<sub>2</sub>), 4.70 (s, 1H, Pyr-CH-Ph), 3.81 (s, 3H, 6-PyrOCH<sub>3</sub>), 3.66 (s, 3H, 2-PyrOCH<sub>3</sub>), 2.74 (dd,  $J$  = 13.7, 5.4 Hz, 1H, CH<sub>a</sub>H<sub>b</sub>-CH=CH<sub>2</sub>), 2.35 – 2.29 (m, 2H, CH<sub>a</sub>H<sub>b</sub>-CH=CH<sub>2</sub>, OH);

$^{13}\text{C}$  NMR (101 MHz,  $\text{CDCl}_3$ )  $\delta$  = 158.6 (2-PyrC-OCH<sub>3</sub>), 156.2 (6-PyrC-OCH<sub>3</sub>), 145.0 (PhC), 144.4 (4-PyrCH), 140.5 (PhC), 133.3 (CH=CH<sub>2</sub>), 130.7 (PhCH), 128.3 (PhCH), 127.8 (PhCH), 126.9 (PhCH), 126.4 (PhCH),

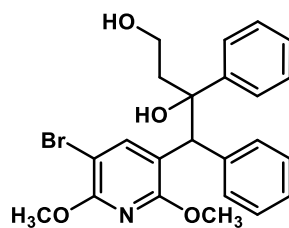
125.8 (Ph $\underline{\text{C}}\text{H}$ ), 120.0 (CH= $\underline{\text{C}}\text{H}_2$ ), 117.5 (3-Pyr $\underline{\text{C}}$ ), 94.9 (5-Pyr $\underline{\text{C}}\text{-Br}$ ), 78.3 ( $\underline{\text{C}}\text{-OH}$ ), 54.0 (6-PyrO $\underline{\text{C}}\text{H}_3$ ), 53.7 (2-PyrO $\underline{\text{C}}\text{H}_3$ ), 52.1 (Pyr- $\underline{\text{C}}\text{H-Ph}$ ), 47.3 ( $\underline{\text{C}}\text{H}_2\text{-CH=CH}_2$ );

Diastereomer B:

$^1\text{H}$  NMR (400 MHz,  $\text{CDCl}_3$ )  $\delta$  = 8.34 (s, 1H, 4-Pyr $\underline{\text{H}}$ ), 7.31 – 7.29 (m, 2H, Ph $\underline{\text{H}}$ ), 7.23 – 7.14 (m, 4H, Ph $\underline{\text{H}}$ ), 7.12 – 7.07 (m, 1H, Ph $\underline{\text{H}}$ ), 7.05 – 6.97 (m, 3H, Ph $\underline{\text{H}}$ ), 5.36 – 5.26 (m, 1H,  $\underline{\text{C}}\text{H=CH}_2$ ), 5.04 – 5.01 (m, 2H, CH= $\underline{\text{C}}\text{H}_2$ ), 4.78 (s, 1H, Pyr- $\underline{\text{C}}\text{H-Ph}$ ), 3.99 (s, 3H, 6-PyrO $\underline{\text{C}}\text{H}_3$ ), 3.97 (s, 3H, 2-PyrO $\underline{\text{C}}\text{H}_3$ ), 2.85 (ddt,  $J$  = 13.7, 5.3, 1.3 Hz, 1H,  $\underline{\text{C}}\text{H}_a\text{H}_b\text{-CH=CH}_2$ ), 2.43 – 2.34 (m, 2H,  $\text{CH}_a\text{H}_b\text{-CH=CH}_2$ , OH);

$^{13}\text{C}$  NMR (101 MHz,  $\text{CDCl}_3$ )  $\delta$  = 159.3 (2-Pyr $\underline{\text{C}}\text{-OCH}_3$ ), 156.8 (6-Pyr $\underline{\text{C}}\text{-OCH}_3$ ), 145.3 (Ph $\underline{\text{C}}$ ), 145.1 (4-Pyr $\underline{\text{C}}\text{H}$ ), 140.6 (Ph $\underline{\text{C}}$ ), 133.4 ( $\underline{\text{C}}\text{H=CH}_2$ ), 130.1 (Ph $\underline{\text{C}}\text{H}$ ), 127.9 (Ph $\underline{\text{C}}\text{H}$ ), 127.8 (Ph $\underline{\text{C}}\text{H}$ ), 126.5 (Ph $\underline{\text{C}}\text{H}$ ), 126.1 (Ph $\underline{\text{C}}\text{H}$ ), 126.0 (Ph $\underline{\text{C}}\text{H}$ ), 120.2 (CH= $\underline{\text{C}}\text{H}_2$ ), 117.01 (3-Pyr $\underline{\text{C}}$ ), 95.7 (5-Pyr $\underline{\text{C}}\text{-Br}$ ), 78.9 ( $\underline{\text{C}}\text{-OH}$ ), 54.3 (6-PyrO $\underline{\text{C}}\text{H}_3$ ), 54.1 (2-PyrO $\underline{\text{C}}\text{H}_3$ ), 52.1 (Pyr- $\underline{\text{C}}\text{H-Ph}$ ), 46.0 ( $\underline{\text{C}}\text{H}_2\text{-CH=CH}_2$ ).

#### 4-(5-bromo-2,6-dimethoxypyridin-3-yl)-3,4-diphenylbutane-1,3-diol (**2.042**)



Step (i) – Oxidative cleavage<sup>[6]</sup>:

To a stirred mixture of **2.040** (5.21 g, 11.5 mmol) in MeCN (60 mL) was added  $\text{RuCl}_3$  (95.2 mg, 4 mol%) and  $\text{NaIO}_4$  (5.40 g, 25.3 mmol) at room temperature. After 5 min, water (6 mL) was added to the reaction mixture at a rate of 0.600 mL every 5 min. After 14 h, the reaction was quenched with  $\text{Na}_2\text{S}_2\text{O}_3$  (saturated, aqueous) and the two layers were separated. The aqueous layer was extracted with  $\text{Et}_2\text{O}$  ( $\times 3$ ), and the combined organic layers washed with brine, dried over anhydrous  $\text{MgSO}_4$ , filtered, and concentrated under reduced pressure. The crude aldehyde product was used in the next step without further purification.

Step (ii) – Aldehyde reduction:

To a ice-cold solution of the crude aldehyde in MeOH (60 mL) was added  $\text{NaBH}_4$  (0.867 g, 23 mmol) portion-wise. The reaction was then warmed to room temperature and stirred for 1 h. After this time, the solvent was removed under reduced pressure, and EtOAc (60 mL) added to the residue. The organic solution was washed with water, and the two layers separated. The aqueous layer was extracted with EtOAc ( $\times 3$ ), and the combined organic layers were washed with brine, dried over anhydrous  $\text{MgSO}_4$ , filtered, and concentrated under reduced pressure. Purification by silica gel flash

chromatography (0–30% EtOAc in Pet. Sp.) afforded the title compound as an off-white foam (2.88 g, 55% over two steps, A:B = 50:50).

LR-MS (ESI+)  $m/z$ : 457.8/459.8  $[M+H]^+$ ;

HR-MS (ESI+)  $m/z$   $[M = C_{23}H_{24}BrNO_4]$ :  $[M+H]^+$  calc'd 458.0961, found 458.0958;

Analytical HPLC (254 nm):  $t_R$  = 8.4 min, 45% (A); 8.5 min 50% (B);

Diastereomer A:

$^1H$  NMR (400 MHz,  $CDCl_3$ )  $\delta$  = 8.35 (s, 1H, PyrH), 7.61 – 7.54 (m, 2H, PhH), 7.48 – 7.39 (m, 2H, PhH), 7.37 – 7.28 (m, 2H, PhH), 7.24 (tt,  $J$  = 7.2, 1.3 Hz, 3H, PhH), 7.17 – 7.07 (m, 1H, PhH), 4.61 (s, 1H, Pyr-CH-Ph), 4.13 (s, 1H, OH), 3.80 (s, 3H, 6-Pyr-OCH<sub>3</sub>), 3.67 (s, 3H, 2-Pyr-OCH<sub>3</sub>), 3.54 (m, 1H, CH<sub>a</sub>H<sub>b</sub>OH), 3.37 (m, 1H, CH<sub>a</sub>H<sub>b</sub>OH), 2.07 (ddd,  $J$  = 15.1, 10.9, 4.4 Hz, 1H, CH<sub>a</sub>H<sub>b</sub>OH), 1.91 (dt,  $J$  = 14.7, 3.3 Hz, 1H, CH<sub>a</sub>H<sub>b</sub>OH), 1.70 (t,  $J$  = 4.4 Hz, 1H, OH);

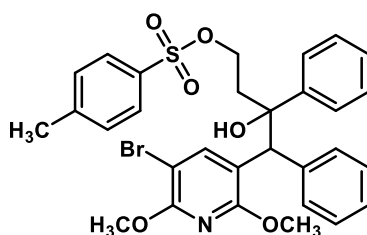
$^{13}C$  NMR (101 MHz,  $CDCl_3$ )  $\delta$  = 158.4 (2-PyrC-OCH<sub>3</sub>), 156.0 (6-PyrC-OCH<sub>3</sub>), 144.9 (PhC), 144.4 (PyrCH), 140.5 (PhC), 130.6 (PhCH), 128.1 (PhCH), 127.8 (PhCH), 126.7 (PhCH), 126.3 (PhCH), 125.7 (PhCH), 117.4 (3-PyrC), 94.8 (5-PyrC-Br), 80.4 (C-OH), 60.3 (CH<sub>2</sub>CH<sub>2</sub>OH), 53.9 (6-PyrOCH<sub>3</sub>), 53.6 (2-PyrOCH<sub>3</sub>), 52.9 (Pyr-CH-Ph), 42.4 (CH<sub>2</sub>CH<sub>2</sub>OH);

Diastereomer B:

$^1H$  NMR (400 MHz,  $CDCl_3$ )  $\delta$  = 8.43 (s, 1H, PyrH), 7.39 – 7.32 (m, 2H, PhH), 7.29 – 7.08 (m, 5H, PhH), 7.07 – 6.95 (m, 3H, PhH), 4.72 (s, 1H, Pyr-CH-Ph), 4.17 (s, 1H, OH), 3.99 (s, 3H, 6-Pyr-OCH<sub>3</sub>), 3.97 (s, 3H, 2-Pyr-OCH<sub>3</sub>), 3.62 (m, 1H, CH<sub>a</sub>H<sub>b</sub>OH), 3.42 (m, 1H, CH<sub>a</sub>H<sub>b</sub>OH), 2.19 (ddd,  $J$  = 15.4, 11.2, 4.4 Hz, 1H, CH<sub>a</sub>H<sub>b</sub>OH), 2.00 (dt,  $J$  = 14.8, 3.1 Hz, 1H, CH<sub>a</sub>H<sub>b</sub>OH), 1.76 (t,  $J$  = 4.3 Hz, 1H, OH);

$^{13}C$  NMR (101 MHz,  $CDCl_3$ )  $\delta$  = 159.3 (2-PyrC-OCH<sub>3</sub>), 156.8 (6-PyrC-OCH<sub>3</sub>), 145.2 (PyrCH), 140.5 (PhC), 130.0 (PhCH), 128.0 (PhCH), 127.7 (PhCH), 126.5 (PhCH), 126.1 (PhCH), 126.0 (PhCH), 117.2 (3-PyrC), 95.7 (5-PyrC-Br), 81.2 (C-OH), 60.7 (CH<sub>2</sub>CH<sub>2</sub>OH), 54.3 (6-PyrOCH<sub>3</sub>), 54.1 (2-PyrOCH<sub>3</sub>), 52.7 (Pyr-CH-Ph), 41.2 (CH<sub>2</sub>CH<sub>2</sub>OH), missing 1  $\times$  PhC.

**4-(5-bromo-2,6-dimethoxypyridin-3-yl)-3-hydroxy-3,4-diphenylbutyl 4-methylbenzenesulfonate (2.043)**



To an ice-cold solution of **2.042** (2.75 g, 6.00 mmol) in CH<sub>2</sub>Cl<sub>2</sub> (30 mL) was added Et<sub>3</sub>N (1.67 mL, 12.0 mmol), followed by the portion-wise addition of *p*-toluenesulfonyl chloride (5.72 g, 30.0 mmol). After stirring for 10 h at room temperature, water was added to quench the reaction, and the two layers separated. The aqueous layer was extracted with CH<sub>2</sub>Cl<sub>2</sub> (×3), and the combined organic extracts were dried over anhydrous MgSO<sub>4</sub>, filtered and concentrated under reduced pressure. Purification by silica gel flash chromatography (0–30% EtOAc in Pet. Sp.) afforded the title compound as an off-white foam (3.08 g, 5.03 mmol, 84%, A:B = 56:44).

LR-MS (ESI+) *m/z*: 612.0/614.0 [M+H]<sup>+</sup>;

HR-MS (ESI+) *m/z* [M = C<sub>30</sub>H<sub>30</sub>BrNO<sub>6</sub>S]: [M+H]<sup>+</sup> calc'd 612.105, found 612.1029;

Analytical HPLC (254 nm): *t*<sub>R</sub> = 8.0 min, 45% (A); 8.2 min 44% (B);

Diastereomer A:

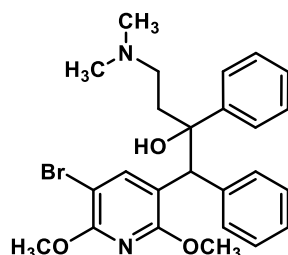
<sup>1</sup>H NMR (400 MHz, CDCl<sub>3</sub>) δ = 8.18 (s, 1H, PyrH), 7.57 (d, *J* = 8.3 Hz, 2H, Ph'H), 7.45 – 7.41 (m, 2H, Ph'H), 7.34 (t, *J* = 7.3 Hz, 2H, PhH), 7.29 – 7.21 (m, 5H, PhH), 7.20 – 7.13 (m, 2H, PhH), 7.08 (t, *J* = 7.2 Hz, 1H, PhH), 4.62 (s, 1H, Pyr-CH-Ph), 3.87 – 3.75 (m, 4H, 6-PyrOCH<sub>3</sub>, CH<sub>a</sub>H<sub>b</sub>OTs), 3.77 – 3.68 (m, 1H, CH<sub>a</sub>H<sub>b</sub>OTs), 3.68 (s, 3H, 2-PyrOCH<sub>3</sub>), 2.52 (s, 1H, OH), 2.42 (s, 3H, PhCH<sub>3</sub>), 2.20 (ddd, *J* = 14.4, 7.6, 5.2 Hz, 1H, CH<sub>a</sub>H<sub>b</sub>OTs), 2.07 (dt, *J* = 14.6, 7.5 Hz, 1H, CH<sub>a</sub>H<sub>b</sub>OTs);

<sup>13</sup>C NMR (101 MHz, CDCl<sub>3</sub>) δ = 158.4 (2-PyrC-OCH<sub>3</sub>), 156.3 (6-PyrC-OCH<sub>3</sub>), 144.8 (PhC), 144.1 (PyrC), 142.8 (PhC), 139.2 (PhC), 132.7 (PhC), 130.4 (PhCH), 129.9 (PhCH), 128.7 (PhCH), 128.1 (PhCH), 127.9 (PhCH), 127.3 (PhCH), 126.8 (PhCH), 125.3 (PhCH), 116.7 (3-PyrC), 94.9 (5-PyrC), 78.2 (C-OH), 67.7 (CH<sub>2</sub>CH<sub>2</sub>OTs), 54.0 (6-PyrOCH<sub>3</sub>), 53.8 (2-PyrOCH<sub>3</sub>), 52.9 (Pyr-CH-Ph), 41.5 (CH<sub>2</sub>CH<sub>2</sub>OTs), 21.7 (PhCH<sub>3</sub>);

Diastereomer B:

<sup>1</sup>H NMR (400 MHz, CDCl<sub>3</sub>) δ = 8.20 (s, 1H, PyrH), 7.60 (d, *J* = 8.4 Hz, 2H, Ph'H), 7.28 – 7.23 (m, 2H, Ph'H), 7.16 (d, *J* = 4.3 Hz, 5H, PhH), 7.04 – 6.98 (m, 5H, PyrH), 4.71 (s, 1H, Pyr-CH-Ph), 4.00 (s, 3H, 6-PyrOCH<sub>3</sub>), 3.96 (s, 3H, 2-PyrOCH<sub>3</sub>), 3.88 (dt, *J* = 10.0, 7.4 Hz, 1H, CH<sub>2</sub>CH<sub>2</sub>OTs), 3.79 (ddd, *J* = 10.1, 7.7, 5.2 Hz, 1H, CH<sub>2</sub>CH<sub>2</sub>OTs), 2.68 (s, 1H, OH), 2.42 (s, 3H, PhCH<sub>3</sub>), 2.31 – 2.12 (m, 2H, CH<sub>2</sub>CH<sub>2</sub>OTs);

<sup>13</sup>C NMR (101 MHz, CDCl<sub>3</sub>) δ = 159.1 (2-PyrC-OCH<sub>3</sub>), 157.0 (6-PyrC-OCH<sub>3</sub>), 144.7 (PhC), 144.7 (PyrC), 143.2 (PhC), 139.3 (PhC), 132.7 (PhC), 129.8 (PhCH), 129.7 (PhCH), 128.1 (PhCH), 127.8 (PhCH), 126.8 (PhCH), 126.3 (PhCH), 125.4 (PhCH), 115.9 (3-PyrC), 95.8 (5-PyrC), 78.9 (C-OH), 67.8 (CH<sub>2</sub>CH<sub>2</sub>OTs), 54.3 (6-PyrOCH<sub>3</sub>), 54.1 (2-PyrOCH<sub>3</sub>), 53.1† (Pyr-CH-Ph), 39.8 (CH<sub>2</sub>CH<sub>2</sub>OTs), 21.6 (PhCH<sub>3</sub>).

**1-(5-bromo-2,6-dimethoxypyridin-3-yl)-4-(dimethylamino)-1,2-diphenylbutan-2-ol<sup>[7]</sup> (**2.044**)**

A solution of **2.043** (3.08 g, 5.02 mmol) and Me<sub>2</sub>NH (20.1 mL, 2.0 M in THF, 40.2 mmol) was stirred at 60 °C for 24 h. After this time, the remaining Me<sub>2</sub>NH and THF were removed under reduced pressure. Purification by silica gel flash chromatography (0–3% MeOH/0.1% NH<sub>3</sub> in CH<sub>2</sub>Cl<sub>2</sub>) afforded the title compound as an off-white foam (2.07 g, 85%, A:B = 50:50).

A portion of this product was further subjected to purification by preparative HPLC to isolate the individual diastereomers as the TFA salt. This was performed using a gradient of 30 to 100% solvent B in solvent A over 12 min.

LR-MS (ESI<sup>+</sup>) *m/z*: 484.8/486.8 [M+H]<sup>+</sup>;

HR-MS (ESI<sup>+</sup>) *m/z* [M = C<sub>25</sub>H<sub>29</sub>BrN<sub>2</sub>O<sub>3</sub>]: [M+H]<sup>+</sup> calc'd 485.1434, found 485.1448;

Diastereomer A:

<sup>1</sup>H NMR (400 MHz, CDCl<sub>3</sub>) δ = 12.64 (br s, 1H, NH<sup>+</sup>), 8.36 (s, 1H, PyrH), 7.47 – 7.42 (m, 4H, PhH), 7.33 (t, *J* = 7.4 Hz, 2H, PhH), 7.29 – 7.22 (m, 3H, PhH), 7.13 (tt, *J* = 7.3, 1.1 Hz, 1H, PhH), 4.64 (s, 1H, Pyr-CH-Ph), 3.80 (s, 3H, 6-PyrOCH<sub>3</sub>), 3.71 (s, 3H, 2-PyrOCH<sub>3</sub>), 3.18 – 3.10 (m, 1H, CH<sub>2</sub>CH<sub>2</sub>N), 2.60 (s, 3H, N(CH<sub>3</sub>)<sub>2</sub>), 2.56 (s, 3H, N(CH<sub>3</sub>)<sub>2</sub>), 2.37 – 2.20 (m, 2H, CH<sub>2</sub>CH<sub>2</sub>N), 2.16 – 2.03 (m, 1H, CH<sub>2</sub>CH<sub>2</sub>N);

<sup>13</sup>C NMR (101 MHz, CDCl<sub>3</sub>) δ = 158.4 (2-PyrC-OCH<sub>3</sub>), 156.3 (6-PyrC-OCH<sub>3</sub>), 144.3 (PyrCH), 143.3 (PhC), 138.9 (PhC), 130.3 (PhCH), 128.7 (PhCH), 128.4 (PhCH), 127.5 (PhCH), 127.0 (PhCH), 125.4 (PhCH), 116.9 (3-PyrC), 95.1 (5-PyrC), 76.7<sup>+</sup> (C-OH), 54.3 (CH<sub>2</sub>CH<sub>2</sub>N), 54.1 (6-PyrOCH<sub>3</sub>), 53.8 (2-PyrOCH<sub>3</sub>), 53.0 (PyrCH-Ph), 44.3 (N(CH<sub>3</sub>)<sub>2</sub>), 42.0 (N(CH<sub>3</sub>)<sub>2</sub>), 37.9 (CH<sub>2</sub>CH<sub>2</sub>N);

Analytical HPLC (254 nm): *t*<sub>R</sub> = 6.8 min, 96%;

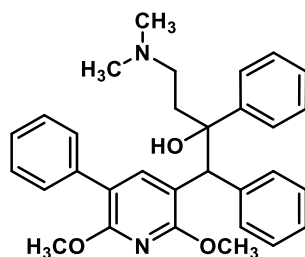
Diastereomer B:

<sup>1</sup>H NMR (400 MHz, CDCl<sub>3</sub>) δ = 11.98 (br s, 1H, NH<sup>+</sup>), 8.05 (s, 1H, PyrH), 7.35 – 7.31 (m, 2H, PhH), 7.23 (t, *J* = 7.6 Hz, 2H, PhH), 7.16 – 7.10 (m, 3H, PhH), 7.06 – 6.99 (m, 3H, PhH), 4.78 (s, 1H, Pyr-CH-Ph), 4.00 (s, 3H, 6-PyrOCH<sub>3</sub>), 3.99 (s, 3H, 2-PyrOCH<sub>3</sub>), 3.21 – 3.12 (m, 1H, CH<sub>2</sub>CH<sub>2</sub>N), 2.64 (s, 3H, N(CH<sub>3</sub>)<sub>2</sub>), 2.62 (s, 3H, N(CH<sub>3</sub>)<sub>2</sub>), 2.43 – 2.28 (m, 2H, CH<sub>2</sub>CH<sub>2</sub>N), 2.28 – 2.16 (m, 1H, CH<sub>2</sub>CH<sub>2</sub>N);

$^{13}\text{C}$  NMR (101 MHz,  $\text{CDCl}_3$ )  $\delta$  = 159.1 (2-Pyr $\underline{\text{C}}$ -OCH $_3$ ), 157.3 (6-Pyr $\underline{\text{C}}$ -OCH $_3$ ), 145.0 (Pyr $\underline{\text{CH}}$ ), 143.2 (Ph $\underline{\text{C}}$ ), 139.9 (Ph $\underline{\text{C}}$ ), 129.9 (Ph $\underline{\text{CH}}$ ), 128.4 (Ph $\underline{\text{CH}}$ ), 128.0 (Ph $\underline{\text{CH}}$ ), 127.0 (Ph $\underline{\text{CH}}$ ), 126.5 (Ph $\underline{\text{CH}}$ ), 125.7 (Ph $\underline{\text{CH}}$ ), 115.3 (3-Pyr $\underline{\text{C}}$ ), 96.2 (5-Pyr $\underline{\text{C}}$ ), 78.1 ( $\underline{\text{C}}$ -OH), 54.6 ( $\text{CH}_2\text{CH}_2\text{N}$ ), 54.4 (2-PyrO $\underline{\text{C}}$ H $_3$ ), 54.2 (6-PyrO $\underline{\text{C}}$ H $_3$ ), 53.2 $^\dagger$  (Pyr- $\underline{\text{CH}}$ -Ph), 44.0 (N( $\underline{\text{C}}$ H $_3$ ) $_2$ ), 42.3 (N( $\underline{\text{C}}$ H $_3$ ) $_2$ ), 36.5 ( $\underline{\text{C}}$ H $_2$ CH $_2$ N);

Analytical HPLC (254 nm):  $t_R$  = 6.9 min, 98%.

**1-(2,6-dimethoxy-5-phenylpyridin-3-yl)-4-(dimethylamino)-1,2-diphenylbutan-2-ol (2.045)**



General method A was used with phenylboronic acid (50.2 mg, 0.412 mmol) to afford the title compound as a light-brown oil (94.2 mg, 0.195 mmol, 95%, A:B = 45:55).

LR-MS (ESI+)  $m/z$ : 483.3  $[\text{M}+\text{H}]^+$ ;

HR-MS (ESI+)  $m/z$   $[\text{M} = \text{C}_{31}\text{H}_{34}\text{N}_2\text{O}_3]$ :  $[\text{M}+\text{H}]^+$  calc'd 483.2642, found 483.2633;

Diastereomer A:

$^1\text{H}$  NMR (400 MHz,  $\text{CDCl}_3$ )  $\delta$  = 12.68 (br s, 1H,  $\text{NH}^+$ ), 8.17 (s, 1H, Pyr $\underline{\text{H}}$ ), 7.49 (d,  $J$  = 8.2 Hz, 4H, Ph $\underline{\text{H}}$ ), 7.42 – 7.22 (m, 10H, Ph $\underline{\text{H}}$ ), 7.13 (tt,  $J$  = 7.3, 1.0 Hz, 1H, Ph $\underline{\text{H}}$ ), 4.73 (s, 1H, Pyr- $\underline{\text{CH}}$ -Ph), 3.79 (s, 3H, 2-PyrO $\underline{\text{C}}$ H $_3$ ), 3.78 (s, 3H, 6-PyrO $\underline{\text{C}}$ H $_3$ ), 3.18 – 3.06 (m, 1H,  $\text{CH}_2\text{CH}_2\text{N}$ ), 2.57 (s, 3H, N( $\underline{\text{C}}$ H $_3$ ) $_2$ ), 2.55 (s, 3H, N( $\underline{\text{C}}$ H $_3$ ) $_2$ ), 2.36 – 2.23 (m, 2H,  $\underline{\text{C}}$ H $_2$ CH $_2$ N), 2.22 – 2.10 (m, 1H,  $\underline{\text{C}}$ H $_2$ CH $_2$ N);

$^{13}\text{C}$  NMR (101 MHz,  $\text{CDCl}_3$ )  $\delta$  = 158.4 (2-Pyr $\underline{\text{C}}$ -OCH $_3$ ), 157.2 (6-Pyr $\underline{\text{C}}$ -OCH $_3$ ), 143.7 (C), 142.5 (4-Pyr $\underline{\text{CH}}$ ), 139.4 (Ph $\underline{\text{C}}$ ), 137.2 (Ph $\underline{\text{C}}$ ), 130.4 (Ph $\underline{\text{CH}}$ ), 129.1 (Ph $\underline{\text{CH}}$ ), 128.7 (Ph $\underline{\text{CH}}$ ), 128.3 (Ph $\underline{\text{CH}}$ ), 128.2 (Ph $\underline{\text{CH}}$ ), 127.3 (Ph $\underline{\text{CH}}$ ), 126.9 (Ph $\underline{\text{CH}}$ ), 126.6 (Ph $\underline{\text{CH}}$ ), 125.5 (Ph $\underline{\text{CH}}$ ), 115.2 (3-Pyr $\underline{\text{C}}$ ), 115.1 (Ph $\underline{\text{C}}$ ), 77.5 $^\dagger$  ( $\underline{\text{C}}$ -OH), 54.4 ( $\text{CH}_2\text{CH}_2\text{N}$ ), 53.7 (Pyr- $\underline{\text{CH}}$ -Ph), 53.6 (2-PyrO $\underline{\text{C}}$ H $_3$ ), 53.3 (6-PyrO $\underline{\text{C}}$ H $_3$ ), 44.0 (N( $\underline{\text{C}}$ H $_3$ ) $_2$ ), 42.2 (N( $\underline{\text{C}}$ H $_3$ ) $_2$ ), 37.8 ( $\underline{\text{C}}$ H $_2$ CH $_2$ N);

Analytical HPLC (254 nm):  $t_R$  = 7.4 min, 100%;

Diastereomer B:

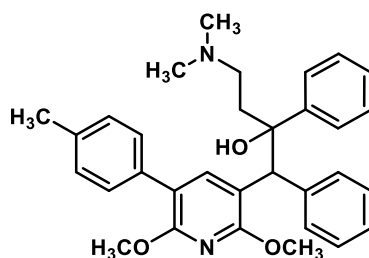
$^1\text{H}$  NMR (400 MHz,  $\text{CDCl}_3$ )  $\delta$  = 12.74 (br s, 1H,  $\text{NH}^+$ ), 7.87 (s, 1H, Pyr $\underline{\text{H}}$ ), 7.55 – 7.49 (m, 2H, Ph $\underline{\text{H}}$ ), 7.42 – 7.34 (m, 4H, Ph $\underline{\text{H}}$ ), 7.31 – 7.16 (m, 5H, Ph $\underline{\text{H}}$ ), 7.13 (t,  $J$  = 7.3 Hz, 1H, Ph $\underline{\text{H}}$ ), 7.05 – 6.94 (m, 3H, Ph $\underline{\text{H}}$ ), 4.86 (s, 1H, Pyr- $\underline{\text{CH}}$ -Ph), 4.08 (br s, 3H, 2-PyrO $\underline{\text{C}}$ H $_3$ ), 3.96 (s, 3H, 6-PyrO $\underline{\text{C}}$ H $_3$ ), 3.24 – 3.13 (m, 1H,  $\text{CH}_2\text{CH}_2\text{N}$ ), 2.60 (s, 6H, N( $\underline{\text{C}}$ H $_3$ ) $_2$ ), 2.49 – 2.38 (m, 1H,  $\underline{\text{C}}$ H $_2$ CH $_2$ N), 2.37 – 2.22 (m, 2H,  $\underline{\text{C}}$ H $_2$ CH $_2$ N);



$^{13}\text{C}$  NMR (101 MHz,  $\text{CDCl}_3$ )  $\delta$  = 159.1 (2-PyrC-OCH<sub>3</sub>), 158.2 (6-PyrC-OCH<sub>3</sub>), 143.5 (PhC), 143.3 (PyrCH), 140.5 (PhC), 137.0 (PhC), 129.9 (PhCH), 129.3 (PhCH), 128.3 (PhCH), 128.2 (PhCH), 127.9 (PhCH), 126.91 (PhCH), 126.85 (PhCH), 126.2 (PhCH), 125.8 (PhCH), 116.5 (PhC), 113.6 (3-PyrC), 78.1 (C-OH), 54.4 (CH<sub>2</sub>CH<sub>2</sub>N), 53.99 (2-PyrOCH<sub>3</sub>), 53.95<sup>+</sup> (Pyr-CH-Ph), 53.6 (6-PyrOCH<sub>3</sub>), 44.0 (N(CH<sub>3</sub>)<sub>2</sub>), 42.1 (N(CH<sub>3</sub>)<sub>2</sub>), 36.8 (CH<sub>2</sub>CH<sub>2</sub>N);

Analytical HPLC (254 nm):  $t_R$  = 7.6 min, 97%.

**1-(2,6-dimethoxy-5-(*p*-tolyl)pyridin-3-yl)-4-(dimethylamino)-1,2-diphenylbutan-2-ol (2.046)**



General method A was used with 4-methylphenylboronic acid (56.0 mg, 0.412 mmol) to afford the title compound as an off-white foam (98.0 mg, 0.197 mmol, 96%, A:B = 52:48).

LR-MS (ESI+)  $m/z$ : 497.0  $[\text{M}+\text{H}]^+$ ;

HR-MS (ESI+)  $m/z$   $[\text{M} = \text{C}_{32}\text{H}_{36}\text{N}_2\text{O}_3]$ :  $[\text{M}+\text{H}]^+$  calc'd 497.2799, found 497.2804;

Diastereomer A:

$^1\text{H}$  NMR (400 MHz,  $\text{CDCl}_3$ )  $\delta$  = 12.48 (br s, 1H, NH<sup>+</sup>), 8.10 (s, 1H, 4-PyrH), 7.48 (d,  $J$  = 7.5 Hz, 4H, PhH), 7.36 – 7.21 (m, 7H, PhH), 7.19 (d,  $J$  = 7.9 Hz, 2H, PhH), 7.12 (t,  $J$  = 7.3 Hz, 1H, PhH), 4.73 (s, 1H, Pyr-CH-Ph), 3.79 (s, 3H, 2-PyrOCH<sub>3</sub>), 3.77 (s, 3H, 6-PyrOCH<sub>3</sub>), 3.17 – 3.05 (m, 1H, CH<sub>2</sub>CH<sub>2</sub>N), 2.62 – 2.52 (m, 6H, N(CH<sub>3</sub>)<sub>2</sub>), 2.37 (s, 3H, Ph-CH<sub>3</sub>), 2.35 – 2.25 (m, 2H, CH<sub>2</sub>CH<sub>2</sub>N), 2.24 – 2.13 (m, 1H, CH<sub>2</sub>CH<sub>2</sub>N);

$^{13}\text{C}$  NMR (101 MHz,  $\text{CDCl}_3$ )  $\delta$  = 158.2 (2-PyrC-OCH<sub>3</sub>), 157.2 (6-PyrC-OCH<sub>3</sub>), 143.7 (PhC), 142.4 (4-PyrCH), 139.4 (PhC), 136.3 (PhC), 134.3 (PhC), 130.4 (PhCH), 129.0 (PhCH), 128.9 (PhCH), 128.6 (PhCH), 128.3 (PhCH), 127.3 (PhCH), 126.9 (PhCH), 125.5 (PhCH), 115.1 (PyrC), 115.0 (PyrC), 77.4 (C-OH), 54.4 (CH<sub>2</sub>CH<sub>2</sub>N), 53.7 (Pyr-CH-Ph), 53.6 (2-PyrOCH<sub>3</sub>), 53.2 (6-PyrOCH<sub>3</sub>), 44.0 (N(CH<sub>3</sub>)<sub>2</sub>), 42.1 (N(CH<sub>3</sub>)<sub>2</sub>), 37.8 (CH<sub>2</sub>CH<sub>2</sub>N), 21.3 (PhCH<sub>3</sub>);

Analytical HPLC (254 nm):  $t_R$  = 8.3 min, 99%;

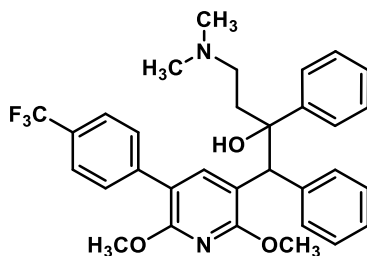
Diastereomer B:

$^1\text{H}$  NMR (400 MHz,  $\text{CDCl}_3$ )  $\delta$  = 11.84 (br s, 1H, NH<sup>+</sup>), 7.83 (s, 1H, PyrH), 7.40 (d,  $J$  = 8.1 Hz, 2H, PhH), 7.35 (d,  $J$  = 7.3 Hz, 2H, PhH), 7.26 – 7.12 (m, 7H, PhH), 7.05 – 6.95 (m, 3H, PhH), 4.85 (s, 1H, Pyr-CH-

Ph), 4.07 (s, 3H, 2-PyrOCH<sub>3</sub>), 3.95 (s, 3H, 6-PyrOCH<sub>3</sub>), 3.22 – 3.12 (m, 1H, CH<sub>2</sub>CH<sub>2</sub>N), 2.65 (br s, 3H, N(CH<sub>3</sub>)<sub>2</sub>), 2.63 (br s, 3H, N(CH<sub>3</sub>)<sub>2</sub>), 2.45 – 2.33 (m, 5H, CH<sub>2</sub>CH<sub>2</sub>N, Ph-CH<sub>3</sub>), 2.31 – 2.22 (m, 1H, CH<sub>2</sub>CH<sub>2</sub>N);  
<sup>13</sup>C NMR (101 MHz, CDCl<sub>3</sub>) δ = 158.9 (2-PyrC-OCH<sub>3</sub>), 158.2 (6-PyrC-OCH<sub>3</sub>), 143.3 (PhC), 143.0 (4-PyrCH), 140.2 (PhC), 136.7 (PhC), 133.9 (PhC), 129.9 (PhCH), 129.1 (PhCH), 129.0 (PhCH), 128.4 (PhCH), 128.0 (PhCH), 127.0 (PhCH), 126.3 (PhCH), 125.8 (PhCH), 116.4 (PyrC), 113.3 (PyrC), 78.2 (C-OH), 54.8 (CH<sub>2</sub>CH<sub>2</sub>N), 54.1<sup>†</sup> (Pyr-CH-Ph), 54.0 (2-PyrOCH<sub>3</sub>), 53.6 (6-PyrOCH<sub>3</sub>), 44.1 (N(CH<sub>3</sub>)<sub>2</sub>), 42.4 (N(CH<sub>3</sub>)<sub>2</sub>), 36.7 (CH<sub>2</sub>CH<sub>2</sub>N), 21.3 (PhCH<sub>3</sub>);

Analytical HPLC (254 nm): *t*<sub>R</sub> = 8.5 min, 95%.

**1-(2,6-dimethoxy-5-(4-(trifluoromethyl)phenyl)pyridin-3-yl)-4-(dimethylamino)-1,2-diphenylbutan-2-ol (2.047)**



General method A was used with 4-trifluoromethylphenylboronic acid (78.3 mg, 0.412 mmol) to afford the title compound as an off-white foam (105 mg, 0.191 mmol, 91%, A:B = 53:47).

LR-MS (ESI+) *m/z*: 551.2 [M+H]<sup>+</sup>;

HR-MS (ESI+) *m/z* [M = C<sub>32</sub>H<sub>33</sub>F<sub>3</sub>N<sub>2</sub>O<sub>3</sub>]: [M+H]<sup>+</sup> calc'd 551.2516, found 551.2531;

Diastereomer A:

<sup>1</sup>H NMR (400 MHz, CDCl<sub>3</sub>) δ = 12.40 (br s, 1H, NH<sup>+</sup>), 8.23 (s, 1H, PyrH), 7.62 (d, *J* = 8.2 Hz, 2H, Ph'H), 7.55 – 7.44 (m, 6H, PhH), 7.36 – 7.22 (m, 5H, PhH), 7.14 (t, *J* = 7.3 Hz, 1H, Ph'H), 4.74 (s, 1H, Pyr-CH-Ph), 3.80 (s, 3H, 2-PyrOCH<sub>3</sub>), 3.79 (s, 3H, 6-PyrOCH<sub>3</sub>), 3.21 – 3.10 (m, 1H, CH<sub>2</sub>CH<sub>2</sub>N), 2.60 (br s, 3H, N(CH<sub>3</sub>)<sub>2</sub>), 2.57 (br s, 3H, N(CH<sub>3</sub>)<sub>2</sub>), 2.36 – 2.24 (m, 2H, CH<sub>2</sub>CH<sub>2</sub>N), 2.22 – 2.10 (m, 1H, CH<sub>2</sub>CH<sub>2</sub>N);

<sup>13</sup>C NMR (101 MHz, CDCl<sub>3</sub>) δ = 159.2 (2-PyrC-OCH<sub>3</sub>), 157.2 (6-PyrC-OCH<sub>3</sub>), 143.7 (PhC), 142.3 (PyrCH), 141.0 (PhC), 139.1 (PhC), 130.3 (PhCH), 129.3 (PhCH), 128.7 (PhCH), 128.44 (q, *J* = 32.4 Hz, Ph'C), 128.38 (PhCH), 127.4 (PhCH), 127.0 (PhCH), 125.4 (PhCH), 125.1 (q, *J* = 3.8 Hz, Ph'CH), 124.6 (q, *J* = 271.8 Hz, CF<sub>3</sub>), 115.7 (3-PyrC), 113.4 (5-PyrC), 77.3 (C-OH), 54.3 (CH<sub>2</sub>CH<sub>2</sub>-N), 53.7 (2-PyrOCH<sub>3</sub>), 53.4 (6-PyrOCH<sub>3</sub>), 53.2 (Pyr-CH-Ph), 44.3 (N(CH<sub>3</sub>)<sub>2</sub>), 42.0 (N(CH<sub>3</sub>)<sub>2</sub>), 38.0 (CH<sub>2</sub>CH<sub>2</sub>N);

Analytical HPLC (254 nm): *t*<sub>R</sub> = 7.9 min, 98%;

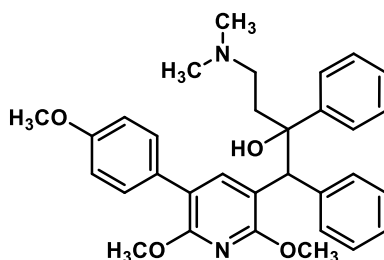
## Diastereomer B:

$^1\text{H}$  NMR (400 MHz,  $\text{CDCl}_3$ )  $\delta$  = 12.36 (br s, 1H,  $\text{NH}^+$ ), 7.88 (s, 1H, s, 1H, 4-Pyr $\underline{\text{H}}$ ), 7.68 – 7.58 (m, 4H, Ph' $\underline{\text{H}}$ ), 7.40 (d,  $J$  = 7.3 Hz, 2H, Ph $\underline{\text{H}}$ ), 7.26 – 7.20 (m, 4H, Ph $\underline{\text{H}}$ ), 7.13 (t,  $J$  = 7.3 Hz, 1H, Ph $\underline{\text{H}}$ ), 7.05 – 6.94 (m, 3H, Ph $\underline{\text{H}}$ ), 4.89 (s, 1H, Pyr- $\underline{\text{CH}}$ -Ph), 4.09 (s, 3H, 2-PyrO $\underline{\text{CH}_3}$ ), 3.97 (s, 3H, 6-PyrO $\underline{\text{CH}_3}$ ), 3.29 – 3.18 (m, 1H,  $\text{CH}_2\text{CH}_2\text{N}$ ), 2.68 – 2.56 (m, 6H, N( $\underline{\text{CH}_3}$ ) $_2$ ), 2.51 – 2.40 (m, 1H,  $\underline{\text{CH}_2}\text{CH}_2\text{N}$ ), 2.34 – 2.20 (m, 2H,  $\underline{\text{CH}_2}\text{CH}_2\text{N}$ );

$^{13}\text{C}$  NMR (101 MHz,  $\text{CDCl}_3$ )  $\delta$  = 159.7 (2-Pyr $\underline{\text{C}}$ -OCH $_3$ ), 158.2 (6-Pyr $\underline{\text{C}}$ -OCH $_3$ ), 143.4 (Ph $\underline{\text{C}}$ ), 143.4 (Pyr $\underline{\text{CH}}$ ), 140.73 (Ph $\underline{\text{C}}$ ), 140.68 (Ph $\underline{\text{C}}$ ), 129.9 (Ph $\underline{\text{CH}}$ ), 129.5 (Ph $\underline{\text{CH}}$ ), 128.7 (q,  $J$  = 32.1 Hz, Ph' $\underline{\text{C}}$ -CF $_3$ ), 128.3 (Ph $\underline{\text{CH}}$ ), 128.0 (Ph $\underline{\text{CH}}$ ), 126.9 (Ph $\underline{\text{CH}}$ ), 126.3 (Ph $\underline{\text{CH}}$ ), 125.8 (Ph $\underline{\text{CH}}$ ), 125.1 (q,  $J$  = 3.7 Hz, Ph' $\underline{\text{CH}}$ ), 124.6 (q,  $J$  = 271.8 Hz,  $\underline{\text{CF}_3}$ ), 115.0 (5-Pyr $\underline{\text{C}}$ ), 114.0 (3-Pyr $\underline{\text{C}}$ ), 78.1 ( $\underline{\text{C}}$ -OH), 54.5 ( $\text{CH}_2\text{CH}_2\text{N}$ ), 54.1 (2-PyrO $\underline{\text{CH}_3}$ ), 53.6 (6-PyrO $\underline{\text{CH}_3}$ ), 53.4 $^\dagger$  (Pyr- $\underline{\text{CH}}$ -Ph) 44.5 (N( $\underline{\text{CH}_3}$ ) $_2$ ), 41.8 (N( $\underline{\text{CH}_3}$ ) $_2$ ), 37.0 ( $\underline{\text{CH}_2}\text{CH}_2\text{N}$ );

Analytical HPLC (254 nm):  $t_R$  = 8.1 min, 97%.

**1-(2,6-dimethoxy-5-(4-methoxyphenyl)pyridin-3-yl)-4-(dimethylamino)-1,2-diphenylbutan-2-ol**  
(**2.048**)



General method A was used with 4-methoxyphenylboronic acid (62.6 mg, 0.412 mmol) to afford the title compound as a brown foam (101 mg, 0.197 mmol, 96%, A:B = 52:48).

LR-MS (ESI+)  $m/z$ : 512.9  $[\text{M}+\text{H}]^+$ ;

HR-MS (ESI+)  $m/z$  [ $\text{M} = \text{C}_{32}\text{H}_{36}\text{N}_2\text{O}_4$ ]:  $[\text{M}+\text{H}]^+$  calc'd 513.2748, found 513.2760;

## Diastereomer A:

$^1\text{H}$  NMR (400 MHz,  $\text{CDCl}_3$ )  $\delta$  = 12.19 (br s, 1H,  $\text{NH}^+$ ), 8.04 (s, 1H, Pyr $\underline{\text{H}}$ ), 7.52 – 7.44 (m, 4H, Ph $\underline{\text{H}}$ ), 7.36 – 7.29 (m, 4H, Ph $\underline{\text{H}}$ , Ph' $\underline{\text{H}}$ ), 7.29 – 7.22 (m, 3H, Ph $\underline{\text{H}}$ ), 7.13 (t,  $J$  = 7.3 Hz, 1H, Ph $\underline{\text{H}}$ ), 6.92 (d,  $J$  = 8.8 Hz, 2H, Ph' $\underline{\text{H}}$ ), 4.71 (s, 1H, Pyr- $\underline{\text{CH}}$ -Ph), 3.84 (s, 3H, Ph'O $\underline{\text{CH}_3}$ ), 3.80 (s, 3H, 2-PyrO $\underline{\text{CH}_3}$ ), 3.78 (s, 3H, 6-PyrO $\underline{\text{CH}_3}$ ), 3.18 – 3.05 (m, 1H,  $\text{CH}_2\text{CH}_2$ ), 2.61 (s, 3H, N( $\underline{\text{CH}_3}$ ) $_2$ ), 2.58 (s, 3H, N( $\underline{\text{CH}_3}$ ) $_2$ ), 2.40 – 2.24 (m, 2H,  $\underline{\text{CH}_2}\text{CH}_2\text{N}$ ), 2.24 – 2.12 (m, 1H,  $\underline{\text{CH}_2}\text{CH}_2\text{N}$ );

$^{13}\text{C}$  NMR (101 MHz,  $\text{CDCl}_3$ )  $\delta$  = 158.5 (Ph' $\underline{\text{C}}$ -OCH $_3$ ), 157.9 (2-Pyr $\underline{\text{C}}$ -OCH $_3$ ), 157.1 (6-Pyr $\underline{\text{C}}$ -OCH $_3$ ), 143.4 (Ph $\underline{\text{C}}$ ), 142.3 (Pyr $\underline{\text{CH}}$ ), 139.3 (Ph $\underline{\text{C}}$ ), 130.3 (Ph $\underline{\text{CH}}$ ), 130.1 (Ph $\underline{\text{CH}}$ ), 129.5 (Ph' $\underline{\text{C}}$ ), 128.6 (Ph $\underline{\text{CH}}$ ), 128.3

(Ph $\underline{\text{C}}\text{H}$ ), 127.3 (Ph $\underline{\text{C}}\text{H}$ ), 127.0 (Ph $\underline{\text{C}}\text{H}$ ), 125.4 (Ph $\underline{\text{C}}\text{H}$ ), 114.9 (5-Pyr $\underline{\text{C}}$ ), 114.8 (3-Pyr $\underline{\text{C}}$ ), 113.7 (Ph' $\underline{\text{C}}\text{H}$ ), 77.6 ( $\underline{\text{C}}\text{-OH}$ ), 55.4 (Ph' $\underline{\text{O}}\underline{\text{C}}\text{H}_3$ ), 54.7 ( $\text{CH}_2\text{CH}_2\text{N}$ ), 54.2 (Pyr- $\underline{\text{C}}\text{H}$ -Ph), 53.6 (2-PyrO $\underline{\text{C}}\text{H}_3$ ), 53.2 (6-PyrO $\underline{\text{C}}\text{H}_3$ ), 44.1 (N( $\underline{\text{C}}\text{H}_3$ ) $_2$ ), 42.4 (N( $\underline{\text{C}}\text{H}_3$ ) $_2$ ), 37.6 ( $\underline{\text{C}}\text{H}_2\text{CH}_2\text{N}$ );

Analytical HPLC (254 nm):  $t_R$  = 7.0 min, 100%;

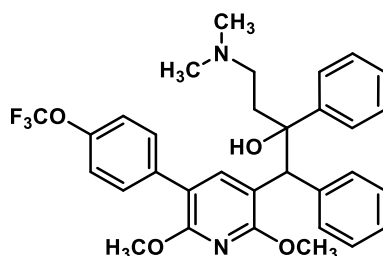
Diastereomer B:

$^1\text{H}$  NMR (400 MHz,  $\text{CDCl}_3$ )  $\delta$  = 12.37 (br s, 1H,  $\text{NH}^+$ ), 7.82 (d,  $J$  = 4.5 Hz, 1H, Pyr $\underline{\text{H}}$ ), 7.45 (d,  $J$  = 8.8 Hz, 2H, Ph' $\underline{\text{H}}$ -O $\underline{\text{C}}\text{H}_3$ ), 7.36 (d,  $J$  = 7.3 Hz, 1H, Ph $\underline{\text{C}}$ ), 7.25 – 7.16 (m, 2H, Ph $\underline{\text{H}}$ ), 7.20 – 7.11 (m, 3H, Ph $\underline{\text{H}}$ ), 7.04 – 6.96 (m, 3H, Ph $\underline{\text{H}}$ ), 6.93 (d,  $J$  = 8.9 Hz, 2H, Ph' $\underline{\text{H}}$ ), 4.84 (s, 1H, Pyr- $\underline{\text{C}}\text{H}$ -Ph), 4.07 (s, 3H, 2-PyrO $\underline{\text{C}}\text{H}_3$ ), 3.95 (s, 3H, 6-PyrO $\underline{\text{C}}\text{H}_3$ ), 3.83 (s, 3H, Ph-O $\underline{\text{C}}\text{H}_3$ ), 3.23 – 3.12 (m, 1H,  $\text{CH}_2\text{-CHHN}$ ), 2.64 (s, 3H, N( $\underline{\text{C}}\text{H}_3$ ) $_2$ ), 2.62 (s, 3H, N( $\underline{\text{C}}\text{H}_3$ ) $_2$ ), 2.47 – 2.21 (m, 3H,  $\text{CH}_2\text{CHHN}$ );

$^{13}\text{C}$  NMR (101 MHz,  $\text{CDCl}_3$ )  $\delta$  = 158.70 $^{\dagger}$  ( $\underline{\text{C}}\text{-OCH}_3$ ), 158.69 $^{\dagger}$  ( $\underline{\text{C}}\text{-OCH}_3$ ), 158.1 (6-Pyr $\underline{\text{C}}\text{-OCH}_3$ ), 143.3 (Ph $\underline{\text{C}}$ ), 142.9 (4-Pyr $\underline{\text{C}}\text{H}$ ), 140.3 (Ph $\underline{\text{C}}$ ), 130.3 (Ph' $\underline{\text{C}}\text{H}$ ), 129.9 (Ph $\underline{\text{C}}\text{H}$ ), 129.3 (Ph' $\underline{\text{C}}$ ), 128.3 (Ph $\underline{\text{C}}\text{H}$ ), 127.9 (Ph $\underline{\text{C}}\text{H}$ ), 127.0 (Ph $\underline{\text{C}}\text{H}$ ), 126.3 (Ph $\underline{\text{C}}\text{H}$ ), 125.8 (Ph $\underline{\text{C}}\text{H}$ ), 116.1 (5-Pyr $\underline{\text{C}}$ ), 113.7 (Ph' $\underline{\text{C}}\text{H}$ ), 133.4 (3-Pyr $\underline{\text{C}}$ ), 78.2 ( $\underline{\text{C}}\text{-OH}$ ), 55.4 (Ph-O $\underline{\text{C}}\text{H}_3$ ), 54.7 ( $\text{CH}_2\text{CH}_2\text{N}$ ), 54.0 $^{\dagger}$  (Pyr- $\underline{\text{C}}\text{H}$ -Ph), 53.9 (2-PyrO $\underline{\text{C}}\text{H}_3$ ), 53.5 (6-PyrO $\underline{\text{C}}\text{H}_3$ ), 44.1 (N( $\underline{\text{C}}\text{H}_3$ ) $_2$ ), 42.2 (N( $\underline{\text{C}}\text{H}_3$ ) $_2$ ), 36.7 ( $\underline{\text{C}}\text{H}_2\text{CH}_2\text{N}$ );

Analytical HPLC (254 nm):  $t_R$  = 7.3 min, 96%.

**1-(2,6-dimethoxy-5-(4-(trifluoromethoxy)phenyl)pyridin-3-yl)-4-(dimethylamino)-1,2-diphenylbutan-2-ol (2.049)**



General method A was used with 4-trifluoromethoxyphenylboronic acid (84.8 mg, 0.412 mmol) to afford the title compound as an off-white solid (110 mg, 0.194 mmol, 94%, A:B = 55:45).

LR-MS (ESI+)  $m/z$ : 566.9  $[\text{M}+\text{H}]^+$ ;

HR-MS (ESI+)  $m/z$   $[\text{M} = \text{C}_{32}\text{H}_{33}\text{F}_3\text{N}_2\text{O}_4]$ :  $[\text{M}+\text{H}]^+$  calc'd 567.2465, found 567.2477;

Diastereomer A:

$^1\text{H}$  NMR (400 MHz,  $\text{CDCl}_3$ )  $\delta$  = 11.33 (br s, 1H,  $\text{NH}^+$ ), 8.06 (s, 1H, Pyr $\underline{\text{H}}$ ), 7.52 – 7.43 (m, 4H, Ph $\underline{\text{H}}$ ), 7.40 (d,  $J$  = 8.7 Hz, 2H, Ph' $\underline{\text{H}}$ ), 7.37 – 7.18 (m, 7H, Ph $\underline{\text{H}}$ ), 7.15 (t,  $J$  = 7.3 Hz, 1H, Ph $\underline{\text{H}}$ ), 4.73 (s, 1H, Pyr- $\underline{\text{C}}\text{H}$ -Ph),

3.81 (s, 3H, 2-PyrOCH<sub>3</sub>), 3.79 (s, 3H, 6-PyrOCH<sub>3</sub>), 3.20 – 3.09 (m, 1H, CH<sub>2</sub>CH<sub>2</sub>N), 2.64 (s, 3H, N(CH<sub>3</sub>)<sub>2</sub>), 2.61 (s, 3H, N(CH<sub>3</sub>)<sub>2</sub>), 2.41 – 2.15 (m, 3H, CH<sub>2</sub>CH<sub>2</sub>NH);

<sup>13</sup>C NMR (101 MHz, CDCl<sub>3</sub>) δ = 158.7 (2-PyrC-OCH<sub>3</sub>), 157.1 (6-PyrC-OCH<sub>3</sub>), 147.9 (m, Ph'C-OCF<sub>3</sub>), 143.4 (PhC), 142.4 (4-PyrCH), 139.0 (PhC), 135.9 (PhC), 130.4 (PhCH), 130.3 (PhCH), 128.7 (PhCH), 128.4 (PhCH), 127.5 (PhCH), 127.1 (PhCH), 125.4 (PhCH), 120.71 (PhCH), 120.70 (q, J = 256.8 Hz, OCF<sub>3</sub>), 115.3 (3-PyrC), 113.6 (5-PyrC), 77.5 (C-OH), 54.8 (CH<sub>2</sub>CH<sub>2</sub>N), 53.74 (2-PyrOCH<sub>3</sub>), 53.74<sup>†</sup> (Pyr-CH-Ph), 53.4 (6-PyrOCH<sub>3</sub>), 44.4 (N(CH<sub>3</sub>)<sub>2</sub>), 42.4 (N(CH<sub>3</sub>)<sub>2</sub>), 37.9 (CH<sub>2</sub>CH<sub>2</sub>N);

Analytical HPLC (254 nm): t<sub>R</sub> = 8.0 min, 100%;

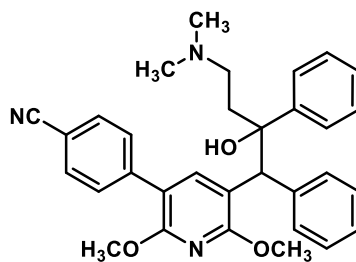
Diastereomer B:

<sup>1</sup>H NMR (400 MHz, CDCl<sub>3</sub>) δ = 11.52 (br s, 1H, NH<sup>+</sup>), 7.84 (s, 1H, PyrH), 7.53 (d, J = 8.8 Hz, 2H, Ph'H), 7.37 (d, J = 7.4 Hz, 2H, PhH), 7.26 – 7.18 (m, 6H, PhH), 7.14 (t, J = 7.3 Hz, 1H, PhH), 7.07 – 6.96 (m, 3H, ArH), 4.87 (s, 1H, Pyr-CH-Ph), 4.08 (s, 3H, 2-PyrOCH<sub>3</sub>), 3.97 (s, 3H, 6-PyrOCH<sub>3</sub>), 3.27 – 3.17 (m, 1H, CH<sub>2</sub>CH<sub>2</sub>N), 2.65 (s, 3H, N(CH<sub>3</sub>)<sub>2</sub>), 2.64 (s, 3H, N(CH<sub>3</sub>)<sub>2</sub>), 2.48 – 2.22 (m, 3H, CH<sub>2</sub>CH<sub>2</sub>NH);

<sup>13</sup>C NMR (101 MHz, CDCl<sub>3</sub>) δ = 159.2 (2-PyrC-OCH<sub>3</sub>), 158.0 (6-PyrC-OCH<sub>3</sub>), 148.0 (m, Ph'C-OCF<sub>3</sub>), 143.1 (PhC), 143.0 (PyrCH), 140.2 (PhC), 135.5 (PhC), 130.4 (PhCH), 129.7 (PhCH), 128.2 (PhCH), 127.9 (PhCH), 126.9 (PhCH), 126.2 (PhCH), 125.6 (PhCH), 120.6 (q, J = 256.8 Hz, OCF<sub>3</sub>), 120.5 (PhCH), 114.9 (PhCH), 113.6 (PhCH), 78.1 (C-OH), 54.7 (CH<sub>2</sub>CH<sub>2</sub>N), 53.9 (2-PyrOCH<sub>3</sub>), 53.7<sup>†</sup> (Pyr-CH-Ph), 53.5 (6-PyrOCH<sub>3</sub>), 44.3 (N(CH<sub>3</sub>)<sub>2</sub>), 42.1 (N(CH<sub>3</sub>)<sub>2</sub>), 36.7 (CH<sub>2</sub>CH<sub>2</sub>N);

Analytical HPLC (254 nm): t<sub>R</sub> = 8.2 min, 95%;

**4-(5-(4-(dimethylamino)-2-hydroxy-1,2-diphenylbutyl)-2,6-dimethoxypyridin-3-yl)benzonitrile (2.050)**



General method A was used with 4-cyanophenylboronic acid (60.5 mg, 0.412 mmol) to afford the title compound as a yellow foam (72.0 mg, 0.142 mmol, 69%, A:B = 29:71).

LR-MS (ESI+) *m/z*: 507.9 [M+H]<sup>+</sup>;

HR-MS (ESI+) *m/z* [M = C<sub>32</sub>H<sub>33</sub>N<sub>3</sub>O<sub>3</sub>]: [M+H]<sup>+</sup> calc'd 508.2595, found 508.2596;

## Diastereomer A:

$^1\text{H}$  NMR (400 MHz,  $\text{CDCl}_3$ )  $\delta$  = 12.38 (br s, 1H,  $\text{NH}^+$ ), 8.27 (s, 1H, 4-Pyr $\underline{\text{H}}$ ), 7.64 (d,  $J$  = 8.4 Hz, 2H, Ph $\underline{\text{H}}$ -CN), 7.56 – 7.44 (m, 6H, Ph $\underline{\text{H}}$ , Ph' $\underline{\text{H}}$ ), 7.32 (t,  $J$  = 7.4 Hz, 2H, Ph $\underline{\text{H}}$ ), 7.29 – 7.22 (m, 3H, Ph $\underline{\text{H}}$ ), 7.13 (t,  $J$  = 7.4 Hz, 1H, Ph $\underline{\text{H}}$ ), 4.73 (s, 1H, Pyr- $\underline{\text{CH}}$ -Ph), 3.82 – 3.76 (m, 6H, Pyr-O $\underline{\text{CH}_3}$ ), 3.22 – 3.12 (m, 1H,  $\text{CH}_2\text{CH}_2\text{N}$ ), 2.61 (s, 3H,  $\text{N}(\underline{\text{CH}_3})_2$ ), 2.58 (s, 3H,  $\text{N}(\underline{\text{CH}_3})_2$ ), 2.37 – 2.22 (m, 2H,  $\underline{\text{CH}_2}\text{CH}_2\text{N}$ ), 2.19 – 2.12 (m, 1H,  $\underline{\text{CH}_2}\text{CH}_2\text{N}$ );

$^{13}\text{C}$  NMR (101 MHz,  $\text{CDCl}_3$ )  $\delta$  = 159.6 (Pyr $\underline{\text{C}}$ -O $\underline{\text{CH}_3}$ ), 157.2 (Pyr $\underline{\text{C}}$ -O $\underline{\text{CH}_3}$ ), 143.7 (Ph $\underline{\text{C}}$ ), 142.2 (Ph $\underline{\text{C}}$ ), 142.1 (Pyr $\underline{\text{CH}}$ ), 139.0 (Ph $\underline{\text{C}}$ ), 132.0 (Ph $\underline{\text{CH}}$ ), 130.3 (Ph $\underline{\text{CH}}$ ), 129.6 (Ph $\underline{\text{CH}}$ ), 128.7 (Ph $\underline{\text{CH}}$ ), 128.4 (Ph $\underline{\text{CH}}$ ), 127.5 (Ph $\underline{\text{CH}}$ ), 127.0 (Ph $\underline{\text{CH}}$ ), 125.4 (Ph $\underline{\text{CH}}$ ), 119.5 (Ph- $\underline{\text{CN}}$ ), 116.0 (3-Pyr $\underline{\text{C}}$ ), 112.9 (Ar $\underline{\text{C}}$ ), 109.8 (Ar $\underline{\text{C}}$ ), 77.3 ( $\underline{\text{C}}$ -OH), 54.3 ( $\text{CH}_2\text{CH}_2\text{N}$ ), 53.8 (PyrO $\underline{\text{CH}_3}$ ), 53.4 (PyrO $\underline{\text{CH}_3}$ ), 53.0 (Pyr- $\underline{\text{CH}}$ -Ph), 44.4 ( $\text{N}(\underline{\text{CH}_3})_2$ ), 42.0 ( $\text{N}(\underline{\text{CH}_3})_2$ ), 38.1 ( $\underline{\text{CH}_2}\text{CH}_2\text{N}$ );

Analytical HPLC (254 nm):  $t_R$  = 6.8 min, 94%;

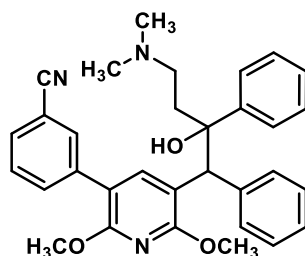
## Diastereomer B:

$^1\text{H}$  NMR (400 MHz,  $\text{CDCl}_3$ )  $\delta$  = 11.80 (br s, 1H,  $\text{NH}^+$ ), 7.89 (s, 1H, Pyr $\underline{\text{H}}$ ), 7.69 – 7.58 (m, 4H, Ph' $\underline{\text{H}}$ ), 7.41 (d,  $J$  = 7.5 Hz, 2H, Ph $\underline{\text{H}}$ ), 7.28 – 7.20 (m, 4H, Ph $\underline{\text{H}}$ ), 7.12 (t,  $J$  = 7.3 Hz, 1H, Ph $\underline{\text{H}}$ ), 7.05 – 6.94 (m, 3H, Ph $\underline{\text{H}}$ ), 4.90 (s, 1H, Pyr- $\underline{\text{CH}}$ -Ph), 4.09 (s, 3H, 2-PyrO $\underline{\text{CH}_3}$ ), 3.97 (s, 3H, 6-PyrO $\underline{\text{CH}_3}$ ), 3.25 (t,  $J$  = 10.8 Hz, 1H,  $\text{CH}_2\text{CH}_2\text{N}$ ), 2.64 (m, 6H,  $\text{N}(\underline{\text{CH}_3})_2$ ), 2.45 (m, 1H,  $\underline{\text{CH}_2}\text{CH}_2\text{N}$ ), 2.36 – 2.18 (m, 2H,  $\underline{\text{CH}_2}\text{CH}_2\text{N}$ );

$^{13}\text{C}$  NMR (101 MHz,  $\text{CDCl}_3$ )  $\delta$  = 160.0 (2-Pyr $\underline{\text{C}}$ -O $\underline{\text{CH}_3}$ ), 158.1 (6-Pyr $\underline{\text{C}}$ -O $\underline{\text{CH}_3}$ ), 143.3 (Ph $\underline{\text{C}}$ ), 143.2 (Pyr $\underline{\text{CH}}$ ), 141.9 (Ph $\underline{\text{C}}$ ), 140.6 (Ph $\underline{\text{C}}$ ), 131.9 (Ph $\underline{\text{CH}}$ ), 129.9 (Ph $\underline{\text{CH}}$ ), 129.8 (Ph $\underline{\text{CH}}$ ), 128.3 (Ph $\underline{\text{CH}}$ ), 128.0 (Ph $\underline{\text{CH}}$ ), 126.9 (Ph $\underline{\text{CH}}$ ), 126.3 (Ph $\underline{\text{CH}}$ ), 125.7 (Ph $\underline{\text{CH}}$ ), 119.5 (Ph- $\underline{\text{CN}}$ ), 114.4 (Ar $\underline{\text{C}}$ ), 114.2 (Ar $\underline{\text{C}}$ ), 109.9 (Ar $\underline{\text{C}}$ ), 78.1 ( $\underline{\text{C}}$ -OH), 54.6 ( $\text{CH}_2\text{CH}_2\text{N}$ ), 54.1 (2-PyrO $\underline{\text{CH}_3}$ ), 53.6 (6-PyrO $\underline{\text{CH}_3}$ ), 53.0 $^{\dagger}$  (Pyr- $\underline{\text{CH}}$ -Ph), 44.7 ( $\text{N}(\underline{\text{CH}_3})_2$ ), 41.8 ( $\text{N}(\underline{\text{CH}_3})_2$ ), 37.0 ( $\underline{\text{CH}_2}\text{CH}_2\text{N}$ );

Analytical HPLC (254 nm):  $t_R$  = 6.9 min, 100%.

**3-(5-(4-(dimethylamino)-2-hydroxy-1,2-diphenylbutyl)-2,6-dimethoxypyridin-3-yl)benzonitrile**  
**(2.051)**



General method A was used with 3-cyanophenylboronic acid (60.5 mg, 0.412 mmol) to afford the title compound as a yellow foam (98.0 mg, 0.206 mmol, 94%, A:B = 33:67).

LR-MS (ESI+)  $m/z$ : 507.9  $[M+H]^+$ ;

HR-MS (ESI+)  $m/z$   $[M = C_{32}H_{33}N_3O_3]$ :  $[M+H]^+$  calc'd 508.2595, found 508.2596;

Diastereomer A:

$^1H$  NMR (400 MHz,  $CDCl_3$ )  $\delta$  = 12.45 (br s, 1H,  $NH^+$ ), 8.21 (s, 1H, PyrH), 7.67 (t,  $J$  = 1.7 Hz, 1H, Ph'H), 7.62 (dt,  $J$  = 7.7, 1.6 Hz, 1H, Ph'H), 7.55 – 7.43 (m, 6H, PhH), 7.35 – 7.23 (m, 5H, PhH), 7.15 (t,  $J$  = 7.3 Hz, 1H, PhH), 4.73 (s, 1H, Pyr-CH-Ph), 3.83 – 3.76 (m, 6H, PyrOCH<sub>3</sub>) 3.23 – 3.10 (m, 1H, CH<sub>2</sub>CH<sub>2</sub>N), 2.61 (s, 3H, N(CH<sub>3</sub>)<sub>2</sub>), 2.58 (s, 3H, N(CH<sub>3</sub>)<sub>2</sub>), 2.37 – 2.22 (m, 2H, CH<sub>2</sub>CH<sub>2</sub>N), 2.22 – 2.08 (m, 1H, CH<sub>2</sub>CH<sub>2</sub>N);

$^{13}C$  NMR (101 MHz,  $CDCl_3$ )  $\delta$  = 159.4 (2-PyrC-OCH<sub>3</sub>), 157.1 (6-PyrC-OCH<sub>3</sub>), 143.7 (PhC), 142.1 (PhC), 139.0 (PyrCH), 138.6 (PhC), 133.4 (PhC), 132.8 (PhCH), 130.4 (PhCH), 129.9 (PhCH), 129.0 (PhCH), 128.7 (PhCH), 128.5 (PhCH), 127.5 (PhCH), 127.1 (PhCH), 125.5 (PhCH), 119.4 (Ph-CN), 115.9 (3-PyrC), 112.5 (ArC), 112.2 (ArC), 77.3 (C-OH), 54.3 (CH<sub>2</sub>CH<sub>2</sub>N), 53.8 (2-PyrOCH<sub>3</sub>), 53.4 (6-PyrOCH<sub>3</sub>), 53.0 (Pyr-CH-Ph), 44.4 (N(CH<sub>3</sub>)<sub>2</sub>), 42.0 (N(CH<sub>3</sub>)<sub>2</sub>), 38.1 (CH<sub>2</sub>CH<sub>2</sub>N);

Analytical HPLC (254 nm):  $t_R$  = 6.8 min, 100%;

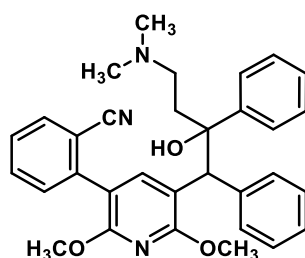
Diastereomer B:

$^1H$  NMR (400 MHz,  $CDCl_3$ )  $\delta$  = 11.47 (br s, 1H,  $NH^+$ ), 7.89 – 7.81 (m, 2H, Ph'H, PyrH), 7.77 (d,  $J$  = 7.6 Hz, 1H, PhH), 7.53 (d,  $J$  = 7.5 Hz, 1H, Ph'H), 7.46 (t,  $J$  = 7.7 Hz, 1H, Ph'H), 7.39 (d,  $J$  = 7.7 Hz, 2H, PhH), 7.14 (t,  $J$  = 7.2 Hz, 1H, PhH), 7.08 – 6.94 (m, 3H, PhH), 4.90 (s, 1H, Pyr-CH-Ph), 4.08 (s, 3H, 2-PyrOCH<sub>3</sub>), 3.97 (s, 3H, 6-PyrOCH<sub>3</sub>), 3.24 (t,  $J$  = 10.8 Hz, 1H, CH<sub>2</sub>CH<sub>2</sub>N), 2.73 – 2.58 (m, 6H, N(CH<sub>3</sub>)<sub>2</sub>), 2.51 – 2.18 (m, 3H, CH<sub>2</sub>CH<sub>2</sub>N);

$^{13}C$  NMR (101 MHz,  $CDCl_3$ )  $\delta$  = 159.7 (2-PyrC-OCH<sub>3</sub>), 158.0 (6-PyrC-OCH<sub>3</sub>), 143.1 (PhC), 142.9 (PyrCH), 140.2 (PhC), 138.1 (PhC), 133.6 (PhCH), 132.7 (PhCH), 130.0 (PhCH), 129.7 (PhCH), 128.9 (PhCH), 128.3 (PhCH), 127.9 (PhCH), 126.9 (PhCH), 126.3 (PhCH), 125.7 (PhCH), 119.2 (Ph-CN), 115.0 (PyrC), 113.9 (PyrC), 112.0 (CNPhC), 78.1 (C-OH), 54.7 (CH<sub>2</sub>CH<sub>2</sub>N), 54.0 (2-PyrOCH<sub>3</sub>), 53.6 (2-PyrOCH<sub>3</sub>), 53.1<sup>†</sup> (Pyr-CH-Ph), 44.6 (N(CH<sub>3</sub>)<sub>2</sub>), 42.1 (N(CH<sub>3</sub>)<sub>2</sub>), 36.8 (CH<sub>2</sub>CH<sub>2</sub>N);

Analytical HPLC (254 nm):  $t_R$  = 7.0 min, 97%.

**2-(5-(4-(dimethylamino)-2-hydroxy-1,2-diphenylbutyl)-2,6-dimethoxypyridin-3-yl)benzonitrile  
(2.052)**



General method A was used with 2-cyanophenylboronic acid (60.5 mg, 0.412 mmol) to afford the title compound as a yellow foam (50.1 mg, 0.098 mmol, 48%, A:B = 56:44).

LR-MS (ESI+)  $m/z$ : 507.9  $[M+H]^+$ ;

HR-MS (ESI+)  $m/z$   $[M = C_{32}H_{33}N_3O_3]$ :  $[M+H]^+$  calc'd 508.2595, found 508.2598;

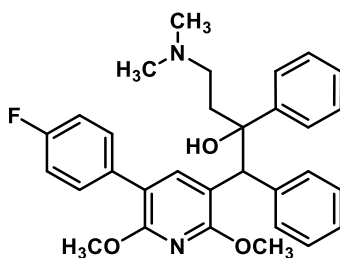
Diastereomer B:

$^1H$  NMR (400 MHz,  $CDCl_3$ )  $\delta$  = 10.72 (br s, 1H,  $NH^+$ ), 8.12 (s, 1H, PyrH), 7.74 (d,  $J$  = 7.6 Hz, 1H, PhH), 7.67 – 7.57 (m, 2H, PhH), 7.42 (ddd,  $J$  = 7.7, 6.0, 2.6 Hz, 1H, PhH), 7.34 (d,  $J$  = 7.8 Hz, 2H, PhH), 7.25 (d,  $J$  = 5.4 Hz, 3H, PhH), 7.20 – 7.10 (m, 3H, PhH), 7.06 – 6.94 (m, 3H, PhH), 4.90 (s, 1H, Pyr-CH-Ph), 4.06 (s, 3H, 2-PyrOCH<sub>3</sub>), 3.96 (s, 3H, 6-PyrOCH<sub>3</sub>), 3.19 – 3.01 (m, 1H, CH<sub>2</sub>CH<sub>2</sub>N), 2.73 – 2.63 (m, 6H, N(CH<sub>3</sub>)<sub>2</sub>), 2.59 – 2.48 (m, 1H, CH<sub>2</sub>CH<sub>2</sub>N), 2.47 – 2.25 (m, 2H, CH<sub>2</sub>CH<sub>2</sub>N);

$^{13}C$  NMR (101 MHz,  $CDCl_3$ )  $\delta$  = 160.7 (2-PyrC-OCH<sub>3</sub>), 158.3 (6-PyrC-OCH<sub>3</sub>), 143.1 (PhC), 143.0 (4-PyrCH), 141.2 (PhC), 139.5 (PhC), 133.1 (PhCH), 132.6 (PhCH), 131.7 (PhCH), 129.9 (PhCH), 128.5 (PhCH), 128.0 (PhCH), 127.5 (PhCH), 127.2 (PhCH), 126.5 (PhCH), 125.6 (PhCH), 125.5 (PhCH), 114.1 (3-PyrC), 112.5 (C), 112.3 (C), 78.9 (C-OH), 54.9 (CH<sub>2</sub>CH<sub>2</sub>N), 54.2 (PyrOCH<sub>3</sub>), 53.7 (PyrOCH<sub>3</sub>), 53.0<sup>†</sup> (Pyr-CH-Ph), 43.6 (2 × N(CH<sub>3</sub>)<sub>2</sub>), 36.0 (CH<sub>2</sub>CH<sub>2</sub>N);

Analytical HPLC (254 nm):  $t_R$  = 6.8 min, 98%.

**4-(dimethylamino)-1-(5-(4-fluorophenyl)-2,6-dimethoxypyridin-3-yl)-1,2-diphenylbutan-2-ol**  
(2.053)



General method A was used with 4-fluorophenylboronic acid (57.7 mg, 0.412 mmol) to afford the title compound as a yellow foam (53.9 mg, 0.107 mmol, 52%, A:B = 47:53).

LR-MS (ESI+)  $m/z$ : 501.2  $[M+H]^+$ ;

HR-MS (ESI+)  $m/z$   $[M = C_{31}H_{33}FN_2O_3]$ :  $[M+H]^+$  calc'd 501.2548, found 501.2558;

Diastereomer A:

$^1H$  NMR (400 MHz,  $CDCl_3$ )  $\delta$  = 12.08 (br s, 1H,  $NH^+$ ), 8.09 (s, 1H, PyrH), 7.51 – 7.45 (m, 4H, PhH), 7.39 – 7.30 (m, 4H, PhH), 7.29 – 7.22 (m, 3H, PhH), 7.14 (t,  $J$  = 7.3 Hz, 1H, PhH), 7.09 – 7.02 (m, 2H, Ph'H), 4.72 (s, 1H, Pyr-CH-Ph), 3.80 (s, 3H, 2-PyrOCH<sub>3</sub>), 3.78 (s, 3H, 6-PyrOCH<sub>3</sub>), 3.20 – 3.08 (m, 1H, CH<sub>2</sub>CH<sub>2</sub>N),



2.61 (br s, 3H, N(CH<sub>3</sub>)<sub>2</sub>), 2.58 (br s, 3H, N(CH<sub>3</sub>)<sub>2</sub>), 2.39 – 2.24 (m, 2H, CH<sub>2</sub>CH<sub>2</sub>N), 2.24 – 2.12 (m, 1H, CH<sub>2</sub>CH<sub>2</sub>N);

<sup>13</sup>C NMR (101 MHz, CDCl<sub>3</sub>) δ = 161.8 (d, *J* = 245.4 Hz, Ph'C-F), 158.5 (2-PyrC-OCH<sub>3</sub>), 157.0 (6-PyrC-OCH<sub>3</sub>), 143.6 (PhC), 142.3 (PyrCH), 139.2 (PhC), 133.1 (d, *J* = 3.2 Hz, Ph'C), 130.7 (d, *J* = 7.9 Hz, Ph'CH), 130.3 (PhCH), 128.7 (PhCH), 128.4 (PhCH), 127.4 (PhCH), 127.0 (PhCH), 125.4 (PhCH), 115.3 (3-PyrC), 115.0 (d, *J* = 21.3 Hz, Ph'CH), 114.0 (5-PyrC), 77.4 (C-OH), 54.5 (CH<sub>2</sub>CH<sub>2</sub>N), 53.8<sup>†</sup> (Pyr-CH-Ph), 53.7 (2-PyrOCH<sub>3</sub>), 53.3 (6-PyrOCH<sub>3</sub>), 44.23 (N(CH<sub>3</sub>)<sub>2</sub>), 42.19 (N(CH<sub>3</sub>)<sub>2</sub>), 37.9 (CH<sub>2</sub>CH<sub>2</sub>N);

Analytical HPLC (254 nm): *t*<sub>R</sub> = 7.3 min, 99%;

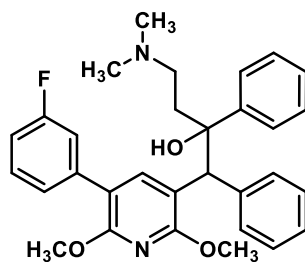
Diastereomer B:

<sup>1</sup>H NMR (400 MHz, CDCl<sub>3</sub>) δ = 11.78 (br s, 1H, NH<sup>+</sup>), 7.81 (s, 1H, PyrH), 7.52 – 7.43 (m, 2H, Ph'H), 7.41 – 7.35 (m, 2H, PhH), 7.25 – 7.17 (m, 4H, PhH), 7.14 (t, *J* = 7.3 Hz, 1H, PhH), 7.10 – 6.95 (m, 5H, PhH), 4.86 (s, 1H, Pyr-CH-Ph), 4.07 (s, 3H, 2-PyrOCH<sub>3</sub>), 3.96 (s, 3H, 6-PyrOCH<sub>3</sub>), 3.21 (t, *J* = 11.6 Hz, 1H, CH<sub>2</sub>CH<sub>2</sub>N), 2.65 (br s, 3H, N(CH<sub>3</sub>)<sub>2</sub>), 2.64 (br s, 3H, N(CH<sub>3</sub>)<sub>2</sub>), 2.48 – 2.20 (m, 3H, CH<sub>2</sub>CH<sub>2</sub>NH);

<sup>13</sup>C NMR (101 MHz, CDCl<sub>3</sub>) δ = 162.0 (d, *J* = 245.6 Hz, Ph'CF), 159.0 (2-PyrC-OCH<sub>3</sub>), 158.1 (6-PyrC-OCH<sub>3</sub>), 143.3 (PhC), 143.1 (PyrCH), 140.4 (PhC), 132.8 (d, *J* = 3.1 Hz, Ph'C), 130.9 (d, *J* = 8.0 Hz, Ph'CH), 129.9 (PhCH), 128.4 (PhCH), 128.0 (PhCH), 127.0 (PhCH), 126.3 (PhCH), 125.8 (PhCH), 115.5 (5-PyrC), 115.1 (d, *J* = 21.3 Hz, Ph'CH), 113.5 (3-PyrC), 78.1 (C-OH), 54.8 (CH<sub>2</sub>CH<sub>2</sub>N), 54.0 (2-PyrOCH<sub>3</sub>), 53.6 (6-PyrOCH<sub>3</sub>), 53.5<sup>†</sup> (Pyr-CH-Ph), 44.4 (N(CH<sub>3</sub>)<sub>2</sub>), 42.2 (N(CH<sub>3</sub>)<sub>2</sub>), 36.9 (CH<sub>2</sub>CH<sub>2</sub>N);

Analytical HPLC (254 nm): *t*<sub>R</sub> = 7.5 min, 97%.

**4-(dimethylamino)-1-(5-(3-fluorophenyl)-2,6-dimethoxypyridin-3-yl)-1,2-diphenylbutan-2-ol**  
(**2.054**)



General method A was used with 3-fluorophenylboronic acid (57.7 mg, 0.412 mmol) to afford the title compound as a pale-yellow foam (85.9 mg, 0.172 mmol, 83%, A:B = 57:43).

LR-MS (ESI<sup>+</sup>) *m/z*: 501.0 [M+H]<sup>+</sup>;

HR-MS (ESI<sup>+</sup>) *m/z* [M = C<sub>31</sub>H<sub>33</sub>FN<sub>2</sub>O<sub>3</sub>]: [M+H]<sup>+</sup> calc'd 501.2548, found 501.2558;

## Diastereomer A:

$^1\text{H}$  NMR (400 MHz,  $\text{CDCl}_3$ )  $\delta$  = 11.74 (br s, 1H,  $\text{NH}^+$ ), 8.11 (s, 1H, PyrH), 7.47 (t,  $J$  = 8.5 Hz, 4H, PhH), 7.37 – 7.28 (m, 4H, PhH), 7.28 – 7.23 (m, 2H, PhH), 7.19 – 7.09 (m, 3H, PhH, Ph'H), 6.96 (tdd,  $J$  = 8.7, 2.6, 0.8 Hz, 1H, Ph'H), 4.72 (s, 1H, Pyr-CH-Ph), 3.81 (s, 3H, 2-PyrOCH<sub>3</sub>), 3.79 (s, 3H, 6-PyrOCH<sub>3</sub>), 3.21 – 3.08 (m, 1H, CH<sub>2</sub>CH<sub>2</sub>N), 2.62 (s, 3H, N(CH<sub>3</sub>)<sub>2</sub>), 2.59 (s, 3H, N(CH<sub>3</sub>)<sub>2</sub>), 2.39 – 2.24 (m, 2H, CH<sub>2</sub>CH<sub>2</sub>N), 2.24 – 2.14 (m, 1H, CH<sub>2</sub>CH<sub>2</sub>N);

$^{13}\text{C}$  NMR (101 MHz,  $\text{CDCl}_3$ )  $\delta$  = 163.7 (d,  $J$  = 244.1 Hz, Ph'CF), 158.8 (2-PyrC-OCH<sub>3</sub>), 157.14 (6-PyrC-OCH<sub>3</sub>), 143.5 (PhC), 142.4 (PyrCH), 139.4 (d,  $J$  = 8.2 Hz, Ph'C), 139.1 (PhC), 130.3 (PhCH), 129.5 (d,  $J$  = 8.5 Hz, Ph'CH), 128.7 (PhCH), 128.4 (PhCH), 127.4 (PhCH), 127.1 (PhCH), 125.4 (PhCH), 124.6 (d,  $J$  = 2.7 Hz, Ph'CH), 116.0 (d,  $J$  = 22.1 Hz, Ph'CH), 115.3 (3-PyrC), 113.8 (d,  $J$  = 2.0 Hz, 5-PyrC), 113.4 (d,  $J$  = 21.1 Hz, Ph'CH), 77.5 (C-OH), 54.7 (CH<sub>2</sub>CH<sub>2</sub>N), 53.9 (Pyr-CH-Ph), 53.7 (2-PyrOCH<sub>3</sub>), 53.3 (6-PyrOCH<sub>3</sub>), 44.3 (N(CH<sub>3</sub>)<sub>2</sub>), 42.3 (N(CH<sub>3</sub>)<sub>2</sub>), 37.9 (CH<sub>2</sub>CH<sub>2</sub>N);

Analytical HPLC (254 nm):  $t_R$  = 7.3 min, 89%;

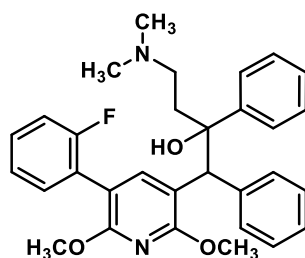
## Diastereomer B:

$^1\text{H}$  NMR (400 MHz,  $\text{CDCl}_3$ )  $\delta$  = 12.30 (br s, 1H,  $\text{NH}^+$ ), 7.86 (s, 1H, PyrH), 7.42 – 7.35 (m, 2H, PhH), 7.35 – 7.17 (m, 7H, PhH), 7.14 (t,  $J$  = 7.3 Hz, 1H, PhH), 7.06 – 6.93 (m, 4H, PhH), 4.87 (s, 1H, Pyr-CH-Ph), 4.07 (s, 3H, 2-PyrOCH<sub>3</sub>), 3.97 (s, 3H, 6-PyrOCH<sub>3</sub>), 3.25 – 3.11 (m, 1H, CH<sub>2</sub>CH<sub>2</sub>N), 2.64 (s, 3H, N(CH<sub>3</sub>)<sub>2</sub>), 2.62 (s, 3H, N(CH<sub>3</sub>)<sub>2</sub>), 2.48 – 2.37 (m, 1H, CH<sub>2</sub>CH<sub>2</sub>N), 2.29 (m, 2H, CH<sub>2</sub>CH<sub>2</sub>N);

$^{13}\text{C}$  NMR (101 MHz,  $\text{CDCl}_3$ )  $\delta$  = 163.7 (d,  $J$  = 244.4 Hz, Ph'CF), 159.4 (2-PyrC-OCH<sub>3</sub>), 158.1 (6-PyrC-OCH<sub>3</sub>), 143.4 (PhC), 143.2 (PyrCH), 140.4 (PhC), 139.1 (d,  $J$  = 8.1 Hz, Ph'C), 129.9 (PhCH), 129.6 (d,  $J$  = 8.4 Hz, Ph'CH), 128.3 (PhCH), 128.0 (PhCH), 127.0 (PhCH), 126.3 (PhCH), 125.8 (PhCH), 124.9 (d,  $J$  = 22.1 Hz, Ph'CH), 115.2 (5-PyrC), 113.7 (3-PyrC), 113.56 (d,  $J$  = 21.0 Hz, Ph'CH), 78.1 (C-OH), 54.6 (CH<sub>2</sub>CH<sub>2</sub>N), 54.0 (2-PyrOCH<sub>3</sub>), 53.8† (Pyr-CH-Ph), 53.6 (6-PyrOCH<sub>3</sub>), 44.3 (N(CH<sub>3</sub>)<sub>2</sub>), 42.1 (N(CH<sub>3</sub>)<sub>2</sub>), 36.9 (CH<sub>2</sub>CH<sub>2</sub>N);

Analytical HPLC (254 nm):  $t_R$  = 7.4 min, 95%.

**4-(dimethylamino)-1-(5-(2-fluorophenyl)-2,6-dimethoxypyridin-3-yl)-1,2-diphenylbutan-2-ol**  
**(2.055)**



General method A was used with 2-fluorophenylboronic acid (57.7 mg, 0.412 mmol) to afford the title compound as a light-brown foam (95.1 mg, 190  $\mu$ mol, 92%, A:B = 55:45).

LR-MS (ESI+)  $m/z$ : 501.0  $[M+H]^+$ ;

HR-MS (ESI+)  $m/z$   $[M = C_{31}H_{33}FN_2O_3]$ :  $[M+H]^+$  calc'd 501.2548, found 501.2561;

Diastereomer A:

$^1H$  NMR (400 MHz,  $CDCl_3$ )  $\delta$  = 12.02 (br s, 1H,  $NH^+$ ), 8.05 (s, 1H, PyrH), 7.51 – 7.42 (m, 4H, PhH), 7.32 (t,  $J$  = 7.4 Hz, 2H, PhH), 7.29 – 7.22 (m, 4H, PhH), 7.19 – 7.05 (m, 4H, PhH), 4.72 (s, 1H, Pyr-CH-Ph), 3.79 (s, 3H, 2-PyrOCH<sub>3</sub>), 3.76 (s, 3H, 6-PyrOCH<sub>3</sub>), 3.15 – 3.07 (m, 1H, CH<sub>2</sub>CH<sub>2</sub>N), 2.61 (s, 3H, N(CH<sub>3</sub>)<sub>2</sub>), 2.59 (s, 3H, N(CH<sub>3</sub>)<sub>2</sub>), 2.40 – 2.25 (m, 2H, CH<sub>2</sub>CH<sub>2</sub>N), 2.25 – 2.12 (m, 1H, CH<sub>2</sub>CH<sub>2</sub>N);

$^{13}C$  NMR (101 MHz,  $CDCl_3$ )  $\delta$  = 160.2 (d,  $J$  = 247.7 Hz, Ph'CF), 159.0 (2-PyrC-OCH<sub>3</sub>), 157.6 (6-PyrC-OCH<sub>3</sub>), 143.4 (PhC), 143.3 (PyrCH), 139.3 (PhC), 132.0 (d,  $J$  = 3.4 Hz, Ph'CH), 130.4 (PhCH), 128.8 (d,  $J$  = 8.1 Hz, Ph'CH), 128.7 (PhCH), 128.3 (PhCH), 127.4 (PhCH), 127.0 (PhCH), 125.5 (PhCH), 125.0 (d,  $J$  = 15.2 Hz, Ph'CH), 123.8 (d,  $J$  = 3.5 Hz, Ph'CH), 115.7 (d,  $J$  = 22.4 Hz, Ph'CH), 114.7 (3-PyrC), 109.4 (5-PyrC), 77.6 (C-OH), 54.6 (CH<sub>2</sub>CH<sub>2</sub>N), 53.7 (Pyr-CH-Ph), 53.6 (2-PyrOCH<sub>3</sub>), 53.4 (6-PyrOCH<sub>3</sub>), 44.1 (N(CH<sub>3</sub>)<sub>2</sub>), 42.3 (N(CH<sub>3</sub>)<sub>2</sub>), 37.7 (CH<sub>2</sub>CH<sub>2</sub>N);

Analytical HPLC (254 nm):  $t_R$  = 7.0 min, 100%;

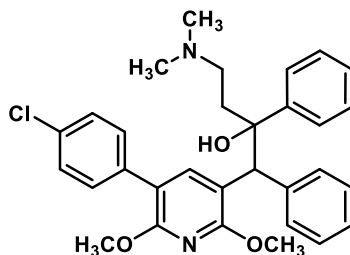
Diastereomer B:

$^1H$  NMR (400 MHz,  $CDCl_3$ )  $\delta$  = 12.29 (br s, 1H,  $NH^+$ ), 8.01 (s, 1H, PyrH), 7.47 (td,  $J$  = 7.6, 1.8 Hz, 1H, Ph'H), 7.35 – 7.22 (m, 5H, PhH), 7.21 – 7.06 (m, 5H, PhH), 7.05 – 6.98 (m, 3H, PhH), 4.86 (s, 1H, Pyr-CH-Ph), 4.04 (s, 3H, 2-PyrOCH<sub>3</sub>), 3.94 (s, 3H, 6-PyrOCH<sub>3</sub>), 3.18 – 3.05 (m, 1H, CH<sub>2</sub>CH<sub>2</sub>N), 2.64 (s, 6H, N(CH<sub>3</sub>)<sub>2</sub>), 2.50 – 2.32 (m, 3H, CH<sub>2</sub>CH<sub>2</sub>N);

$^{13}C$  NMR (101 MHz,  $CDCl_3$ )  $\delta$  = 160.0 (d,  $J$  = 247.5 Hz, Ph'CF), 159.8 (2-PyrC-OCH<sub>3</sub>), 158.5 (6-PyrC-OCH<sub>3</sub>), 143.8 (PyrCH), 143.5 (PhC), 139.7 (PhC), 132.4 (d,  $J$  = 3.3 Hz, Ph'CH), 129.9 (PhCH), 129.0 (d,  $J$  = 8.3 Hz, Ph'CH), 128.4 (PhCH), 128.0 (PhCH), 127.1 (PhCH), 126.4 (PhCH), 125.7 (PhCH), 124.6 (d,  $J$  = 14.8 Hz, Ph'CH), 124.0 (d,  $J$  = 3.5 Hz, Ph'CH), 115.7 (d,  $J$  = 22.6 Hz, Ph'CH), 113.3 (3-PyrC), 110.1 (5-PyrC), 78.4 (C-OH), 54.5 (CH<sub>2</sub>CH<sub>2</sub>N), 54.0 (2-PyrOCH<sub>3</sub>), 53.7 (6-PyrOCH<sub>3</sub>), 53.6<sup>†</sup> (Pyr-CH-Ph), 43.6 (N(CH<sub>3</sub>)<sub>2</sub>), 42.6 (N(CH<sub>3</sub>)<sub>2</sub>), 36.0 (CH<sub>2</sub>CH<sub>2</sub>N);

Analytical HPLC (254 nm):  $t_R$  = 7.2 min, 97%.

**1-(5-(4-chlorophenyl)-2,6-dimethoxypyridin-3-yl)-4-(dimethylamino)-1,2-diphenylbutan-2-ol**  
**(2.056)**



General method A was used with 4-chlorophenylboronic acid (64.4 mg, 0.412 mmol) to afford the title compound as a light-brown oil (102 mg, 0.197 mmol, 96%, A:B = 52:48)

LR-MS (ESI+)  $m/z$ : 516.9  $[M+H]^+$ ;

HR-MS (ESI+)  $m/z$   $[M = C_{31}H_{33}ClN_2O_3]$ :  $[M+H]^+$  calc'd 517.2252, found 517.2258;

Diastereomer A:

$^1H$  NMR (400 MHz,  $CDCl_3$ )  $\delta$  = 12.45 (br s, 1H,  $NH^+$ ), 8.08 (s, 1H, PyrH), 7.44 – 7.37 (m, 4H, PhH), 7.27 – 7.23 (m, 5H, PhH), 7.21 – 7.15 (m, 4H, PhH), 7.06 (t,  $J$  = 7.3 Hz, 1H, PhH), 4.65 (s, 1H, Pyr-CH-Ph), 3.72 (s, 3H, 2-PyrOCH<sub>3</sub>), 3.70 (s, 3H, 6-PyrOCH<sub>3</sub>), 3.13 – 3.02 (m, 1H, CH<sub>2</sub>CH<sub>2</sub>N), 2.52 (s, 3H, N(CH<sub>3</sub>)<sub>2</sub>), 2.49 (s, 3H, N(CH<sub>3</sub>)<sub>2</sub>), 2.29 – 2.16 (m, 2H, CH<sub>2</sub>CH<sub>2</sub>N), 2.15 – 2.03 (m, 1H, CH<sub>2</sub>CH<sub>2</sub>N);

$^{13}C$  NMR (101 MHz,  $CDCl_3$ )  $\delta$  = 158.8 (2-PyrC-OCH<sub>3</sub>), 157.1 (6-PyrC-OCH<sub>3</sub>), 143.7 (PhC), 142.2 (4-PyrCH), 139.3 (PhC), 135.7 (PhC), 132.5 (PhC), 130.38 (PhCH), 130.36 (PhCH), 128.7 (PhCH), 128.33 (PhCH), 128.30 (PhCH), 127.4 (PhCH), 127.0 (PhCH), 125.5 (PhCH), 115.5 (PyrC), 113.8 (PyrC), 77.4 (C-OH), 54.3 (CH<sub>2</sub>CH<sub>2</sub>N), 53.7 (2-PyrOCH<sub>3</sub>), 53.4 (Pyr-CH-Ph), 53.3 (6-PyrOCH<sub>3</sub>), 44.2 (N(CH<sub>3</sub>)<sub>2</sub>), 42.0 (N(CH<sub>3</sub>)<sub>2</sub>), 38.0 (CH<sub>2</sub>CH<sub>2</sub>N);

Analytical HPLC (254 nm):  $t_R$  = 7.7 min, 100%;

Diastereomer B:

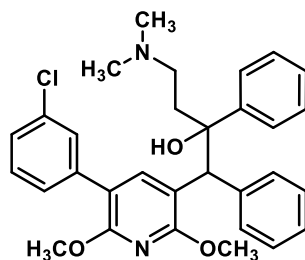
$^1H$  NMR (400 MHz,  $CDCl_3$ )  $\delta$  = 12.19 (br s, 1H,  $NH^+$ ), 7.82 (s, 1H, PyrH), 7.45 (d,  $J$  = 8.5 Hz, 2H, Ph'H), 7.38 (d,  $J$  = 7.3 Hz, 2H, PhH), 7.33 (d,  $J$  = 8.5 Hz, 2H, Ph'H), 7.26 – 7.18 (m, 4H, PhH), 7.13 (t,  $J$  = 7.3 Hz, 1H, PhH), 7.05 – 6.94 (m, 3H, PhH), 4.87 (s, 1H, (Pyr-CH-Ph)), 4.07 (s, 4H, 2-PyrOCH<sub>3</sub>), 3.96 (s, 3H, 6-PyrOCH<sub>3</sub>), 3.22 (t,  $J$  = 10.6 Hz, 1H, CH<sub>2</sub>CH<sub>2</sub>N), 2.63 (s, 3H, N(CH<sub>3</sub>)<sub>2</sub>), 2.62 (s, 3H, N(CH<sub>3</sub>)<sub>2</sub>), 2.47 – 2.38 (m, 1H, CH<sub>2</sub>CH<sub>2</sub>N), 2.35 – 2.20 (m, 2H, CH<sub>2</sub>CH<sub>2</sub>N);

$^{13}C$  NMR (101 MHz,  $CDCl_3$ )  $\delta$  = 159.3 (2-PyrC-OCH<sub>3</sub>), 158.1 (6-PyrC-OCH<sub>3</sub>), 143.4 (PhC), 143.1 (PyrCH), 140.5 (PhC), 135.4 (PhC), 132.7 (PhC), 130.6 (Ph'CH), 129.9 (PhCH), 128.34 (Ph'CH), 128.31 (PhCH), 128.0 (PhCH), 126.9 (PhCH), 126.3 (PhCH), 125.8 (PhCH), 115.3 (PyrC), 113.7 (PyrC), 78.1 (C-OH), 54.6

(CH<sub>2</sub>CH<sub>2</sub>N), 54.0 (2-PyrOCH<sub>3</sub>), 53.7<sup>†</sup> (Pyr-CH-Ph), 53.6 (6-PyrOCH<sub>3</sub>), 44.4 (N(CH<sub>3</sub>)<sub>2</sub>), 42.0 (N(CH<sub>3</sub>)<sub>2</sub>), 36.93 (CH<sub>2</sub>CH<sub>2</sub>N);

Analytical HPLC (254 nm): *t*<sub>R</sub> = 7.8 min, 93%.

**1-(5-(3-chlorophenyl)-2,6-dimethoxypyridin-3-yl)-4-(dimethylamino)-1,2-diphenylbutan-2-ol**  
(2.057)



General method A was used with 3-fluorophenylboronic acid (64.4 mg, 0.412 mmol) to afford the title compound as a pale-yellow foam (74.2 mg, 0.143 mmol, 70%, A:B = 57:43).

LR-MS (ESI+) *m/z*: 516.9 [M+H]<sup>+</sup>;

HR-MS (ESI+) *m/z* [M = C<sub>31</sub>H<sub>33</sub>ClN<sub>2</sub>O<sub>3</sub>]: [M+H]<sup>+</sup> calc'd 517.2252, found 517.2255;

Diastereomer A:

<sup>1</sup>H NMR (401 MHz, CDCl<sub>3</sub>) δ = 11.81 (br s, 1H, NH<sup>+</sup>), 8.08 (s, 1H, PyrH), 7.49 (d, *J* = 7.4 Hz, 2H, PhH), 7.45 (d, *J* = 7.2 Hz, 2H, PhH), 7.36 – 7.21 (m, 9H, PhH), 7.15 (t, *J* = 7.3 Hz, 1H, PhH), 4.72 (s, 1H, Pyr-CH-Ph), 3.80 (s, 3H, 2-PyrOCH<sub>3</sub>), 3.79 (s, 3H, 6-PyrOCH<sub>3</sub>), 3.21 – 3.09 (m, 1H, CH<sub>2</sub>CH<sub>2</sub>N), 2.62 (s, 3H, N(CH<sub>3</sub>)<sub>2</sub>), 2.59 (s, 3H, N(CH<sub>3</sub>)<sub>2</sub>), 2.39 – 2.24 (m, 2H, CH<sub>2</sub>CH<sub>2</sub>N), 2.24 – 2.14 (m, 1H, CH<sub>2</sub>CH<sub>2</sub>N);

<sup>13</sup>C NMR (101 MHz, CDCl<sub>3</sub>) δ = 158.9 (2-PyrC-OCH<sub>3</sub>), 157.1 (6-PyrC-OCH<sub>3</sub>), 143.5 (PhC), 142.4 (PyrCH), 139.04 (PhC), 139.03 (PhC), 133.9 (PhC), 130.3 (PhCH), 129.4 (PhCH), 129.2 (PhCH), 128.7 (PhCH), 128.5 (PhCH), 127.4 (PhCH), 127.2 (PhCH), 127.1 (PhCH), 126.6 (PhCH), 125.4 (PhCH), 115.4 (3-PyrC), 113.6 (5-PyrC), 77.4 (C-OH), 54.6 (CH<sub>2</sub>CH<sub>2</sub>N), 53.7 (2-PyrOCH<sub>3</sub>), 53.6<sup>†</sup> (Pyr-CH-Ph), 53.4 (6-PyrOCH<sub>3</sub>), 44.3 (N(CH<sub>3</sub>)<sub>2</sub>), 42.3 (N(CH<sub>3</sub>)<sub>2</sub>), 37.9 (CH<sub>2</sub>CH<sub>2</sub>N);

Analytical HPLC (254 nm): *t*<sub>R</sub> = 7.7 min, 98%;

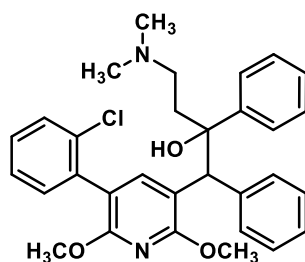
Diastereomer B:

<sup>1</sup>H NMR (401 MHz, CDCl<sub>3</sub>) δ = 12.26 (br s, 1H, NH<sup>+</sup>), 7.82 (s, 1H, PyrH), 7.50 (t, *J* = 1.7 Hz, 1H, PhH), 7.42 – 7.35 (m, 3H, PhH), 7.30 (t, *J* = 7.8 Hz, 1H, PhH), 7.26 – 7.21 (m, 3H, PhH), 7.21 – 7.12 (m, 3H, PhH), 7.06 – 6.96 (m, 3H, PhH), 4.86 (s, 1H, Pyr-CH-Ph), 4.08 (s, 3H, 2-PyrOCH<sub>3</sub>), 3.97 (s, 3H, 6-PyrOCH<sub>3</sub>), 3.21 (t, *J* = 10.7 Hz, 1H, CH<sub>2</sub>CH<sub>2</sub>N), 2.65 (s, 3H, N(CH<sub>3</sub>)<sub>2</sub>), 2.61 (s, 3H, N(CH<sub>3</sub>)<sub>2</sub>), 2.50 – 2.38 (m, 1H, CH<sub>2</sub>CH<sub>2</sub>N), 2.28 (m, 2H, CH<sub>2</sub>CH<sub>2</sub>N);

$^{13}\text{C}$  NMR (101 MHz,  $\text{CDCl}_3$ )  $\delta$  = 159.4 (2-PyrC-OCH<sub>3</sub>), 158.1 (6-PyrC-OCH<sub>3</sub>), 143.3 (PhC), 143.2 (PyrCH), 140.4 (PhC), 138.8 (PhC), 133.9 (PhC), 129.9 (PhCH), 129.5 (PhCH), 129.2 (PhCH), 128.4 (PhCH), 128.0 (PhCH), 127.5 (PhCH), 127.0 (PhCH), 126.9 (PhCH), 126.3 (PhCH), 125.8 (PhCH), 115.0 (PyrC), 113.7 (PyrC), 78.1 (C-OH), 54.6 (CH<sub>2</sub>CH<sub>2</sub>N), 54.1 (2-PyrOCH<sub>3</sub>), 53.8<sup>†</sup> (Pyr-CH-Ph), 53.7 (6-PyrOCH<sub>3</sub>), 44.3 (N(CH<sub>3</sub>)<sub>2</sub>), 42.1 (N(CH<sub>3</sub>)<sub>2</sub>), 36.8 (CH<sub>2</sub>CH<sub>2</sub>N);

Analytical HPLC (254 nm):  $t_R$  = 7.9 min, 95%.

**1-(5-(2-chlorophenyl)-2,6-dimethoxypyridin-3-yl)-4-(dimethylamino)-1,2-diphenylbutan-2-ol**  
**(2.058)**



General method A was used with 2-chlorophenylboronic acid (64.4 mg, 0.412 mmol) to afford the title compound as a light-brown foam (59.1 mg, 0.114 mmol, 55%, A:B = 55:45).

LR-MS (ESI+)  $m/z$ : 516.9  $[\text{M}+\text{H}]^+$ ;

HR-MS (ESI+)  $m/z$  [ $\text{M} = \text{C}_{31}\text{H}_{33}\text{ClN}_2\text{O}_3$ ]:  $[\text{M}+\text{H}]^+$  calc'd 517.2252, found 517.2262;

Diastereomer A:

$^1\text{H}$  NMR (400 MHz,  $\text{CDCl}_3$ )  $\delta$  = 12.53 (br s, 1H, NH<sup>+</sup>), 7.99 (s, 1H, PyrH), 7.54 – 7.46 (m, 2H, PhH), 7.46 – 7.38 (m, 3H, PhH), 7.33 (t,  $J$  = 7.4 Hz, 2H, PhH), 7.29 – 7.20 (m, 4H, PhH), 7.13 (tt,  $J$  = 7.3, 1.3 Hz, 1H, PhH), 7.11 – 7.07 (m, 1H, PhH), 4.73 (s, 1H, Pyr-CH-Ph), 3.78 (d,  $J$  = 5.1 Hz, 3H, 2-PyrOCH<sub>3</sub>), 3.73 (s, 3H, 6-PyrOCH<sub>3</sub>), 3.14 – 3.04 (m, 1H, CH<sub>2</sub>CH<sub>2</sub>N), 2.58 (s, 3H, N(CH<sub>3</sub>)<sub>2</sub>), 2.56 (s, 3H, N(CH<sub>3</sub>)<sub>2</sub>), 2.38 – 2.25 (m, 2H, CH<sub>2</sub>CH<sub>2</sub>N), 2.21 – 2.10 (m, 1H, CH<sub>2</sub>CH<sub>2</sub>N);

$^{13}\text{C}$  NMR (101 MHz,  $\text{CDCl}_3$ )  $\delta$  = 159.0 (2-PyrC-OCH<sub>3</sub>), 157.4 (6-PyrC-OCH<sub>3</sub>), 143.4 (PhC), 143.1 (PyrCH), 139.3 (PhC), 136.3 (PhC), 134.3 (PhC), 132.1 (PhCH), 130.4 (PhCH), 129.5 (PhCH), 128.7 (PhCH), 128.6 (PhCH), 128.3 (PhCH), 127.4 (PhCH), 126.9 (PhCH), 126.5 (PhCH), 125.6 (PhCH), 114.5 (PyrC), 113.1 (PyrC), 77.6 (C-OH), 54.5 (CH<sub>2</sub>CH<sub>2</sub>N), 53.7 (Pyr-CH-Ph), 53.6 (2-PyrOCH<sub>3</sub>), 53.4 (6-PyrOCH<sub>3</sub>), 44.0 (N(CH<sub>3</sub>)<sub>2</sub>), 42.3 (N(CH<sub>3</sub>)<sub>2</sub>), 37.7 (CH<sub>2</sub>CH<sub>2</sub>N);

Analytical HPLC (254 nm):  $t_R$  = 7.3 min, 95%;

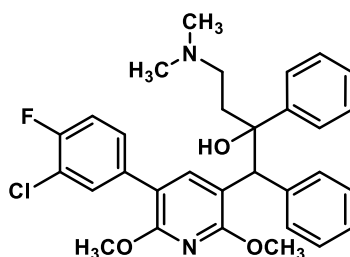
## Diastereomer B:

$^1\text{H}$  NMR (400 MHz,  $\text{CDCl}_3$ )  $\delta$  = 12.63 (br s, 1H,  $\text{NH}^+$ ), 7.84 (s, 1H, PyrH), 7.38 (dd,  $J$  = 7.7, 1.5 Hz, 1H, PhH), 7.34 (dd,  $J$  = 7.4, 1.9 Hz, 1H, PhH), 7.29 – 7.22 (m, 3H, PhH), 7.22 – 7.15 (m, 3H, PhH), 7.12 – 7.03 (m, 3H, PhH), 6.99 – 6.91 (m, 3H, PhH), 4.82 (s, 1H, Pyr-CH-Ph), 4.00 (s, 3H, 2-PyrOCH<sub>3</sub>), 3.87 (s, 3H, 6-PyrOCH<sub>3</sub>), 3.04 (d,  $J$  = 9.1 Hz, 1H, CH<sub>2</sub>CH<sub>2</sub>N), 2.56 (s, 6H, N(CH<sub>3</sub>)<sub>2</sub>), 2.41 – 2.22 (m, 3H, CH<sub>2</sub>CH<sub>2</sub>N);

$^{13}\text{C}$  NMR (101 MHz,  $\text{CDCl}_3$ )  $\delta$  = 159.8 (2-PyrC-OCH<sub>3</sub>), 158.4 (6-PyrC-OCH<sub>3</sub>), 143.7 (4-PyrCH), 143.5 (PhC), 139.7 (PhC), 135.9 (PhC), 134.0 (PhC), 132.5 (PhCH), 130.0 (PhCH), 129.6 (PhCH), 128.8 (PhCH), 128.4 (PhCH), 128.0 (PhCH), 127.1 (PhCH), 126.7 (PhCH), 126.4 (PhCH), 125.7 (PhCH), 113.8 (PyrC), 113.0 (PyrC), 78.4 (C-OH), 54.5 (CH<sub>2</sub>CH<sub>2</sub>N), 54.0 (2-PyrOCH<sub>3</sub>), 53.7 (6-PyrOCH<sub>3</sub>), 53.6<sup>†</sup> (Pyr-CH-Ph), 43.6 (N(CH<sub>3</sub>)<sub>2</sub>), 42.6 (N(CH<sub>3</sub>)<sub>2</sub>), 36.2 (CH<sub>2</sub>CH<sub>2</sub>N);

Analytical HPLC (254 nm):  $t_R$  = 7.5 min, 94%.

**1-(5-(3-chloro-4-fluorophenyl)-2,6-dimethoxypyridin-3-yl)-4-(dimethylamino)-1,2-diphenylbutan-2-ol (2.059)**



General method A was used with 3-chloro-4-fluorophenylboronic acid (71.8 mg, 0.412 mmol) to afford the title compound as a light-yellow foam (72.3 mg, 0.135 mmol, 66%, A:B = 54:46).

LR-MS (ESI+)  $m/z$ : 534.9  $[\text{M}+\text{H}]^+$ ;

HR-MS (ESI+)  $m/z$   $[\text{M} = \text{C}_{31}\text{H}_{32}\text{ClFN}_2\text{O}_3]$ :  $[\text{M}+\text{H}]^+$  calc'd 535.2158, found 535.2167;

## Diastereomer A:

$^1\text{H}$  NMR (400 MHz,  $\text{CDCl}_3$ )  $\delta$  = 12.68 (br s, 1H,  $\text{NH}^+$ ), 8.15 (s, 1H, PyrH), 7.50 (d,  $J$  = 7.9 Hz, 2H, PhH), 7.46 (d,  $J$  = 7.7 Hz, 2H, PhH), 7.39 (d,  $J$  = 7.1 Hz, 1H, PhH), 7.26 (s, 6H, PhH), 7.18 – 7.09 (m, 2H, PhH), 4.72 (s, 1H, Pyr-CH-Ph), 3.78 (s, 6H, PyrOCH<sub>3</sub>), 3.28 – 3.02 (m, 1H, CH<sub>2</sub>CH<sub>2</sub>N), 2.59 (s, 3H, N(CH<sub>3</sub>)<sub>2</sub>), 2.57 (s, 3H, N(CH<sub>3</sub>)<sub>2</sub>), 2.35 – 2.21 (m, 2H, CH<sub>2</sub>CH<sub>2</sub>N), 2.21 – 2.07 (m, 1H, CH<sub>2</sub>CH<sub>2</sub>N);

$^{13}\text{C}$  NMR (101 MHz,  $\text{CDCl}_3$ )  $\delta$  = 159.0 (2-PyrC-OCH<sub>3</sub>), 157.0 (d,  $J$  = 248.0 Hz, Ph'CF), 156.9 (6-PyrC-OCH<sub>3</sub>), 143.8 (PhC), 142.1 (PyrCH), 139.2 (PhC), 134.5 (d,  $J$  = 4.0 Hz, Ph'C), 131.2 (PhCH), 130.4 (PhCH), 128.8 (d,  $J$  = 6.9 Hz, Ph'CH), 128.6 (PhCH), 128.4 (PhCH), 127.4 (PhCH), 127.0 (PhCH), 125.5 (PhCH), 120.5 (d,  $J$  = 17.6 Hz, Ph'Cl), 116.2 (d,  $J$  = 20.9 Hz, Ph'CH), 115.7 (PyrC), 112.7 (PyrC), 77.3 (C-OH), 54.2 (CH<sub>2</sub>CH<sub>2</sub>N), 53.7 (PyrOCH<sub>3</sub>), 53.3 (PyrOCH<sub>3</sub>), 53.1 (Pyr-CH-Ph), 44.2 (N(CH<sub>3</sub>)<sub>2</sub>), 41.9 (N(CH<sub>3</sub>)<sub>2</sub>), 38.1 (CH<sub>2</sub>CH<sub>2</sub>N);

Analytical HPLC (254 nm):  $t_R$  = 7.8 min, 91%;

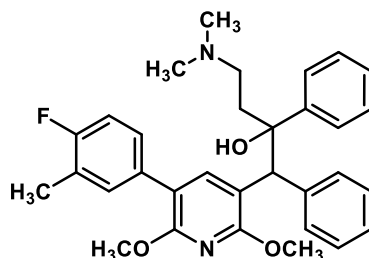
Diastereomer B:

$^1\text{H}$  NMR (400 MHz,  $\text{CDCl}_3$ )  $\delta$  = 12.32 (br s, 1H,  $\text{NH}^+$ ), 7.79 (s, 1H,  $\text{PyrH}$ ), 7.55 (dd,  $J$  = 7.2, 1.9 Hz, 1H,  $\text{PhH}$ ), 7.42 – 7.35 (m, 3H,  $\text{PhH}$ ), 7.26 – 7.19 (m, 4H,  $\text{PhH}$ ), 7.17 – 7.10 (m, 2H,  $\text{PhH}$ ), 7.06 – 6.94 (m,  $J$  = 14.2, 7.0 Hz, 3H,  $\text{PhH}$ ), 4.87 (s, 1H,  $\text{Pyr-CH-Ph}$ ), 4.07 (d,  $J$  = 7.3 Hz, 3H, 2- $\text{PyrOCH}_3$ ), 3.96 (s, 3H, 6- $\text{PyrOCH}_3$ ), 3.29 – 3.20 (m, 1H,  $\text{CH}_2\text{CH}_2\text{N}$ ), 2.65 (s, 3H,  $\text{N}(\text{CH}_3)_2$ ), 2.63 (s, 3H,  $\text{N}(\text{CH}_3)_2$ ), 2.49 – 2.39 (m, 1H,  $\text{CH}_2\text{CH}_2\text{N}$ ), 2.35 – 2.23 (m, 2H,  $\text{CH}_2\text{CH}_2\text{N}$ );

$^{13}\text{C}$  NMR (101 MHz,  $\text{CDCl}_3$ )  $\delta$  = 159.4 (2- $\text{PyrC-OCH}_3$ ), 158.0 (6- $\text{PyrC-OCH}_3$ ), 157.2 (d,  $J$  = 248.0 Hz,  $\text{Ph}'\text{CF}$ ), 143.4 ( $\text{PhC}$ ), 143.1 ( $\text{PyrCH}$ ), 140.6 ( $\text{PhC}$ ), 134.1 (d,  $J$  = 4.0 Hz,  $\text{Ph}'\text{C}$ ), 131.3 ( $\text{PhCH}$ ), 129.9 ( $\text{PhCH}$ ), 129.2 (d,  $J$  = 7.1 Hz,  $\text{Ph}'\text{CH}$ ), 128.3 ( $\text{PhCH}$ ), 128.0 ( $\text{PhCH}$ ), 126.9 ( $\text{PhCH}$ ), 126.3 ( $\text{PhCH}$ ), 125.9 ( $\text{PhCH}$ ), 120.4 (d,  $J$  = 17.8 Hz,  $\text{Ph}'\text{C}$ ), 116.2 (d,  $J$  = 21.0 Hz,  $\text{Ph}'\text{CH}$ ), 114.3 ( $\text{PyrC}$ ), 113.9 ( $\text{PyrC}$ ), 78.1 ( $\text{C-OH}$ ), 54.6 ( $\text{CH}_2\text{CH}_2\text{N}$ ), 54.1 (2- $\text{PyrOCH}_3$ ), 53.67 (6- $\text{PyrOCH}_3$ ), 53.66<sup>†</sup> ( $\text{Pyr-CH-Ph}$ ), 44.6 ( $\text{N}(\text{CH}_3)_2$ ), 42.0 ( $\text{N}(\text{CH}_3)_2$ ), 37.0 ( $\text{CH}_2\text{CH}_2\text{N}$ );

Analytical HPLC (254 nm):  $t_R$  = 7.9 min, 94%.

**4-(dimethylamino)-1-(5-(4-fluoro-3-methylphenyl)-2,6-dimethoxypyridin-3-yl)-1,2-diphenylbutan-2-ol (2.060)**



General method A was used with 4-fluoro-3-methylphenylboronic acid (63.4 mg, 0.412 mmol) to afford the title compound as an off-white foam (97.0 mg, 0.188 mmol, 91%, A:B = 55:45).

LR-MS (ESI+)  $m/z$ : 515.0  $[\text{M}+\text{H}]^+$ ;

HR-MS (ESI+)  $m/z$  [ $\text{M} = \text{C}_{31}\text{H}_{34}\text{N}_2\text{O}_3$ ]:  $[\text{M}+\text{H}]^+$  calc'd 515.2704, found 515.2715;

Diastereomer A:

$^1\text{H}$  NMR (400 MHz,  $\text{CDCl}_3$ )  $\delta$  = 8.04 (s, 1H,  $\text{PyrH}$ ), 7.51 – 7.44 (m, 4H,  $\text{PhH}$ ), 7.32 (t,  $J$  = 7.4 Hz, 2H,  $\text{PhH}$ ), 7.29 – 7.21 (m, 3H,  $\text{PhH}$ ), 7.18 – 7.11 (m, 3H,  $\text{PhH}$ ,  $\text{Ph}'\text{H}$ ), 7.03 – 6.96 (m, 1H,  $\text{Ph}'\text{H}$ ), 4.71 (s, 1H,  $\text{Pyr-CH-Ph}$ ), 3.79 (s, 3H,  $\text{PyrOCH}_3$ ), 3.77 (s, 3H,  $\text{PyrOCH}_3$ ), 3.18 – 3.09 (m, 1H,  $\text{CH}_2\text{CH}_2\text{N}$ ), 2.61 (s, 3H,  $\text{N}(\text{CH}_3)_2$ ), 2.58 (s, 3H,  $\text{N}(\text{CH}_3)_2$ ), 2.37 – 2.25 (m, 2H,  $\text{CH}_2\text{CH}_2\text{N}$ ), 2.31 (d,  $J$  = 1.7 Hz, 3H,  $\text{Ph}'\text{CH}_3$ ), 2.23 – 2.14 (m, 1H,  $\text{CH}_2\text{CH}_2\text{N}$ );



$^{13}\text{C}$  NMR (101 MHz,  $\text{CDCl}_3$ )  $\delta$  = 160.5 (d,  $J$  = 244.4 Hz,  $\text{Ph}'\text{CF}$ ), 158.4 (Pyr $\text{C}$ - $\text{OCH}_3$ ), 157.0 (Pyr $\text{C}$ - $\text{OCH}_3$ ), 143.7 (Ph $\text{C}$ ), 142.4 (Pyr $\text{CH}$ ), 139.3 (Ph $\text{C}$ ), 132.9 (d,  $J$  = 3.5 Hz,  $\text{Ph}'\text{C}$ ), 132.2 (d,  $J$  = 5.2 Hz,  $\text{Ph}'\text{CH}$ ), 130.4 (Ph $\text{CH}$ ), 128.6 (Ph $\text{CH}$ ), 128.3 (Ph $\text{CH}$ ), 128.1 (d,  $J$  = 7.7 Hz,  $\text{Ph}'\text{CH}$ ), 127.4 (Ph $\text{CH}$ ), 127.0 (Ph $\text{CH}$ ), 125.5 (Ph $\text{CH}$ ), 124.4 (d,  $J$  = 17.5 Hz,  $\text{Ph}'\text{C}$ ), 115.2 (Pyr $\text{C}$ ), 114.7 (d,  $J$  = 22.3 Hz,  $\text{Ph}'\text{CH}$ ), 114.3 (Pyr $\text{C}$ ), 77.4 ( $\text{C}$ -OH), 54.4 ( $\text{CH}_2\text{CH}_2\text{N}$ ), 53.7 $^\dagger$  (Pyr- $\text{CH}$ -Ph), 53.6 (Pyr $\text{OCH}_3$ ), 53.3 (Pyr $\text{OCH}_3$ ), 44.1 ( $\text{N}(\text{CH}_3)_2$ ), 42.1 ( $\text{N}(\text{CH}_3)_2$ ), 37.9 ( $\text{CH}_2\text{CH}_2\text{N}$ ), 14.8 (d,  $J$  = 3.6 Hz,  $\text{Ph}'\text{CH}_3$ );

Analytical HPLC (254 nm):  $t_R$  = 7.7 min, 100%;

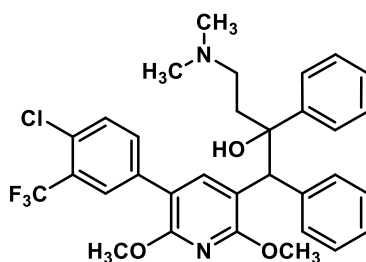
Diastereomer B:

$^1\text{H}$  NMR (400 MHz,  $\text{CDCl}_3$ )  $\delta$  = 12.21 (br s, 1H,  $\text{NH}^+$ ), 7.76 (s, 1H, Pyr $\text{H}$ ), 7.37 (d,  $J$  = 7.3 Hz, 2H, Ph $\text{H}$ ), 7.33 – 7.11 (m, 7H, Ph $\text{H}$ ), 7.06 – 6.95 (m, 4H, Ph $\text{H}$ ), 4.85 (s, 1H, Pyr- $\text{CH}$ -Ph), 4.08 (s, 3H, Pyr $\text{OCH}_3$ ), 3.96 (s, 3H, Pyr $\text{OCH}_3$ ), 3.21 (td,  $J$  = 11.2, 2.3 Hz, 1H,  $\text{CH}_2\text{CH}_2\text{N}$ ), 2.65 (s, 3H,  $\text{N}(\text{CH}_3)_2$ ), 2.63 (s, 3H,  $\text{N}(\text{CH}_3)_2$ ), 2.49 – 2.37 (m, 1H,  $\text{CH}_2\text{CH}_2\text{N}$ ), 2.30 (d,  $J$  = 1.7 Hz, 3H,  $\text{Ph}'\text{CH}_3$ ), 2.36 – 2.21 (m, 2H,  $\text{CH}_2\text{CH}_2\text{N}$ );

$^{13}\text{C}$  NMR (101 MHz,  $\text{CDCl}_3$ )  $\delta$  = 160.6 (d,  $J$  = 244.5 Hz,  $\text{Ph}'\text{CF}$ ), 159.0 $^\dagger$  (Pyr $\text{C}$ - $\text{OCH}_3$ ), 158.1 (Pyr $\text{C}$ - $\text{OCH}_3$ ), 143.4 (Ph $\text{C}$ ), 143.3 (Pyr $\text{CH}$ ), 140.5 (Ph $\text{C}$ ), 132.5 ( $\text{Ph}'\text{C}$ ), 132.3 (d,  $J$  = 4.9 Hz,  $\text{Ph}'\text{CH}$ ), 129.9 (Ph $\text{CH}$ ), 128.3 (Ph $\text{CH}$ ), 128.2 (d,  $J$  = 7.6 Hz,  $\text{Ph}'\text{CH}$ ), 127.9 (Ph $\text{CH}$ ), 126.9 (Ph $\text{CH}$ ), 126.3 (Ph $\text{CH}$ ), 125.8 (Ph $\text{CH}$ ), 124.4 (d,  $J$  = 17.5 Hz,  $\text{Ph}'\text{C}$ ), 115.8 (Pyr $\text{C}$ ), 114.7 (d,  $J$  = 22.2 Hz,  $\text{Ph}'\text{CH}$ ), 113.5 (Pyr $\text{C}$ ), 78.1 ( $\text{C}$ -OH), 54.6 ( $\text{CH}_2\text{CH}_2\text{N}$ ), 54.0 (Pyr $\text{OCH}_3$ ), 53.9 $^\dagger$  (Pyr- $\text{CH}$ -Ph), 53.6 (Pyr $\text{OCH}_3$ ), 44.3 ( $\text{N}(\text{CH}_3)_2$ ), 42.1 ( $\text{N}(\text{CH}_3)_2$ ), 36.9 ( $\text{CH}_2\text{CH}_2\text{N}$ ), 14.7 ( $\text{Ph}'\text{CH}_3$ );

Analytical HPLC (254 nm):  $t_R$  = 7.8 min, 100%.

**1-(5-(4-chloro-3-(trifluoromethyl)phenyl)-2,6-dimethoxypyridin-3-yl)-4-(dimethylamino)-1,2-diphenylbutan-2-ol (2.061)**



General method A was used with 4-chloro-3-trifluoromethylphenylboronic acid (92.4 mg, 0.412 mmol) to afford the title compound as a yellow foam (117 mg, mmol, 97%, A:B = 57:43).

LR-MS (ESI+)  $m/z$ : 585.2  $[\text{M}+\text{H}]^+$ .

HR-MS (ESI+)  $m/z$   $[\text{M} = \text{C}_{32}\text{H}_{32}\text{ClF}_3\text{N}_2\text{O}_3]$ :  $[\text{M}+\text{H}]^+$  calc'd 585.2126, found 585.2134;

## Diastereomer A:

$^1\text{H}$  NMR (400 MHz,  $\text{CDCl}_3$ )  $\delta$  = 12.47 (br s, 1H,  $\text{NH}^+$ ), 8.20 (s, 1H,  $\text{PyrH}$ ), 7.64 (d,  $J$  = 2.0 Hz, 1H,  $\text{PhH}$ ), 7.57 – 7.40 (m, 6H,  $\text{PhH}$ ), 7.36 – 7.23 (m, 5H,  $\text{PhH}$ ), 7.15 (t,  $J$  = 7.3 Hz, 1H,  $\text{PhH}$ ), 4.73 (s, 1H,  $\text{Pyr-CH-Ph}$ ), 3.794 (s, 3H, 2-PyrOCH<sub>3</sub>), 3.786 (s, 3H, 6-PyrOCH<sub>3</sub>), 3.25 – 3.12 (m, 1H,  $\text{CH}_2\text{CH}_2\text{N}$ ), 2.61 (br s, 3H,  $\text{N}(\text{CH}_3)_2$ ), 2.58 (br s, 3H,  $\text{N}(\text{CH}_3)_2$ ), 2.35 – 2.21 (m, 2H,  $\text{CH}_2\text{CH}_2\text{N}$ ), 2.21 – 2.12 (m, 1H,  $\text{CH}_2\text{CH}_2\text{N}$ );

$^{13}\text{C}$  NMR (101 MHz,  $\text{CDCl}_3$ )  $\delta$  = 159.4 (2-PyrC-OCH<sub>3</sub>), 157.0 (6-PyrC-OCH<sub>3</sub>), 143.7 ( $\text{PhC}$ ), 142.0 ( $\text{PyrCH}$ ), 138.9 ( $\text{PhC}$ ), 136.3 ( $\text{PhC}$ ), 133.3 ( $\text{PhCH}$ ), 131.1 ( $\text{PhCH}$ ), 130.4 ( $\text{PhCH}$ ), 130.0 (m,  $\text{Ph}'\text{C}$ ), 128.7 ( $\text{PhCH}$ ), 128.5 ( $\text{PhCH}$ ), 128.11 (q,  $J$  = 5.3 Hz,  $\text{Ph}'\text{CH}$ ), 128.07 (q,  $J$  = 31.0 Hz,  $\text{Ph}'\text{C}$ ), 127.5 ( $\text{PhCH}$ ), 127.1 ( $\text{PhCH}$ ), 125.4 ( $\text{PhCH}$ ), 123.2 (q,  $J$  = 273.2,  $\text{Ph}'\text{-CF}_3$ ), 115.9 ( $\text{PyrC}$ ), 112.2 ( $\text{PyrC}$ ), 77.3 ( $\text{C-OH}$ ), 54.3 ( $\text{CH}_2\text{CH}_2\text{N}$ ), 53.8 (2-PyrOCH<sub>3</sub>), 53.4 (6-PyrOCH<sub>3</sub>), 53.1 ( $\text{Pyr-CH-Ph}$ ), 44.4 ( $\text{N}(\text{CH}_3)_2$ ), 42.0 ( $\text{N}(\text{CH}_3)_2$ ), 38.2 ( $\text{CH}_2\text{CH}_2\text{N}$ );

Analytical HPLC (254 nm):  $t_R$  = 8.8 min, 99%;

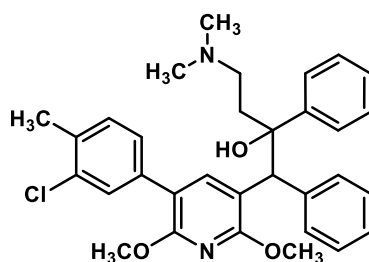
## Diastereomer B:

$^1\text{H}$  NMR (400 MHz,  $\text{CDCl}_3$ )  $\delta$  = 11.72 (br s, 1H,  $\text{NH}^+$ ), 7.85 – 7.79 (m, 2H,  $\text{PhH}$ ,  $\text{PyrH}$ ), 7.63 (dd,  $J$  = 8.3, 2.0 Hz, 1H,  $\text{PhH}$ ), 7.48 (d,  $J$  = 8.3 Hz, 1H,  $\text{PhH}$ ), 7.39 (d,  $J$  = 7.3 Hz, 2H,  $\text{PhH}$ ), 7.25 – 7.19 (m, 4H,  $\text{PhH}$ ), 7.14 (t,  $J$  = 7.3 Hz, 1H,  $\text{PhH}$ ), 7.06 – 6.95 (m, 3H,  $\text{PhH}$ ), 4.89 (s, 1H,  $\text{Pyr-CH-Ph}$ ), 4.08 (s, 3H, 2-PyrOCH<sub>3</sub>), 3.97 (s, 3H, 6-PyrOCH<sub>3</sub>), 3.32 – 3.18 (m, 1H,  $\text{CH}_2\text{CH}_2\text{N}$ ), 2.66 (br s, 3H,  $\text{N}(\text{CH}_3)_2$ ), 2.65 (br s, 3H,  $\text{N}(\text{CH}_3)_2$ ), 2.49 – 2.37 (m, 1H,  $\text{CH}_2\text{CH}_2\text{N}$ ), 2.35 – 2.19 (m, 2H,  $\text{CH}_2\text{CH}_2\text{N}$ );

$^{13}\text{C}$  NMR (101 MHz,  $\text{CDCl}_3$ )  $\delta$  = 159.8 (2-PyrC-OCH<sub>3</sub>), 158.1 (6-PyrC-OCH<sub>3</sub>), 143.2 ( $\text{PhC}$ ), 143.0 (4-PyrCH), 140.5 ( $\text{PhC}$ ), 136.0 ( $\text{PhC}$ ), 133.5 ( $\text{PhCH}$ ), 131.3 ( $\text{PhCH}$ ), 130.4 (m,  $\text{Ph}'\text{C}$ ), 129.9 ( $\text{PhCH}$ ), 128.4 ( $\text{PhCH}$ ), 128.3 (q,  $J$  = 5.4 Hz,  $\text{Ph}'\text{CH}$ ), 128.03 ( $\text{PhCH}$ ), 127.94 (q,  $J$  = 30.9 Hz,  $\text{Ph}'\text{C}$ ), 127.0 ( $\text{PhCH}$ ), 126.4 ( $\text{PhCH}$ ), 125.8 ( $\text{PhCH}$ ), 123.2 (q,  $J$  = 273.3,  $\text{Ph}'\text{-CF}_3$ ), 114.0 ( $\text{PyrC}$ ), 113.9 ( $\text{PyrC}$ ), 78.1 ( $\text{C-OH}$ ), 54.8 ( $\text{CH}_2\text{CH}_2\text{N}$ ), 54.1 (2-PyrOCH<sub>3</sub>), 53.7 (2-PyrOCH<sub>3</sub>), 53.3<sup>+</sup> ( $\text{Pyr-CH-Ph}$ ), 44.6 ( $\text{N}(\text{CH}_3)_2$ ), 42.1 ( $\text{N}(\text{CH}_3)_2$ ), 37.0 ( $\text{CH}_2\text{CH}_2\text{N}$ );

Analytical HPLC (254 nm):  $t_R$  = 8.9 min, 97%.

**1-(5-(3-chloro-4-methylphenyl)-2,6-dimethoxypyridin-3-yl)-4-(dimethylamino)-1,2-diphenylbutan-2-ol (**2.062**)**



General method A was used with 3-chloro-4-methylphenylboronic acid (70.2 mg, 0.412 mmol) to afford the title compound as a yellow foam (53.1 mg, 0.109 mmol, 51%, A:B = 56:44).

LR-MS (ESI+)  $m/z$ : 531.2  $[M+H]^+$ ;

HR-MS (ESI+)  $m/z$   $[M+H]^+$  calc'd 531.2409, found 531.2419;

Diastereomer A:

$^1\text{H}$  NMR (401 MHz,  $\text{CDCl}_3$ )  $\delta$  = 12.45 (br s, 1H,  $\text{NH}^+$ ), 8.10 (s, 1H, PyrH), 7.53 – 7.43 (m, 4H, PhH), 7.36 – 7.29 (m, 4H, PhH), 7.28 – 7.17 (m, 4H, PhH), 7.14 (tt,  $J$  = 7.3, 1 Hz, 1H, PhH), 4.72 (s, 1H, Pyr-CH-Ph), 3.79 (s, 3H, 2-PyrOCH<sub>3</sub>), 3.78 (s, 3H, 6-PyrOCH<sub>3</sub>), 3.20 – 3.09 (m, 1H, CH<sub>2</sub>CH<sub>2</sub>N), 2.59 (s, 3H, N(CH<sub>3</sub>)<sub>2</sub>), 2.57 (s, 3H, N(CH<sub>3</sub>)<sub>2</sub>), 2.39 (s, 3H, Ph-CH<sub>3</sub>), 2.36 – 2.25 (m, 2H, CH<sub>2</sub>CH<sub>2</sub>N), 2.23 – 2.12 (m, 1H, CH<sub>2</sub>CH<sub>2</sub>N);

$^{13}\text{C}$  NMR (101 MHz,  $\text{CDCl}_3$ )  $\delta$  = 158.7 (2-PyrC-OCH<sub>3</sub>), 157.1 (6-PyrC-OCH<sub>3</sub>), 143.6 (PhC), 142.2 (PyrCH), 139.2 (PhC), 136.4 (PhC), 134.2 (PhC), 134.1 (PhC), 130.6 (PhCH), 130.4 (PhCH), 129.5 (PhCH), 128.6 (PhCH), 128.4 (PhCH), 127.4 (PhCH), 127.3 (PhCH), 127.0 (PhCH), 125.5 (PhCH), 115.3 (PyrC), 113.6 (PyrC), 77.3 (C-OH), 54.4 (CH<sub>2</sub>CH<sub>2</sub>N), 53.7 (2-PyrOCH<sub>3</sub>), 53.5<sup>†</sup> (Pyr-CH-Ph), 53.3 (6-PyrOCH<sub>3</sub>), 44.1 (N(CH<sub>3</sub>)<sub>2</sub>), 42.01 (N(CH<sub>3</sub>)<sub>2</sub>), 38.0 (CH<sub>2</sub>CH<sub>2</sub>N), 19.9 (Ph-CH<sub>3</sub>);

Analytical HPLC (254 nm):  $t_R$  = 8.1 min, 100%;

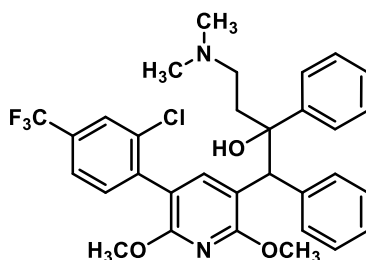
Diastereomer B:

$^1\text{H}$  NMR (400 MHz,  $\text{CDCl}_3$ )  $\delta$  = 12.48 (br s, 1H,  $\text{NH}^+$ ), 7.80 (s, 1H, PyrH), 7.49 (d,  $J$  = 1.6 Hz, 1H, PhH), 7.37 (d,  $J$  = 7.4 Hz, 2H, PhH), 7.31 (dd,  $J$  = 7.8, 1.7 Hz, 1H, PhH), 7.23 (d,  $J$  = 7.8 Hz, 3H, PhH), 7.20 – 7.11 (m,  $J$  = 15.9, 7.4 Hz, 3H, PhH), 7.06 – 6.96 (m, 3H, PhH), 4.85 (s, 1H, Pyr-CH-Ph), 4.07 (s, 3H, 2-PyrOCH<sub>3</sub>), 3.96 (s, 3H, 6-PyrOCH<sub>3</sub>), 3.20 (t,  $J$  = 11.3 Hz, 1H, CH<sub>2</sub>CH<sub>2</sub>N), 2.64 (s, 3H, N(CH<sub>3</sub>)<sub>2</sub>), 2.62 (s, 3H, N(CH<sub>3</sub>)<sub>2</sub>), 2.47 – 2.40 (m, 1H, CH<sub>2</sub>CH<sub>2</sub>N), 2.38 (s, 3H, Ph-CH<sub>3</sub>), 2.35 – 2.22 (m, 2H, CH<sub>2</sub>CH<sub>2</sub>N);

$^{13}\text{C}$  NMR (101 MHz,  $\text{CDCl}_3$ )  $\delta$  = 159.2 (2-PyrC-OCH<sub>3</sub>), 158.1 (6-PyrC-OCH<sub>3</sub>), 143.4 (PhC), 143.1 (PyrCH), 140.4 (PhC), 136.1 (PhC), 134.4 (PhC), 134.1 (PhC), 130.7 (PhCH), 129.9 (PhCH), 129.6 (PhCH), 128.3 (PhCH), 128.0 (PhCH), 127.5 (PhCH), 127.0 (PhCH), 126.3 (PhCH), 125.8 (PhCH), 115.1 (PyrC), 113.6 (PyrC), 78.1 (C-OH), 54.5 (CH<sub>2</sub>CH<sub>2</sub>N), 54.0 (2-PyrOCH<sub>3</sub>), 53.7 (6-PyrOCH<sub>3</sub>), 53.3 (Pyr-CH-Ph), 44.2 (N(CH<sub>3</sub>)<sub>2</sub>), 42.1 (N(CH<sub>3</sub>)<sub>2</sub>), 36.8 (CH<sub>2</sub>CH<sub>2</sub>N), 19.90 (Ph-CH<sub>3</sub>), missing 1 × CH peak (Pyr-CH-Ph);

Analytical HPLC (254 nm):  $t_R$  = 8.2 min, 97%.

**1-(5-(2-chloro-4-(trifluoromethyl)phenyl)-2,6-dimethoxypyridin-3-yl)-4-(dimethylamino)-1,2-diphenylbutan-2-ol (2.063)**



General method A was used with 2-chloro-4-trifluoromethylphenylboronic acid (92.4 mg, 0.412 mmol) to afford the title compound as an off-white foam (75.8 mg, 0.130 mmol, 63%, A:B = 72:28).

LR-MS (ESI+)  $m/z$ : 585.2  $[M+H]^+$ ;

HR-MS (ESI+)  $m/z$   $[M = C_{32}H_{32}ClF_3N_2O_3]$ :  $[M+H]^+$  calc'd 587.2113, found 587.2128;

Diastereomer A:

$^1H$  NMR (400 MHz,  $CDCl_3$ )  $\delta$  = 12.06 (br s, 1H,  $NH^+$ ), 8.02 (s, 1H, PyrH), 7.69 (d,  $J$  = 0.8 Hz, 1H, PhH), 7.54 – 7.40 (m, 5H, PhH), 7.33 (t,  $J$  = 7.4 Hz, 2H, PhH), 7.29 – 7.19 (m, 4H, PhH), 7.14 (t,  $J$  = 7.3 Hz, 1H, PhH), 4.75 (s, 1H, Pyr-CH-Ph), 3.80 (s, 3H, 2-PyrOCH<sub>3</sub>), 3.74 (s, 3H, 6-PyrOCH<sub>3</sub>), 3.19 – 3.05 (m, 1H, CH<sub>2</sub>CH<sub>2</sub>N), 2.61 (s, 3H, N(CH<sub>3</sub>)<sub>2</sub>), 2.58 (s, 3H, N(CH<sub>3</sub>)<sub>2</sub>), 2.38 – 2.24 (m, 2H, CH<sub>2</sub>CH<sub>2</sub>N), 2.24 – 2.09 (m, 1H, CH<sub>2</sub>CH<sub>2</sub>N);

$^{13}C$  NMR (101 MHz,  $CDCl_3$ )  $\delta$  = 159.6 (2-PyrC-OCH<sub>3</sub>), 157.3 (6-PyrC-OCH<sub>3</sub>), 143.4 (PhC), 142.8 (PyrCH), 140.2 (PhC), 139.1 (PhC), 134.9 (PhC), 132.6 (PhCH), 130.8 (q,  $J$  = 33.0 Hz, Ph'C-CF<sub>3</sub>), 130.4 (PhCH), 128.7 (PhCH), 128.3 (PhCH), 127.4 (PhCH), 127.0 (PhCH), 126.6 (q,  $J$  = 3.7 Hz, Ph'CH), 125.5 (PhCH), 123.6 (q,  $J$  = 272.5 Hz, Ph'-CF<sub>3</sub>), 123.4 (q,  $J$  = 3.5 Hz, Ph'CH), 114.9 (PyrC), 111.7 (PyrC), 77.5 (C-OH), 54.5 (CH<sub>2</sub>CH<sub>2</sub>N), 53.7 (2-PyrOCH<sub>3</sub>), 53.4 (6-PyrOCH<sub>3</sub>), 53.3 (Pyr-CH-Ph), 44.23 (N(CH<sub>3</sub>)<sub>2</sub>), 42.21 (N(CH<sub>3</sub>)<sub>2</sub>), 37.8 (CH<sub>2</sub>CH<sub>2</sub>N);

Analytical HPLC (254 nm):  $t_R$  = 7.8 min, 94%;

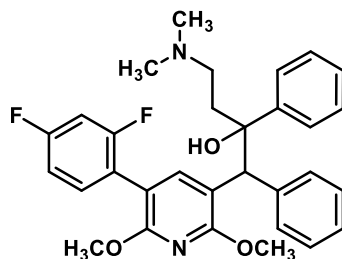
Diastereomer B:

$^1H$  NMR (400 MHz,  $CDCl_3$ )  $\delta$  = 12.19 (br s, 1H,  $NH^+$ ), 7.87 (s, 1H, 4-PyrH), 7.68 (s, 1H, PhH), 7.59 – 7.53 (m, 2H, PhH), 7.35 (d,  $J$  = 7.6 Hz, 2H, PhH), 7.27 – 7.21 (m, 2H, PhH), 7.17 – 7.11 (m, 3H, PhH), 7.06 – 6.95 (m, 3H, PhH), 4.90 (s, 1H, Pyr-CH-Ph), 4.07 (s, 3H, 2-PyrOCH<sub>3</sub>), 3.93 (s, 3H, 6-PyrOCH<sub>3</sub>), 3.17 (s, 1H, CH<sub>2</sub>CH<sub>2</sub>N), 2.66 (s, 6H, N(CH<sub>3</sub>)<sub>2</sub>), 2.49 – 2.29 (m, 3H, CH<sub>2</sub>CH<sub>2</sub>N);

$^{13}C$  NMR (101 MHz,  $CDCl_3$ )  $\delta$  = 160.2 (2-PyrC-OCH<sub>3</sub>), 158.2 (6-PyrC-OCH<sub>3</sub>), 143.7 (PyrCH), 143.3 (PhC), 140.0 (PhC), 139.8 (PhC), 134.6 (PhC), 133.1 (PhCH), 130.9 (q,  $J$  = 33.0 Hz, Ph'C-CF<sub>3</sub>), 130.0 (PhCH), 128.4 (PhCH), 128.0 (PhCH), 127.1 (PhCH), 126.7 (q,  $J$  = 3.6 Hz, PhCH), 126.4 (PhCH), 125.7 (PhCH), 123.62 (q,  $J$  = 272.2 Hz, Ph'-CF<sub>3</sub>), 123.55 (q,  $J$  = 3.5 Hz, Ph'CH), 113.3 (PyrC), 112.6 (PyrC), 78.3 (C-OH), 54.7 (CH<sub>2</sub>CH<sub>2</sub>N), 54.1 (2-PyrOCH<sub>3</sub>), 53.7 (6-PyrOCH<sub>3</sub>), 53.3† (Pyr-CH-Ph), 44.1 (N(CH<sub>3</sub>)<sub>2</sub>), 42.3 (N(CH<sub>3</sub>)<sub>2</sub>), 36.6 (CH<sub>2</sub>CH<sub>2</sub>N);

Analytical HPLC (254 nm):  $t_R$  = 7.9 min, 91%.

**1-(5-(2,4-difluorophenyl)-2,6-dimethoxypyridin-3-yl)-4-(dimethylamino)-1,2-diphenylbutan-2-ol**  
**(2.064)**



General method A was used with 2,4-difluorophenylboronic acid (65.1 mg, 0.412 mmol) to afford the title compound as a light-brown foam (69.9 mg, 0.135 mmol, 55%, A:B = 47:53).

LR-MS (ESI+)  $m/z$ : 518.9  $[M+H]^+$ ;

HR-MS (ESI+)  $m/z$   $[M = C_{31}H_{32}F_2N_2O_3]$ :  $[M+H]^+$  calc'd 519.2454, found 519.2458;

Diastereomer A:

$^1H$  NMR (400 MHz,  $CDCl_3$ )  $\delta$  = 12.60 (br s, 1H,  $NH^+$ ), 8.11 (s, 1H, PyrH), 7.47 (t,  $J$  = 7.2 Hz, 4H, PhH), 7.32 (t,  $J$  = 7.4 Hz, 2H, PhH), 7.29 – 7.21 (m, 3H, PhH), 7.17 – 7.09 (m, 2H, ArH), 6.86 (dtd,  $J$  = 12.0, 9.1, 2.6 Hz, 2H, PhH), 4.72 (s, 1H, Pyr-CH-Ph), 3.78 (s, 3H, 2-PyrOCH<sub>3</sub>), 3.74 (s, 3H, 6-PyrOCH<sub>3</sub>), 3.18 – 3.04 (m, 1H, CH<sub>2</sub>CH<sub>2</sub>N), 2.56 (br s, 6H, N(CH<sub>3</sub>)<sub>2</sub>), 2.34 – 2.22 (m, 2H, CH<sub>2</sub>CH<sub>2</sub>), 2.19 – 2.10 (m, 1H, CH<sub>2</sub>CH<sub>2</sub>N);

$^{13}C$  NMR (101 MHz,  $CDCl_3$ )  $\delta$  = 162.3 (dd,  $J$  = 247.8, 11.6 Hz, Ph'CF), 160.2 (dd,  $J$  = 250.5, 11.9 Hz, 2-Ph'CF), 159.2 (2-PyrC-OCH<sub>3</sub>), 157.6 (6-PyrC-OCH<sub>3</sub>), 143.5 (PhC), 143.2 (PyrCH), 139.2 (PhC), 132.6 (dd,  $J$  = 9.4, 5.1 Hz, Ph'CH), 130.4 (PhCH), 128.7 (PhCH), 128.3 (PhCH), 127.4 (PhCH), 126.9 (PhCH), 125.5 (Ph'CH), 121.1 (dd,  $J$  = 15.6, 3.7 Hz, Ph'C), 115.0 (PhC), 111.0 (dd,  $J$  = 21.0, 3.6 Hz, PhCH), 108.5 (PyrC), 104.0 (t,  $J$  = 25.9, PhCH), 77.6 (C-OH), 54.4 (CH<sub>2</sub>CH<sub>2</sub>N), 53.6 (2-PyrOCH<sub>3</sub>), 53.4 (6-PyrOCH<sub>3</sub>), 53.3<sup>†</sup> (Pyr-CH-Ph) 44.2 (N(CH<sub>3</sub>)<sub>2</sub>), 42.1 (N(CH<sub>3</sub>)<sub>2</sub>), 37.8 (CH<sub>2</sub>CH<sub>2</sub>N);

Analytical HPLC (254 nm):  $t_R$  = 7.3 min, 95%;

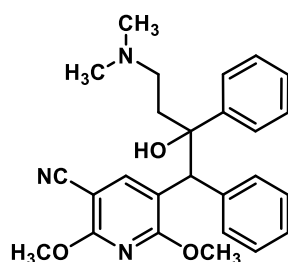
Diastereomer B:

$^1H$  NMR (400 MHz,  $CDCl_3$ )  $\delta$  = 12.16 (br s, 1H,  $NH^+$ ), 7.93 (s, 1H, PyrH), 7.44 (td,  $J$  = 8.6, 6.7 Hz, 1H, PhH), 7.34 (d,  $J$  = 7.4 Hz, 2H, PhH), 7.23 (d,  $J$  = 7.9 Hz, 2H, PhH), 7.15 (d,  $J$  = 7.3 Hz, 1H, PhH), 7.14 – 7.09 (m, 2H, PhH), 7.05 – 6.97 (m, 3H, PhH), 6.92 (td,  $J$  = 8.1, 1.9 Hz, 1H, PhH), 6.84 (ddd,  $J$  = 10.2, 9.1, 2.5 Hz, 1H, PhH), 4.86 (s, 1H, Pyr-CH-Ph), 4.04 (s, 3H, 2-PyrOCH<sub>3</sub>), 3.93 (s, 3H, 6-PyrOCH<sub>3</sub>), 3.21 – 3.07 (m, 1H, CH<sub>2</sub>CH<sub>2</sub>N), 2.65 (br s, 3H, N(CH<sub>3</sub>)<sub>2</sub>), 2.64 (br s, 3H, N(CH<sub>3</sub>)<sub>2</sub>), 2.44 – 2.30 (m, 3H, CH<sub>2</sub>CH<sub>2</sub>N);

$^{13}\text{C}$  NMR (101 MHz,  $\text{CDCl}_3$ )  $\delta$  = 162.4 (dd,  $J$  = 247.2, 11.9 Hz,  $\text{Ph}'\text{C}\text{F}$ ), 160.1 (dd,  $J$  = 249.1, 12.0 Hz, 2- $\text{Ph}'\text{C}\text{F}$ ), 159.8 (2-Pyr $\text{C}\text{-OCH}_3$ ), 158.5 (6-Pyr $\text{C}\text{-OCH}_3$ ), 143.8 (Pyr $\text{CH}$ ), 143.5 (Ph $\text{C}$ ), 139.9 (Ph $\text{C}$ ), 133.1 (dd,  $J$  = 9.4, 4.8 Hz,  $\text{Ph}'\text{CH}$ ), 129.9 (Ph $\text{CH}$ ), 128.4 (Ph $\text{CH}$ ), 128.0 (Ph $\text{CH}$ ), 127.1 (Ph $\text{CH}$ ), 126.4 (Ph $\text{CH}$ ), 125.7 (Ph $\text{CH}$ ), 113.4 (Pyr $\text{C}$ ), 111.2 (dd,  $J$  = 21.0, 3.6 Hz,  $\text{Ph}'\text{CH}$ ), 109.4 (Pyr $\text{C}$ ), 104.0 (t,  $J$  = 26.0 Hz,  $\text{Ph}'\text{CH}$ ), 78.3 ( $\text{C}\text{-OH}$ ), 54.6 ( $\text{CH}_2\text{CH}_2\text{N}$ ), 54.0 (2-Pyr $\text{OCH}_3$ ), 53.7 (2-Pyr $\text{OCH}_3$ ), 53.2 $^{\dagger}$  (Pyr- $\text{CH}\text{-Ph}$ ), 43.9 ( $\text{N}(\text{CH}_3)_2$ ), 42.4 ( $\text{N}(\text{CH}_3)_2$ ), 36.3 ( $\text{CH}_2\text{CH}_2\text{N}$ );

Analytical HPLC (254 nm):  $t_R$  = 7.4 min, 99%.

**5-(4-(dimethylamino)-2-hydroxy-1,2-diphenylbutyl)-2,6-dimethoxynicotinonitrile<sup>[8]</sup> (**2.065**)**



To an oven dried tube under nitrogen was added **2.044**,  $\text{Pd}_2(\text{dba})_3$  (9.43 mg, 5 mol%), X-Phos (9.82 mg, 10 mol%),  $\text{K}_4[\text{Fe}(\text{CN})_6]\cdot 3\text{H}_2\text{O}$  (43.5 mg, 0.103 mmol), dioxane (0.5 mL) and 0.05 M KOAc in degassed water (0.5 mL). The tube was then heated to 100 °C for 2 h. After this time the reaction mixture was cooled to room temperature, diluted with EtOAc and washed with brine. The layers were separated and the aqueous layer extracted with EtOAc ( $\times 2$ ) and the combined organic layers were dried over anhydrous  $\text{MgSO}_4$ , filtered, and concentrated under reduced pressure. Purification by silica gel flash chromatography (0–3% MeOH/0.1%  $\text{NH}_3$  in  $\text{CH}_2\text{Cl}_2$ ) afforded the title product as an orange-brown foam (88.0 mg, 0.204 mmol, 99%, A:B = 55:45).

A portion of this product was further subjected to purification by preparative HPLC to isolate the individual diastereomers as the TFA salt. This was performed using a gradient of 30 to 100% solvent B in solvent A over 12 min.

LR-MS (ESI $^+$ )  $m/z$ : 432.0  $[\text{M}+\text{H}]^+$ ;

HR-MS (ESI $^+$ )  $m/z$  [ $\text{M} = \text{C}_{26}\text{H}_{29}\text{N}_3\text{O}_3$ ]:  $[\text{M}+\text{H}]^+$  calc'd 432.2282, found 432.2289;

Diastereomer A:

$^1\text{H}$  NMR (400 MHz,  $\text{CDCl}_3$ )  $\delta$  = 12.51 (br s, 1H,  $\text{NH}^+$ ), 8.53 (s, 1H, Pyr $\text{H}$ ), 7.43 (t,  $J$  = 7.0 Hz, 4H, Ph $\text{H}$ ), 7.33 (t,  $J$  = 7.4 Hz, 2H, Ph $\text{H}$ ), 7.29 – 7.21 (m, 3H, Ph $\text{H}$ ), 7.13 (t,  $J$  = 7.3 Hz, 1H, Ph $\text{H}$ ), 4.65 (s, 1H, Pyr- $\text{CH}\text{-Ph}$ ), 3.83 (s, 3H, 6-Pyr $\text{OCH}_3$ ), 3.76 (s, 3H, 2-Pyr $\text{OCH}_3$ ), 3.22 – 3.10 (m, 1H,  $\text{CH}_2\text{CH}_2\text{N}$ ), 2.59 (s, 3H,  $\text{N}(\text{CH}_3)_2$ ), 2.56 (s, 3H,  $\text{N}(\text{CH}_3)_2$ ), 2.33 – 2.17 (m, 2H,  $\text{CH}_2\text{CH}_2\text{N}$ ), 2.11 – 2.00 (m, 1H,  $\text{CH}_2\text{CH}_2\text{N}$ );

$^{13}\text{C}$  NMR (101 MHz,  $\text{CDCl}_3$ )  $\delta$  = 162.6 (6-PyrC-OCH<sub>3</sub>), 162.4 (2-PyrC-OCH<sub>3</sub>), 144.5 (4-PyrCH), 143.1 (PhC), 138.2 (PhC), 130.2 (PhCH), 128.8 (PhCH), 128.5 (PhCH), 127.7 (PhCH), 127.1 (PhCH), 125.3 (PhCH), 116.67 (PyrC), 116.65 (PyrC), 86.4 (CN-Ph), 77.1 (C-OH), 54.3 (2-PyrOCH<sub>3</sub>), 54.09 (6-PyrOCH<sub>3</sub>), 54.07 (CH<sub>2</sub>CH<sub>2</sub>N), 52.3 (Pyr-CH-Ph), 44.4 (N(CH<sub>3</sub>)<sub>2</sub>), 41.8 (N(CH<sub>3</sub>)<sub>2</sub>), 38.0 (CH<sub>2</sub>CH<sub>2</sub>N);

Analytical HPLC (254 nm):  $t_R$  = 6.2 min, 96%;

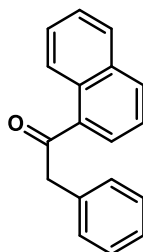
Diastereomer B:

$^1\text{H}$  NMR (400 MHz,  $\text{CDCl}_3$ )  $\delta$  = 11.87 (br s, 1H, NH<sup>+</sup>), 8.16 (s, 1H, PyrH), 7.37 – 7.30 (m, 2H, PhH), 7.23 (t,  $J$  = 7.6 Hz, 2H, PhH), 7.18 – 7.10 (m, 3H, PhH), 7.08 – 6.97 (m, 3H, PhH), 4.83 (s, 1H, Pyr-CH-Ph), 4.06 (s, 3H, 2-PyrOCH<sub>3</sub>), 4.02 (s, 3H, 6-PyrOCH<sub>3</sub>), 3.24 – 3.12 (m, 1H, CH<sub>2</sub>CH<sub>2</sub>N), 2.68 (s, 3H, N(CH<sub>3</sub>)<sub>2</sub>), 2.64 (s, 3H, N(CH<sub>3</sub>)<sub>2</sub>), 2.47 – 2.31 (m, 2H, CH<sub>2</sub>CH<sub>2</sub>N), 2.23 – 2.11 (m, 1H, CH<sub>2</sub>CH<sub>2</sub>N);

$^{13}\text{C}$  NMR (101 MHz,  $\text{CDCl}_3$ )  $\delta$  = 163.3 (6-PyrC-OCH<sub>3</sub>), 163.1 (2-PyrC-OCH<sub>3</sub>), 145.7 (PyrCH), 142.8 (PhC), 139.5 (PhC), 129.8 (PhCH), 128.5 (PhCH), 128.2 (PhCH), 127.2 (PhCH), 126.7 (PhCH), 125.6 (PhCH), 116.4 (PyrC), 115.2 (PyrC), 87.6 (CN-Ph), 78.2 (C-OH), 54.7 (2-PyrOCH<sub>3</sub>), 54.5 (CH<sub>2</sub>CH<sub>2</sub>N), 54.4 (6-PyrOCH<sub>3</sub>), 52.5 (Pyr-CH-Ph), 44.1 (N(CH<sub>3</sub>)<sub>2</sub>), 42.6 (N(CH<sub>3</sub>)<sub>2</sub>), 36.4 (CH<sub>2</sub>CH<sub>2</sub>N);

Analytical HPLC (254 nm):  $t_R$  = 6.4 min, 97%.

#### 1-(naphthalen-1-yl)-2-phenylethan-1-one<sup>[9]</sup> (**2.091**)



To an oven dried flask under nitrogen was added  $\text{Pd}(\text{OAc})_2$  (67.4 mg, 1.0 mol%),  $\text{P}(t\text{-Bu})_3\cdot\text{HBF}_4$  (174 mg, 2.0 mol%), sodium *tert*-butoxide (7.21 mg, 75.0 mmol) and THF (40 mL, anhydrous, degassed). After stirring for 5 min, iodobenzene (3.70 mL, 33.0 mmol) and 1-acetonaphthone (5.11 g, 30.0 mmol) were added, and the reaction mixture was stirred for 12 h at 60 °C. After this time, the reaction mixture was cooled to room temperature, diluted with EtOAc and filtered through a pad of Celite with the aid of EtOAc. The filtrate was washed with  $\text{NH}_4\text{Cl}$  (saturated, aqueous) and the organic phase extracted with EtOAc (x5). The combined organic layers were washed with brine, dried over anhydrous  $\text{MgSO}_4$ , filtered, and concentrated under reduced pressure. Purification by silica gel flash chromatography (0–10% EtOAc in Pet. Sp.) afforded the title compound which was further recrystallised from EtOH to give grey rocks (6.66 g, 27.1 mmol, 90%). Spectroscopic data are in agreement with the literature reported values.<sup>[9]</sup>

$^1\text{H}$  NMR (400 MHz,  $\text{CDCl}_3$ )  $\delta$  = 8.55 – 8.49 (m, 1H, Naph $\underline{\text{H}}$ ), 7.96 – 7.87 (m, 2H, Naph $\underline{\text{H}}$ ), 7.81 (dd,  $J$  = 8.3, 1.1 Hz, 1H, Naph $\underline{\text{H}}$ ), 7.56 – 7.40 (m, 3H, Naph $\underline{\text{H}}$ ), 7.31 – 7.17 (m, 5H, Ph $\underline{\text{H}}$ ), 4.33 (s, 2H, CH $\underline{2}$ );

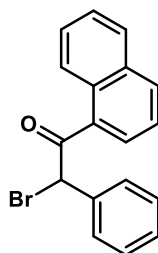
LR-MS (ESI+)  $m/z$ : 247.0  $[\text{M}+\text{H}]^+$ ;

HR-MS (ESI+)  $m/z$  [ $\text{M} = \text{C}_{18}\text{H}_{14}\text{O}$ ]:  $[\text{M}+\text{H}]^+$  calc'd 247.1117, found 247.1118;

Analytical HPLC (254 nm):  $t_R$  = 6.7 min, 97%;

MP: 65.3 – 67.8 °C.

**2-bromo-(naphthalen-1-yl)-2-phenylethan-1-one<sup>[9]</sup> (2.095)**

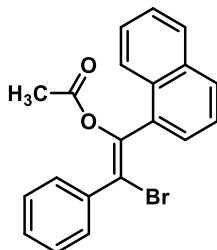


To a solution of ketone **2.091** (1.23 g, 5.0 mmol) in  $\text{CH}_2\text{Cl}_2$  (10 mL) was added a solution of  $\text{Br}_2$  (0.959 g, 6.0 mmol) in AcOH (30 mL), and the resultant mixture stirred for 16 h at room temperature. After this time, the volatiles were removed under reduced pressure and purification by silica gel column chromatography (1:1 PhMe/Pet. Sp.) afforded the title compound as a clear oil (1.38 g, 4.25 mmol, 85%). Spectroscopic data are in agreement with the literature reported values.<sup>[9]</sup>

$^1\text{H}$  NMR ( $\text{CDCl}_3$ )  $\delta$  = 8.43 (d,  $J$  = 8.2 Hz, 1H, Naph $\underline{\text{H}}$ ), 7.98 (d,  $J$  = 8.2 Hz, 1H, Naph $\underline{\text{H}}$ ), 7.86 (d,  $J$  = 8.2 Hz, 1H, Naph $\underline{\text{H}}$ ), 7.82 (d,  $J$  = 6.7 Hz, 1H, Naph $\underline{\text{H}}$ ), 7.52 – 7.62 (m, 4H, Naph $\underline{\text{H}}$ , Ph $\underline{\text{H}}$ ), 7.45 (t,  $J$  = 7.9 Hz, 1H, Naph $\underline{\text{H}}$ ), 7.30 – 7.39 (m, 3H, Ph $\underline{\text{H}}$ ), 6.39 (s, 1H, CH-Br);

LR-MS (ESI+)  $m/z$ : 325.0/327.0  $[\text{M}+\text{H}]^+$ .

**(E)-2-bromo-1-(naphthalen-1-yl)-2-phenylvinyl acetate<sup>[10]</sup> (2.096)**



To a solution of NaH (240 mg, 60% dispersion in oil, 6.00 mmol) in  $\text{Et}_2\text{O}$  (5 mL) was added MeOH (96.0 mg, 3.00 mmol, anhydrous) dropwise and the resultant mixture stirred for 30 min at room temperature. After this time, the reaction mixture was cooled to  $-10$  °C, and a solution of bromoketone **2.095** (976 mg, 3.00 mmol) in  $\text{Et}_2\text{O}$  (5 mL) was added dropwise. The reaction mixture

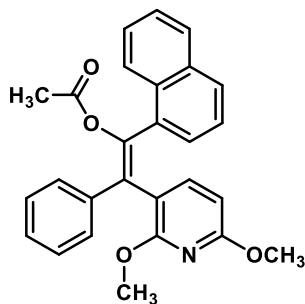


was stirred for 30 min at  $-10\text{ }^{\circ}\text{C}$ , after which time acetyl chloride (471 mg, 6.00 mmol) was added and stirring continued for an additional 10 min. The reaction mixture was filtered and the filtrate concentrated under reduced pressure. Purification by silica gel column chromatography (1:1 PhMe/Pet. Sp.) afforded the title compound as a clear oil (980 mg, 2.67 mmol, 89%). Spectroscopic data are in agreement with the literature reported values.<sup>[9]</sup>

$^1\text{H}$  NMR ( $\text{CDCl}_3$ )  $\delta$  = 8.05 (dd,  $J$  = 1.0 and 8.7 Hz, 1H, Naph $\underline{\text{H}}$ ), 7.71 – 7.73 (m, 1H, Naph $\underline{\text{H}}$ ), 7.66 (d,  $J$  = 8.2 Hz, 1H, Naph $\underline{\text{H}}$ ), 7.45 (ddd,  $J$  = 1.4, 6.8 and 8.4 Hz, 1H, Naph $\underline{\text{H}}$ ), 7.39 (ddd,  $J$  = 1.4, 6.8 and 8.0 Hz, 1H, Naph $\underline{\text{H}}$ ), 7.34 (dd,  $J$  = 1.2 and 7.1 Hz, 1H, Naph $\underline{\text{H}}$ ), 7.18 (dd,  $J$  = 7.1 and 8.2 Hz, 1H, Naph $\underline{\text{H}}$ ), 7.08 – 7.11 (m, 2H, Ph $\underline{\text{H}}$ ), 6.91 – 6.99 (m, 3H, Ph $\underline{\text{H}}$ ), 2.10 (s, 3H, COCH $\underline{\text{H}}$ );

LR-MS (ESI+)  $m/z$ : 389.0/391.0  $[\text{M}+\text{H}]^+$ .

**(Z)-2-(2,6-dimethoxypyridin-3-yl)-1-(naphthalen-1-yl)-2-phenylvinyl acetate (2.097)**



To a reaction tube under nitrogen was sequentially added  $\text{Pd}(\text{OAc})_2$  (102 mg, 5 mol%), XPhos (434 mg, 10 mol%),  $\text{K}_3\text{PO}_4$  (5.80 mg, 27.3 mmol), bromo-enol acetate **2.096** (3.35 g, 9.11 mmol) and PhMe (20 mL). After stirring for 5 min, 2,6-dimethoxy-3-pyridineboronic acid (5.00 g, 27.3 mmol) was added and the reaction mixture was stirred at reflux for 20 h. After this time, the reaction mixture was diluted with EtOAc and filtered through a pad of Celite with the aid of EtOAc. The filtrate was washed with  $\text{NH}_4\text{Cl}$  (saturated, aqueous) and the organic phase extracted with EtOAc ( $\times 2$ ). The combined organic layers were washed with brine, dried over anhydrous  $\text{MgSO}_4$ , filtered, and concentrated under reduced pressure. Purification by silica gel flash chromatography (0–30%  $\text{Et}_2\text{O}$  in Pet. Sp.) afforded the title compound as a pale-yellow solid (1.96 g, 4.60 mmol, 50%).

$^1\text{H}$  NMR (400 MHz,  $\text{CDCl}_3$ )  $\delta$  = 8.27 – 8.23 (m, 1H, Naph $\underline{\text{H}}$ ), 7.81 – 7.77 (m, 1H, Naph $\underline{\text{H}}$ ), 7.74 (d,  $J$  = 8.2 Hz, 1H, Naph $\underline{\text{H}}$ ), 7.55 – 7.50 (m, 2H, Naph $\underline{\text{H}}$ , 4-Pyr $\underline{\text{H}}$ ), 7.49 – 7.40 (m, 2H, Naph $\underline{\text{H}}$ ), 7.31 (dd,  $J$  = 8.2, 7.2 Hz, 1H, Naph $\underline{\text{H}}$ ), 6.96 – 6.89 (m, 5H, Ph $\underline{\text{H}}$ ), 6.35 (d,  $J$  = 8.0 Hz, 1H, 5-Pyr $\underline{\text{H}}$ ), 3.97 (s, 3H, PyrOCH $\underline{\text{H}}$ ), 3.91 (s, 3H, PyrOCH $\underline{\text{H}}$ ), 1.87 (s, 3H, C=OCH $\underline{\text{H}}$ );

$^{13}\text{C}$  NMR (101 MHz,  $\text{CDCl}_3$ )  $\delta$  = 169.2 ( $\text{C}=\text{O}$ ), 162.7 (Pyr $\underline{\text{C}}$ -OCH $\underline{\text{H}}$ ), 160.0 (Pyr $\underline{\text{C}}$ -OCH $\underline{\text{H}}$ ), 144.5 (Ar $\underline{\text{C}}$ ), 142.1 (4-Pyr $\underline{\text{CH}}$ ), 139.0 (Ar $\underline{\text{C}}$ ), 133.6 (Ar $\underline{\text{C}}$ ), 133.3 (Ar $\underline{\text{C}}$ ), 131.8 (Ar $\underline{\text{C}}$ ), 130.0 (Naph $\underline{\text{CH}}$ ), 129.5 (Ph $\underline{\text{CH}}$ ), 129.3

(ArC), 129.0 (NaphCH), 128.4 (NaphCH), 127.6 (PhCH), 126.8 (PhCH), 126.4 (NaphCH), 126.0 (NaphCH), 125.8 (NaphCH), 125.2 (NaphCH), 113.7 (3-PyrC), 100.6 (5-PyrCH), 53.7 (PyrOCH<sub>3</sub>), 53.63 (PyrOCH<sub>3</sub>), 20.9 (COCH<sub>3</sub>);

LR-MS (ESI+)  $m/z$ : 425.9 [M+H]<sup>+</sup>;

HR-MS (ESI+)  $m/z$  [M = C<sub>27</sub>H<sub>23</sub>NO<sub>4</sub>]: [M+H]<sup>+</sup> calc'd 426.1700, found 426.1710;

Analytical HPLC (254 nm):  $t_R$  = 8.4 min, 100%.

### 2,2',6,6'-tetramethoxy-3,3'-bipyridine (**2.098**)



This compound was isolated from the synthesis of **2.097** as yellow needles following recrystallisation from EtOH.

<sup>1</sup>H NMR (400 MHz, CDCl<sub>3</sub>)  $\delta$  = 7.52 (d,  $J$  = 8.0 Hz, 2H, 4-PyrH), 6.36 (d,  $J$  = 8.0 Hz, 2H, 5-PyrH), 3.95 (s, 6H, 2-PyrOCH<sub>3</sub>), 3.92 (s, 6H, 2-PyrOCH<sub>3</sub>);

<sup>13</sup>C NMR (101 MHz, CDCl<sub>3</sub>)  $\delta$  = 162.3 (6-PyrC), 159.8 (2-PyrC), 142.7 (4-PyrCH), 110.8 (3-PyrC), 100.6 (5-PyrCH), 53.7 (2-PyrOCH<sub>3</sub>), 53.56 (6-PyrOCH<sub>3</sub>);

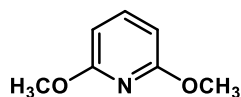
LR-MS (ESI+)  $m/z$ : 276.9 [M+H]<sup>+</sup>;

HR-MS (ESI+)  $m/z$  [M = C<sub>14</sub>H<sub>16</sub>N<sub>2</sub>O<sub>4</sub>]: [M+H]<sup>+</sup> calc'd 277.1183, found 277.1192;

Analytical HPLC (254 nm):  $t_R$  = 7.9 min, 100%;

MP: 143.9 – 145.3 °C.

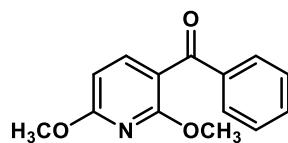
### 2,6-dimethoxypyridine (**2.037**)



This compound was isolated from the synthesis of **2.097** as a clear oil. Spectroscopic data are in agreement with the literature reported values.<sup>[11]</sup>

<sup>1</sup>H NMR (400 MHz, CDCl<sub>3</sub>)  $\delta$  = 7.48 (t,  $J$  = 7.9 Hz, 1H, 4-PyrH), 6.29 (d,  $J$  = 7.9 Hz, 2H, 3,4-PyrH), 3.91 (s, 6H, 2,6-PyrOCH<sub>3</sub>);

LR-MS (ESI+)  $m/z$ : mass not found.

**(2,6-dimethoxypyridin-3-yl)(phenyl)methanone (2.099)****Method 1**

To a solution of **2.097** (426 mg, 1.00 mmol) in EtOH (15 mL) was added a solution of NaOH (15 mL, 2 M aqueous, 30.0 mmol). The reaction was stirred at room temperature for 1 h. After this time the reaction mixture was extracted with CH<sub>2</sub>Cl<sub>2</sub> (×5), dried over anhydrous MgSO<sub>4</sub>, filtered, and concentrated under reduced pressure. Purification by silica gel flash chromatography (0–3% Et<sub>2</sub>O in PhMe) afforded the title compound as a light-brown solid (197 mg, 0.810 mmol, 81%). A portion of this product was further recrystallised from EtOH to give orange crystals.

**Method 2**

To a solution of **2.097** (426 mg, 1.00 mmol) in MeOH (5 mL) was added K<sub>2</sub>CO<sub>3</sub> (276 mg, 2.00 mmol). The reaction was stirred at room temperature for 15 min. After this time the reaction mixture was extracted with CH<sub>2</sub>Cl<sub>2</sub> (×5), dried over anhydrous MgSO<sub>4</sub>, filtered, and concentrated under reduced pressure to give the title compound.

<sup>1</sup>H NMR (400 MHz, CDCl<sub>3</sub>) δ = 7.79 – 7.73 (m, 3H, Ph<sub>H</sub>, 4-Pyr<sub>H</sub>), 7.53 (tt, *J* = 7.4, 1.3 Hz, 1H, Ph<sub>H</sub>), 7.45 – 7.40 (m, 2H, Ph<sub>H</sub>), 6.38 (d, *J* = 8.2 Hz, 1H, 5-Pyr<sub>H</sub>), 3.99 (s, 3H, 2-PyrOCH<sub>3</sub>), 3.87 (s, 3H, 6-PyrOCH<sub>3</sub>);

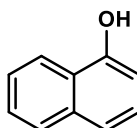
<sup>13</sup>C NMR (101 MHz, CDCl<sub>3</sub>) δ = 194.4 (C=O), 165.1 (2-PyrC), 161.7 (6-PyrC), 143.4 (4-PyrCH), 138.8 (PhC=O), 132.5 (PhCH), 129.62 (PhCH), 128.2 (PhCH), 113.7 (3-PyrC), 101.7 (5-PyrCH), 54.0 (2-PyrOCH<sub>3</sub>), 53.7 (6-PyrOCH<sub>3</sub>);

LR-MS (ESI+) *m/z*: 243.9 [M+H]<sup>+</sup>;

HR-MS (ESI+) *m/z* [M = C<sub>14</sub>H<sub>13</sub>NO<sub>3</sub>]: [M+H]<sup>+</sup> calc'd 244.0968, found 244.0973;

Analytical HPLC (254 nm): *t*<sub>R</sub> = 7.0 min, 100%,

MP: 92.1 – 93.1 °C.

**Naphthalen-1-ol (2.100)**

This compound was isolated from the synthesis of **2.099** (Method 2). The aqueous phase was acidified to pH 2, extracted with EtOAc (×3), dried over anhydrous MgSO<sub>4</sub>, filtered, and concentrated under reduced pressure. Recrystallisation from H<sub>2</sub>O gave the title compound as pearlescent purple flakes. Spectroscopic data are in agreement with the literature reported values.<sup>[12]</sup>

<sup>1</sup>H NMR (400 MHz, CDCl<sub>3</sub>) δ = 8.21 – 8.16 (m, 1H, H8), 7.86 – 7.79 (m, 1H, H5), 7.52 – 7.47 (m, 2H, H7, H8), 7.45 (d, *J* = 8.3 Hz, 1H, H4), 7.35 – 7.28 (m, 1H, H3), 6.82 (dd, *J* = 7.4, 0.9 Hz, 1H, H2), 5.25 (s, 1H, OH);

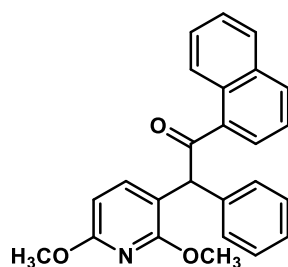
<sup>13</sup>C NMR (101 MHz, CDCl<sub>3</sub>) δ = 151.5 (NaphC-OH), 134.9 (NaphC), 127.8 (NaphCH), 126.6 (NaphCH), 126.0 (NaphCH), 125.4 (NaphCH), 124.5 (NaphC), 121.7 (NaphCH), 120.9 (NaphCH), 108.8 (NaphCH);

LR-MS (ESI+) *m/z*: mass not found;

Analytical HPLC (254 nm): *t*<sub>R</sub> = 5.8 min, 95%;

MP: 93.3 – 95.3 °C (lit. 93 – 95 °C)<sup>[13]</sup>.

**2-(2,6-dimethoxypyridin-3-yl)-1-(naphthalen-1-yl)-2-phenylethan-1-one<sup>[14]</sup> (**2.088**)**



To a stirred solution of **2.097** (1.87 g, 4.40 mmol) in MeOH (10 mL) and CH<sub>2</sub>Cl<sub>2</sub> (10 mL) was added acetyl chloride (0.940 mL, 13.2 mmol) dropwise. The reaction was stirred at room temperature until completion after 20 h. After this time, the reaction was quenched with a solution of NaHCO<sub>3</sub> (saturated, aqueous) and the aqueous layer separated and extracted with CH<sub>2</sub>Cl<sub>2</sub> (×3). The combined organic extracts were dried over anhydrous MgSO<sub>4</sub>, filtered and concentrated under reduced pressure. Purification by silica gel flash chromatography (0–5% Et<sub>2</sub>O in PhMe) afforded the title compound as a viscous orange oil (1.59 g, 4.15 mmol, 94%).

LR-MS (ESI+) *m/z*: 383.9 [M+H]<sup>+</sup>;

HR-MS (ESI+) *m/z* [M = C<sub>25</sub>H<sub>21</sub>NO<sub>3</sub>]: [M+H]<sup>+</sup> calc'd 384.1594, found 384.1607;

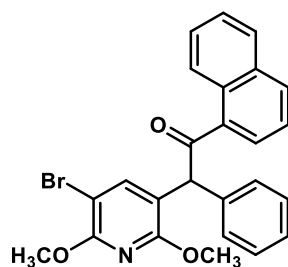
Analytical HPLC (254 nm): *t*<sub>R</sub> = 8.8 min, 95%;

<sup>1</sup>H NMR (400 MHz, CDCl<sub>3</sub>) δ = 8.61 (d, *J* = 8.3 Hz, 1H, NaphH), 8.04 (d, *J* = 7.2 Hz, 1H, ArCH), 7.95 (d, *J* = 8.2 Hz, 1H, ArCH), 7.86 (d, *J* = 7.9 Hz, 1H, ArCH), 7.62 – 7.55 (m, 1H, ArCH), 7.52 (t, *J* = 7.5 Hz, 1H, ArCH),

7.48 – 7.35 (m, 5H, ArCH), 7.31 (d,  $J = 7.1$  Hz, 1H, ArCH), 7.28 (d,  $J = 7.2$  Hz, 1H, 5-PyrCH), 6.29 (d,  $J = 8.1$  Hz, 1H, 4-PyrCH), 6.19 (s, 1H, Pyr-CH-Ph), 3.93 (s, 3H, 6-PyrOCH<sub>3</sub>), 3.91 (s, 3H, 3-PyrOCH<sub>3</sub>);

<sup>13</sup>C NMR (101 MHz, CDCl<sub>3</sub>)  $\delta = 202.3$  (C=O), 162.3 (6-PyrC-OCH<sub>3</sub>), 159.6 (2-PyrC-OCH<sub>3</sub>), 141.0 (5-PyrCH), 137.3 (PhC), 136.6 (NaphC), 134.1 (NaphC), 132.5 (ArCH), 130.7 (NaphC), 129.6 (ArCH), 129.1 (ArCH), 128.4 (ArCH), 127.8 (ArCH), 127.7 (ArCH), 127.5 (ArCH), 126.4 (ArCH), 126.0 (ArCH), 124.4 (ArCH), 114.3 (3-PyrC), 100.6 (4-PyrCH), 55.8 (Pyr-CH-Ph), 53.7 (2-PyrOCH<sub>3</sub>), 53.6 (6-PyrOCH<sub>3</sub>).

**2-(5-bromo-2,6-dimethoxypyridin-3-yl)-1-(naphthalen-1-yl)-2-phenylethan-1-one<sup>[2]</sup> (2.101)**



To a solution of **2.088** (1.59 g, 4.15 mmol) in MeCN (20 mL) was added *N*-bromosuccinimide (0.813 g, 4.57 mmol). The resulting mixture was stirred at reflux for 3 h. After this time, the solvent was evaporated under reduced pressure, and the residue purified by silica gel flash chromatography (0–30% Et<sub>2</sub>O in Pet. Sp.) to afford the title compound as a pale-yellow foam (1.52 g, 3.28 mmol, 79%).

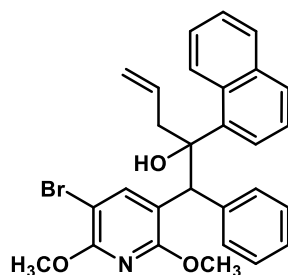
<sup>1</sup>H NMR (400 MHz, CDCl<sub>3</sub>)  $\delta = 8.56$  –  $8.53$  (m, 1H, NaphH), 7.98 (dd,  $J = 7.2, 1.2$  Hz, 1H, NaphH), 7.94 (d,  $J = 8.3$  Hz, 1H, NaphH), 7.87 – 7.82 (m, 1H, NaphH), 7.56 (ddd,  $J = 8.5, 6.8, 1.6$  Hz, 1H, NaphH), 7.51 (ddd,  $J = 8.1, 6.8, 1.4$  Hz, 1H, NaphH), 7.43 (dd,  $J = 8.2, 7.2$  Hz, 1H, NaphH), 7.42 – 7.33 (m, 5H, PyrH, 4 × PhH), 7.33 – 7.27 (m, 1H, PhH), 6.10 (s, 1H, Pyr-CH-Ph), 4.00 (s, 3H, 6-PyrOCH<sub>3</sub>), 3.88 (s, 3H, 2-PyrOCH<sub>3</sub>);

<sup>13</sup>C NMR (101 MHz, CDCl<sub>3</sub>)  $\delta = 201.7$  (C=O), 158.6 (2-PyrC-OCH<sub>3</sub>), 157.7 (6-PyrC-OCH<sub>3</sub>), 143.6 (PyrCH), 136.5 (PhC), 136.3 (NaphC), 134.1 (NaphC), 132.7 (NaphCH), 130.7 (NaphC), 129.6 (PhCH), 129.4 (PhCH), 128.5 (NaphCH), 128.0 (ArCH), 127.9 (ArCH), 127.8 (NaphCH), 126.5 (NaphCH), 125.9 (NaphCH), 124.4 (NaphCH), 116.2 (PyrC-CH-Ph), 95.5 (PyrC-Br), 55.7 (Pyr-CH-Ph), 54.5 (6-PyrOCH<sub>3</sub>), 54.0 (2-PyrOCH<sub>3</sub>);

LR-MS (ESI+)  $m/z$ : 461.8/463.7 [M+H]<sup>+</sup>;

HR-MS (ESI+)  $m/z$  [M = C<sub>25</sub>H<sub>20</sub>BrNO<sub>3</sub>]: [M+H]<sup>+</sup> calc'd 462.0699, found 462.0708;

Analytical HPLC (254 nm):  $t_R = 9.3$  min, 100%.

**1-(5-bromo-2,6-dimethoxypyridin-3-yl)-2-(naphthalen-1-yl)-1-phenylpent-4-en-2-ol<sup>[5]</sup> (2.102)****Step (i) – Preparation of allylzinc bromide:**

To an oven-dried reaction tube under nitrogen was added zinc powder (501 mg, 7.66 mmol), which was then heated to 70 °C. After 2 min, 1,2-dibromoethane (66  $\mu$ L, 0.766 mmol) in THF (1.3 mL, anhydrous) was added, and the temperature was maintained for 10 min. The reaction mixture was then cooled to room temperature, followed by the addition of trimethylsilyl chloride (70  $\mu$ L, 0.555 mmol) in THF (0.65 mL, anhydrous). The mixture was stirred at room temperature for 15 min. After this step, allyl bromide (0.551 mL, 6.38 mmol) in THF (3.2 mL, anhydrous) was added dropwise over 50 min to give a milky-white suspension.

**Step (ii) – Addition of allylzinc bromide:**

In an open atmosphere, compound **2.101** (2.36 g, 5.10 mmol) was added as a powder to the freshly prepared solution of allyl zinc bromide and stirred for 30 min at room temperature. After this time, the reaction was quenched by the addition of H<sub>2</sub>O, diluted with EtOAc, washed with a solution of NH<sub>4</sub>Cl (saturated, aqueous), and the aqueous layer extracted with EtOAc ( $\times 3$ ). The combined organic layers were washed with brine, dried over anhydrous MgSO<sub>4</sub>, filtered and concentrated under reduced pressure. Purification by silica gel flash chromatography (0–30% EtOAc in Pet. Sp.) afforded the title compound as a white foam (1.67 g, 3.31 mmol, 65%, A:B = 50:50).

**Diastereomer A:**

<sup>1</sup>H NMR (400 MHz, CDCl<sub>3</sub>)  $\delta$  = 8.51 (d,  $J$  = 8.6 Hz, 1H, Naph<sub>H</sub>), 8.29 (s, 1H, Pyr<sub>H</sub>), 7.82 (d,  $J$  = 8.3 Hz, 1H, Naph<sub>H</sub>), 7.77 – 7.68 (m, 3H, Naph<sub>H</sub>), 7.65 (d,  $J$  = 8.1 Hz, 1H, Naph<sub>H</sub>), 7.61 – 7.52 (m, 1H, Naph<sub>H</sub>), 7.5 – 7.3 (m, 6H, Naph<sub>H</sub>, Ph<sub>H</sub>), 5.55 (s, 1H, Pyr-CH-Ph), 5.19 – 5.00 (m, 1H, CH=CH<sub>2</sub>), 4.97 – 4.81 (m, 2H, CH=CH<sub>2</sub>), 3.70 (s, 3H, PyrOCH<sub>3</sub>), 3.53 (d,  $J$  = 13.9 Hz, 1H, C(OH)-CH<sub>2</sub>), 3.16 (s, 3H, PyrOCH<sub>3</sub>), 2.66 – 2.41 (m, 2H, C(OH)-CH<sub>2</sub>, OH);

<sup>13</sup>C NMR (101 MHz, CDCl<sub>3</sub>)  $\delta$  = 158.6 (PyrC-OCH<sub>3</sub>), 156.1 (PyrC-OCH<sub>3</sub>), 140.4 (PyrCH), 134.7 (ArC), 133.4 (CH=CH<sub>2</sub>), 131.1 (NaphCH), 129.6 (NaphCH), 128.35<sup>†</sup> (NaphCH), 128.34 (PhCH), 127.0 (PhCH), 126.4 (NaphCH), 125.07<sup>†</sup> (NaphCH), 125.10 (NaphCH), 124.9 (PhCH), 124.8 (NaphCH), 119.7 (CH=CH<sub>2</sub>), 94.7

(PyrC), 78.8 (C-OH), 54.0 (PyrOCH<sub>3</sub>), 53.1 (PyrOCH<sub>3</sub>), 50.5 (Pyr-CH-Ph), 45.5 (C(OH)-CH<sub>2</sub>), missing 4 × ArC;

Diastereomer B:

<sup>1</sup>H NMR (400 MHz, CDCl<sub>3</sub>) δ = 8.61 (d, *J* = 8.7 Hz, 1H, NaphH), 8.44 (s, 1H, PyrH), 7.85 (d, *J* = 8.1 Hz, 1H, NaphH), 7.64 (d, *J* = 8.1 Hz, 2H, NaphH), 7.55 (dd, *J* = 7.6, 1.3 Hz, 1H, NaphH), 7.48 (t, *J* = 7.5 Hz, 1H, NaphH), 7.25 (t, *J* = 7.7 Hz, 1H, NaphH), 7.00 (br s, 2H, PhH), 6.97 – 6.84 (m, 3H, PhH), 5.71 (s, 1H, Pyr-CH-Ph), 5.06 (br s, 1H, CH=CH<sub>2</sub>), 5.0 – 4.9 (m, 2H, CH=CH<sub>2</sub>), 4.08 (s, 3H, PyrOCH<sub>3</sub>), 4.03 (s, 3H, PyrOCH<sub>3</sub>), 3.56 (d, *J* = 13.9 Hz, 1H, C(OH)CH<sub>2</sub>), 2.59 (s, 1H, OH), 2.43 (t, *J* = 11.7 Hz, 1H, C(OH)CH<sub>2</sub>);

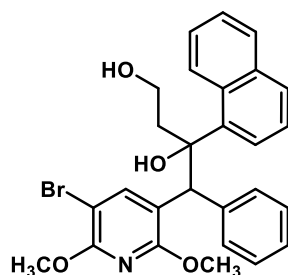
<sup>13</sup>C NMR (101 MHz, CDCl<sub>3</sub>) δ = 159.5 (PyrC-OCH<sub>3</sub>), 156.9 (PyrC-OCH<sub>3</sub>), 145.6 (PyrCH), 140.5 (ArC), 140.3 (ArC), 134.7 (ArC), 133.5 (CH=CH<sub>2</sub>), 129.9<sup>+</sup> (NaphCH), 129.8 (PhCH), 128.5 (NaphCH), 127.7 (PhCH), 126.4 (NaphCH), 126.2 (PhCH), 125.6 (NaphCH), 125.0<sup>+</sup> (NaphCH), 124.94 (NaphCH), 124.86 (NaphCH), 119.8 (CH=CH<sub>2</sub>), 116.7 (PyrC), 95.8 (PyrC), 79.1 (C-OH), 54.4 (PyrOCH<sub>3</sub>), 54.4 (PyrOCH<sub>3</sub>), 49.3 (Pyr-CH-Ph), 44.5 (C(OH)CH<sub>2</sub>), missing 1 × ArC;

LR-MS (ESI<sup>+</sup>) *m/z*: 503.9/505.9 [M+H]<sup>+</sup>;

HR-MS (ESI<sup>+</sup>) *m/z* [M = C<sub>28</sub>H<sub>26</sub>BrNO<sub>3</sub>]: [M+H]<sup>+</sup> calc'd 504.1169, found 504.1179;

Analytical HPLC (254 nm): *t<sub>R</sub>* = 8.6 min, 54% (A); 8.7 min, 46% (B).

#### 4-(5-bromo-2,6-dimethoxypyridin-3-yl)-3-(naphthalen-1-yl)-4-phenylbutane-1,3-diol<sup>[6]</sup> (**2.103**)



Step (i) – Oxidative cleavage:

To a stirred solution of **2.102** (1.18 g, 2.33 mmol) in MeCN (12.5 mL) was added RuCl<sub>3</sub> (19.3 mg, 4 mol%) and NaIO<sub>4</sub> (1.10 g, 5.12 mmol) at room temperature. Following this, water (1.25 mL) was added to the reaction mixture at a rate of 0.125 mL every 5 min. After 14 h, the reaction was quenched with a solution of Na<sub>2</sub>S<sub>2</sub>O<sub>3</sub> (saturated, aqueous), and the two layers were separated. The aqueous layer was extracted with EtOAc (×3), and the combined organic layers washed with brine, dried over anhydrous MgSO<sub>4</sub>, filtered, and concentrated under reduced pressure. The crude aldehyde product was isolated as a golden foam and was used in the next step without further purification.

## Step (ii) – Aldehyde reduction:

To an ice-cold solution of the crude aldehyde in MeOH (15 mL) was added NaBH<sub>4</sub> (0.176 g, 4.66 mmol) portion-wise. The reaction was warmed to room temperature and stirred 2 h. After this time, the solvent was removed under reduced pressure, and EtOAc added to the residue. The organic solution was washed with water, and the two layers separated. The aqueous layer was extracted with EtOAc (×3), and the combined organic layers were washed with brine, dried over anhydrous MgSO<sub>4</sub>, filtered, and concentrated under reduced pressure. Purification by silica gel flash chromatography (0–30% EtOAc in Pet. Sp.) afforded the title compound as a white foam (0.676 g, 57% over two steps, A:B = 50:50).

LR-MS (ESI+) *m/z*: 507.9/509.8 [M+H]<sup>+</sup>;

HR-MS (ESI+) *m/z* [M = C<sub>27</sub>H<sub>26</sub>BrNO<sub>4</sub>]: [M+H]<sup>+</sup> calc'd 508.1118, found 508.1126;

Analytical HPLC (254 nm): *t<sub>R</sub>* = 7.7 min, 55% (A); 7.9 min, 45% (B);

## Diastereomer A:

<sup>1</sup>H NMR (400 MHz, CDCl<sub>3</sub>) δ = 8.35 (d, *J* = 8.7 Hz, 1H, NaphH), 8.28 (s, 1H, PyrH), 7.94 (d, *J* = 7.4 Hz, 1H, NaphH), 7.82 (d, *J* = 8.1 Hz, 1H, NaphH), 7.74 (d, *J* = 7.5 Hz, 2H, NaphH), 7.66 (d, *J* = 8.1 Hz, 1H, NaphH), 7.53 (t, *J* = 7.6 Hz, 1H, NaphH), 7.48 – 7.27 (m, 5H, PhH), 5.44 (s, 1H, Pyr-CH-Ph), 4.31 (s, 1H, OH), 3.70 (s, 3H, PyrOCH<sub>3</sub>), 3.58 – 3.48 (m, 1H, CH<sub>2</sub>CH<sub>2</sub>OH), 3.27 – 3.15 (m, 1H, CH<sub>2</sub>CH<sub>2</sub>OH), 3.11 (s, 3H, PyrOCH<sub>3</sub>), 2.70 (br d, *J* = 15.1 Hz, 1H, CH<sub>2</sub>CH<sub>2</sub>OH), 2.28 (ddd, *J* = 15.3, 11.2, 4.4 Hz, 1H, CH<sub>2</sub>CH<sub>2</sub>OH), 2.1 – 1.4 (br s, 2H, OH);

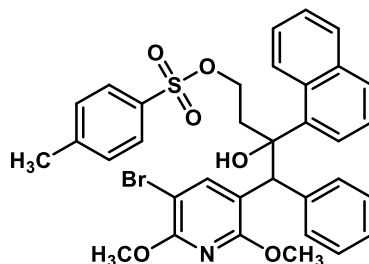
<sup>13</sup>C NMR (101 MHz, CDCl<sub>3</sub>) δ = 158.6 (PyrC-OCH<sub>3</sub>), 156.1 (PyrC-OCH<sub>3</sub>), 144.8 (PyrCH), 140.7 (ArC), 140.3 (ArC), 134.7 (ArC), 131.1 (ArCH), 129.7 (ArCH), 128.5 (ArCH), 128.4 (ArCH), 127.0 (ArCH), 126.8 (ArCH), 125.3 (ArCH), 125.2 (ArCH), 125.1 (ArCH), 124.7 (ArCH), 116.9 (PyrC), 94.7 (PyrC), 77.3<sup>†</sup> (C-OH) 60.7 (CH<sub>2</sub>CH<sub>2</sub>OH), 53.9 (PyrCH<sub>3</sub>), 53.1 (PyrCH<sub>3</sub>), 51.0 (Pyr-CH-Ph), 41.0 (CH<sub>2</sub>CH<sub>2</sub>OH), missing 1 × ArC;

## Diastereomer B:

<sup>1</sup>H NMR (400 MHz, CDCl<sub>3</sub>) δ = 8.56 (s, 1H, PyrH), 8.45 (d, *J* = 8.7 Hz, 1H, NaphH), 7.87 (d, *J* = 8.1 Hz, 1H, NaphH), 7.74 (d, *J* = 7.4 Hz, 1H, NaphH), 7.67 (d, *J* = 8.1 Hz, 1H, NaphH), 7.62 – 7.27 (m, 3H, NaphH), 7.01 – 6.94 (m, 2H, PhH), 6.94 – 6.85 (m, 3H, PhH), 5.62 (s, 1H, Pyr-CH-Ph), 4.27 (s, 1H, OH), 4.05 (s, 3H, PyrOCH<sub>3</sub>), 4.02 (s, 3H, PyrOCH<sub>3</sub>), 3.58 – 3.48 (m, 1H, CH<sub>2</sub>CH<sub>2</sub>OH), 3.27 – 3.15 (m, 1H, CH<sub>2</sub>CH<sub>2</sub>OH), 2.72 (br d, *J* = 15.2 Hz, 1H, CH<sub>2</sub>CH<sub>2</sub>OH), 2.34 – 2.19 (m, 1H, CH<sub>2</sub>CH<sub>2</sub>OH) 1.61 (s, 1H, OH).



**1-(5-bromo-2,6-dimethoxypyridin-3-yl)-2-(naphthalen-1-yl)-1-phenyl-4-(p-tolyloxy)butan-2-ol**  
**(2.104)**



To an ice-cold solution of **2.103** (0.676 g, 1.33 mmol) in  $\text{CH}_2\text{Cl}_2$  (10 mL) was added  $\text{Et}_3\text{N}$  (0.370 mL, 2.66 mmol), followed by the portion-wise addition of *p*-toluenesulfonyl chloride (2.53 g, 13.3 mmol). After stirring for a total of 63 h at room temperature, water was added to quench the reaction and the organic layer separated. The aqueous layer was extracted with  $\text{CH}_2\text{Cl}_2$  (x3) and the combined organic extracts were dried over anhydrous  $\text{MgSO}_4$ , filtered and concentrated under reduced pressure. Purification by silica gel flash chromatography (0–40% EtOAc in Pet. Sp.) afforded the title compound as an off-white foam (3.08 g, 5.03 mmol, 69%, A:B = 50:50).

LR-MS (ESI+)  $m/z$ : 661.9/663.8  $[\text{M}+\text{H}]^+$ ;

HR-MS (ESI+)  $m/z$   $[\text{M} = \text{C}_{34}\text{H}_{32}\text{BrNO}_6\text{S}]$ :  $[\text{M}+\text{H}]^+$  calc'd 662.1206, found 662.1219;

Analytical HPLC (254 nm):  $t_R$  = 7.7 min, 53% (A); 7.9 min, 41% (B);

Diastereomer A:

$^1\text{H}$  NMR (400 MHz,  $\text{CDCl}_3$ )  $\delta$  = 8.22 (s, 1H, Naph $\underline{\text{H}}$ ), 8.10 (s, 1H, Pyr $\underline{\text{H}}$ ), 7.78 (d,  $J$  = 8.0 Hz, 1H, Naph $\underline{\text{H}}$ ), 7.74 – 7.68 (m, 1H, Naph $\underline{\text{H}}$ ), 7.64 – 7.55 (m, 3H, Ar $\underline{\text{H}}$ ), 7.48 (d,  $J$  = 8.0 Hz, 1H, Ar $\underline{\text{H}}$ ), 7.46 – 7.34 (m, 5H, Ar $\underline{\text{H}}$ ), 7.31 (t,  $J$  = 7.3 Hz, 1H, Ar $\underline{\text{H}}$ ), 7.28 – 7.22 (m, 1H, Ar $\underline{\text{H}}$ ), 7.12 (d,  $J$  = 8.0 Hz, 2H, Ar $\underline{\text{H}}$ ), 5.41 (s, 1H, Pyr- $\underline{\text{CH}}$ -Ph), 3.82 – 3.53 (m, 5H, PyrO $\underline{\text{CH}}_3$ ,  $\text{CH}_2\text{CH}_2\text{OTs}$ ), 3.19 (s, 3H, PyrO $\underline{\text{CH}}_3$ ), 2.99 – 2.87 (m, 1H,  $\text{CH}_2\text{CH}_2\text{OTs}$ ), 2.72 ( $\underline{\text{OH}}$ ), 2.39 (s, 3H, Ph'- $\underline{\text{CH}}_3$ ), 2.27 (dt,  $J$  = 15.0, 7.6 Hz, 1H,  $\text{CH}_2\text{CH}_2\text{OTs}$ );

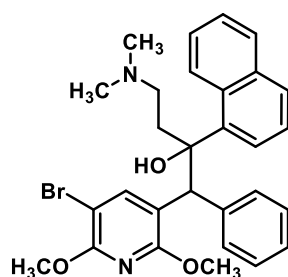
$^{13}\text{C}$  NMR (101 MHz,  $\text{CDCl}_3$ )  $\delta$  = 158.5 (Pyr $\underline{\text{C}}$ -O $\underline{\text{CH}}_3$ ), 156.3 (Pyr $\underline{\text{C}}$ -O $\underline{\text{CH}}_3$ ), 144.7 (Ar $\underline{\text{C}}$ ), 144.4 (Pyr $\underline{\text{CH}}$ ), 139.3 (Ar $\underline{\text{C}}$ ), 138.0 (Ar $\underline{\text{C}}$ ), 134.5 (Ar $\underline{\text{C}}$ ), 132.6 (Ar $\underline{\text{C}}$ ), 130.9 (Ar $\underline{\text{CH}}$ ), 129.8 (Ar $\underline{\text{CH}}$ ), 129.7 $^\dagger$  (Ar $\underline{\text{CH}}$ ), 128.8 (Ar $\underline{\text{CH}}$ ), 128.8 (Ar $\underline{\text{CH}}$ ), 127.8 (Ar $\underline{\text{CH}}$ ), 127.5 (Ar $\underline{\text{CH}}$ ), 126.3 (Ar $\underline{\text{CH}}$ ), 125.6 (Ar $\underline{\text{CH}}$ ), 125.0 (Ar $\underline{\text{CH}}$ ), 124.9 (Ar $\underline{\text{CH}}$ ), 124.4 (Ar $\underline{\text{CH}}$ ), 94.6 $^\dagger$  (Pyr $\underline{\text{C}}$ ), 78.5 $^\dagger$  ( $\underline{\text{C}}$ -OH), 68.0 ( $\text{CH}_2\text{CH}_2\text{OTs}$ ), 54.0 (PyrO $\underline{\text{CH}}_3$ ), 53.3 (PyrO $\underline{\text{CH}}_3$ ), 51.4 (Pyr- $\underline{\text{CH}}$ -Ph), 39.8 ( $\text{CH}_2\text{CH}_2\text{OTs}$ ), 21.8 (Ph'- $\underline{\text{CH}}_3$ );

$^1\text{H}$  NMR (400 MHz,  $\text{CDCl}_3$ )  $\delta$  = 8.38 (s, 1H, Pyr $\underline{\text{H}}$ ), 8.33 (d,  $J$  = 8.9 Hz, 1H, Naph $\underline{\text{H}}$ ), 7.85 (d,  $J$  = 8.1 Hz, 1H, Naph $\underline{\text{H}}$ ), 7.64 (d,  $J$  = 8.1 Hz, 1H, Naph $\underline{\text{H}}$ ), 7.61 – 7.53 (m, 1H, Naph $\underline{\text{H}}$ ), 7.49 (t,  $J$  = 7.3 Hz, 1H, Naph $\underline{\text{H}}$ ), 7.46 – 7.41 (m, 2H, Ph' $\underline{\text{H}}$ ), 7.41 – 7.35 (m, 1H, Naph $\underline{\text{H}}$ ), 7.21 – 7.09 (m, 3H, Ph' $\underline{\text{H}}$ , Naph $\underline{\text{H}}$ ), 6.96 – 6.86 (m, 3H, Ph' $\underline{\text{H}}$ ), 6.86 – 6.76 (m, 2H, Ph' $\underline{\text{H}}$ ), 5.60 (s, 1H, Pyr- $\underline{\text{CH}}$ -Ph), 4.03 (s, 6H, PyrO $\underline{\text{CH}}_3$ ), 3.79 – 3.67 (m,

$^1\text{H}$ ,  $\text{CH}_2\text{CH}_2\text{OTs}$ ), 3.60 (br s, 1H,  $\text{CH}_2\text{CH}_2\text{OTs}$ ), 3.02 – 2.61 (m, 2H,  $\text{CH}_2\text{CH}_2\text{OTs}$ , OH), 2.39 (s, 3H,  $\text{Ph}'\text{-CH}_3$ ), 2.27 (dt,  $J = 15.3$ , 7.8 Hz, 1H,  $\text{CH}_2\text{CH}_2\text{OTs}$ );

$^{13}\text{C}$  NMR (101 MHz,  $\text{CDCl}_3$ )  $\delta = 159.5$  (PyrC-OCH<sub>3</sub>), 157.3 (PyrC-OCH<sub>3</sub>), 145.3 (PyrCH), 144.7 (ArC), 138.7 (ArC), 134.6 (ArC), 132.7 (ArC), 130.1 (NaphCH), 129.8 (Ph'CH), 129.6 (PhCH), 128.9 (NaphH), 127.82 (PhCH), 127.80 (Ph'CH), 126.6 (PhCH), 126.09 (NaphCH), 126.05<sup>†</sup> (NaphCH), 125.12 (NaphCH), 125.07<sup>†</sup> (NaphCH), 124.4 (NaphCH), 115.6 (ArC), 96.0 (ArC), 79.5<sup>†</sup> (C-OH), 68.1 ( $\text{CH}_2\text{CH}_2\text{OTs}$ ), 54.5 (PyrOCH<sub>3</sub>), 54.4 (PyrOCH<sub>3</sub>), 50.2<sup>†</sup> (Pyr-CH-Ph), 38.5 ( $\text{CH}_2\text{CH}_2\text{OTs}$ ), 21.8 ( $\text{Ph}'\text{-CH}_3$ ), missing 2  $\times$  ArC.

**1-(5-bromo-2,6-dimethoxy-pyridin-3-yl)-4-(dimethylamino)-2-(naphthalen-1-yl)-1-phenylbutan-2-ol<sup>[7]</sup> (2.105)**



To a flask containing **2.104** (1.59 g, 2.40 mmol) was added a solution of  $\text{Me}_2\text{NH}$  (18.0 mL, 2.0 M in THF, 36.1 mmol) and the reaction mixture was stirred at 60 °C for 34 h. After this time, the remaining  $\text{Me}_2\text{NH}$  and THF were removed under reduced pressure. Purification by silica gel flash chromatography (0–5% MeOH in  $\text{CH}_2\text{Cl}_2$ ) afforded the title compound as an off-white foam (1.12 g, 90%, A:B = 52:48).

A portion of this product was further subjected to purification by preparative HPLC to isolate the individual diastereomers as the TFA salt. This was performed using a gradient of 30 to 100% solvent B in solvent A over 12 min.

LR-MS (ESI+)  $m/z$ : 534.9/536.9  $[\text{M}+\text{H}]^+$ ;

HR-MS (ESI+)  $m/z$   $[\text{M} = \text{C}_{29}\text{H}_{31}\text{BrN}_2\text{O}_3]$ :  $[\text{M}+\text{H}]^+$  calc'd 535.1591, found 535.1607;

Analytical HPLC (254 nm):  $t_R = 6.7$  min, 54% (A); 6.9 min, 45% (B);

$^1\text{H}$  NMR (400 MHz,  $\text{CDCl}_3$ )  $\delta = 11.88$  (br s, 1H,  $\text{NH}^+$ ), 8.37 (d,  $J = 8.8$  Hz, 1H, NaphH), 8.23 (s, 1H, PyrH), 8.00 (d,  $J = 7.4$  Hz, 1H, NaphH), 7.83 (d,  $J = 8.0$  Hz, 1H, NaphH), 7.67 (d,  $J = 8.0$  Hz, 1H, NaphH), 7.64 – 7.52 (m, 3H, PhH, NaphH), 7.46 (t,  $J = 7.4$  Hz, 1H, NaphH), 7.42 – 7.35 (m, 3H, PhH, NaphH), 7.30 (t,  $J = 7.3$  Hz, 1H, PhH), 5.47 (s, 1H, Pyr-CH-Ph), 3.68 (s, 3H, 6-PyrOCH<sub>3</sub>), 3.28 (s, 3H, 2-PyrOCH<sub>3</sub>), 3.14 (t,  $J = 11.7$  Hz, 1H,  $\text{CH}_2\text{CH}_2\text{N}$ ), 3.02 (td,  $J = 12.3$ , 11.7, 5.5 Hz, 1H,  $\text{CH}_2\text{CH}_2\text{N}$ ), 2.54 (s, 6H,  $\text{N}(\text{CH}_3)_2$ ), 2.49 (s, 3H,  $\text{N}(\text{CH}_3)_2$ ), 2.30 (t,  $J = 11.2$  Hz, 1H,  $\text{CH}_2\text{CH}_2\text{N}$ ), 2.13 – 1.98 (m, 2H,  $\text{CH}_2\text{CH}_2\text{N}$ );

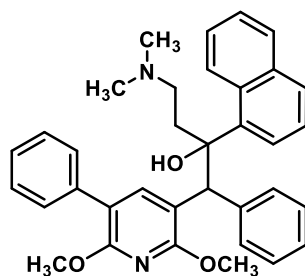
$^{13}\text{C}$  NMR (101 MHz,  $\text{CDCl}_3$ )  $\delta$  = 158.4 (2-PyrC-OCH<sub>3</sub>), 156.2 (6-PyrC-OCH<sub>3</sub>), 144.4 (PyrCH), 138.8 (PhC), 137.8 (NaphC), 134.6 (NaphC), 130.7 (PhCH), 130.0 (NaphCH), 129.4 (NaphC), 129.0 (PhCH), 128.9 (NaphCH), 127.7 (PhCH), 127.2 (NaphCH), 125.8 (NaphCH), 125.2 (NaphCH), 125.1 (NaphCH), 123.8 (NaphCH), 116.1 (3-PyrC), 94.8 (5-PyrC), 77.7 (C-OH), 54.7 (CH<sub>2</sub>CH<sub>2</sub>N), 54.0 (6-PyrOCH<sub>3</sub>), 53.3 (2-PyrOCH<sub>3</sub>), 51.5 (Pyr-CH-Ph), 44.6 (N(CH<sub>3</sub>)<sub>2</sub>), 41.8 (N(CH<sub>3</sub>)<sub>2</sub>), 35.5 (CH<sub>2</sub>CH<sub>2</sub>N);

Diastereomer B:

$^1\text{H}$  NMR (400 MHz,  $\text{CDCl}_3$ )  $\delta$  = 12.84 (br s, 1H, NH<sup>+</sup>), 8.44 (d,  $J$  = 8.8 Hz, 1H, NaphH), 8.23 (s, 1H, NaphH), 7.86 (d,  $J$  = 8.1 Hz, 1H, NaphH), 7.78 (d,  $J$  = 7.4 Hz, 1H, NaphH), 7.70 – 7.59 (m, 2H, NaphH), 7.53 – 7.47 (m, 1H, NaphH), 7.32 – 7.27 (m, 1H, NaphH), 7.06 – 6.94 (m, 2H, PhH), 6.97 – 6.86 (m, 3H, PhH), 5.61 (s, 1H, Pyr-CH-Ph), 4.10 (s, 3H, PyrOCH<sub>3</sub>), 4.02 (s, 3H, PyrOCH<sub>3</sub>), 3.19 – 2.95 (m, 2H, CH<sub>2</sub>CH<sub>2</sub>N), 2.66 – 2.38 (m, 6H, N(CH<sub>3</sub>)<sub>2</sub>), 2.39 – 2.17 (m, 1H, CH<sub>2</sub>CH<sub>2</sub>N), 2.15 – 1.96 (m, 1H, CH<sub>2</sub>CH<sub>2</sub>N);

$^{13}\text{C}$  NMR (101 MHz,  $\text{CDCl}_3$ )  $\delta$  = 159.3 (PyrC-OCH<sub>3</sub>), 157.3 (PyrC-OCH<sub>3</sub>), 145.6 (PyrCH), 139.9 (ArC), 138.2 (ArC), 134.6 (ArC), 130.2 (NaphCH), 129.7 (PhCH), 129.3 (ArC), 128.9 (NaphCH), 127.7 (PhCH), 127.2 (NaphCH), 126.4 (PhCH), 126.2 (NaphCH), 125.2 (NaphCH), 125.1 (NaphCH), 123.6 (NaphCH), 115.2 (PyrC), 96.3 (PyrC), 78.4 (C-OH), 54.6 (CH<sub>2</sub>CH<sub>2</sub>N), 54.3 (PyrOCH<sub>3</sub>), 54.3 (PyrOCH<sub>3</sub>), 50.6 (Pyr-CH-Ph), 44.3<sup>+</sup> (N(CH<sub>3</sub>)<sub>2</sub>), 41.8<sup>+</sup> (N(CH<sub>3</sub>)<sub>2</sub>), 34.3 (CH<sub>2</sub>CH<sub>2</sub>N).

**1-(2,6-dimethoxy-5-phenylpyridin-3-yl)-4-(dimethylamino)-2-(naphthalen-1-yl)-1-phenylbutan-2-ol**  
(**2.106**)



General method B was used with phenylboronic acid (61.0 mg, 0.5 mmol) to afford the title compound as pale-yellow foam (94.2 mg, 0.195 mmol, 71%, A:B = 52:48).

LR-MS (ESI<sup>+</sup>)  $m/z$ : 533.1 [M+H]<sup>+</sup>;

HR-MS (ESI<sup>+</sup>)  $m/z$  [M = C<sub>35</sub>H<sub>36</sub>N<sub>2</sub>O<sub>3</sub>]: [M+H]<sup>+</sup> calc'd 533.2799, found 533.2807;

Diastereomer A:

$^1\text{H}$  NMR (400 MHz,  $\text{CDCl}_3$ )  $\delta$  = 11.23 (br s, 1H, NH<sup>+</sup>), 8.42 (d,  $J$  = 8.6 Hz, 1H, NaphH), 8.06 (d,  $J$  = 7.3 Hz, 1H, NaphH), 7.87 (br s, 1H, PyrCH), 7.83 (d,  $J$  = 8.0 Hz, 1H, NaphH), 7.68 (d,  $J$  = 8.0 Hz, 1H, NaphH), 7.61 (m, 3H, ArH), 7.51 – 7.19 (m, 9H, ArCH), 5.52 (s, 1H, Pyr-CH-Ph), 3.67 (s, 3H, 6-PyrOCH<sub>3</sub>), 3.52 (s, 3H,

2-PyrOCH<sub>3</sub>), 3.25 – 2.90 (m, 2H, CH<sub>2</sub>CH<sub>2</sub>N), 2.58 (s, 3H, N(CH<sub>3</sub>)<sub>2</sub>), 2.51 (s, 3H, N(CH<sub>3</sub>)<sub>2</sub>), 2.47 – 2.37 (m, 1H, CH<sub>2</sub>CH<sub>2</sub>N), 2.26 – 2.12 (m, 2H, CH<sub>2</sub>CH<sub>2</sub>N);

<sup>13</sup>C NMR (101 MHz, CDCl<sub>3</sub>) δ = 158.2 (2-PyrC-OCH<sub>3</sub>), 157.2 (6-PyrC-OCH<sub>3</sub>), 142.7 (PyrCH), 139.0 (ArC), 138.3 (ArC), 137.0 (ArC), 134.7 (NaphC), 130.8 (ArCH), 130.1 (ArCH), 129.5 (NaphC), 129.2 (NaphCH), 129.1 (ArCH), 128.8 (ArCH), 128.1 (ArCH), 127.7 (ArCH), 127.6 (ArCH), 126.7 (ArCH), 126.6 (NaphCH), 126.0 (ArCH), 125.2 (ArCH), 125.0 (ArCH), 124.1 (NaphCH), 114.9 (5-PyrC), 114.2 (3-PyrC), 78.2 (C-OH), 55.2 (CH<sub>2</sub>CH<sub>2</sub>N), 53.3 (2-PyrOCH<sub>3</sub>), 53.10 (6-PyrOCH<sub>3</sub>), 53.06<sup>†</sup> (PyrCH-Ph), 44.4 (N(CH<sub>3</sub>)<sub>2</sub>), 42.3 (N(CH<sub>3</sub>)<sub>2</sub>), 35.2 (CH<sub>2</sub>CH<sub>2</sub>N);

Analytical HPLC (254 nm): *t*<sub>R</sub> = 7.0 min, 95%;

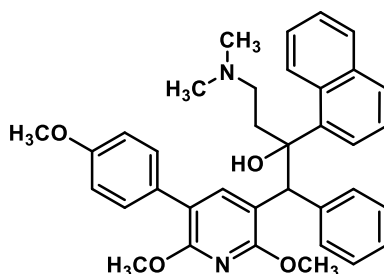
Diastereomer B:

<sup>1</sup>H NMR (400 MHz, CDCl<sub>3</sub>) δ = 11.51 (br s, 1H, NH<sup>+</sup>), 8.49 (d, *J* = 8.7 Hz, 1H, NaphH), 8.10 (s, 1H, PyrH), 7.88 (d, *J* = 7.7 Hz, 1H, NaphH), 7.78 – 7.61 (m, 3H, ArH), 7.55 (m, 3H, ArH), 7.41 (t, *J* = 7.5 Hz, 2H, NaphH), 7.30 (t, *J* = 7.7 Hz, 2H, NaphH), 7.03 – 6.95 (m, 4H, 2H, ArH), 6.95 – 6.84 (m, 3H, ArH), 5.71 (s, 1H, PyrCH-Ph), 4.17 (s, 3H, 2-PyrOCH<sub>3</sub>), 4.00 (s, 3H, 6-PyrOCH<sub>3</sub>), 3.20 – 3.01 (m, 2H, CH<sub>2</sub>CH<sub>2</sub>N), 2.55 (s, 3H, N(CH<sub>3</sub>)<sub>2</sub>), 2.52 (s, 3H, N(CH<sub>3</sub>)<sub>2</sub>), 2.43 – 2.30 (m, 1H, CH<sub>2</sub>CH<sub>2</sub>N), 2.17 – 2.00 (m, 2H, CH<sub>2</sub>CH<sub>2</sub>N);

<sup>13</sup>C NMR (101 MHz, CDCl<sub>3</sub>) δ = 159.3 (2-PyrC-OCH<sub>3</sub>), 158.4 (6-PyrC-OCH<sub>3</sub>), 143.5 (PyrCH), 139.7 (ArC), 138.2 (NaphC), 136.9 (NaphC), 134.7 (NaphC), 130.3 (NaphCH), 129.7 (ArCH), 129.4 (ArC), 129.3 (ArCH), 129.1 (ArCH), 128.3 (NaphCH), 127.8 (ArCH), 127.0 (ArCH), 126.5 (ArCH), 126.4 (ArCH), 125.3 (NaphCH), 125.2 (ArCH), 123.8 (NaphCH), 116.6 (PyrC), 113.1 (PyrC), 78.6 (C-OH), 55.0 (CH<sub>2</sub>CH<sub>2</sub>N), 54.2 (2-PyrOCH<sub>3</sub>), 53.6 (6-PyrOCH<sub>3</sub>), 51.1<sup>†</sup> (PyrCH-Ph), 44.3 (N(CH<sub>3</sub>)<sub>2</sub>), 42.1 (N(CH<sub>3</sub>)<sub>2</sub>), 34.7 (CH<sub>2</sub>CH<sub>2</sub>N<sub>2</sub>), missing 1 × ArCH due to overlap;

Analytical HPLC (254 nm): *t*<sub>R</sub> = 7.3 min, 95%.

**1-(2,6-dimethoxy-5-(4-methoxyphenyl)pyridin-3-yl)-4-(dimethylamino)-2-(naphthalen-1-yl)-1-phenylbutan-2-ol (2.107)**



General method B was used with 4-methoxyphenylboronic acid (76.0 mg, 0.5 mmol) to afford the title compound an orange foam (135 mg, 0.240 mmol, 96%, A:B = 56:44).

LR-MS (ESI+)  $m/z$ : 562.9  $[M+H]^+$ ;

HR-MS (ESI+)  $m/z$   $[M = C_{36}H_{38}N_2O_4]$ :  $[M+H]^+$  calc'd 563.2904, found 563.2909;

Diastereomer A:

$^1H$  NMR (400 MHz,  $CDCl_3$ )  $\delta$  = 11.07 (br s, 1H,  $NH^+$ ), 8.41 (d,  $J$  = 8.7 Hz, 1H, NaphH), 8.03 (d,  $J$  = 7.5 Hz, 1H, NaphH), 7.82 (d,  $J$  = 7.7 Hz, 1H, NaphH), 7.77 (s, 1H, PyrH), 7.68 (d,  $J$  = 8.1 Hz, 1H, NaphH), 7.65 – 7.56 (m, 3H, ArH), 7.48 (t,  $J$  = 7.4 Hz, 1H, NaphH), 7.44 – 7.33 (m, 3H, ArH), 7.30 (d,  $J$  = 7.3 Hz, 1H, ArH), 7.14 (d,  $J$  = 8.2 Hz, 2H, ArH), 6.88 (d,  $J$  = 8.6 Hz, 2H, ArH), 5.50 (s, 1H, Pyr-CH-Ph), 3.83 (s, 3H, OCH<sub>3</sub>), 3.67 (s, 3H, OCH<sub>3</sub>), 3.52 (s, 3H, OCH<sub>3</sub>), 3.21 – 2.95 (m, 2H, CH<sub>2</sub>CH<sub>2</sub>N), 2.59 (s, 3H, N(CH<sub>3</sub>)<sub>2</sub>), 2.52 (s, 3H, N(CH<sub>3</sub>)<sub>2</sub>), 2.50 – 2.38 (m, 1H, CH<sub>2</sub>CH<sub>2</sub>N), 2.31 – 2.14 (m, 1H, CH<sub>2</sub>CH<sub>2</sub>N);

$^{13}C$  NMR (101 MHz,  $CDCl_3$ )  $\delta$  = 158.5 (C-OCH<sub>3</sub>), 157.8 (C-OCH<sub>3</sub>), 157.1 (C-OCH<sub>3</sub>), 142.4 (PyrCH), 139.1 (ArC), 138.3 (ArC), 134.7 (NaphC), 130.8 (NaphCH), 130.1 (NaphCH), 130.0 (ArC), 129.5 (ArC), 129.3 (NaphCH), 129.2 (ArCH), 128.8 (NaphCH), 127.6 (NaphCH), 126.6 (NaphCH), 126.0 (ArCH), 125.2 (NaphCH), 125.0 (ArCH), 124.1 (NaphCH), 114.6 (PyrC), 114.1 (PyrC), 113.6 (PhCH-OCH<sub>3</sub>), 78.3 (C-OH), 55.4 (OCH<sub>3</sub>), 55.3 (CH<sub>2</sub>CH<sub>2</sub>N), 53.31<sup>†</sup> (Pyr-CH-Ph), 53.30 (OCH<sub>3</sub>), 53.2 (OCH<sub>3</sub>), 44.4 (N(CH<sub>3</sub>)<sub>2</sub>), 42.4 (N(CH<sub>3</sub>)<sub>2</sub>), 35.1 (CH<sub>2</sub>CH<sub>2</sub>N);

Analytical HPLC (254 nm):  $t_R$  = 7.4 min, 95%;

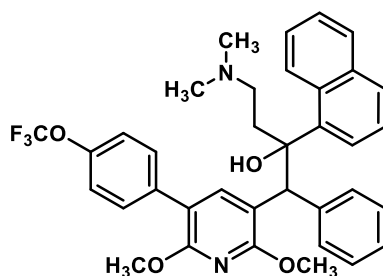
Diastereomer B:

$^1H$  NMR (400 MHz,  $CDCl_3$ )  $\delta$  = 11.3 (br s, 1H,  $NH^+$ ), 8.48 (d,  $J$  = 8.7 Hz, 1H, NaphH), 8.06 (s, 1H, PyrH), 7.88 (d,  $J$  = 8.1 Hz, 1H, NaphH), 7.76 – 7.59 (m, 3H, ArCH), 7.58 – 7.45 (m, 3H, ArCH), 7.30 (t,  $J$  = 7.7 Hz, 1H, NaphH), 7.05 – 6.82 (m, 7H, ArCH), 5.70 (s, 1H, Pyr-CH-Ph), 4.16 (s, 3H, Pyr-OCH<sub>3</sub>), 4.00 (s, 3H, Pyr-OCH<sub>3</sub>), 3.84 (s, 3H, Ph-OCH<sub>3</sub>), 3.18 – 3.04 (m, 2H, CH<sub>2</sub>CH<sub>2</sub>N), 2.55 (s, 3H, N(CH<sub>3</sub>)<sub>2</sub>), 2.52 (s, 3H, N(CH<sub>3</sub>)<sub>2</sub>), 2.43 – 2.30 (m, 1H, CH<sub>2</sub>CH<sub>2</sub>N), 2.18 – 2.07 (m, 1H, CH<sub>2</sub>CH<sub>2</sub>N);

$^{13}C$  NMR (101 MHz,  $CDCl_3$ )  $\delta$  = 159.0 (PyrC-OCH<sub>3</sub>), 158.7 (PhC-OCH<sub>3</sub>), 158.3 (PyrC-OCH<sub>3</sub>), 143.1 (PyrC), 139.6 (ArC), 138.2 (ArC), 134.7 (ArC), 130.4 (ArCH), 130.3 (NaphCH), 129.7 (ArCH), 129.4 (ArC), 129.3 (ArC), 129.1 (ArCH), 127.8 (ArCH), 127.0 (ArCH), 126.5 (ArCH), 126.4 (ArCH), 125.3 (ArCH), 125.2 (NaphCH), 123.8 (NaphCH), 116.2 (5-PyrC), 113.8 (PhCH-OCH<sub>3</sub>), 112.9 (3-PyrC), 78.6 (C-OH), 55.4 (Ph-OCH<sub>3</sub>), 55.1 (CH<sub>2</sub>CH<sub>2</sub>N), 54.2 (Pyr-OCH<sub>3</sub>), 53.6 (Pyr-OCH<sub>3</sub>), 51.2<sup>†</sup> (Pyr-CH-Ph), 44.3 (N(CH<sub>3</sub>)<sub>2</sub>), 42.1 (N(CH<sub>3</sub>)<sub>2</sub>), 34.6 (CH<sub>2</sub>CH<sub>2</sub>N);

Analytical HPLC (254 nm):  $t_R$  = 7.7 min, 96%.

**1-(2,6-dimethoxy-5-(4-(trifluoromethoxy)phenyl)pyridin-3-yl)-4-(dimethylamino)-2-(naphthalen-1-yl)-1-phenylbutan-2-ol (2.108)**



General method B was used with 4-trifluoromethoxyphenylboronic acid (103 mg, 0.5 mmol) to afford the title compound an orange foam (145 mg, 0.235 mmol, 94%, A:B = 50:50).

LR-MS (ESI+)  $m/z$ : 616.9  $[M+H]^+$ ;

HR-MS (ESI+)  $m/z$   $[M = C_{36}H_{35}F_3N_2O_4]$ :  $[M+H]^+$  calc'd 617.2622, found 617.2623;

Diastereomer A:

$^1H$  NMR (401 MHz,  $CDCl_3$ )  $\delta$  = 12.23 (br s, 1H,  $NH^+$ ), 8.43 (d,  $J$  = 8.6 Hz, 1H, Naph $\underline{H}$ ), 8.10 (d,  $J$  = 7.6 Hz, 1H, Naph $\underline{H}$ ), 8.00 (s, 1H, Pyr $\underline{H}$ ), 7.83 (d,  $J$  = 8.1 Hz, 1H, Naph $\underline{H}$ ), 7.68 (d,  $J$  = 8.0 Hz, 1H, Naph $\underline{H}$ ), 7.66 – 7.57 (m, 3H, Ar $\underline{H}$ ), 7.51 – 7.44 (m, 1H, Naph $\underline{H}$ ), 7.44 – 7.35 (m, 3H, Ar $\underline{H}$ ), 7.32 – 7.27 (m, 3H, Ph' $\underline{H}$ -OCF $_3$ , Ar $\underline{H}$ ), 7.19 (d,  $J$  = 8.2 Hz, 2H, Ph' $\underline{H}$ -OCF $_3$ ), 5.53 (s, 1H, Pyr- $\underline{CH}$ -Ph), 3.67 (s, 3H, 6-PyrOCH $_3$ ), 3.46 (s, 3H, 2-PyrOCH $_3$ ), 3.24 – 2.99 (m, 2H,  $\underline{CH_2CH_2N}$ ), 2.58 (s, 3H, N( $\underline{CH_3}$ ) $_2$ ), 2.52 (s, 3H, N( $\underline{CH_3}$ ) $_2$ ), 2.46 – 2.29 (m, 1H,  $\underline{CH_2CH_2N}$ ), 2.23 – 2.07 (m, 1H,  $\underline{CH_2CH_2N}$ );

$^{13}C$  NMR (101 MHz,  $CDCl_3$ )  $\delta$  = 158.7 (2-Pyr $\underline{C}$ -OCH $_3$ ), 157.0 (6-Pyr $\underline{C}$ -OCH $_3$ ), 147.9 (Ph' $\underline{C}$ -OCF $_3$ ), 142.4 (Pyr $\underline{CH}$ ), 139.0 (Ar $\underline{C}$ ), 138.4 (Ar $\underline{C}$ ), 135.9 (Ph $\underline{C}$ ), 134.6 (Ar $\underline{C}$ ), 130.8 (Ar $\underline{CH}$ ), 130.3 (Ar $\underline{CH}$ ), 130.0 (Naph $\underline{CH}$ ), 129.6 (Ar $\underline{C}$ ), 129.1 (Ar $\underline{CH}$ ), 128.8 (Ar $\underline{CH}$ ), 127.6 (Ar $\underline{CH}$ ), 126.9 (Ar $\underline{CH}$ ), 125.9 (Ar $\underline{CH}$ ), 125.2 (Ar $\underline{CH}$ ), 125.0 (Ar $\underline{CH}$ ), 124.1 (Naph $\underline{H}$ ), 120.7 (q,  $J$  = 256.6 Hz, Ph' $\underline{OCF_3}$ ), 120.7 (Ph' $\underline{CH}$ ), 114.7 (3-Pyr $\underline{C}$ ), 113.3 (5-Pyr $\underline{C}$ ), 78.0 ( $\underline{C}$ -OH), 54.8 ( $\underline{CH_2CH_2N}$ ), 53.31 $^+$  (Pyr- $\underline{CH}$ -Ph), 53.30 (2-Pyr-O $\underline{CH_3}$ ), 53.25 (6-Pyr-O $\underline{CH_3}$ ), 44.5 (N( $\underline{CH_3}$ ) $_2$ ), 41.9 (N( $\underline{CH_3}$ ) $_2$ ), 35.5 ( $\underline{CH_2CH_2N}$ );

Analytical HPLC (254 nm):  $t_R$  = 8.1 min, 93%;

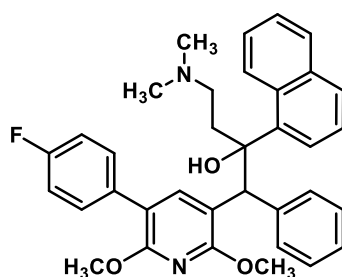
Diastereomer B:

$^1H$  NMR (400 MHz,  $CDCl_3$ )  $\delta$  = 12.31 (br s, 1H,  $NH^+$ ), 8.52 (d,  $J$  = 8.2 Hz, 1H, Naph $\underline{H}$ ), 8.09 (s, 1H, Pyr $\underline{H}$ ), 7.95 – 7.77 (m, 2H, Ar $\underline{CH}$ ), 7.73 – 7.56 (m, 4H, Ar $\underline{CH}$ , Ph' $\underline{H}$ ), 7.51 (t,  $J$  = 7.3 Hz, 1H, Naph $\underline{H}$ ), 7.30 (t,  $J$  = 7.4 Hz, 1H, Naph $\underline{H}$ ), 7.23 (d,  $J$  = 7.9 Hz, 2H, Ph' $\underline{H}$ ), 7.07 (s, 2H, Ar $\underline{H}$ ), 6.95 – 6.80 (m, 3H, Ar $\underline{H}$ ), 5.70 (s, 1H, Pyr- $\underline{CH}$ -Ph), 4.17 (s, 3H, 2-PyrOCH $_3$ ), 4.00 (s, 3H, 6-PyrOCH $_3$ ), 3.29 – 3.08 (m, 2H,  $\underline{CH_2CH_2N}$ ), 2.66 – 2.49 (m, 6H, N( $\underline{CH_3}$ ) $_2$ ), 2.43 – 2.30 (m, 1H,  $\underline{CH_2CH_2N}$ ), 2.13 – 1.98 (m, 1H,  $\underline{CH_2CH_2N}$ );

$^{13}\text{C}$  NMR (101 MHz,  $\text{CDCl}_3$ )  $\delta$  = 159.6 (6-Pyr $\text{C}$ - $\text{OCH}_3$ ), 158.2 (2-Pyr $\text{C}$ - $\text{OCH}_3$ ), 148.2 (Ph' $\text{C}$ - $\text{OCF}_3$ ), 143.5 (Pyr $\text{C}$ ), 140.1 (Ar $\text{C}$ ), 138.3 (Ar $\text{C}$ ), 135.7 (Ph $\text{C}$ -Pyr), 134.6 (Ar $\text{C}$ ), 130.7 (Ph' $\text{CH}$ ), 130.3 (Ar $\text{CH}$ ), 129.8 (Ar $\text{CH}$ ), 129.5 (Ar $\text{C}$ ), 129.0 (Ar $\text{CH}$ ), 127.7 (Ar $\text{CH}$ ), 127.3 (Ar $\text{CH}$ ), 126.4 (Ar $\text{CH}$ ), 126.3 (Ar $\text{CH}$ ), 125.3 (Naph $\text{CH}$ ), 125.2 (Naph $\text{CH}$ ), 123.7 (Naph $\text{CH}$ ), 120.73 (q,  $J$  = 256.8 Hz,  $\text{OCF}_3$ ), 120.68 (3,5-Ph $\text{CH}$ - $\text{OCF}_3$ ), 115.3 (5-Pyr $\text{C}$ ), 113.6 (3-Pyr $\text{C}$ ), 78.5 ( $\text{C}$ -OH), 54.8 ( $\text{CH}_2\text{CH}_2\text{N}$ ), 54.2 (2-Pyr- $\text{OCH}_3$ ), 53.6 (6-Pyr- $\text{OCH}_3$ ), 50.7 $^\dagger$  (Pyr- $\text{CH}$ -Ph), 44.6 ( $\text{N}(\text{CH}_3)_2$ ), 41.6 ( $\text{N}(\text{CH}_3)_2$ ), 34.9 ( $\text{CH}_2\text{CH}_2\text{N}$ );

Analytical HPLC (254 nm):  $t_R$  = 8.3 min, 93%.

**4-(dimethylamino)-1-(5-(4-fluorophenyl)-2,6-dimethoxypyridin-3-yl)-2-(naphthalen-1-yl)-1-phenylbutan-2-ol (2.109)**



General method B was used with 4-fluorophenylboronic acid (61.0 mg, 0.5 mmol) to afford the title compound as pale-yellow foam (128 mg, 0.232 mmol, 93%, A:B = 50:50).

LR-MS (ESI+)  $m/z$ : 551.0  $[\text{M}+\text{H}]^+$ ;

HR-MS (ESI+)  $m/z$  [ $\text{M} = \text{C}_{35}\text{H}_{35}\text{FN}_2\text{O}_3$ ]:  $[\text{M}+\text{H}]^+$  calc'd 551.2704, found 551.2713;

Diastereomer A:

$^1\text{H}$  NMR (400 MHz,  $\text{CDCl}_3$ )  $\delta$  = 10.60 (br s, 1H,  $\text{NH}^+$ ), 8.40 (d,  $J$  = 8.7 Hz, 1H, Naph $\text{H}$ ), 8.03 (d,  $J$  = 7.3 Hz, 1H, Naph $\text{H}$ ), 7.83 (d,  $J$  = 7.5 Hz, 1H, Naph $\text{H}$ ), 7.74 (br s, 1H, Pyr $\text{H}$ ), 7.69 (d,  $J$  = 8.1 Hz, 1H, Naph $\text{H}$ ), 7.65 – 7.57 (m, 3H, Ar $\text{H}$ ), 7.48 (t,  $J$  = 7.4 Hz, 1H, Naph $\text{H}$ ), 7.44 – 7.35 (m, 3H, Ar $\text{H}$ ), 7.30 (t,  $J$  = 7.3 Hz, 1H, Naph $\text{H}$ ), 7.20 – 7.10 (m, 2H, Ph' $\text{H}$ ), 7.05 – 6.97 (m, 2H, Ph' $\text{H}$ ), 5.50 (s, 1H, Pyr- $\text{CH}$ -Ph), 3.67 (s, 3H, 6-Pyr $\text{OCH}_3$ ), 3.55 (s, 3H, 2-Pyr $\text{OCH}_3$ ), 3.19 – 3.09 (m, 1H,  $\text{CH}_2\text{CH}_2\text{N}$ ), 3.09 – 2.95 (m, 1H,  $\text{CH}_2\text{CH}_2\text{N}$ ), 2.62 (s, 3H,  $\text{N}(\text{CH}_3)_2$ ), 2.54 (s, 3H,  $\text{N}(\text{CH}_3)_2$ ), 2.50 – 2.39 (m, 1H,  $\text{CH}_2\text{CH}_2\text{N}$ ), 2.31 – 2.16 (m, 1H,  $\text{CH}_2\text{CH}_2\text{N}$ );

$^{13}\text{C}$  NMR (101 MHz,  $\text{CDCl}_3$ )  $\delta$  = 161.9 (d,  $J$  = 245.6 Hz, Ph' $\text{CF}$ ), 158.2 (2-Pyr $\text{C}$ - $\text{OCH}_3$ ), 157.2 (6-Pyr $\text{C}$ - $\text{OCH}_3$ ), 142.6 (Pyr $\text{CH}$ ), 138.9 (Ar $\text{C}$ ), 138.2 (Ar $\text{C}$ ), 134.7 (Ar $\text{C}$ ), 132.82 (d,  $J$  = 3.3 Hz, Ph' $\text{C}$ -Pyr), 130.8 (Ar $\text{CH}$ ), 130.5 (d,  $J$  = 8.0 Hz, Ph' $\text{CH}$ ), 130.1 (Naph $\text{CH}$ ), 129.5 (Ar $\text{C}$ ), 129.3 (Naph $\text{CH}$ ), 128.9 (Ar $\text{CH}$ ), 127.7 (Naph $\text{CH}$ ), 126.5 (Naph $\text{CH}$ ), 126.1 (Ar $\text{CH}$ ), 125.3 (Naph $\text{CH}$ ), 125.0 (Ar $\text{CH}$ ), 124.0 (Naph $\text{CH}$ ), 115.00 (d,  $J$  = 21.1 Hz, Ph' $\text{CH}$ ), 114.2 (Pyr $\text{C}$ ), 114.0 (Pyr $\text{C}$ ), 78.4 ( $\text{C}$ -OH), 55.5 ( $\text{CH}_2\text{CH}_2\text{N}$ ), 53.6 $^\dagger$  (Pyr- $\text{CH}$ -Ph), 53.5 (6-Pyr $\text{OCH}_3$ ), 53.3 (2-Pyr $\text{OCH}_3$ ), 44.7 ( $\text{N}(\text{CH}_3)_2$ ), 42.5 ( $\text{N}(\text{CH}_3)_2$ ), 35.1 ( $\text{CH}_2\text{CH}_2\text{N}(\text{CH}_3)_2$ );

Analytical HPLC (254 nm):  $t_R$  = 7.2 min, 98%;

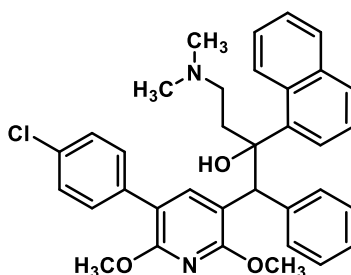
Diastereomer B:

$^1\text{H}$  NMR (400 MHz,  $\text{CDCl}_3$ )  $\delta$  = 11.31 (br s, 1H,  $\text{NH}^+$ ), 8.50 (d,  $J$  = 8.7 Hz, 1H, Naph $\underline{\text{H}}$ ), 8.06 (s, 1H, Pyr $\underline{\text{H}}$ ), 7.88 (d,  $J$  = 8.1 Hz, 1H, Naph $\underline{\text{H}}$ ), 7.76 (d,  $J$  = 7.4 Hz, 1H, Naph $\underline{\text{H}}$ ), 7.72 – 7.62 (m, 2H, Ar $\underline{\text{H}}$ ), 7.59 – 7.46 (m, 3H, Ar $\underline{\text{H}}$ , Ph' $\underline{\text{H}}$ ), 7.31 (t,  $J$  = 7.8 Hz, 1H, Naph $\underline{\text{H}}$ ), 7.09 (t,  $J$  = 8.6 Hz, 3H, Ph' $\underline{\text{H}}$ ), 7.05 – 6.98 (m, 2H, Ar $\underline{\text{H}}$ ), 6.93 – 6.87 (m, 3H, Ar $\underline{\text{H}}$ ), 5.71 (s, 1H, Pyr- $\underline{\text{CH}}$ -Ph), 4.17 (s, 3H, 6-PyrO $\underline{\text{CH}_3}$ ), 4.00 (s, 3H, 2-PyrO $\underline{\text{CH}_3}$ ), 3.25 – 3.04 (m, 2H,  $\underline{\text{CH}_2\text{CH}_2\text{N}}$ ), 2.55 (s, 3H, N( $\underline{\text{CH}_3}$ ) $_2$ ), 2.53 (s, 3H, N( $\underline{\text{CH}_3}$ ) $_2$ ), 2.42 – 2.26 (m, 1H,  $\underline{\text{CH}_2\text{CH}_2\text{N}}$ ), 2.17 – 2.03 (m, 1H,  $\underline{\text{CH}_2\text{CH}_2\text{N}}$ );

$^{13}\text{C}$  NMR (101 MHz,  $\text{CDCl}_3$ )  $\delta$  = 162.1 (d,  $J$  = 245.7 Hz, Ph' $\underline{\text{CF}}$ ), 159.4 (6-Pyr $\underline{\text{C}}$ -O $\underline{\text{CH}_3}$ ), 158.2 (2-Pyr $\underline{\text{C}}$ -O $\underline{\text{CH}_3}$ ), 143.3 (Pyr $\underline{\text{CH}}$ ), 139.8 (Ar $\underline{\text{C}}$ ), 138.1 (Naph $\underline{\text{C}}$ ), 134.7 (Naph $\underline{\text{C}}$ ), 132.9 (d,  $J$  = 3.3 Hz, Ph' $\underline{\text{C}}$ ), 130.9 (d,  $J$  = 7.9 Hz, Ph' $\underline{\text{CH}}$ ), 130.3 (Naph $\underline{\text{CH}}$ ), 129.7 (Ar $\underline{\text{CH}}$ ), 129.4 (Ar $\underline{\text{C}}$ ), 129.1 (Naph $\underline{\text{CH}}$ ), 127.8 (Ar $\underline{\text{CH}}$ ), 127.0 (Naph $\underline{\text{CH}}$ ), 126.44 (Ar $\underline{\text{CH}}$ ), 126.37 (Ar $\underline{\text{CH}}$ ), 125.3 (Ar $\underline{\text{CH}}$ ), 125.2 (Naph $\underline{\text{CH}}$ ), 123.7 (Naph $\underline{\text{CH}}$ ), 115.6 (5-Pyr $\underline{\text{C}}$ ), 115.11 (d,  $J$  = 21.4 Hz, Ph' $\underline{\text{CH}}$ ), 113.2 (3-Pyr $\underline{\text{C}}$ ), 78.6 ( $\underline{\text{C}}$ -OH), 55.1 ( $\underline{\text{CH}_2\text{CH}_2\text{N}}$ ), 54.2 (6-PyrO $\underline{\text{CH}_3}$ ), 53.6 (2-PyrO $\underline{\text{CH}_3}$ ), 50.8 $^+$  (Pyr- $\underline{\text{CH}}$ -Ph), 44.5 (N( $\underline{\text{CH}_3}$ ) $_2$ ), 41.9 (N( $\underline{\text{CH}_3}$ ) $_2$ ), 34.8 ( $\underline{\text{CH}_2\text{CH}_2\text{N}}$ );

Analytical HPLC (254 nm):  $t_R$  = 7.4 min, 96%.

**1-(5-(4-chlorophenyl)-2,6-dimethoxypyridin-3-yl)-4-(dimethylamino)-2-(naphthalen-1-yl)-1-phenylbutan-2-ol (2.110)**



General method B was used with 4-chlorophenylboronic acid (78.2 mg, 0.5 mmol) to afford the title compound as pale-yellow foam (108 mg, 0.192 mmol, 77%, A:B = 52:48).

LR-MS (ESI $^+$ )  $m/z$ : 566.9 [ $\text{M}+\text{H}$ ] $^+$ ;

HR-MS (ESI $^+$ )  $m/z$  [ $\text{M} = \text{C}_{35}\text{H}_{35}\text{ClN}_2\text{O}_3$ ]: [ $\text{M}+\text{H}$ ] $^+$  calc'd 567.2409, found 567.2410;

Diastereomer A:

$^1\text{H}$  NMR (400 MHz, MeOD)  $\delta$  = 8.60 (d,  $J$  = 8.8 Hz, 1H, Naph $\underline{\text{H}}$ ), 8.09 – 7.97 (m, 2H, Naph $\underline{\text{H}}$ , Pyr $\underline{\text{H}}$ ), 7.86 (d,  $J$  = 8.1 Hz, 1H, Naph $\underline{\text{H}}$ ), 7.77 – 7.68 (m, 3H, Ar $\underline{\text{H}}$ ), 7.66 (t,  $J$  = 7.4 Hz, 1H, Naph $\underline{\text{H}}$ ), 7.49 (t,  $J$  = 7.5 Hz, 1H, Naph $\underline{\text{H}}$ ), 7.45 – 7.21 (m, 8H, Ar $\underline{\text{H}}$ , Ph' $\underline{\text{H}}$ ), 5.64 (s, 1H, Pyr- $\underline{\text{CH}}$ -Ph), 3.66 (s, 3H, 6-PyrO $\underline{\text{CH}_3}$ ), 3.44 (s,



3H, 2-PyrOCH<sub>3</sub>), 3.25 – 3.13 (m, 1H, CH<sub>2</sub>CH<sub>2</sub>N), 3.09 – 3.00 (m, 1H, CH<sub>2</sub>CH<sub>2</sub>N), 2.61 (br s, 6H, N(CH<sub>3</sub>)<sub>2</sub>), 2.42 – 2.31 (m, 2H, CH<sub>2</sub>CH<sub>2</sub>N);

<sup>13</sup>C NMR (101 MHz, MeOD) δ = 160.0 (2-PyrC-OCH<sub>3</sub>), 158.2 (6-PyrC-OCH<sub>3</sub>), 143.6 (PyrCH), 141.2 (PhC), 140.1 (ArC), 137.1 (ArC), 136.2 (NaphC), 133.3 (ArC), 132.4 (PhCH), 131.4 (Ph'CH), 131.0 (ArC), 130.8 (NaphCH), 130.1 (ArCH), 129.4 (ArCH), 129.0 (ArCH), 128.1 (ArCH), 127.6 (NaphCH), 127.0 (NaphCH), 126.2 (NaphCH), 125.8 (ArCH), 125.7 (NaphCH), 116.3 (3-PyrC), 114.4 (5-PyrC), 79.6 (C-OH), 56.0 (CH<sub>2</sub>CH<sub>2</sub>N), 53.6 (2-PyrOCH<sub>3</sub>), 53.5 (2-PyrOCH<sub>3</sub>), 53.4<sup>†</sup> (PyrCH-Ph), 44.0 (N(CH<sub>3</sub>)<sub>2</sub>), 42.9 (N(CH<sub>3</sub>)<sub>2</sub>), 36.3 (CH<sub>2</sub>CH<sub>2</sub>N);

Analytical HPLC (254 nm): *t*<sub>R</sub> = 8.0 min, 97%;

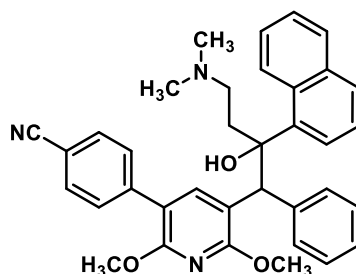
Diastereomer B:

<sup>1</sup>H NMR (400 MHz, MeOD) δ = 8.66 (br s, 1H, NaphH), 8.31 (br s, 1H, PyrH), 7.90 (d, *J* = 8.2 Hz, 1H, NaphH), 7.74 – 7.66 (m, 3H, ArH), 7.61 – 7.47 (m, 3H, ArH), 7.43 – 7.37 (m, 2H, Ph'H), 7.30 (t, *J* = 7.8 Hz, 1H, NaphCH), 7.02 (br s, 2H, ArH), 6.91 – 6.82 (m, 3H, ArH), 5.78 (s, 1H, Pyr-CH-Ph), 4.17 (s, 3H, PyrOCH<sub>3</sub>), 4.00 (s, 3H, PyrOCH<sub>3</sub>), 3.22 – 3.09 (m, 1H, CH<sub>2</sub>CH<sub>2</sub>N), 3.08 – 3.00 (m, 1H, CH<sub>2</sub>CH<sub>2</sub>N), 2.61 (s, 3H, N(CH<sub>3</sub>)<sub>2</sub>), 2.59 (s, 3H, N(CH<sub>3</sub>)<sub>2</sub>), 2.43 – 2.21 (m, 2H, CH<sub>2</sub>CH<sub>2</sub>N);

<sup>13</sup>C NMR (101 MHz, MeOD) δ = 161.2 (PyrC-OCH<sub>3</sub>), 159.3 (PyrC-OCH<sub>3</sub>), 144.6 (PyrCH), 141.42 (ArC), 141.37 (ArC), 139.9 (NaphC), 137.0 (Ph'C), 136.3 (NaphC), 133.6 (Ph'C), 131.5 (ArCH), 131.1 (NaphCH), 130.8 (ArCH), 130.1 (ArCH), 129.3 (Ph'CH), 128.6 (ArCH), 127.7 (ArCH), 127.32 (ArCH), 127.25 (ArCH), 126.3 (ArCH), 125.9 (NaphCH), 125.3<sup>†</sup> (NaphCH), 115.7 (PyrC), 115.6 (PyrC), 71.4 (C-OH), 56.0 (CH<sub>2</sub>CH<sub>2</sub>N), 54.7 (PyrOCH<sub>3</sub>), 54.0 (PyrOCH<sub>3</sub>), 51.1<sup>†</sup> (Pyr-CH-Ph), 44.1 (N(CH<sub>3</sub>)<sub>2</sub>), 43.0 (N(CH<sub>3</sub>)<sub>2</sub>), 30.72 (CH<sub>2</sub>CH<sub>2</sub>N);

Analytical HPLC (254 nm): *t*<sub>R</sub> = 8.2 min, 91%.

**4-(5-(4-(dimethylamino)-2-hydroxy-2-(naphthalen-1-yl)-1-phenylbutyl)-2,6-dimethoxypyridin-3-yl)benzonitrile (2.111)**



General method B was used with 4-cyanophenylboronic acid (73.5 mg, 0.5 mmol) afforded the title compound as a yellow foam (85.0 mg, 0.152 mmol, 61%, A:B = 53:47).

LR-MS (ESI+)  $m/z$ : 558.0  $[M+H]^+$ ;

HR-MS (ESI+)  $m/z$   $[M = C_{36}H_{35}N_3O_3]$ :  $[M+H]^+$  calc'd 558.2751, found 558.2761;

Diastereomer A:

$^1H$  NMR (400 MHz,  $CDCl_3$ )  $\delta$  = 8.41 (d,  $J$  = 8.7 Hz, 1H, NaphH), 8.07 (d,  $J$  = 7.3 Hz, 1H, NaphH), 7.98 (br s, 1H, PyrH), 7.83 (d,  $J$  = 7.7 Hz, 1H, NaphH), 7.69 (d,  $J$  = 8.2 Hz, 1H, NaphH), 7.64 – 7.57 (m, 5H, ArH), 7.48 (t,  $J$  = 7.0 Hz, 2H, ArH), 7.45 – 7.27 (m, 6H, ArH), 5.54 (s, 1H, Pyr-CH-Ph), 3.68 (s, 3H, 6-PyrOCH<sub>3</sub>), 3.51 (s, 3H, 2-PyrOCH<sub>3</sub>), 3.21 – 2.99 (m, 2H, CH<sub>2</sub>CH<sub>2</sub>N), 2.59 (s, 3H, N(CH<sub>3</sub>)<sub>2</sub>), 2.53 (s, 3H, N(CH<sub>3</sub>)<sub>2</sub>), 2.46 – 2.36 (m, 1H, CH<sub>2</sub>CH<sub>2</sub>N), 2.23 – 2.10 (m, 1H, CH<sub>2</sub>CH<sub>2</sub>N);

$^{13}C$  NMR (101 MHz,  $CDCl_3$ )  $\delta$  = 159.3 (2-PyrC-OCH<sub>3</sub>), 157.2 (6-PyrC-OCH<sub>3</sub>), 142.3 (PyrC), 142.0 (ArC), 138.7 (ArC), 138.1 (ArC), 134.7 (NaphC), 131.9 (ArCH), 130.8 (ArCH), 130.1 (NaphCH), 129.5 (ArCH), 129.3 (ArCH), 128.9 (ArCH), 127.7 (ArCH), 126.7 (NaphCH), 126.0 (ArCH), 125.3 (ArCH), 125.0 (ArCH), 124.0 (NaphCH), 119.4 (ArC), 114.9 (3-PyrC), 112.7 (ArC), 109.7 (ArC), 78.1 (C-OH), 55.1 (CH<sub>2</sub>CH<sub>2</sub>N), 53.5 (6-PyrOCH<sub>3</sub>), 53.3 (2-PyrOCH<sub>3</sub>), 52.4<sup>†</sup> (Pyr-CH-Ph), 44.7 (N(CH<sub>3</sub>)<sub>2</sub>), 42.2 (N(CH<sub>3</sub>)<sub>2</sub>), 35.3 (CH<sub>2</sub>CH<sub>2</sub>N);

Analytical HPLC (254 nm):  $t_R$  = 6.9 min, 98%;

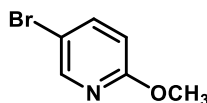
Diastereomer B:

$^1H$  NMR (400 MHz,  $CDCl_3$ )  $\delta$  = 11.38 (br s, 1H, NH<sup>+</sup>), 8.50 (d,  $J$  = 8.7 Hz, 1H, NaphH), 8.12 (s, 1H, PyrH), 7.87 (d,  $J$  = 7.9 Hz, 2H, NaphH), 7.82 (d,  $J$  = 7.4 Hz, 1H, NaphH), 7.75 – 7.61 (m, 5H, ArH), 7.51 (t,  $J$  = 7.6 Hz, 1H, NaphH), 7.31 (t,  $J$  = 7.8 Hz, 1H, NaphH), 7.07 (s, 2H, ArH), 6.94 – 6.82 (m, 3H, ArH), 5.72 (s, 1H, Pyr-CH-Ph), 4.18 (s, 3H, 2-PyrOCH<sub>3</sub>), 4.00 (s, 3H, 6-PyrOCH<sub>3</sub>), 3.28 – 3.10 (m, 2H, CH<sub>2</sub>CH<sub>2</sub>N), 2.56 (s, 3H, N(CH<sub>3</sub>)<sub>2</sub>), 2.54 (s, 3H, N(CH<sub>3</sub>)<sub>2</sub>), 2.38 – 2.29 (m, 1H, CH<sub>2</sub>CH<sub>2</sub>N), 2.12 – 1.98 (m, 1H, CH<sub>2</sub>CH<sub>2</sub>N);

$^{13}C$  NMR (101 MHz,  $CDCl_3$ )  $\delta$  = 160.3 (2-PyrC-OCH<sub>3</sub>), 158.3 (6-PyrC-OCH<sub>3</sub>), 143.4 (PyrC), 141.9 (ArC), 139.9 (ArC), 138.0 (ArC), 134.6 (NaphC), 132.0 (ArCH), 130.4 (NaphCH), 129.9 (ArCH), 129.7 (ArCH), 129.1 (ArCH), 127.8 (ArCH), 127.2 (ArCH), 126.5 (ArCH), 126.4 (ArCH), 125.27 (NaphCH), 125.2 (NaphCH), 123.6 (NaphCH), 119.5 (ArC), 114.6 (ArCH), 113.9 (3-PyrC), 110.0 (ArC), 78.6 (C-OH), 55.0 (CH<sub>2</sub>CH<sub>2</sub>N), 54.4 (2-PyrOCH<sub>3</sub>), 53.7 (6-PyrOCH<sub>3</sub>), 50.2<sup>†</sup> (Pyr-CH-Ph), 44.8 (N(CH<sub>3</sub>)<sub>2</sub>), 41.8 (N(CH<sub>3</sub>)<sub>2</sub>), 34.8 (CH<sub>2</sub>CH<sub>2</sub>N);

Analytical HPLC (254 nm):  $t_R$  = 7.2 min, 95%.

## 6.1.4 Chapter 3 compounds

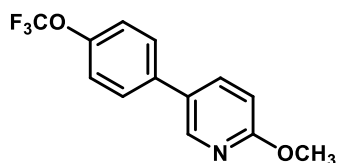
5-bromo-2-methoxypyridine<sup>[2]</sup> (**3.05**)

To a solution of 2-methoxypyridine (2.18 g, 20.0 mmol) in MeCN (25 mL) was added *N*-bromosuccinimide (3.92 g, 22.0 mmol), and the reaction stirred at reflux for 36 h. After this time, the solvent was evaporated under reduced pressure, and the residue purified by silica gel flash chromatography (0–10% Et<sub>2</sub>O in Pet. Sp.) to afford the title compound as a clear oil (3.06 g, 16.3 mmol, 81%). Spectroscopic data are in agreement with the literature reported values.<sup>[15]</sup>

<sup>1</sup>H NMR (400 MHz, CDCl<sub>3</sub>)  $\delta$  = 8.20 (d, *J* = 2.5 Hz, 1H, 6-PyrH), 7.63 (dd, *J* = 8.8, 2.5 Hz, 1H, 4-PyrH), 6.66 (d, *J* = 8.8 Hz, 1H, 3-PyrH), 3.91 (s, 3H, OCH<sub>3</sub>);

LR-MS (ESI+) *m/z*: 187.9/189.9 [M+H]<sup>+</sup>;

Analytical HPLC (254 nm): *t*<sub>R</sub> = 5.6 min, 98%.

2-methoxy-5-(4-(trifluoromethoxy)phenyl)pyridine (**3.11**)

To flask under nitrogen was added Pd(OAc)<sub>2</sub> (0.068 g, 5 mol%), X-Phos (0.288 g, 10 mol%), K<sub>3</sub>PO<sub>4</sub> (3.85 g, 18.1 mmol) and degassed PhMe (10 mL). After stirring for 5 min, 4-trifluoromethoxyphenylboronic acid (2.49 g, 12.08 mmol) and **3.05** (1.14 g, 6.04 mmol) were added and the reaction mixture was stirred at reflux for 20 h. After this time the reaction was cooled to room temperature, diluted with EtOAc, and filtered through a pad of Celite with the aid of EtOAc. The filtrate was washed with a solution of NH<sub>4</sub>Cl (saturated, aqueous), the layers separated and the aqueous layer extracted with EtOAc (×3). The combined organic layers were washed with brine, dried over anhydrous MgSO<sub>4</sub>, filtered, and concentrated under reduced pressure. Purification by silica gel flash chromatography (0–10% EtOAc in Pet. Sp.) afforded the title compound as a yellow oil (1.54 g, 5.7 mmol, 95%).

<sup>1</sup>H NMR (400 MHz, CDCl<sub>3</sub>)  $\delta$  = 8.36 (d, *J* = 2.3 Hz, 1H, 6-PyrH), 7.75 (dd, *J* = 8.6, 2.6 Hz, 1H, 4-PyrH), 7.55 – 7.50 (m, 2H, Ph'H-OCF<sub>3</sub>), 7.29 (d, *J* = 8.0 Hz, 2H, Ph'H-OCF<sub>3</sub>), 6.83 (d, *J* = 8.6 Hz, 1H, 3-PyrH), 3.99 (s, *J* = 2.6 Hz, 3H, OCH<sub>3</sub>);

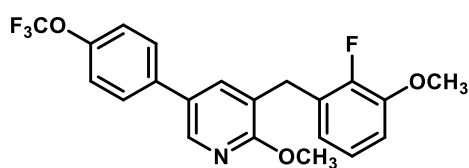
$^{13}\text{C}$  NMR (101 MHz,  $\text{CDCl}_3$ )  $\delta$  = 164.0 (2-PyrC-O $\text{CH}_3$ ), 148.9 (q,  $J$  = 1.8 Hz, PhC-OCF $_3$ ), 145.2 (6-PyrCH), 137.5 (4-PyrCH), 136.9 (PhC), 129.0 (5-PyrC), 128.2 (PhCH), 121.6 (PhCH), 120.7 (q,  $J$  = 257.2 Hz, OCF $_3$ ), 111.2 (3-PyrCH), 53.8 (Pyr-O $\text{CH}_3$ );

LR-MS (ESI+)  $m/z$ : 269.9  $[\text{M}+\text{H}]^+$ ;

Analytical HPLC (254 nm):  $t_R$  = 7.5 min, 97%;

HR-MS (ESI+)  $m/z$   $[\text{M} = \text{C}_{13}\text{H}_{10}\text{F}_3\text{NO}_2]$ :  $[\text{M}+\text{H}]^+$  calc'd 270.0736, found 270.0739.

### 3-(2-fluoro-3-methoxybenzyl)-2-methoxy-5-(4-(trifluoromethoxy)phenyl)pyridine (**3.04**)



Step (i) - Addition of 2-fluoro-3-methoxybenzaldehyde:

To a solution of 2,2,6,6-tetramethylpiperidine (0.760 mL, 4.48 mmol, anhydrous) in THF (10 mL, anhydrous) cooled to  $-10\text{ }^\circ\text{C}$  and under an atmosphere of nitrogen was added  $n\text{-BuLi}$  (2.50 mL, 1.64 M in hexanes, 4.11 mmol) dropwise over 30 min. The mixture was maintained at this temperature for 1 h, followed by cooling to  $-78\text{ }^\circ\text{C}$ . To the reaction mixture was added a solution of **3.11** (1.00 g, 3.73 mmol) in THF (5 mL, anhydrous) dropwise over 30 min, and the resultant mixture was stirred at  $-78\text{ }^\circ\text{C}$  for 4 h. A solution of 2-fluoro-3-methoxybenzaldehyde (0.690 g, 4.48 mmol) in THF (5 mL, anhydrous) was then added dropwise over 30 min and the mixture was stirred for an additional 6 h. After this time, the reaction was quenched with a solution of  $\text{NH}_4\text{Cl}$  (saturated, aqueous), the organic phase separated and the aqueous phase extracted with EtOAc ( $\times 3$ ). The combined organic layers were washed with brine, dried over anhydrous  $\text{MgSO}_4$ , filtered, and concentrated under reduced pressure. Purification by silica gel flash chromatography (0–30% EtOAc in Pet. Sp.) afforded a mixture of regioisomers (2:1 ratio, **3.13** to **3.14**) as a clear yellow semi-solid, which was used in the next step without further purification (0.586 g, 1.38 mmol, 37%).

Step (ii) - Reduction of alcohol:

To a solution of the isomeric mixture from step 1 (0.586 g, 1.38 mmol) in  $\text{CH}_2\text{Cl}_2$  (3 mL) was added  $\text{Et}_3\text{SiH}$  (0.880 mL, 5.53 mmol) and  $\text{BF}_3\cdot\text{OEt}_2$  (0.510 mL, 4.15 mmol) and was stirred at reflux for 16 h. Upon completion, the reaction mixture was cooled to room temperature and added to an ice-cold solution of  $\text{K}_2\text{CO}_3$  (20% w/v, aqueous). The aqueous phase was extracted with  $\text{CH}_2\text{Cl}_2$  ( $\times 3$ ), and the combined organic layers were dried over anhydrous  $\text{MgSO}_4$ , filtered, and concentrated under reduced

pressure. Purification by silica gel flash chromatography (0–10% Et<sub>2</sub>O in PhMe) afforded the title compound as a white solid on standing (0.354 g, 0.836 mmol, 23% over two steps).

<sup>1</sup>H NMR (400 MHz, CDCl<sub>3</sub>) δ = 8.22 (d, *J* = 2.4 Hz, 1H, 6-PyrH), 7.51 (br s, 1H, 4-PyrH), 7.49 – 7.44 (m, 2H, PhH-OCF<sub>3</sub>), 7.25 (d, *J* = 7.9 Hz, 2H, PhH-OCF<sub>3</sub>), 7.00 (td, *J* = 8.0, 1.4 Hz, 1H, PhH), 6.86 (td, *J* = 8.1, 1.4 Hz, 1H, Ph'H), 6.83 – 6.78 (m, 1H, Ph'H), 4.02 (s, 3H, PyrOCH<sub>3</sub>), 4.00 (br s, 2H, Pyr-CH<sub>2</sub>-Ph), 3.88 (s, 3H, Ph'OCH<sub>3</sub>);

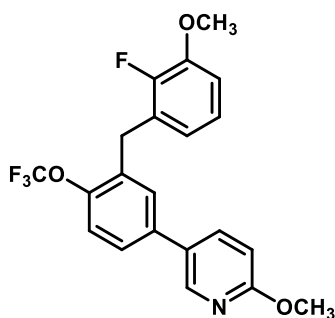
<sup>13</sup>C NMR (101 MHz, CDCl<sub>3</sub>) δ = 161.8 (2-PyrC-OCH<sub>3</sub>), 151.1 (d, *J* = 244.9 Hz, Ph'C-F), 148.8 (q, *J* = 1.7 Hz, PhC-OCF<sub>3</sub>), 147.9 (d, *J* = 11.0 Hz, Ph'C-OCH<sub>3</sub>), 142.9 (6-PyrCH), 137.1 (4-PyrCH), 137.0 (ArC), 129.1 (ArC), 128.2 (PhCH), 127.3 (d, *J* = 13.0 Hz, PhC-CH<sub>2</sub>-Pyr), 123.9 (d, *J* = 4.7 Hz, Ph'CH), 122.8, (ArC), 122.7 (d, *J* = 3.4 Hz, Ph'CH), 121.5 (PhCH), 120.7 (q, *J* = 257.1 Hz, Ph-OCF<sub>3</sub>), 111.7 (d, *J* = 1.3 Hz, Ph'CH), 56.4 (Ph'-OCH<sub>3</sub>), 53.9 (Pyr-OCH<sub>3</sub>), 28.8 (d, *J* = 3.8 Hz, Pyr-CH<sub>2</sub>-Ph');

LR-MS (ESI+) *m/z*: 407.9 [M+H]<sup>+</sup>;

HR-MS (ESI+) *m/z* [M = C<sub>21</sub>H<sub>17</sub>F<sub>4</sub>NO<sub>3</sub>]: [M+H]<sup>+</sup> calc'd 408.1217, found 408.1222;

Analytical HPLC (254 nm): *t*<sub>R</sub> = 8.9 min, 95%.

#### **5-(3-(2-fluoro-3-methoxybenzyl)-4-(trifluoromethoxy)phenyl)-2-methoxypyridine (3.15)**



This compound was isolated from the synthesis of **3.04** as a light-yellow oil (0.157 g, 0.385 mmol, 10% over two-steps).

<sup>1</sup>H NMR (400 MHz, CDCl<sub>3</sub>) δ = 8.28 (d, *J* = 2.5 Hz, 1H, 6-PyrH), 7.69 (dd, *J* = 8.6, 2.6 Hz, 1H, 4-PyrH), 7.38 (dd, *J* = 8.4, 2.3 Hz, 1H, PhH), 7.35 – 7.28 (m, 2H, PhH), 7.00 (td, *J* = 8.0, 1.5 Hz, 1H, Ph'H), 6.86 (td, *J* = 8.1, 1.5 Hz, 1H, Ph'H), 6.81 – 6.73 (m, 2H, Ph'H, 3-PyrH), 4.10 (br s, 2H, Ph-CH<sub>2</sub>-Ph'), 3.96 (s, 3H, 2-Pyr-OCH<sub>3</sub>), 3.88 (s, 3H, Ph'-OCH<sub>3</sub>);

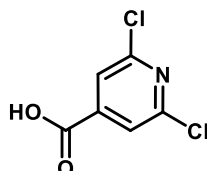
<sup>13</sup>C NMR (101 MHz, CDCl<sub>3</sub>) δ = 163.9 (2-PyrC-OCH<sub>3</sub>), 151.0 (d, *J* = 245.1 Hz, Ph'C-F), 148.0 (d, *J* = 11.0 Hz, Ph'C-OCH<sub>3</sub>), 147.1 (q, *J* = 1.2 Hz, PhC-OCF<sub>3</sub>), 145.1 (6-PyrCH), 137.5 (4-PyrCH), 136.8 (ArC), 133.1 (ArC), 129.4 (PhCH), 129.0 (5-PyrC-Ph), 127.2 (d, *J* = 13.0 Hz, PhC-CH<sub>2</sub>-Pyr), 126.1 (PhCH), 124.0 (d, *J* = 4.7 Hz, Ph'CH), 122.5 (d, *J* = 3.4 Hz, Ph'CH), 121.0 (q, *J* = 1.1 Hz, 5-PhCH), 120.8 (q, *J* = 257.7 Hz, OCF<sub>3</sub>), 111.9

(d,  $J = 1.1$  Hz, 5-Ph'CH), 111.1 (3-PyrCH), 56.4 (Ph'-OCH<sub>3</sub>), 53.7 (Pyr-OCH<sub>3</sub>), 29.0 (d,  $J = 3.8$  Hz, Ph-CH<sub>2</sub>-Ph');  
 LR-MS (ESI+)  $m/z$ : 407.9 [M+H]<sup>+</sup>;

Analytical HPLC (254 nm):  $t_R = 8.4$  min, 97%;

HR-MS (ESI+)  $m/z$  [M = C<sub>21</sub>H<sub>17</sub>F<sub>4</sub>NO<sub>3</sub>]: [M+H]<sup>+</sup> calc'd 408.1217, found 408.1221.

### 2,6-dichloroisonicotinic acid<sup>[16]</sup> (3.20)



Citrazinic acid (1.55 g, 10 mmol), benzyltriethylammonium chloride (2.51 g, 11.0 mmol) and POCl<sub>3</sub> (3.00 mL, 32.1 mmol) were combined in a sealed tube and the mixture stirred at 145 °C for 24 h. After cooling to room temperature, the mixture was concentrated under reduced pressure to remove excess POCl<sub>3</sub>, and the resulting residue was further quenched with ice-cold NaHCO<sub>3</sub> (saturated, aqueous). The aqueous mixture was extracted with EtOAc (×5) and the combined organic layers were washed with brine, dried over anhydrous MgSO<sub>4</sub>, filtered, and concentrated under reduced pressure to give the title compound as a pale-brown solid (1.64 g, 8.53 mmol, 85%). A portion of this product was further recrystallised from EtOH to give pale-yellow needles for melting point analysis. Spectroscopic data are in agreement with the literature reported values.<sup>[17]</sup>

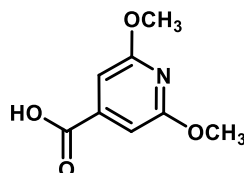
<sup>1</sup>H NMR (400 MHz, DMSO-*d*<sub>6</sub>)  $\delta = 7.86$  (s, 2H, PyrH);

LR-MS (ESI+)  $m/z$ : 192.1 [M+H]<sup>+</sup>;

Analytical HPLC (254 nm):  $t_R = 5.1$  min, 93%;

MP: 206.4 – 208.7 °C.

### 2,6-dimethoxyisonicotinic acid<sup>[18]</sup> (3.21)



Sodium metal (1.66 g, 72.3 mmol) was added portion-wise to ice-cold MeOH (15 mL, anhydrous) under an atmosphere of nitrogen. Once the sodium was dissolved, the resulting sodium methoxide solution was added to a flask containing **3.20** (3.47 g, 18.1 mmol) in DMF (20 mL, anhydrous) and the reaction was heated at 145 °C for 16 h. After this time, the reaction mixture was cooled to room temperature,

quenched with ice-cold water and acidified to pH 3 using a solution of HCl (4 M, aqueous). The resulting precipitate was collected by filtration, washed with water, and dried to give the title compound as a pale-yellow solid (3.12 g, 17.0 mmol, 94%).

$^1\text{H}$  NMR (400 MHz, DMSO- $d_6$ )  $\delta$  = 13.52 (br s, 1H, OH), 6.74 (s, 2H, PyrH), 3.88 (s, 6H, PyrOCH<sub>3</sub>);

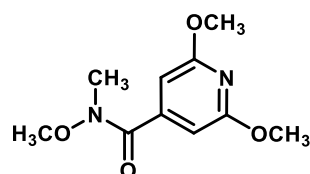
$^{13}\text{C}$  NMR (101 MHz, DMSO- $d_6$ )  $\delta$  = 165.7 (COOH), 163.3 (PyrC-OCH<sub>3</sub>), 144.2 (PyrC), 100.7 (PyrCH), 53.7 (PyrOCH<sub>3</sub>);

LR-MS (ESI+)  $m/z$ : 184.0 [M+H]<sup>+</sup>;

HR-MS (ESI+)  $m/z$  [M = C<sub>8</sub>H<sub>9</sub>NO<sub>4</sub>]: [M+H]<sup>+</sup> calc'd 184.0604, found 184.0605;

Analytical HPLC (254 nm):  $t_R$  = 5.0 min, 95%.

### ***N*,2,6-trimethoxy-*N*-methylisonicotinamide<sup>[19]</sup> (3.22)**



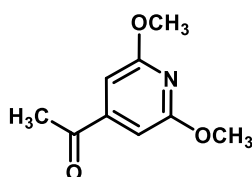
To a suspension of **3.21** (3.12 g, 17.0 mmol) in CH<sub>2</sub>Cl<sub>2</sub> (40 mL) was added 1,1'-carbonyldiimidazole (3.05 g, 18.7 mmol), and the resulting solution was stirred at room temperature for 1 h. After this time, *N*,*O*-dimethylhydroxylamine hydrochloride (1.83 g, 18.7 mmol) was added to the mixture and the reaction was left to stir at room temperature for 16 h. After this time, the reaction was quenched with NaOH (1 M, aqueous) and extracted with CH<sub>2</sub>Cl<sub>2</sub> (×2). The combined organic layers were dried over anhydrous MgSO<sub>4</sub>, filtered, and concentrated under reduced pressure. Purification by silica gel flash chromatography (0–30% EtOAc in Pet. Sp.) afforded the title compound as an off-white solid on standing (2.76 g, 12.2 mmol, 72%). Spectroscopic data are in agreement with the literature reported values.<sup>[20]</sup>

$^1\text{H}$  NMR (400 MHz, CDCl<sub>3</sub>)  $\delta$  = 6.46 (s, 2H, PyrH), 3.92 (s, 6H, Pyr-OCH<sub>3</sub>), 3.57 (br s, 3H, N-OCH<sub>3</sub>), 3.30 (s, 3H, NCH<sub>3</sub>);

LR-MS (ESI+)  $m/z$ : 226.9 [M+H]<sup>+</sup>;

Analytical HPLC (254 nm):  $t_R$  = 4.9 min, 95%.

### **1-(2,6-dimethoxypyridin-4-yl)ethan-1-one<sup>[21]</sup> (3.23)**



To an solution of **3.21** (634 mg, 2.38 mmol) in THF (5 mL, anhydrous) at 0 °C and under an atmosphere of nitrogen was added MeMgBr (1.40 mL, 3 M in diethyl ether, 4.20 mmol), dropwise. After stirring for 1 h, the reaction was quenched with the addition of an NH<sub>4</sub>Cl solution (saturated, aqueous), and the mixture extracted with EtOAc (×3). The combined organic fractions were then washed with brine, dried over anhydrous MgSO<sub>4</sub>, filtered, and concentrated under reduced pressure. Purification by silica gel flash chromatography (0–20% EtOAc in Pet. Sp.) afforded the title compound as a white solid (477 mg, 2.63 mmol, 94%). A portion of this product was further recrystallised from EtOH to give a pale-yellow crystals for melting point analysis. Spectroscopic data are in agreement with the literature reported values.<sup>[21]</sup>

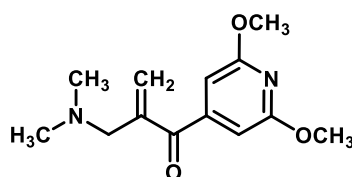
<sup>1</sup>H NMR (400 MHz, CDCl<sub>3</sub>) δ = 6.73 (s, 2H, PyrH), 3.95 (s, 6H, OCH<sub>3</sub>), 2.54 (s, 3H, (CO)CH<sub>3</sub>);

LR-MS (ESI+) *m/z*: 182.0 [M+H]<sup>+</sup>;

Analytical HPLC (254 nm): *t<sub>R</sub>* = 5.6 min, 99%;

MP: 65.8 – 67.2 °C.

**1-(2,6-dimethoxypyridin-4-yl)-2-((dimethylamino)methyl)prop-2-en-1-one<sup>[22,23]</sup> (3.25)**



To a microwave tube was added **3.23** (135 mg, 1.00 mmol), paraformaldehyde (39.0 mg, 1.30 mmol), dimethylamine hydrochloride (106 mg, 1.30 mmol), 1,4-dioxane (200 μL), and HCl (2.5 μL, concentrated), and the reaction was heated in a microwave reactor at 130 °C for 2 h. The reaction mixture was then partitioned between a solution of EtOAc and Na<sub>2</sub>CO<sub>3</sub> (10% aqueous), the layers separated, and the aqueous layer extracted with EtOAc (×3). The combined organic fractions were dried over anhydrous MgSO<sub>4</sub>, filtered, and concentrated under reduced pressure. Purification by silica gel flash chromatography (0–5% MeOH in CH<sub>2</sub>Cl<sub>2</sub>) afforded the title compound as an orange viscous oil (30.0 mg, 0.126 mmol, 13%).

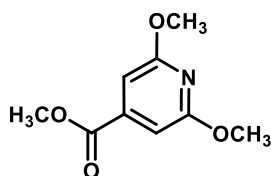
<sup>1</sup>H NMR (400 MHz, CDCl<sub>3</sub>) δ = 6.53 (s, 2H, PyrH), 6.07 (q, *J* = 1.2 Hz, 1H, C=CH<sub>2</sub>), 5.86 (d, *J* = 0.9 Hz, 1H, C=CH<sub>2</sub>), 3.94 (s, 6H, PyrOCH<sub>3</sub>), 3.28 (s, 2H, CH<sub>2</sub>N), 2.27 (s, 6H, N(CH<sub>3</sub>)<sub>2</sub>);

LR-MS (ESI+) *m/z*: 251.1 [M+H]<sup>+</sup>;

HR-MS (ESI+) *m/z* [M = C<sub>13</sub>H<sub>18</sub>N<sub>2</sub>O<sub>3</sub>]: [M+H]<sup>+</sup> calc'd 251.1390, found 251.1388;

Analytical HPLC (254 nm): *t<sub>R</sub>* = 4.2 min, 79%.



**Methyl 2,6-dimethoxyisonicotinate<sup>[24]</sup> (3.32)**

Step (i) – Pyridine methoxylation:

A solution of **3.20** (0.960 g, 5.00 mmol) and sodium methoxide (2.16 g, 40.0 mmol) in MeOH (20 mL, anhydrous) were heated in a microwave reactor at 145 °C for 4 h. After this time, the reaction mixture was cooled to room temperature and transferred into a round bottom flask with an additional 20 mL MeOH.

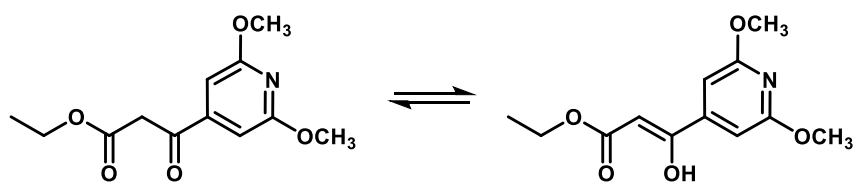
Step (ii) – Esterification:

The crude reaction mixture from step 1 was cooled to 0 °C, followed by the dropwise addition of concentrated H<sub>2</sub>SO<sub>4</sub> (1 mL, 18.8 mmol), and the reaction stirred at reflux for 6 h. After this time, the reaction was cooled to room temperature and concentrated under reduced pressure. The resulting residue was resuspended in CH<sub>2</sub>Cl<sub>2</sub> and slowly added to an ice cold solution of Na<sub>2</sub>CO<sub>3</sub> (saturated, aqueous). The mixture was filtered through a pad of Celite and the aqueous layer was extracted with CH<sub>2</sub>Cl<sub>2</sub> (×3). The combined organic phases were dried over anhydrous MgSO<sub>4</sub>, filtered, and concentrated under reduced pressure. Purification by silica gel flash chromatography (0–5% EtOAc in Pet. Sp.) afforded the title compound as a white solid (0.745 g, 3.78 mmol, 76%). A portion of this product was further recrystallised from EtOH to give colourless needles for melting point analysis. Spectroscopic data are in agreement with the literature reported values.<sup>[25]</sup>

<sup>1</sup>H NMR (400 MHz, CDCl<sub>3</sub>) δ = 6.85 (s, 2H, PyrH), 3.94 (s, 6H, PyrOCH<sub>3</sub>), 3.91 (s, 3H, (CO)OCH<sub>3</sub>);

LR-MS (ESI+) *m/z*: 198.0 [M+H]<sup>+</sup>;

MP: 72.8 – 73.6 °C.

**Ethyl 3-(2,6-dimethoxypyridin-4-yl)-3-oxopropanoate<sup>[26]</sup> (3.33)**

To a solution of **3.32** (2.22 g, 11.3 mmol) in EtOAc (81.5 mmol, 8 mL) and THF (20 mL, anhydrous) at –40 °C was added LiHMDS (33.7 mL, 1 M in THF, 33.7 mmol) and stirred at this temperature for 1 h.

After this time the reaction was quenched with acetic acid (1.30 mL, 22.5 mmol) and water 25 mL, basified with  $\text{NaHCO}_3$  (saturated, aqueous) and extracted with ethyl acetate ( $\times 3$ ). The combined organic extracts were washed with brine, dried over anhydrous  $\text{MgSO}_4$ , filtered, and concentrated under reduced pressure. Purification by silica gel flash chromatography (0–15%  $\text{Et}_2\text{O}$  in Pet. Sp.) afforded the title compound as a yellow crystalline semi-solid as a 52:48 mixture of keto-enol tautomers (2.18 g, 8.62 mmol, 77%).

Ketone peaks:

$^1\text{H}$  NMR (400 MHz,  $\text{CDCl}_3$ )  $\delta$  = 6.72 (s, 2H, PyrH), 4.21 (q,  $J$  = 7.2 Hz, 2H, CH<sub>2</sub>CH<sub>3</sub>), 3.95 (s, 6H, Pyr-OCH<sub>3</sub>), 3.89 (s, 2H, CH<sub>2</sub>CH<sub>3</sub>), 1.26 (t,  $J$  = 7.1 Hz, 3H, CH<sub>2</sub>CH<sub>3</sub>);

$^{13}\text{C}$  NMR (101 MHz,  $\text{CDCl}_3$ )  $\delta$  = 192.1 (Pyr-CO-CH<sub>2</sub>), 167.0 (CH<sub>2</sub>-CO-CH<sub>2</sub>), 164.3 (PyrC-OCH<sub>3</sub>), 147.8 (4-PyrC), 100.0 (PyrCH), 61.8 (CH<sub>2</sub>CH<sub>3</sub>), 54.1 (PyrOCH<sub>3</sub>), 46.4 (CO-CH<sub>2</sub>-CO), 14.18 (CH<sub>2</sub>CH<sub>3</sub>);

Enol peaks:

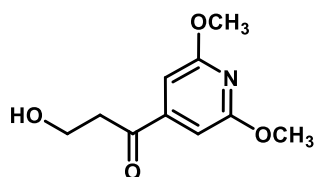
$^1\text{H}$  NMR (400 MHz,  $\text{CDCl}_3$ )  $\delta$  = 12.37 (s, 1H, OH), 6.62 (s, 2H, PyrH), 5.65 (s, 1H, CH=C-OH), 4.26 (q,  $J$  = 7.2 Hz, 2H, CH<sub>2</sub>CH<sub>3</sub>), 3.93 (s, 6H, Pyr-OCH<sub>3</sub>), 1.33 (t,  $J$  = 7.1 Hz, 3H, CH<sub>2</sub>CH<sub>3</sub>);

$^{13}\text{C}$  NMR (101 MHz,  $\text{CDCl}_3$ )  $\delta$  = 172.9 ((CO)O), 169.1 (C-OH), 163.9 (PyrC-OCH<sub>3</sub>), 146.4 (4-PyrC), 98.2 (PyrCH), 89.8 (CH=C-OH), 60.8 (CH<sub>2</sub>CH<sub>3</sub>), 53.9 (PyrOCH<sub>3</sub>), 14.4 (CH<sub>2</sub>CH<sub>3</sub>);

LR-MS (ESI+)  $m/z$ : 253.9  $[\text{M}+\text{H}]^+$ , 207.9  $[\text{M} - \text{CH}_3\text{CH}_2\text{O}]$ ;

HR-MS (ESI+)  $m/z$   $[\text{M} = \text{C}_{12}\text{H}_{15}\text{NO}_5]$ :  $[\text{M}+\text{H}]^+$  calc'd 254.1023, found 254.1023.

### 1-(2,6-dimethoxypyridin-4-yl)-3-hydroxypropan-1-one<sup>[26]</sup> (**3.36**)



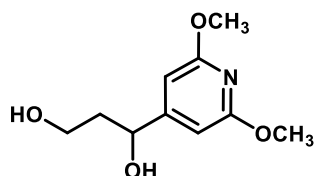
To a solution of **3.33** (507 mg, 2.00 mmol) in THF (4 mL, anhydrous) at 0 °C and under an atmosphere of nitrogen was added LiHMDS (2.00 mL, 1 M in THF, 2.00 mmol) dropwise. After stirring at this temperature for 30 min LAH (152 mg, 4.00 mmol) was added at 0 °C and stirred at this temperature for 4 h. The reaction was monitored by TLC. After completion of the reaction, the reaction mixture was quenched with EtOAc and cold water and the resulting solid was filtered through a pad of Celite with the aid of EtOAc. The filtrate was dried over anhydrous  $\text{MgSO}_4$ , filtered, and concentrated under reduced pressure. Purification by silica gel flash chromatography (0–30% Acetone in PhMe) afforded the title compound as a clear oil (64 mg, 0.303 mmol, 15%).

$^1\text{H}$  NMR (400 MHz,  $\text{CDCl}_3$ )  $\delta$  = 6.72 (s, 2H, PyrH), 3.99 (t,  $J$  = 5.4 Hz, 2H, CH<sub>2</sub>-OH), 3.94 (s, 6H, PyrOCH<sub>3</sub>), 3.13 (t,  $J$  = 5.4 Hz, 2H, CO-CH<sub>2</sub>), 2.53 (s, 1H, OH);

LR-MS (ESI+)  $m/z$ : 211.9  $[\text{M}+\text{H}]^+$ ;

HR-MS (ESI+)  $m/z$  [ $\text{M} = \text{C}_{10}\text{H}_{13}\text{NO}_4$ ]:  $[\text{M}+\text{H}]^+$  calc'd 212.0917, found 212.0917.

### 1-(2,6-dimethoxypyridin-4-yl)propane-1,3-diol (**3.35**)



By-product isolated from synthesis of **3.36** as a yellow oil (0.121 g, 0.567 mmol, 28%).

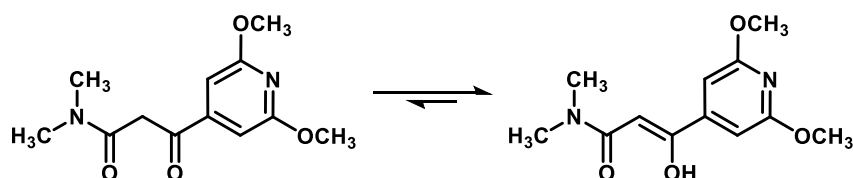
$^1\text{H}$  NMR (400 MHz,  $\text{CDCl}_3$ )  $\delta$  = 6.30 (d,  $J$  = 0.6 Hz, 2H, PyrH), 4.86 (dd,  $J$  = 7.6, 4.4 Hz, 1H, Pyr-CH-OH), 3.90 (s, 6H, PyrOCH<sub>3</sub>), 3.87 – 3.82 (m, 2H, CH<sub>2</sub>OH), 3.32 (br s, 1H, Pyr-CH-OH), 2.45 (br s, 1H, CH<sub>2</sub>OH), 1.97 – 1.88 (m, 2H, CH<sub>2</sub>C(OH)Pyr);

$^{13}\text{C}$  NMR (101 MHz,  $\text{CDCl}_3$ )  $\delta$  = 163.6 (PyrC-OCH<sub>3</sub>), 159.1 (4-PyrC), 98.0 (PyrCH), 73.1 (Pyr-CH-OH), 61.3 (CH<sub>2</sub>OH), 53.7 (PyrOCH<sub>3</sub>), 39.8 (CH<sub>2</sub>C(OH)Pyr);

LR-MS (ESI+)  $m/z$ : 214.0  $[\text{M}+\text{H}]^+$ ;

HR-MS (ESI+)  $m/z$  [ $\text{M} = \text{C}_{10}\text{H}_{15}\text{NO}_4$ ]:  $[\text{M}+\text{H}]^+$  calc'd 214.1074, found 214.1075.

### 3-(2,6-Dimethoxypyridin-4-yl)-*N,N*-dimethyl-3-oxopropanamide<sup>[27]</sup> (**3.39**)



To a solution of anhydrous diisopropylamine (5.93 mL, 42.0 mmol) in THF (100 mL, anhydrous) at  $-78^\circ\text{C}$  and under an atmosphere of nitrogen was slowly added *n*-BuLi (29.1 mL, 1.34 M in hexanes, 39.0 mmol). The mixture was stirred at  $-78^\circ\text{C}$  for 1 h, after which *N,N*-dimethylacetamide (3.07 mL, 33.0 mmol) was added dropwise. The reaction mixture was kept stirring at  $-78^\circ\text{C}$  for 1 h, followed by the dropwise addition of a solution of **3.32** (5.92 g, 30.0 mmol) in THF (30 mL, anhydrous). The resulting yellow solution was reacted for an additional 1 h, followed by the addition of an  $\text{NH}_4\text{Cl}$  solution (saturated, aqueous) to quench the reaction. The reaction mixture was diluted with additional THF, and the organic phase was separated. The aqueous phase was saturated with NaCl and extracted with THF ( $\times 5$ ). The combined organic layers were dried over anhydrous  $\text{MgSO}_4$ , filtered, and concentrated under reduced pressure. Purification by silica gel flash chromatography (0–10% MeOH in  $\text{CH}_2\text{Cl}_2$ )

afforded the title compound as a pale-yellow solid as a *ca.* 1:4 mixture of keto-enol tautomers (6.72 g, 26.7 mmol, 89%).

Ketone peaks:

$^1\text{H}$  NMR (400 MHz,  $\text{CDCl}_3$ )  $\delta$  = 6.77 (s, 2H, PyrH), 4.00 (s, 2H, CH<sub>2</sub>CO), 3.95 (s, 6H, PyrOCH<sub>3</sub>), 3.02 (s, 3H, N(CH<sub>3</sub>)<sub>2</sub>), 2.99 (s, 3H, N(CH<sub>3</sub>)<sub>2</sub>);

$^{13}\text{C}$  NMR (101 MHz,  $\text{CDCl}_3$ )  $\delta$  = 193.5 (Pyr-CO-CH<sub>2</sub>), 166.6 (CO-N(CH<sub>3</sub>)<sub>2</sub>), 164.3 (PyrC-OCH<sub>3</sub>), 100.1 (PyrCH), 54.1 (PyrOCH<sub>3</sub>), 46.1 (CH<sub>2</sub>CO), 38.1 (N(CH<sub>3</sub>)<sub>2</sub>), 35.7 (N(CH<sub>3</sub>)<sub>2</sub>), missing 1  $\times$  PyrC;

Enol peaks:

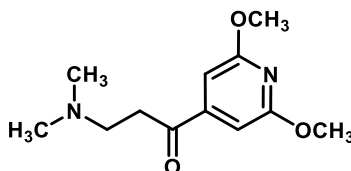
$^1\text{H}$  NMR (400 MHz,  $\text{CDCl}_3$ )  $\delta$  = 15.21 (s, 1H, OH), 6.64 (s, 2H, PyrH), 5.79 (s, 1H, COH=CH), 3.94 (s, 6H, PyrOCH<sub>3</sub>), 3.06 (br. s, 6H, N(CH<sub>3</sub>)<sub>2</sub>);

$^{13}\text{C}$  NMR (101 MHz,  $\text{CDCl}_3$ )  $\delta$  = 172.0 (CO-N(CH<sub>3</sub>)<sub>2</sub>), 169.0 (C-OH), 163.8 (PyrC-OCH<sub>3</sub>), 148.1 (4-PyrC), 98.1 (PyrCH), 86.7 (COH=CH), 53.9 (PyrOCH<sub>3</sub>), 37.2<sup>†</sup> (N(CH<sub>3</sub>)<sub>2</sub>), 35.1<sup>†</sup> (N(CH<sub>3</sub>)<sub>2</sub>);

LR-MS (ESI<sup>+</sup>)  $m/z$ : 253.0  $[\text{M}+\text{H}]^+$ , 208.0  $[\text{M} - \text{N}(\text{CH}_3)_2]$ , 275.0  $[\text{M} + \text{Na}]^+$ ;

HR-MS (ESI<sup>+</sup>)  $m/z$   $[\text{M} = \text{C}_{12}\text{H}_{16}\text{N}_2\text{O}_4]$ :  $[\text{M}+\text{H}]^+$  calc'd 253.1183, found 253.1183.

### 1-(2,6-Dimethoxypyridin-4-yl)-3-(dimethylamino)propan-1-one (**3.03**)



#### Method 1 (Scheme 3.12)

##### Step (ii) – Reduction:

A solution of **3.39** (3.00 g, 11.89 mmol) in THF (15 mL, anhydrous) was added dropwise to a vigorously stirred suspension of LAH in THF (20 mL, anhydrous) at  $-10\text{ }^\circ\text{C}$  and under an atmosphere of nitrogen. The reaction mixture was warmed to room temperature and stirred for 4 h. Upon completion, the reaction mixture was cooled to  $-10\text{ }^\circ\text{C}$  and treated sequentially with the dropwise addition of  $\text{H}_2\text{O}$  (1.5 mL), NaOH (1.5 mL, 4 M, aqueous) and  $\text{H}_2\text{O}$  (4.5 mL). The mixture was warmed to room temperature, stirred for 15 min, dried over  $\text{Na}_2\text{SO}_4$  for 30 min, filtered, and concentrated under reduced pressure to give 2.78 g of a viscous orange oil as a 65:35 mixture of alcohol to ketone which was carried onto the next step without further purification.

## Step (ii) – Oxidation

To a flask containing the crude mixture of alcohol and ketone was added  $\text{CH}_2\text{Cl}_2$  (30 mL) and  $\text{BaMnO}_4$  (20.8 g, 80.98 mmol). The reaction stirred at room temperature and monitored by TLC. After 18 h, the reaction mixture was filtered through a pad of Celite with the aid of MeOH, and the filtrate concentrated under reduced pressure. Purification of the crude mixture by silica gel flash chromatography (0–10% MeOH in  $\text{CH}_2\text{Cl}_2$ ) afforded the title compound as a yellow oil (1.14 g, 4.78 mmol, 41%).

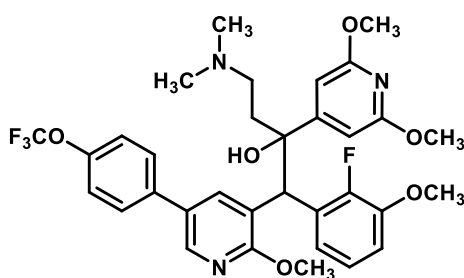
Method 2<sup>[28]</sup> (Scheme 3.21)

To a flask containing **3.39** in  $\text{CH}_2\text{Cl}_2$  (12.5 mL) was added  $\text{BPh}_3$  (0.121 mg, 0.500 mmol) and TMS (1.80 mL, 10.0 mmol). The reaction was stirred at room temperature and monitored by TLC. After 1 h, the solvent was removed under reduced pressure, and purification of the crude mixture by silica gel flash chromatography (0–2% MeOH/1%  $\text{Et}_3\text{N}$  in  $\text{CH}_2\text{Cl}_2$ ) afforded the title compound as a yellow oil (0.911 g, 4.16 mmol, 83%). Spectroscopic data are in agreement with the literature reported values.<sup>[20]</sup>

$^1\text{H}$  NMR (400 MHz,  $\text{CDCl}_3$ )  $\delta$  = 6.73 (s, 2H, PyrH), 3.94 (s, 6H, PyrOCH<sub>3</sub>), 3.06 (t,  $J$  = 7.2 Hz, 2H, CH<sub>2</sub>), 2.73 (t,  $J$  = 7.2 Hz, 2H, CH<sub>2</sub>), 2.27 (s, 6H, N(CH<sub>3</sub>)<sub>2</sub>);

LR-MS (ESI+)  $m/z$ : 239.0  $[\text{M}+\text{H}]^+$ .

**4-(dimethylamino)-1-(2-fluoro-3-methoxyphenyl)-1-(2-methoxy-5-(4-(trifluoromethoxy)phenyl)pyridin-3-yl)-2-(2-methoxy-6-methylpyridin-4-yl)butan-2-ol (3.02)**



To a solution of 2,2,6,6-tetramethylpiperidine (0.430 mL, 2.54 mmol, anhydrous) in THF (6 mL, anhydrous) at  $-10\text{ }^\circ\text{C}$  and under an atmosphere of nitrogen was added  $n\text{-BuLi}$  (2.10 mL, 1.14 M in hexanes, 2.38 mmol), dropwise. The mixture was stirred at  $-10\text{ }^\circ\text{C}$  for 1 h. Following this time, the mixture was cooled to  $-78\text{ }^\circ\text{C}$ , and a solution of **3.04** (647 mg, 1.59 mmol) in THF (3 mL, anhydrous) was added dropwise to give a deep rust coloured solution. The reaction mixture was kept stirring at  $-78\text{ }^\circ\text{C}$  for 1.5 h, after which a solution of **3.03** (454 mg, 1.91 mmol) in THF (3 mL, anhydrous) was added dropwise. The mixture was stirred at  $-78\text{ }^\circ\text{C}$  for 4 h, and upon completion the reaction was quenched with an  $\text{NH}_4\text{Cl}$  solution (saturated, aqueous) and diluted with EtOAc. The organic phase was

separated, and the aqueous layer extracted with EtOAc (×3). The combined organic layers were washed with brine, dried over anhydrous MgSO<sub>4</sub>, filtered, and concentrated under reduced pressure. Purification by silica gel flash chromatography (0–40% Acetone in PhMe) afforded the title compound as a 1:1 mixture of diastereomers (252 mg, 0.390 mmol, 25%).

Diastereomer B was further subjected to chiral purification by our collaborators at TCG Lifesciences using HPLC to isolate the individual enantiomers. Isocratic elution was used with a solvent system of Hexane/IPA/CH<sub>2</sub>Cl<sub>2</sub>/diethylamine (80/10/10/0.1) over 10 min with a flow rate of 1 mL/min.

LR-MS (ESI+) *m/z*: 645.8 [M+H]<sup>+</sup>;

HR-MS (ESI+) *m/z* [M = C<sub>33</sub>H<sub>35</sub>F<sub>4</sub>N<sub>3</sub>O<sub>6</sub>]: [M+H]<sup>+</sup> calc'd 646.2535, found 646.2538;

Diastereomer A:

<sup>1</sup>H NMR (401 MHz, CDCl<sub>3</sub>) δ = 12.29 (br s, 1H, NH<sup>+</sup>), 8.63 (d, *J* = 2.5 Hz, 1H, PyrH), 8.06 (d, *J* = 2.4 Hz, 1H, PyrH), 7.44 (d, *J* = 8.7 Hz, 2H, PhH-OCF<sub>3</sub>), 7.28 (d, *J* = 8.0 Hz, 2H, PhH-OCF<sub>3</sub>), 7.03 – 6.92 (m, 2H, Ph'H), 6.86 (td, *J* = 8.0, 1.7 Hz, 1H, Ph'H), 6.54 (br s, 2H, Pyr'H), 5.25 (s, 1H, Pyr-CH-Ph'), 3.89 (s, 3H, Ph'OCH<sub>3</sub>), 3.84 (s, 9H, PyrOCH<sub>3</sub>), 3.34 (t, *J* = 11.1 Hz, 1H, CH<sub>2</sub>CHHN), 2.65 (s, 3H, NCH<sub>3</sub>), 2.63 (s, 3H, NCH<sub>3</sub>), 2.38 – 2.21 (m, 2H, CHHCHHN), 2.05 (t, *J* = 10.9 Hz, 1H, CHHCH<sub>2</sub>N);

<sup>13</sup>C NMR (101 MHz, CDCl<sub>3</sub>) δ = 163.8, 160.9, 158.7, 151.1 (d, *J* = 243.1 Hz), 148.7 (q, *J* = 1.4 Hz), 147.4 (d, *J* = 12.1 Hz), 142.3, 138.1, 137.0, 128.6, 128.2, 125.5 (d, *J* = 12.0 Hz), 124.2 (d, *J* = 4.5 Hz), 123.5, 123.0 (d, *J* = 2.0 Hz), 121.6, 120.7 (q, *J* = 257.1 Hz), 112.2, 98.4, 77.0, 56.2, 54.2, 53.7, 53.6, 45.1, 43.3, 41.4, 37.1;

Analytical HPLC (254 nm): *t*<sub>R</sub> = 7.4 min, 98%;

Diastereomer B:

<sup>1</sup>H NMR (400 MHz, CDCl<sub>3</sub>) δ = 12.19 (br s, 1H, NH<sup>+</sup>), 8.14 (s, 1H, PyrH), 7.85 (d, *J* = 2.3 Hz, 1H, PyrH), 7.63 (t, *J* = 6.8 Hz, 1H, Ph'H), 7.45 (d, *J* = 8.6 Hz, 2H, PhH-OCF<sub>3</sub>), 7.16 (d, *J* = 8.1 Hz, 2H, PhH-OCF<sub>3</sub>), 6.77 (t, *J* = 7.7 Hz, 1H, Ph'H), 6.57 (t, *J* = 7.9 Hz, 1H, Ph'H), 6.45 (br s, 2H, Pyr'H), 5.31 (s, 1H, Pyr-CH-Ph'), 4.03 (s, 3H, PyrOCH<sub>3</sub>), 3.79 (s, 6H, Pyr'OCH<sub>3</sub>), 3.64 (s, 3H, Ph'OCH<sub>3</sub>), 3.21 (t, *J* = 11.2 Hz, 1H, CH<sub>2</sub>CHHN), 2.57 (s, 3H, NCH<sub>3</sub>), 2.52 (s, 3H, NCH<sub>3</sub>), 2.44 – 2.30 (m, 1H, CHHCH<sub>2</sub>N), 2.19 (s, 1H, CH<sub>2</sub>CHHN), 2.00 (t, *J* = 11.1 Hz, 1H, CHHCH<sub>2</sub>N);

<sup>13</sup>C NMR (101 MHz, CDCl<sub>3</sub>) δ = 163.7, 161.4, 158.7, 150.4 (d, *J* = 244.3 Hz), 148.8 (q, *J* = 1.4 Hz), 147.2 (d, *J* = 11.5 Hz), 143.6, 140.0, 136.9, 130.0, 128.9 (d, *J* = 11.1 Hz), 128.7, 123.5 (d, *J* = 4.6 Hz), 121.6, 121.3, 120.7 (q, *J* = 257.1 Hz, CF<sub>3</sub>), 111.5, 98.5, 77.4, 56.1, 54.5, 53.7, 53.7, 45.1, 43.0, 41.2, 37.0;

Analytical HPLC (254 nm): *t*<sub>R</sub> = 7.4 min, 99%;

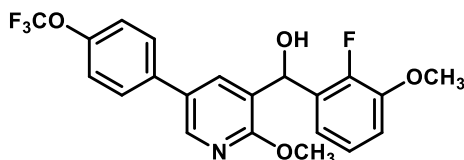
Enantiomer B1:

Chiral HPLC (260 nm):  $t_R$  = 3.5 min, 100%;

Enantiomer B2:

Chiral HPLC (260 nm):  $t_R$  = 4.5 min, 99%.

**(2-fluoro-3-methoxyphenyl)(2-methoxy-5-(4-(trifluoromethoxy)phenyl)pyridin-3-yl)methanol**  
**(3.13)**



By-product isolated from synthesis of **3.02** as an orange oil (0.227 g, 0.536 mmol, 34%).

$^1\text{H}$  NMR (400 MHz,  $\text{CDCl}_3$ )  $\delta$  = 8.29 (d,  $J$  = 2.5 Hz, 1H, PyrH), 7.85 – 7.79 (m, 1H, PyrH), 7.50 (d,  $J$  = 8.7 Hz, 2H, PhH- $\text{OCF}_3$ ), 7.30 – 7.24 (m, 2H, PhH- $\text{OCF}_3$ ), 7.08 (td,  $J$  = 8.0, 1.4 Hz, 1H, Ph'H), 7.00 (ddd,  $J$  = 7.9, 6.0, 1.7 Hz, 1H, Ph'H), 6.92 (td,  $J$  = 8.1, 1.7 Hz, 1H, Ph'H), 6.31 (s, 1H, Pyr-CH-Ph'), 4.53 (s, 1H, OH), 4.01 (s, 3H, PyrOCH<sub>3</sub>), 3.88 (s, 3H, Ph'OCH<sub>3</sub>);

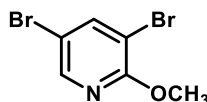
$^{13}\text{C}$  NMR (101 MHz,  $\text{CDCl}_3$ )  $\delta$  = 160.5 (PyrC- $\text{OCH}_3$ ), 150.0 (d,  $J$  = 246.9 Hz, Ph'CF), 149.0 (q,  $J$  = 1.8 Hz, PhC- $\text{OCF}_3$ ), 147.8 (d,  $J$  = 10.8 Hz, Ph'C- $\text{OCH}_3$ ), 143.6 (6-PyrCH), 136.6 (Ph'C-Pyr), 135.3 (4-PyrCH), 129.8 (d,  $J$  = 10.8 Hz, Ph'C), 129.4 (PyrC), 128.3 (PhCH), 125.4 (PyrC), 124.12 (d,  $J$  = 4.7 Hz, Ph'CH), 121.6 (PhCH), 119.4 (d,  $J$  = 2.7 Hz, PhCH), 113.0 (d,  $J$  = 2.1 Hz, PhCH), 65.9 (d,  $J$  = 4.6 Hz, Pyr-CH-Ph') 56.4 (Ph'OCH<sub>3</sub>), 54.2 (PyrOCH<sub>3</sub>), missing  $\text{OCF}_3$ ;

LR-MS (ESI+)  $m/z$ : 423.8  $[\text{M}+\text{H}]^+$ ;

HR-MS (ESI+)  $m/z$   $[\text{M} = \text{C}_{21}\text{H}_{17}\text{F}_4\text{NO}_4]$ :  $[\text{M}+\text{H}]^+$  calc'd 424.1166, found 424.1169;

Analytical HPLC (254 nm):  $t_R$  = 7.5 min, 91%.

**3,5-dibromo-2-methoxypyridine<sup>[29]</sup> (3.42)**



To a solution of 2-methoxypyridine (3.27 g, 30.0 mmol) in acetic acid (20 mL) was slowly added sodium acetate (4.92 g, 60.0 mmol) to prevent the formation of lumps. This was followed by the addition of  $\text{Br}_2$  (5.41 mL, 105 mmol) at a rate which ensured the temperature remained below 35 °C. After this addition, the reaction mixture was heated to 80 °C and stirred for 5 h, followed by cooling to room temperature and stirring for an additional 15 h. After this time, the reaction was quenched with an

addition of water (30 mL), extracted with Et<sub>2</sub>O (×3) and the combined organic fractions were washed with NaOH (1 M, aqueous), Na<sub>2</sub>S<sub>2</sub>O<sub>3</sub> (saturated, aqueous) and brine. The organic phase was then dried over MgSO<sub>4</sub>, filtered, and concentrated under reduced pressure. Purification by silica gel flash chromatography (0–8% Et<sub>2</sub>O in Pet. Sp.) afforded the title compound pale-yellow solid (3.43 g, 12.8 mmol, 43%). A portion of this product was further recrystallised from EtOH to give short colourless needles for melting point analysis. Spectroscopic data are in agreement with the literature reported values.<sup>[29]</sup>

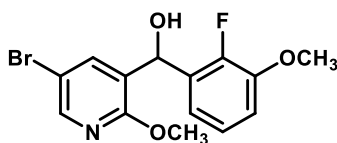
<sup>1</sup>H NMR (400 MHz, CDCl<sub>3</sub>) δ = 8.13 (d, *J* = 2.2 Hz, 1H, 6-PyrH), 7.92 (d, *J* = 2.2 Hz, 1H, 4-PyrH), 3.99 (s, 3H, PyrOCH<sub>3</sub>);

LR-MS (ESI+) *m/z*: 267.9 [M+H]<sup>+</sup>;

Analytical HPLC (254 nm): *t*<sub>R</sub> = 6.4 min, 98%;

MP: 49.5 – 50.8 °C.

**(5-Bromo-2-methoxypyridin-3-yl)(2-fluoro-3-methoxyphenyl)methanol (3.44)**



**Method 1 (Scheme 3.15)**

To a solution of 2,2,6,6-tetramethylpiperidine (0.200 mL, 2.60 mmol, anhydrous) in THF (2 mL, anhydrous) at –10 °C and under an atmosphere of nitrogen was added *n*-BuLi (1.70 mL, 1.30 M in hexanes, 2.20 mmol), dropwise. The mixture was stirred at –10 °C for 0.5 h. Following this time, the mixture was cooled to –78 °C, and a solution of **3.05** (376 mg, 2.00 mmol) in THF (3 mL, anhydrous) was added dropwise over 5 min. The reaction mixture was kept stirring at –78 °C for 1.5 h, after which a solution of 2-fluoro-3-methoxybenzaldehyde (370 mg, 2.40 mmol) in THF (3 mL, anhydrous) was added dropwise over 10 min. The mixture was stirred at –78 °C for a total of 3.5 h. After this time, the reaction was quenched with an NH<sub>4</sub>Cl solution (saturated, aqueous) and diluted with EtOAc, the organic phase separated, and the aqueous layer extracted with EtOAc (×3). The combined organic layers were washed with brine, dried over anhydrous MgSO<sub>4</sub>, filtered, and concentrated under reduced pressure. Purification by silica gel flash chromatography (0–40% EtOAc in Pet. Sp.) afforded the title compound a pale-yellow viscous oil which solidified on standing (108 mg, 0.316 mmol, 16%).



Method 2 (**Scheme 3.17**)<sup>[29]</sup>

To a solution of **3.42** (1.33 g, 5.00 mmol) in THF (10 mL, anhydrous) at  $-78\text{ }^{\circ}\text{C}$  and under an atmosphere of nitrogen was added *n*-BuLi (3.50 mL, 1.57 M in hexanes, 5.50 mmol) dropwise over 15 min, and the reaction was stirred at this temperature for 1 h. After this time, a solution of 2-fluoro-3-methoxybenzaldehyde (0.848 g, 5.50 mmol) in THF (4 mL, anhydrous) was added dropwise over 25 min, and the reaction mixture was stirred  $-78\text{ }^{\circ}\text{C}$  for 0.5 h and then slowly allowed to warm to room temperature over 1 h. The reaction was quenched with a solution of  $\text{NH}_4\text{Cl}$  (saturated, aqueous), the organic phase separated and the aqueous phase extracted with EtOAc ( $\times 3$ ). The combined organic layers were washed with brine, dried over anhydrous  $\text{MgSO}_4$ , filtered, and concentrated under reduced pressure. Purification by silica gel flash chromatography (0–35%  $\text{Et}_2\text{O}$  in PhMe) afforded the title compound as a pale-yellow viscous oil (70 mg, 1.90 mmol, 5%).

Method 3 (**Scheme 3.18**)<sup>[30]</sup>

To a solution of **3.42** (8.01 g, 30.0 mmol) in THF (60 mL, anhydrous) at  $-78\text{ }^{\circ}\text{C}$  and under an atmosphere of nitrogen was added *i*-PrMgCl $\cdot$ LiCl (42.7 mL, 0.84 M in THF, 36.0 mmol) dropwise, and the reaction was stirred at this temperature for 2 h. After this time, a solution of 2-fluoro-3-methoxybenzaldehyde (6.94 g, 45.0 mmol) in THF (25 mL, anhydrous) was added dropwise, and the reaction mixture was stirred  $-78\text{ }^{\circ}\text{C}$  for an additional 2.5 h. The reaction was quenched with a solution of  $\text{NH}_4\text{Cl}$  (saturated, aqueous), the organic phase separated and the aqueous phase extracted with EtOAc ( $\times 3$ ). The combined organic layers were washed with brine, dried over anhydrous  $\text{MgSO}_4$ , filtered, and concentrated under reduced pressure. Purification by silica gel flash chromatography (0–20% EtOAc in Pet. Sp.) afforded the title compound as a viscous oil which solidified to a white solid on standing (4.65 g, 13.6 mmol, 45%). A small portion of crystals were isolated from slow evaporation of a single column chromatography fraction to give colourless rocks which were used for melting point analysis.

$^1\text{H}$  NMR (400 MHz,  $\text{CDCl}_3$ )  $\delta$  = 8.12 (d,  $J$  = 2.4 Hz, 1H, 6-PyrH), 7.66 (dt,  $J$  = 2.4, 0.8 Hz, 1H, 4-PyrH), 7.08 (td,  $J$  = 8.0, 1.5 Hz, 1H, PhH), 6.98 – 6.90 (m, 2H, PhH), 6.22 (s, 1H, CH-OH), 3.92 (s, 3H, PyrOCH<sub>3</sub>), 3.89 (s, 3H, PhOCH<sub>3</sub>), 3.01 (br s, 1H, OH);

$^{13}\text{C}$  NMR (101 MHz,  $\text{CDCl}_3$ )  $\delta$  = 159.8 (PyrC-OCH<sub>3</sub>), 149.92 (d,  $J$  = 247.0 Hz, CF), 147.72 (d,  $J$  = 10.8 Hz, PhC-OCH<sub>3</sub>), 146.5 (6-PyrCH), 138.4 (d,  $J$  = 1.4 Hz, 4-PyrCH), 129.36 (d,  $J$  = 10.7 Hz, PhC-COH), 126.9 (3-PyrC), 124.2 (d,  $J$  = 4.6 Hz, PhCH), 119.3 (d,  $J$  = 2.8 Hz, PhCH), 113.0 (d,  $J$  = 2.0 Hz, PhCH), 112.2 (5-PyrC-Br), 65.1 (d,  $J$  = 4.8 Hz, CH-OH), 56.4 (PhOCH<sub>3</sub>), 54.0 (PyrOCH<sub>3</sub>);

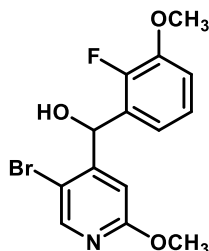
LR-MS (ESI+)  $m/z$ : 341.9/343.8 [ $\text{M}+\text{H}$ ]<sup>+</sup>;

HR-MS (ESI+)  $m/z$  [ $\text{M} = \text{C}_{14}\text{H}_{13}\text{BrFNO}_3$ ]: [ $\text{M}+\text{H}$ ]<sup>+</sup> calc'd 342.0136, found 342.0138;

Analytical HPLC (254 nm):  $t_R$  = 6.1 min, 95%;

MP: 110.0 – 111.5 °C.

**(5-bromo-2-methoxypyridin-4-yl)(2-fluoro-3-methoxyphenyl)methanol (3.47)**



By-product isolated from synthesis of **3.44** (Method 1) as an off-white powder (0.402 g, 1.17 mmol, 59%). A small portion of crystals were isolated from slow evaporation of a single column chromatography fraction to give colourless cubes which were used for melting point analysis.

By-product isolated from synthesis of **3.44** (Method 2) as a pale-yellow crystalline solid (0.213 g, 0.623 mmol, 12%).

$^1\text{H}$  NMR (400 MHz,  $\text{CDCl}_3$ )  $\delta$  = 8.16 (d,  $J$  = 0.5 Hz, 1H, 6-PyrH), 7.08 (s, 1H, 3-PyrH), 7.02 (td,  $J$  = 8.0, 1.5 Hz, 1H, PhH), 6.93 (td,  $J$  = 8.1, 1.6 Hz, 1H, PhH), 6.70 (ddd,  $J$  = 7.9, 6.1, 1.6 Hz, 1H, PhH), 6.26 (d,  $J$  = 3.4 Hz, 1H, CHOH), 3.92 (s, 3H, PyrOCH<sub>3</sub>), 3.89 (s, 3H, PhOCH<sub>3</sub>), 2.65 (d,  $J$  = 4.1 Hz, 1H, OH);

$^{13}\text{C}$  NMR (101 MHz,  $\text{CDCl}_3$ )  $\delta$  = 164.1 (PyrC-OCH<sub>3</sub>), 152.2 (4-PyrC), 150.6 (d,  $J$  = 248.1 Hz, CF), 148.6 (6-PyrCH), 147.87 (d,  $J$  = 10.7 Hz, PhC-OCH<sub>3</sub>), 128.6 (d,  $J$  = 11.4 Hz, PhC-COH), 124.32 (d,  $J$  = 4.7 Hz, PhCH), 119.8 (d,  $J$  = 2.6 Hz, PhCH), 113.6 (d,  $J$  = 2.2 Hz, PhCH), 111.9 (5-PyrC), 110.6 (3-PyrCH), 68.2 (d,  $J$  = 5.1 Hz, CHOH), 56.5 (PhOCH<sub>3</sub>), 54.0 (PyrOCH<sub>3</sub>);

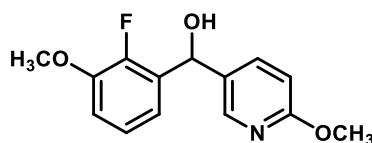
LR-MS (ESI+)  $m/z$ : 341.9/343.9 [ $\text{M}+\text{H}$ ]<sup>+</sup>;

HR-MS (ESI+)  $m/z$  [ $\text{M} = \text{C}_{14}\text{H}_{13}\text{BrFNO}_3$ ]: [ $\text{M}+\text{H}$ ]<sup>+</sup> calc'd 342.0136, found 342.0141;

Analytical HPLC (254 nm):  $t_R$  = 5.6 min, 99%;

MP: 143.1 – 145.1 °C.

**(2-fluoro-3-methoxyphenyl)(6-methoxypyridin-3-yl)methanol (3.50)**



By-product isolated from synthesis of **3.44** (Method 2) as a light-brown oil (0.500 g, 1.90 mmol, 38%).

$^1\text{H}$  NMR (400 MHz,  $\text{CDCl}_3$ )  $\delta$  = 8.18 (d,  $J$  = 2.4 Hz, 1H, 2-PyrH), 7.60 (dd,  $J$  = 8.6, 2.5 Hz, 1H, 4-PyrH), 7.13 – 7.06 (m, 2H, 5,6-PhH), 6.94 – 6.87 (m, 1H, 4-PhH), 6.70 (d,  $J$  = 8.5 Hz, 1H, 5-PyrH), 6.13 (s, 1H, CHOH), 3.92 (s, 3H, PyrOCH<sub>3</sub>), 3.86 (s, 3H, PhOCH<sub>3</sub>), 2.39 (s, 1H, OH);

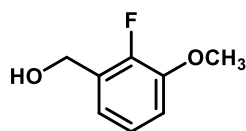
$^{13}\text{C}$  NMR (101 MHz,  $\text{CDCl}_3$ )  $\delta$  = 163.8 (PyrC-OCH<sub>3</sub>), 149.6 (d,  $J$  = 245.9 Hz, CF), 147.8 (d,  $J$  = 10.5 Hz, PhC-OCH<sub>3</sub>), 145.1 (2-PyrCH), 137.5 (4-PyrCH), 131.6 (d,  $J$  = 10.3 Hz, 1-PhC), 131.3 (3-PyrC), 124.4 (d,  $J$  = 4.7 Hz, PhH), 118.4 (d,  $J$  = 3.0 Hz, PhH), 112.8 (d,  $J$  = 1.9 Hz, 4-PyrCH), 111.0 (5-PyrCH), 67.9 (d,  $J$  = 4.6 Hz, CHOH), 56.4 (PhOCH<sub>3</sub>), 53.8 (PyrOCH<sub>3</sub>);

LR-MS (ESI+)  $m/z$ : 263.9  $[\text{M}+\text{H}]^+$ ;

HR-MS (ESI+)  $m/z$   $[\text{M} = \text{C}_{14}\text{H}_{14}\text{FNO}_3]$ :  $[\text{M}+\text{H}]^+$  calc'd 264.1030, found 264.1038;

Analytical HPLC (254 nm):  $t_R$  = 4.1 min, 93%.

### (2-fluoro-3-methoxyphenyl)methanol (**3.52**)



By-product isolated from synthesis of **3.44** (Method 3). A portion of this product was further recrystallised from  $\text{Et}_2\text{O}$  to give an off-white needles for melting point analysis. Spectroscopic data are in agreement with the reported literature values.<sup>[31]</sup>

$^1\text{H}$  NMR (400 MHz,  $\text{CDCl}_3$ )  $\delta$  = 7.07 (td,  $J$  = 7.9, 1.4 Hz, 1H, PhH), 7.02 – 6.97 (m, 1H, PhH), 6.91 (td,  $J$  = 8.2, 1.8 Hz, 1H, PhH), 4.76 (d,  $J$  = 1.3 Hz, 2H, CH<sub>2</sub>OH), 3.88 (s, 3H, OCH<sub>3</sub>), 1.89 (s, 1H, OH);

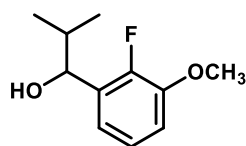
$^{13}\text{C}$  NMR (101 MHz,  $\text{CDCl}_3$ )  $\delta$  = 150.4 (d,  $J$  = 245.4 Hz, CF), 147.7 (d,  $J$  = 10.7 Hz, PhC-OCH<sub>3</sub>), 128.9 (d,  $J$  = 12.1 Hz, PhC-CH<sub>2</sub>), 124.2 (d,  $J$  = 4.7 Hz, PhCH), 120.6 (d,  $J$  = 3.3 Hz, PhCH), 113.0 (d,  $J$  = 2.0 Hz, PhCH), 59.4 (d,  $J$  = 5.4 Hz, CH<sub>2</sub>OH), 56.5 (OCH<sub>3</sub>);

LR-MS (ESI+)  $m/z$ : mass not found;

Analytical HPLC (254 nm):  $t_R$  = 3.7 min, 90%;

MP: 54.5 – 57.0 °C.

### 1-(2-fluoro-3-methoxyphenyl)-2-methylpropan-1-ol (**3.53**)

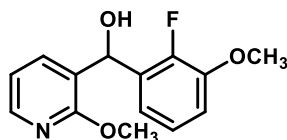


By-product isolated from synthesis of **3.44** (Method 3).

$^1\text{H}$  NMR (401 MHz,  $\text{CDCl}_3$ )  $\delta$  = 7.12 – 6.84 (m, 1H, PhH), 4.73 (dd,  $J$  = 7.0, 4.6 Hz, 1H, CHOH), 3.88 (s, 3H, OCH<sub>3</sub>), 2.00 (m, 1H, CH-(CH<sub>3</sub>)<sub>2</sub>), 1.85 (dd,  $J$  = 4.6, 0.9 Hz, 1H, OH), 1.02 (d,  $J$  = 6.4 Hz, 1H, CHCH<sub>3</sub>), 0.85 (dd,  $J$  = 6.8, 0.9 Hz, 1H, CHCH<sub>3</sub>);

LR-MS (ESI+)  $m/z$ : mass not found.

**(2-fluoro-3-methoxyphenyl)(2-methoxypyridin-3-yl)methanol (3.48)**



To a solution of 2,2,6,6-tetramethylpiperidine (1.00 mL, 6.00 mmol, anhydrous) in THF (10 mL, anhydrous) at  $-10\text{ }^\circ\text{C}$  and under an atmosphere of nitrogen was added  $n\text{-BuLi}$  (3.50 mL, 1.57 M in hexanes, 5.50 mmol), dropwise. The mixture was stirred at  $-10\text{ }^\circ\text{C}$  for 0.5 h. Following this time, the mixture was cooled to  $-78\text{ }^\circ\text{C}$ , and a solution of 2-methoxypyridine (546 mg, 5.00 mmol) in THF (6 mL, anhydrous) was added dropwise over 20 min. The reaction mixture was kept stirring at  $-78\text{ }^\circ\text{C}$  for 2 h, after which a solution of 2-fluoro-3-methoxybenzaldehyde (925 mg, 6.00 mmol) in THF (5 mL, anhydrous) was added dropwise over 20 min. The mixture was stirred at  $-78\text{ }^\circ\text{C}$  for a total of 3 h. After this time, the reaction was quenched with a solution of  $\text{NH}_4\text{Cl}$  (saturated, aqueous) and diluted with EtOAc, the organic phase separated, and the aqueous layer extracted with EtOAc ( $\times 3$ ). The combined organic layers were washed with brine, dried over anhydrous  $\text{MgSO}_4$ , filtered, and concentrated under reduced pressure. Purification by silica gel flash chromatography (0–50%  $\text{Et}_2\text{O}$  in PhMe) afforded the title compound a yellow solid (663 mg, 2.52 mmol, 50%). A portion of this product was further recrystallised from  $\text{Et}_2\text{O}$  to give short colourless pearlescent rocks for melting point analysis.

$^1\text{H}$  NMR (400 MHz,  $\text{CDCl}_3$ )  $\delta$  = 8.06 (dd,  $J$  = 5.0, 1.9 Hz, 1H, 6-PyrH), 7.50 (ddt,  $J$  = 7.3, 1.9, 0.9 Hz, 1H, 4-PyrH), 7.06 (td,  $J$  = 7.9, 1.4 Hz, 1H, 4-PhH), 7.00 (ddd,  $J$  = 7.8, 6.0, 1.4 Hz, 1H, 5-PhH), 6.90 (td,  $J$  = 8.1, 1.8 Hz, 1H, 3-PhH), 6.85 (dd,  $J$  = 7.3, 5.0 Hz, 1H, 5-PyrH), 3.95 (s, 3H, PyrOCH<sub>3</sub>), 3.87 (s, 3H, PhOCH<sub>3</sub>), 3.33 (br s, 1H, OH);

$^{13}\text{C}$  NMR (101 MHz,  $\text{CDCl}_3$ )  $\delta$  = 161.0 (PyrC-OCH<sub>3</sub>), 149.9 (d,  $J$  = 246.6 Hz, CF), 147.6 (d,  $J$  = 10.8 Hz, PhC-OCH<sub>3</sub>), 146.0 (6-PyrCH), 136.1 (d,  $J$  = 1.4 Hz, 4-PyrCH), 130.0 (d,  $J$  = 10.8 Hz, PhC-COH), 125.1 (3-PyrC), 124.0 (d,  $J$  = 4.7 Hz, PhCH), 119.4 (d,  $J$  = 3.0 Hz, PhCH), 117.1 (5-PyrCH), 112.7 (d,  $J$  = 1.9 Hz, PhCH), 65.8 (d,  $J$  = 4.7 Hz, COH), 56.4 (PhOCH<sub>3</sub>), 53.6 (PhOCH<sub>3</sub>);

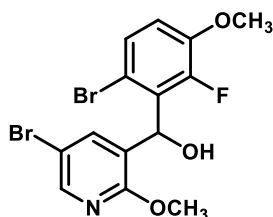
LR-MS (ESI+)  $m/z$ : 263.9  $[\text{M}+\text{H}]^+$ ;

HR-MS (ESI+)  $m/z$   $[\text{M} = \text{C}_{14}\text{H}_{14}\text{FNO}_3]$ :  $[\text{M}+\text{H}]^+$  calc'd 264.1030, found 264.1034;

Analytical HPLC (254 nm):  $t_R$  = 5.0 min, 94%;

MP: 105.2 – 107.2 °C.

**(6-bromo-2-fluoro-3-methoxyphenyl)(5-bromo-2-methoxypyridin-3-yl)methanol<sup>[2]</sup> (3.49)**



To a solution of **3.48** (600 mg, 2.28 mmol) in MeCN (12 mL) was added *N*-bromosuccinimide (446 mg, 2.51 mmol), and the reaction stirred at reflux for 16 h. After this time, the solvent was evaporated under reduced pressure, and the residue purified by silica gel flash chromatography (0–50% EtOAc in Pet. Sp.) to afford the title compound as a pale-yellow solid (706 mg, 2.06 mmol, 91%). A portion of this product was further recrystallised from EtOH to give short colourless needles for melting point analysis.

<sup>1</sup>H NMR (400 MHz, CDCl<sub>3</sub>) δ = 8.11 (dd, *J* = 2.4, 0.7 Hz, 1H, 6-PyrH), 7.92 (td, *J* = 2.3, 1.0 Hz, 2H, 4-PyrCH), 7.31 (dd, *J* = 8.9, 2.0 Hz, 1H, 5-PhH), 6.81 (t, *J* = 8.8 Hz, 1H, 4-PhH), 6.33 (s, 1H, CHOH), 3.854 (s, 3H, PyrOCH<sub>3</sub>), 3.85 (s, 3H, PhOCH<sub>3</sub>), 2.93 (s, 1H, OH);

<sup>13</sup>C NMR (101 MHz, CDCl<sub>3</sub>) δ = 159.6 (PyrC-OCH<sub>3</sub>), 151.7 (d, *J* = 253.1 Hz, CF), 148.0 (d, *J* = 11.2 Hz, PhC-OCH<sub>3</sub>), 146.3 (6-PyrCH), 138.53 (d, *J* = 3.7 Hz, 4-PyrCH), 128.7 (d, *J* = 11.2 Hz, PhC-CHOH), 128.3 (d, *J* = 4.3 Hz, 5-PhCH), 125.7 (d, *J* = 1.1 Hz, 3-PyrC), 114.11 (d, *J* = 3.1 Hz, 4-PhCH), 114.07 (6-PhC-Br), 111.9 (5-PyrC-Br), 69.1 (d, *J* = 2.0 Hz, CHOH), 56.7 (PhOCH<sub>3</sub>), 53.8 (PyrOCH<sub>3</sub>);

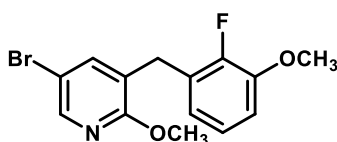
LR-MS (ESI+) *m/z*: 421.6 [M+H]<sup>+</sup>;

HR-MS (ESI+) *m/z* [M = C<sub>14</sub>H<sub>12</sub>Br<sub>2</sub>FNO<sub>3</sub>]: [M+H]<sup>+</sup> calc'd 419.9241, found 419.9247;

Analytical HPLC (254 nm): *t*<sub>R</sub> = 6.3 min, 93%;

MP: 165.2 – 167.0 °C.

**5-Bromo-3-(2-fluoro-3-methoxybenzyl)-2-methoxypyridine<sup>[32]</sup> (3.45)**



To a solution of **3.44** (5.73 g, 16.7 mmol) in CH<sub>2</sub>Cl<sub>2</sub> (55 mL, anhydrous) under an atmosphere of nitrogen was added triethylsilane (21.4 mL, 134 mmol), and the mixture cooled to 0 °C. Boron trifluoride diethyl etherate (16.5 mL, 133.9 mmol) was added dropwise to the cooled reaction mixture, and the solution stirred at reflux for 19 h. Upon completion, the reaction mixture was cooled to room

temperature and added to an ice-cold solution of  $\text{K}_2\text{CO}_3$  (20% w/v, aqueous). The solution was filtered through a pad of Celite with the aid of  $\text{CH}_2\text{Cl}_2$ , and the organic phase was separated. The aqueous phase was extracted with  $\text{CH}_2\text{Cl}_2$  ( $\times 3$ ) and the combined organic layers dried over anhydrous  $\text{MgSO}_4$ , filtered, and concentrated under reduced pressure. Purification by silica gel flash chromatography (0–15% EtOAc in Pet. Sp.) afforded the title compound as a white solid on standing (5.05 g, 15.5 mmol, 93%). A portion of this product was further recrystallised from slow evaporation of  $\text{Et}_2\text{O}$  to give short colourless needles for melting point analysis.

$^1\text{H}$  NMR (400 MHz,  $\text{CDCl}_3$ )  $\delta$  = 8.05 (d,  $J$  = 2.4 Hz, 1H, 6-PyrH), 7.36 (dq,  $J$  = 2.1, 0.9 Hz, 1H, 4-PyrH), 7.00 (td,  $J$  = 8.0, 1.5 Hz, 1H, PhH), 6.87 (td,  $J$  = 8.1, 1.5 Hz, 1H, PhH), 6.79 – 6.70 (m, 1H, PhH), 3.94 (s, 3H, PyrOCH<sub>3</sub>), 3.90 (br. s, 2H, Pyr-CH<sub>2</sub>-Ph), 3.89 (s, 3H, PhOCH<sub>3</sub>);

$^{13}\text{C}$  NMR (101 MHz,  $\text{CDCl}_3$ )  $\delta$  = 160.9 (PyrC-OCH<sub>3</sub>), 151.0 (d,  $J$  = 245.2 Hz, CF), 148.0 (d,  $J$  = 11.0 Hz, PhC-OCH<sub>3</sub>), 145.3 (6-PyrC), 140.3 (d,  $J$  = 1.4 Hz, 4-PyrH), 126.57 (d,  $J$  = 13.2 Hz, PhC-CH<sub>2</sub>), 124.7 (3-PyrC), 124.0 (d,  $J$  = 4.7 Hz, PhCH), 122.6 (d,  $J$  = 3.2 Hz, PhCH), 111.9 (d,  $J$  = 1.8 Hz, PhCH), 111.8 (5-PyrC-Br), 56.4 (PhOCH<sub>3</sub>), 53.9 (PhOCH<sub>3</sub>), 28.6 (d,  $J$  = 4.0 Hz, Pyr-CH<sub>2</sub>);

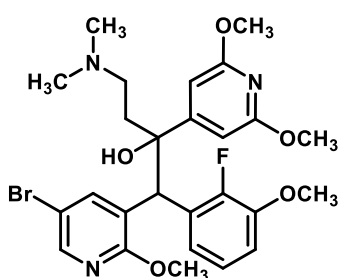
LR-MS (ESI+)  $m/z$ : 325.9  $[\text{M}+\text{H}]^+$ ;

HR-MS (ESI+)  $m/z$  [ $\text{M} = \text{C}_{14}\text{H}_{13}\text{BrFNO}_2$ ]:  $[\text{M}+\text{H}]^+$  calc'd 326.0186, found 326.0188;

Analytical HPLC (254 nm):  $t_R$  = 7.6 min, 100%;

MP: 87.5 – 89.6 °C.

**1-(5-bromo-2-methoxypyridin-3-yl)-2-(2,6-dimethoxypyridin-4-yl)-4-(dimethylamino)-1-(2-fluoro-3-methoxyphenyl)butan-2-ol (**3.46**)**



To a solution of 2,2,6,6-tetramethylpiperidine (1.18 mL, 7.00 mmol, anhydrous) in THF (5 mL, anhydrous) at  $-10$  °C and under an atmosphere of nitrogen was added  $n$ -BuLi (4.00 mL, 1.37 M in hexanes, 5.50 mmol), dropwise. The mixture was stirred at  $-10$  °C for 0.5 h. Following this time, the mixture was cooled to  $-78$  °C, and a solution of **3.45** (1.63 g, 5.00 mmol) in THF (7 mL, anhydrous) was added dropwise over 20 min to give a fluorescent orange solution. The reaction mixture was kept stirring at  $-78$  °C for 2 h, after which a solution of **3.03** (1.79 g, 7.50 mmol) in THF (7 mL, anhydrous) was added dropwise over 15 min. The mixture was stirred at  $-78$  °C for a total of 4 h. After this time,

the reaction was quenched with a solution of  $\text{NH}_4\text{Cl}$  (saturated, aqueous) and diluted with EtOAc, the organic phase separated, and the aqueous layer extracted with EtOAc ( $\times 3$ ). The combined organic layers were washed with brine, dried over anhydrous  $\text{MgSO}_4$ , filtered, and concentrated under reduced pressure. Purification by silica gel flash chromatography (0–10% MeOH in  $\text{CH}_2\text{Cl}_2$ ) afforded the title compound a pale-yellow foam (1.79 g, 3.18 mmol, 64%).

LR-MS (ESI+)  $m/z$ : 563.9/565.9  $[\text{M}+\text{H}]^+$ ;

HR-MS (ESI+)  $m/z$   $[\text{M} = \text{C}_{26}\text{H}_{31}\text{BrFN}_3\text{O}_5]$ :  $[\text{M}+\text{H}]^+$  calc'd 564.1504, found 564.1517;

Analytical HPLC (254 nm):  $t_R$  = 6.2 min, 42% (A); 6.3 min, 55%;

Diastereomer A:

$^1\text{H}$  NMR (400 MHz,  $\text{CDCl}_3$ )  $\delta$  = 12.35 (br s, 1H,  $\text{NH}^+$ ), 8.07 (d,  $J$  = 2.4 Hz, 1H,  $\text{PyrH}$ ), 7.81 (d,  $J$  = 2.4 Hz, 1H,  $\text{PyrH}$ ), 7.60 (ddd,  $J$  = 7.6, 6.0, 1.4 Hz, 1H,  $\text{PhH}$ ), 6.86 (td,  $J$  = 8.2, 1.6 Hz, 1H,  $\text{PhH}$ ), 6.68 (td,  $J$  = 8.2, 1.4 Hz, 1H,  $\text{PhH}$ ), 6.47 (s, 2H,  $\text{Pyr}'\text{H}$ ), 5.27 (s, 1H,  $\text{Pyr-CH-Ph}$ ), 4.02 (s, 3H,  $\text{PyrOCH}_3$ ), 3.85 (s, 6H,  $\text{Pyr}'\text{OCH}_3$ ), 3.74 (s, 3H,  $\text{PhOCH}_3$ ), 3.26 (t,  $J$  = 11.5 Hz, 1H,  $\text{CH}_2\text{CHHN}$ ), 2.65 (s, 3H,  $\text{NCH}_3$ ), 2.59 (s, 3H,  $\text{NCH}_3$ ), 2.41 – 2.31 (m, 1H,  $\text{CHHCH}_2\text{N}$ ), 2.30 – 2.19 (m, 1H,  $\text{CH}_2\text{CHHN}$ ), 2.07 – 1.94 (m, 1H,  $\text{CHHCH}_2\text{N}$ );

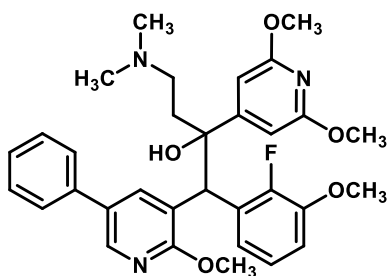
$^{13}\text{C}$  NMR (101 MHz,  $\text{CDCl}_3$ )  $\delta$  = 163.7, 160.6, 158.5, 150.4 (d,  $J$  = 244.4 Hz), 147.2 (d,  $J$  = 11.5 Hz), 146.4, 143.1, 128.4 (d,  $J$  = 10.9 Hz), 123.6 (d,  $J$  = 4.7 Hz), 123.4, 122.2 (d,  $J$  = 1.8 Hz), 112.7, 111.8, 98.4, 77.2, 56.2, 54.4, 53.7, 53.7, 44.9, 43.0, 41.3, 37.0;

Diastereomer B:

$^1\text{H}$  NMR (400 MHz,  $\text{CDCl}_3$ )  $\delta$  = 11.91 (br s, 1H,  $\text{NH}^+$ ), 8.50 (d,  $J$  = 2.4 Hz, 1H,  $\text{PyrH}$ ), 7.89 (d,  $J$  = 2.5 Hz, 1H,  $\text{PyrH}$ ), 7.03 (td,  $J$  = 8.1, 1.4 Hz, 1H,  $\text{PhH}$ ), 6.95 – 6.84 (m, 2H,  $\text{PhH}$ ), 6.48 (s, 2H,  $\text{Pyr}'\text{H}$ ), 5.16 (s, 1H,  $\text{Pyr-CH-Ph}$ ), 3.89 (s, 3H,  $\text{PhOCH}_3$ ), 3.87 (s, 6H,  $\text{Pyr}'\text{OCH}_3$ ), 3.76 (s, 3H,  $\text{PyrOCH}_3$ ), 3.39 – 3.25 (m, 1H,  $\text{CH}_2\text{CHHN}$ ), 2.66 (s, 3H,  $\text{NCH}_3$ ), 2.63 (s, 3H,  $\text{NCH}_3$ ), 2.35 – 2.17 (m, 2H,  $\text{CHHCHHN}$ ), 2.05 – 1.91 (m, 1H,  $\text{CHHCH}_2\text{N}$ );

$^{13}\text{C}$  NMR (101 MHz,  $\text{CDCl}_3$ )  $\delta$  = 163.9, 160.1, 158.2, 151.0 (d,  $J$  = 243.4 Hz), 147.4 (d,  $J$  = 11.6 Hz), 145.1, 141.4, 125.1, 125.0, 124.3 (d,  $J$  = 4.8 Hz), 122.8 (d,  $J$  = 1.2 Hz), 112.3 (d,  $J$  = 1.2 Hz), 111.7, 98.2, 76.9†, 56.2, 54.1, 53.8, 53.7, 45.2, 43.2 (d,  $J$  = 2.6 Hz), 41.5, 37.0.

**2-(2,6-dimethoxypyridin-4-yl)-4-(dimethylamino)-1-(2-fluoro-3-methoxyphenyl)-1-(2-methoxy-5-phenylpyridin-3-yl)butan-2-ol (3.54)**



General method C was used with phenylboronic acid (122 mg, 1.00 mmol) to afford the title compound an off-white foam (211 mg, 0.375 mmol, 75%, A:B = 55:45).

A portion of this product was further subjected to purification by our collaborators at HangZhou (China) using preparative HPLC to isolate the individual diastereomers as the TFA salt. This was performed using an Agilent 1260 Infinity HPLC system fitted with a Bondysil-C8 column (10  $\mu$ m, 250  $\times$  20 mm). Isocratic elution was used with a solvent system of 40% ultrapure H<sub>2</sub>O (0.1% TFA) in MeOH (0.1% TFA) over 30 min with a flow rate of 22 mL/min.

LR-MS (ESI+)  $m/z$ : 561.9 [M+H]<sup>+</sup>;

HR-MS (ESI+)  $m/z$  [M = C<sub>32</sub>H<sub>36</sub>FN<sub>3</sub>O<sub>5</sub>]: [M+H]<sup>+</sup> calc'd 562.2712, found 562.2721;

Diastereomer A:

<sup>1</sup>H NMR (400 MHz, CDCl<sub>3</sub>)  $\delta$  = 12.57 (br s, 1H, NH<sup>+</sup>), 8.65 (d,  $J$  = 2.4 Hz, 1H, PyrH), 8.08 (d,  $J$  = 2.4 Hz, 1H, PyrH), 7.46 – 7.42 (m, 4H, Ph'H), 7.38 – 7.29 (m, 1H, Ph'H), 7.03 – 6.96 (m, 2H, PhH), 6.89 – 6.82 (m, 1H, PhH), 6.56 (s, 2H, Pyr'H), 5.26 (s, 1H, Pyr-CH-Ph), 3.89 (s, 3H, PhOCH<sub>3</sub>), 3.84 (s, 9H, Pyr'OCH<sub>3</sub>, PyrOCH<sub>3</sub>), 3.34 (t,  $J$  = 11.4 Hz, 1H, CH<sub>2</sub>CHHN), 2.71 – 2.55 (m, 6H, N(CH<sub>3</sub>)<sub>2</sub>), 2.39 – 2.19 (m, 2H, CHHCHHN), 2.04 (t,  $J$  = 11.1 Hz, 1H, CH<sub>2</sub>CHHN);

<sup>13</sup>C NMR (101 MHz, CDCl<sub>3</sub>)  $\delta$  = 163.6, 160.5, 158.7, 150.9 (d,  $J$  = 242.7 Hz), 147.2 (d,  $J$  = 12.1 Hz), 142.3, 138.1, 138.0, 129.7, 128.9, 127.1, 126.7, 125.5 (d,  $J$  = 11.8 Hz), 124.0 (d,  $J$  = 4.6 Hz), 123.0, 123.0 (d,  $J$  = 2.0 Hz), 111.9, 98.2, 76.9, 56.0, 53.9, 53.5, 53.4, 44.9, 43.2, 41.2, 37.0;

HangZhou HPLC (290 nm):  $t_R$  = 10.0 min, 99% (isocratic 40% solvent A in solvent B, 1.5 mL/min);

Diastereomer B:

<sup>1</sup>H NMR (400 MHz, CDCl<sub>3</sub>)  $\delta$  = 12.03 (br s, 1H, NH<sup>+</sup>), 8.27 (d,  $J$  = 2.4 Hz, 1H, PyrH), 7.98 (d,  $J$  = 2.1 Hz, 1H, PyrH), 7.67 (ddd,  $J$  = 7.8, 6.2, 1.5 Hz, 1H, PhH), 7.53 – 7.46 (m, 2H, Ph'H), 7.40 (t,  $J$  = 7.5 Hz, 2H, Ph'H), 7.32 (t,  $J$  = 7.3 Hz, 1H, Ph'H), 6.84 (td,  $J$  = 8.2, 1.5 Hz, 1H, PhH), 6.65 (td,  $J$  = 8.1, 1.3 Hz, 1H, PhH), 6.51 (s, 2H, Pyr'H), 5.38 (s, 1H, Pyr-CH-Ph), 4.12 (s, 3H, PyrOCH<sub>3</sub>), 3.86 (s, 6H, Pyr'OCH<sub>3</sub>), 3.72 (s, 3H,

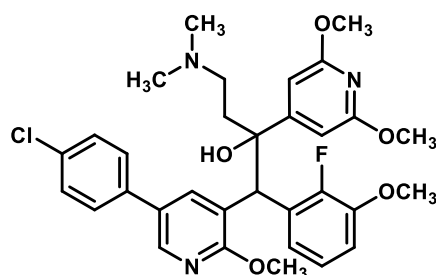


PhOCH<sub>3</sub>), 3.28 (t, *J* = 11.8 Hz, 1H, CH<sub>2</sub>CHHN), 2.66 (s, 3H, NCH<sub>3</sub>), 2.63 (s, 3H, NCH<sub>3</sub>), 2.47 – 2.36 (m, 1H, CHHCH<sub>2</sub>N), 2.35 – 2.23 (m, 1H, CH<sub>2</sub>CHHN), 2.09 (t, *J* = 11.6 Hz, 1H, CHHCH<sub>2</sub>N);

<sup>13</sup>C NMR (101 MHz, CDCl<sub>3</sub>) δ = 163.7, 161.1, 158.6, 150.4 (d, *J* = 244.5 Hz), 147.2 (d, *J* = 11.4 Hz), 143.3, 140.4, 137.8, 131.4, 128.9, 127.5, 127.3, 123.5 (d, *J* = 4.9 Hz), 122.3 (d, *J* = 1.3 Hz), 121.7, 111.6 (d, *J* = 1.1 Hz), 98.4, 77.9, 56.1, 54.7, 53.9, 53.7, 45.0, 43.2, 41.4, 37.1, missing 1 × PhC;

HangZhou HPLC (290 nm): *t*<sub>R</sub> = 12.0 min, 98% (isocratic 40% solvent A in solvent B, 1.5 mL/min).

**1-(5-(4-chlorophenyl)-2-methoxypyridin-3-yl)-2-(2,6-dimethoxypyridin-4-yl)-4-(dimethylamino)-1-(2-fluoro-3-methoxyphenyl)butan-2-ol (3.55)**



General method D was used with 4-chlorophenylboronic acid (93.8 mg, 0.600 mmol) to afford the title compound a yellow foam (197 mg, 0.330 mmol, 66%, A:B = 52:48).

A portion of this product was further subjected to purification by our collaborators at HangZhou (China) using preparative HPLC to isolate the individual diastereomers as the TFA salt. This was performed using a Generik HP30 and Gilson FC204 HPLC system fitted with a Bondysil-C18 column (10 μm, 250 × 20 mm). Isocratic elution was used with a solvent system of 20% ultrapure H<sub>2</sub>O (0.1% TFA) in MeOH (0.1% TFA) over 15 min with a flow rate of 20 mL/min.

Diastereomer B was further subjected to chiral purification by our collaborators at TCG Lifesciences using HPLC to isolate the individual enantiomers. Isocratic elution was used with a solvent system of Hexane/EtOH/Isopropylamine (80/20/0.1) over 10 min with a flow rate of 1 mL/min.

LR-MS (ESI+) *m/z*: 596.0 [M+H]<sup>+</sup>;

HR-MS (ESI+) *m/z* [M = C<sub>32</sub>H<sub>35</sub>ClFN<sub>3</sub>O<sub>5</sub>]: [M+H]<sup>+</sup> calc'd 596.2322, found 596.2335;

Diastereomer A:

<sup>1</sup>H NMR (400 MHz, CDCl<sub>3</sub>) δ = 12.70 (br s, 1H, NH<sup>+</sup>), 8.61 (d, *J* = 2.2 Hz, 1H, PyrH), 8.03 (d, *J* = 2.3 Hz, 1H, PyrH), 7.40 (d, *J* = 8.6 Hz, 2H, Ph'H), 7.36 (d, *J* = 8.6 Hz, 2H, Ph'H), 6.98 (p, *J* = 7.2, 6.5 Hz, 2H, PhH), 6.86 (t, *J* = 8.1 Hz, 1H, PhH), 6.55 (s, 2H, Pyr'H), 5.24 (s, 1H, Pyr-CH-Ph), 3.89 (s, 3H, PhOCH<sub>3</sub>), 3.84 (s, 6H, Pyr'OCH<sub>3</sub>), 3.82 (s, 3H, PyrOCH<sub>3</sub>), 3.34 (t, *J* = 11.2 Hz, 1H, CH<sub>2</sub>CHHN), 2.67 – 2.58 (m, 6H, N(CH<sub>3</sub>)<sub>2</sub>), 2.40 – 2.18 (m, 2H, CHHCHHN), 2.11 – 1.96 (m, 1H, CHHCH<sub>2</sub>N);

$^{13}\text{C}$  NMR (101 MHz,  $\text{CDCl}_3$ )  $\delta$  = 163.8, 160.9, 158.8, 151.0 (d,  $J$  = 243.0 Hz), 147.3 (d,  $J$  = 12.0 Hz), 142.5, 137.7, 136.8, 133.3, 129.2, 128.6, 128.0, 125.6 (d,  $J$  = 12.0 Hz), 124.2 (d,  $J$  = 4.5 Hz), 123.3, 123.1 (d,  $J$  = 2.1 Hz), 112.1, 98.4, 77.0, 56.2, 53.9, 53.7, 53.5, 45.0, 43.3, 41.2, 37.1;

Analytical HPLC (290 nm):  $t_R$  = 16.5 min, 99% (isocratic 35% solvent A in solvent B, 1.0 mL/min);

Diastereomer B:

$^1\text{H}$  NMR (400 MHz,  $\text{CDCl}_3$ )  $\delta$  = 12.48 (br s, 1H,  $\text{NH}^+$ ), 8.20 (d,  $J$  = 2.4 Hz, 1H,  $\text{PyrH}$ ), 7.89 (d,  $J$  = 2.3 Hz, 1H,  $\text{PyrH}$ ), 7.71 (t,  $J$  = 7.1 Hz, 1H,  $\text{PhH}$ ), 7.43 (d,  $J$  = 8.5 Hz, 2H,  $\text{Ph'H}$ ), 7.35 (d,  $J$  = 8.4 Hz, 2H,  $\text{Ph'H}$ ), 6.84 (td,  $J$  = 8.1, 1.3 Hz, 1H,  $\text{PhH}$ ), 6.64 (td,  $J$  = 8.1, 1.1 Hz, 2H,  $\text{PhH}$ ), 6.53 (s, 2H,  $\text{Pyr'H}$ ), 5.38 (s, 1H,  $\text{Pyr-CH-Ph}$ ), 4.10 (s, 3H,  $\text{PyrOCH}_3$ ), 3.86 (s, 6H,  $\text{Pyr'OCH}_3$ ), 3.72 (s, 3H,  $\text{PhOCH}_3$ ), 3.29 (t,  $J$  = 11.8 Hz, 1H,  $\text{CH}_2\text{CHHN}$ ), 2.64 (s, 3H,  $\text{NCH}_3$ ), 2.59 (s, 3H,  $\text{NCH}_3$ ), 2.50 – 2.36 (m, 1H,  $\text{CHHCH}_2\text{N}$ ), 2.32 – 2.17 (m, 1H,  $\text{CH}_2\text{CHHN}$ ), 2.05 (t,  $J$  = 11.4 Hz, 1H,  $\text{CHHCH}_2\text{N}$ );

HangZhou HPLC (290 nm):  $t_R$  = 15.1 min, 98% (isocratic 35% solvent A in solvent B, 1.0 mL/min);

Chiral HPLC (266 nm):  $t_R$  = 4.4 min, 51% (B1); 5.2 min 49% (B2);

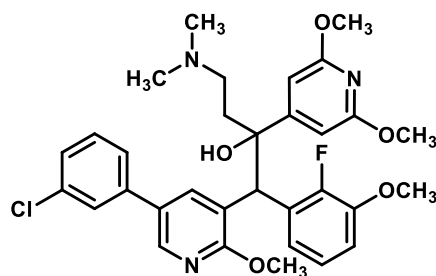
Enantiomer B1:

Chiral HPLC (266 nm):  $t_R$  = 4.4 min, 100%;

Enantiomer B2:

Chiral HPLC (266 nm):  $t_R$  = 5.2 min, 97%.

**1-(5-(3-chlorophenyl)-2-methoxypyridin-3-yl)-2-(2,6-dimethoxypyridin-4-yl)-4-(dimethylamino)-1-(2-fluoro-3-methoxyphenyl)butan-2-ol (3.56)**



General method D was used with 3-chlorophenylboronic acid (93.8 mg, 0.600 mmol) to afford the title compound a yellow foam (229 mg, 0.384 mmol, 77%, A:B = 52:48).

LR-MS (ESI+)  $m/z$ : 596.0  $[\text{M}+\text{H}]^+$ ;

HR-MS (ESI+)  $m/z$  [ $\text{M} = \text{C}_{32}\text{H}_{35}\text{ClFN}_3\text{O}_5$ ]:  $[\text{M}+\text{H}]^+$  calc'd 596.2322, found 596.2337;

Analytical HPLC (254 nm):  $t_R$  = 6.9 min, 80% (A + B overlapping);

## Diastereomer A:

$^1\text{H}$  NMR (400 MHz,  $\text{CDCl}_3$ )  $\delta$  = 12.33 (br s, 1H,  $\text{NH}^+$ ), 8.60 (d,  $J$  = 2.4 Hz, 1H,  $\text{PyrH}$ ), 8.04 (d,  $J$  = 2.4 Hz, 1H,  $\text{PyrH}$ ), 7.39 – 7.28 (m, 4H,  $\text{Ph}'\text{H}$ ), 7.00 (t,  $J$  = 8.0 Hz, 1H,  $\text{PhH}$ ), 6.94 (ddd,  $J$  = 7.8, 5.9, 1.6 Hz, 1H,  $\text{PhH}$ ), 6.86 (t,  $J$  = 7.5 Hz, 1H,  $\text{PhH}$ ), 6.56 (br s, 2H,  $\text{PyrH}$ ), 5.24 (s, 1H,  $\text{Pyr-CH-Ph}$ ), 3.89 (s, 3H,  $\text{PhOCH}_3$ ), 3.85 (s, 6H,  $\text{Pyr}'\text{OCH}_3$ ), 3.83 (s, 3H,  $\text{PyrOCH}_3$ ), 3.35 (t,  $J$  = 11.4 Hz, 1H,  $\text{CH}_2\text{CHHN}$ ), 2.65 (s, 3H,  $\text{NCH}_3$ ), 2.63 (s, 3H,  $\text{NCH}_3$ ), 2.40 – 2.20 (m, 2H,  $\text{CHHCHHN}$ ), 2.05 (t,  $J$  = 11.6 Hz, 1H,  $\text{CHHCH}_2\text{N}$ );

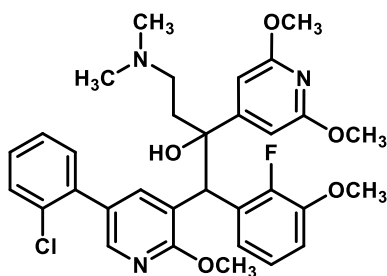
$^{13}\text{C}$  NMR (101 MHz,  $\text{CDCl}_3$ )  $\delta$  = 163.8, 161.0, 158.7, 151.0 (d,  $J$  = 243.2 Hz), 147.3 (d,  $J$  = 11.9 Hz), 142.5, 140.1, 138.0, 134.9, 130.2, 128.5, 127.3, 126.9, 125.4 (d,  $J$  = 12.0 Hz), 125.0, 124.2 (d,  $J$  = 4.2 Hz), 123.4, 123.0, 112.1, 98.3, 76.9, 56.1, 54.1, 53.7, 53.6, 45.0, 43.4, 41.3, 37.1;

## Diastereomer B:

$^1\text{H}$  NMR (400 MHz,  $\text{CDCl}_3$ )  $\delta$  = 12.23 (br s, 1H,  $\text{NH}^+$ ), 8.21 (d,  $J$  = 2.3 Hz, 1H,  $\text{PyrH}$ ), 7.90 (d,  $J$  = 2.1 Hz, 1H,  $\text{PyrH}$ ), 7.70 (ddd,  $J$  = 7.9, 6.1, 1.5 Hz, 1H,  $\text{PhH}$ ), 7.45 (t,  $J$  = 1.8 Hz, 1H,  $\text{Ph}'\text{H}$ ), 7.39 (dt,  $J$  = 7.3, 1.5 Hz, 1H,  $\text{Ph}'\text{H}$ ), 7.35 – 7.26 (m, 2H,  $\text{Ph}'\text{H}$ ), 6.85 (td,  $J$  = 8.1, 1.5 Hz, 1H,  $\text{PhH}$ ), 6.65 (td,  $J$  = 8.2, 1.4 Hz, 1H,  $\text{PhH}$ ), 6.52 (s, 2H,  $\text{Pyr}'\text{H}$ ), 5.38 (s, 1H,  $\text{Pyr-CH-Ph}$ ), 4.10 (s, 3H,  $\text{PyrOCH}_3$ ), 3.86 (s, 6H,  $\text{Pyr}'\text{OCH}_3$ ), 3.72 (s, 3H,  $\text{PhOCH}_3$ ), 3.29 (t,  $J$  = 11.7 Hz, 1H,  $\text{CH}_2\text{CHHN}$ ), 2.65 (s, 3H,  $\text{NCH}_3$ ), 2.61 (s, 3H,  $\text{NCH}_3$ ), 2.49 – 2.34 (m, 1H,  $\text{CHHCH}_2\text{N}$ ), 2.34 – 2.18 (m, 1H,  $\text{CH}_2\text{CHHN}$ ), 2.12 – 2.04 (m, 1H,  $\text{CHHCH}_2\text{N}$ );

$^{13}\text{C}$  NMR (101 MHz,  $\text{CDCl}_3$ )  $\delta$  = 163.6, 161.5, 158.6, 149.2, 147.1 (d,  $J$  = 11.8 Hz), 143.6, 140.0, 139.9, 134.6, 130.1, 129.9, 128.8 (d,  $J$  = 10.8 Hz), 127.4, 127.2, 125.6, 123.5 (d,  $J$  = 4.5 Hz), 122.2, 121.6, 111.6, 98.4, 77.3, 56.1, 54.5, 53.7, 53.7, 45.0, 43.0, 41.2, 37.1.

**1-(5-(2-chlorophenyl)-2-methoxypyridin-3-yl)-2-(2,6-dimethoxypyridin-4-yl)-4-(dimethylamino)-1-(2-fluoro-3-methoxyphenyl)butan-2-ol (3.57)**



General method D was used with 2-chlorophenylboronic acid (93.8 mg, 0.600 mmol) to afford the title compound a yellow foam (261 mg, 0.438 mmol, 88%, A:B = 48:52).

LR-MS (ESI+)  $m/z$ : 596.0  $[\text{M}+\text{H}]^+$ ;

HR-MS (ESI+)  $m/z$   $[\text{M} = \text{C}_{32}\text{H}_{35}\text{ClFN}_3\text{O}_5]$ :  $[\text{M}+\text{H}]^+$  calc'd 596.2322, found 596.2335;

Analytical HPLC (254 nm):  $t_R$  = 6.6 min, 88% (A + B overlapping);

## Diastereomer A:

$^1\text{H}$  NMR (400 MHz,  $\text{CDCl}_3$ )  $\delta$  = 12.8 (br s, 1H,  $\text{NH}^+$ ), 8.17 (d,  $J$  = 2.4 Hz, 1H, Pyr $\underline{\text{H}}$ ), 7.89 (s, 1H, Pyr $\underline{\text{H}}$ ), 7.64 (t,  $J$  = 7.0 Hz, 1H, Ar $\underline{\text{H}}$ ), 7.50 – 7.36 (m, 3H, Ar $\underline{\text{H}}$ ), 7.33 – 7.27 (m, 2H, Ar $\underline{\text{H}}$ ), 6.84 – 6.79 (m, 1H, Ph $\underline{\text{H}}$ ), 6.64 (t,  $J$  = 8.2 Hz, 1H, Ph $\underline{\text{H}}$ ), 6.50 (s, 1H, Pyr' $\underline{\text{H}}$ ), 5.38 (s, 1H, Pyr-CH $\underline{\text{H}}$ -Ph), 4.10 (s, 3H, PyrOCH $\underline{\text{H}}_3$ ), 3.85 (s, 6H, Pyr'OCH $\underline{\text{H}}_3$ ), 3.73 (s, 3H, PhOCH $\underline{\text{H}}_3$ ), 3.29 – 3.10 (m, 1H, CH $\underline{\text{H}}$ CH $\underline{\text{H}}$ N), 2.68 – 2.56 (m, 6H, N(CH $\underline{\text{H}}_3$ ) $_2$ ), 2.52 – 2.22 (m, 2H, CH $\underline{\text{H}}$ CH $\underline{\text{H}}$ N), 2.20 – 2.05 (m, 1H, CH $\underline{\text{H}}$ CH $\underline{\text{H}}$ N);

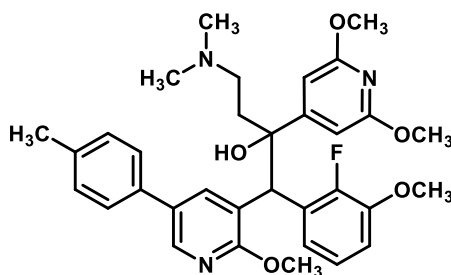
$^{13}\text{C}$  NMR – insufficient sample;

## Diastereomer B:

$^1\text{H}$  NMR (400 MHz,  $\text{CDCl}_3$ )  $\delta$  = 10.92 (br s, 1H,  $\text{NH}^+$ ), 8.62 (s, 1H, Pyr $\underline{\text{H}}$ ), 8.01 (d,  $J$  = 2.3 Hz, 1H, Pyr $\underline{\text{H}}$ ), 7.49 – 7.46 (m, 1H, Ph' $\underline{\text{H}}$ ), 7.35 – 7.31 (m, 2H, Ph' $\underline{\text{H}}$ ), 7.19 – 7.15 (m, 1H, Ph' $\underline{\text{H}}$ ), 7.01 (td,  $J$  = 8.0, 1.3 Hz, 1H, Ph $\underline{\text{H}}$ ), 6.94 – 6.85 (m, 2H, Ph $\underline{\text{H}}$ ), 6.48 (s, 2H, Pyr' $\underline{\text{H}}$ ), 5.27 (s, 1H, Pyr-CH $\underline{\text{H}}$ -Ph), 3.98 (s, 3H, PyrOCH $\underline{\text{H}}_3$ ), 3.90 (s, 3H, PhOCH $\underline{\text{H}}_3$ ), 3.87 (s, 6H, Pyr'OCH $\underline{\text{H}}_3$ ), 3.40 – 3.27 (m, 1H, CH $\underline{\text{H}}$ CH $\underline{\text{H}}$ N), 2.70 (s, 3H, NCH $\underline{\text{H}}_3$ ), 2.68 (s, 3H, NCH $\underline{\text{H}}_3$ ), 2.44 – 2.24 (m, 2H, CH $\underline{\text{H}}$ CH $\underline{\text{H}}$ N), 2.20 – 1.98 (m, 1H, CH $\underline{\text{H}}$ CH $\underline{\text{H}}$ N);

$^{13}\text{C}$  NMR (101 MHz,  $\text{CDCl}_3$ )  $\delta$  = 163.9, 159.5, 157.6, 150.9 (d,  $J$  = 243.9 Hz), 147.6 (d,  $J$  = 11.8 Hz), 143.1, 141.3, 135.7, 132.9, 132.6, 131.3, 130.2, 129.7, 129.4, 129.2, 127.3, 124.6 (d,  $J$  = 11.6 Hz), 124.5, 122.4, 112.5, 98.2, 77.0, 56.14, 56.11, 53.7, 45.2, 43.6 $^{\dagger}$ , 41.8, 36.9.

**2-(2,6-dimethoxy-pyridin-4-yl)-4-(dimethylamino)-1-(2-fluoro-3-methoxyphenyl)-1-(2-methoxy-5-(*p*-tolyl)pyridin-3-yl)butan-2-ol (3.58)**



General method C was used with 4-tolylboronic acid (136 mg, 1.00 mmol) to afford the title compound a yellow foam (261 mg, 0.453 mmol, 91%, A:B = 50:50).

A portion of this product was further subjected to purification by our collaborators at HangZhou (China) using preparative HPLC to isolate the individual diastereomers as the TFA salt. This was performed using an Agilent 1260 Infinity HPLC system fitted with a Bondysil-C8 column (10  $\mu\text{m}$ , 250  $\times$  20 mm). Isocratic elution was used with a solvent system of 40% ultrapure  $\text{H}_2\text{O}$  (0.05% TFA) in MeOH (0.05% TFA) over 60 min with a flow rate of 23 mL/min.

LR-MS (ESI+)  $m/z$ : 575.9  $[\text{M}+\text{H}]^+$ ;

HR-MS (ESI+)  $m/z$  [ $M = C_{33}H_{38}FN_3O_5$ ]: [ $M+H$ ] $^+$  calc'd 576.2868, found 576.2876;

Diastereomer A:

$^1H$  NMR (400 MHz,  $CDCl_3$ )  $\delta$  = 11.06 (br s, 1H,  $NH^+$ ), 8.81 (s, 1H, PyrH), 8.12 (s, 1H, PyrH), 7.27 (d,  $J$  = 8.0 Hz, 2H, Ph'H), 7.20 (d,  $J$  = 9.6 Hz, 2H, Ph'H), 6.94 (t,  $J$  = 8.0 Hz, 1H, PhH), 6.86 – 6.75 (m, 2H, PhH), 6.45 (br s, 2H, Pyr'H), 5.15 (s, 1H, Pyr-CH-Ph), 3.94 (s, 3H,  $PhOCH_3$ ), 3.83 (s, 3H,  $PyrOCH_3$ ), 3.79 (s, 6H,  $Pyr'OCH_3$ ), 3.35 – 3.21 (m, 1H,  $CH_2CHHN$ ), 2.64 (s, 3H,  $NCH_3$ ), 2.62 (s, 3H,  $NCH_3$ ), 2.34 (s, 3H,  $Ph'CH_3$ ), 2.31 – 2.18 (m, 2H,  $CHHCHHN$ ), 2.09 – 1.92 (m, 1H,  $CHHCH_2N$ );

$^{13}C$  NMR (101 MHz,  $CDCl_3$ )  $\delta$  = 164.0, 158.7, 157.8, 150.9 (d,  $J$  = 243.8 Hz), 147.5 (d,  $J$  = 11.2 Hz), 141.5, 138.4, 137.7, 133.0, 131.0, 130.0, 126.7, 125.7, 124.4 (d,  $J$  = 3.3 Hz), 124.3 (d,  $J$  = 11.1 Hz), 122.4, 112.6, 98.1, 76.9, 56.7, 56.1, 53.9, 53.7, 45.2, 43.5, 41.7, 36.8, 21.2;

HangZhou HPLC (290 nm):  $t_R$  = 12.0 min, 99% (isocratic 40% solvent A in solvent B, 1.5 mL/min);

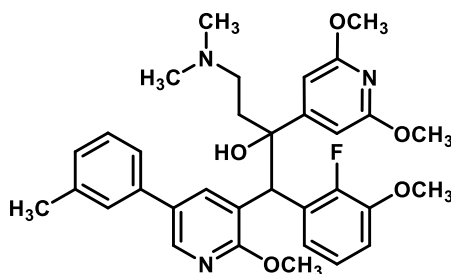
Diastereomer B:

$^1H$  NMR (400 MHz,  $CDCl_3$ )  $\delta$  = 11.09 (br s, 1H,  $NH^+$ ), 8.29 (s, 1H, PyrH), 8.11 (s, 1H, PyrH), 7.61 (t,  $J$  = 7.1 Hz, 1H, PhH), 7.38 (d,  $J$  = 7.8 Hz, 2H, Ph'H), 7.22 (d,  $J$  = 7.6 Hz, 2H, Ph'H), 6.85 (t,  $J$  = 8.1 Hz, 1H, PhH), 6.67 (t,  $J$  = 8.1 Hz, 1H, Ph'H), 6.49 (s, 2H, Pyr'H), 5.37 (s, 1H, Pyr-CH-Ph), 4.21 (s, 3H,  $PyrOCH_3$ ), 3.87 (s, 6H,  $Pyr'OCH_3$ ), 3.73 (s, 3H,  $PhOCH_3$ ), 3.33 – 3.21 (m, 1H,  $CH_2CHHN$ ), 2.69 (s, 3H,  $NCH_3$ ), 2.67 (s, 3H,  $NCH_3$ ), 2.45 – 2.27 (m, 5H,  $CHHCHHN$ ,  $Ph'CH_3$ ), 2.18 – 2.02 (m, 1H,  $CHHCH_2N$ );

$^{13}C$  NMR (101 MHz,  $CDCl_3$ )  $\delta$  = 163.7, 159.9, 158.2, 150.3 (d,  $J$  = 244.2 Hz), 147.3 (d,  $J$  = 11.5 Hz), 142.6, 140.2, 138.1, 133.5, 131.9, 129.8, 128.1 (d,  $J$  = 10.8 Hz), 127.0, 123.7 (d,  $J$  = 4.6 Hz), 123.5, 121.9, 111.9, 77.5 $\dagger$ , 98.3, 56.3, 56.1, 54.0, 53.8, 44.9, 43.2 $\dagger$ , 41.8, 37.0, 21.2;

HangZhou HPLC (290 nm):  $t_R$  = 17.7 min, 99% (isocratic 40% solvent A in solvent B, 1.5 mL/min).

**2-(2,6-dimethoxypyridin-4-yl)-4-(dimethylamino)-1-(2-fluoro-3-methoxyphenyl)-1-(2-methoxy-5-(*m*-tolyl)pyridin-3-yl)butan-2-ol (3.59)**



General method C was used with 3-tolylboronic acid (136 mg, 1.00 mmol) to afford the title compound a yellow foam (261 mg, 0.453 mmol, 91%, A:B = 50:50).

LR-MS (ESI+)  $m/z$ : 575.9 [ $M+H$ ] $^+$ ;

HR-MS (ESI+)  $m/z$  [ $M = C_{33}H_{38}FN_3O_5$ ]: [ $M+H$ ] $^+$  calc'd 576.2868, found 576.2879;

Analytical HPLC (254 nm):  $t_R = 6.7$  min, 97% (A + B overlapping);

Diastereomer A:

$^1H$  NMR (400 MHz,  $CDCl_3$ )  $\delta = 12.62$  (br s, 1H,  $NH^+$ ), 8.61 (d,  $J = 2.4$  Hz, 1H, PyrH), 8.05 (d,  $J = 2.4$  Hz, 1H, PyrH), 7.31 (t,  $J = 7.5$  Hz, 1H, Ph'H), 7.25 – 7.20 (m, 2H, Ph'H), 7.15 (d,  $J = 7.6$  Hz, 1H, Ph'H), 7.03 – 6.93 (m, 2H, PhH), 6.90 – 6.81 (m, 1H, PhH), 6.57 (s, 2H, Pyr'H), 5.25 (s, 1H, Pyr-CH-Ph), 3.89 (s, 3H, PhOCH<sub>3</sub>), 3.84 (s, 6H, Pyr'OCH<sub>3</sub>), 3.82 (s, 3H, PyrOCH<sub>3</sub>), 3.41 – 3.28 (m, 1H, CH<sub>2</sub>CHHN), 2.69 – 2.58 (m, 6H, N(CH<sub>3</sub>)<sub>2</sub>), 2.44 (s, 3H, Ph'CH<sub>3</sub>), 2.39 – 2.20 (m, 2H, CHHCHHN), 2.11 – 1.99 (m, 1H, CHHCH<sub>2</sub>N);

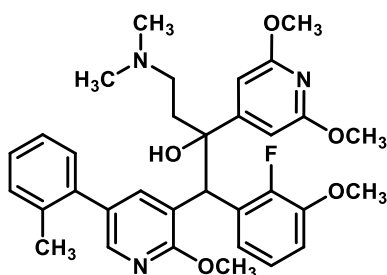
$^{13}C$  NMR (101 MHz,  $CDCl_3$ )  $\delta = 163.8, 160.6, 158.8, 151.0$  (d,  $J = 243.1$  Hz), 147.3 (d,  $J = 12.0$  Hz), 142.5, 138.6, 138.2, 138.1, 129.9, 128.9, 128.0, 127.8, 125.7 (d,  $J = 12.0$  Hz), 124.1 (d,  $J = 4.4$  Hz), 123.9, 123.2, 123.0, 112.0, 97.8 $^\dagger$ , 76.9 (d,  $J = 1.4$  Hz), 56.2, 53.6, 53.5, 45.0, 43.4, 41.3, 37.2, 21.6;

Diastereomer B:

$^1H$  NMR (400 MHz,  $CDCl_3$ )  $\delta = 11.17$  (br s, 1H,  $NH^+$ ), 8.29 (s, 1H, PyrH), 8.08 (s, 1H, PyrH), 7.62 (ddd,  $J = 7.8, 6.2, 1.5$  Hz, 1H, Ph'H), 7.35 – 7.25 (m, 3H, Ph'H), 7.16 (d,  $J = 7.0$  Hz, 1H, Ph'H), 6.86 (td,  $J = 8.1, 1.5$  Hz, 1H, PhH), 6.67 (td,  $J = 8.2, 1.4$  Hz, 1H, PhH), 6.49 (s, 2H, PyrH), 5.37 (s, 1H, Pyr-CH-Ph), 4.20 (s, 3H, PyrOCH<sub>3</sub>), 3.87 (s, 6H, Pyr'OCH<sub>3</sub>), 3.73 (s, 3H, PhOCH<sub>3</sub>), 3.27 (t,  $J = 11.5$  Hz, 1H, CH<sub>2</sub>CHHN), 2.70 (s, 3H, NCH<sub>3</sub>), 2.67 (s, 3H, NCH<sub>3</sub>), 2.48 – 2.22 (m, 5H, CHHCHHN, Ph'CH<sub>3</sub>), 2.10 (t,  $J = 11.0$  Hz, 1H, CHHCH<sub>2</sub>N);

$^{13}C$  NMR (101 MHz,  $CDCl_3$ )  $\delta = 163.7, 160.1, 158.2, 150.4$  (d,  $J = 244.1$  Hz), 147.3 (d,  $J = 11.4$  Hz), 142.8, 140.5, 138.9, 136.4, 132.2, 129.01, 128.96, 128.0 (d,  $J = 10.8$  Hz), 127.9, 124.4, 123.7 (d,  $J = 4.7$  Hz), 123.5, 121.9, 111.9, 98.3, 77.7 $^\dagger$ , 56.4, 56.1, 54.1, 53.8, 45.0, 43.3 $^\dagger$ , 41.8, 37.0, 21.5.

**2-(2,6-dimethoxypyridin-4-yl)-4-(dimethylamino)-1-(2-fluoro-3-methoxyphenyl)-1-(2-methoxy-5-(*o*-tolyl)pyridin-3-yl)butan-2-ol (3.60)**



General method C was used with 2-tolylboronic acid (136 mg, 1.00 mmol) to afford the title compound a yellow foam (249 mg, 0.433 mmol, 87%, A:B = 50:50).

LR-MS (ESI+)  $m/z$ : 575.9 [ $M+H$ ] $^+$ ;

HR-MS (ESI+)  $m/z$  [ $M = C_{33}H_{38}FN_3O_5$ ]: [ $M+H$ ] $^+$  calc'd 576.2868, found 576.2882;

Analytical HPLC (254 nm):  $t_R$  = 6.6 min, 96% (A + B overlapping);

Diastereomer A:

$^1\text{H}$  NMR (400 MHz,  $\text{CDCl}_3$ )  $\delta$  = 11.69 (br s, 1H,  $\text{NH}^+$ ), 8.07 (s, 1H, PyrH), 7.80 (d,  $J$  = 1.9 Hz, 1H, PyrH), 7.55 (t,  $J$  = 6.7 Hz, 1H, PhH), 7.23 (t,  $J$  = 2.8 Hz, 4H, Ph'H), 6.82 (td,  $J$  = 8.2, 1.5 Hz, 1H, PhH), 6.65 (td,  $J$  = 8.1, 1.3 Hz, 1H, PhH), 6.48 (s, 2H, Pyr'H), 5.37 (s, 1H, Pyr-CH-Ph), 4.15 (s, 3H, PyrOCH<sub>3</sub>), 3.86 (s, 6H, Pyr'OCH<sub>3</sub>), 3.73 (s, 3H, PhOCH<sub>3</sub>), 3.26 (t,  $J$  = 11.4 Hz, 1H, CH<sub>2</sub>CHHN), 2.68 (s, 3H, NCH<sub>3</sub>), 2.66 (s, 3H, NCH<sub>3</sub>), 2.50 – 2.37 (m, 1H, CHHCH<sub>2</sub>N), 2.34 – 2.22 (m, 1H, CH<sub>2</sub>CHHN), 2.19 – 2.07 (m, 4H, CHHCH<sub>2</sub>N, Ph'OCH<sub>3</sub>);

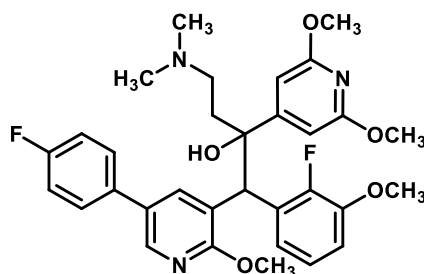
$^{13}\text{C}$  NMR (101 MHz,  $\text{CDCl}_3$ )  $\delta$  = 163.7, 160.3, 158.4, 150.3 (d,  $J$  = 244.4 Hz), 147.2 (d,  $J$  = 11.4 Hz), 144.3, 143.2, 137.3, 135.8, 131.6, 130.6, 130.3, 130.0 (d,  $J$  = 5.5 Hz), 128.5 (d,  $J$  = 12.0 Hz), 127.9, 126.2, 123.5 (d,  $J$  = 4.6 Hz), 122.2, 121.4, 111.7, 98.3, 77.5, 56.2, 55.0, 54.0, 53.7, 44.9, 43.5<sup>†</sup>, 41.6, 37.3;

Diastereomer B:

$^1\text{H}$  NMR (400 MHz,  $\text{CDCl}_3$ )  $\delta$  = 11.76 (br s, 1H,  $\text{NH}^+$ ), 8.36 (d,  $J$  = 1.9 Hz, 1H, PyrH), 7.80 (d,  $J$  = 2.3 Hz, 1H, PyrH), 7.26 – 7.12 (m, 3H, 2 × Ph'H, 1 × PhH), 6.98 (dd,  $J$  = 7.3, 1.3 Hz, 1H, Ph'H), 6.94 (d,  $J$  = 7.9 Hz, 1H, Ph'H), 6.89 (t,  $J$  = 6.8 Hz, 1H, PhH), 6.81 (t,  $J$  = 8.0 Hz, 1H, PhH), 6.42 (s, 2H, PyrH), 5.22 (s, 1H, Pyr-CH-Ph), 3.85 (s, 3H, PyrOCH<sub>3</sub>), 3.83 (s, 3H, Ph'OCH<sub>3</sub>), 3.80 (s, 6H, Pyr'OCH<sub>3</sub>), 3.32 – 3.17 (m, 1H, CH<sub>2</sub>CHHN), 2.59 (s, 3H, NCH<sub>3</sub>), 2.57 (s, 3H, NCH<sub>3</sub>), 2.29 – 2.15 (m, 2H, CHHCHHN), 2.02 (s, 3H, Ph'CH<sub>3</sub>), 2.01 – 1.89 (m, 1H, CHHCH<sub>2</sub>N);

$^{13}\text{C}$  NMR (101 MHz,  $\text{CDCl}_3$ )  $\delta$  = 163.8, 159.8, 158.3, 151.0 (d,  $J$  = 243.7 Hz), 147.5 (d,  $J$  = 12.1 Hz), 142.8, 141.4, 137.7, 136.0, 131.0, 130.5, 130.1, 128.0, 126.1, 125.3 (d,  $J$  = 11.6 Hz), 124.3 (d,  $J$  = 4.4 Hz), 123.3, 122.7, 112.3, 98.3, 77.0, 56.2, 54.9, 53.8, 53.7, 45.1, 43.3, 41.6, 37.0, 20.3.

**2-(2,6-dimethoxypyridin-4-yl)-4-(dimethylamino)-1-(2-fluoro-3-methoxyphenyl)-1-(5-(4-fluorophenyl)-2-methoxypyridin-3-yl)butan-2-ol (3.61)**



General method C was used with 4-fluorophenylboronic acid (140 mg, 1.00 mmol) to afford the title compound a yellow foam (249 mg, 0.430 mmol, 86%, A:B = 50:50).

A portion of this product was further subjected to purification by our collaborators at HangZhou (China) using preparative HPLC to isolate the individual diastereomers as the TFA salt. This was performed using an Agilent 1260 Infinity HPLC system fitted with a Bondysil-C8 column (10  $\mu$ m, 250  $\times$  20 mm). Isocratic elution was used with a solvent system of 42% ultrapure H<sub>2</sub>O (0.05% TFA) in MeOH (0.05% TFA) over 60 min with a flow rate of 17 mL/min.

LR-MS (ESI+)  $m/z$ : 579.8 [M+H]<sup>+</sup>;

HR-MS (ESI+)  $m/z$  [M = C<sub>32</sub>H<sub>35</sub>F<sub>2</sub>N<sub>3</sub>O<sub>5</sub>]: [M+H]<sup>+</sup> calc'd 580.2618, found 580.2625;

Diastereomer A:

<sup>1</sup>H NMR (400 MHz, CDCl<sub>3</sub>)  $\delta$  = 11.35 (br s, 1H, NH<sup>+</sup>), 8.72 (d,  $J$  = 1.7 Hz, 1H, PyrH), 8.12 (d,  $J$  = 2.1 Hz, 1H, PyrH), 7.44 – 7.34 (m, 2H, Ph'H), 7.14 (t,  $J$  = 8.6 Hz, 2H, Ph'H), 7.01 (t,  $J$  = 8.0 Hz, 1H, PhH), 6.92 – 6.85 (m, 2H, PhH), 6.52 (br s, 2H, Pyr'H), 5.23 (s, 1H, Pyr-CH-Ph), 3.93 (s, 3H, PyrOCH<sub>3</sub>), 3.90 (s, 3H, Ph'OCH<sub>3</sub>), 3.86 (s, 6H, Pyr'OCH<sub>3</sub>), 3.43 – 3.27 (m, 1H, CH<sub>2</sub>CHHN), 2.70 (s, 3H, NCH<sub>3</sub>), 2.68 (s, 3H, NCH<sub>3</sub>), 2.42 – 2.23 (m, 2H, CHHCH<sub>2</sub>N), 2.14 – 1.94 (m, 1H, CHHCH<sub>2</sub>N);

<sup>13</sup>C NMR (101 MHz, CDCl<sub>3</sub>)  $\delta$  = 163.9, 162.8 (d,  $J$  = 247.5 Hz), 159.9, 158.2, 151.0 (d,  $J$  = 243.6 Hz), 147.5 (d,  $J$  = 12.0 Hz), 140.1, 139.8, 133.2 (d,  $J$  = 3.3 Hz), 130.0 (d,  $J$  = 5.9 Hz), 129.5, 128.5 (d,  $J$  = 8.1 Hz), 124.9 (d,  $J$  = 11.9 Hz), 124.6, 124.4 (d,  $J$  = 4.4 Hz), 122.6, 116.1 (d,  $J$  = 21.8 Hz), 112.5, 98.2, 56.2, 55.5, 53.9, 53.7, 45.2, 43.6, 41.7, 37.0;

HangZhou HPLC (290 nm):  $t_R$  = 5.9 min, 99% (isocratic 40% solvent A in solvent B, 1.2 mL/min);

Diastereomer B:

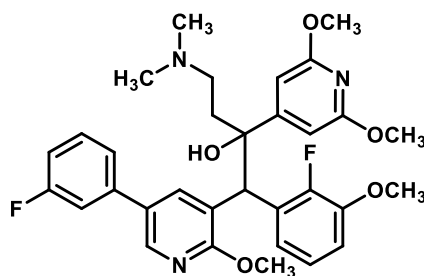
<sup>1</sup>H NMR (400 MHz, CDCl<sub>3</sub>)  $\delta$  = 11.11 (br s, 1H, NH<sup>+</sup>), 8.26 (d,  $J$  = 1.3 Hz, 1H, PyrH), 8.02 (d,  $J$  = 1.7 Hz, 1H, PyrH), 7.63 (ddd,  $J$  = 7.8, 6.1, 1.5 Hz, 1H, PhH), 7.45 (dd,  $J$  = 8.6, 5.3 Hz, 2H, Ph'H), 7.09 (t,  $J$  = 8.6 Hz, 2H, Ph'H), 6.86 (td,  $J$  = 8.2, 1.3 Hz, 1H, PhH), 6.67 (td,  $J$  = 8.2, 1.4 Hz, 1H, PhH), 6.50 (s, 2H, Pyr'H), 5.37 (s, 1H, Pyr-CH-Ph), 4.17 (s, 3H, PyrOCH<sub>3</sub>), 3.87 (s, 6H, Pyr'OCH<sub>3</sub>), 3.73 (s, 3H, PhOCH<sub>3</sub>), 3.29 (t,  $J$  = 11.4 Hz, 1H, CH<sub>2</sub>CHHN), 2.70 (s, 3H, NCH<sub>3</sub>), 2.67 (s, 3H, NCH<sub>3</sub>), 2.50 – 2.22 (m, 2H, CHHCHHN), 2.08 (t,  $J$  = 11.2 Hz, 1H, CHHCH<sub>2</sub>N);

<sup>13</sup>C NMR (101 MHz, CDCl<sub>3</sub>)  $\delta$  = 163.7, 162.9 (d,  $J$  = 247.2 Hz), 160.5, 158.3, 150.4 (d,  $J$  = 244.4 Hz), 147.3 (d,  $J$  = 11.8 Hz), 141.7 (d,  $J$  = 3.9 Hz), 141.5 (d,  $J$  = 4.4 Hz), 133.0, 130.8, 128.9 (d,  $J$  = 8.1 Hz), 128.3 (d,  $J$  = 11.5 Hz), 123.7 (d,  $J$  = 4.6 Hz), 122.9 (d,  $J$  = 3.9 Hz), 121.9, 115.9 (d,  $J$  = 21.7 Hz), 111.8, 98.3, 77.7<sup>†</sup>, 56.1, 55.8, 54.1, 53.8, 45.1, 43.1<sup>†</sup>, 41.7, 37.0;

HangZhou HPLC (290 nm):  $t_R$  = 7.0 min, 97% (isocratic 40% solvent A in solvent B, 1.2 mL/min).



**2-(2,6-dimethoxypyridin-4-yl)-4-(dimethylamino)-1-(2-fluoro-3-methoxyphenyl)-1-(5-(3-fluorophenyl)-2-methoxypyridin-3-yl)butan-2-ol (3.62)**



General method C was used with 3-fluorophenylboronic acid (140 mg, 1.00 mmol) to afford the title compound a yellow foam (228 mg, 0.393 mmol, 79%, A:B = 50:50).

LR-MS (ESI+)  $m/z$ : 580.1  $[M+H]^+$ ;

HR-MS (ESI+)  $m/z$   $[M = C_{32}H_{35}F_2N_3O_5]$ :  $[M+H]^+$  calc'd 580.2618, found 580.2631;

Analytical HPLC (254 nm):  $t_R$  = 6.6 min, 99% (A + B overlapping);

Diastereomer A:

$^1H$  NMR (400 MHz,  $CDCl_3$ )  $\delta$  = 12.09 (br s, 1H,  $NH^+$ ), 8.63 (d,  $J$  = 2.4 Hz, 1H, PyrH), 8.08 (d,  $J$  = 2.5 Hz, 1H, PyrH), 7.39 (td,  $J$  = 8.0, 6.0 Hz, 1H, Ph'H), 7.21 (dt,  $J$  = 7.7, 1.2 Hz, 1H, Ph'H), 7.11 (dt,  $J$  = 10.1, 2.1 Hz, 1H, Ph'H), 7.08 – 6.96 (m, 2H, PhH, Ph'H), 6.93 (ddd,  $J$  = 7.9, 5.9, 1.7 Hz, 1H, PhH), 6.86 (td,  $J$  = 8.1, 1.3 Hz, 1H, PhH), 6.55 (br s, 2H, Pyr'H), 5.24 (s, 1H, Pyr-CH-Ph), 3.89 (s, 3H, PhOCH<sub>3</sub>), 3.85 (s, 9H, PyrOCH<sub>3</sub>, Pyr'OCH<sub>3</sub>), 3.40 – 3.30 (m, 1H, CH<sub>2</sub>CHHN), 2.67 (s, 3H, NCH<sub>3</sub>), 2.64 (s, 3H, NCH<sub>3</sub>), 2.39 – 2.20 (m, 2H, CHHCHHN), 2.15 – 1.93 (m, 1H, CHHCH<sub>2</sub>N);

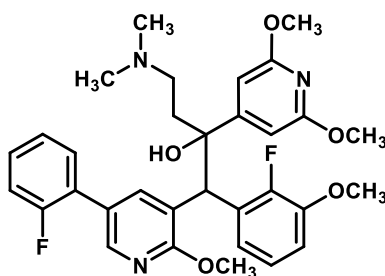
$^{13}C$  NMR (101 MHz,  $CDCl_3$ )  $\delta$  = 163.7, 163.2 (d,  $J$  = 245.9 Hz), 160.8, 158.4, 150.9 (d,  $J$  = 243.2 Hz), 147.3 (d,  $J$  = 12.0 Hz), 142.0, 140.2 (d,  $J$  = 7.7 Hz), 138.1, 130.4 (d,  $J$  = 8.2 Hz), 128.6 (d,  $J$  = 1.8 Hz), 125.3 (d,  $J$  = 11.4 Hz), 124.1 (d,  $J$  = 4.5 Hz), 123.4, 122.8, 122.3 (d,  $J$  = 2.9 Hz), 114.0 (d,  $J$  = 21.3 Hz), 113.5 (d,  $J$  = 22.2 Hz), 112.1, 98.2, 76.9, 56.0, 54.2, 53.6, 53.5, 44.9, 43.3, 41.3, 37.0;

Diastereomer B:

$^1H$  NMR (400 MHz,  $CDCl_3$ )  $\delta$  = 12.64 (br s, 1H,  $NH^+$ ), 8.22 (d,  $J$  = 2.3 Hz, 1H, PyrH), 7.91 (d,  $J$  = 2.4 Hz, 1H, PyrH), 7.72 (ddd,  $J$  = 7.9, 6.1, 1.6 Hz, 1H, PhH), 7.35 (td,  $J$  = 7.9, 5.9 Hz, 1H, Ph'H), 7.30 – 7.27 (m, 1H, Ph'H), 7.20 (dt,  $J$  = 10.1, 2.1 Hz, 1H, Ph'H), 7.04 – 6.96 (m, 1H, Ph'H), 6.85 (td,  $J$  = 8.2, 1.6 Hz, 1H, PhH), 6.65 (td,  $J$  = 8.3, 1.5 Hz, 1H, PhH), 6.53 (s, 2H, Pyr'H), 5.38 (s, 1H, Pyr-CH-Ph), 4.10 (s, 3H, PyrOCH<sub>3</sub>), 3.86 (s, 6H, Pyr'OCH<sub>3</sub>), 3.72 (s, 3H, PhOCH<sub>3</sub>), 3.29 (t,  $J$  = 11.7 Hz, 1H, CH<sub>2</sub>CHHN), 2.64 (s, 3H, NCH<sub>3</sub>), 2.59 (s, 3H, NCH<sub>3</sub>), 2.42 (td,  $J$  = 12.1, 6.9 Hz, 1H, CHHCH<sub>2</sub>N), 2.23 (t,  $J$  = 7.6 Hz, 1H, CH<sub>2</sub>CHHN), 2.09 – 2.04 (m, 1H, CHHCH<sub>2</sub>N);

$^{13}\text{C}$  NMR (101 MHz,  $\text{CDCl}_3$ )  $\delta$  = 163.7, 163.2 (d,  $J$  = 245.7 Hz), 161.6, 158.8, 150.4 (d,  $J$  = 244.3 Hz), 147.2, 144.1, 143.8, 140.4 (d,  $J$  = 8.0 Hz), 139.9, 130.3 (d,  $J$  = 8.6 Hz), 129.0, 123.5 (d,  $J$  = 4.5 Hz), 123.0 (d,  $J$  = 2.9 Hz), 122.3 (d,  $J$  = 2.0 Hz), 121.4, 114.2 (d,  $J$  = 5.2 Hz), 114.0 (d,  $J$  = 4.1 Hz), 111.5, 98.5, 77.3, 56.1, 54.3, 53.7, 53.6, 45.0, 42.9, 41.1, 37.1.

**2-(2,6-dimethoxypyridin-4-yl)-4-(dimethylamino)-1-(2-fluoro-3-methoxyphenyl)-1-(5-(2-fluorophenyl)-2-methoxypyridin-3-yl)butan-2-ol (3.62)**



General method C was used with 2-fluorophenylboronic acid (140 mg, 1.00 mmol) to afford the title compound a yellow foam (245 mg, 0.423 mmol, 85%, A:B = 50:50).

LR-MS (ESI+)  $m/z$ : 580.0  $[\text{M}+\text{H}]^+$ ;

HR-MS (ESI+)  $m/z$  [ $\text{M} = \text{C}_{32}\text{H}_{35}\text{F}_2\text{N}_3\text{O}_5$ ]:  $[\text{M}+\text{H}]^+$  calc'd 580.2618, found 580.2627;

Analytical HPLC (254 nm):  $t_R$  = 6.5 min, 100% (A + B overlapping);

Diastereomer A:

$^1\text{H}$  NMR (400 MHz,  $\text{CDCl}_3$ )  $\delta$  = 12.47 (br s, 1H,  $\text{NH}^+$ ), 8.60 (d,  $J$  = 0.8 Hz, 1H,  $\text{PyrH}$ ), 8.06 (t,  $J$  = 2.0 Hz, 1H,  $\text{PyrH}$ ), 7.35 – 7.25 (m, 2H,  $\text{PhH}$ ,  $\text{Ph'H}$ ), 7.24 – 7.15 (m, 1H,  $\text{PhH}$ ), 7.18 – 7.08 (m, 1H,  $\text{Ph'H}$ ), 7.03 – 6.96 (m, 2H,  $\text{PhH}$ ,  $\text{Ph'H}$ ), 6.91 – 6.80 (m, 1H,  $\text{Ph'H}$ ), 6.53 (br s, 2H,  $\text{PyrH}$ ), 5.27 (s, 1H,  $\text{Pyr-CH-Ph}$ ), 3.89 (s, 3H,  $\text{PhOCH}_3$ ), 3.85 (s, 6H,  $\text{Pyr'OCH}_3$ ), 3.84 (s, 3H,  $\text{PyrOCH}_3$ ), 3.38 – 3.27 (m, 1H,  $\text{CH}_2\text{CHHN}$ ), 2.63 (s, 3H,  $\text{NCH}_3$ ), 2.61 (s, 3H,  $\text{NCH}_3$ ), 2.41 – 2.17 (m, 2H,  $\text{CHHCHHN}$ ), 2.10 – 1.93 (m, 1H,  $\text{CHHCH}_2\text{N}$ );

$^{13}\text{C}$  NMR (101 MHz,  $\text{CDCl}_3$ )  $\delta$  = 163.6, 160.5, 159.7 (d,  $J$  = 247.9 Hz), 158.5, 150.9 (d,  $J$  = 243.1 Hz), 147.2 (d,  $J$  = 12.0 Hz), 144.1 (d,  $J$  = 4.6 Hz), 139.6, 130.3 (d,  $J$  = 3.4 Hz), 129.0 (d,  $J$  = 8.1 Hz), 125.9 (d,  $J$  = 13.8 Hz), 125.5 (d,  $J$  = 11.8 Hz), 124.5, 124.5, 124.0 (d,  $J$  = 4.6 Hz), 122.9, 122.9, 116.1 (d,  $J$  = 22.6 Hz), 111.9, 98.3, 76.9, 56.0, 53.9, 53.5, 53.4, 44.8, 43.0, 41.1, 36.9;

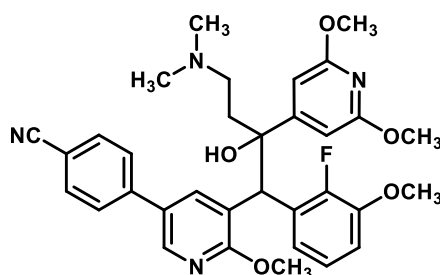
Diastereomer B:

$^1\text{H}$  NMR (400 MHz,  $\text{CDCl}_3$ )  $\delta$  = 12.02 (br s, 1H,  $\text{NH}^+$ ), 8.27 (t,  $J$  = 2.1 Hz, 1H,  $\text{PyrH}$ ), 7.99 (dd,  $J$  = 2.5, 1.2 Hz, 1H,  $\text{PyrH}$ ), 7.61 (ddd,  $J$  = 7.9, 6.2, 1.5 Hz, 1H,  $\text{PhH}$ ), 7.46 (td,  $J$  = 7.8, 1.9 Hz, 1H,  $\text{Ph'H}$ ), 7.33 – 7.25 (m, 1H,  $\text{Ph'H}$ ), 7.19 (td,  $J$  = 7.5, 1.3 Hz, 1H,  $\text{Ph'H}$ ), 7.09 (ddd,  $J$  = 10.7, 8.2, 1.3 Hz, 1H,  $\text{Ph'H}$ ), 6.84 (td,  $J$  = 8.1, 1.5 Hz, 1H,  $\text{PhH}$ ), 6.65 (td,  $J$  = 8.2, 1.5 Hz, 1H,  $\text{PhH}$ ), 6.49 (s, 2H,  $\text{PyrH}$ ), 5.37 (s, 1H,  $\text{Pyr-CH-Ph}$ ), 4.10

(s, 3H, PyrOCH<sub>3</sub>), 3.86 (s, 6H, Pyr'OCH<sub>3</sub>), 3.72 (s, 3H, PhOCH<sub>3</sub>), 3.30 – 3.18 (m, 1H, CH<sub>2</sub>CHHN), 2.66 (s, 3H, NCH<sub>3</sub>), 2.63 (s, 3H, NCH<sub>3</sub>), 2.46 – 2.28 (m, 2H, CHHCHHN), 2.16 – 2.06 (m, 1H, CHHCH<sub>2</sub>N);

<sup>13</sup>C NMR (101 MHz, CDCl<sub>3</sub>) δ = 163.6, 159.8 (d, *J* = 247.6 Hz), 158.9, 150.4 (d, *J* = 244.4 Hz), 147.1 (d, *J* = 11.6 Hz), 145.6 (d, *J* = 4.4 Hz), 141.3, 131.0 (d, *J* = 3.3 Hz), 130.0 (d, *J* = 3.3 Hz), 129.1 (d, *J* = 8.1 Hz), 128.8 (d, *J* = 11.2 Hz), 125.8 (d, *J* = 13.5 Hz), 125.6 (d, *J* = 1.2 Hz), 124.6 (d, *J* = 3.5 Hz), 123.4 (d, *J* = 4.7 Hz), 122.3, 121.2, 115.9 (d, *J* = 22.7 Hz), 111.5, 98.4, 77.3†, 56.1, 54.2, 53.7, 53.6, 44.7†, 43.1†, 41.2†, 36.9.

**4-(5-(2-(2,6-dimethoxyphenyl)-4-(dimethylamino)-1-(2-fluoro-3-methoxyphenyl)-2-hydroxybutyl)-6-methoxypyridin-3-yl)benzonitrile (3.64)**



General method C was used with 4-cyanophenylboronic acid (147 mg, 1.00 mmol) to afford the title compound a yellow foam (160 mg, 0.273 mmol, 55%, A:B = 57:43).

A portion of this product was further subjected to purification by our collaborators at HangZhou (China) using preparative HPLC to isolate the individual diastereomers as the TFA salt. This was performed using a Generik HP30 and Gilson FC204 HPLC system fitted with a Bondysil-C8 column (10 μm, 250 × 20 mm). Isocratic elution was used with a solvent system of 45% MeCN (0.05% TFA) in ultrapure H<sub>2</sub>O (0.05% TFA) over 20 min with a flow rate of 20 mL/min.

Diastereomer B was further subjected to chiral purification by our collaborators at TCG Lifesciences using HPLC to isolate the individual enantiomers. Isocratic elution was used with a solvent system of Hexane/EtOH/Isopropylamine (80/20/0.1) over 10 min with a flow rate of 1 mL/min.

LR-MS (ESI+) *m/z*: 587.0 [M+H]<sup>+</sup>;

HR-MS (ESI+) *m/z* [M = C<sub>33</sub>H<sub>35</sub>FN<sub>4</sub>O<sub>5</sub>]: [M+H]<sup>+</sup> calc'd 587.2664, found 588.2674;

Diastereomer A:

<sup>1</sup>H NMR (400 MHz, CDCl<sub>3</sub>) δ = 11.31 (br s, 1H, NH<sup>+</sup>), 8.68 (d, *J* = 2.3 Hz, 1H, PyrH), 8.14 (d, *J* = 2.5 Hz, 1H, PyrH), 7.72 (d, *J* = 8.4 Hz, 2H, Ph'H), 7.53 (d, *J* = 8.4 Hz, 2H, Ph'H), 6.99 (t, *J* = 8.0 Hz, 1H, PhH), 6.87 (t, 2H, PhH), 6.53 (br s, 2H, Pyr'H), 5.24 (s, 1H, Pyr-CH-Ph), 3.89 (s, 3H, PhOCH<sub>3</sub>), 3.87 (s, 3H, PyrOCH<sub>3</sub>),

3.85 (s, 6H, Pyr'OCH<sub>3</sub>), 3.42 – 3.30 (m, 1H, CH<sub>2</sub>CHHN), 2.70 (s, 3H, NCH<sub>3</sub>), 2.68 (s, 3H, NCH<sub>3</sub>), 2.42 – 2.21 (m, 2H, CHHCHHN), 2.13 – 1.95 (m, 1H, CHHCH<sub>2</sub>N);

<sup>13</sup>C NMR (101 MHz, CDCl<sub>3</sub>) δ = 163.8, 161.2, 158.2, 151.0 (d, *J* = 243.8 Hz), 147.4 (d, *J* = 11.7 Hz), 142.3, 142.1, 138.5 (d, *J* = 2.1 Hz), 132.9, 128.0, 127.2, 125.0 (d, *J* = 11.7 Hz), 124.2 (d, *J* = 4.0 Hz), 124.1, 122.5, 118.9, 112.3, 110.9, 98.1, 77.0, 56.1, 54.7 (d, *J* = 3.1 Hz), 53.8, 53.6, 45.1, 43.4, 41.6, 36.9;

HangZhou HPLC (290 nm): *t*<sub>R</sub> = 20.5 min, 94% (isocratic 45% solvent A in solvent B, 1.0 mL/min);

Diastereomer B:

<sup>1</sup>H NMR (400 MHz, CDCl<sub>3</sub>) δ = 11.88 (br s, 1H, NH<sup>+</sup>), 8.25 (d, *J* = 2.4 Hz, 1H, PyrH), 7.94 (d, *J* = 2.3 Hz, 1H, PyrH), 7.75 – 7.64 (m, 3H, 2 × Ph'H, 1 × PhH), 7.61 (d, *J* = 8.5 Hz, 2H, Ph'H), 6.85 (td, *J* = 8.2, 1.5 Hz, 1H, PhH), 6.66 (td, *J* = 8.2, 1.4 Hz, 1H, PhH), 6.52 (s, 2H, Pyr'H), 5.39 (s, 1H, Pyr-CH-Ph), 4.11 (s, 3H, PyrOCH<sub>3</sub>), 3.86 (s, 6H, Pyr'OCH<sub>3</sub>), 3.72 (s, 3H, PhOCH<sub>3</sub>), 3.31 (t, *J* = 11.8 Hz, 1H, CH<sub>2</sub>CHHN), 2.66 (s, 3H, NCH<sub>3</sub>), 2.61 (s, 3H, NCH<sub>3</sub>), 2.49 – 2.38 (m, 1H, CHHCH<sub>2</sub>N), 2.32 – 2.19 (m, 1H, CH<sub>2</sub>CHHN), 2.12 – 1.94 (m, 1H, CHHCH<sub>2</sub>N);

<sup>13</sup>C NMR (101 MHz, CDCl<sub>3</sub>) δ = 163.7, 162.0, 158.4, 150.4 (d, *J* = 244.4 Hz), 147.2 (d, *J* = 11.6 Hz), 143.8, 142.6, 140.0, 132.6, 129.3, 128.8 (d, *J* = 10.8 Hz), 127.8, 123.5 (d, *J* = 4.5 Hz), 122.0, 122.0, 119.2, 111.6, 110.9, 98.4, 77.3, 56.1, 54.6, 53.8, 53.7, 45.2, 42.8, 41.2, 37.1;

HangZhou HPLC (290 nm): *t*<sub>R</sub> = 22.4 min, 97% (isocratic 45% solvent A in solvent B, 1.0 mL/min);

Chiral HPLC (224 nm): *t*<sub>R</sub> = 6.6 min, 50% (B1); 8.6 min 50% (B2);

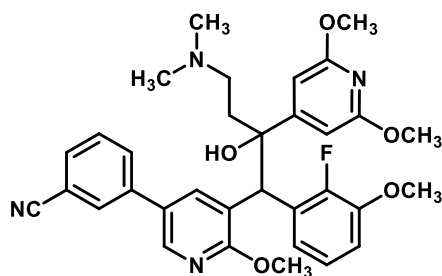
Enantiomer B1:

Chiral HPLC (224 nm): *t*<sub>R</sub> = 6.6 min, 100%;

Enantiomer B2:

Chiral HPLC (224 nm): *t*<sub>R</sub> = 8.7min, 99%.

**3-(5-(2-(2,6-dimethoxypyridin-4-yl)-4-(dimethylamino)-1-(2-fluoro-3-methoxyphenyl)-2-hydroxybutyl)-6-methoxypyridin-3-yl)benzonitrile (3.65)**



General method C was used with 3-cyanophenylboronic acid (147 mg, 1.00 mmol) to afford the title compound a yellow foam (123 mg, 0.210 mmol, 42%, A:B = 67:33).

LR-MS (ESI+)  $m/z$ : 587.0  $[M+H]^+$ ;

HR-MS (ESI+)  $m/z$   $[M = C_{33}H_{35}FN_4O_5]$ :  $[M+H]^+$  calc'd 587.2664, found 587.2672;

Analytical HPLC (254 nm):  $t_R$  = 6.3 min, 86% (A + B overlapping);

Diastereomer A:

$^1H$  NMR (400 MHz,  $CDCl_3$ )  $\delta$  = 10.83 (br s, 1H,  $NH^+$ ), 8.66 (d,  $J$  = 2.0 Hz, 1H, PyrH), 8.12 (d,  $J$  = 2.4 Hz, 1H, PyrH), 7.69 – 7.62 (m, 3H, Ph'H), 7.56 (t,  $J$  = 7.7 Hz, 1H, Pyr'H), 7.00 (t,  $J$  = 8.0 Hz, 1H, PhH), 6.89 (t,  $J$  = 8.0 Hz, 1H, PhH), 6.82 (t,  $J$  = 6.9 Hz, 1H, PhH), 6.54 (br s, 2H, Pyr'H), 5.22 (s, 1H, Pyr-CH-Ph), 3.91 (s, 3H, PyrOCH<sub>3</sub>), 3.90 (s, 3H, PhOCH<sub>3</sub>), 3.88 (s, 6H, Pyr'OCH<sub>3</sub>), 3.44 – 3.29 (m, 1H, CH<sub>2</sub>CHHN), 2.72 (s, 3H, NCH<sub>3</sub>), 2.71 (s, 3H, NCH<sub>3</sub>), 2.40 – 2.28 (m, 2H, CHHCHHN), 2.17 – 2.05 (m, 1H, CHHCH<sub>2</sub>N);

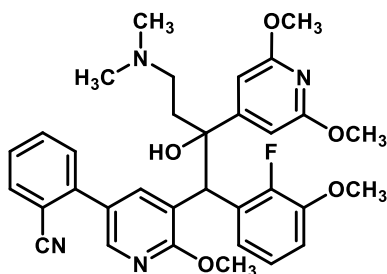
$^{13}C$  NMR (101 MHz,  $CDCl_3$ )  $\delta$  = 164.0, 160.7, 158.0, 151.0 (d,  $J$  = 243.9 Hz), 147.6 (d,  $J$  = 11.7 Hz), 141.0, 139.4, 138.7, 137.9 (d,  $J$  = 13.0 Hz), 131.3, 130.4 (2  $\times$  Ph'CH), 130.1, 128.2, 124.6 (d,  $J$  = 11.2 Hz), 124.4, 122.4, 118.6, 113.4, 112.5, 98.2, 77.0, 56.1, 55.4 (d,  $J$  = 1.8 Hz), 54.1, 53.8, 45.3, 43.7, 41.9, 37.0;

Diastereomer B:

$^1H$  NMR (400 MHz,  $CDCl_3$ )  $\delta$  = 12.07 (br s, 1H,  $NH^+$ ), 8.22 (d,  $J$  = 2.3 Hz, 1H, PyrH), 7.90 (d,  $J$  = 2.3 Hz, 1H, PyrH), 7.79 – 7.68 (m, 3H, 2  $\times$  Ph'H, 1  $\times$  PhH), 7.59 (d,  $J$  = 7.6 Hz, 1H, Ph'H), 7.50 (t,  $J$  = 7.8 Hz, 1H, Ph'H), 6.87 (td,  $J$  = 8.1, 1.5 Hz, 1H, PhH), 6.66 (td,  $J$  = 8.2, 1.4 Hz, 1H, PhH), 6.53 (br s, 2H, Pyr'H), 5.39 (s, 1H, Pyr-CH-Ph), 4.11 (s, 3H, PyrOCH<sub>3</sub>), 3.86 (s, 6H, Pyr'OCH<sub>3</sub>), 3.73 (s, 3H, PhOCH<sub>3</sub>), 3.31 (t,  $J$  = 11.7 Hz, 1H, CH<sub>2</sub>CHHN), 2.67 (s, 3H, NCH<sub>3</sub>), 2.61 (s, 3H, NCH<sub>3</sub>), 2.50 – 2.36 (m, 1H, CHHCH<sub>2</sub>N), 2.32 – 2.19 (m, 1H, CH<sub>2</sub>CHHN), 2.09 – 2.02 (m, 1H, CHHCH<sub>2</sub>N);

$^{13}C$  NMR (101 MHz,  $CDCl_3$ )  $\delta$  = 163.7, 161.8, 158.5, 150.4 (d,  $J$  = 244.4 Hz), 147.2 (d,  $J$  = 11.5 Hz), 143.7, 140.0, 139.3, 131.8, 130.8, 130.7, 129.7, 129.1, 128.8 (d,  $J$  = 10.7 Hz), 123.6 (d,  $J$  = 4.6 Hz), 122.1, 121.9, 119.0, 112.9, 111.6, 98.4, 77.3, 56.1, 54.6, 53.8, 53.7, 45.2, 43.9 $\dagger$ , 41.2, 37.1.

**2-(5-(2-(2,6-dimethoxyppyridin-4-yl)-4-(dimethylamino)-1-(2-fluoro-3-methoxyphenyl)-2-hydroxybutyl)-6-methoxyppyridin-3-yl)benzonitrile (3.66)**



General method C was used with 2-cyanophenylboronic acid (147 mg, 1.00 mmol) to afford the title compound a yellow foam (133 mg, 0.227 mmol, 45%, A:B = 50:50).

LR-MS (ESI+)  $m/z$ : 587.0  $[M+H]^+$ ;

HR-MS (ESI+)  $m/z$   $[M = C_{33}H_{35}FN_4O_5]$ :  $[M+H]^+$  calc'd 587.2664, found 587.2672;

Analytical HPLC (254 nm):  $t_R$  = 6.1 min, 44% (A); 6.2 min, 46% (B);

Diastereomer A:

$^1H$  NMR (400 MHz,  $CDCl_3$ )  $\delta$  = 11.67 (br s, 1H,  $NH^+$ ), 8.52 (d,  $J$  = 2.3 Hz, 1H, PyrH), 8.11 (d,  $J$  = 2.4 Hz, 1H, PyrH), 7.75 (d,  $J$  = 7.8 Hz, 1H, Ph'H), 7.65 (td,  $J$  = 7.7, 1.3 Hz, 1H, Ph'H), 7.44 (t,  $J$  = 7.6 Hz, 1H, Ph'H), 7.32 (d,  $J$  = 7.8 Hz, 1H, Ph'H), 7.09 (t,  $J$  = 6.8 Hz, 1H, PhH), 7.03 (t,  $J$  = 8.0 Hz, 1H, PhH), 6.87 (t,  $J$  = 8.0 Hz, 1H, PhH), 6.49 (s, 2H, Pyr'H), 5.30 (s, 1H, Pyr-CH-Ph), 3.89 (s, 3H, PhOCH3), 3.86 (s, 3H, PyrOCH3), 3.85 (s, 6H, Pyr'OCH3), 3.34 – 3.22 (m, 1H, CH<sub>2</sub>CHHN), 2.66 (s, 3H, NCH3), 2.64 (s, 3H, NCH3), 2.38 – 2.21 (m, 2H, CHHCHHN), 2.08 (d,  $J$  = 12.4 Hz, 1H, CHHCH2N);

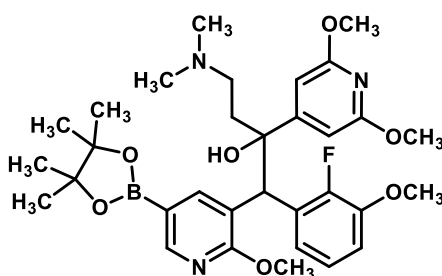
$^{13}C$  NMR (101 MHz,  $CDCl_3$ )  $\delta$  = 163.8, 161.4, 158.2, 151.0 (d,  $J$  = 243.4 Hz), 147.4 (d,  $J$  = 11.8 Hz), 144.1, 142.2, 139.4, 133.9, 133.1, 130.1, 127.8, 127.1, 125.4 (d,  $J$  = 11.7 Hz), 124.4 (d,  $J$  = 4.5 Hz), 123.3, 122.9, 118.7, 112.3, 111.2, 98.3, 77.2, 56.2, 54.3, 53.8, 53.7, 44.9, 43.2, 41.7, 36.8;

Diastereomer B:

$^1H$  NMR (400 MHz,  $CDCl_3$ )  $\delta$  = 11.64 (br s, 1H,  $NH^+$ ), 8.25 (d,  $J$  = 2.3 Hz, 1H, PyrH), 8.05 (d,  $J$  = 2.3 Hz, 1H, PyrH), 7.72 (dd,  $J$  = 7.8, 1.2 Hz, 1H, Ph'H), 7.66 (td,  $J$  = 7.6, 1.3 Hz, 1H, PhH), 7.62 – 7.56 (m, 2H, Ph'H), 7.44 (td,  $J$  = 7.5, 1.3 Hz, 1H, Ph'H), 6.83 (td,  $J$  = 8.0, 1.3 Hz, 1H, PhH), 6.66 (td,  $J$  = 8.2, 1.3 Hz, 1H, PhH), 6.48 (s, 2H, Pyr'H), 5.37 (s, 1H, Pyr-CH-Ph), 4.11 (s, 3H, PyrOCH3), 3.86 (s, 6H, Pyr'OCH3), 3.73 (s, 3H, Ph'OCH3), 3.20 – 3.10 (m, 1H, CH<sub>2</sub>CHHN), 2.66 (s, 3H, NCH3), 2.65 (s, 3H, NCH3), 2.49 – 2.34 (m, 2H, CHHCHHN), 2.18 – 2.06 (m, 1H, CHHCH2N);

$^{13}C$  NMR (101 MHz,  $CDCl_3$ )  $\delta$  = 163.7, 162.0, 158.2, 150.5 (d,  $J$  = 244.7 Hz), 147.3 (d,  $J$  = 11.6 Hz), 145.2, 142.1, 140.7, 133.5, 133.3, 130.3, 127.9, 127.9, 123.5 (d,  $J$  = 4.5 Hz), 122.2, 121.8, 111.8, 111.3, 98.3, 77.9, 56.2, 54.5, 53.9, 53.7, 44.3, 43.1, 42.2, 36.6, missing 2  $\times$  ArC.

**2-(2,6-dimethoxypyridin-4-yl)-4-(dimethylamino)-1-(2-fluoro-3-methoxyphenyl)-1-(2-methoxy-5-(4,4,5,5-tetramethyl-1,3,2-dioxaborolan-2-yl)pyridin-3-yl)butan-2-ol (3.68)**



To a reaction flask was added **3.46** (1.00 g, 1.77 mmol), B<sub>2</sub>pin<sub>2</sub> (0.810 g, 3.19 mmol), Pd(dppf)Cl<sub>2</sub> (0.129 mg, 10 mol%), KOAc (0.782 g, 7.97 mmol), and 1,4-dioxane (10 mL, degassed), and the reaction mixture was heated at 85 °C for 21 h. After this time the reaction mixture was cooled to room temperature and filtered through a pad of Celite with the aid of EtOAc. The filtrate washed with a solution of NH<sub>4</sub>Cl (saturated, aqueous). The layers were separated, the aqueous layer extracted with EtOAc (×2), and the combined organic layers were washed with brine, dried over anhydrous MgSO<sub>4</sub>, filtered, and concentrated under reduced pressure. Purification by silica gel flash chromatography (0–5% MeOH in CH<sub>2</sub>Cl<sub>2</sub>) afforded the title compound as brown residue (0.940 mg, 1.54 mmol, 87%, A:B = 50:50).

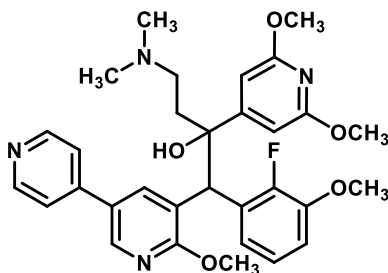
LR-MS (ESI+) *m/z*: 612.5 [M+H]<sup>+</sup>;

HR-MS (ESI+) *m/z* [M = C<sub>32</sub>H<sub>43</sub>BFN<sub>3</sub>O<sub>7</sub>]: [M+H]<sup>+</sup> calc'd 612.3257, found 612.3264;

Diastereomer A:

<sup>1</sup>H NMR (400 MHz, CDCl<sub>3</sub>) δ = 8.66 (d, *J* = 1.9 Hz, 1H, Pyr<sub>H</sub>), 8.19 (d, *J* = 1.9 Hz, 1H, Pyr<sub>H</sub>), 7.18 (ddd, *J* = 7.9, 6.2, 1.6 Hz, 1H, Ph<sub>H</sub>), 6.95 (td, *J* = 8.1, 1.5 Hz, 1H, Ph<sub>H</sub>), 6.81 (td, *J* = 8.1, 1.7 Hz, 1H, Ph<sub>H</sub>), 6.58 (br s, 2H, Pyr'<sub>H</sub>), 5.11 (s, 1H, Pyr-CH-Ph), 3.90 (s, 3H, OCH<sub>3</sub>), 3.84 (s, 6H, Pyr'OCH<sub>3</sub>), 3.76 (s, 3H, OCH<sub>3</sub>), 2.35 – 2.23 (m, 1H, CH<sub>2</sub>CH<sub>2</sub>N), 2.08 – 1.85 (m, 8H, CH<sub>2</sub>CH<sub>2</sub>N, N(CH<sub>3</sub>)<sub>2</sub>), 1.69 (d, *J* = 14.7 Hz, 1H, CH<sub>2</sub>CH<sub>2</sub>N), 1.31 (s, 6H, PinCH<sub>3</sub>), 1.30 (s, 6H, PinCH<sub>3</sub>).

**2-(2,6-dimethoxypyridin-4-yl)-4-(dimethylamino)-1-(2-fluoro-3-methoxyphenyl)-1-(6-methoxy-[3,4'-bipyridin]-5-yl)butan-2-ol (**3.69**)**



General method E was used with 4-bromopyridine hydrochloride (58.3 mg, 0.600 mmol) to afford the title compound brown foam (103 mg, 0.183 mmol, 92%, A:B = 54:46).

LR-MS (ESI+) *m/z*: 563.4 [M+H]<sup>+</sup>;

HR-MS (ESI+) *m/z* [M = C<sub>31</sub>H<sub>35</sub>FN<sub>4</sub>O<sub>5</sub>]: [M+H]<sup>+</sup> calc'd 563.2664, found 563.2675;

Diastereomer A:

<sup>1</sup>H NMR (400 MHz, CDCl<sub>3</sub>) δ = 11.73 (br s, 1H, NH<sup>+</sup>), 8.90 – 8.73 (m, 3H, Pyr<sub>H</sub>, 2 × Pyr''<sub>H</sub>), 8.32 (d, *J* = 2.4 Hz, 1H, Pyr<sub>H</sub>), 7.91 (s, 2H, Pyr''<sub>H</sub>), 6.99 (t, *J* = 8.0 Hz, 1H, Ph<sub>H</sub>), 6.92 – 6.80 (m, 2H, Ph<sub>H</sub>), 6.53 (br s, 2H, Pyr'<sub>H</sub>), 5.23 (s, 1H, Pyr-CH-Ph), 3.89 (s, 3H, PhOCH<sub>3</sub>), 3.88 (s, 3H, PyrOCH<sub>3</sub>), 3.84 (s, 6H, Pyr'OCH<sub>3</sub>),

3.40 – 3.25 (m, 1H, CH<sub>2</sub>CHHN), 2.70 (s, 3H, NCH<sub>3</sub>), 2.66 (s, 3H, NCH<sub>3</sub>), 2.43 – 2.22 (m, 2H, CHHCHHN), 2.15 – 2.01 (m, 1H, CHHCH<sub>2</sub>N);

<sup>13</sup>C NMR (101 MHz, CDCl<sub>3</sub>) δ = 164.0, 163.8, 158.4, 154.8, 151.1 (d, *J* = 243.7 Hz), 147.5 (d, *J* = 11.9 Hz), 144.6, 142.2, 137.4, 124.8 (d, *J* = 2.8 Hz), 124.6, 124.3 (d, *J* = 4.4 Hz), 123.3, 123.0, 122.6, 112.4, 98.2†, 77.0, 56.2, 54.7, 53.7, 53.6, 45.2, 43.3, 41.5, 36.9;

Analytical HPLC (254 nm): *t*<sub>R</sub> = 4.5 min, 97%;

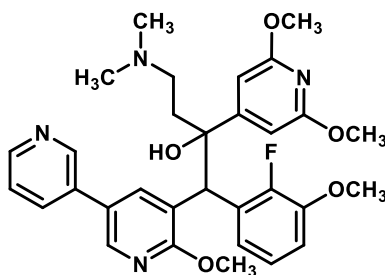
Diastereomer B:

<sup>1</sup>H NMR (400 MHz, CDCl<sub>3</sub>) δ = 11.91 (br s, 1H, NH<sup>+</sup>), 8.69 (s, 2H, Pyr''H), 8.35 (d, *J* = 2.3 Hz, 1H, PyrH), 8.03 (d, *J* = 2.3 Hz, 1H, PyrH), 7.96 (s, 2H, Pyr''H), 7.66 (t, *J* = 6.8 Hz, 1H, PhH), 6.80 (td, *J* = 8.2, 1.4 Hz, 1H, PhH), 6.60 (td, *J* = 8.3, 1.3 Hz, 1H, PhH), 6.46 (br s, 2H, Pyr'H), 5.33 (s, 1H, Pyr-CH-Ph), 4.09 (s, 3H, PyrOCH<sub>3</sub>), 3.80 (s, 6H, Pyr'OCH<sub>3</sub>), 3.65 (s, 3H, PhOCH<sub>3</sub>), 3.24 (t, *J* = 11.7 Hz, 1H, CH<sub>2</sub>CHHN), 2.61 (s, 3H, NCH<sub>3</sub>), 2.56 (s, 3H, NCH<sub>3</sub>), 2.41 – 2.31 (m, 1H, CHHCH<sub>2</sub>N), 2.27 – 2.15 (m, 1H, CH<sub>2</sub>CHHN), 1.94 (t, *J* = 11.4 Hz, 1H, CHHCH<sub>2</sub>N);

<sup>13</sup>C NMR (101 MHz, CDCl<sub>3</sub>) δ = 164.0, 163.6, 158.0, 154.6, 150.2 (d, *J* = 244.8 Hz), 147.1 (d, *J* = 11.5 Hz), 144.9, 141.7, 139.9, 128.5 (d, *J* = 11.0 Hz), 124.8, 123.8, 123.6 (d, *J* = 4.6 Hz), 123.0, 121.6, 111.6, 98.2, 77.1, 55.9, 54.8, 53.5, 53.3, 45.1, 42.4, 41.0, 36.8;

Analytical HPLC (254 nm): *t*<sub>R</sub> = 4.9 min, 98%.

**2-(2,6-dimethoxypyridin-4-yl)-4-(dimethylamino)-1-(2-fluoro-3-methoxyphenyl)-1-(6-methoxy-[3,3'-bipyridin]-5-yl)butan-2-ol (3.70)**



General method E was used with 3-bromopyridine (47.4 mg, 0.300 mmol) to afford the title compound brown foam (64.0 mg, 0.114 mmol, 57%, A:B = 48:52).

LR-MS (ESI+) *m/z*: 563.4 [M+H]<sup>+</sup>;

HR-MS (ESI+) *m/z* [M = C<sub>31</sub>H<sub>35</sub>FN<sub>4</sub>O<sub>5</sub>]: [M+H]<sup>+</sup> calc'd 563.2664, found 563.2677;

Diastereomer A:

<sup>1</sup>H NMR (400 MHz, CDCl<sub>3</sub>) δ = 11.75 (br s, 1H, NH<sup>+</sup>), 8.85 (m, 2H, Pyr''H), 8.71 (s, 1H, PyrH), 8.34 (d, *J* = 7.9 Hz, 1H, Pyr''H), 8.15 (s, 1H, PyrH), 7.91 (br s, 1H, PyrH), 7.00 (t, *J* = 7.9 Hz, 1H, PhH), 6.88 (m, 2H,



Ph $\underline{\text{H}}$ ), 6.53 (s, 2H, Pyr' $\underline{\text{H}}$ ), 5.25 (s, 1H, Pyr-CH $\underline{\text{H}}$ -Ph), 3.90 (s, 3H, PhOCH $\underline{\text{H}}$ ), 3.87 (s, 3H, PyrOCH $\underline{\text{H}}$ ), 3.85 (s, 6H, Pyr'OCH $\underline{\text{H}}$ ), 3.41 – 3.26 (m, 1H, CH $\underline{\text{H}}$ CHN), 2.69 (s, 3H, NCH $\underline{\text{H}}$ ), 2.66 (s, 3H, NCH $\underline{\text{H}}$ ), 2.38 – 2.22 (m, 2H, CH $\underline{\text{H}}$ CH $\underline{\text{H}}$ N), 2.11 – 2.01 (m, 1H, CH $\underline{\text{H}}$ CH $\underline{\text{H}}$ N);

$^{13}\text{C}$  NMR (101 MHz, CDCl $_3$ )  $\delta$  = 163.9, 162.5, 158.4, 151.1 (d,  $J$  = 243.8 Hz), 147.5 (d,  $J$  = 12.0 Hz), 143.3, 141.2, 141.0, 140.4, 140.0, 137.4, 126.7, 124.9 (d,  $J$  = 11.8 Hz), 124.5, 124.3 (d,  $J$  = 4.6 Hz), 123.0, 122.6, 112.4, 98.2, 77.0, 56.2, 54.5, 53.72, 53.67, 45.2, 43.2, 41.5, 37.0;

Analytical HPLC (254 nm):  $t_{\text{R}}$  = 4.5 min, 95%;

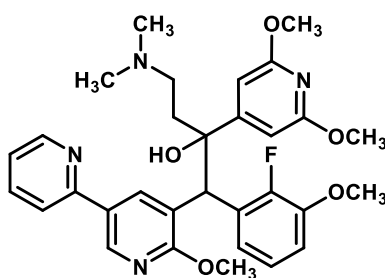
Diastereomer B:

$^1\text{H}$  NMR (400 MHz, CDCl $_3$ )  $\delta$  = 12.15 (br s, 1H, NH $^+$ ), 8.93 (br s, 1H, Pyr'' $\underline{\text{H}}$ ), 8.79 (br s, 1H, Pyr'' $\underline{\text{H}}$ ), 8.58 (d,  $J$  = 7.6 Hz, 1H, Pyr'' $\underline{\text{H}}$ ), 8.27 (s, 1H, Pyr $\underline{\text{H}}$ ), 7.99 (s, 1H, Pyr $\underline{\text{H}}$ ), 7.84 (br s, 1H, Pyr'' $\underline{\text{H}}$ ), 7.72 (t,  $J$  = 7.1 Hz, 1H, Ph $\underline{\text{H}}$ ), 6.84 (t,  $J$  = 8.0, 1H, Ph $\underline{\text{H}}$ ), 6.66 (t,  $J$  = 7.9 Hz, 1H, Ph $\underline{\text{H}}$ ), 6.54 (br s, 2H, Pyr' $\underline{\text{H}}$ ), 5.40 (s, 1H, Pyr-CH $\underline{\text{H}}$ -Ph), 4.13 (s, 3H, PyrOCH $\underline{\text{H}}$ ), 3.85 (s, 6H, Pyr'OCH $\underline{\text{H}}$ ), 3.72 (s, 3H, PhOCH $\underline{\text{H}}$ ), 3.32 (t,  $J$  = 11.6 Hz, 1H, CH $\underline{\text{H}}$ CHN), 2.67 (s, 3H, NCH $\underline{\text{H}}$ ), 2.60 (s, 3H, NCH $\underline{\text{H}}$ ), 2.51 – 2.35 (m, 1H, CH $\underline{\text{H}}$ CH $\underline{\text{H}}$ N), 2.28 (s, 1H, CH $\underline{\text{H}}$ CH $\underline{\text{H}}$ N), 2.02 (t,  $J$  = 11.3 Hz, 1H, CH $\underline{\text{H}}$ CH $\underline{\text{H}}$ N);

$^{13}\text{C}$  NMR (101 MHz, CDCl $_3$ )  $\delta$  = 163.7, 163.1, 158.2, 150.4 (d,  $J$  = 244.8 Hz), 147.2 (d,  $J$  = 11.5 Hz), 144.1, 142.9, 140.4, 140.0, 139.9, 138.1, 128.6 (d,  $J$  = 10.9 Hz), 126.6, 124.2, 123.7 (d,  $J$  = 4.6 Hz), 122.9, 121.8, 111.7, 98.4, 77.3, 56.1, 54.8, 53.7, 53.6, 45.3, 42.6, 41.2, 36.9;

Analytical HPLC (254 nm):  $t_{\text{R}}$  = 4.9 min, 95%.

**2-(2,6-dimethoxypyridin-4-yl)-4-(dimethylamino)-1-(2-fluoro-3-methoxyphenyl)-1-(6'-methoxy-[2,3'-bipyridin]-5'-yl)butan-2-ol (3.71)**



General method E was used with 2-bromopyridine (47.4 mg, 0.300 mmol) to afford the title compound brown foam (104 mg, 0.185 mmol, 92%, A:B = 45:55).

LR-MS (ESI+)  $m/z$ : 563.4  $[\text{M}+\text{H}]^+$ ;

HR-MS (ESI+)  $m/z$   $[\text{M} = \text{C}_{31}\text{H}_{35}\text{FN}_4\text{O}_5]$ :  $[\text{M}+\text{H}]^+$  calc'd 563.2664, found 563.2674;

## Diastereomer A:

$^1\text{H}$  NMR (400 MHz,  $\text{CDCl}_3$ )  $\delta$  = 11.73 (br s, 1H,  $\text{NH}^+$ ), 9.15 (br s, 1H, PyrH), 8.77 (s, 1H, PyrH), 8.51 (s, 1H, PyrH), 8.29 (s, 1H, PyrH), 7.86 (d,  $J$  = 7.3 Hz, 1H, PyrH), 7.70 (s, 1H, PyrH), 7.13 (s, 1H, PhH), 7.03 (s, 1H, PhH), 6.88 (t,  $J$  = 7.3 Hz, 1H, PhH), 6.48 (s, 2H, PyrH), 5.30 (s, 1H, Pyr-CH-Ph), 3.88 (s, 6H,  $\text{PhOCH}_3$ ,  $\text{PyrOCH}_3$ ), 3.83 (s, 6H,  $\text{PyrOCH}_3$ ), 3.33 – 3.17 (m, 1H,  $\text{CH}_2\text{CHHN}$ ), 2.80 – 2.54 (m, 6H,  $(\text{NCH}_3)_2$ ), 2.46 – 2.23 (m, 2H,  $\text{CHHCHHN}$ ), 2.19 – 2.03 (m, 1H,  $\text{CHHCH}_2\text{N}$ );

$^{13}\text{C}$  NMR (101 MHz,  $\text{CDCl}_3$ )  $\delta$  = 163.9, 163.5, 158.1, 152.5, 151.1 (d,  $J$  = 243.8 Hz), 147.6 (d,  $J$  = 12.1 Hz), 145.3, 144.5, 143.8, 137.6, 125.3 (d,  $J$  = 11.7 Hz), 124.5 (d,  $J$  = 4.5 Hz), 124.3, 124.2, 123.8, 122.5, 121.5, 112.5, 98.2, 77.2 $^\dagger$ , 56.2, 54.7, 53.9, 53.7, 44.6, 42.9, 42.0, 36.5;

Analytical HPLC (254 nm):  $t_R$  = 4.7 min, 96%;

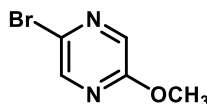
## Diastereomer B:

$^1\text{H}$  NMR (400 MHz,  $\text{CDCl}_3$ )  $\delta$  = 11.46 (br s, 1H,  $\text{NH}^+$ ), 9.08 (s, 1H, Pyr''H), 8.50 (d,  $J$  = 2.2 Hz, 1H, PyrH), 8.35 (t,  $J$  = 7.8 Hz, 1H, Pyr''H), 8.31 – 8.22 (m, 1H, PyrH), 8.03 (d,  $J$  = 8.0 Hz, 1H, Pyr''H), 7.77 (t,  $J$  = 6.1 Hz, 1H, Pyr''H), 7.70 (ddd,  $J$  = 7.8, 6.1, 1.5 Hz, 1H, PhH), 6.82 (td,  $J$  = 8.1, 1.5 Hz, 1H, PhH), 6.64 (td,  $J$  = 8.2, 1.4 Hz, 1H, PhH), 6.51 (s, 2H, Pyr'H), 5.41 (s, 1H, Pyr-CH-Ph), 4.15 (s, 3H,  $\text{PyrOCH}_3$ ), 3.86 (s, 6H,  $\text{Pyr}'\text{OCH}_3$ ), 3.70 (s, 3H,  $\text{PhOCH}_3$ ), 3.26 – 3.12 (m, 1H,  $\text{CH}_2\text{CHHN}$ ), 2.65 (s, 3H,  $\text{NCH}_3$ ), 2.63 (s, 3H,  $\text{NCH}_3$ ), 2.52 – 2.37 (m, 2H,  $\text{CHHCHHN}$ ), 2.07 – 1.95 (m, 1H,  $\text{CHHCH}_2\text{N}$ );

$^{13}\text{C}$  NMR (101 MHz,  $\text{CDCl}_3$ )  $\delta$  = 164.5, 163.7, 158.0, 152.2, 150.4 (d,  $J$  = 245.2 Hz), 147.2 (d,  $J$  = 11.5 Hz), 146.0, 145.0, 143.4, 139.2, 128.3 (d,  $J$  = 10.5 Hz), 125.4, 124.4, 123.7, 123.6, 121.9, 121.5, 111.8, 98.4, 77.6, 56.1, 55.1, 53.9, 53.7, 43.7, 43.1, 42.8 $^\dagger$ , 36.5;

Analytical HPLC (254 nm):  $t_R$  = 5.1 min, 98%.

## 6.1.5 Chapter 4 compounds

2-bromo-5-methoxypyrazine<sup>[33]</sup> (4.01)

To a solution of 2-amino-5-bromopyrazine (3.48 g, 20.0 mmol) in MeOH (50 mL, anhydrous) at  $-10\text{ }^\circ\text{C}$  under nitrogen was added HCl (0.480 mL, 1 M in MeOH, 0.600 mmol) and isopentyl nitrite (8.00 mL, 60.0 mmol) sequentially. The reaction mixture was stirred at this temperature for 1.5 h, followed by an additional 16 h at room temperature. After this time, the solution was concentrated under reduced pressure, the residue diluted with  $\text{CH}_2\text{Cl}_2$ , and partitioned between  $\text{Na}_2\text{CO}_3$  (saturated, aqueous) and  $\text{CH}_2\text{Cl}_2$  ( $\times 3$ ). The combined organic fractions were dried over anhydrous  $\text{MgSO}_4$ , filtered, and

concentrated under reduced pressure. Purification by silica gel flash chromatography (0–10% EtOAc in Pet. Sp.) afforded the title compound as an off-white solid (2.72 g, 14.4 mmol, 72%).

$^1\text{H}$  NMR (400 MHz,  $\text{CDCl}_3$ )  $\delta$  = 8.19 (d,  $J$  = 1.4 Hz, 1H, 3-PyzH), 8.01 (d,  $J$  = 1.4 Hz, 1H, 6-PyzH), 3.95 (s, 3H, OCH<sub>3</sub>);

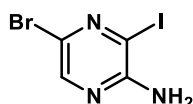
$^{13}\text{C}$  NMR (101 MHz,  $\text{CDCl}_3$ )  $\delta$  = 160.0 (PyzC-OCH<sub>3</sub>), 143.0 (3-PyzCH), 135.5 (6-PyzCH), 130.3 (PyzC-Br), 54.4 (Pyz-OCH<sub>3</sub>);

LR-MS (ESI+)  $m/z$ : 188.8/190.9;

HR-MS (ESI+)  $m/z$  [ $\text{M} = \text{C}_5\text{H}_5\text{BrN}_2\text{O}$ ]: [ $\text{M}+\text{H}$ ]<sup>+</sup> calc'd 188.9658, found 188.9657;

Analytical HPLC (254 nm):  $t_R$  = 4.3 min, 98%.

### 5-bromo-3-iodopyrazin-2-amine<sup>[34]</sup> (4.08)



To an ice-cold solution of 2-amino-5-bromopyrazine (2.61 g, 15.0 mmol) in MeCN (25 mL) were added trifluoroacetic acid (0.570 mL, 7.50 mmol) and *N*-iodosuccinimide (4.05 g, 18.0 mmol), and the reaction mixture was then stirred at reflux for 36 h. After this time, the mixture was poured onto a solution of  $\text{Na}_2\text{S}_2\text{O}_5$  (saturated, aqueous) and extracted with EtOAc (×3). The combined organic layers were washed with brine, dried over anhydrous  $\text{MgSO}_4$ , filtered, and concentrated under reduced pressure. Purification of the crude mixture by silica gel flash chromatography (0–65% EtOAc in Pet. Sp.) followed by recrystallisation from EtOH afforded the title compound as yellow needles (1.38 g, 4.61 mmol, 31%). Spectroscopic data are in agreement with the reported literature values.<sup>[34]</sup>

$^1\text{H}$  NMR (400 MHz,  $\text{CDCl}_3$ )  $\delta$  = 7.98 (s, 1H, PyzH), 5.03 (br s, 2H, Pyz-NH<sub>2</sub>);

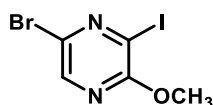
$^{13}\text{C}$  NMR (101 MHz,  $\text{CDCl}_3$ )  $\delta$  = 154.4 (PyzC-NH<sub>2</sub>), 143.4 (PyzCH), 124.5 (PyzC-Br), 101.8 (PyzC-I);

LR-MS (ESI+)  $m/z$ : mass not found;

Analytical HPLC (254 nm):  $t_R$  = 4.6 min, 92%;

MP: 131.6 – 133.6 °C.

### 3,5-dibromo-2-methoxypyrazine<sup>[35]</sup> (4.02)



To a solution of **4.08** (1.20 g, 4.00 mmol) in MeOH (10 mL, anhydrous) under nitrogen were added isopentyl nitrite (1.60 mL, 12.0 mmol) and HCl (0.640 mL, 1 M in MeOH, 0.800 mmol). The reaction mixture was heated to reflux and stirred for 23 h. After this time, the solution was concentrated under reduced pressure, the residue diluted with CH<sub>2</sub>Cl<sub>2</sub>, and partitioned between NaHCO<sub>3</sub> (saturated, aqueous) and CH<sub>2</sub>Cl<sub>2</sub> (×3). The combined organic fractions were dried over anhydrous MgSO<sub>4</sub>, filtered, and concentrated under reduced pressure. The crude product was recrystallised from EtOH to afford the title compound as orange crystals (0.896 mg, 2855 μmol, 71%).

<sup>1</sup>H NMR (400 MHz, CDCl<sub>3</sub>) δ = 8.07 (s, 1H, PyzH), 4.00 (s, 3H, OCH<sub>3</sub>);

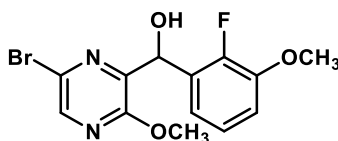
<sup>13</sup>C NMR (101 MHz, CDCl<sub>3</sub>) δ = 159.3 (PyzC-OCH<sub>3</sub>), 141.6 (PyzCH), 128.5 (PyzC-Br), 105.5 (PyzC-I), 55.8 (Pyz-OCH<sub>3</sub>);

LR-MS (ESI+) *m/z*: 314.6/316.8;

HR-MS (ESI+) *m/z* [M = C<sub>5</sub>H<sub>4</sub>BrIN<sub>2</sub>O]: [M+H]<sup>+</sup> calc'd 314.8624, found 314.8617;

Analytical HPLC (254 nm): *t*<sub>R</sub> = 5.9 min, 90%.

**(6-bromo-3-methoxypyrazin-2-yl)(2-fluoro-3-methoxyphenyl)methanol (**4.04**)**



**Method 1 (Scheme 4.3)**<sup>[36]</sup>

To a solution of 2,2,6,6-tetramethylpiperidine (0.300 mL, 1.80 mmol, anhydrous) in THF (2 mL, anhydrous) cooled to −10 °C and under an atmosphere of nitrogen was added *n*-BuLi (0.830 mL, 1.44 M in hexanes, 1.20 mmol) dropwise over 5 min. The mixture was maintained at this temperature for 30 min, followed by cooling to −78 °C. To the reaction mixture was added a solution of **4.01** (189 mg, 1.00 mmol) in THF (2 mL, anhydrous) dropwise over 10 min, and the resultant mixture was stirred at −78 °C for 2 h. A solution of 2-fluoro-3-methoxybenzaldehyde (185 mg, 1.20 mmol) in THF (2 mL, anhydrous) was then added dropwise over 5 min and the mixture was stirred for an additional 3 h. After this time, the reaction was quenched with a solution of NH<sub>4</sub>Cl (saturated, aqueous), the organic phase separated and the aqueous phase extracted with EtOAc (×3). The combined organic layers were washed with brine, dried over anhydrous MgSO<sub>4</sub>, filtered, and concentrated under reduced pressure. Purification by silica gel flash chromatography (0–75% EtOAc in Pet. Sp.), afforded the title compound as a pale yellow crystalline solid (89.0 mg, 0.259 mmol, 26%).

Method 2 (**Scheme 4.4**)<sup>[37]</sup>

To a solution of  $\text{TMP}_2\text{MgCl}\cdot 2\text{LiCl}$  (2.00 mL, 0.610 M in THF/PhMe, 1.20 mmol) at  $-50\text{ }^\circ\text{C}$  and under an atmosphere of nitrogen was added a solution of **4.01** (189 mg, 1.00 mmol) in THF (2 mL, anhydrous) dropwise over 10 min. The reaction was stirred at this temperature for 2 h, followed by the addition of a solution of 2-fluoro-3-methoxybenzaldehyde (185 mg, 1.20 mmol) in THF (2 mL) dropwise over 5 min. The reaction mixture was allowed to warm to room temperature and react for a total of 3 h. After this time, the reaction was quenched with a solution of  $\text{NH}_4\text{Cl}$  (saturated, aqueous), the organic phase separated and the aqueous phase extracted with EtOAc ( $\times 3$ ). The combined organic layers were washed with brine, dried over anhydrous  $\text{MgSO}_4$ , filtered, and concentrated under reduced pressure. Purification by silica gel flash chromatography (0–40% EtOAc in Pet. Sp.) afforded the title compound as an off-white solid (67.0 mg, 0.195 mmol, 20%).

Method 3 (**Scheme 4.7**)<sup>[38]</sup>

To a solution of **4.02** (315 mg, 1.00 mmol) in THF (2 mL, anhydrous) at  $0\text{ }^\circ\text{C}$  and under an atmosphere of nitrogen was added  $i\text{-PrMgCl}\cdot\text{LiCl}$  (1.20 mL, 0.950 M in THF, 1.10 mmol) dropwise over 10 min. The reaction was stirred at this temperature for 30 min, followed by the dropwise addition of a solution of 2-fluoro-3-methoxybenzaldehyde (185 mg, 1.20 mmol) in THF (2 mL, anhydrous). The reaction was stirred for an additional 4 h, after which time it was quenched with a solution of  $\text{NH}_4\text{Cl}$  (saturated, aqueous). The organic phase was separated, the aqueous phase extracted with EtOAc ( $\times 3$ ) and the combined organic layers were washed with brine, dried over anhydrous  $\text{MgSO}_4$ , filtered, and concentrated under reduced pressure. Purification by silica gel flash chromatography (0–30% EtOAc in Pet. Sp.) afforded the title compound as a white solid (58.0 mg, 0.169 mmol, 17%).

Method 4 (**Scheme 4.7**)<sup>[39]</sup>

To a solution of  $n$ -butyl-magnesium chloride (0.250 mL, 1.34 M, 0.33 mmol) in THF (5 mL, anhydrous) cooled to  $-10\text{ }^\circ\text{C}$  and under an atmosphere of nitrogen was added  $n\text{-BuLi}$  (0.420 mL, 1.56 M in hexanes, 2.20 mmol) dropwise over 5 min. After 1 h the reaction mixture was cooled to  $-50\text{ }^\circ\text{C}$  followed by the dropwise addition of a solution of **4.02** (189 mg, 1 mmol) in THF (2 mL). The mixture was warmed to  $-10\text{ }^\circ\text{C}$  and stirred at this temperature for 3 h. After this time, a solution of 2-fluoro-3-methoxybenzaldehyde (230 mg, 1.5 mmol) in THF (2 mL, anhydrous) was added to the reaction dropwise at  $-10\text{ }^\circ\text{C}$ . The reaction was stirred at this temperature for 1 h, and was then allowed to warm to room temperature to react for an additional 17 h. After this time, the reaction was quenched with a solution of  $\text{NH}_4\text{Cl}$  (saturated, aqueous), and diluted with EtOAc. The organic layer was washed with brine, dried over  $\text{MgSO}_4$  and concentrated under reduced pressure. Purification of the crude

mixture by silica gel flash chromatography (0–30% EtOAc in Pet. Sp.) afforded the title compound as a pale-yellow oil (43.0 mg, 0.125 mmol, 13%).

$^1\text{H}$  NMR (400 MHz,  $\text{CDCl}_3$ )  $\delta$  = 8.14 (d,  $J$  = 0.6 Hz, 1H, PyzH), 7.01 (td,  $J$  = 8.0, 1.5 Hz, 1H, 5-PhH), 6.88 (td,  $J$  = 8.1, 1.6 Hz, 1H, 4-PhH), 6.78 (ddd,  $J$  = 7.7, 6.0, 1.6 Hz, 1H, 6-PhH), 6.15 (d,  $J$  = 5.4 Hz, 1H, CH-OH), 4.40 (d,  $J$  = 7.2 Hz, 1H, OH), 3.88 (s, 3H, Pyz-OCH<sub>3</sub>), 3.88 (s, 3H, Ph-OCH<sub>3</sub>);

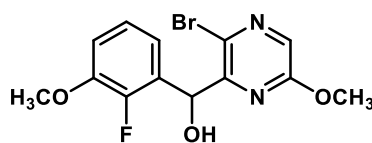
$^{13}\text{C}$  NMR (101 MHz,  $\text{CDCl}_3$ )  $\delta$  = 156.6 (PyzC-OCH<sub>3</sub>), 150.7 (d,  $J_{\text{CF}}$  = 248.7 Hz, PhC-F), 147.9 (d,  $J_{\text{CF}}$  = 11.0 Hz, PhC-OCH<sub>3</sub>), 145.9 (PyzC-CHOH), 142.3 (PyzCH), 128.7 (d,  $J_{\text{CF}}$  = 10.9 Hz, PhC-CHOH), 128.5 (PyzC-Br), 124.0 (d,  $J_{\text{CF}}$  = 4.7 Hz, 5-PhCH), 120.1 (d,  $J_{\text{CF}}$  = 2.8 Hz, 6-PhCH), 113.1 (d,  $J_{\text{CF}}$  = 2.0 Hz, 4-PhCH), 65.2 (d,  $J_{\text{CF}}$  = 4.7 Hz, CH-OH), 56.5 (Ph-OCH<sub>3</sub>), 54.5 (Pyz-OCH<sub>3</sub>);

LR-MS (ESI+)  $m/z$ : 324.9/326.9 [ $\text{M-OH}$ ]<sup>+</sup>, 364.8/366.8 [ $\text{M+Na}$ ]<sup>+</sup>

HR-MS (ESI+)  $m/z$  [ $\text{M} = \text{C}_{13}\text{H}_{12}\text{BrFN}_2\text{O}_3$ ]: [ $\text{M+H}$ ]<sup>+</sup> calc'd 343.0088, found 343.0091;

Analytical HPLC (254 nm):  $t_{\text{R}}$  = 5.7 min, 97%.

**(3-bromo-6-methoxypyrazin-2-yl)(2-fluoro-3-methoxyphenyl)methanol (4.06)**



By-product isolated from synthesis of **4.04** (Method 1 and 2) as a pale-yellow crystalline solid.

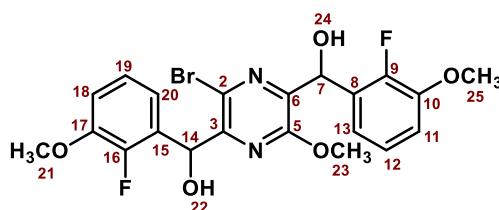
$^1\text{H}$  NMR (400 MHz,  $\text{CDCl}_3$ )  $\delta$  = 8.00 (s, 1H, PyzH), 7.02 (td,  $J$  = 8.0, 1.5 Hz, 1H, 5-PhH), 6.92 (td,  $J$  = 8.1, 1.6 Hz, 1H, 4-PhH), 6.79 (ddd,  $J$  = 7.8, 6.0, 1.6 Hz, 1H, 6-PhH), 6.15 (d,  $J$  = 8.3 Hz, 1H, CH-OH), 4.37 (dd,  $J$  = 8.4, 1H, OH), 4.06 (s, 3H, Pyz-OCH<sub>3</sub>), 3.88 (s, 3H, Ph-OCH<sub>3</sub>);

$^{13}\text{C}$  NMR (101 MHz,  $\text{CDCl}_3$ )  $\delta$  = 158.9 (PyzC-OCH<sub>3</sub>), 150.8 (d,  $J_{\text{CF}}$  = 248.7 Hz, PhC-F), 150.7 (PyzC-CHOH), 148.0 (d,  $J_{\text{CF}}$  = 10.8 Hz, PhC-OCH<sub>3</sub>), 134.3 (PyzCH), 128.42 (PyzC-Br), 128.39 (d,  $J_{\text{CF}}$  = 10.9 Hz, PhC-CHOH), 123.9 (d,  $J_{\text{CF}}$  = 4.7 Hz, 5-PhCH), 120.5 (d,  $J_{\text{CF}}$  = 3.0 Hz, 6-PhCH), 113.3 (d,  $J_{\text{CF}}$  = 2.1 Hz, 4-PhCH), 68.1 (d,  $J_{\text{CF}}$  = 3.5 Hz, CH-OH), 56.3 (Ph-OCH<sub>3</sub>), 54.5 (Pyz-OCH<sub>3</sub>);

LR-MS (ESI+)  $m/z$ : 324.9/326.9 [ $\text{M-OH}$ ]<sup>+</sup>, 364.8/366.8 [ $\text{M+Na}$ ]<sup>+</sup>

HR-MS (ESI+)  $m/z$  [ $\text{M} = \text{C}_{13}\text{H}_{12}\text{BrFN}_2\text{O}_3$ ]: [ $\text{M+H}$ ]<sup>+</sup> calc'd 343.0088, found 343.0095;

Analytical HPLC (254 nm):  $t_{\text{R}}$  = 5.4 min, 92%.

**(3-bromo-6-methoxypyrazine-2,5-diyl)bis((2-fluoro-3-methoxyphenyl)methanol) (4.07)**

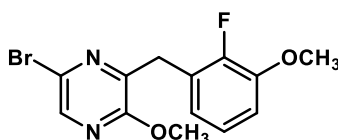
By-product isolated from synthesis of **4.04** (Method 1) as an off-white powder.

$^1\text{H}$  NMR (400 MHz,  $\text{CDCl}_3$ )  $\delta$  = 7.05 – 6.97 (m, 2H, **H12**, **H19**), 6.94 – 6.85 (m, 2H, **H11**, **H18**), 6.84 – 6.76 (m, 2H, **H13**, **H20**), 6.20 – 6.14 (m, 2H, **H7**, **H14**), 4.38 – 4.30 (m, 1H, **H24**), 4.27 – 4.17 (m, 1H, **H20**), 3.98 – 3.96 (m, 3H, **H23**), 3.90 – 3.84 (m, 6H, **H21**, **H25**);

$^{13}\text{C}$  NMR (101 MHz,  $\text{CDCl}_3$ )  $\delta$  = 155.6 (**C5**), 150.8 (d,  $J_{\text{CF}}$  = 248.5 Hz, **C9/C16**), 150.6 (d,  $J_{\text{CF}}$  = 248.6 Hz, **C9/C16**), 150.3 (**C3**), 148.0 (d,  $J_{\text{CF}}$  = 10.7 Hz, **C10/C17**), 147.9 (d,  $J_{\text{CF}}$  = 10.8 Hz, **C10/C17**), 145.1 (**C2**), 128.5 (d,  $J_{\text{CF}}$  = 2.4 Hz, **C15**), 128.4 (d,  $J_{\text{CF}}$  = 2.3 Hz, **C8**), 126.7 (**C6**), 124.1 (**C19**), 124.0 (**C12**), 120.5 (d,  $J_{\text{CF}}$  = 13.4 Hz, **C20**), 120.0 (d,  $J_{\text{CF}}$  = 7.4, **C13**), 113.3 (d,  $J_{\text{CF}}$  = 8.56 Hz, **C18**), 113.1 (d,  $J_{\text{CF}}$  = 6.2 Hz, **C11**), 68.2 (d,  $J_{\text{CF}}$  = 22.7 Hz, **C14**), 65.1 (d,  $J_{\text{CF}}$  = 16.6 Hz, **C7**), 56.5 (**C21/C25**), 56.4 (**C21/C25**), 54.7 (**C23**);

LR-MS (ESI+)  $m/z$ : 478.8/480.8  $[\text{M}-\text{OH}]^+$ , 496.9/498.9  $[\text{M}+\text{H}]^+$ , 518.8/520.8  $[\text{M}+\text{Na}]^+$

HR-MS (ESI+)  $m/z$   $[\text{M} = \text{C}_{21}\text{H}_{19}\text{BrF}_2\text{N}_2\text{O}_5]$ :  $[\text{M}+\text{H}]^+$  calc'd 497.0518, found 497.0525.

**5-bromo-3-(2-fluoro-3-methoxybenzyl)-2-methoxypyrazine<sup>[32]</sup> (4.09)**

To a solution of **4.04** (0.789 g, 2.30 mmol) in  $\text{CH}_2\text{Cl}_2$  (12 mL, anhydrous) under an atmosphere of nitrogen was added triethylsilane (2.20 mL, 13.8 mmol), and the mixture cooled to 0 °C. Boron trifluoride diethyl etherate (1.70 mL, 13.8 mmol) was added dropwise to the cooled reaction mixture, and the solution stirred at reflux for 14 h. After this time, an additional amount of triethylsilane (1.10 mL, 6.90 mmol) was added and the reaction stirred at reflux for a further 13 h. After this time, an additional amount of triethylsilane (1.10 mL, 6.90 mmol) was added and the reaction stirred at reflux for a further 11 h. Upon completion, the reaction mixture was cooled to room temperature and added to an ice-cold solution of  $\text{K}_2\text{CO}_3$  (20% w/v, aqueous). The solution was filtered through a pad of Celite with the aid of  $\text{CH}_2\text{Cl}_2$ , and the organic phase was separated. The aqueous phase was extracted with  $\text{CH}_2\text{Cl}_2$  ( $\times 3$ ) and the combined organic layers dried over anhydrous  $\text{MgSO}_4$ , filtered, and concentrated

under reduced pressure. Purification by silica gel flash chromatography (0–10% EtOAc in Pet. Sp.) afforded the title compound as a white solid on standing (0.478 g, 1.46 mmol, 64%).

$^1\text{H}$  NMR (400 MHz,  $\text{CDCl}_3$ )  $\delta$  = 8.06 (s, 1H, PyzH), 6.96 (td,  $J$  = 8.0, 1.5 Hz, 1H, PhH), 6.84 (td,  $J$  = 8.1, 1.5 Hz, 1H, PhH), 6.74 (ddd,  $J$  = 7.8, 6.2, 1.6 Hz, 1H, PhH), 4.15 (br s, 1H, Pyz-CH<sub>2</sub>-Ph), 3.93 (s, 3H, Pyz-OCH<sub>3</sub>), 3.88 (s, 3H, Ph-OCH<sub>3</sub>);

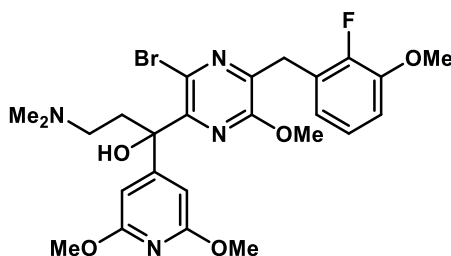
$^{13}\text{C}$  NMR (101 MHz,  $\text{CDCl}_3$ )  $\delta$  = 158.1 (PyzC-OCH<sub>3</sub>), 150.9 (d,  $J_{\text{CF}}$  = 245.9 Hz, PhC-F), 147.9 (d,  $J_{\text{CF}}$  = 11.0 Hz, PhC-OCH<sub>3</sub>), 145.8 (PyzC-CH<sub>2</sub>), 141.1 (PyzCH), 129.2 (PyzC-Br), 125.3 (d,  $J_{\text{CF}}$  = 13.4 Hz, 1-PhC), 123.7 (d,  $J_{\text{CF}}$  = 4.7 Hz, PhCH), 122.3 (d,  $J_{\text{CF}}$  = 3.3 Hz, PhCH), 111.9 (PhCH, d,  $J_{\text{CF}}$  = 1.8 Hz), 56.4 (Ph-OCH<sub>3</sub>), 54.4 (Pyz-OCH<sub>3</sub>), 31.5 (d,  $J$  = 3.9 Hz, Pyz-CH<sub>2</sub>-Ph);

LR-MS (ESI+)  $m/z$ : 326.9 / 328.9  $[\text{M}+\text{H}]^+$ ;

HR-MS (ESI+)  $m/z$   $[\text{M} = \text{C}_{13}\text{H}_{12}\text{BrFN}_2\text{O}_2]$ :  $[\text{M}+\text{H}]^+$  calc'd 327.0139, found 327.0146;

Analytical HPLC (254 nm):  $t_{\text{R}}$  = 6.8 min, 95%.

**1-(6-bromo-3-methoxypyrazin-2-yl)-2-(2,6-dimethoxypyridin-4-yl)-4-(dimethylamino)-1-(2-fluoro-3-methoxyphenyl)butan-2-ol (**4.11**)**



To a solution of anhydrous 2,2,6,6-tetramethylpiperidine (0.490 mL, 2.93 mmol) in THF (3 mL, anhydrous) at  $-10\text{ }^{\circ}\text{C}$  and under an atmosphere of nitrogen was added *n*-BuLi (1.2 mL, 1.93 M in hexanes, 2.20 mmol) dropwise. The mixture was stirred at  $-78\text{ }^{\circ}\text{C}$  for 1 h, after which a solution of **4.09** (599 mg, 1.20 mmol) in THF (3 mL, anhydrous) was added dropwise to give a bright orange solution. The reaction mixture was kept stirring at  $-78\text{ }^{\circ}\text{C}$  for 2 h, followed by the dropwise addition of a solution of **3.03** (654 mg, 2.75 mmol) in THF (3 mL, anhydrous). The reaction mixture was stirred at  $-78\text{ }^{\circ}\text{C}$  for 5 h, quenched with a solution of  $\text{NH}_4\text{Cl}$  (saturated, aqueous) and warmed to room temperature. The mixture was diluted with EtOAc, the organic phase separated, and the aqueous layer extracted with EtOAc ( $\times 3$ ). The combined organic layers were then washed with brine, dried over anhydrous  $\text{MgSO}_4$ , filtered, and concentrated under reduced pressure. Purification by silica gel flash chromatography (0–10% MeOH in  $\text{CH}_2\text{Cl}_2$ ) afforded the title compound as a pale brown foam (78.0 mg, 0.138 mmol, 8%).

$^1\text{H}$  NMR (400 MHz,  $\text{CDCl}_3$ )  $\delta$  = 6.94 (td,  $J$  = 8.0, 1.5 Hz, 1H, PhH), 6.82 (td,  $J$  = 8.1, 1.6 Hz, 1H, PhH), 6.74 (ddd,  $J$  = 8.0, 6.3, 1.6 Hz, 1H, PhH), 6.34 (s, 2H, 2  $\times$  PyrH), 4.23 – 4.03 (m, 2H, Pyz-CH<sub>2</sub>-Ph), 3.96 (s, 3H,



Pyz-OCH<sub>3</sub>), 3.89 (s, 6H, 2 × Pyr-OCH<sub>3</sub>), 3.86 (s, 3H, Ph-OCH<sub>3</sub>), 2.73 – 2.62 (m, 1H, N(CH<sub>3</sub>)<sub>2</sub>-CH<sub>3</sub>H<sub>b</sub>), 2.55 – 2.41 (m, 2H, N(CH<sub>3</sub>)<sub>2</sub>-CH<sub>2</sub>CH<sub>2</sub>), 2.25f (s, 6H, N(CH<sub>3</sub>)<sub>2</sub>-CH<sub>2</sub>), 2.20 – 2.15 (m, 1H, N(CH<sub>3</sub>)<sub>2</sub>-CH<sub>3</sub>H<sub>b</sub>);

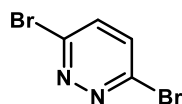
<sup>13</sup>C NMR (101 MHz, CDCl<sub>3</sub>) δ = 163.1 (2 × Pyr-C-OCH<sub>3</sub>), 160.4 (Pyz-C-OH), 155.5 (Pyz-C-OCH<sub>3</sub>), 150.8 (d, *J*<sub>CF</sub> = 245.9 Hz, Pyz-C-F), 147.8 (d, *J*<sub>CF</sub> = 11.1 Hz, Ph-C-OCH<sub>3</sub>), 142.9 (Pyz-C-CH<sub>2</sub>), 128.3 (Pyz-C-Br), 125.3 (d, *J*<sub>CF</sub> = 13.2 Hz, Ph-C-CH<sub>2</sub>), 123.6 (d, *J*<sub>CF</sub> = 4.7 Hz, Ph-CH), 122.4 (d, *J*<sub>CF</sub> = 3.2 Hz, Ph-CH), 111.8 (d, *J*<sub>CF</sub> = 1.8 Hz, Ph-CH), 99.1 (2 × Pyr-CH), 80.2 (C-OH), 56.4 (Ph-OCH<sub>3</sub>), 55.9 (N(CH<sub>3</sub>)<sub>2</sub>-CH<sub>2</sub>CH<sub>2</sub>), 54.2 (Pyz-OCH<sub>3</sub>), 53.6 (2 × Pyr-OCH<sub>3</sub>), 45.0 (N(CH<sub>3</sub>)<sub>2</sub>-CH<sub>2</sub>CH<sub>2</sub>), 35.5 (N(CH<sub>3</sub>)<sub>2</sub>-CH<sub>2</sub>CH<sub>2</sub>), 30.8 (d, *J*<sub>CF</sub> = 4.1 Hz, Pyz-CH<sub>2</sub>-Ph);

LR-MS (ESI+) *m/z*: 564.9/566.9 [M+H]<sup>+</sup>;

HR-MS (ESI+) *m/z* [M = C<sub>25</sub>H<sub>30</sub>BrFN<sub>4</sub>O<sub>5</sub>]: [M+H]<sup>+</sup> calc'd 565.1456, found 565.1467;

Analytical HPLC (254 nm): *t*<sub>R</sub> = 6.1 min, 79%.

### 3,6-dibromopyridazine<sup>[40]</sup> (4.13)



A mixture of maleic hydrazide (1.12 g, 10.0 mmol) and phosphorus oxybromide (3.15 g, 11.0 mmol) was heated at 200 °C for 30 min, and then allowed to cool to room temperature. The residue was poured over ice, made basic with NaHCO<sub>3</sub> (saturated, aqueous), and extracted with CH<sub>2</sub>Cl<sub>2</sub> (×3). The combined organic layers were dried over MgSO<sub>4</sub>, filtered and concentrated under reduced pressure. Purification by silica gel flash chromatography (0–60% EtOAc in Pet. Sp.) afforded the title compound as a white solid (1.27 g, 5.36 mmol, 54%). Spectroscopic data are in agreement with the literature reported values.<sup>[41]</sup>

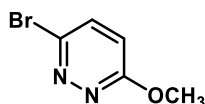
<sup>1</sup>H NMR (400 MHz, CDCl<sub>3</sub>) δ = 7.52 (s, 2H, Pydz-H);

<sup>13</sup>C NMR (101 MHz, CDCl<sub>3</sub>) δ = 147.8 (Pydz-C-Br), 133.41 (Pydz-CH);

LR-MS (ESI+) *m/z*: 236.8/236.7/240.8 [M+H]<sup>+</sup>;

Analytical HPLC (254 nm): *t*<sub>R</sub> = 3.3 min, 99%.

### 3-bromo-6-methoxypyridazine<sup>[42]</sup> (4.14)



To a solution of **4.13** (1.19 g, 5.00 mmol) in a THF (10 mL, anhydrous) and MeOH (10 mL, anhydrous) was added sodium methoxide (1.08 g, 20.0 mmol) at 0 °C. The resulting mixture was slowly warmed to room temperature and stirred for a total of 16 h. After this time, the reaction was diluted with

water and extracted with EtOAc (×3). The combined organic layers were dried over MgSO<sub>4</sub>, filtered and concentrated under reduced pressure to give the title compound as a white solid (0.800 g, 4.24 mmol, 85%) which was used in the next step without further purification. Spectroscopic data are in agreement with the reported literature values.<sup>[42]</sup>

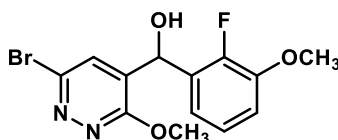
<sup>1</sup>H NMR (400 MHz, CDCl<sub>3</sub>) δ = 7.47 (d, *J* = 9.1 Hz, 1H, 4-PydzH), 6.86 (d, *J* = 9.1 Hz, 1H, 5-PydzH), 4.11 (s, 3H, Pydz-OCH<sub>3</sub>);

<sup>13</sup>C NMR (101 MHz, CDCl<sub>3</sub>) δ = 164.8 (PydzC-OCH<sub>3</sub>), 141.6 (PydzC-Br), 134.0 (4-PydzCH), 120.0 (5-PydzCH), 55.5 (Pydz-OCH<sub>3</sub>);

LR-MS (ESI+) *m/z*: 188.9/190.9 [M+H]<sup>+</sup>;

Analytical HPLC (254 nm): *t*<sub>R</sub> = 3.3 min, 98%.

**(6-bromo-3-methoxypyridazin-4-yl)(2-fluoro-3-methoxyphenyl)methanol<sup>[43]</sup> (4.15)**



To a solution of 2,2,6,6-tetramethylpiperidine (0.470 mL, 2.80 mmol, anhydrous) in THF (2.5 mL, anhydrous) cooled to −10 °C and under an atmosphere of nitrogen was added *n*-BuLi (1.48 mL, 1.49 M in hexanes, 2.20 mmol) dropwise over 5 min. The mixture was maintained at this temperature for 30 min, followed by cooling to −78 °C. To the reaction mixture was added a solution of **4.14** (189 mg, 1.00 mmol) in THF (2 mL, anhydrous) dropwise over 5 min, and the resultant reaction mixture was stirred at −78 °C for 30 min. After this time, a solution of 2-fluoro-3-methoxybenzaldehyde (170 mg, 1.10 mmol) in THF (2 mL, anhydrous) was added dropwise over 5 min and the mixture was left to react for 3 h. After this time the reaction was quenched with a solution of NH<sub>4</sub>Cl (saturated, aqueous), the organic phase separated and the aqueous phase extracted with EtOAc (×3). The combined organic layers were washed with brine, dried over anhydrous MgSO<sub>4</sub>, filtered, and concentrated under reduced pressure. Purification by silica gel flash chromatography (0–40% EtOAc in PhMe), followed by recrystallisation from EtOH afforded the title compound as an off-white powder (191 mg, 0.567 mmol, 56%).

<sup>1</sup>H NMR (400 MHz, DMSO-*d*<sub>6</sub>) δ = 7.90 (d, *J* = 1.1 Hz, 1H, PydzH), 7.14 – 7.01 (m, 2H, PhH), 6.77 – 6.71 (m, 1H, PhH), 6.40 (d, *J* = 4.0 Hz, 1H, OH), 5.95 (d, *J* = 3.5 Hz, 1H, CH-OH), 3.90 (s, 3H, Pydz-OCH<sub>3</sub>), 3.82 (s, 3H, Ph-OCH<sub>3</sub>);

<sup>13</sup>C NMR (101 MHz, DMSO-*d*<sub>6</sub>) δ = 161.6 (PydzC-OCH<sub>3</sub>), 149.3 (d, *J*<sub>CF</sub> = 246.9 Hz, PhC-F), 147.1 (d, *J*<sub>CF</sub> = 10.7 Hz, PhC-OCH<sub>3</sub>), 141.9 (PydzC-Br), 136.4 (PydzC-CHOH), 129.8 (PydzCH), 128.7 (d, *J*<sub>CF</sub> = 11.3 Hz,

Ph $\underline{\text{C}}$ -CHOH), 124.1 (d,  $J_{\text{CF}} = 4.3$  Hz, Ph $\underline{\text{C}}$ H), 119.8 (d,  $J_{\text{CF}} = 2.7$  Hz, Ph $\underline{\text{C}}$ H), 113.3 (5-Ph $\underline{\text{C}}$ H), 62.0 (d,  $J_{\text{CF}} = 4.7$  Hz,  $\underline{\text{C}}$ H-OH), 56.0 (Ph-O $\underline{\text{C}}$ H<sub>3</sub>), 55.0 (Pydz-O $\underline{\text{C}}$ H<sub>3</sub>);

LR-MS (ESI+)  $m/z$ : 342.9/344.9 [M+H]<sup>+</sup>;

HR-MS (ESI+)  $m/z$  [M = C<sub>13</sub>H<sub>12</sub>BrFN<sub>2</sub>O<sub>3</sub>]: [M+H]<sup>+</sup> calc'd 343.0088, found 343.0096;

Analytical HPLC (254 nm):  $t_R = 5.0$  min, 97%.

## 6.2 Biological assays

### 6.2.1 Resazurin microtitre assay

#### Protocol A

*Performed by Dr. Gayathri Nagalingam in the group of Prof. James Triccas at the Centenary Institute (University of Sydney).*

The *M.tb* strain H37Rv was grown at 37 °C in complete Middlebrook 7H9 media (Bacto, Australia) containing albumin, dextrose, and catalase (ADC), 20% Tween 80, and 50% glycerol (Sigma-Aldrich, Australia) to an optical density (OD) of 0.6–0.8 (determined by spectrophotometry or comparison with McFarland standard). On the day of the assay the grown *M.tb* culture was diluted to an OD of 0.001.

The minimal inhibitory concentration (MIC<sub>90</sub>) of compounds was determined using a modified version of the resazurin viability assay (REMA). All compounds were initially prepared as 100 mM stocks in 100% DMSO and then adjusted to the required concentration in diluent (0.1% DMSO). Compounds were added to a 96-well plate in 2-fold dilutions (usually 100 – 0.2  $\mu\text{M}$ ) with a final volume of 10  $\mu\text{L}$ . Rifampicin was used as the positive control. To the compound wells was added 90  $\mu\text{L}$  of diluted bacterial suspension. Compounds and *M.tb* were incubated in complete 7H9 media supplemented with ADC enrichment for 7 days. Resazurin (10  $\mu\text{L}$ ; 0.05% w/v; Sigma-Aldrich, Australia) was then added, and plates were incubated for 24 h at 37 °C. Detection of fluorescence at 590 nm was performed using a FLUOstar Omega microplate reader (BMG Labtech, Germany). After subtraction of background fluorescence from all wells, the percentage mycobacterial survival was determined by comparing the fluorescence of wells containing test compounds of rifampicin with control wells not treated with compound. The MIC<sub>90</sub> was determined using non-linear regression to produce a line of best fit (GraphPad Prism version 7.0).

#### Protocol B

*Performed by Dr. Lendl Tan in the group of Assoc. Prof. Nick West (University of Queensland)*

Virulent *Mt* H37Rv was grown in Middlebrook 7H9 broth medium supplemented with 10% ADC, 0.5% glycerol and 0.02% tyloxapol. Cultures were grown at 37 °C to mid-exponential phase (OD<sub>600</sub> 0.4–0.8)

and diluted to OD<sub>600</sub> 0.002 in 7H9S media (Middlebrook 7H9 with 10% ADC, 0.5% glycerol, 0.75% tween-80, 1% tryptone). 96-well microtitre plates were setup with 100 µl of inhibitors, serially diluted (10 – 0.02 µM) into 7H9S media. 100 µl of diluted *M.tb*, representing *ca.*  $2 \times 10^4$  CFU/mL was added to each well. Plates were incubated for five days at 37 °C. 42.5 µl of resazurin solution (30 µl of 0.02% resazurin, 12.5 µl of 20% Tween 80) was added to each well. Fluorescence was measured after 24 h on a FluoroStar Omega fluorescent plate reader (BMG) with an excitation wavelength of 530 nm and an emission wavelength of 590 nm. Changes in fluorescence relative to positive control wells (H37Rv with no inhibitor) minus negative control wells (no H37Rv) were plotted using non-linear regression to produce a line of best fit (GraphPad Prism version 7.0) for determination of MIC<sub>90</sub>.

### 6.2.2 *In vitro* hERG inhibition assay

FASTPatch® hERG assay protocol

*Performed by Charles River Laboratories (U.S.A)*

The hERG potassium channels (KCNH2 gene, a surrogate for IKr, the rapidly activating, delayed rectifier cardiac potassium current) were stably expressed in HEK293 cells. Test articles were prepared by diluting stock solutions into an appropriate HEPES-buffered physiological saline solution with no more than 0.3% DMSO. Each test article formulation was sonicated (Model 2510/5510, Branson Ultrasonics, Danbury, CT) at room temperature to facilitate dissolution. A glass-lined 96-well compound plate was loaded with the appropriate amounts of test and control solutions, and placed in the plate well of the QPatch HT® or QPatch HTX® (Sophion Bioscience A/S, Denmark). In preparation for a recording session, intracellular solution (130 mM K-Asp, 5 mM MgCl<sub>2</sub>, 5 mM EGTA, 4 mM Tris-ATP) was loaded into the intracellular compartments of the QPlate and cell suspension was pipetted into the extracellular compartments. Vehicle was applied *via* the QPatch robot pipetting system to naïve cells for a 5–10 minute exposure interval. After vehicle application, the test article concentrations were applied in at least three minute intervals in at least two cells ( $n \geq 2$ , where  $n$  = the number of cells/concentration). Each solution exchange was performed multiple times through the microfluidic flow channel, which resulted in 100% replacement of the compound in the QPlate. Onset and block of hERG current was measured using a stimulus voltage pattern consisting of a 500 ms prepulse to –40 mV (leakage subtraction), a 2-second activating pulse to +40 mV followed by a 2-second test pulse to –40 mV. The pulse pattern was repeated continuously at 10 s intervals from a holding potential of –80 mV. Peak tail current was measured during the –40 mV test pulse. Leakage current was calculated from the current amplitude evoked by the –40 mV prepulse and subtracted from the total membrane current record.

Concentration-response data were fit to an equation of the form:

$$\% \text{ Inhibition} = \{1 - 1/[1 + ([\text{Test}]/\text{IC}_{50})^N]\} * 100$$

Where [Test] was the test article concentration,  $\text{IC}_{50}$  was the test article concentration at half-maximal inhibition, N was the Hill coefficient and % Inhibition was the percentage of current inhibited at each test article concentration. Nonlinear least squares fits were solved with the Solver add-in for Excel 2003 (Microsoft, WA) and the  $\text{IC}_{50}$  was calculated.

Bedaquiline was evaluated at 0.01, 0.03, 0.1, 0.3, 1, 3 and 10  $\mu\text{M}$ . Compounds **3.55-B** and **3.64-B** were evaluated at 0.1, 1, 3, 10, 33.33, 50, 75 and 100  $\mu\text{M}$ . Cisapride (0.05  $\mu\text{M}$ ) was used as a positive control.

### 6.3 References

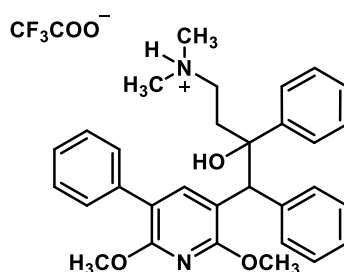
- [1] T. Ishiyama, N. Matsuda, N. Miyaura, A. Suzuki, *J. Am. Chem. Soc.* **1993**, *115*, 11018–11019.
- [2] V. Cañibano, J. F. Rodríguez, M. Santos, M. A. Sanz-Tejedor, M. C. Carreño, G. González, J. L. García-Ruano, *Synthesis*. **2001**, *2001*, 2175–2179.
- [3] M. Shimizu, I. Nagao, Y. Tomioka, T. Hiyama, *Angew. Chem. Int. Ed. Engl.* **2008**, *47*, 8096–9.
- [4] H. R. Kim, J. Yun, *Chem. Commun.* **2011**, *47*, 2943–2945.
- [5] Y. Zhang, X. Jia, J.-X. Wang, *European J. Org. Chem.* **2009**, *2009*, 2983–2986.
- [6] D. Yang, C. Zhang, *J. Org. Chem.* **2001**, *66*, 4814–4818.
- [7] S. Chandrasekhar, G. S. K. Babu, D. K. Mohapatra, *European J. Org. Chem.* **2011**, *2011*, 2057–2061.
- [8] T. D. Senecal, W. Shu, S. L. Buchwald, *Angew. Chemie Int. Ed.* **2013**, *52*, 10035–10039.
- [9] D. L. Priebbenow, L. Barbaro, J. B. Baell, *Org. Biomol. Chem.* **2016**, *14*, 9622–9628.
- [10] D. J. Cooper, L. N. Owen, *J. Chem. Soc. C* **1966**, *0*, 533–540.
- [11] L. Testaferri, M. Tiecco, M. Tingoli, D. Bartoli, A. Massoli, *Tetrahedron* **1985**, *41*, 1373–1384.
- [12] F. Damkaci, C. Sigindere, T. Sobiech, E. Vik, J. Malone, *Tetrahedron Lett.* **2017**, *58*, 3559–3564.
- [13] M. P. Sibi, J. W. Dankwardt, V. Snieckus, *J. Org. Chem.* **1986**, *51*, 271–273.
- [14] C.-E. Yeom, S. Lee, Y. Kim, B. Kim, *Synlett* **2005**, *2005*, 1527–1530.
- [15] A. Palmgren, A. L. E. Larsson, J.-E. Bäck andvall, P. Helquist, *J. Org. Chem.* **1999**, *64*, 836–842.
- [16] C. Klein, E. Baranoff, M. Grätzel, M. K. Nazeeruddin, *Tetrahedron Lett.* **2011**, *52*, 584–587.
- [17] K. E. Henegar, S. W. Ashford, T. A. Baughman, J. C. Sih, R.-L. Gu, *J. Org. Chem.* **1997**, *62*, 6588–6597.
- [18] E. L. Stogryn, *J. Heterocycl. Chem.* **1974**, *11*, 251–253.
- [19] D. M. Rudzinski, C. B. Kelly, N. E. Leadbeater, *Chem. Commun.* **2012**, *48*, 9610.
- [20] H. S. Sutherland, A. S. T. Tong, P. J. Choi, A. Blaser, D. Conole, S. G. Franzblau, M. U. Lotlikar, C. B. Cooper, A. M. Upton, W. A. Denny, et al., *Bioorganic Med. Chem.* **2019**, *27*, 1292–1307.
- [21] F. Xu, W. Li, W. Shuai, L. Yang, Y. Bi, C. Ma, H. Yao, S. Xu, Z. Zhu, J. Xu, *Eur. J. Med. Chem.* **2019**, *173*, 1–14.
- [22] I. Katsuhiko, M. Hamada, A. Terauchi, S. Ozaki, J.-I. Goto, E. Ebisu, A. Suzuki, *Inhibitor of Protein Crosslinking and Use of the Same*, **2009**, US8937091B2.
- [23] S. Ozaki, E. Ebisui, K. Hamada, J.-I. Goto, A. Z. Suzuki, A. Terauchi, K. Mikoshiba, *Bioorg. Med. Chem. Lett.* **2010**, *20*, 1141–1144.
- [24] M. Frank, H. Haeberle, M. Henry, T. Pachur, M. Santagostino, U. Stertz, T. Trebing, U. Werthmann, *Co-Crystals and Salts of Ccr3-Inhibitors*, **2011**, WO2012045803A1.

- [25] S. Erbas-Cakmak, F. P. Cakmak, S. D. Topel, T. B. Uyar, E. U. Akkaya, *Chem. Commun.* **2015**, 51, 12258–12261.
- [26] K. Sivagurunathan, S. Raja Mohamed Kamil, S. Syed Shafi, F. Liakth Ali Khan, R. V. Ragavan, *Tetrahedron Lett.* **2011**, 52, 1205–1207.
- [27] A. M. Goldys, M. G. Núñez, D. J. Dixon, *Org. Lett.* **2014**, 16, 6294–6297.
- [28] D. Mukherjee, S. Shirase, K. Mashima, J. Okuda, *Angew. Chemie Int. Ed.* **2016**, 55, 13326–13329.
- [29] T. M. Bargar, J. K. Dulworth, M. T. Kenny, R. Massad, J. K. Daniel, T. Wilson, R. N. Sargent, *J. Med. Chem.* **1986**, 29, 1590–1595.
- [30] M. Peters, M. Trobe, R. Breinbauer, *Chem. - A Eur. J.* **2013**, 19, 2450–2456.
- [31] M. C. Pirrung, K. Park, L. N. Tumey, *J. Comb. Chem.* **2002**, 4, 3298–344.
- [32] M. R. Witten, L. Wissler, M. Snow, S. Geschwindner, J. A. Read, N. J. Brandon, A. C. Nairn, P. J. Lombroso, H. Käck, J. A. Ellman, *J. Med. Chem.* **2017**, 60, 9299–9319.
- [33] V. Lotti, G. A. Showell, *Substituted Pyrazines, Pyrimidines and Pyridazines for Use in the Treatment of Glaucoma*, **1991**, US5219849A.
- [34] Y. Younis, F. Douelle, D. González Cabrera, C. Le Manach, A. T. Nchinda, T. Paquet, L. J. Street, K. L. White, K. M. Zabiulla, J. T. Joseph, et al., *J. Med. Chem.* **2013**, 56, 8860–8871.
- [35] J. Kehler, L. K. Rasmussen, M. Jessing, *Triazolopyrazinones as Pde1 Inhibitors*, **2015**, WO2016055618A1.
- [36] F. Toudic, A. Turck, N. Plé, G. Quéguiner, M. Darabantu, T. Lequeux, J. C. Pommelet, *J. Heterocycl. Chem.* **2003**, 40, 855–860.
- [37] A. Krasovskiy, V. Krasovskaya, P. Knochel, *Angew. Chemie Int. Ed.* **2006**, 45, 2958–2961.
- [38] A. Leprêtre, A. Turck, N. Plé, P. Knochel, G. Quéguiner, *Tetrahedron* **2000**, 56, 265–273.
- [39] F. Buron, N. Plé, A. Turck, F. Marsais, *Synlett* **2006**, 2006, 1586–1588.
- [40] N. J. Dewdney, Y. Lou, E. B. Sjogren, M. Soth, *Novel Phenyl-Imidazopyridines and Pyridazines*, **2009**, WO2010006947A1.
- [41] Y. S. Park, D. Kim, H. Lee, B. Moon, *Org. Lett.* **2006**, 8, 4699–4702.
- [42] W. P. Dankulich, D. G. McGarry, C. Burns, T. F. Gallagher, F. A. Volz, *Substituted (Aminoiminomethyl or Aminomethyl) Benzoheteroaryl Compounds*, **1999**, WO2000039087A2.
- [43] L. Mojovic, A. Turck, N. Plé, M. Dorsy, B. Ndzi, G. Quéguiner, *Tetrahedron* **1996**, 52, 10417–10426.

## Appendices

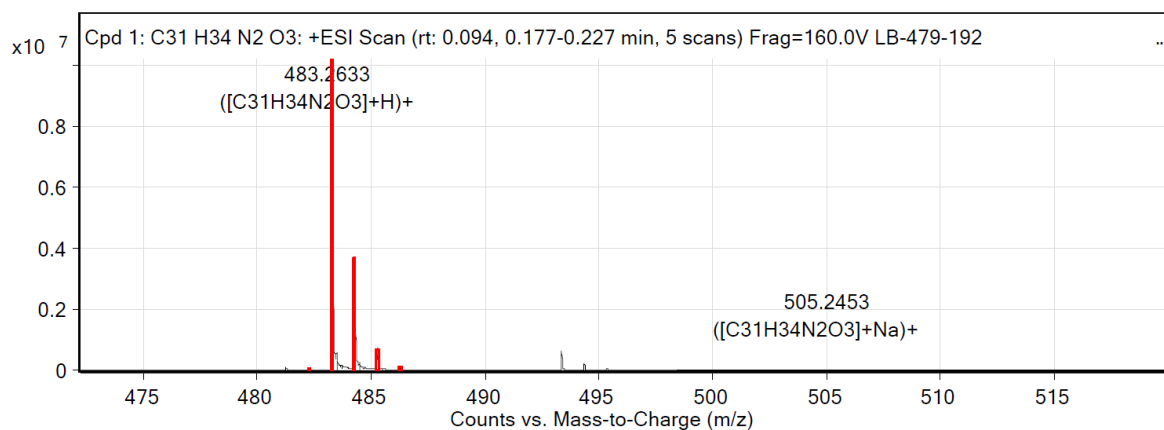
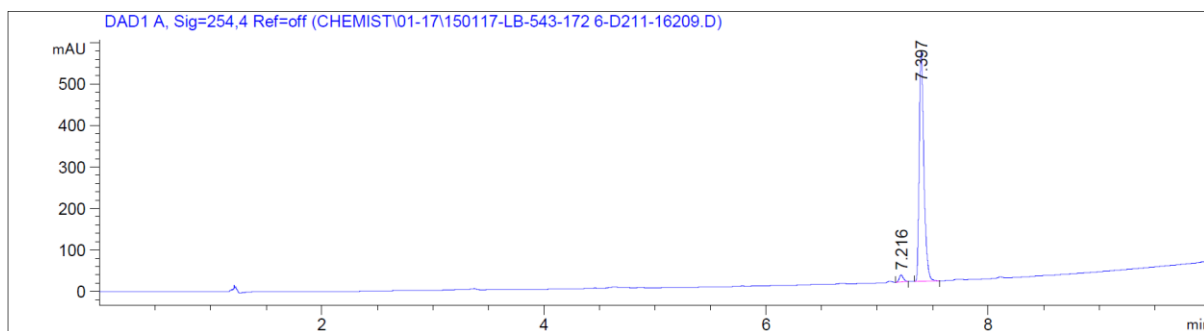
### Appendix 1: Characterisation for representative final compounds

#### A1.1 Compound 2.045-B

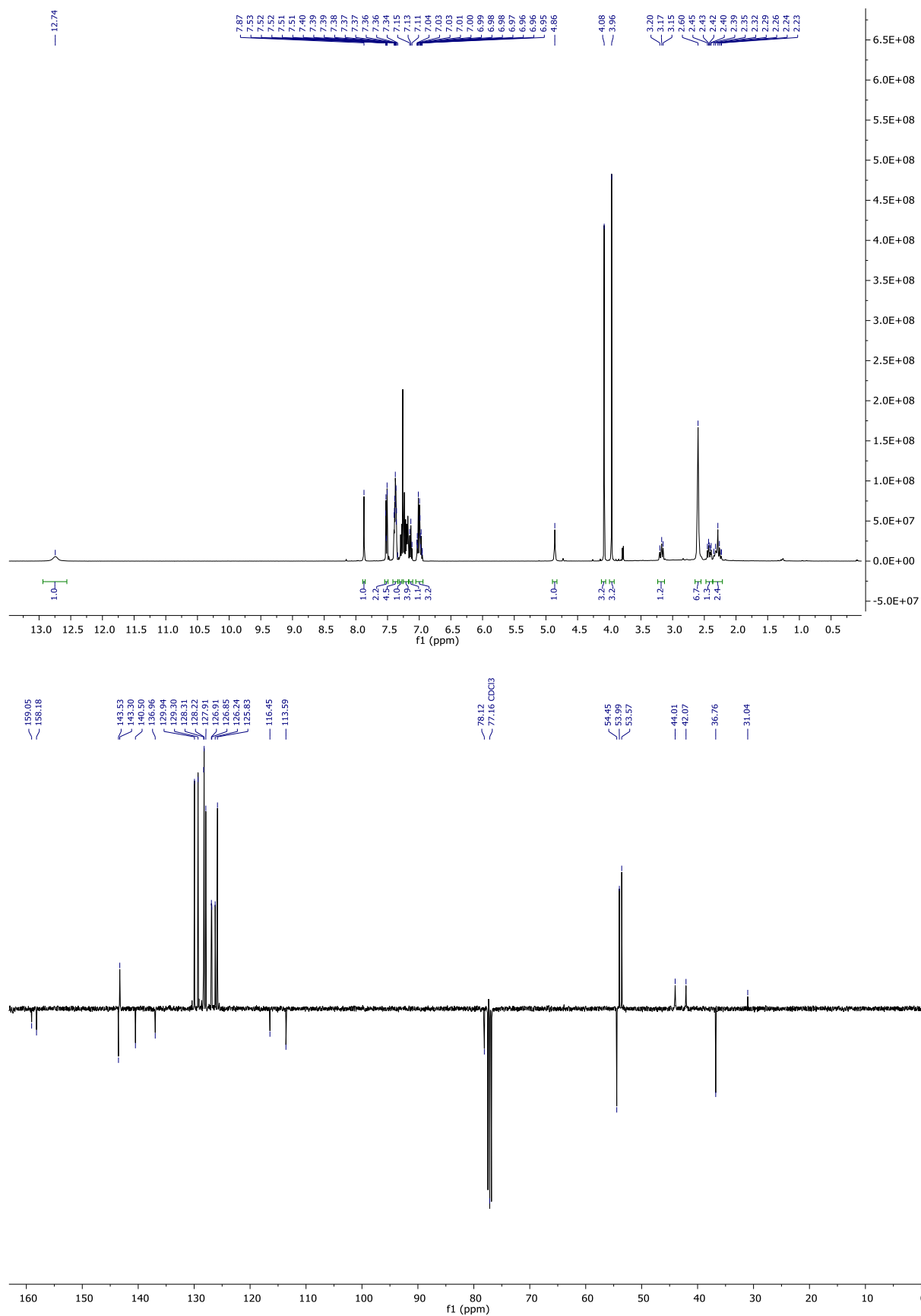


2.045-B

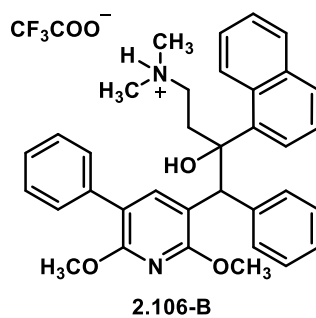
Exact Mass: 483.2642



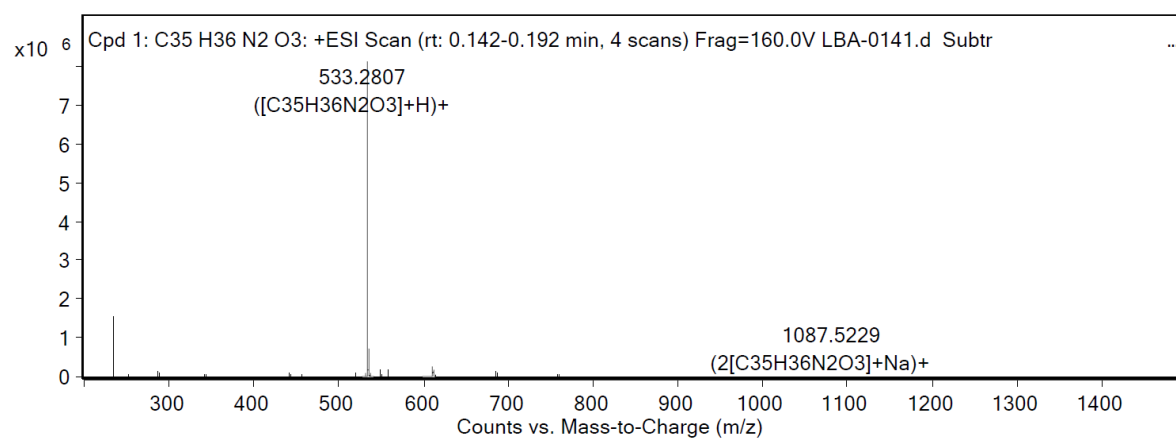
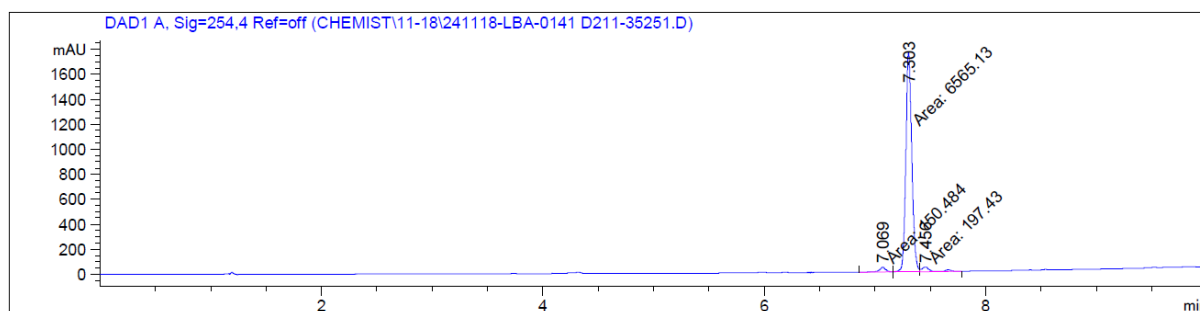


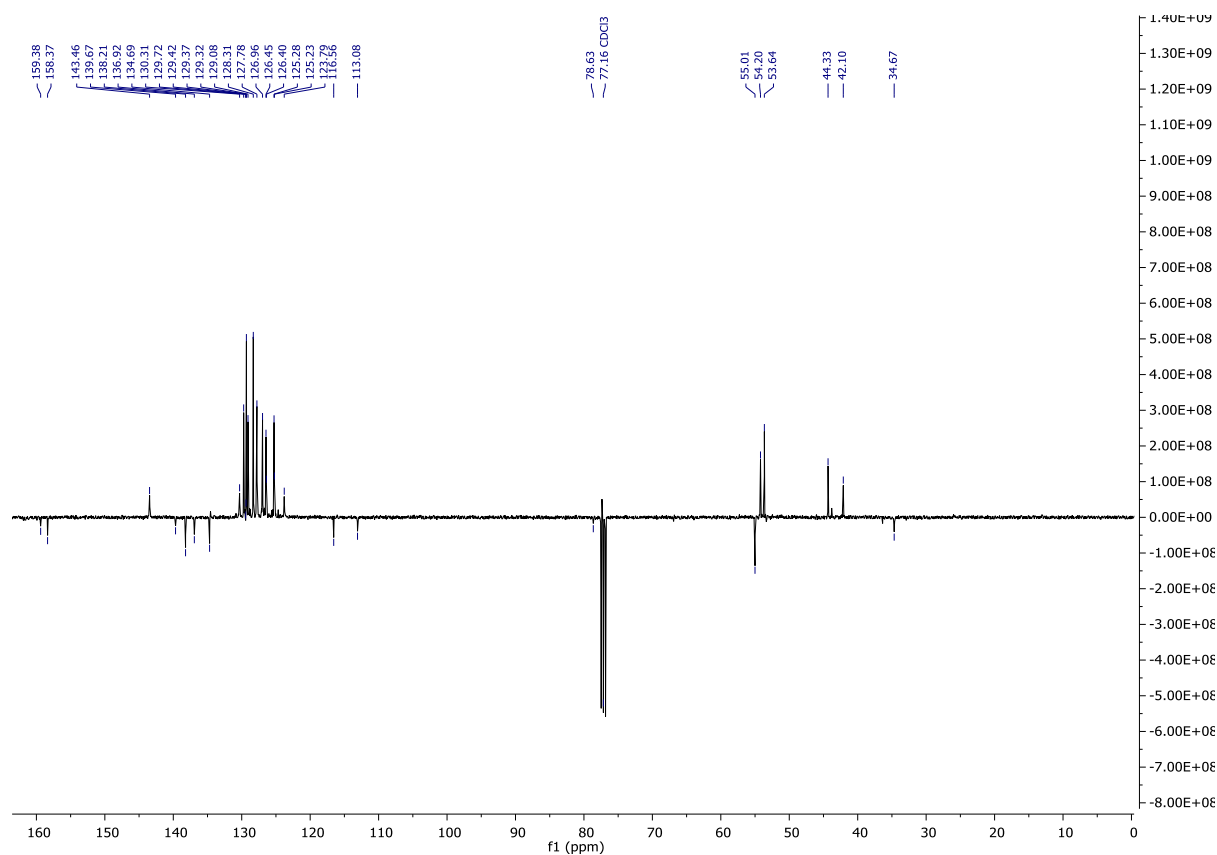
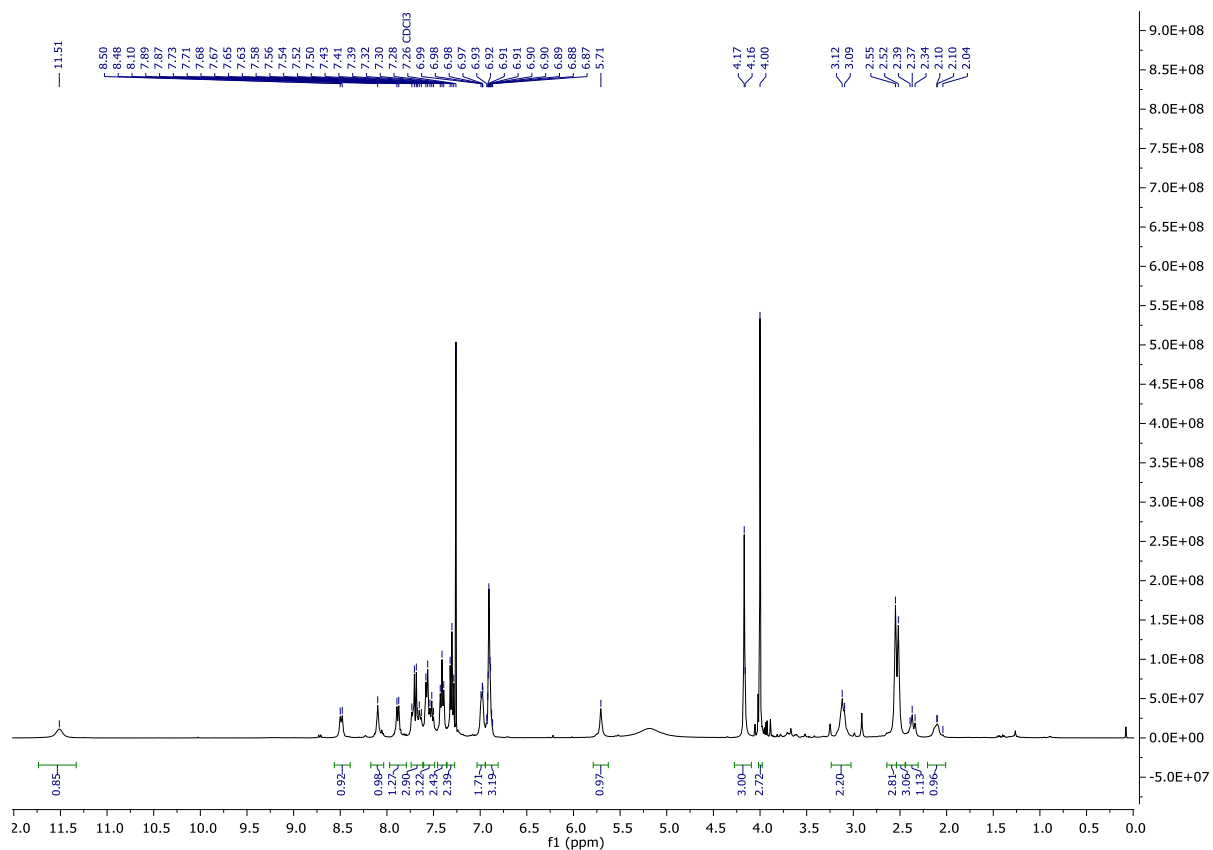


## A1.2 Compound 2.106-B

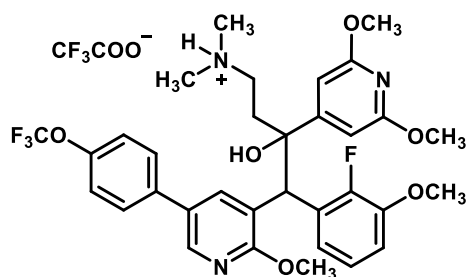


Exact Mass: 533.2799



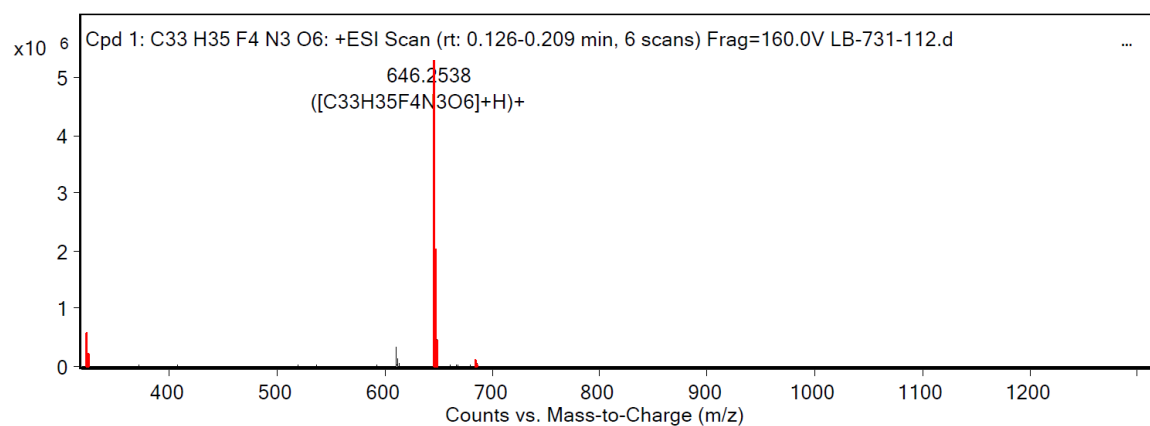
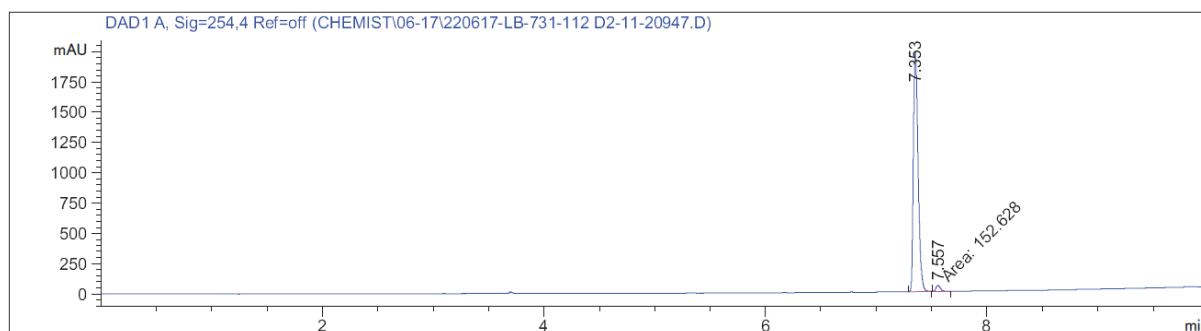


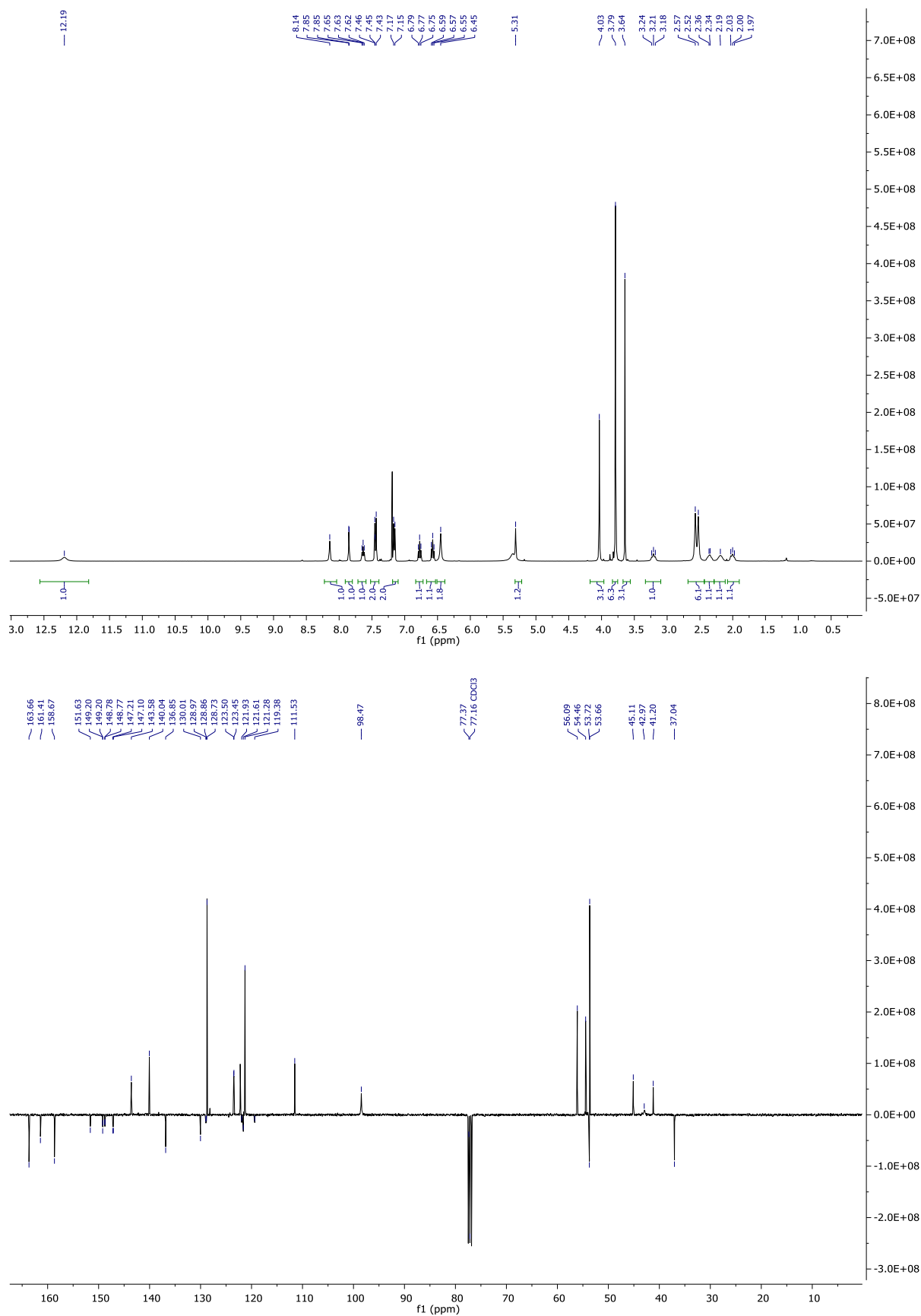
### A1.3 Compound 3.02-B



3.02-B

Exact Mass: 646.2535



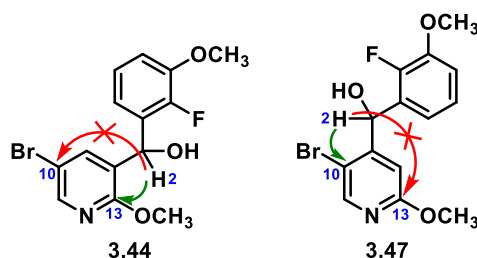


## Appendix 2: NMR assignments for selected compounds

### A2.1 Compounds 3.44 and 3.47

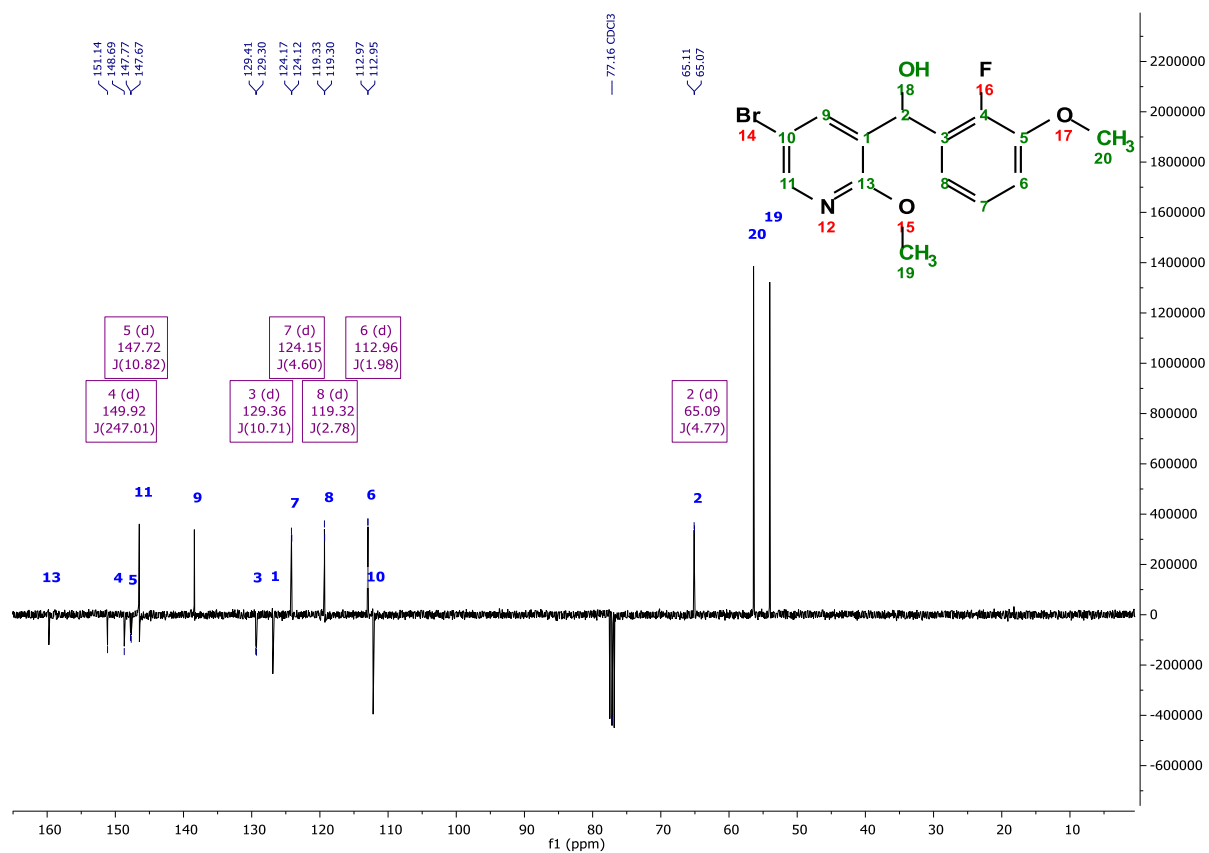
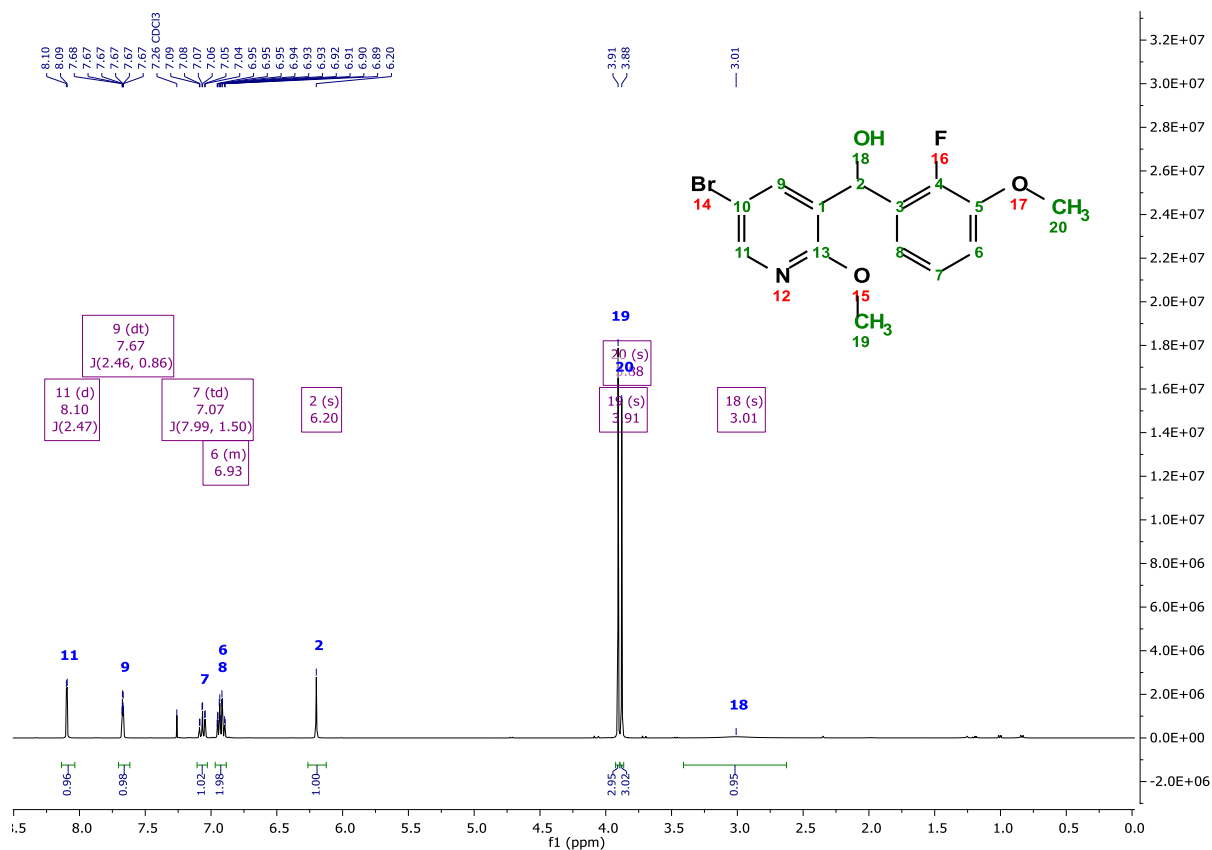
Additional evidence for structure for 3.44 is the presence of an HMBC  $^3J_{C-H}$  cross-peak between H2 and C13. This peak would be missing if the structure was 3.47 as these atoms would be too far away ( $^4J_{C-H}$ ). Additionally, there is an absence of an HMBC  $^3J_{C-H}$  cross-peak between H2 and C10 as these atoms are too far away.

Additional evidence for structure for 3.47 is the presence of an HMBC  $^3J_{C-H}$  cross-peak between H2 and C10. This peak would be missing if the structure was 3.44 as these atoms would be too far away ( $^4J_{C-H}$ ). Additionally, there is an absence of an HMBC  $^3J_{C-H}$  cross-peak between H2 and C13 as these atoms are too far away.



### Compound 3.44

| Atom  | Chemical Shift | Splitting, $J$ (Hz)  | HSQC | HMBC     |
|-------|----------------|----------------------|------|----------|
| 1 C   | 126.91         |                      |      | 2        |
| 2 C   | 64.97          | d, 4.77              | 2    |          |
| H     | 6.20           |                      | 2    | 8, 13, 1 |
| 3 C   | 129.48         | d, 10.71             |      | 7        |
| 4 C   | 148.09..151.77 | d, 247.01            |      | 8        |
| 5 C   | 147.79         | d, 10.82             |      | 7        |
| 6 C   | 112.83         | d, 1.98              | 6    |          |
| H     | 6.93           |                      | 6    |          |
| 7 C   | 124.03         | d, 4.60              | 7    |          |
| H     | 7.07           | td, 1.50, 7.99, 7.97 | 7    | 3, 5     |
| 8 C   | 119.01         | d, 2.78              |      | 2        |
| H     | 6.87..6.99     |                      |      | 4        |
| 9 C   | 138.29         |                      | 9    |          |
| H     | 7.67           | dt, 0.86, 0.86, 2.46 | 9    | 13, 10   |
| 10 C  | 112.19         |                      |      | 9, 11    |
| 11 C  | 146.25         | d, 2.47              | 11   |          |
| H     | 8.10           |                      | 11   | 13, 10   |
| 12 N  |                |                      |      |          |
| 13 C  | 159.75         |                      |      | 2, 11, 9 |
| 14 Br |                |                      |      |          |
| 15 O  |                |                      |      |          |
| 16 F  |                |                      |      |          |
| 17 O  |                |                      |      |          |
| 18 O  |                |                      |      |          |
| H     | 3.01           |                      |      |          |
| 19 C  | 53.87          |                      | 19   |          |
| H3    | 3.91           |                      | 19   |          |
| 20 C  | 56.28          |                      | 20   |          |
| H3    | 3.88           |                      | 20   |          |

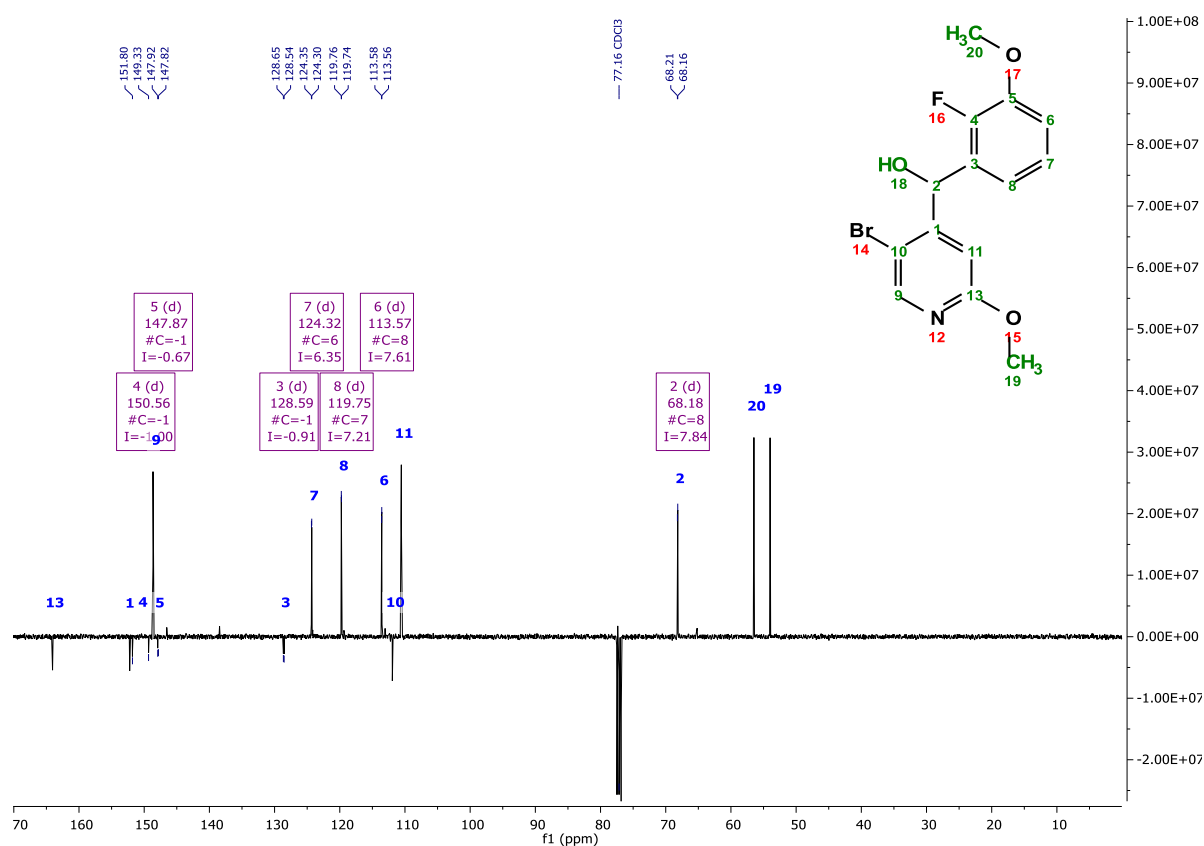
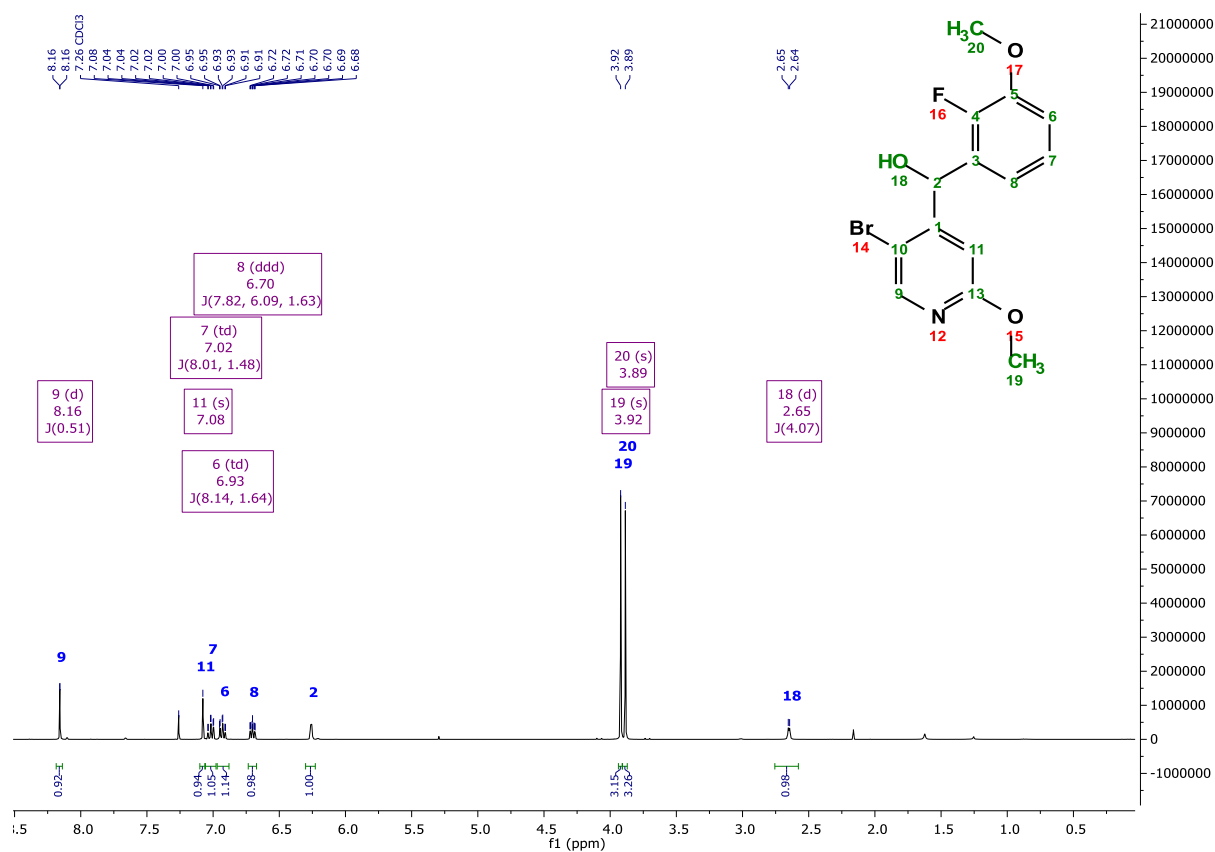


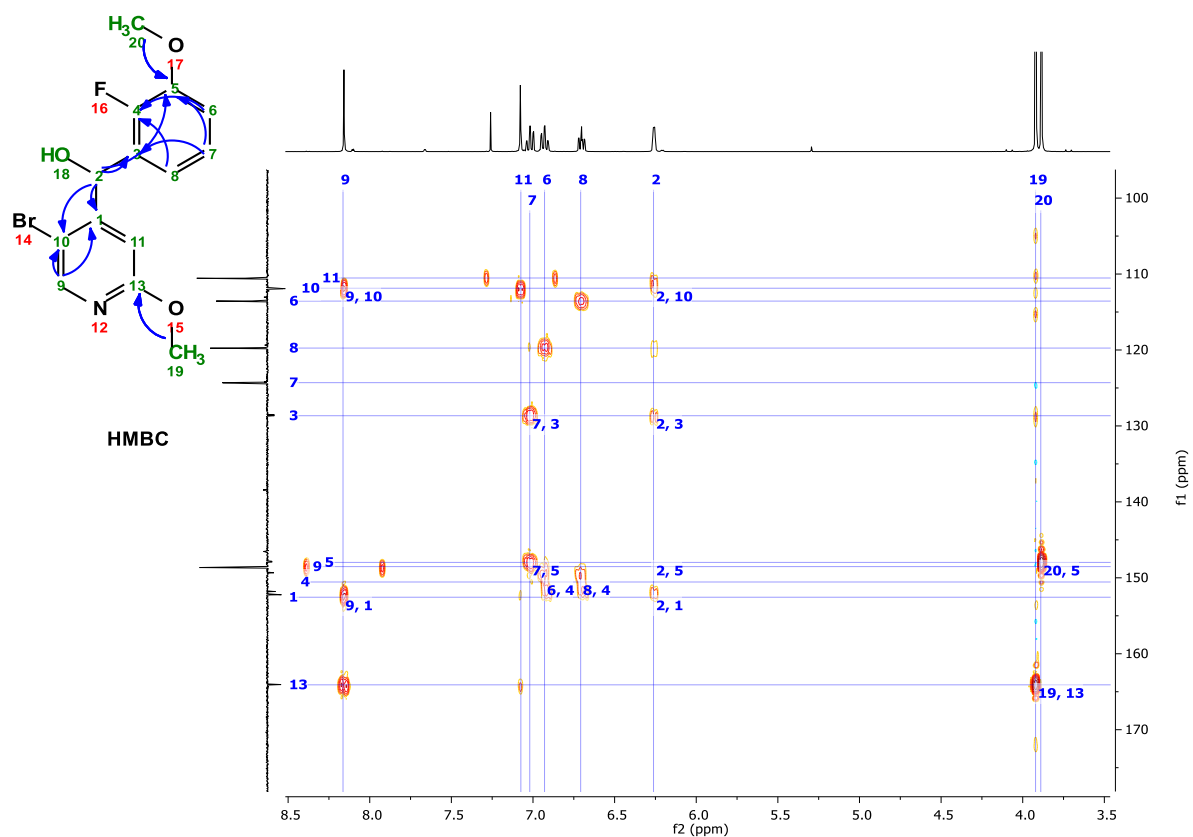
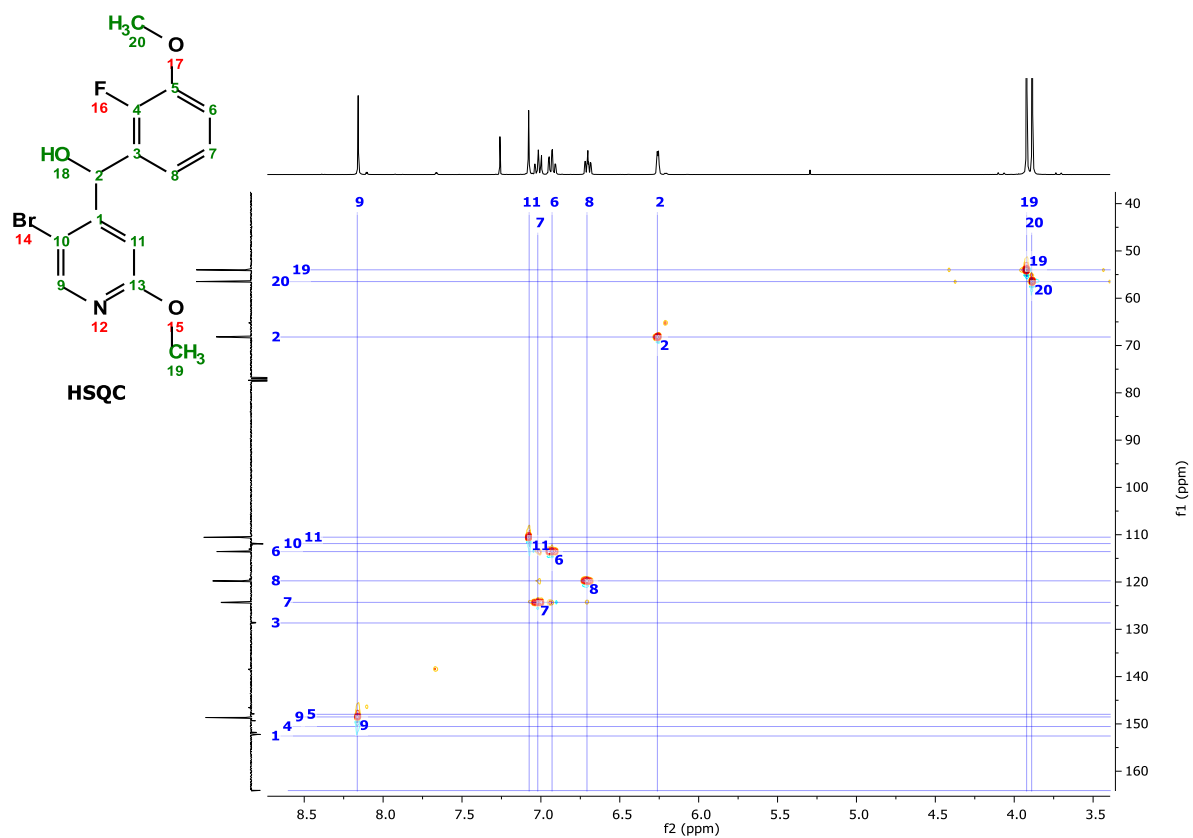




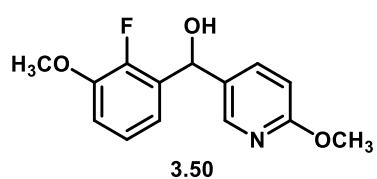
### Compound 3.47

| Atom  | Chemical Shift | Splitting, <i>J</i> (Hz) | HSQC | HMBC        |
|-------|----------------|--------------------------|------|-------------|
| 1 C   | 152.56         |                          |      | 9, 2        |
| 2 C   | 68.20          | d, 5.15                  | 2    |             |
| H     | 6.26           |                          | 2    | 1, 5, 3, 10 |
| 3 C   | 128.66         | d, 11.35                 |      | 7, 2        |
| 4 C   | 149.16..151.93 | d, 248.12                |      | 8, 6        |
| 5 C   | 147.97         | d, 10.70                 |      | 20, 2, 7    |
| 6 C   | 113.56         | d, 2.16                  | 6    |             |
| H     | 6.93           | td, 1.64, 8.14, 8.19     | 6    | 4           |
| 7 C   | 124.30         | d, 4.69                  | 7    |             |
| H     | 7.02           | td, 1.48, 8.01, 7.95     | 7    | 5, 3        |
| 8 C   | 119.75         | d, 2.58                  | 8    |             |
| H     | 6.71           | ddd, 1.63, 6.09, 7.82    | 8    | 4           |
| 9 C   | 148.52         |                          | 9    |             |
| H     | 8.16           | d, 0.51                  | 9    | 1, 10       |
| 10 C  | 111.87         |                          |      | 9, 2        |
| 11 C  | 110.52         |                          | 11   |             |
| H     | 7.07           |                          | 11   |             |
| 12 N  |                |                          |      |             |
| 13 C  | 164.09         |                          |      | 19          |
| 14 Br |                |                          |      |             |
| 15 O  |                |                          |      |             |
| 16 F  |                |                          |      |             |
| 17 O  |                |                          |      |             |
| 18 O  |                |                          |      |             |
| H     | 2.62..2.67     | d, 4.07                  |      |             |
| 19 C  | 53.99          |                          | 19   |             |
| H3    | 3.92           |                          | 19   | 13          |
| 20 C  | 56.48          |                          | 20   |             |
| H3    | 3.89           |                          | 20   | 5           |



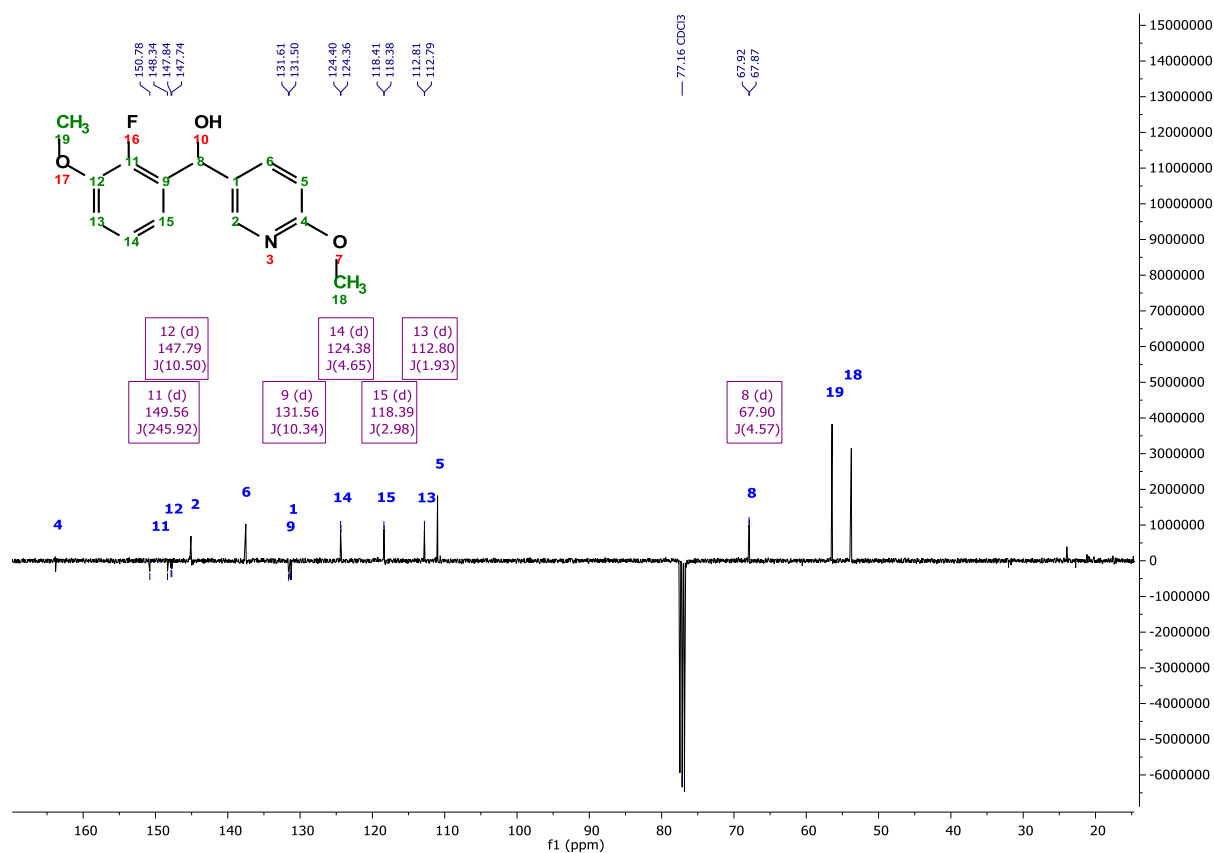
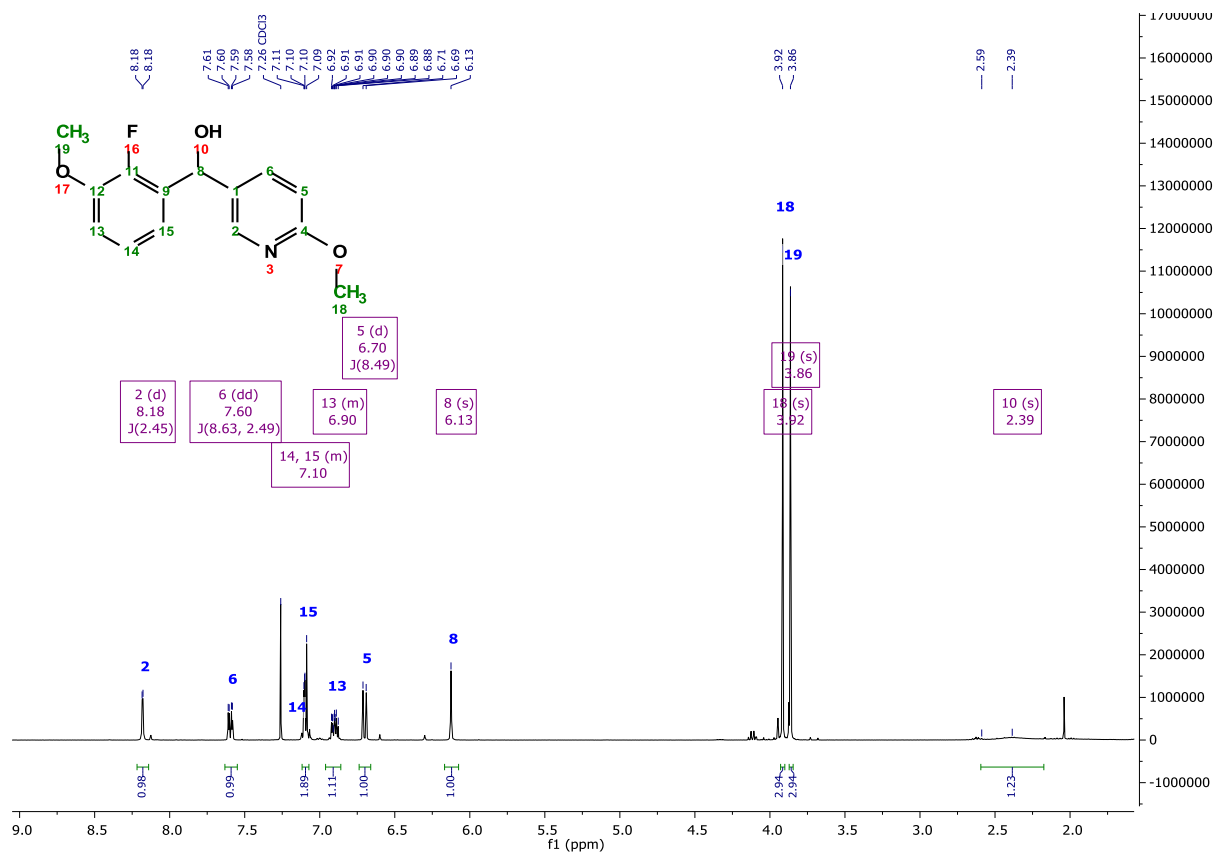


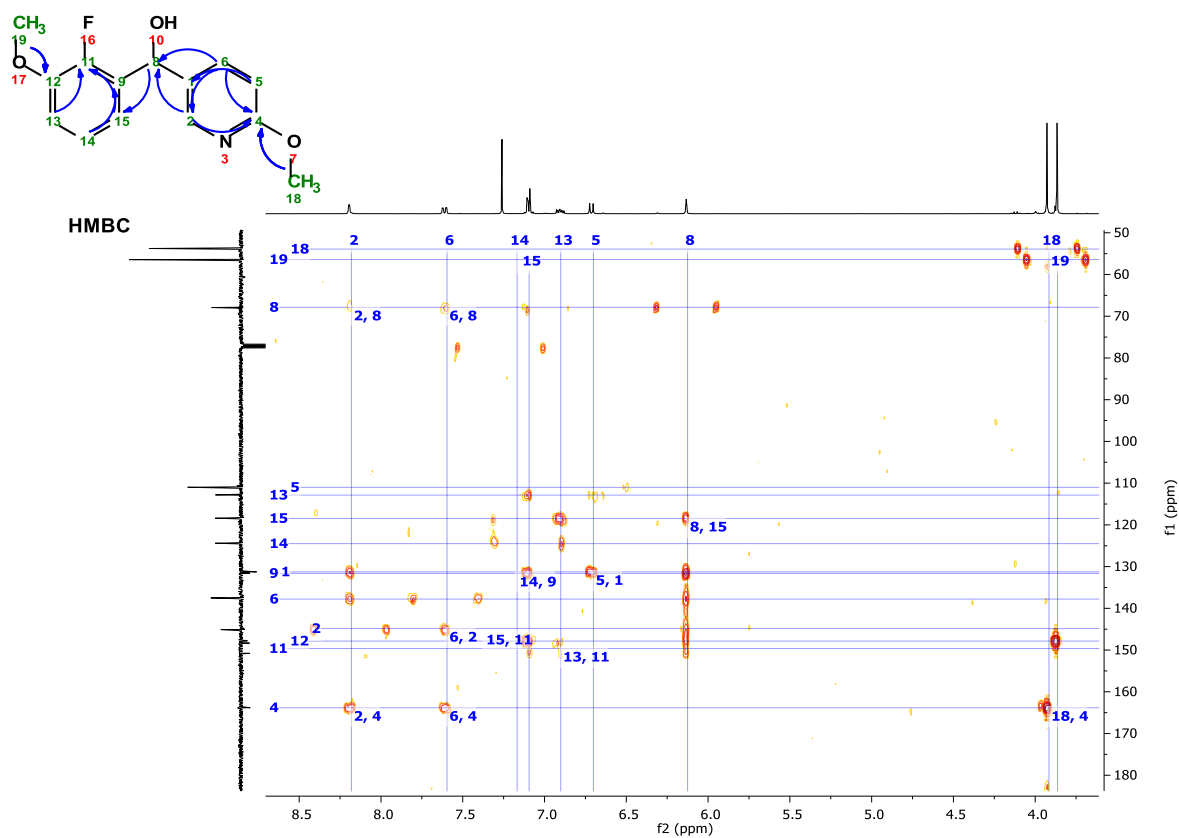
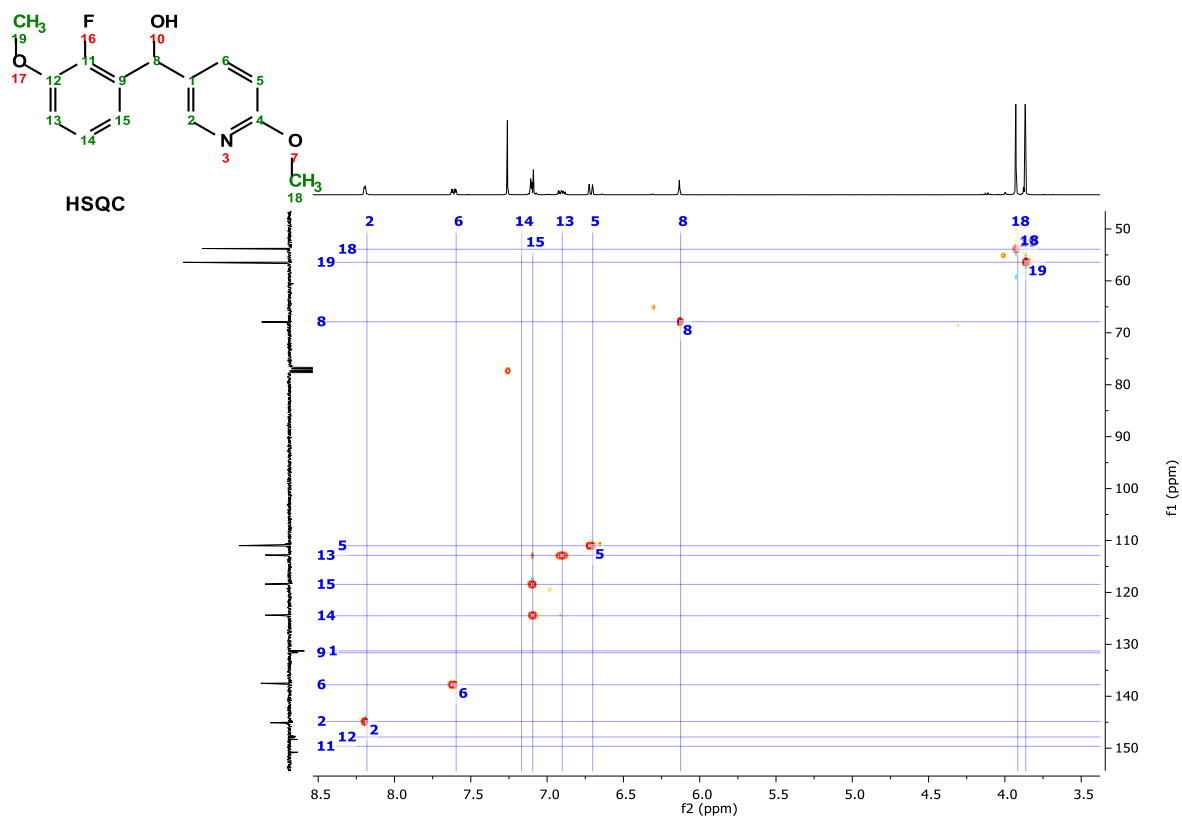
## A2.2 Compound 3.50



Exact Mass: 263.0958

| Atom | Chemical Shift | Splitting, <i>J</i> (Hz) | HSQC | HMBC     |
|------|----------------|--------------------------|------|----------|
| 1 C  | 131.26         |                          |      | 5        |
| 2 C  | 144.85         |                          | 2    | 6        |
| H    | 8.18           | d, 2.45                  | 2    | 4, 8     |
| 3 N  |                |                          |      |          |
| 4 C  | 163.82         |                          |      | 18, 6, 2 |
| 5 C  | 111.00         |                          | 5    |          |
| H    | 6.70           | d, 8.49                  | 5    | 1        |
| 6 C  | 137.78         |                          | 6    |          |
| H    | 7.60           | dd, 2.49, 8.63           | 6    | 4, 2, 8  |
| 7 O  |                |                          |      |          |
| 8 C  | 67.87          | d, 4.57                  | 8    | 2, 6     |
| H    | 6.13           |                          | 8    | 15       |
| 9 C  | 131.49..131.76 | d, 10.34                 |      | 14       |
| 10 O |                |                          |      |          |
| H    | 2.21..2.56     |                          |      |          |
| 11 C | 148.25..151.02 | d, 245.92                |      | 13, 15   |
| 12 C | 147.84         | d, 10.50                 |      | 19       |
| 13 C | 112.46..113.27 | d, 1.93                  |      |          |
| H    | 6.90           |                          |      | 11       |
| 14 C | 124.18..124.80 | d, 4.65                  |      |          |
| H    | 7.17           |                          |      | 9        |
| 15 C | 118.09..118.82 | d, 2.98                  |      | 8        |
| H    | 7.06..7.13     |                          |      | 11       |
| 16 F |                |                          |      |          |
| 17 O |                |                          |      |          |
| 18 C | 53.91          |                          | 18   |          |
| H3   | 3.92           |                          | 18   | 4        |
| 19 C | 56.42          |                          | 19   |          |
| H3   | 3.86           |                          | 19   | 12       |





## Appendix 3: Report of crystal structure for compound 4.04

SoC X-Ray Facility ID: [rwg2019\\_1b](#)

Dr Robert W. Gable  
School of Chemistry  
University of Melbourne  
Victoria 3010  
AUSTRALIA  
[23 January 2019](#)

### Crystal Quality (Information):

Colourless crystals were grown by slow evaporation from petroleum spirit 40°-60°/Ethyl Acetate. Crystals were very large plates. Attempts to cut the crystals resulted in them becoming disordered, however a small fragment was found that was not disordered. The structure was as indicated.

### Crystallography:

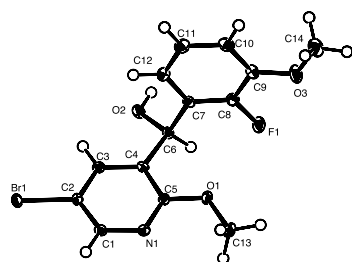
Colourless single crystals of  $C_{13}H_{12}BrFN_2O_3$  [rwg2019\\_1b](#) were crystallized by slow evaporation from petroleum spirit 40°-60°/Ethyl Acetate. Data collection for [rwg2018\\_44b](#) was carried out on an XtaLAB Synergy, Dualflex, HyPix diffractometer using mirror monochromated Mo K $\alpha$  radiation ( $\lambda = 0.71073 \text{ \AA}$ ) at 100 K. Using Olex2<sup>[1]</sup>, the structure was solved with the ShelXT<sup>[2]</sup> structure solution program using Intrinsic Phasing and refined with the ShelXL<sup>[3]</sup> refinement package using Least Squares minimization on  $F^2$ , using all data. Gaussian absorption corrections were applied to the data (CrysAlisPro 1.171.40.36a, Rigaku Oxford Diffraction, 2018). All non-hydrogen atoms were refined with anisotropic displacement parameters, while all hydrogen atoms on carbon atoms were placed at geometrical estimates and refined using the riding model; the hydroxyl hydrogen atoms were refined.

### Description of the Structure:

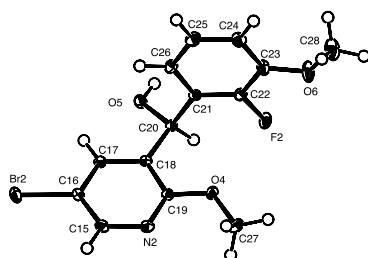
The crystal structure confirms the structure to be as indicated, there are two crystallographically unique molecules in the asymmetric unit. The conformation of both molecules are similar, the pyrazine (1,4-diazine) rings are in an almost perpendicular orientation to the attached [2-flouro-3-methoxyphenyl](#) ring, the dihedral angle between these two rings is 77.38(5)° and 79.59(6)°. The methoxy groups trans to the bromine are almost coplanar with the attached aromatic rings, and oriented away from the fluorine substituted ring [C12-O1-C4-N1 -0.6(3)° and C25-O4-C17-N3 -1.1(3)°], while the methoxy groups in the fluorine substituted ring are also slightly non-planar, the torsion angles C13-O3-C8-C7 and C26-O6-C21-C20 being 178.86(16)° and 176.90(17)°, respectively.

The hydroxyl group in each molecule is involved in an intramolecular H-bond with a nitrogen atom from the adjacent aromatic ring. As well, the hydroxyl group of molecule 2 is involved in an intermolecular H-bond with the hydroxyl group of molecule 1, while this hydroxyl group is also involved in a weak H-bond with the bromine atom of molecule 2, giving rise to a hydrogen bonded dimer. Weaker C-H...O, and C-H...F hydrogen bonds link the molecules into a 3D network. There is also a Br...Br interaction between adjacent molecules [Br1...Br2 3.5344(3)Å, C2-Br1...Br2 91.92(6)°; Br1...Br2-C15 166.05(6)°; C2-Br1...Br2-C15 12.1(3)°].

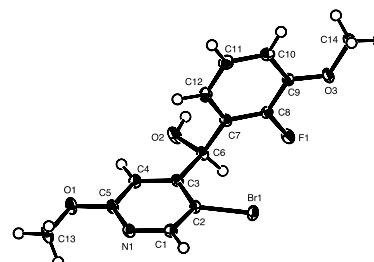
The conformations of the molecules are similar to those of the two molecules of [rwg2018\\_42](#).



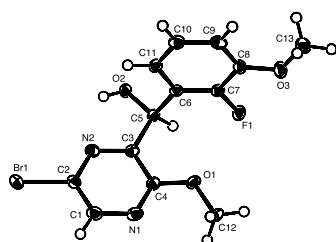
rwg2018\_42b Molecule 1



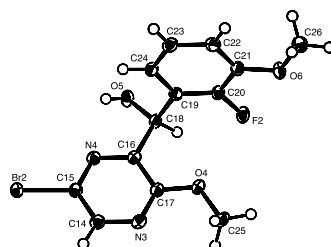
rwg2018\_42b Molecule 2



rwg2018\_44



rwg2019\_1b Molecule 1



rwg2018\_1b Molecule 2

A search through CSD Version 5.39 (August 2018 Update)<sup>[4]</sup> found only one similar compound, (4-bromophenyl)(pyridin-3-yl)methanol<sup>[5]</sup>.

**Table 1 Crystal data and structure refinement for rwg2019\_1aGau.**

|                                    |  |
|------------------------------------|--|
| Identification code                | rwg2019_1aGau  |
| Empirical formula                  | C <sub>13</sub> H <sub>12</sub> BrFN <sub>2</sub> O <sub>3</sub> |
| Formula weight                     | 343.16   |
| Temperature/K                      | 100.00(10)   |
| Crystal system                     | triclinic  |
| Space group                        | P-1  |
| a/Å                                | 8.76464(19)  |
| b/Å                                | 9.66017(19)  |
| c/Å                                | 16.2338(4)   |
| α/°                                | 105.7202(19)   |
| β/°                                | 93.6451(19)  |
| γ/°                                | 90.5667(17)  |
| Volume/Å <sup>3</sup>              | 1319.87(5)   |
| Z                                  | 4  |
| ρ <sub>calc</sub> /cm <sup>3</sup> | 1.727  |
| μ/mm <sup>-1</sup>                 | 4.465  |
| F(000)                             | 688.0  |



---

|   |   |
|---|---|
| Crystal size/mm <sup>3</sup>                | 0.073 × 0.046 × 0.032   |
| Radiation                                   | CuKα (λ = 1.54184)  |
| 2θ range for data collection/°              | 5.67 to 155.984   |
| Index ranges                                | -11 ≤ h ≤ 10, -12 ≤ k ≤ 10, -20 ≤ l ≤ 20                      |
| Reflections collected                       | 21049   |
| Independent reflections                     | 5535 [R <sub>int</sub> = 0.0355, R <sub>sigma</sub> = 0.0328] |
| Data/restraints/parameters                  | 5535/0/373  |
| Goodness-of-fit on F <sup>2</sup>           | 1.083   |
| Final R indexes [I ≥ 2σ (I)]                | R <sub>1</sub> = 0.0259, wR <sub>2</sub> = 0.0651             |
| Final R indexes [all data]                  | R <sub>1</sub> = 0.0296, wR <sub>2</sub> = 0.0668             |
| Largest diff. peak/hole / e Å <sup>-3</sup> | 0.44/-0.40  |

**Table 2 Fractional Atomic Coordinates ( $\times 10^4$ ) and Equivalent Isotropic Displacement Parameters ( $\text{\AA}^2 \times 10^3$ ) for rwg2019\_1aGau.  $U_{\text{eq}}$  is defined as 1/3 of the trace of the orthogonalised  $U_{ij}$  tensor.**

| Atom | <i>x</i>     | <i>y</i>     | <i>z</i>     | $U(\text{eq})$ |
|------|--------------|--------------|--------------|----------------|
| Br1  | 0.64601(2)   | 0.55014(2)   | 0.22744(2)   | 0.02223(7)     |
| F1   | 0.90447(12)  | -0.24508(12) | 0.14258(7)   | 0.0205(2)      |
| O1   | 1.01435(15)  | 0.03287(15)  | 0.12796(9)   | 0.0197(3)      |
| O2   | 0.61328(15)  | 0.03897(15)  | 0.25845(9)   | 0.0186(3)      |
| O3   | 0.82773(17)  | -0.45082(15) | 0.00348(9)   | 0.0240(3)      |
| N1   | 0.98259(19)  | 0.27147(19)  | 0.12946(11)  | 0.0223(3)      |
| N2   | 0.71345(18)  | 0.26298(17)  | 0.21010(10)  | 0.0174(3)      |
| C1   | 0.8968(2)    | 0.3878(2)    | 0.15263(14)  | 0.0227(4)      |
| C2   | 0.7643(2)    | 0.3826(2)    | 0.19323(12)  | 0.0183(4)      |
| C3   | 0.7959(2)    | 0.1470(2)    | 0.18679(11)  | 0.0155(3)      |
| C4   | 0.9340(2)    | 0.1532(2)    | 0.14687(12)  | 0.0167(4)      |
| C5   | 0.7382(2)    | 0.00972(19)  | 0.20546(12)  | 0.0152(3)      |
| C6   | 0.6914(2)    | -0.10590(19) | 0.12334(12)  | 0.0148(3)      |
| C7   | 0.7758(2)    | -0.2273(2)   | 0.09585(12)  | 0.0163(3)      |
| C8   | 0.7332(2)    | -0.3377(2)   | 0.02179(12)  | 0.0182(4)      |
| C9   | 0.5992(2)    | -0.3237(2)   | -0.02571(12) | 0.0201(4)      |
| C10  | 0.5120(2)    | -0.2019(2)   | 0.00178(13)  | 0.0203(4)      |
| C11  | 0.5564(2)    | -0.0941(2)   | 0.07446(13)  | 0.0186(4)      |
| C12  | 1.1558(2)    | 0.0377(2)    | 0.08695(13)  | 0.0229(4)      |
| C13  | 0.7842(3)    | -0.5656(2)   | -0.07108(14) | 0.0271(4)      |
| Br2  | 0.34868(2)   | 0.35496(2)   | 0.28699(2)   | 0.02082(7)     |
| F2   | 0.08293(13)  | -0.37375(12) | 0.35334(7)   | 0.0212(2)      |
| O4   | -0.02507(15) | -0.08787(15) | 0.37207(9)   | 0.0199(3)      |
| O5   | 0.35547(17)  | -0.19098(16) | 0.22537(9)   | 0.0210(3)      |
| O6   | 0.16871(16)  | -0.44543(15) | 0.49252(9)   | 0.0215(3)      |
| N3   | 0.00677(18)  | 0.15289(18)  | 0.37755(11)  | 0.0194(3)      |
| N4   | 0.27293(18)  | 0.08028(17)  | 0.29282(10)  | 0.0168(3)      |
| C14  | 0.0934(2)    | 0.2533(2)    | 0.35773(13)  | 0.0200(4)      |
| C15  | 0.2249(2)    | 0.2148(2)    | 0.31598(12)  | 0.0176(4)      |
| C16  | 0.1891(2)    | -0.0197(2)   | 0.31093(11)  | 0.0154(3)      |
| C17  | 0.0538(2)    | 0.0198(2)    | 0.35511(12)  | 0.0165(4)      |
| C18  | 0.2418(2)    | -0.1737(2)   | 0.28488(12)  | 0.0173(4)      |
| C19  | 0.2976(2)    | -0.21706(19) | 0.36488(12)  | 0.0164(3)      |
| C20  | 0.2151(2)    | -0.3117(2)   | 0.39633(12)  | 0.0170(4)      |
| C21  | 0.2627(2)    | -0.3504(2)   | 0.47057(12)  | 0.0179(4)      |
| C22  | 0.3999(2)    | -0.2920(2)   | 0.51427(13)  | 0.0199(4)      |
| C23  | 0.4855(2)    | -0.1976(2)   | 0.48290(13)  | 0.0212(4)      |
| C24  | 0.4362(2)    | -0.1601(2)   | 0.40966(13)  | 0.0191(4)      |
| C25  | -0.1622(2)   | -0.0493(2)   | 0.41751(14)  | 0.0239(4)      |
| C26  | 0.2194(2)    | -0.4923(2)   | 0.56607(14)  | 0.0246(4)      |

**Table 3 Anisotropic Displacement Parameters ( $\text{\AA}^2 \times 10^3$ ) for rwg2019\_1aGau. The Anisotropic displacement factor exponent takes the form:  $-2\pi^2[h^2a^{*2}U_{11}+2hka^*b^*U_{12}+...]$ .**

| Atom | $U_{11}$    | $U_{22}$    | $U_{33}$    | $U_{23}$   | $U_{13}$   | $U_{12}$    |
|------|-------------|-------------|-------------|------------|------------|-------------|
| Br1  | 0.02443(11) | 0.01494(10) | 0.02790(12) | 0.00658(8) | 0.00287(8) | 0.00004(7)  |
| F1   | 0.0164(5)   | 0.0205(5)   | 0.0234(6)   | 0.0048(5)  | -0.0030(4) | 0.0048(4)   |
| O1   | 0.0144(6)   | 0.0231(7)   | 0.0226(7)   | 0.0073(6)  | 0.0051(5)  | 0.0008(5)   |
| O2   | 0.0198(6)   | 0.0161(7)   | 0.0206(7)   | 0.0049(5)  | 0.0077(5)  | 0.0027(5)   |
| O3   | 0.0250(7)   | 0.0189(7)   | 0.0246(7)   | 0.0003(6)  | 0.0002(6)  | 0.0049(6)   |
| N1   | 0.0180(8)   | 0.0262(9)   | 0.0255(9)   | 0.0117(7)  | 0.0023(6)  | -0.0021(7)  |
| N2   | 0.0179(7)   | 0.0179(7)   | 0.0155(7)   | 0.0035(6)  | 0.0002(6)  | -0.0020(6)  |
| C1   | 0.0226(9)   | 0.0207(9)   | 0.0269(10)  | 0.0107(8)  | 0.0003(8)  | -0.0032(8)  |
| C2   | 0.0197(9)   | 0.0156(8)   | 0.0187(9)   | 0.0041(7)  | -0.0015(7) | -0.0011(7)  |
| C3   | 0.0150(8)   | 0.0179(9)   | 0.0128(8)   | 0.0033(7)  | -0.0018(6) | -0.0016(7)  |
| C4   | 0.0152(8)   | 0.0191(9)   | 0.0155(8)   | 0.0043(7)  | 0.0000(7)  | 0.0003(7)   |
| C5   | 0.0135(8)   | 0.0163(8)   | 0.0167(9)   | 0.0056(7)  | 0.0027(7)  | 0.0013(7)   |
| C6   | 0.0135(8)   | 0.0160(8)   | 0.0165(8)   | 0.0069(7)  | 0.0022(6)  | -0.0014(6)  |
| C7   | 0.0136(8)   | 0.0184(9)   | 0.0182(9)   | 0.0077(7)  | -0.0012(7) | 0.0000(7)   |
| C8   | 0.0201(9)   | 0.0162(9)   | 0.0193(9)   | 0.0057(7)  | 0.0049(7)  | 0.0012(7)   |
| C9   | 0.0220(9)   | 0.0210(9)   | 0.0168(9)   | 0.0053(7)  | -0.0016(7) | -0.0048(7)  |
| C10  | 0.0178(9)   | 0.0237(10)  | 0.0200(9)   | 0.0080(8)  | -0.0033(7) | -0.0016(7)  |
| C11  | 0.0154(8)   | 0.0193(9)   | 0.0232(9)   | 0.0095(7)  | 0.0006(7)  | 0.0015(7)   |
| C12  | 0.0151(9)   | 0.0304(11)  | 0.0238(10)  | 0.0068(8)  | 0.0069(7)  | 0.0006(8)   |
| C13  | 0.0295(11)  | 0.0193(10)  | 0.0279(11)  | -0.0030(8) | 0.0086(8)  | -0.0011(8)  |
| Br2  | 0.01870(10) | 0.01656(11) | 0.02813(12) | 0.00737(8) | 0.00318(8) | -0.00118(7) |
| F2   | 0.0188(5)   | 0.0219(6)   | 0.0231(6)   | 0.0080(5)  | -0.0036(4) | -0.0078(4)  |
| O4   | 0.0160(6)   | 0.0222(7)   | 0.0229(7)   | 0.0079(6)  | 0.0054(5)  | -0.0005(5)  |
| O5   | 0.0250(7)   | 0.0173(6)   | 0.0201(7)   | 0.0022(5)  | 0.0099(6)  | -0.0013(6)  |
| O6   | 0.0237(7)   | 0.0206(7)   | 0.0218(7)   | 0.0092(6)  | 0.0001(5)  | -0.0051(5)  |
| N3   | 0.0155(7)   | 0.0210(8)   | 0.0200(8)   | 0.0027(6)  | 0.0009(6)  | -0.0003(6)  |
| N4   | 0.0157(7)   | 0.0188(8)   | 0.0158(7)   | 0.0048(6)  | -0.0003(6) | -0.0005(6)  |
| C14  | 0.0178(9)   | 0.0188(9)   | 0.0218(9)   | 0.0032(7)  | -0.0003(7) | 0.0001(7)   |
| C15  | 0.0162(8)   | 0.0160(8)   | 0.0195(9)   | 0.0035(7)  | -0.0005(7) | -0.0019(7)  |
| C16  | 0.0149(8)   | 0.0176(9)   | 0.0128(8)   | 0.0030(7)  | -0.0006(6) | -0.0007(7)  |
| C17  | 0.0152(8)   | 0.0208(9)   | 0.0139(8)   | 0.0057(7)  | -0.0009(6) | -0.0012(7)  |
| C18  | 0.0165(8)   | 0.0170(9)   | 0.0182(9)   | 0.0035(7)  | 0.0045(7)  | -0.0008(7)  |
| C19  | 0.0167(8)   | 0.0139(8)   | 0.0176(9)   | 0.0021(7)  | 0.0037(7)  | 0.0018(7)   |
| C20  | 0.0149(8)   | 0.0143(8)   | 0.0198(9)   | 0.0019(7)  | -0.0011(7) | -0.0032(7)  |
| C21  | 0.0188(9)   | 0.0143(8)   | 0.0202(9)   | 0.0029(7)  | 0.0052(7)  | 0.0005(7)   |
| C22  | 0.0194(9)   | 0.0188(9)   | 0.0210(9)   | 0.0050(7)  | -0.0001(7) | 0.0019(7)   |
| C23  | 0.0158(8)   | 0.0202(9)   | 0.0255(10)  | 0.0033(8)  | -0.0007(7) | -0.0011(7)  |
| C24  | 0.0163(8)   | 0.0166(8)   | 0.0245(10)  | 0.0053(7)  | 0.0036(7)  | -0.0006(7)  |
| C25  | 0.0150(9)   | 0.0340(11)  | 0.0260(10)  | 0.0128(9)  | 0.0060(7)  | 0.0010(8)   |
| C26  | 0.0256(10)  | 0.0288(10)  | 0.0240(10)  | 0.0140(9)  | 0.0049(8)  | 0.0031(8)   |

**Table 4 Bond Lengths for rwg2019\_1aGau.**

| Atom | Atom | Length/Å | Atom | Atom | Length/Å   |
|------|------|----------|------|------|------------|
| Br1  | C2   | 1.903(2) | Br2  | C15  | 1.9003(18) |
| F1   | C7   | 1.358(2) | F2   | C20  | 1.358(2)   |
| O1   | C4   | 1.339(2) | O4   | C17  | 1.342(2)   |
| O1   | C12  | 1.450(2) | O4   | C25  | 1.449(2)   |
| O2   | C5   | 1.419(2) | O5   | C18  | 1.411(2)   |
| O3   | C8   | 1.357(2) | O6   | C21  | 1.359(2)   |
| O3   | C13  | 1.430(2) | O6   | C26  | 1.434(2)   |
| N1   | C1   | 1.339(3) | N3   | C14  | 1.344(3)   |
| N1   | C4   | 1.321(3) | N3   | C17  | 1.316(3)   |
| N2   | C2   | 1.337(2) | N4   | C15  | 1.332(3)   |
| N2   | C3   | 1.320(3) | N4   | C16  | 1.314(2)   |
| C1   | C2   | 1.378(3) | C14  | C15  | 1.377(3)   |
| C3   | C4   | 1.417(3) | C16  | C17  | 1.427(3)   |
| C3   | C5   | 1.527(2) | C16  | C18  | 1.517(3)   |
| C5   | C6   | 1.519(3) | C18  | C19  | 1.523(3)   |
| C6   | C7   | 1.377(3) | C19  | C20  | 1.381(3)   |
| C6   | C11  | 1.405(3) | C19  | C24  | 1.401(3)   |
| C7   | C8   | 1.401(3) | C20  | C21  | 1.396(3)   |
| C8   | C9   | 1.392(3) | C21  | C22  | 1.389(3)   |
| C9   | C10  | 1.394(3) | C22  | C23  | 1.393(3)   |
| C10  | C11  | 1.377(3) | C23  | C24  | 1.379(3)   |

**Table 5 Bond Angles for rwg2019\_1aGau.**

| Atom | Atom | Atom | Angle/°    | Atom | Atom | Atom | Angle/°    |
|------|------|------|------------|------|------|------|------------|
| C4   | O1   | C12  | 117.13(15) | C17  | O4   | C25  | 116.59(15) |
| C8   | O3   | C13  | 116.60(16) | C21  | O6   | C26  | 116.44(15) |
| C4   | N1   | C1   | 117.12(17) | C17  | N3   | C14  | 116.94(16) |
| C3   | N2   | C2   | 117.49(16) | C16  | N4   | C15  | 117.59(16) |
| N1   | C1   | C2   | 120.68(18) | N3   | C14  | C15  | 120.04(18) |
| N2   | C2   | Br1  | 117.48(14) | N4   | C15  | Br2  | 115.93(14) |
| N2   | C2   | C1   | 122.54(19) | N4   | C15  | C14  | 123.33(17) |
| C1   | C2   | Br1  | 119.98(14) | C14  | C15  | Br2  | 120.74(15) |
| N2   | C3   | C4   | 119.95(17) | N4   | C16  | C17  | 119.30(17) |
| N2   | C3   | C5   | 117.79(16) | N4   | C16  | C18  | 118.35(16) |
| C4   | C3   | C5   | 122.25(17) | C17  | C16  | C18  | 122.34(16) |
| O1   | C4   | C3   | 116.55(16) | O4   | C17  | C16  | 115.92(16) |
| N1   | C4   | O1   | 121.26(17) | N3   | C17  | O4   | 121.29(16) |
| N1   | C4   | C3   | 122.19(18) | N3   | C17  | C16  | 122.79(17) |
| O2   | C5   | C3   | 110.59(15) | O5   | C18  | C16  | 111.33(15) |
| O2   | C5   | C6   | 109.86(14) | O5   | C18  | C19  | 111.71(15) |
| C6   | C5   | C3   | 111.55(14) | C16  | C18  | C19  | 109.18(15) |
| C7   | C6   | C5   | 121.62(16) | C20  | C19  | C18  | 122.08(17) |
| C7   | C6   | C11  | 117.83(17) | C20  | C19  | C24  | 117.62(17) |
| C11  | C6   | C5   | 120.51(17) | C24  | C19  | C18  | 120.30(16) |
| F1   | C7   | C6   | 119.77(16) | F2   | C20  | C19  | 119.75(17) |
| F1   | C7   | C8   | 117.24(17) | F2   | C20  | C21  | 117.27(16) |
| C6   | C7   | C8   | 122.97(17) | C19  | C20  | C21  | 122.97(17) |
| O3   | C8   | C7   | 116.00(17) | O6   | C21  | C20  | 115.59(16) |
| O3   | C8   | C9   | 125.79(18) | O6   | C21  | C22  | 125.96(18) |
| C9   | C8   | C7   | 118.21(18) | C22  | C21  | C20  | 118.44(17) |
| C8   | C9   | C10  | 119.41(18) | C21  | C22  | C23  | 119.36(18) |
| C11  | C10  | C9   | 121.44(18) | C24  | C23  | C22  | 121.31(18) |
| C10  | C11  | C6   | 120.14(18) | C23  | C24  | C19  | 120.30(17) |

**Table 6 Hydrogen Bonds for rwg2019\_1aGau.**

| D   | H    | A               | d(D-H)/Å | d(H-A)/Å | d(D-A)/Å   | D-H-A/° |
|-----|------|-----------------|----------|----------|------------|---------|
| O2  | H2   | N2              | 0.80(3)  | 2.15(3)  | 2.653(2)   | 121(2)  |
| O2  | H2   | Br2             | 0.80(3)  | 3.06(3)  | 3.7975(15) | 155(2)  |
| C13 | H13B | F1 <sup>1</sup> | 0.98     | 2.52     | 3.390(2)   | 147.8   |
| O5  | H5A  | O2              | 0.78(3)  | 2.32(3)  | 3.071(2)   | 162(3)  |
| O5  | H5A  | N4              | 0.78(3)  | 2.27(3)  | 2.678(2)   | 113(3)  |
| C14 | H14  | O6 <sup>2</sup> | 0.95     | 2.48     | 3.166(2)   | 128.7   |
| C25 | H25C | O2 <sup>3</sup> | 0.98     | 2.50     | 3.442(3)   | 161.3   |
| C26 | H26C | F2 <sup>4</sup> | 0.98     | 2.53     | 3.421(2)   | 150.7   |

<sup>1</sup>2-X,-1-Y,-Z; <sup>2</sup>+X,1+Y,+Z; <sup>3</sup>-1+X,+Y,+Z; <sup>4</sup>-X,-1-Y,1-Z

**Table 7 Torsion Angles for rwg2019\_1aGau.**

| A   | B   | C   | D   | Angle/°     | A   | B   | C   | D   | Angle/°     |
|-----|-----|-----|-----|-------------|-----|-----|-----|-----|-------------|
| F1  | C7  | C8  | O3  | -1.2(2)     | F2  | C20 | C21 | O6  | -1.0(2)     |
| F1  | C7  | C8  | C9  | 178.10(16)  | F2  | C20 | C21 | C22 | 178.01(17)  |
| O2  | C5  | C6  | C7  | -127.66(17) | O5  | C18 | C19 | C20 | -128.90(18) |
| O2  | C5  | C6  | C11 | 50.1(2)     | O5  | C18 | C19 | C24 | 51.5(2)     |
| O3  | C8  | C9  | C10 | 178.95(17)  | O6  | C21 | C22 | C23 | 178.80(18)  |
| N1  | C1  | C2  | Br1 | 178.87(15)  | N3  | C14 | C15 | Br2 | 179.78(14)  |
| N1  | C1  | C2  | N2  | -1.2(3)     | N3  | C14 | C15 | N4  | 0.4(3)      |
| N2  | C3  | C4  | O1  | 177.58(16)  | N4  | C16 | C17 | O4  | -179.40(16) |
| N2  | C3  | C4  | N1  | -2.0(3)     | N4  | C16 | C17 | N3  | 1.3(3)      |
| N2  | C3  | C5  | O2  | -9.3(2)     | N4  | C16 | C18 | O5  | -14.8(2)    |
| N2  | C3  | C5  | C6  | 113.26(18)  | N4  | C16 | C18 | C19 | 108.98(18)  |
| C1  | N1  | C4  | O1  | -178.33(18) | C14 | N3  | C17 | O4  | -179.95(17) |
| C1  | N1  | C4  | C3  | 1.2(3)      | C14 | N3  | C17 | C16 | -0.7(3)     |
| C2  | N2  | C3  | C4  | 1.1(3)      | C15 | N4  | C16 | C17 | -1.0(3)     |
| C2  | N2  | C3  | C5  | -179.71(16) | C15 | N4  | C16 | C18 | 179.86(16)  |
| C3  | N2  | C2  | Br1 | -179.64(13) | C16 | N4  | C15 | Br2 | -179.20(13) |
| C3  | N2  | C2  | C1  | 0.4(3)      | C16 | N4  | C15 | C14 | 0.2(3)      |
| C3  | C5  | C6  | C7  | 109.34(19)  | C16 | C18 | C19 | C20 | 107.5(2)    |
| C3  | C5  | C6  | C11 | -72.9(2)    | C16 | C18 | C19 | C24 | -72.0(2)    |
| C4  | N1  | C1  | C2  | 0.3(3)      | C17 | N3  | C14 | C15 | -0.1(3)     |
| C4  | C3  | C5  | O2  | 169.87(16)  | C17 | C16 | C18 | O5  | 166.06(16)  |
| C4  | C3  | C5  | C6  | -67.5(2)    | C17 | C16 | C18 | C19 | -70.1(2)    |
| C5  | C3  | C4  | O1  | -1.6(3)     | C18 | C16 | C17 | O4  | -0.3(3)     |
| C5  | C3  | C4  | N1  | 178.85(17)  | C18 | C16 | C17 | N3  | -179.61(17) |
| C5  | C6  | C7  | F1  | -0.2(3)     | C18 | C19 | C20 | F2  | 2.8(3)      |
| C5  | C6  | C7  | C8  | 178.10(16)  | C18 | C19 | C20 | C21 | -178.59(17) |
| C5  | C6  | C11 | C10 | -177.67(16) | C18 | C19 | C24 | C23 | 178.93(17)  |
| C6  | C7  | C8  | O3  | -179.54(16) | C19 | C20 | C21 | O6  | -179.65(17) |
| C6  | C7  | C8  | C9  | -0.2(3)     | C19 | C20 | C21 | C22 | -0.6(3)     |
| C7  | C6  | C11 | C10 | 0.2(3)      | C20 | C19 | C24 | C23 | -0.6(3)     |
| C7  | C8  | C9  | C10 | -0.3(3)     | C20 | C21 | C22 | C23 | -0.1(3)     |
| C8  | C9  | C10 | C11 | 0.7(3)      | C21 | C22 | C23 | C24 | 0.5(3)      |
| C9  | C10 | C11 | C6  | -0.7(3)     | C22 | C23 | C24 | C19 | -0.1(3)     |
| C11 | C6  | C7  | F1  | -178.00(15) | C24 | C19 | C20 | F2  | -177.58(17) |
| C11 | C6  | C7  | C8  | 0.3(3)      | C24 | C19 | C20 | C21 | 1.0(3)      |
| C12 | O1  | C4  | N1  | -0.6(3)     | C25 | O4  | C17 | N3  | -1.1(3)     |
| C12 | O1  | C4  | C3  | 179.90(16)  | C25 | O4  | C17 | C16 | 179.54(16)  |
| C13 | O3  | C8  | C7  | 178.86(16)  | C26 | O6  | C21 | C20 | 176.90(17)  |
| C13 | O3  | C8  | C9  | -0.4(3)     | C26 | O6  | C21 | C22 | -2.1(3)     |

**Table 8 Hydrogen Atom Coordinates ( $\text{\AA} \times 10^4$ ) and Isotropic Displacement Parameters ( $\text{\AA}^2 \times 10^3$ ) for rwg2019\_1aGau.**

| Atom | x         | y         | z          | U(eq)    |
|------|-----------|-----------|------------|----------|
| H2   | 0.582(3)  | 0.116(3)  | 0.2577(18) | 0.027(7) |
| H1   | 0.927528  | 0.47475   | 0.140968   | 0.027    |
| H5   | 0.823111  | -0.027544 | 0.236864   | 0.018    |
| H9   | 0.567373  | -0.396428 | -0.076398  | 0.024    |
| H10  | 0.419923  | -0.19306  | -0.030343  | 0.024    |
| H11  | 0.495743  | -0.011642 | 0.091595   | 0.022    |
| H12A | 1.224187  | 0.113531  | 0.123664   | 0.034    |
| H12B | 1.133613  | 0.058018  | 0.031523   | 0.034    |
| H12C | 1.205299  | -0.05529  | 0.077942   | 0.034    |
| H13A | 0.682284  | -0.60344  | -0.065572  | 0.041    |
| H13B | 0.858164  | -0.642464 | -0.076705  | 0.041    |
| H13C | 0.782222  | -0.529574 | -0.122045  | 0.041    |
| H5A  | 0.406(3)  | -0.120(3) | 0.2369(19) | 0.032    |
| H14  | 0.06391   | 0.350834  | 0.37253    | 0.024    |
| H18  | 0.151829  | -0.237368 | 0.256869   | 0.021    |
| H22  | 0.435079  | -0.316205 | 0.56504    | 0.024    |
| H23  | 0.579749  | -0.158177 | 0.512552   | 0.025    |
| H24  | 0.496392  | -0.095459 | 0.389482   | 0.023    |
| H25A | -0.135446 | 0.020224  | 0.473031   | 0.036    |
| H25B | -0.209617 | -0.135685 | 0.426724   | 0.036    |
| H25C | -0.23419  | -0.006351 | 0.383495   | 0.036    |
| H26A | 0.228114  | -0.409487 | 0.61695    | 0.037    |
| H26B | 0.319415  | -0.536289 | 0.55697    | 0.037    |
| H26C | 0.145424  | -0.563024 | 0.574542   | 0.037    |

**Table 9. Least-squares planes (x,y,z in crystal coordinates) and deviations from them (\* indicates atom used to define plane) for rwg2019\_1aGau**

Plane 1:  $3.967(6) x + 0.236(8) y + 13.300(7) z = 5.685(4)$

Rms deviation of fitted atoms = 0.0066

|      |             |
|------|-------------|
| * N1 | -0.0017(13) |
| * C1 | -0.0064(14) |
| * C2 | 0.0067(14)  |
| * C3 | -0.0090(12) |
| * C4 | 0.0093(13)  |
| * N2 | 0.0012(12)  |
| Br1  | 0.032(3)    |
| O1   | 0.048(3)    |
| C12  | 0.065(4)    |
| C5   | -0.022(3)   |

Plane 2:  $4.817(6) x + 6.066(6) y - 11.853(8) z = 1.225(5)$

Rms deviation of fitted atoms = 0.0025

|       |             |
|-------|-------------|
| * C6  | 0.0013(12)  |
| * C7  | -0.0026(13) |
| * C8  | 0.0005(13)  |
| * C9  | 0.0028(13)  |
| * C10 | -0.0041(13) |
| * C11 | 0.0021(13)  |
| F1    | -0.045(2)   |
| O3    | -0.014(3)   |
| C13   | -0.036(4)   |
| C5    | -0.045(3)   |

Plane 3:  $4.103(5) x - 0.884(8) y + 13.609(6) z = 5.0310(14)$

Rms deviation of fitted atoms = 0.0038

|       |             |
|-------|-------------|
| * N3  | -0.0003(12) |
| * C14 | -0.0033(13) |
| * C15 | 0.0020(13)  |
| * C16 | -0.0062(12) |
| * C17 | 0.0050(13)  |
| * N4  | 0.0028(12)  |
| Br2   | -0.008(3)   |
| O4    | 0.007(3)    |
| C25   | 0.029(4)    |
| C18   | -0.009(3)   |



Plane 4: 4.658(6) x - 6.259(6) y - 6.318(12) z = 0.444(7)

Rms deviation of fitted atoms = 0.0032

|       |             |
|-------|-------------|
| * C19 | -0.0048(13) |
| * C20 | 0.0045(13)  |
| * C21 | -0.0005(13) |
| * C22 | -0.0031(14) |
| * C23 | 0.0027(14)  |
| * C24 | 0.0012(14)  |
| F2    | 0.049(3)    |
| O6    | 0.018(3)    |
| C26   | 0.082(4)    |
| C18   | -0.031(3)   |

Dihedral Angle (with approximate esd) between Planes 1 & 2: 77.38(5)°

Dihedral Angle (with approximate esd) between Planes 1 & 3: 6.73(9)°

Dihedral Angle (with approximate esd) between Planes 1 & 4: 74.34(6)°

Dihedral Angle (with approximate esd) between Planes 2 & 3: 73.93(5)°

Dihedral Angle (with approximate esd) between Planes 2 & 4: 79.31(5)°

Dihedral Angle (with approximate esd) between Planes 3 & 4: 79.59(6)°

## Experimental

Single crystals of  $C_{13}H_{12}BrFN_2O_3$  [rwg2019\_1aGau] were grown by slow evaporation from petroleum spirit 40–60 and Ethyl Acetate. A suitable crystal was selected and mounted on a MiTeGen mount on a XtaLAB Synergy, Dualflex, HyPix diffractometer. The crystal was kept at 100.00(10) K during data collection. Using Olex2<sup>[1]</sup>, the structure was solved with the ShelXT<sup>[2]</sup> structure solution program using Intrinsic Phasing and refined with the ShelXL<sup>[3]</sup> refinement package using Least Squares minimisation.

## Crystal structure determination of [rwg2019\_1aGau]

**Crystal Data** for  $C_{13}H_{12}BrFN_2O_3$  ( $M = 343.16$  g/mol): triclinic, space group P-1 (no. 2),  $a = 8.76464(19)$  Å,  $b = 9.66017(19)$  Å,  $c = 16.2338(4)$  Å,  $\alpha = 105.7202(19)^\circ$ ,  $\beta = 93.6451(19)^\circ$ ,  $\gamma = 90.5667(17)^\circ$ ,  $V = 1319.87(5)$  Å<sup>3</sup>,  $Z = 4$ ,  $T = 100.00(10)$  K,  $\mu(\text{CuK}\alpha) = 4.465$  mm<sup>-1</sup>,  $D_{\text{calc}} = 1.727$  g/cm<sup>3</sup>, 21049 reflections measured ( $5.67^\circ \leq 2\theta \leq 155.984^\circ$ ), 5535 unique ( $R_{\text{int}} = 0.0355$ ,  $R_{\text{sigma}} = 0.0328$ ) which were used in all calculations. The final  $R_1$  was 0.0259 ( $I > 2\sigma(I)$ ) and  $wR_2$  was 0.0668 (all data).

## Refinement model description

Number of restraints - 0, number of constraints - unknown.

### Details:

1. Fixed Uiso
  - At 1.2 times of:
    - All C(H) groups
  - At 1.5 times of:
    - All C(H,H,H) groups, All O(H) groups
- 2.a Ternary CH refined with riding coordinates:
  - C5(H5), C18(H18)
- 2.b Aromatic/amide H refined with riding coordinates:
  - C1(H1), C9(H9), C10(H10), C11(H11), C14(H14), C22(H22), C23(H23), C24(H24)
- 2.c Idealised Me refined as rotating group:
  - C12(H12A,H12B,H12C), C13(H13A,H13B,H13C), C25(H25A,H25B,H25C), C26(H26A,H26B,H26C)

## References:

- [1] O. V. Dolomanov, L. J. Bourhis, R. J. Gildea, J. A. K. Howard, H. Puschmann, *IUCr, J. Appl. Crystallogr.* **2009**, *42*, 339–341.
- [2] G. M. Sheldrick, *Acta Crystallogr. Sect. A Found. Adv.* **2015**, *71*, 3–8.
- [3] G. M. Sheldrick, *Acta Crystallogr. Sect. C Struct. Chem.* **2015**, *71*, 3–8.
- [4] C. R. Groom, I. J. Bruno, M. P. Lightfoot, S. C. Ward, *Acta Crystallogr. Sect. B Struct. Sci. Cryst. Eng. Mater.* **2016**, *72*, 171–179.